LEYBOLD
VACUUM HANDBOOK

BY

K. DIELS AND R. JAECKEL

TRANSLATED BY

H. ADAM AND J. EDWARDS

PERGAMON PRESS
OXFORD · LONDON · EDINBURGH · NEW YORK
TORONTO · PARIS · BRAUNSCHWEIG

Pergamon Press Ltd., Headington Hill Hall, Oxford
4 & 5 Fitzroy Square, London W. 1
Pergamon Press (Scotland) Ltd., 2 & 3 Teviot Place, Edinburgh 1
Pergamon Press Inc., 44-01 21st Street, Long Island City, New York 11101
Pergamon of Canada, Ltd., 6 Adelaide Street East, Toronto, Ontario
Pergamon Press S.A.R.L., 24 rue des Écoles, Paris 5^e
Vieweg & Sohn GmbH, Burgplatz 1, Braunschweig

First English edition 1966

This is a translation of the second edition of the German
Leybold Vakuum-Taschenbuch published by Springer-Verlag, Berlin

Library of Congress Catalog Card No. 64-23680

1846/66

Foreword

VACUUM technology in general and high vacuum technology in particular have undergone such rapid and progressive development in the last decade that they constitute today a sphere of work which requires a continually widening range of specialized knowledge for one to have command of it. This specialized knowledge is not confined solely to the handling of pumps and gauges, it also extends to many physico-chemical problems and others arising out of the physics of solids, which must be mastered, otherwise not even the best of pumps will give the desired results. Conversely, the accumulation of deeper knowledge has led to an advance into pressure ranges which but a few years ago were considered to be technically inaccessible.

I am convinced that the authors of the Vacuum Handbook will reap the thanks of all readers for the valuable and critical information which they have so diligently and carefully compiled. It is for me a great pleasure that the name of my company is associated with this handbook.

Cologne,
January 1958

M. DUNKEL

Preface to the Second Edition

We are delighted that the first edition of this handbook was received with such wide and keen interest at home and abroad. In the second edition we have made every endeavour to eliminate all errors and shortcomings that arose in the first edition. We are grateful to all colleagues who helped us to realize this endeavour by providing us with information and suggestions for improvements.

Apart from the inclusion of new data and the improvements, the revised second edition differs from its predecessor by the rearrangement of certain chapters. The high vacuum processes and plants have meanwhile grown so much in importance that they must be treated at far greater length than was the case in the first edition. We have, therefore, decided to omit them completely in the text of the second edition, although we would draw readers' attention to the long lists of references on high vacuum processes and plants given in the bibliography. Besides these, we have included in the chapter on materials a number of important tables extracted from the chapter on high vacuum processes and plants in the first edition. Ion getter pumps, cryogenic pumps and ultra-high vacuum have acquired such technical significance in recent years that we have treated these subjects in chapters of their own.

We are most grateful to the many co-workers who have again helped us in preparing the second edition. Besides those already mentioned in the first edition, special thanks are extended to Messrs. Forth, Nöller, Reinke and Schieffer.

Cologne and Bonn,
September 1962

K. Diels and R. Jaeckel

Preface to the First Edition

IN recent decades vacuum technology has advanced from the purely empirical treatment of problems to a technical science in which existing problems are dealt with by quantitative means. The data required today for the numerical calculation of vacuum plants and vacuum processes are, however, widely scattered in a very large number of journals, book publications and company catalogues. In consequence, it is most laborious, time-wasting and extremely difficult for the individual to trace the necessary numerical data. A collection of the numerical material needed for such purposes, compiled in the same way as already successfully accomplished in other fields, appeared, therefore, to be most useful. We realize that such a screening of data will at the first attempt be subject to shortcomings. We should be most grateful to colleagues for helpful suggestions and additional information.

The subjects on which we have compiled data in this handbook include: the gas-kinetic processes, the use and the treatment of vacuum pumps and vacuum gauges, the calculation and dimensioning of pipelines, and data on high vacuum processes (here, too, we considered that a collection of the available material would even now be of much benefit).

With respect to materials, a large number of very good monographs already exist, although they mainly refer to the manufacture of tubes*. But as this handbook is intended both for the designer of tubes as well as for the process engineer, we believe that the best solution is to provide summarized extracts of the data on materials used for tube manufacture together with the already available material for process engineering. We have purposely omitted those values which at some time were obtained in special conditions, solely including significant values proved by experience. For these reasons, we have also decided not to devote special chapters to fields that are still in the stage of brisk development (ion pumps, getter pumps etc.) nor to the extremely low pressures of less than 10^{-9} Torr. We have merely made occasional brief reference to these questions wherever they appeared relevant.

In view of its special importance, a separate chapter has been written on the subject of outgassing and gas sorption.

---

* These publications also include Vol. 2 of *Tabellen für Elektronenphysik, Ionenphysik und Übermikroskopie* by MANFRED VON ARDENNE; chapter D contains an excellent and comprehensive collection of numerical data of importance to high vacuum technology.

A comprehensive bibliography is provided with the object of helping readers to find information not reproduced in this handbook for lack of space.

We gratefully acknowledge the very great assistance we received from our following co-workers in preparing and compiling this handbook: Messrs. Bächler, vom Berg, Eschbach, Florin, Gross, Holländer, Mirgel, Peperle, Rettinghaus, Reylander, Schittko, Strier, Thees and Treupel. Special thanks are extended to Dr. Manfred Dunkel for his valued help, encouragement and advice, as well as for placing at our disposal information and records in the possession of Messrs. Leybold. Finally, we are greatly indebted to the German publishers, Messrs. Springer, for the understanding they showed for our wishes in the printing of the German edition of this handbook.

Cologne and Bonn,
January 1958

K. DIELS and R. JAECKEL

1 Vacuum Physics

1.1 Nomenclature

1.1.1 Symbols used in Formulae*

Term	Symbol	Dimension	cf. page
Impingement rate (rate of incidence)	A	$\text{sec}^{-1}\,\text{cm}^{-2}$	14
Collision radius	$a = r_1 + r_2$	cm	17
Gas ballast	B	litre/sec	5
Specific heat at const. pressure	C_p	$\text{cal deg}^{-1}\,\text{mol}^{-1}$	
Specific heat at const. volume	C_v	$\text{cal deg}^{-1}\,\text{mol}^{-1}$	
Velocity of sound	c	cm sec^{-1}	40
Volume concentration of gas in solution in liquid	c_{Fl}	cm^{-3}	251
Volume concentration of gas in solution in the gas phase	c_g	cm^{-3}	251
Diffusion coefficient	D	$\text{cm}^2\,\text{sec}^{-1}$	4
Diameter	d, D	cm	
Heat of absorption	E_A	cal	251
Area, cross section	F	cm^2	
Rate of flow (throughput)	G	g sec^{-1} Torr litre/sec	
Gas desorption rate	g	$\text{g sec}^{-1}\,\text{cm}^{-2}$ $\text{Torr litre sec}^{-1}\,\text{cm}^{-2}$ $\text{mol sec}^{-1}\,\text{cm}^{-2}$	
Heat of adsorption	H	cal	252
Enthalpy per unit mass	i	erg g^{-1}	38
Ion current	i^+	A	
Pumping efficiency of the condenser	$K = S_K \cdot p$	Torr litre/sec	
BOLTZMANN's constant	k	erg deg^{-1}	10
Conductance	$L = 1/W$	litre/sec	4

---

* It is unavoidable that in some sections a few formula symbols have a different meaning from that given in the table. Appropriate definitions are given in the respective sections.

Term	Symbol	Dimension	cf. page
Length	l	cm	
Molecular weight	M	g mol^{-1}	
MACH number	Ma	—	40
Mass of molecule	m	g	
Number of molecules per cc.	n	cm^{-3}	55
Pressure	p, P	Torr (dyn cm^{-2})	
Atmospheric pressure	p_{at}	Torr	
Partial vapour pressure	p_d	Torr	
Partial gas pressure	p_g	Torr	
Saturation vapour pressure	p_s	Torr	7
Intake pressure of high vacuum pump	p_H	Torr	67
Intake pressure of forepump	p_V	Torr	67
Throughput (load)	Q	Torr litre/sec	7
Rate of flow, capacity		g sec^{-1}	
Gas constant per mole	R	erg deg^{-1} mol^{-1} Torr litre deg^{-1} mol^{-1}	10
Radius of molecule	r	cm	
Pumping speed	S	litre/sec	20
Speed of a high vacuum pump	S_H	litre/sec	
Speed of the condenser	S_K	litre/sec	
Speed of the forepump	S_V	litre/sec	
Absol. temperature	T	°K	
SUTHERLAND constant	T_v	°K	17
Time	t	sec	
Circumference of cross section	U	cm	
Volume	V	cm^3, litre	
Specific volume (per unit mass)	v	cm^3 g^{-1}	22
Impedance (resistance) of flow	$W = 1/L$	sec litre^{-1}	5
Velocity	w	cm sec^{-1}	
Mean velocity	$\overline{w}$	cm sec^{-1}	11
Mean square velocity	$\overline{w^2}$	cm^2 sec^{-2}	11
Most probable velocity	$w_{\max}$	cm sec^{-1}	10
Collision rate (collision frequency per molecule)	z	sec^{-1}	16
Accommodation coefficient	α	—	3
OSTWALD's coefficient of solubility	$\Gamma = c_{Fl}/c_g$	—	251

Term	Symbol	Dimension	cf. page
Coefficient of viscosity	η	P, g cm^{-1} sec^{-1}	17
Ratio of specific heats	$\varkappa = C_p/C_v$	–	
Mean free path	Λ	cm	15
Heat conductivity	λ	cal deg^{-1} cm^{-1} sec^{-1}	18
Mass of gas per unit time and surface area	μ	g sec^{-1} cm^{-2}	14
Micron	$1\,\mu = 10^{-3}$ Torr		
Number of revolutions, frequency	ν	sec^{-1}	
Density	ϱ	g cm^{-3}	
Throughput per unit area, specific rate of flow	$\psi = G/F$	g sec^{-1} cm^{-2} Torr litre sec^{-1} cm^{-2}	22

1.1.2 General Terms and Symbols used in Vacuum Technology*

Accommodation Coefficient (for free-molecule heat transfer). The ratio of the energy actually transferred between impinging gas molecules and a surface and the energy which would be theoretically transferred if the impinging molecules reached complete thermal equilibrium with the surface.

Back Streaming. The direct flight of vapour molecules by scattering from the hot vapour jet or evaporation from hot nozzle parts in the direction of the mouth or intake port of a vapour pump.

Baffle. A system of cooled walls, plates, or tubing placed near the inlet of a vapour pump to condense back-streaming vapour at a temperature below that of the room and return the fluid to the boiler. The baffle plates may be located in the "head" of the pump or in a separate housing attached to the inlet.

Booster Pump. A vapour pump or a specially designed mechanical pump used between a vapour pump and a forepump to increase the maximum gas throughput which can be handled. The limiting or breaking forepressure of the booster at this maximum throughput must be appreciably greater than that of the vapour pump which it backs.

Cold-cathode Ion Pump. A gettering pump in which the gettering surface is produced by cathode sputtering.

Cold Trap. A vessel designed to hold a refrigerant, or cooled by coils in which a refrigerant circulates, inserted into a vacuum system so as to condense on its inner surface vapours present in the system.

Collision Rate. The average number of collisions per second suffered by a molecule or other particle through a gas. Also called the *collision frequency per molecule*.

Compression Chamber. The decreasing space within a mechanical pump in which the gas is compressed before discharging through the outlet.

---

* The definitions given in this section are – wherever available – in accordance with the *Glossary of Terms used in Vacuum Technology*, issued by the Committee on Standards of the AMERICAN VACUUM SOCIETY INC. and published by PERGAMON PRESS INC., and/or in accordance with DIN 28·400.

Condensation Coefficient. The ratio of condensation rate to impingement rate.

Condenser. Part of a vacuum system with large cooling surfaces (usually water-cooled) for the condensation of large quantities of vapour (frequently water vapour).

Conductance (measured value). The throughput under steady-state limited conditions divided by the measured difference in pressure between two specified cross sections inside a pumping system.

Critical Backing Pressure. The value of the backing pressure at any stated throughput which, if exceeded, causes an abrupt increase of pressure on the high vacuum side of the pump. In certain pumps the increase does not occur abruptly and this pressure is not precisely determinable.

Cryogenic Pump. Device for pumping gases by condensation on extremely cold surfaces ($T \leqq 20\,^\circ$K).

Diffusion Coefficient. The absolute value of the ratio of the molecular flux per unit area to the concentration gradient of a gas diffusing through a gas or a porous medium where the molecular flux is evaluated across a surface perpendicular to the direction of the concentration gradient.

Diffusion Pump. A vapour pump with a vapour stream of low density, capable of pumping gas with full efficiency at intake pressures below 10^{-2} Torr. The pumping action of each vapour jet occurs by the diffusion of gas molecules through the low-density scattered vapour into the denser forward moving core of a freely expanding vapour jet.

Ejector Pump. A vapour pump with a dense vapour stream. The operating range depends on the pump fluid and is between 10^{-4} and 10^2 Torr. At higher pressures the mixing of entrained gas and vapour is effected by turbulence, at lower pressures by diffusion of gas into the vapour at the boundary of the dense vapour stream.

Evaporator-Ion Pump. An evaporator pump in which the gas is ionized in order to increase the sorption effect.

Evaporator Pump. A gettering pump in which the gas and vapour trapping surface is produced by means of thermal evaporation of a suitable metal.

Evaporation Rate. The number of molecules of a given substance evaporated per second per square centimetre from the free surface of the condensed phase.

Fluid Operated Pumps (stream pumps). Vacuum pumps which use a liquid, gaseous or vapour fluid of high velocity to effect pumping.

Forepressure. The total pressure on the outlet side of a pump measured near the outlet port. Sometimes called the *backing pressure.*

Forepump. The pump which produces the necessary fore-vacuum for a pump which is incapable of discharging gases at atmospheric pressure. Sometimes called the *backing pump.*

Fractionating Pump. A multi-stage vapour pump in which the vapour supplied to the first stage (jet nearest the high vacuum) has been purged of the more volatile impurities, resulting from decomposition or contamination, by the partial condensation and refluxing of vapour in the condenser and the circulating of the condensed pump fluid through a series of boilers feeding the various stages so that the unwanted volatile constituents will be ejected in the stages closest to the fore-vacuum.

Free Air Displacement (for mechanical pumps). (a) – Measured value – the volume of air passed per unit time through a mechanical pump when the pressure on the intake and exhaust sides is equal to atmospheric pressure. Also called *free air capacity.* (b) – Calculated value – product of the geometric volume of the compression chamber × atmospheric pressure × revs/min of the pump.

Gas Ballast. The venting of the compression chamber of a mechanical pump to the atmosphere to prevent condensation of condensable vapours within the pump. Also called *vented exhaust.*

Getter. (a) (noun) – a material which is included in a vacuum system or device for removing gas by sorption. (b) (verb) – to remove gas by sorption.

Getter-Ion Pump. An ion-sorption pump in which a getter is continuously or intermittently vaporized and condensed on the trapping surface to give a fresh deposit of sorbent.

Gettering Pump. A device in which gases are pumped by means of a getter contained in the device.

Harmful Space. Free space in the compression chamber of a mechanical pump at the end of the compression cycle. In oil-sealed mechanical pumps this free space is filled with oil for further reduction of its volume.

High-vacuum Pumps. Diffusion pumps, getter-ion pumps, ion pumps, molecular pumps.

HO-Coefficient (speed factor). Ratio of the speed (or admittance) to the product of the throat (or nozzle clearance area) and the maximum flow rate per unit area as given by the effusion law.

Impedance of Flow. The reciprocal of the conductance. Also called *resistance.* $W = 1/L$

Impingement Rate. The number of molecules which strike a plane surface per square centimetre per second in a gas at rest. Also known as *rate of incidence.*

Inlet Pressure. The total static pressure measured in a standard testing chamber by a vacuum gauge located near the inlet port of a vacuum pump (or: pressure in the inlet port of an operative vacuum pump.)

Ion Pump. An electrical device for pumping gas, comprising a means for ionizing the gas and a system of electrodes at suitable potentials, and in some cases also a magnetic field, which causes the ions formed to move towards an auxiliary pump or trap.

Ion-Sorption Pump. A pump which combines the action of an ion pump and a sorption pump by driving the ions into the sorbent.

Leak. In vacuum technology a hole, or porosity, in the wall of an enclosure capable of passing gas from one side of the wall to the other under action of a pressure or concentration differential existing across the wall.

Leak Rate. In leak detection practice, *leak rate* is defined as the rate of flow (in pressure × volume units per unit time) through a leak with gas at a specified high pressure (usually atmospheric pressure) on the inlet side and gas at a pressure on the exit side which is low enough to have negligible effect on the rate of flow.

Liquid Ring Pump. A pump for liquids or gases which entrains the fluid between the teeth of a pair of gears and the wall of the pump casing which fits closely around the gears except in the exhaust region where the teeth engage and the intake region where the teeth disengage.

Load of a Pump. The quantity of gas (not including pump fluid vapour) in mass units flowing across the inlet port of a pump in unit time. Typical units are pounds per hour or grams per hour.

Mean free path (of any particle). The average distance that a particle travels between successive collisions with the other particles of an assembly. In vacuum technology the assembly of particles of interest comprises only the molecules in the gas phase.

Mean Molecular Velocity. The average velocity of molecules in a gas at rest under equilibrium conditions.

Mechanical Pump. A pump which moves the gas by the cyclic motion of a system of mechanical parts such as pistons, eccentric rotors, vanes, valves, etc.

Modes of Flow. (a) – *supersonic flow* – flow of a compressive medium with large relative variations of density, characterized by high MACH numbers (e. g. supersonic flow in nozzles of an ejector pump). (b) – *turbulent flow* – flow of viscous matter accompanied by eddy currents so that the REYNOLDS number exceeds a certain critical value (i. e. $R_e \approx 2300$ for cylindrical ducts). (c) – *laminar flow* – flow of viscous matter without eddy currents (streamline flow) with small REYNOLDS numbers. (d) – POISEUILLE *flow* – the particular case of laminar viscous flow through a long pipe of circular section. (e) – *molecular flow* – the flow of gas through a duct under conditions such that the mean free path is greater than the largest dimension of a transverse section of the duct. The impedance is independent of pressure. (f) – *Knudsen flow* – the flow of gases through ducts and tubes under conditions intermediate between laminar flow and molecular flow.

Molecular Effusion. The passage of gas through a single opening in a plane wall of negligible thickness where the largest dimension of the hole is smaller than the mean free path.

Molecular (drag) Pump. A mechanical vacuum pump which creates a gas flow toward a suitable forepump by imparting to gas molecules which strike a rapidly moving surface a component of momentum tangential to the moving surface.

Oil Separator. An oil purification system attached to the oil reservoir of oil-sealed mechanical pumps to remove absorbed water vapour, solvents, etc.

Partial Pressure. The pressure of a designated component of a gaseous mixture. The total pressure in a mixture of perfect gases is equal to the sum of the pressures exerted by the component gases were each to occupy the same volume by itself.

Pressure after Compression. The pressure at the exhaust port of an operating vacuum pump.

Pump Fluid. The operating fluid used in vapour pumps or in liquid-sealed mechanical pumps.

Reciprocating Pump. A pump which moves the gas by means of a system of reciprocating pistons and valves.

Residual Gas Pressure. The pressure of all non-condensable gases in a container in which ultimate pressure has been obtained.

Residual Vapour Pressure. The vapour pressure in a system which has reached the ultimate or limiting value of total pressure.

Reynolds Number. As applied to the flow of gas through a circular tube the Reynold's number is a dimensionless quantity equal to the product of the gas density in grams per cubic centimetre times the flow velocity in centimetres per second times the tube diameter in centimetres divided by the viscosity coefficient in poises, $R_e = \varrho v d / \eta$.

Roots (blower) Pump. A rotary blower pump having a pair of two-lobe interengaging impellers of special design.

Rotary Blower Pump. A pump without a discharge valve which moves the gas by the propelling action of one or more rapidly rotating members provided with lobes, blades, or vanes. Sometimes called a *mechanical booster pump* when used in series with a mechanical forepump. Rotary blowers are sometimes classified as either *axial flow* or *cross flow* types depending on the direction of flow of gas.

Sliding Vane Rotary Pump. A liquid-sealed mechanical pump employing a rotor, stator and sliding vanes, dividing the pump chamber in three compartments.

Rotary Piston Pump. A liquid-sealed mechanical pump having a cylindrical plunger (or piston) which is moved by an eccentric rotor in a sliding rotary motion with a liquid seal against the walls of a cylindrical stator and which divides the stator into two compartments by means of an attached vane or blade which slides through a slot in a cylindrical bearing in the stator wall.

Saturation Vapour Pressure. The vapour pressure in an isolated system under equilibrium conditions in the presence of the condensed phase.

Separator (trap). Reservoir for separating two intermixed materials (e.g. water–oil; oil–air) by centrifugal force or by deposition under the influence of gravity.

Sorption Pump. A pump with a renewable trapping surface which reduces the partial pressure of gases by adsorption, absorption, or chemisorption.

Specific Speed. Pumping speed of a diffusion pump per unit area of nozzle clearance area.

Speed of Exhaust. The magnitude of the rate of reduction of pressure in the system multiplied by the volume and divided by the measured pressure.

Speed of a Pump. The pumping speed for a given gas is the ratio of the throughput of that gas to the partial pressure of that gas at a specified point near the mouth (or inlet port) of a pump.

Sputtering Pump. A gettering pump in which the gettering surface is produced by sputtering the getter material in an electric gas discharge.

Standard Atmosphere. (a) – the *standard atmosphere*, or *normal atmosphere* – is defined (independently of barometric height) as a pressure of 1,013,250 dyn/cm^2. (b) – the *normal atmosphere* – has also been defined as the pressure exerted by a mercury column 760 mm in height at 0 °C under standard acceleration of gravity of 980·665 cm/sec^2. Assuming a density of mercury at 0 °C of 13·59509 g/cm^3, this is equal to 1,013,249 dyn/cm^2.

Throughput. Under conditions of steady-state conservative flow the throughput across the entrance to a pipe is equal to the throughput at the exit. In this case the throughput can be defined as the quantity of gas flowing through a pipe in pressure× volume units per unit time at room temperature.

Time of Evacuation. The time required to pump a given system from atmospheric pressure to a specified pressure. Also known as *pump-down time*.

Torr. The Torr is defined as 1/760 of a standard atmosphere or 1,013,250/760 dyn/cm^2. This is equivalent to defining the Torr as 1333·22 microbars and differs by only one part in seven million from the International Standard millimetre of mercury. 1 mm Hg $=$ 1·00000014 Torr. Other units see page 102/103.

Total Pressure. Total pressure usually refers to the pressure determined by all of the molecular species crossing the imaginary surface.

Ultimate Pressure. The *limiting pressure* approached in the vacuum system after sufficient pumping time to establish that further reductions in pressure will be negligible.

Vapour. A gas whose temperature is below its critical temperature, so that it can be condensed to the liquid or solid state by increase of pressure alone.

Vapour Pressure. (a) – the sum of the partial pressures of all the vapours in a system. (b) – the partial pressure of a specified vapour.

Vapour (stream) Pump. Any pump employing a vapour jet as the pumping means. Applies to ejector pumps as well as to diffusion pumps.

Symbols for Vacuum Components

Symbols	Meaning
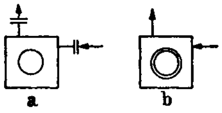	Rotary piston pump *a* -- single-stage *b* – two-stage
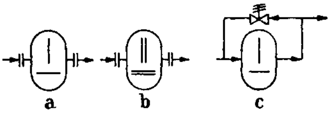	Roots blower pump *a* – single-stage *b* – two-stage *c* – single-stage with by-pass line
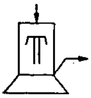	Diffusion pump
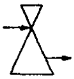	Diffusion ejector pump or ejector pump
	Condenser
	Buffer volume with stopcocks
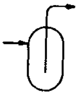	Cold trap

Fig. 1.1.1.

Symbols	Meaning
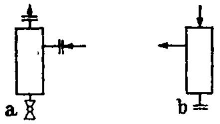	Oil separator *a* – on the exhaust port *b* – on the intake port
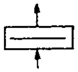	Baffle
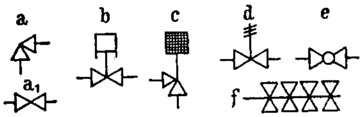	*a* – right angle valve a_1 – straight through valve *b* – pneumatic valve *c* – electro-magnetic valve *d* – overpressure valve *e* – tap *f* – valve combination
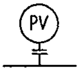 *e. g. Penning gauge*	Vacuum gauges e. g., AV – alphatron JV – ionization gauge KV – McLeod gauge FV – spring vacuum gauge PV – Penning gauge TV – thermoelectric gauge UV – U-tube manometer
	Flexible pipe
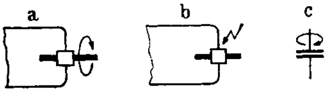	*a* – rotary lead-in *b* – current lead-in *c* – rotary flange
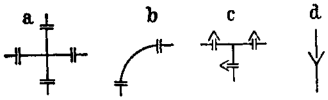	*a* – cross piece } with flanges *b* – bend } *c* – T-piece with small flanges *d* – conical ground joint

FIG. 1.1.2.

1.2 Kinetic Theory of Gases: Formulae and Tables

1.2.1 MAXWELL's Distribution of Molecular Velocities

Law of distribution for one single component (x component):

$$\frac{dn_{w_x}}{n} = \sqrt{\frac{M}{2\pi RT}}\, e^{-\frac{Mw_x^2}{2RT}}\, dw_x \qquad (1.2.1)$$

The formula gives the fraction of molecules for which the x component (w_x) of the resultant velocity is between w_x and $w_x + dw_x$.

Distribution law for the resultant velocity w

$$\frac{dn_w}{n} = \sqrt{\frac{2}{\pi}\left(\frac{M}{RT}\right)^3}\, e^{-\frac{Mw^2}{2RT}}\, w^2 dw \qquad (1.2.2)$$

The formula gives the fraction of molecules having a resultant velocity between w and $w + dw$.

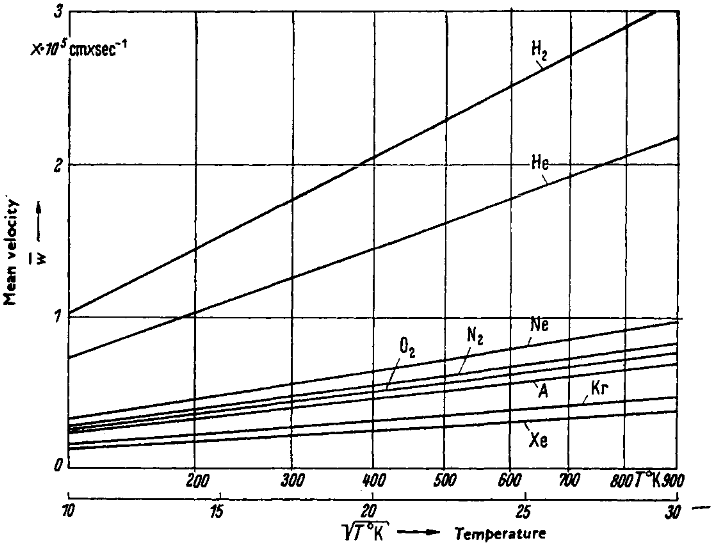

FIG. 1.2.1. Mean velocity $\bar{w}$ as a function of temperature T for various gases.

$w_{\max}$ **(cm/sec).** *Most probable velocity* $w_{\max}$ (velocity in the maximum of the distribution curve)

$$w_{\max} = \sqrt{\frac{2kT}{m}} = \sqrt{\frac{2RT}{M}} = 1{\cdot}29 \times 10^4 \sqrt{\frac{T}{M}} \quad (\text{cm sec}^{-1}) \qquad (1.2.3)$$

k – BOLTZMANN's constant $= 1{\cdot}371 \times 10^{-16}$ erg deg^{-1},
R – gas constant per mole $= 8{\cdot}315 \times 10^7$ erg deg^{-1} mol^{-1},
$= 62{\cdot}37$ Torr litre deg^{-1} mol^{-1}.

Mean velocities (cm/sec).

1. Mean velocity

$$\bar{w} = \sqrt{\frac{8kT}{\pi m}} = \sqrt{\frac{8RT}{\pi M}} = 1{\cdot}455 \times 10^4 \sqrt{\frac{T}{M}} \quad (\mathrm{cm\,sec^{-1}}). \tag{1.2.4}$$

2. Arithmetical mean of square velocities

$$\overline{w^2} = \frac{3kT}{m} = \frac{3RT}{M} = 2{\cdot}49 \times 10^8 \frac{T}{M} \quad (\mathrm{cm^2\,sec^{-2}}). \tag{1.2.5}$$

3. Root mean square velocity

$$\sqrt{\overline{w^2}} = \sqrt{\frac{3kT}{m}} = \sqrt{\frac{3RT}{M}} = 1{\cdot}58 \times 10^4 \sqrt{\frac{T}{M}} \quad (\mathrm{cm\,sec^{-1}}). \tag{1.2.6}$$

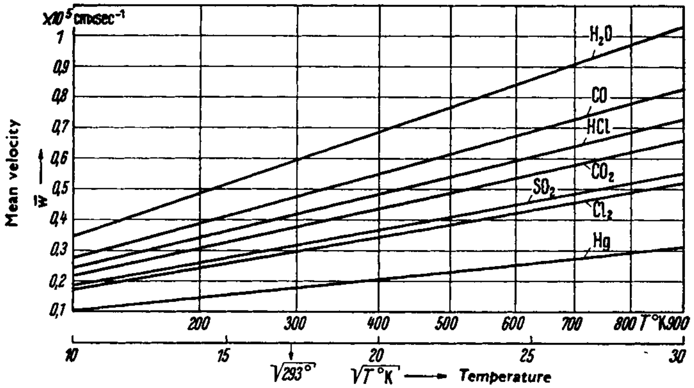

Fig. 1.2.2. Mean velocity $\bar{w}$ as a function of temperature T for various gases.

Table 1.2.1 Mean velocity $\bar{w}$ at 0 °C, 20 °C and 100 °C

Gas		H_2	N_2	O_2	Air	He	Ne	A
$\bar{w} \times 10^{-4}$ (cm/sec)	at 0 °C	16·93	4·542	4·252	4·468	12·01	5·355	3·805
$\bar{w} \times 10^{-4}$ (cm/sec)	at 20 °C	17·54	4·707	4·403	4·642	12·45	5·545	3·942
$\bar{w} \times 10^{-4}$ (cm/sec)	at 100 °C	19·79	5·310	4·968	5·238	14·05	6·256	4·447

Gas		Kr	Xe	Hg	H_2O	CO	CO_2	HCl
$\bar{w} \times 10^{-4}$ (cm/sec)	at 0 °C	2·629	2·099	1·698	5·565	4·543	3·624	3·981
$\bar{w} \times 10^{-4}$ (cm/sec)	at 20 °C	2·723	2·174	1·759	5·869	4·707	3·755	4·125
$\bar{w} \times 10^{-4}$ (cm/sec)	at 100 °C	3·072	2·453	1·984	6·620	5·310	4·236	4·653

Gas		SO_2	Cl_2	C_2H_5OH	NH_3
$\bar{w} \times 10^{-4}$ (cm/sec)	at 0 °C	3·004	2·856	3·543	5·829
$\bar{w} \times 10^{-4}$ (cm/sec)	at 20 °C	3·113	2·958	3·670	6·036
$\bar{w} \times 10^{-4}$ (cm/sec)	at 100 °C	3·512	3·337	4·141	6·810

TABLE 1.2.2. $\sqrt{\overline{w^2}}$ at 0°C, 20°C and 100°C.

Gas	H_2	N_2	O_2	Air	He	Ne	A
$\sqrt{\overline{w^2}} \times 10^{-4}$ (cm/sec) at 0°C	18·38	4·928	4·613	4·849	13·05	5·811	4·133
$\sqrt{\overline{w^2}} \times 10^{-4}$ (cm/sec) at 20°C	19·04	5·106	4·778	5·023	13·52	6·021	4·282
$\sqrt{\overline{w^2}} \times 10^{-4}$ (cm/sec) at 100°C	21·50	5·766	5·390	5·688	15·25	6·793	4·830

Gas	Kr	Xe	Hg	H_2O	CO	CO_2	HCl
$\sqrt{\overline{w^2}} \times 10^{-4}$ (cm/sec) at 0°C	2·854	2·278	1·842	6·148	4·933	3·933	4·323
$\sqrt{\overline{w^2}} \times 10^{-4}$ (cm/sec) at 20°C	2·957	2·361	1·908	6·368	5·109	4·076	4·479
$\sqrt{\overline{w^2}} \times 10^{-4}$ (cm/sec) at 100°C	3·336	2·663	2·155	7·190	5·766	4·600	5·053

Gas	SO_2	Cl_2	C_2H_5OH	NH_3
$\sqrt{\overline{w^2}} \times 10^{-4}$ (cm/sec) at 0°C	3·262	3·100	3·847	6·328
$\sqrt{\overline{w^2}} \times 10^{-4}$ (cm/sec) at 20°C	3·380	3·212	3·986	6·554
$\sqrt{\overline{w^2}} \times 10^{-4}$ (cm/sec) at 100°C	3·813	3·624	4·497	7·395

Relations of mean velocities and most probable velocities:

$$\overline{w^2} = \frac{3\pi}{8}\,\bar{w}^2 = \frac{3}{2}\,w_{\max}^2 .$$

$$\bar{w} = 1{\cdot}128\,w_{\max}, \qquad \overline{w^2} = \frac{3}{2}\,w_{\max}^2, \qquad \sqrt{\overline{w^2}} = 1{\cdot}223\,w_{\max} . \tag{1.2.7}$$

By inserting the most probable velocity $w_{\max} = \sqrt{\frac{2RT}{M}}$ in the MAXWELL'S distribution law one obtains:

$$\frac{dn_w}{n} = \frac{4}{\sqrt{\pi}}\left(\frac{w}{w_{\max}}\right)^2 e^{-\left(\frac{w}{w_{\max}}\right)^2} d\left(\frac{w}{w_{\max}}\right) = f\left(\frac{w}{w_{\max}}\right) d\left(\frac{w}{w_{\max}}\right). \tag{1.2.8}$$

By integration between $\left(\frac{w}{w_{\max}}\right)$ and ∞ one obtains the fraction $\frac{n_w}{n}$ of all molecules with a velocity higher than w:

$$\frac{n_w}{n} = \int\limits_{\left(\frac{w}{w_{\max}}\right)}^{\infty} f\left(\frac{w}{w_{\max}}\right) d\left(\frac{w}{w_{\max}}\right). \tag{1.2.9}$$

Table 1.2.3. Law of velocity distribution.

Maxwell's distribution law			Distribution of the relative impact velocity		
$\frac{w}{w_{\mathrm{max}}}$	$f\left(\frac{w}{w_{\mathrm{max}}}\right)$	$\frac{n_w}{n} = \int_{\left(\frac{w}{w_{\mathrm{max}}}\right)}^{\infty} f\left(\frac{w}{\mathrm{m\ ax}}\right) d\left(\frac{w}{w_{\mathrm{max}}}\right)$	$\frac{w_{rs}}{w_{\mathrm{max}}}$	$f\left(\frac{w_{rs}}{w_{\mathrm{max}}}\right)$	$\frac{n_{rs}}{n} = \int_{\left(\frac{w_{rs}}{w_{\mathrm{max}}}\right)}^{\infty} f\left(\frac{w_{rs}}{w_{\mathrm{max}}}\right) d\left(\frac{w_{rs}}{w_{\mathrm{max}}}\right)$
0·0	0·0000	1·000	0·0	0·00000	1·000
0·1	0·0224	0·999	0·1	0·00050	1·000
0·2	0·0866	0·994	0·2	0·00392	0·999
0·3	0·186	0·983	0·3	0·0129	0·999
0·4	0·308	0·956	0·4	0·0295	0·998
0·5	0·440	0·919	0·5	0·0552	0·994
0·6	0·567	0·869	0·6	0·0920	0·989
0·7	0·678	0·806	0·7	0·134	0·975
0·8	0·761	0·734	0·8	0·185	0·959
0·9	0·813	0·655	0·9	0·243	0·939
1·0	0·831	0·572	1·0	0·303	0·910
1·1	0·814	0·490	1·1	0·364	0·876
1·2	0·770	0·411	1·2	0·420	0·838
1·3	0·702	0·336	1·3	0·472	0·792
1·4	0·623	0·271	1·4	0·514	0·743
1·5	0·534	0·212	1·5	0·550	0·689
1·6	0·446	0·1633	1·6	0·570	0·634
1·7	0·362	0·1229	1·7	0·576	0·576
1·8	0·286	0·0906	1·8	0·577	0·519
1·9	0·220	0·0652	1·9	0·566	0·464
2·0	0·165	0·0460	2·0	0·540	0·405
2·1	0·121	0·0320	2·1	0·509	0·356
2·2	0·0864	0·0215	2·2	0·474	0·304
2·3	0·0601	0·0142	2·3	0·433	0·259
2·4	0·0408	0·0092	2·4	0·389	0·218
2·5	0·0272	0·0058	2·5	0·344	0·182
2·6	0·0177	0·0036	2·6	0·300	0·149
2·7	0·0112	0·0022	2·7	0·256	0·121
2·8	0·0069	0·0012	2·8	0·218	0·097
2·9	0·0040	0·0007	2·9	0·183	0·078
3·0	0·0024	0·0004	3·0	0·150	0·061
			3·1	0·122	0·048
			3·2	0·098	0·037
			3·3	0·077	0·028
			3·4	0·061	0·021
			3·5	0·047	0·016

In analogy the fraction $\frac{n_{rs}}{n}$ of molecules which have a velocity higher than the relative impact velocity w_{rs} is given by:

$$\frac{n_{rs}}{n} = \int\limits_{\left(\frac{w_{rs}}{w_{\max}}\right)}^{\infty} f\left(\frac{w_{rs}}{w_{\max}}\right) d\left(\frac{w_{rs}}{w_{\max}}\right). \qquad (1.2.10)$$

Calculated values are given in Table 1.2.3. It is evident that e. g. 57·2 percent of the total number of molecules have a higher velocity than the most probable velocity $w_{\max}$. 4·6 percent have a higher velocity than twice the most probable velocity, i. e. $2\,w_{\max}$.

1.2.2 Impingement Rate *A*

A (sec^{-1} cm^{-2})

$$A = \frac{1}{4} n \bar{w},$$

$$A = 2{\cdot}653 \times 10^{19} \frac{p}{\sqrt{MT}}, \quad p\,(\mathrm{dyn\,cm^{-2}}), \qquad (1.2.11)$$

$$A = 3{\cdot}535 \times 10^{22} \frac{p}{\sqrt{MT}}, \quad p\,(\mathrm{Torr}).$$

TABLE 1.2.4. Impingement rate at $p = 1$ Torr and 25 °C.

Gas	H_2	N_2	O_2	Air	He	Ne	A	Kr	Xe
$A \times 10^{-20}$ (sec^{-1} cm^{-2})	14·42	3·869	3·62	3·816	10·24	4·558	3·241	2·238	1·787

Gas	Hg	H_2O	CO	CO_2	HCl	SO_2	Cl_2	C_2H_5OH	NH_3
$A \times 10^{-20}$ (sec^{-1} cm^{-2})	1·446	4·826	3·869	3·087	3·391	2·559	2·431	3·017	4·962

1.2.3 Mass μ of Gas per unit Time and unit Area

μ (g sec^{-1} cm^{-2})

$$\mu = \frac{1}{4} n m \bar{w} = \frac{1}{4} \varrho \bar{w},$$

$$\mu = 43{\cdot}74 \times 10^{-6} p \sqrt{\frac{M}{T}}, \quad p\,(\mathrm{dyn\,cm^{-2}}), \qquad (1.2.12)$$

$$\mu = 58{\cdot}33 \times 10^{-3} p \sqrt{\frac{M}{T}}, \quad p\,(\mathrm{Torr}).$$

1.2.4 Pressure p of Molecules Impinging on a Wall

p (Torr)

p (dyn cm^{-2}) 1 Torr = 1333 dyn cm^{-2}

$$p = \frac{1}{3} n m \overline{w^2} = \frac{1}{3} \varrho \overline{w^2}. \tag{1.2.13}$$

1.2.5 Mean Free Path Λ $\Lambda \sim \frac{1}{p}$

Λ (cm)

(a) for identical molecules of radius r

$$\Lambda = \frac{1}{\sqrt{2} \times 4 \pi n r^2}, \tag{1.2.14}$$

(b) for gas mixtures

$$\Lambda_1 = \frac{1}{\pi \sum n_\nu 4 r_{1,\nu}^2 \sqrt{1 + \frac{M_1}{M_\nu}}} \tag{1.2.15}$$

mean free path of the first component

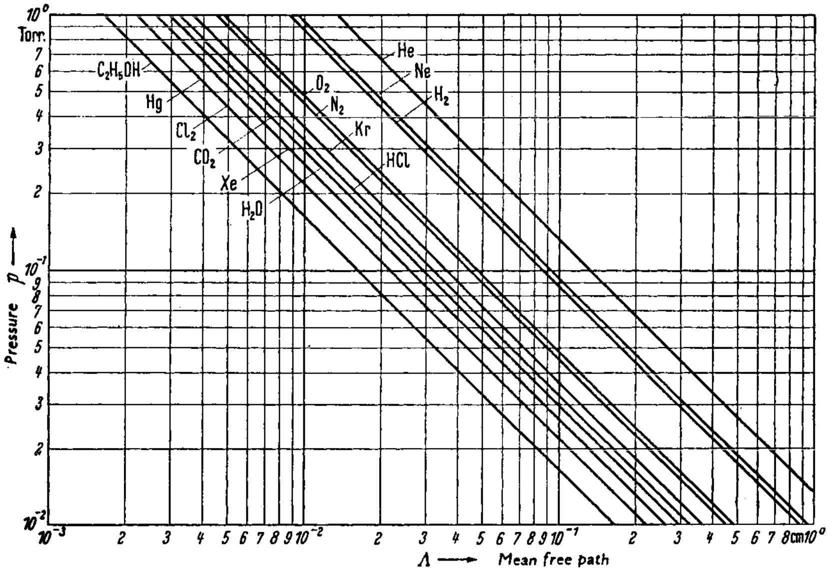

FIG. 1.2.3. Mean free path Λ vs. pressure p for various gases at 20 °C.

(c) for ions

$$\Lambda_i = \sqrt{2} \Lambda, \tag{1.2.16}$$

(d) for electrons

$$\Lambda_e = 4 \times \sqrt{2} \Lambda = \frac{1}{\pi r^2 n} \tag{1.2.17}$$

r radius of molecule; radius of electron neglected.

TABLE 1.2.5. Mean free path Λ at 20 °C and 1 micron.

Gas	H_2	N_2	O_2	Air	He	Ne	A	Kr	Xe	Hg	H_2O	CO	CO_2	HCl	SO_2	Cl_2	C_2H_5OH	NH_3
Λ(cm)	8·81	4·50	4·82	4·56	13·32	9·40	4·73	3·63	2·62	2·20	2·96	4·48	2·96	3·24	2·30	2·20	1·65	3·40

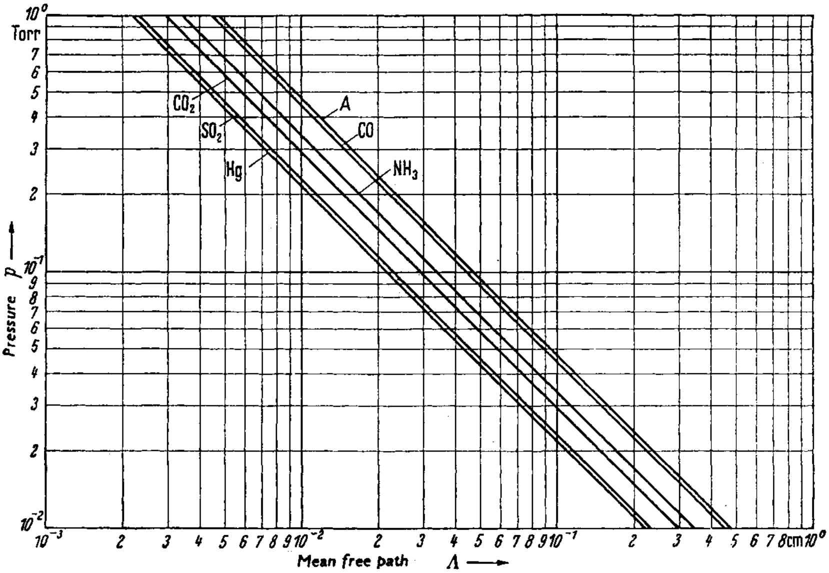

FIG. 1.2.4. Mean free path Λ vs. pressure p for various gases at 20 °C.

1.2.6 Collision Rate z

z (sec^{-1})

Average number of collisions per molecule in 1 sec:

$$z = \frac{\overline{w}}{\Lambda}. \tag{1.2.18}$$

TABLE 1.2.6. Collision rate z at 20 °C and 1 micron

Gas	H_2	N_2	O_2	Air	He	Ne	A	Kr	Xe	Hg	H_2O	CO	CO_2	HCl	SO_2	Cl_2	C_2H_5OH	NH_3
$z \times 10^{-3}$ (sec^{-1})	19·9	10·5	9·14	10·2	9·35	5·90	8·33	7·50	8·10	8·00	19·8	10·5	12·7	12·7	14·0	14·0	22·3	17·8

Relation of mean free path to temperature:

$$\Lambda = \frac{\Lambda_\infty}{1 + \frac{T_v}{T}}, \tag{1.2.19}$$

where Λ_∞ is the mean free path at $T = \infty$, and
T_v SUTHERLAND's constant.

Relation of collision radius a to temperature: $a = r_1 + r_2$,

$$a^2 = \left(1 + \frac{T_v}{T}\right) a_\infty^2, \tag{1.2.20}$$

where a_∞ is the collision radius at $T = \infty$.

TABLE 1.2.7. Λ_∞, a_∞ and T_v values (after JAECKEL)

Gas	H_2	N_2	O_2	He	Ne	A	Kr
$\Lambda_\infty \times 10^3$ at 1 Torr (cm)	10·56	6·1	6·87	16·0	11·19	7·03	5·96
$a_\infty \times 10^8$ (cm)	1·21	1·60	1·48	0·97	1·23	1·43	1·68
T_v (°K)	76	112	132	79	56	169	142

Gas	Xe	Hg	H_2O	CO	CO_2	HCl
$\Lambda_\infty \times 10^3$ at 1 Torr (cm)	4·87	9·5	9·5	6·02	5·7	7·22
$a_\infty \times 10^8$ (cm)	1·78	1·34	1·34	1·68	1·73	1·54
T_v (°K)	252	942	600	100	273	360

1.2.7 Viscosity η

η **(P)** 1 Poise = 1 g cm^{-1} sec^{-1}.

Coefficient of viscosity $\eta = \frac{n\overline{w}}{3} \Lambda m$, (1.2.21)

expressed more accurately $\eta = 21{\cdot}2 \times 10^{-22} \frac{\sqrt{MT}}{\pi a^2}$, (1.2.22)

$$\eta = 21{\cdot}2 \times 10^{-22} \frac{\sqrt{M}}{\pi a_\infty^2} \frac{T^{3/2}}{T + T_v}.$$

The approximate formula for *gas mixtures* containing two components is

$$\eta = \frac{1}{3} n_1 \overline{w}_1 \Lambda_1 m_1 + \frac{1}{3} n_2 \overline{w}_2 \Lambda_2 m_2, \tag{1.2.23}$$

$$\eta = \frac{1}{3} \sum n_v \overline{w}_v \Lambda_v m_v. \tag{1.2.24}$$

1.2.8 Heat Conductivity λ

λ (cal deg^{-1} cm^{-1} sec^{-1})

$$\lambda = \eta \frac{C_v}{M} \text{ for high pressures} \qquad (1.2.25)$$

or expressed more accurately

$$\lambda = 2{\cdot}52\, \eta \frac{C_v}{M} \text{ for monatomic gases,} \qquad (1.2.26)$$

also applies approximately to polyatomic gases (after CHAPMAN).

TABLE 1.2.8. η and λ values.

Gas	H_2	N_2	O_2	Air	He	Ne	A
$\eta \times 10^4$ at 20 °C (g sec^{-1} cm^{-1})	0·88	1·75	2·03	1·81	1·96	3·10	2·22
$\lambda \times 10^4$ at 0 °C (cal deg^{-1} cm^{-1} sec^{-1})	4·19	0·57	0·58	0·58	3·43	1·09	0·39

Gas	Kr	Xe	Hg	H_2O	CO	CO_2	HCl
$\eta \times 10^4$ at 20 °C (g sec^{-1} cm^{-1})	2·46	2·26	2·28	8·80	1·77	1·47	1·43
$\lambda \times 10^4$ at 0 °C (cal deg^{-1} cm^{-1} sec^{-1})	0·21	0·12	0·12	—	0·53	0·34	—

Gas	SO_2	Cl_2	C_2H_5OH	NH_3
$\eta \times 10^4$ at 20 °C (g sec^{-1} cm^{-1})	1·3	1·4	—	1·0
$\lambda \times 10^4$ at 0 °C (cal deg^{-1} cm^{-1} sec^{-1})	0·2	0·19	0·33	0·52

TABLE 1.2.9. Gas density ϱ at 0 °C and 760 Torr.

Gas	H_2	N_2	O_2	Air	He	Ne	A
$\varrho \times 10^3$ (g cm^{-3})	0·0899	1·2505	1·42895	1·2928	0·1785	0·8999	1·7839

Gas	Kr	Xe	Hg	H_2O	CO	CO_2	HCl
$\varrho \times 10^3$ (g cm^{-3})	3·74	5·89	9·021	0·768	1·25	1·9768	1·6391

Gas	SO_2	Cl_2	C_2H_5OH	NH_3
$\varrho \times 10^3$ (g cm^{-3})	2·9263	3·22	2·043	0·7714

TABLE 1.2.10. Boiling points.

Gas	H_2	N_2	O_2	Air	He	Ne	A	Kr	Xe
Boiling temp. in °C at 760 Torr	−253	−195·8	−183	−194·5	−269	−246	−186	−153	−108
Boiling temp. in °K at 760 Torr	20	77	90	78·5	4	27	87	120	165

Gas	Hg	H_2O	CO	CO_2	HCl	SO_2	Cl_2	C_2H_5OH	NH_3
Boiling temp. in °C at 760 Torr	+357	+ 100·0	−192	−78·5	− 85	−10	−34	+78	−33
Boiling temp. in °K at 760 Torr	630	373	81	194·5	188	263	239	351	240

TABLE 1.2.11. First ionization potentials.

Gas	H_2	N_2	O_2	He	Ne	A	Kr	Xe	Hg
First ionization potential in volts	15·4	15·8	12·5	24·5	21·5	15·7	14·0	12·08	10·4

Gas	H_2O	CO	CO_2	HCl	SO_2	Cl_2	NH_3
First ionization potential in volts	13·0	14·1	14·4	13·8	12·1	13·0	11·2

TABLE 1.2.12. Lowest excitation potentials.

Gas	H_2	N_2	O_2	He	Ne	A	Kr	Xe	Hg	CO	CO_2
Lowest excitation potential in volts	11·1	7·9	6·1	19·4	16·6	11·6	9·9	8·3	4·7	6·4	11·2

Examples of applications of gases.

H_2	N_2	He, Ne, A, Kr, Xe	Hg	CO_2
For filling barretter tubes and mercury arc switches, also as reducing protective gas atmosphere	Neutral protective gas atmosphere	Thyratrons, photoelectric cells, overload arresters and glow discharge tubes of all types, also resonant gate tubes without electrodes, additional filling for mercury arc rectifiers (Argonal)	Mercury arc rectifiers	Pilot lamps

1.3 Flow Phenomena

1.3.1 Impedance

Each flow in vacuum pipelines is expressed by the continuity equation

$$Q = p_1 S_1 = p_2 S_2 \tag{1.3.1}$$

according to which the same throughput of gas Q (in torr litre/sec.) flows through each of a number of successive cross sections 1, 2 etc. up to n. The impedance formula

$$p_1 - p_2 = S\,p\,W \text{ (analogous to Ohm's law)} \tag{1.3.2}$$

is of equally general validity; it expresses that the difference of pressure between the ends of a pipeline $p_1 - p_2$ is proportional to the product of the throughput flowing through the pipeline ($S\,p$) and the impedance (W) of the pipeline. On the other hand, the pumping speed (S) is not constant for all cross sections. The relation between the pumping speed at the inlet of a pipeline (S_1), at the outlet (S_2) and the impedance (W) or conductance (L) of the pipeline is given by the equation

$$S_1 = \frac{1}{\frac{1}{S_2} + W} = \frac{1}{\frac{1}{S_2} + \frac{1}{L}} \tag{1.3.3}$$

(see Fig. 1.3.1), which states that the pumping speed at the inlet of a pipeline S_1 is all the smaller the larger the impedance W of the pipeline. From this it follows that exact knowledge of factor W is necessary for estimating the efficiency of vacuum systems. For calculating the pipeline impedances W in sec/litre and the rates of flow G in g/sec, the following expressions are applied:

$$S\,p = \frac{G}{M} R\,T\,, \tag{1.3.4}$$

$$p_1 - p_2 = \frac{G}{M} R\,T\,W\,, \tag{1.3.5}$$

$$W = \frac{1}{G}\,\frac{(p_1 - p_2)\,M}{R\,T} = \frac{10^3 \varrho}{G} \tag{1.3.6}$$

(R = 62.37 Torr × litre × deg^{-1} × mol^{-1}).

1.3.1.1 At High Pressures ($\Lambda \ll 2r$)

1.3.1.1.1 Turbulent Flow

Cases of turbulent flow do not occur in the ranges of medium-high and high vacuum; this can easily be proved by calculating Reynold's number.

1.3.1.1.2 Laminar Flow

1.3.1.1.2.1 For long pipelines ($l \gg r$) and small differences of pressure between the ends of the pipeline $\left(p_1 - p_2 \ll \frac{p_1 + p_2}{2}\right)$ laminar flow is expressed by HAGEN-POISEUILLE's equation:

$$W = \frac{l\,\eta}{r^4}\,\frac{8 \times 10^3 \times 2}{\pi \times 1333\,(p_1 + p_2)} = \frac{l\,\eta}{F\,r^2}\,\frac{8 \times 10^3 \times 2}{1333\,(p_1 + p_2)} = 12\,\frac{l\,\eta}{F\,r^2\,(p_1 + p_2)} \quad \text{(sec/litre)} \tag{1.3.7}$$

$$G = \frac{10^3\,\varrho}{W} \quad \text{(g/sec)}, \tag{1.3.8}$$

l, r (cm), η (P), p (Torr), F cross section of pipe (cm^2), ϱ gas density (g/cm^3).

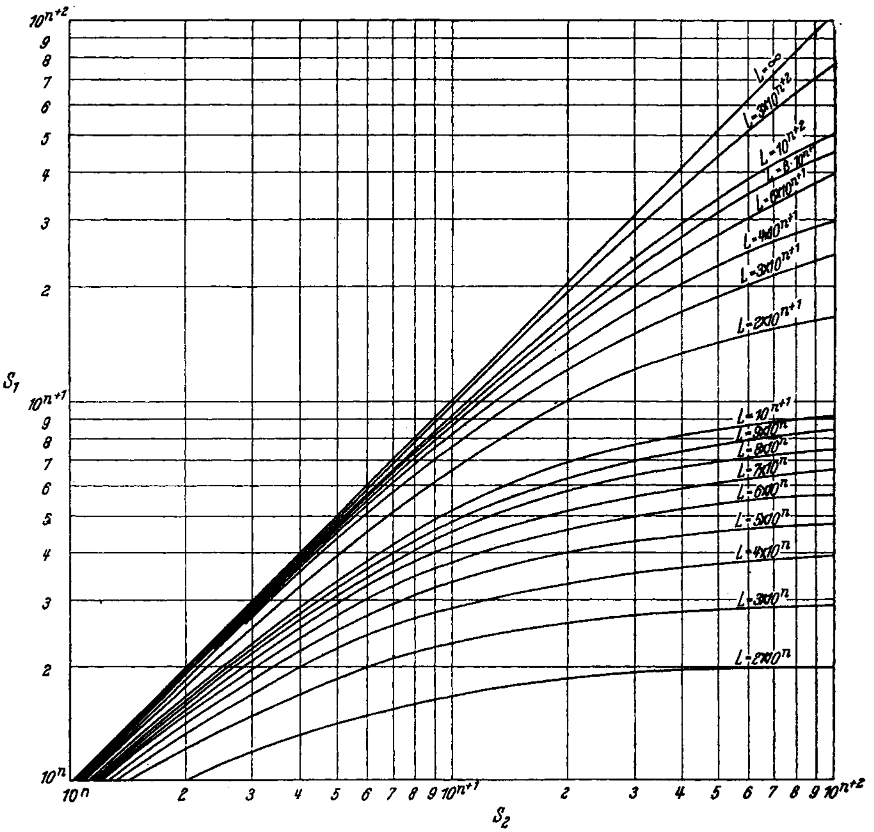

FIG. 1.3.1. Effective pumping speed S_1 at inlet of a pipeline of conductance L as a function of pumping speed S_2 at outlet of pipeline (cf. equation (1.3.3)).

For this case of flow, the graph of Harries (Fig. 1.3.2.) can be used to estimate whether a pipeline (l, r), for which the impedance of flow W has been calculated from equation (1.3.7), is suitable for a pump with a pumping speed S at a pressure p. Criterion: $S_1 \geqq 0.7\,S_2$.

1.3.1.1.2.2 For short pipelines. The processes in short pipelines ($l \simeq r$), with large differences of pressure between the ends of the pipe $\left(p_1 - p_2 \geqq \frac{p_1}{2}\right)$, can be treated analogous to flow through nozzles. The rate of flow in this case is expressed by the equation

$$G = F\left(\frac{p_2}{p_1}\right)^{\frac{1}{\varkappa}} \sqrt{\frac{\varkappa}{\varkappa-1}\left[1-\left(\frac{p_2}{p_1}\right)^{\frac{\varkappa-1}{\varkappa}}\right] 2\times 1333\,\frac{p_1}{v_1}} \quad \text{(g/sec)}. \tag{1.3.9}$$

where v_1 is the specific volume (cm³/g).

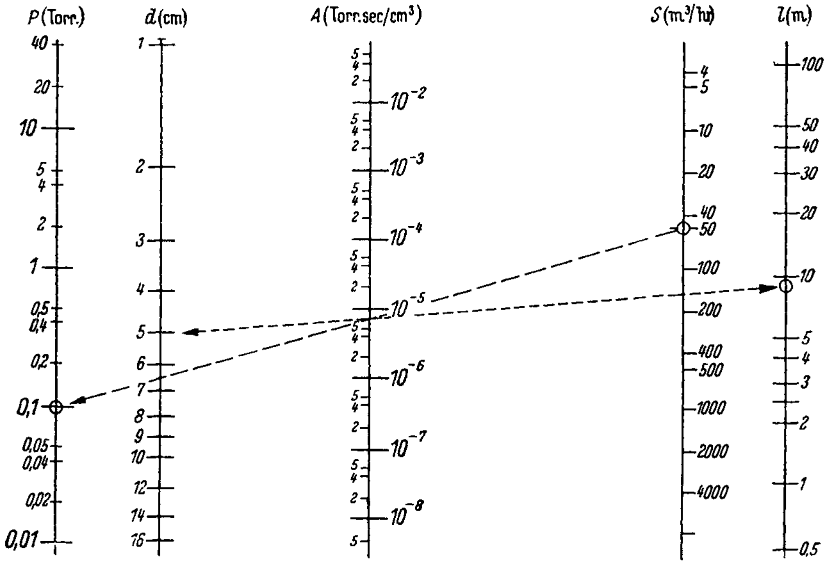

FIG. 1.3.2. HARRIES' graph shows how the pipeline (l, d) must be dimensioned for a pump with a pumping speed S at an intake pressure p so that the pumping speed will not be reduced by more than 30 percent, and, conversely, which pumping speed is admissible for the connected pump using the given pipeline (l, d) and a given intake pressure p. If three of the factors S, p, l, d are known, the fourth can be found from the graph. It is shown in the example that for a pipeline with a length of $l = 9$ m and a dia. of $d = 5$ cm; the line joining these two scale values intersects the scale A at one point. For an intake pressure of $p = 0{\cdot}1$ Torr, a second straight line extended from the scale value of 0·1 Torr through the above point of intersection on the scale A shows that the maximum admissible pumping speed S in the given conditions is 50 m³/hr.

The impedance W of the pipeline is calculated from equation (1.3.6) just as in the following cases, too, in which only the rate of flow G is given. The specific rate of flow ψ is expressed by the equation

$$\psi = \frac{G}{F} \quad (\text{g sec}^{-1}\,\text{cm}^{-2}) \tag{1.3.10}$$

1.3.1.1.2.3 For the intermediate range. The intermediate range between equation (1.3.7) resp. (1.3.8) and (1.3.9) is expressed, according to Günther, Jaeckel and Oetjen*, by the approximate equation

$$G = F\,\frac{M r^2 \frac{\varkappa}{\varkappa+1}}{R T_1 l \times 8\eta}\,\frac{\left[p_1^2 - p_2^2\left(\frac{p_1}{p_2}\right)^{\frac{\varkappa-1}{\varkappa}}\right]}{\left[1+\frac{G}{F}\,\frac{1}{6\eta\varkappa}\,\frac{r^2}{l}\ln\frac{p_1}{p_2}\right]}$$

$$= F \times 2{\cdot}68 \times 10^{-2}\,\frac{M r^2 \frac{\varkappa}{\varkappa+1}}{T_1 l \eta}\,\frac{\left[p_1^2 - p_2^2\left(\frac{p_1}{p_2}\right)^{\frac{\varkappa-1}{\varkappa}}\right]}{\left[1+\frac{G}{F}\,\frac{1}{6\eta\varkappa}\,\frac{r^2}{l}\ln\frac{p_1}{p_2}\right]} \quad \text{(g/sec)} \qquad (1.3.11)$$

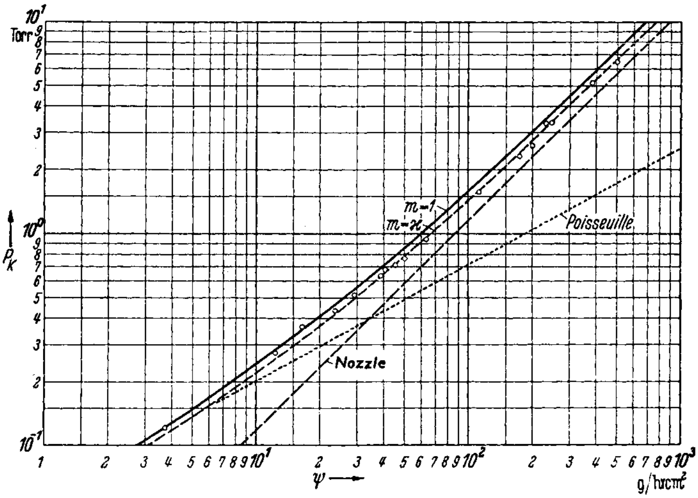

Fig. 1.3.3 shows, for a cylindrical pipeline, the relation of the specific rate of flow $\psi = G/F$ in relation to pressure at the inlet of the pipeline p_k. It is assumed that a polytropic line with the polytropic exponent m is valid for the phenomena in this case, i.e. for isothermal phenomena the polytropic exponent has a value of $m = 1$, and for adiabatic phenomena a value of $m = \varkappa$. The phenomena are described in all cases by Poiseuille's flow at low pressures and low throughputs, whereas at high pressures and large throughputs the inter-relationships valid for flow through nozzles become closer.

Figure 1.3.3 shows that in the case of large rates of flow and high pressures, equation 1.3.11 becomes equation 1.3.9 which expresses flow through nozzles, while in the case of small rates of flow and low pressures it becomes Hagen–Poiseuille's flow equation 1.3.7 or 1.3.8.

---

* *Z. angew. Phys.*, 7, 71 (1955).

The rate of flow through an orifice in a thin wall where the difference of pressure between both sides is small is derived from equation 1.3.11 $p_1 \to p_2$ and $l \to 0$, and is written

$$G = F \times 1333\, p_1 \sqrt{\frac{3}{4}\varkappa \frac{M}{R\,T_1}} = F \times 12{\cdot}66 \times 10^{-2} p_1 \sqrt{\varkappa \frac{M}{T_1}} \quad \text{(g/sec)}. \qquad (1.3.12)$$

Equation 1.3.11 can be evaluated from Fig. 1.3.4. to 1.3.7.

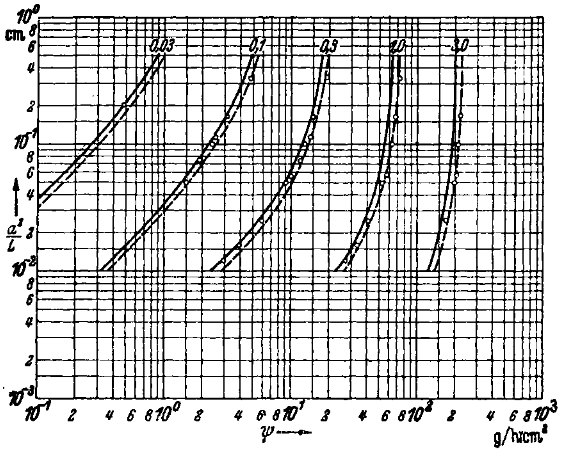

FIG. 1.3.4. Specific rate of flow ψ for water vapour in relation to pipe radius a, pipe length l and inlet pressure p_k (in Torr as parameter according to equation (1.3.11)).
$m = 1$, solid curve; $m = \varkappa$, dashed-line curve

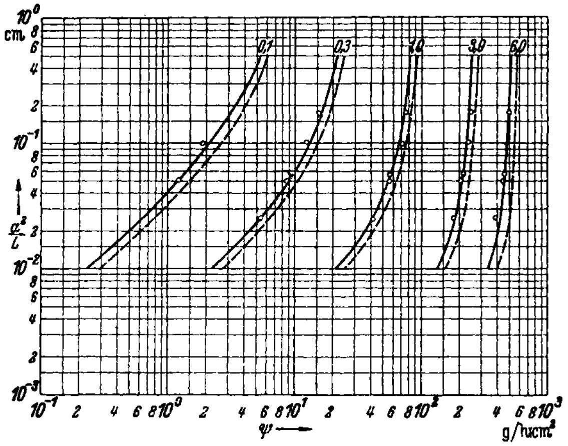

FIG. 1.3.5. Specific rate of flow ψ for air in relation to pipe radius a, pipe length l and inlet pressure p_k (as parameter in Torr according to equation 1.3.11).
$m = 1$, solid curve; $m = \varkappa$, dashed-line curve

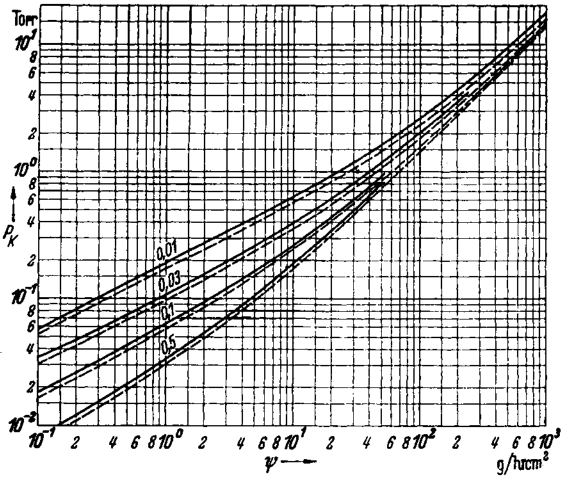

FIG. 1.3.6. Specific rate of flow ψ for water vapour in relation to inlet pressure p_k and the pipe dimension r^2/l (as parameter in cm according to equation 1.3.11). $m = 1$, solid curve; $m = \varkappa$, dashed-line curve

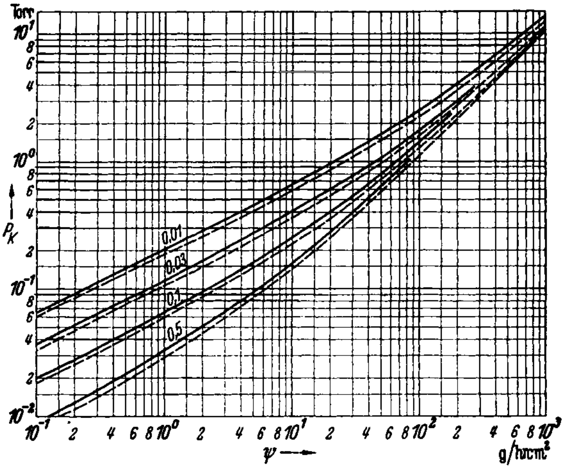

FIG. 1.3.7. Specific rate of flow ψ for air in relation to inlet pressure p_k and the pipe dimension r^2/l (as parameter in cm according to equation 1.3.11). $m = 1$ solid curve; $m = \varkappa$ dashed-line curve

1.3.1.2 At Low Pressures ($\Lambda \gg 2r$)

1.3.1.2.1 For long pipes ($l \gg r$)

$$W = \frac{3\times 10^3}{8} \frac{lU}{F^2} \sqrt{\frac{\pi M}{2RT}} = 5{\cdot}15 \times 10^{-2} \frac{lU}{F^2} \sqrt{\frac{M}{T}} \quad \text{(sec/litre)} \tag{1.3.13}$$

for any gases, any cross-sectional shape,

$$W \approx \frac{l}{r^3} \frac{1}{100} \quad \text{(sec/litre)} \tag{1.3.14}$$

for air at 20 °C, circular cross section.

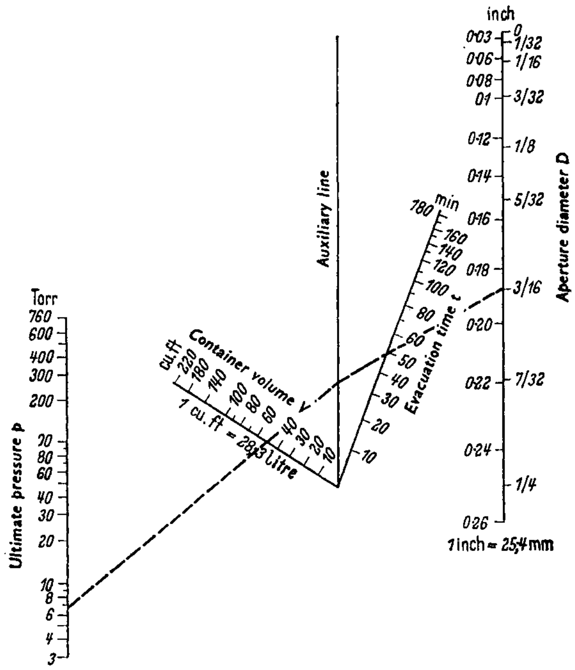

Fig. 1.3.8a. Evacuation time t in relation to container volume V, ultimate pressure p and aperture dia. D. The correlated values of p and V and t and D, respectively lie on two straight lines which intersect on the auxiliary line (after R. E. Greenhalgh and J. W. Miller, *Chem. Engng.*, 63, 222 (1956)).

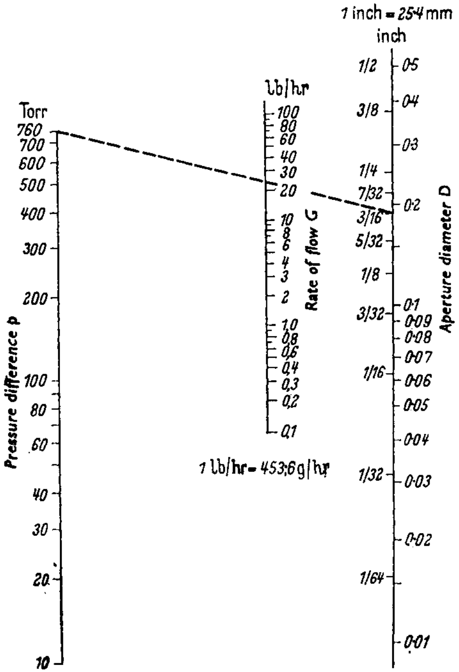

Fig. 1.3.8b. Rate of flow G through an aperture of dia. D at a pressure difference p (after R. E. Greenhalgh and J. W. Miller, *Chem. Engng.* 63, 222 (1956)).

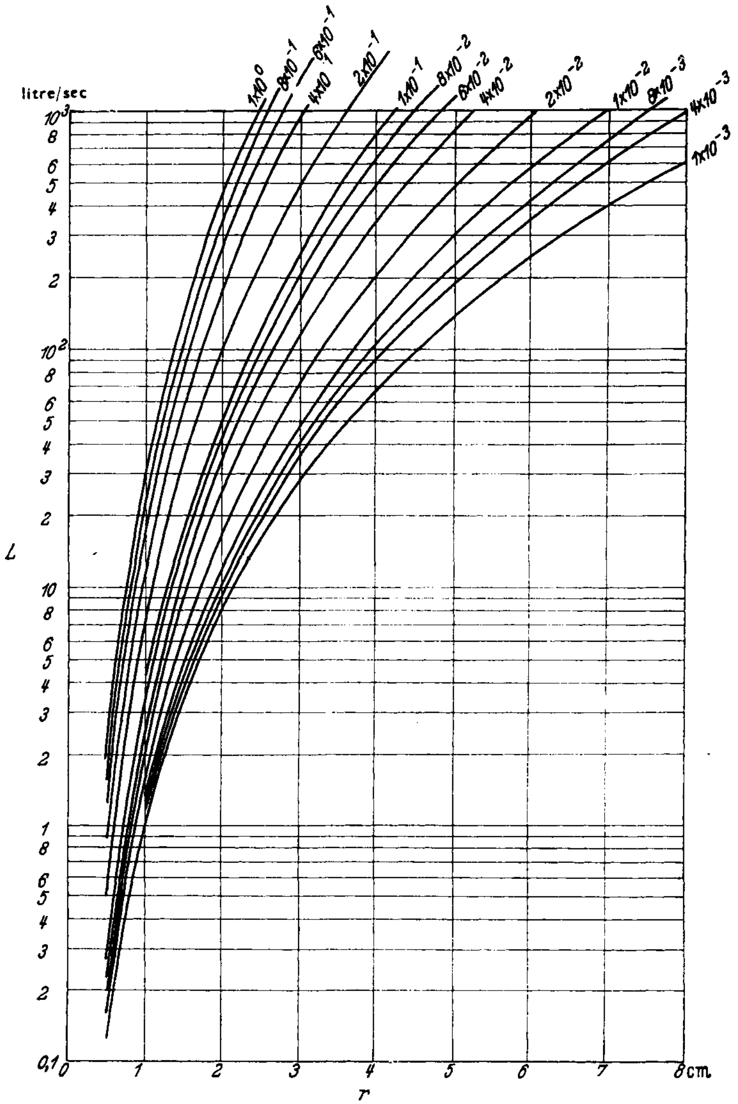

FIG. 1.3.9. Conductance L for l m long pipelines in relation to pipe radius r at different pressures (as parameter in Torr) for air at 20°C according to equation 1.3.20.

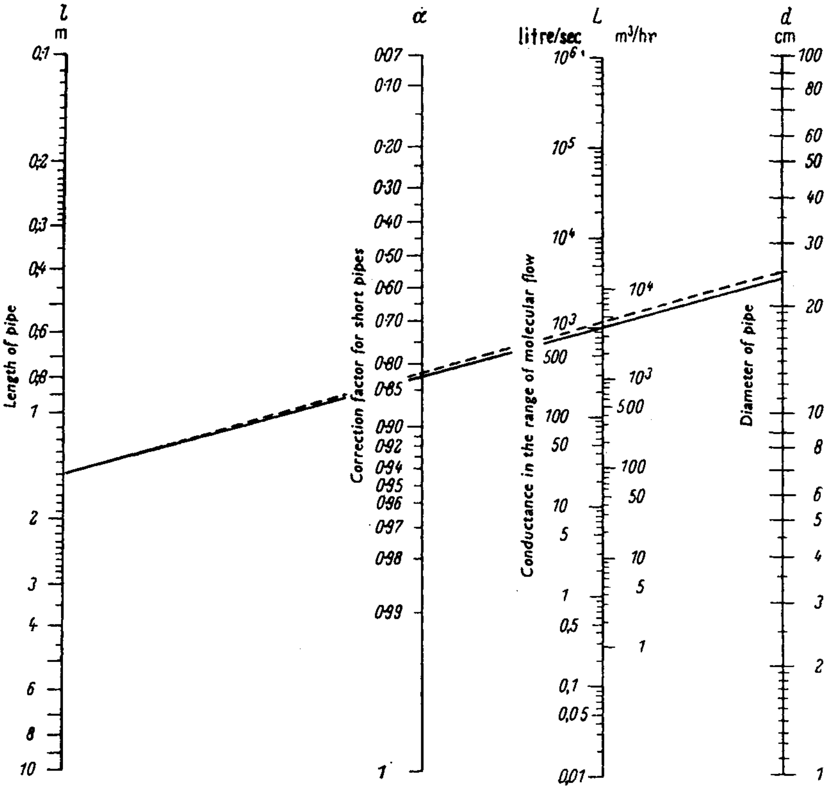

Fig. 1.3.10a. Nomogram for determining the conductances of pipes of circular cross section for air at 20 °C in the range of molecular flow (after J. Delafosse and G. Mongodin: Les calculs de la Technique du Vide, special edition *Le Vide*, 1961).

Example: What must be the dia. d of an $l = 1{\cdot}5$ m long pipeline for it to have a conductance of approximately $L = 1000$ litre/sec in the range of molecular flow?

The points $l = 1{\cdot}5$ m and $L = 1000$ litre/sec are joined together by a straight line which is extended to the point of intersection on the scale for dia. d. A value of $d = 24$ cm is obtained. The conductance at the entrance of the pipe, which depends on the ratio d/l and must not be neglected in short pipes, is allowed for by a correction factor α. For $d/l < 0{\cdot}1$ (both quantities inserted in terms of cm), α can be made equal to 1. In our example, $d/l = 0{\cdot}16$ and $\alpha = 0{\cdot}83$ (point at which straight line intersects the α scale), the effective conductance of the pipeline is thus reduced to

$$L \times \alpha = 1000 \times 0{\cdot}83 = 830 \text{ litre/sec.}$$

When d is increased to 25 cm, the value for the conductance will be

$$1200 \times 0{\cdot}82 = 985 \text{ litre/sec}$$

(dash-line).

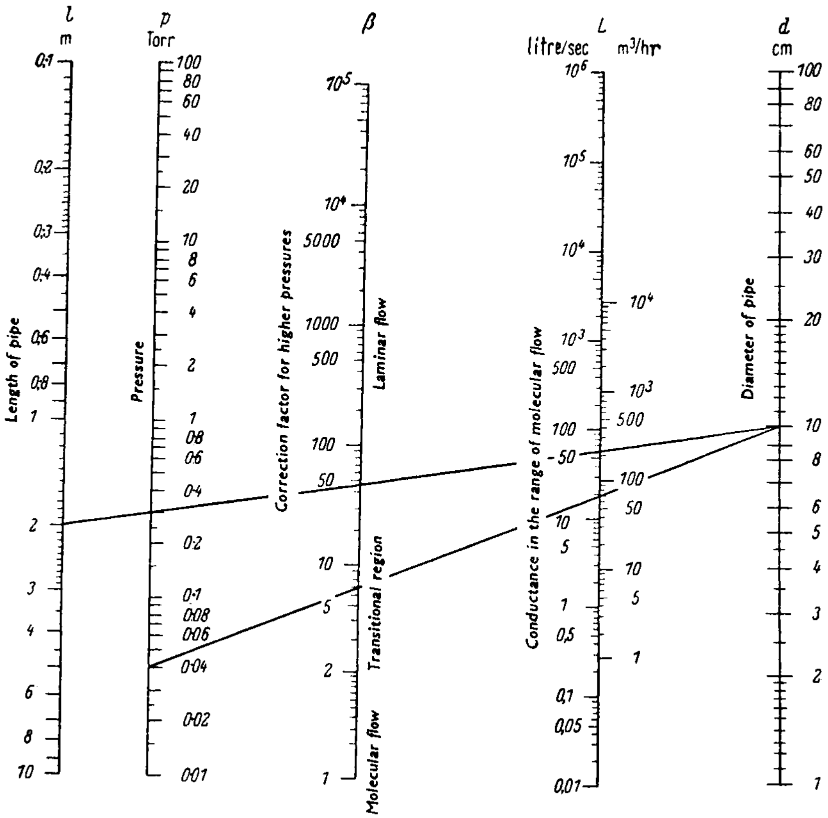

Fig. 1.3.10b. Nomogram for determining the conductances of pipes of circular cross section for air at 20°C in the whole pressure range (after J. Delafosse and G. Mongodin: Les calculs de la Technique du Vide, special edition *Le Vide*, 1961).

Example: How large is the conductance L of an $l = 2$ m long pipe of $d = 10$ cm dia.

(a) in the range of molecular flow?

(b) at an average working pressure of 4×10^{-2} Torr?

(a): The points $l = 2$ m and $d = 10$ cm are joined together by a straight line which intersects the L scale at $L = 60$ litre/sec. As $d/l < 0{\cdot}1$ in this case, a correction is not necessary (see example for Fig. 1.3.10a). Therefore, the conductance in the range of molecular flow is

$$L = 60 \text{ litre/sec.}$$

(b): At higher working pressures, the conductance calculated for molecular flow increases by the factor β. On joining together the points $p = 4 \times 10^{-2}$ Torr and $d = 10$ cm, a value of 6·8 is obtained for the factor β. Thus, the conductance is found to be

$$L = 60 \times \beta = 60 \times 6{\cdot}8 = 408 \text{ litre/sec.}$$

1.3.1.2.2 For short pipes ($l \cong r$)

$$W = \left(\frac{3}{16}\frac{l\,U}{F} + 1\right)\frac{10^3}{F}\sqrt{\frac{2\pi M}{R\,T}} = 0{\cdot}275\left(\frac{3}{16}\frac{l\,U}{F} + 1\right)\frac{1}{F}\sqrt{\frac{M}{T}} \quad \text{(sec/litre)} \tag{1.3.15}$$

for any gases, any cross-sectional shape

$$W = \frac{\frac{3}{8}\frac{l}{r} + 1}{36{\cdot}3\,r^2} \quad \text{(sec/litre)} \tag{1.3.16}$$

for air at 20 °C, circular cross section.

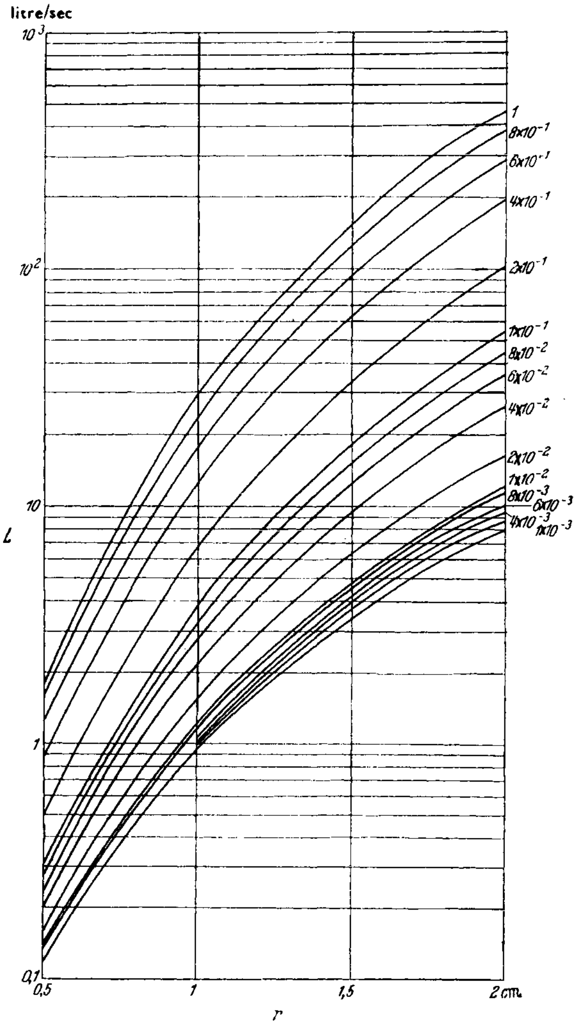

FIG. 1.3.11. Conductance L for l m long pipelines in relation to pipe radius r at different pressures (as parameter in Torr) for air at 20 °C according to equation 1.3.20.

1.3.1.2.3 For orifices in a thin wall ($l \ll r$)

$$W = \frac{10^3}{F}\sqrt{\frac{2\pi M}{RT}} = 0{\cdot}275\frac{1}{F}\sqrt{\frac{M}{T}} \quad \text{(sec/litre)} \qquad (1.3.17)$$

for any gases, any cross sectional shape

$$W = \frac{1}{36{\cdot}3 r^2} \quad \text{(sec/litre)} \qquad (1.3.18)$$

for air at 20 °C, circular cross section.

1.3.1.3 For the Whole Pressure Range

Finally, an equation is given which expresses the impedance of *long circular pipes* for the **whole** pressure range:

$$W = \frac{l}{r^3}\,\frac{10^3}{\frac{\pi r}{8\eta}\,1333\,\frac{(p_1+p_2)}{2} + \frac{8}{3}\sqrt{\frac{\pi R T}{2M}}} \quad \text{(sec/litre)} \qquad (1.3.19)$$

for any gases

$$W = \frac{l}{r^3}\,\frac{10^3}{2{\cdot}9\times 10^6\, r\,\frac{(p_1+p_2)}{2} + 9{\cdot}7\times 10^4} \quad \text{(sec/litre)} \qquad (1.3.20)$$

for air at 20 °C

To determine $L = \frac{1}{W}$ see also Figs. 1.3.9 to 1.3.11.

1.3.1.4 Compound Pipelines

Series connection of pipelines with the respective individual impedances $W_1, W_2, \ldots, W_n$. $W_{\text{total}} = W_1 + W_2 + \ldots W_n = \sum_1^n W_v$.

Example (see FIG. 1.3.12):

$$W_1 = \frac{50}{1{\cdot}5^3} \times \frac{1}{100} = 0{\cdot}148 \text{ sec/litre} \quad \text{(according to equation 1.3.14)}$$

$$W_2 = \frac{\frac{3}{8} \times \frac{12}{6} + 1}{36{\cdot}3 \times 6^2} = 0{\cdot}0013 \text{ sec/litre} \quad \text{(according to equation 1.3.16)}$$

$$W_3 = \frac{1}{36{\cdot}3 \times 0{\cdot}5^2} = 0{\cdot}11 \text{ sec/litre} \quad \text{(according to equation 1.3.18)}$$

$$W_4 = \frac{100}{3^3} \times \frac{1}{100} = 0{\cdot}037 \text{ sec/litre} \quad \text{(according to equation 1.3.14)}$$

$$W_1 + W_2 + W_3 + W_4 = 0{\cdot}2963 \approx 0{\cdot}3 \text{ sec/litre}.$$

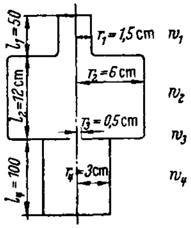

FIG. 1.3.12

For a diffusion pump with a pumping speed of $S_2 = 1$ litre/sec, the pipelines schematically assumed above would reduce this pumping speed, according to equation 1.3.3, to a value of

$$S_1 = \frac{1}{1 + 0{\cdot}3} = 0{\cdot}77 \text{ litre/sec}.$$

Such a reduction of the pumping speed by the flow resistance of the pipeline, amounting to about 23 percent of the initial value, is just tolerable.

For a diffusion pump with a higher pumping speed of $S_2 = 10$ litre/sec, an effective pumping speed of

$$S_1 = \frac{1}{0{\cdot}1 + 0{\cdot}3} = \frac{1}{0{\cdot}4} = 2{\cdot}5 \text{ litre/sec}.$$

would remain at the end of the same pipeline. The flow impedance of the pipeline is too large for this pump because the effective pumping speed is reduced by 75 percent.

This analysis shows how essential it is to make a detailed quantitative calculation of pipeline impedances in vacuum plants.

Parallel connection of pipelines with the respective individual impedances $W_1, W_2, \ldots, W_n$,

$$L_1 = \frac{1}{W_1}, \quad L_2 = \frac{1}{W_2}, \quad L_n = \frac{1}{W_n},$$

$$L = L_1 + L_2 + \cdots L_n,$$

$$W_{\text{total}} = \frac{1}{L} = \frac{1}{L_1 + L_2 + \cdots L_n} = \frac{1}{\frac{1}{W_1} + \frac{1}{W_2} + \cdots \frac{1}{W_n}}.$$

1.3.2 Nomographic Representation of Phenomena in Vacuum Systems

For solving flow phenomena in vacuum systems, SANTELER and NORTON* have developed a graphical method which can be applied in the pressure range of 760 to 10^{-7} Torr and below. The characteristics or the flow curves of the different component parts of a system, such as pumps, valves, lines etc., which can be derived either from the technical data or from the geometrical dimensions of the components, are separately plotted in a special graph with a coordinate scheme already printed on it †, and the resultant characteristic of the whole system is determined by combination. It is essential to note that the characteristic of the component which operates at the lowest pressure prevailing in the system must always be entered first in the graph. That component is usually the pump.

The resultant curve shows what a vacuum system, which consists of many component parts, is capable of performing, i.e. how large the total quantitative throughput Q will be at a given pressure p.

---

* D. I. SANTELER and J. F. NORTON, *Vacuum* 4, 176 (1954).

† Obtainable from GENERAL ELECTRIC Co.

The abscissae and ordinates of the graph (Fig. 1.3.13) are divided logarithmically. The lower abscissa and the right-hand ordinate carry the scales for the pressure p (in Torr) and the rate of flow Q (in Torr × litre/sec), while the upper abscissa and the left-hand ordinate carry the scales for the length l (in cm) and the radius a (in cm) of a pipeline.

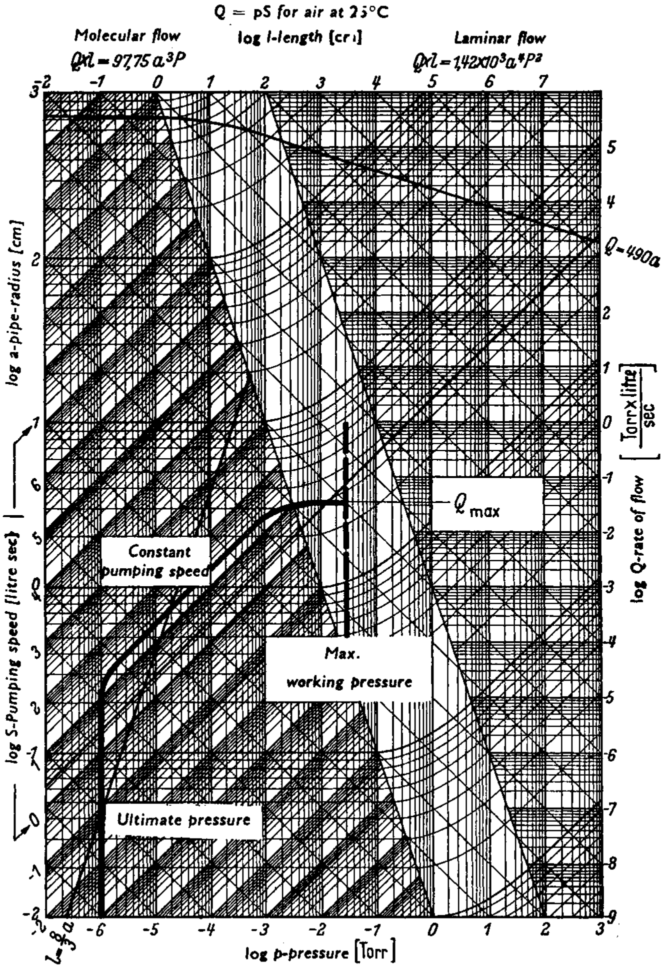

FIG. 1.3.13. Characteristic of a diffusion pump.

The left-hand section of the graph is for the pressure range of molecular flow, the right-hand section for laminar flow. In between these is the (lighter shades, diagonal) section for the transition range. Its boundaries are marked on the left by that line for which the pressure is equivalent to a mean free path Λ of the molecule of $a/2$, and on the right by a line at those pressures for which Λ is $\lesssim 2a$.

According to equation 1.3.1

$$Q = pS \quad (S \text{ pumping speed in litre/sec}).$$

On the graph every straight line which runs from bottom left to top right at 45° represents a value for $\log S = \text{const.}$, and hence also for $S = \text{const.}$, since $\log Q = \log p + \log S$, and these scales are divided in equal units.

The characteristic of a diffusion pump, derived from the data on ultimate pressure, the range of constant pumping speed and the rate of flow (capacity or throughput), is plotted in Fig. 1.3.13. S is constant between $p = 10^{-6}$ Torr (ultimate pressure) and $p = 10^{-3}$ Torr. Here, the maximum working pressure is already in the transition range.

Figure 1.3.14 illustrates the flow curve for a pipeline within the whole pressure range. According to equation 1.3.14 the impedance W of a pipeline at low pressures (molecular flow) for air at 25°C is

$$W = \frac{l}{a^3}\,\frac{1}{97{\cdot}75} \quad (\text{sec/litre}) \quad (a \text{ is the pipeline radius (cm)}).$$

According to equations 1.3.1 and 1.3.2 the rate of flow Q through this pipeline is given by

$$Q = pS = \frac{p_1 - p_2}{W} = 97{\cdot}75\,\frac{a^3}{l}\,(p_1 - p_2)$$

or when $p_1 \gg p_2$ and $p_1 = p$ by

$$Q = 97{\cdot}75\,\frac{a^3}{l}\,p \tag{1.3.21}$$

As the radius a appears as a^3, the unit of the $\log a$ scale in the graph is larger by a factor of 3 than in the scales for $\log p$ and $\log Q$.

In the given example (Fig. 1.3.14), $l = 100$ cm ($\log l = 2$) and $a = 1$ cm ($\log a = 0$). Upon substituting the values for l and a in equation 1.3.21, the following equation is obtained:

$$Q = 97{\cdot}75\,\frac{1}{100}\,p \approx p\,.$$

The lines for l and a should, therefore, intersect on that straight line at 45° for which $Q = p$ or $Q = pS$, where $S = 1$ and $\log S = 0$, respectively.

In the range of laminar flow the impedance according to equation 1.3.7 is expressed by

$$W = 7{\cdot}05 \times 10^{-4}\,\frac{l}{a^4(p_1 + p_2)}\,,$$

hence

$$Q = \frac{p_1 - p_2}{W} = 1{\cdot}42 \times 10^3\,\frac{a^4}{l}\,(p_1^2 - p_2^2) \approx 1{\cdot}42 \times 10^3\,\frac{a^4}{l}\,p^2\,.$$

Here, Q is $\sim a^4 p^2$, i. e. $Q = f(p)$ rises more sharply in this range. The change from a^3 to a^4 is compensated by traversing the lines for $a = \text{const.}$ by 45°. In consequence the unit of the $\log a$ scale becomes larger by a factor 4 than that of the $\log p$ and $\log Q$ scales.

The line for $Q = 490 \times$ radius a, imprinted in every graph, gives that rate of flow which, from experience, must not be exceeded if laminar flow is not to change to turbulent flow.

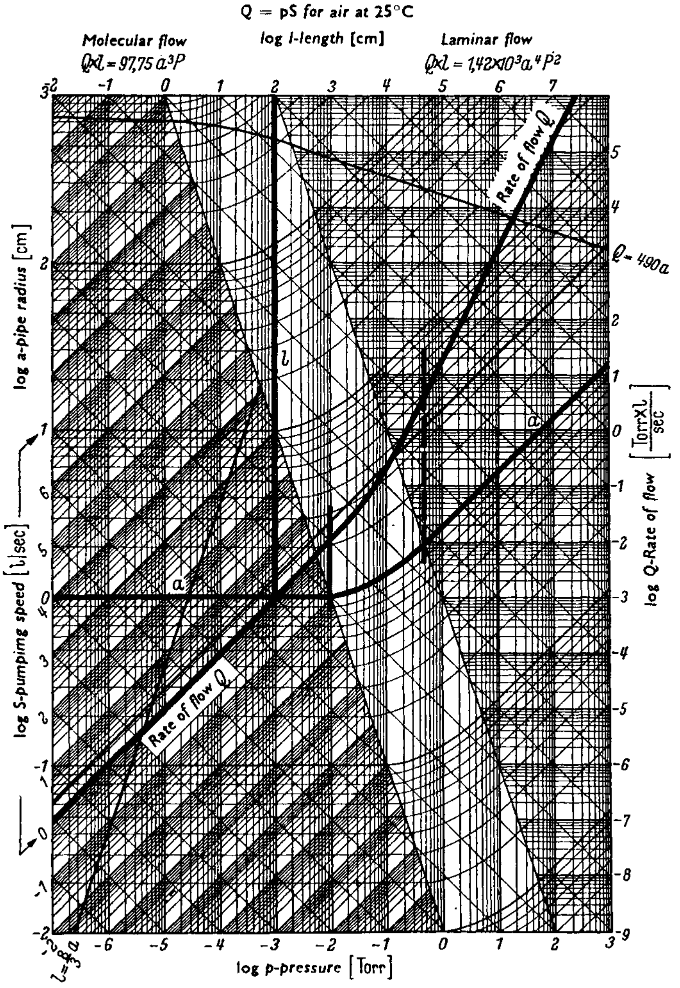

FIG. 1.3.14. Flow curve of a pipeline.

The line $l = 8/3a$, imprinted in the range of molecular flow, gives as an approximation the length which, in special cases, must be added to the true length l as an equivalent in order to compensate losses which occur when gases enter a pipeline and which are comparable with normal constrictions within a pipeline. The correction need only be made when the point of intersection of the a and l lines is on the left of or close to this imprinted line.

Figure 1.3.15 illustrates the flow curve of the same pipeline shown in Fig. 1.3.14, together with a plot of the characteristic of a backing pump. From atmospheric pressure down to almost ultimate pressure ($p = 10^{-4}$ Torr) the backing pump has an approximately constant pumping speed S, i. e.

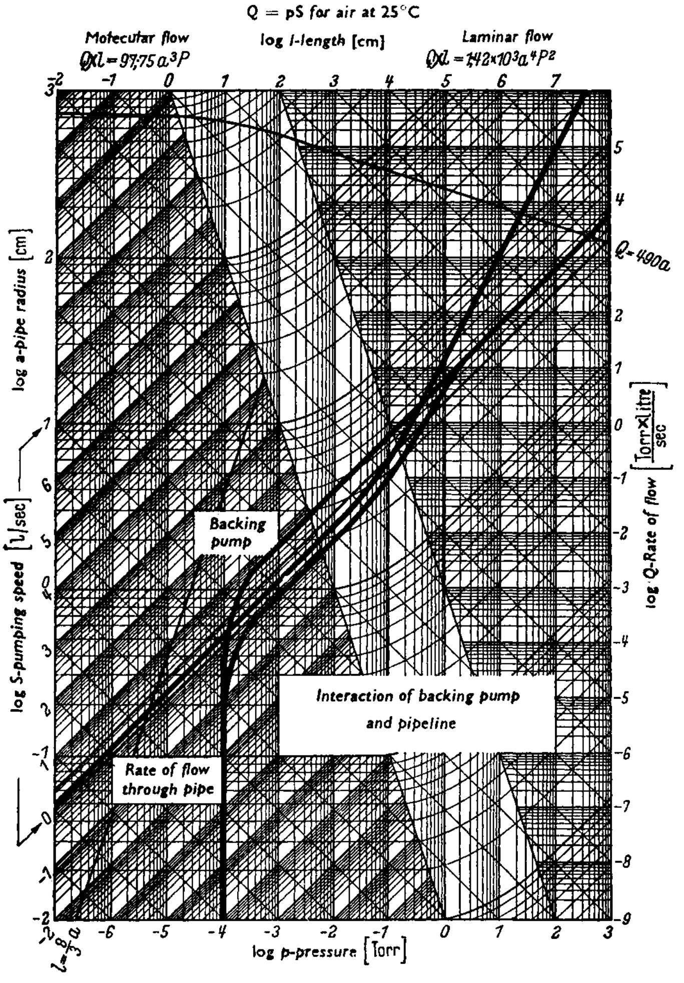

FIG. 1.3.15. Interaction of backing pump and pipeline.

$Q = f(p)$, follows the same run as in Fig. 1.3.13 (for the diffusion pump) at 45°.

$Q = f(p)$ of the pipeline (rate of flow through the pipeline) is of interest only within the range from $\log p = -4$ to about $\log p = -0{\cdot}5$. In this range the rate of flow through the pipeline is smaller than through the backing pump. The rate of flow through the pipeline first becomes larger at higher pressures; this, however, is only of theoretical importance since the rate of flow cannot be greater than the throughput of the pump. Always decisive for the overall rate of flow is the component part with the smallest rate of flow. The resultant plot of the characteristic for the combination

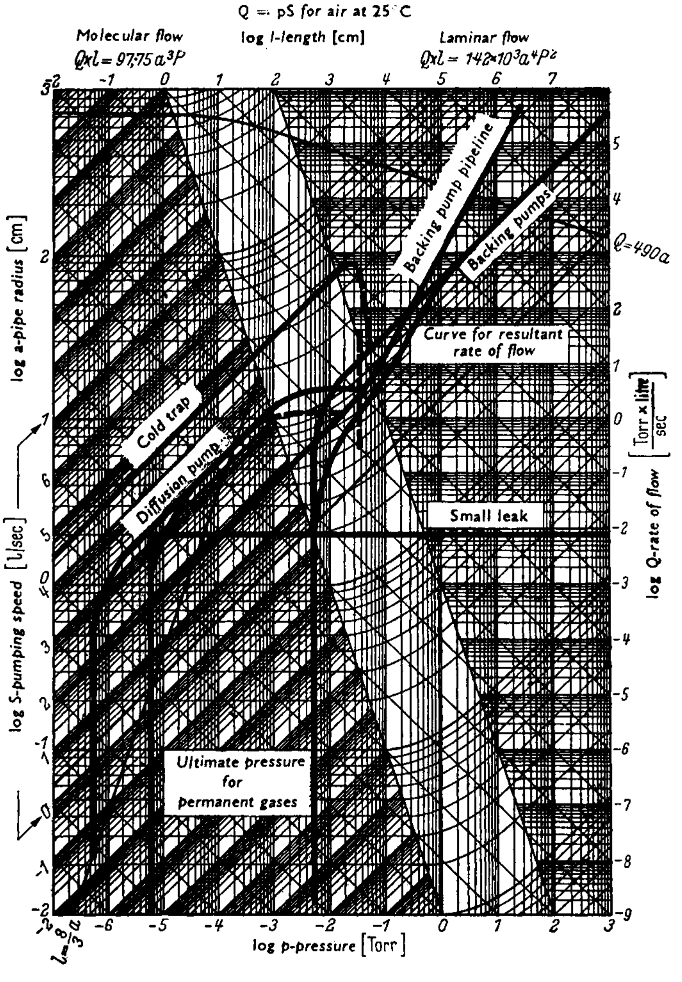

FIG. 1.3.16. Interaction of different components of a vacuum system.

backing-pump pipeline runs, therefore, below the curves plotted for the backing pump and for the pipeline.

Figure 1.3.16 illustrates the interaction of different components of a vacuum system.

Further details will be found in the original study.

1.3.3 Thermodynamics of Nozzle Phenomena and Supersonic Flow

1.3.3.1 Nozzle Discharge

The quantity of gas or vapour G (g) that flows in a steady state per unit of time (sec) through every cross section F (cm^2) of a stream tube (Fig. 1.3.17) is the same, when not taking into account the viscosity and thermal conductivity of the flowing medium, the force of gravity and other external forces. The flow is expressed by the continuity equation

$$G = F_1 w_1 \frac{1}{v_1} = F_2 w_2 \frac{1}{v_2} = F w \frac{1}{v} = F w \varrho = \text{const} \tag{1.3.22}$$

where

w is the flow velocity (cm/sec), averaged across F,
ϱ the density (g/cm^3),
$v = 1/\varrho$ (cm^3/g) = specific volume of flow through F,

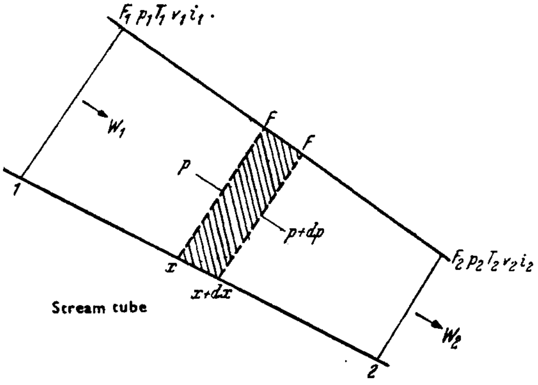

FIG. 1.3.17. Stream tube.

and by the energy law written as

$$q_{1,2} = i_2 - i_1 - \int_1^2 v p d = i_2 - i_1 + \frac{w_2^2 - w_1^2}{2} \tag{1.3.23}$$

q being the specific quantity of heat supplied (erg/g),
$i = u + pv$ = specific enthalpy (erg/g).

In the direction of flow indicated in Fig. 1.3.17, the flow velocity is $w_2 > w_1$ since $p_1 > p_2$ and $F_1 > F_2$.

The adiabatic discharge ($q = 0$) from a nozzle (Fig. 1.3.18) is thus given by the equation

$$\frac{w_1^2 - w_0^2}{2} = i_0 - i_1 \tag{1.3.24}$$

(using the symbols in Fig. 1.3.18).

TABLE 1.3.1. Frequently used functions of $\varkappa$.

$\varkappa$	$\frac{1}{\varkappa}$	$\frac{1}{\varkappa-1}$	$\frac{\varkappa-1}{\varkappa}$	$\sqrt{\frac{\varkappa+1}{2}}$	$\sqrt{\frac{\varkappa+1}{\varkappa-1}}$	$\left(\frac{2}{\varkappa+1}\right)^{\varkappa/(\varkappa-1)}$	
1·67	0·600	1·5	0·4	1·155	2·000	0·487	Monatomic gases
1·5	0·667	2	0·333	1·118	2·236	0·512	
1·4	0·714	2·5	0·286	1·095	2·449	0·528	Diatomic gases (air)
1·3	0·769	3·3	0·231	1·072	2·768	0·546	Superheated water vapour
1·2	0·833	5	0·167	1·049	3·317	0·564	

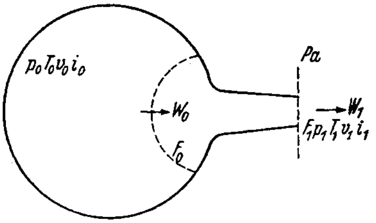

FIG. 1.3.18. Discharge from a nozzle at a pressure p_1 in the nozzle mouth, a pressure p_a in the surroundings of the nozzle mouth and a boiler pressure p_0. All quantities with the index 1 refer to the state in the nozzle mouth, all quantities with the index 0 to the state in the boiler.

TABLE 1.3.2. Critical velocity w_s and maximum velocity $w_{\max}$ at the initial temperature T_0.

$$w_s = \sqrt{2\frac{\varkappa}{\varkappa+1}\frac{R}{M}T_0} \quad (\text{cm/sec})\,, \qquad w_{\max} = \sqrt{2\frac{\varkappa}{\varkappa-1}\frac{R}{M}T_0} \quad (\text{cm/sec})\,.$$

	air $\varkappa = 1{\cdot}4$		water vapour (saturated) $\varkappa = 1{\cdot}135$		Hg vapour (superheated) $\varkappa = 1{\cdot}67$	
	$T_0 = 273\,°\text{K}$	$T_0 = 500\,°\text{K}$	$T_0 = 273\,°\text{K}$	$T_0 = 383\,°\text{K}$	$T_0 = 273\,°\text{K}$	$T_0 = 540\,°\text{K}$
w_s in m/sec	302	409	366	433	118·6	166·9
$w_{\max}$ in m/sec	741	1001	1455	1720	237	333

$$R = 8{\cdot}313 \times 10^7 \text{ erg deg}^{-1}\text{ mol}^{-1}$$

For $w_1 > w_0$ it follows that

$$\frac{w_1^2}{2} = C_p(T_0 - T_1) = \frac{\varkappa}{\varkappa - 1} p_0 v_0 \left[1 - \left(\frac{p_1}{p_0}\right)^{\frac{\varkappa-1}{\varkappa}}\right]. \tag{1.3.25}$$

Upon discharge into vacuum ($p_1 = 0$), w_1 attains its maximum value

$$w_{\max} = \sqrt{2\frac{\varkappa}{\varkappa - 1} p_0 v_0} = \sqrt{2\frac{\varkappa}{\varkappa - 1}\frac{R}{M} T_0}\,. \tag{1.3.26}$$

C_p spec. heat at constant pressure	R gas constant per mol
$\varkappa$ adiabatic exponent	M molecular weight

Table 1.3.2. includes several values for $w_{\max}$.

This value of $w_{\max}$ can only be attained with Laval nozzles, and not with simple, conically constricted ones (see Fig. 1.3.19.) Decisive is the specific cross section $f = F/G$ of the nozzle, which is found from equation 1.3.22 to be

$$f = \frac{v}{w}\cdot \tag{1.3.27}$$

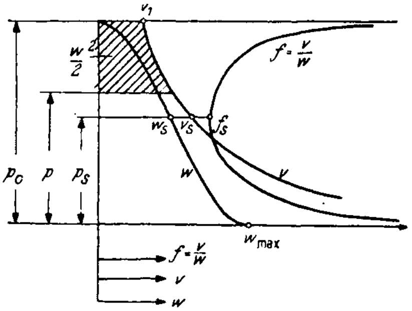

FIG. 1.3.19. Diagram for discharge from a Laval nozzle.

In the initial state ($p = p_0$, $w = w_0 = 0$), the gas has a finite specific volume $v = v_1$ so that f becomes infinite. w increases proportional to the growth of v, and the decrease of p along an adiabatic. f thus assumes finite values. Whereas v continually grows, the upper limit of w is $w_{\max}$, i. e. f ultimately becomes infinite again. Therefore, to attain as high a flow velocity as possible the nozzle must be so designed that f first decreases and then increases (Laval nozzle). At the minimum $f = f_s$, and accordingly $v = v_s$, $p = p_s$ and $w = w_s$. This so-called critical state corresponds to a critical cross section of the nozzle of $F = F_s$. At this point (as a first approximation) the flow velocity w attains the value of the local sonic speed c, i. e. for $w = w_s$ then $w = c$. When the nozzle widens again, w becomes $> c$, and the gas flows at supersonic speed. The ratio w/c is designated as the MACH number Ma. In the range $w < w_s$ (Fig. 1.3.19), Ma is, therefore, < 1, and in the range $w > w_s$, Ma is > 1. Using the value given for w in equation 1.3.26, and the relation

$$c = \sqrt{\varkappa \frac{p}{\varrho}} = \sqrt{\varkappa\, p_0 v_0 \left(\frac{p}{p_0}\right)^{\frac{\varkappa-1}{\varkappa}}} \tag{1.3.28}$$

it follows that

$$\frac{w}{c} = Ma = \sqrt{\frac{2}{\varkappa-1}\left[\left(\frac{p}{p_0}\right)^{\frac{1-\varkappa}{\varkappa}} - 1\right]}\,. \tag{1.3.29}$$

In Fig. 1.3.20, w/c is plotted as the function of p/p_0 for $\varkappa = 1.1$.

At $w = w_s$, $c = c^*$ [1]. c^* is designated as the critical sonic speed, and accordingly $w/c^* = Ma^*$ as the critical MACH number.

---

[1] An asterisk * indicates all quantities which refer to the critical state (flow velocity = sonic speed); the index s indicates all quantities which refer to the narrowest cross section of a Laval nozzle.

The quantity of gas G issuing out of the nozzle, is given by the equations 1.3.22 and 1.3.26 and by the adiabatic equation

$$\frac{p}{p_0} = \left(\frac{v_0}{v}\right)^{\varkappa} = \left(\frac{T}{T_0}\right)^{\frac{\varkappa}{\varkappa-1}} = \left(\frac{\varrho}{\varrho_0}\right)^{\varkappa}; \tag{1.3.30}$$

$$G = F\frac{w}{v} = F\left(\frac{p}{p_0}\right)^{\frac{1}{\varkappa}} \sqrt{\frac{\varkappa}{\varkappa-1}\left[1-\left(\frac{p}{p_0}\right)^{\frac{\varkappa-1}{\varkappa}}\right]}\sqrt{2\frac{p_0}{v_0}} = F\psi\sqrt{2\frac{p_0}{v_0}} \tag{1.3.31}$$

whereby

$$\psi = \left(\frac{p}{p_0}\right)^{\frac{1}{\varkappa}} \sqrt{\frac{\varkappa}{\varkappa-1}\left[1-\left(\frac{p}{p_0}\right)^{\frac{\varkappa-1}{\varkappa}}\right]}.$$

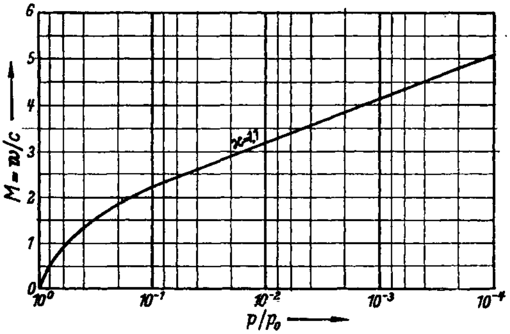

FIG. 1.3.20. Mach number in relation to expansion ratio p/p_0 for substances of high molecular weight ($\varkappa = 1{\cdot}1$).

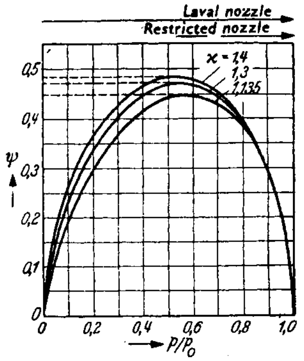

FIG. 1.3.21. Plot of the function ψ in relation to expansion ratio p/p_0.

G is, therefore, only dependent on the initial state p_0/v_0 and on ψ, i. e. on the nature of the gas ($\varkappa$) and on the expansion ratio p/p_0. Hence, ψ is equal to zero for $p/p_0 = 0$ and $p/p_0 = 1$, with a maximum in between (critical expansion ratio p_s/p_0, see Fig. 1.3.21).

p_s/p_0 is calculated from $d\,\psi/d\,(p/p_0) = 0$ to be

$$\frac{p_s}{p_0} = \left(\frac{2}{\varkappa + 1}\right)^{\frac{\varkappa}{\varkappa - 1}}$$

(For values see Table 1.3.3)

TABLE 1.3.3. Values for $\varkappa$ and p_s/p_0.

	Monatomic gases	Diatomic gases	Polyatomic gases	Saturated water vapour
$\varkappa$	1·67	1·4	1·3	1·135
p_s/p_0	0·437	0·528	0·546	0·577

The critical flow velocity amounts to

$$w_s = \sqrt{\frac{2\varkappa}{\varkappa + 1}\,\frac{R}{M}\,T_0}\,. \qquad (1.3.33)$$

(For values see Table 1.3.2).

Beyond the critical cross section F_s, the expansion of the gas from p_s to the value p takes place; this is dependent on the respective nozzle cross section F, and can be derived from

$$\frac{F_s}{F} = \frac{f_s}{f} = \left(\frac{\varkappa + 1}{2}\right)^{\frac{1}{\varkappa - 1}} \sqrt{\frac{\varkappa + 1}{\varkappa - 1}\left[\left(\frac{p}{p_0}\right)^{\frac{2}{\varkappa}} - \left(\frac{p}{p_0}\right)^{\frac{\varkappa + 1}{\varkappa}}\right]}\,. \qquad (1.3.34)$$

This ratio is plotted in Fig. 1.3.22 for $\varkappa = 1·1$. and $\varkappa = 1·4$ (see also Table 1.3.4.).

TABLE 1.3.4. Widening ratio F/F_s and velocity ratio w/w_s in Laval nozzles for diatomic gases ($\varkappa = 1·4$), overheated water vapour ($\varkappa = 1·3$) and dry saturated water vapour ($\varkappa = 1·135$)

p_0/p	$\varkappa = 1·4$		$\varkappa = 1·3$		$\varkappa = 1·135$	
	F/F_s	w/w_s	F/F_s	w/w_s	F/F_s	w/w_s
∞	∞	2·45	∞	2·77	∞	3·98
100	8·13	2·10	9·71	2·24	13·80	2·58
80	7·04	2·07	8·26	2·21	11·56	2·54
60	5·82	2·03	6·76	2·17	9·16	2·47
50	5·16	2·01	5·97	2·14	7·98	2·43
40	4·46	1·98	5·12	2·10	6·75	2·37
30	3·72	1·93	4·20	2·04	5·28	2·30
20	2·90	1·86	3·22	1·96	3·97	2·18
10	1·94	1·72	2·08	1·78	2.44	1·92
8	1·70	1·64	1·82	1·71	2·07	1·86
6	1·47	1·55	1·55	1·61	1·72	1·74
4	1·21	1·40	1·26	1·45	1·35	1·55
2	1·02	1·04	1·03	1·07	1·02	1·12

According to equations 1.3.26 and 1.3.33, the critical velocity ratio w/w_s is

$$\frac{w}{w_s} = \sqrt{\frac{\varkappa+1}{\varkappa-1}\left[1-\left(\frac{p}{p_0}\right)^{\frac{\varkappa-1}{\varkappa}}\right]}. \tag{1.3.35}$$

(For values see Table 1.3.4).

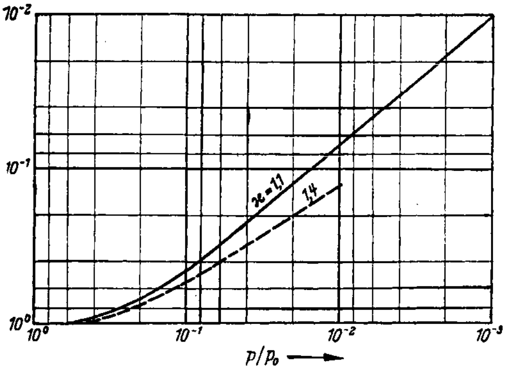

FIG. 1.3.22. Expansion ratio, i.e. ratio of pressure in nozzle mouth (p) to boiler pressure (p_0) as a function of the ratio of nozzle cross sections (F^*/F).

The critical sonic speed

$$c^* = \sqrt{\frac{2\varkappa}{\varkappa+1}\,\frac{R}{M}\,T_0} \tag{1.3.36}$$

is equal to the critical flow velocity (equation 1.3.33).

1.3.3.2 Construction of the Patterns of Two-dimensional Supersonic Flow *

Here, the following basic relations hold in the first instance. MACH angle α:

$$\sin\alpha = \frac{c}{w} = \frac{1}{Ma}; \quad \frac{c^*}{w} = \frac{1}{Ma^*}, \tag{1.3.37}$$

$$Ma^2 = \frac{2}{\varkappa-1}\left[\left(\frac{p_0}{p}\right)^{\frac{\varkappa-1}{\varkappa}} - 1\right], \tag{1.3.38}$$

$$Ma^{*2} = \frac{\varkappa+1}{\varkappa-1}\left[1-\left(\frac{p}{p_0}\right)^{\frac{\varkappa-1}{\varkappa}}\right] = \frac{(\varkappa+1)\,Ma^2}{(\varkappa-1)\,Ma^2+2}. \tag{1.3.39}$$

In the absence of viscosity ($\eta = 0$), $\mathfrak{w} = \operatorname{grad}\varphi$ can be applied. Furthermore, $\mathfrak{w}$ must conform with the BERNOULLI equation and the continuity equation.

---

* See e.g., R. SAUER: *Einführung in die theoretische Gasdynamik*, 2nd ed., Springer Berlin, Göttingen, Heidelberg 1951.

Linearized equation for small distortions. Let $\bar{\mathfrak{w}}$ and $\bar{\varphi}$ represent the velocity vector and potential of the undistorted main flow, and $\mathfrak{w}$ and φ represent the corresponding quantities of the distorted flow to be investigated. Then (cf. Fig. 1.3.24)

$$\mathfrak{w} = \bar{\mathfrak{w}} + \mathfrak{w}', \quad w_1 = \bar{w} + w_1',$$

$$\varphi = \bar{\varphi} + \varphi', \quad w_2 = w_2'.$$

In the case of supersonic flow ($\overline{Ma} > 1$), the linear potential equation for the additional potential φ to be superimposed on the main flow is

$$\frac{\partial^2 \varphi'}{\partial x^2} \left(\overline{Ma}^2 - 1\right) - \frac{\partial^2 \varphi'}{\partial y^2} = 0 . \tag{1.3.40}$$

The solution of this differential equation is written in the form

$$\varphi' = F_1(y - x \tan \bar{\alpha}) + F_2(y + x \tan \bar{\alpha}) \tag{1.3.41}$$

where

$$\tan \bar{\alpha} = \frac{1}{\sqrt{\overline{Ma}^2 - 1}} \cdot \tag{1.3.42}$$

F_1, F_2: Arbitrary functions of the variables $y \mp x \tan \bar{\alpha}$, determinable from the respective boundary conditions.

The two parallel bands of straight lines from equation 1.3.41

$$y - x \tan \bar{\alpha} = \text{const}, \quad y + x \tan \bar{\alpha} = \text{const}, \tag{1.3.43}$$

which are inclined against the main flow $\bar{\mathfrak{w}}$ by $\mp \bar{\alpha}$, are termed **Mach** lines (see m in Fig. 1.3.24). They produce the straight-line **Mach** system of linear supersonic flow.

$\bar{w} = f(\bar{\alpha})$ is given by

$$\sin^2 \bar{\alpha} = \frac{\bar{c}^2}{\bar{w}^2} = \frac{\varkappa - 1}{2} \, \frac{w_{\max}^2 - \bar{w}^2}{\bar{w}^2} \cdot \tag{1.3.44}$$

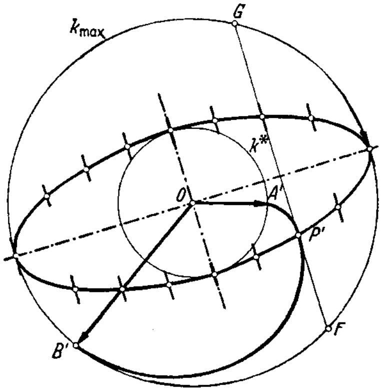

FIG. 1.3.23. Adiabatic ellipse and directional field of velocity pattern (after SAUER). The small circle k^* corresponds to the critical velocity $w = c^*$, the large circle $k_{\max}$ to the maximum velocity $w_{\max}$.

From this, it follows, after change over to rectangular coordinates, that:

$$\bar{u} = \bar{w}\cos\bar{\alpha}\,, \qquad \bar{v} = \bar{w}\sin\bar{\alpha}\,,$$

$$\frac{\bar{u}^2}{w_{\max}^2} + \frac{\bar{v}^2}{c^{*2}} = 1\,. \tag{1.3.45}$$

This equation represents the adiabatic ellipse (Fig. 1.3.23) with the semi-axes $w_{\max}$ and c^*.

Flow around a flat convex angle. In cases where the main flow is deflected by a small angle $\Delta\vartheta$, the following relations hold (Fig. 1.3.24):

$$\left.\begin{aligned} u' &= +\Delta\vartheta\,\bar{u}\tan\bar{\alpha} \\ v' &= -\Delta\vartheta\,\bar{u} \end{aligned}\right\} \frac{u'}{v'} = -\tan\bar{\alpha}\,, \tag{1.3.46}$$

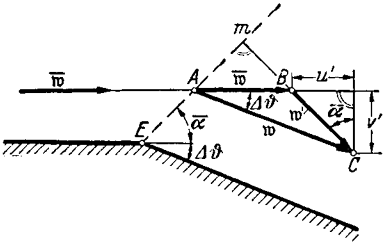

FIG. 1.3.24. Supersonic flow around a flat angle (after SAUER).

i.e. the constant additional vector $\mathfrak{w}'$ is perpendicular to the MACH line m. In consequence, $\mathfrak{w}$ (deflected flow) can be directly derived from $\bar{\mathfrak{w}}$ (main flow) and $\bar{\alpha}$. Because

$$\frac{v'}{\bar{u} + u'} \approx \frac{v'}{\bar{u}} = -\Delta\vartheta\,,$$

this additional flow produces a parallel flow deflected by the angle $\Delta\vartheta$; the increase of velocity is

$$\Delta w = u' = \bar{u}\tan\bar{\alpha}\,\Delta\vartheta\,. \tag{1.3.47}$$

The difference of pressure before and beyond the MACH line m is expressed by

$$\begin{aligned} \Delta p = p - \bar{p} &= -\int_{\bar{w}}^{w} \varrho w\,dw = -\bar{\varrho}\bar{w}(w - \bar{w}) = -\bar{\varrho}\bar{w}u' \\ &= -\bar{\varrho}\bar{u}^2\tan\bar{\alpha}\,\Delta\vartheta = -2\bar{q}\tan\bar{\alpha}\,\Delta\vartheta \end{aligned} \tag{1.3.48}$$

where $\bar{q} = \frac{\bar{\varrho}}{2}\bar{u}^2$, the pressure head of the main flow.

Non-linear flow. Definition of symbols:

α is the MACH angle between the direction of flow and the MACH line m,
ϑ is the angle of deflection of the streamlines,
ω is the polar angle of the MACH line with E as the zero point (see Fig. 1.3.25, left-hand diagram). For $\omega = 0$, $\bar{w} = c^*$, i.e. ω begins to count at A on that line $\bar{m}$ on which c^* is just reached.

The relation between these quantities is defined by the equation

$$\omega + \alpha = \vartheta + \frac{\pi}{2} \tag{1.3.49}$$

Figure 1.3.25 shows the relationship between the flow pattern (**Mach** system m) and the velocity curve ($\mathfrak{w}$). The diagram of characteristics after **Prandtl—Busemann** (Fig. 1.3.26) is used for the step-by-step construction of the flow pattern based on the adiabatic ellipse (Fig. 1.3.23) or the velocity curve (Fig. 1.3.25, right-hand diagram). The different characteristics (epicycloids) are consecutively numbered (**Mach** coordinates m_0).

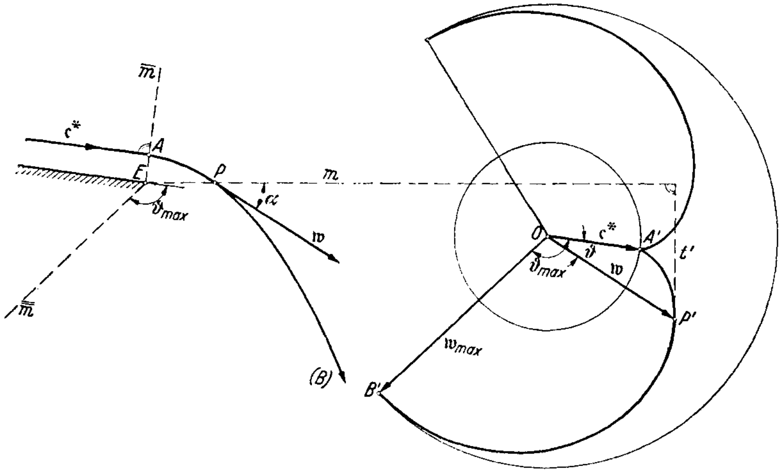

Fig. 1.3.25. Velocity curve (after **Sauer**).
Left: Flow pattern (**Mach** system m). Right: Velocity curve $\mathfrak{w}$ (the velocities are entered here in polar coordinates according to magnitude and direction). The velocity curve $A'P'B'$ is obtained by rotating the adiabatic ellipse in the velocity pattern (see Fig. 1.3.23). The tangent at every point p' on the velocity curve is parallel to the small ellipse axis, the **Mach** line is parallel to the large ellipse axis.

Epicycloids displaced two by two degrees relatively to each other differ by $m_0 = 1$. By adding the **Mach** coordinates of two epicycloids in their points of intersection, a number is obtained which is directly related to the **Mach** number Ma (Fig. 1.3.27). The difference between the **Mach** coordinates gives the direction of flow.

Compression impact. If the distortion assumes the form of a flat, concave angle, a compression (compression impact) will take place along a line of impact s instead of the expansion along a **Mach** line m.

p, ϱ, T, $\mathfrak{w}$, ..., = characteristic values of state before the line of impact s

$\hat{p}$, $\hat{\varrho}$, $\hat{T}$, $\hat{\mathfrak{w}}$, ..., = characteristic values of state beyond the line of impact s

angle of impact σ = angle between line of impact s and approach direction of flow

angle of deflection ϑ = angle between $\mathfrak{w}$ and $\hat{\mathfrak{w}}$.

The following equations hold (Fig. 1.3.29):

$$\varrho w_n = \hat{\varrho}\hat{w}_n\,; \qquad w_t = \hat{w}_t\,. \tag{1.3.50}$$

$$i_0 = \hat{i}_0\,; \quad T_0 = \hat{T}_0\,; \quad \frac{p_0}{\varrho_0} = \frac{\hat{p}_0}{\hat{\varrho}_0}\,. \tag{1.3.51}$$

$$c^* = \hat{c}^*\,; \qquad w_{\max} = \hat{w}_{\max}\,, \tag{1.3.52}$$

$$\frac{\Delta p}{\Delta \varrho} = \frac{\hat{p} - p}{\hat{\varrho} - \varrho} = \varkappa \frac{p + \dfrac{\Delta p}{2}}{\varrho + \dfrac{\Delta \varrho}{2}}\,. \tag{1.3.53}$$

$$\Delta p = \varrho w^2 \sin^2 \sigma \frac{\Delta \varrho}{\varrho + \Delta \varrho}\,. \tag{1.3.54}$$

$$\frac{\varrho + \Delta \varrho}{\varrho} = \frac{\tan \alpha}{\tan(\sigma - \vartheta)}\,. \tag{1.3.55}$$

The compression impact (impact polar curves) can be fully computed from the above equations:

$$\frac{\Delta p}{\Delta \varrho} = c^{*2} - \frac{\varkappa - 1}{\varkappa + 1} w_t^2\,. \tag{1.3.56}$$

Vertical compression impact:
In this case

$$\vartheta = 0\,, \qquad \sigma = \frac{\pi}{2}\,, \tag{1.3.57}$$

$$w_t = \hat{w}_t = 0\,, \quad w_n = w\,, \quad \hat{w}_n = \hat{w}\,. \tag{1.3.58}$$

Supersonic velocity w prevails before, and subsonic velocity $\bar{w}$ after impact. The following equation holds:

$$w\hat{w} = c^{*2}\,. \tag{1.3.59}$$

TABLE 1.3.5. Flow density Θ and MACH number Ma for different expansion ratios p/p_0 at supersonic velocity for monatomic gases and Hg vapour ($\varkappa = 1{\cdot}67$) (after WASSERRAB).

p/p_0	$Ma = w/c$	$Ma^* = w/c^*$	$\Theta = \dfrac{\varrho w}{\varrho^* w_s}$	$f/f^* = 1/\Theta$
0·488	1·000	1·000	1·000	1·000
0·450	1·050	1·038	0·991	1·010
0·400	1·148	1·104	0·980	1·021
0·350	1·26	1·173	0·955	1·049
0·300	1·36	1·237	0·918	1·090
0·250	1·49	1·305	0·877	1·142
0·200	1·64	1·378	0·806	1·241
0·150	1·84	1·451	0·720	1·390
0·100	2·12	1·550	0·598	1·675
0·050	2·64	1·720	0·420	2·381
0·000	∞	2·00	0·000	∞

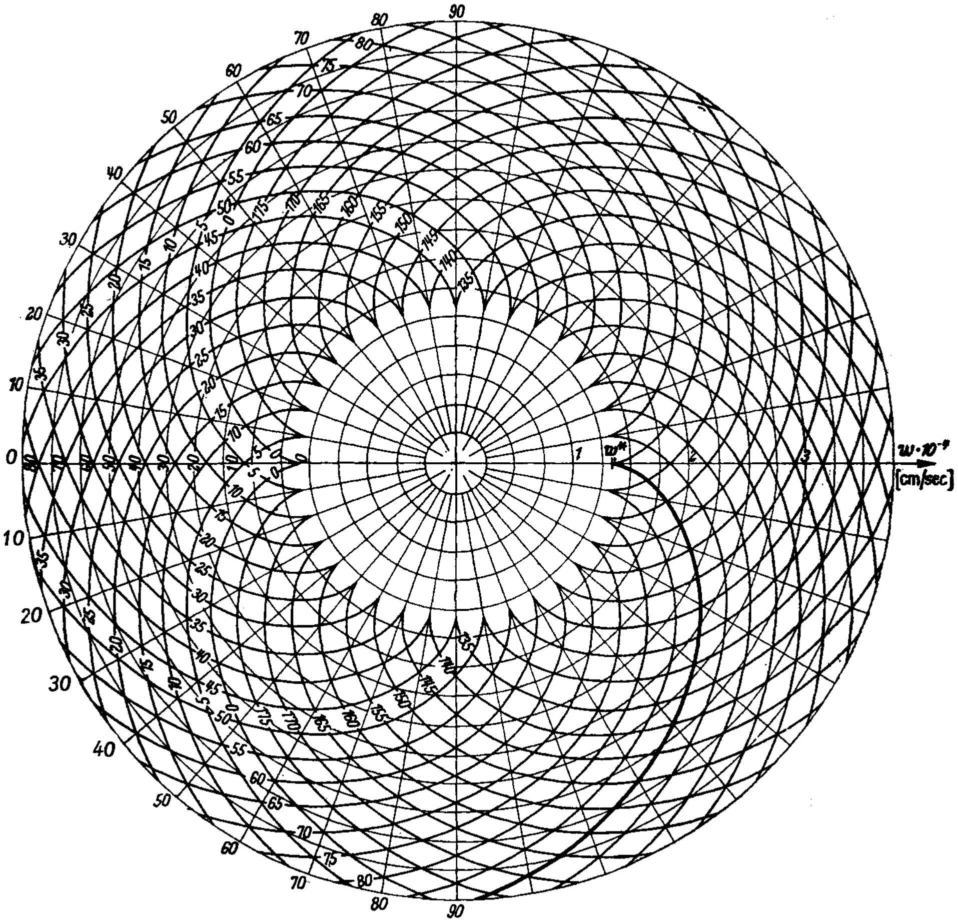

Fig. 1.3.26. Diagram of characteristics after Prandtl–Busemann for substances of high molecular weight (such as organic vapours used as pump fluids for diffusion pumps and ejector booster pumps) ($\varkappa = 1{\cdot}1$) (after Kutscher). See Fig. 1.3.27 for meaning of Mach coordinates used in this diagram.

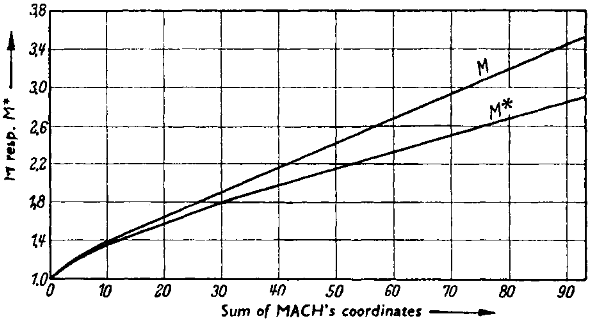

Fig. 1.3.27. Values of Mach coordinates used in Fig. 1.3.26.

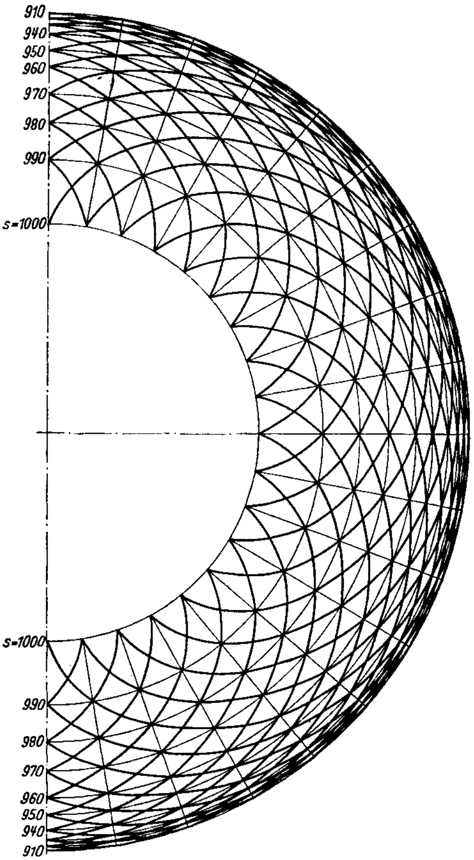

FIG. 1.3.28. Diagram of characteristics after PRANDTL–BUSEMANN for mercury vapour or monatomic gases ($\varkappa = 1{\cdot}67$) (after WASSERRAB). See Table 1.3.6 for coordinates s.

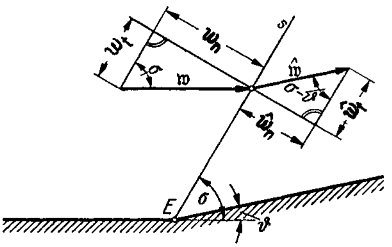

FIG. 1.3.29. Compression for supersonic flow, compression impact (designations after SAUER)

TABLE 1.3.6. Hg vapour and monatomic gases. Characteristic quantities of a two-dimensional supersonic flow ($\varkappa = 1{\cdot}67$) (after WASSERRAB).

s	ϑ °	ω °	α °	p/p_0	$Ma = w/c$	$Ma^* = w/c^*$	$\frac{1}{2}\frac{\varrho w^2}{p_0}$	$\frac{p}{p_0} + \frac{1}{2}\frac{\varrho w^2}{p_0}$	Θ
1000	0	0·00	90·00	0·488	1·000	1·000	0·405	0·893	1·000
990	10	57·5	42·5	0·285	1·395	1·255	0·470	0 755	0·911
980	20	78·0	32·0	0·178	1·72	1·41	0·470	0·648	0·774
970	30	95·5	24·5	0·102	2·14	1·55	0·383	0·485	0·596
960	40	111·5	18·5	0·051	2·60	1·66	0·287	0·339	0·436
950	50	126	14	0·0244	3·19	1·76	0·207	0·232	0·292
940	60	140	10	0·0093	4·05	1·85	0·125	0·135	0·172
910	90	180	0	0	∞	2·00	0	0	0

As the compression impact is not an adiabatic process, the original static pressure p_0 cannot be restored behind the direct impact, but instead only a static pressure of $\hat{p}_0 < p_0$ is obtained. The ratio $\hat{p}_0/p_0$ is clearly given by the pressure ratio p/p_0 immediately before the impact (Fig. 1.3.30).

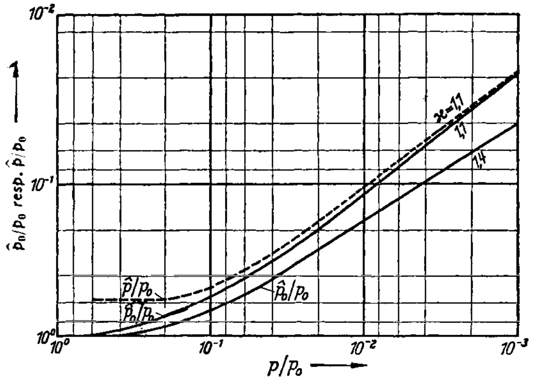

FIG. 1.3.30. Pressure loss $\hat{p}/p_0$ and static pressure loss $\hat{p}_0/p_0$ in relation to the expansion ratio p/p_0 for perpendicular compression impacts (after KUTSCHER).

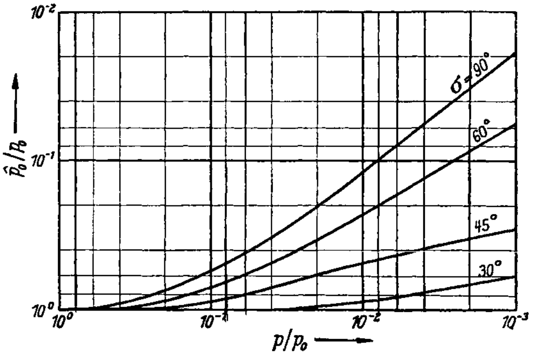

FIG. 1.3.31. Static pressure loss $\hat{p}_0/p_0$ as a function of the expansion ratio p/p_0 for oblique compression impacts (after KUTSCHER).

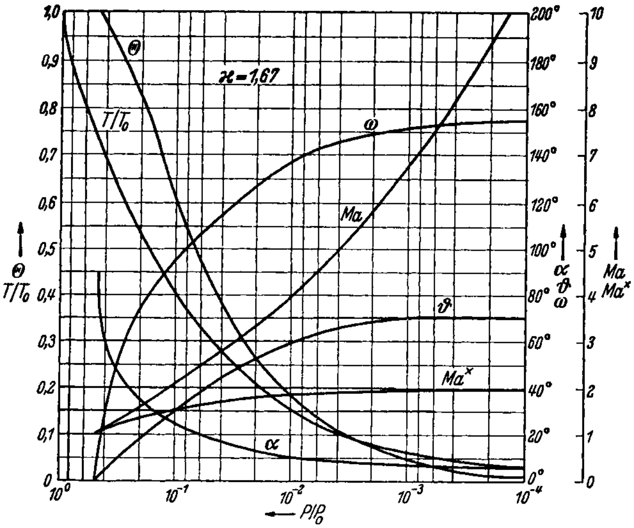

FIG. 1.3.32. Variables of state of mercury vapour ($\varkappa = 1{\cdot}67$) in relation to the expansion ratio p/p_0 (after NÖLLER)

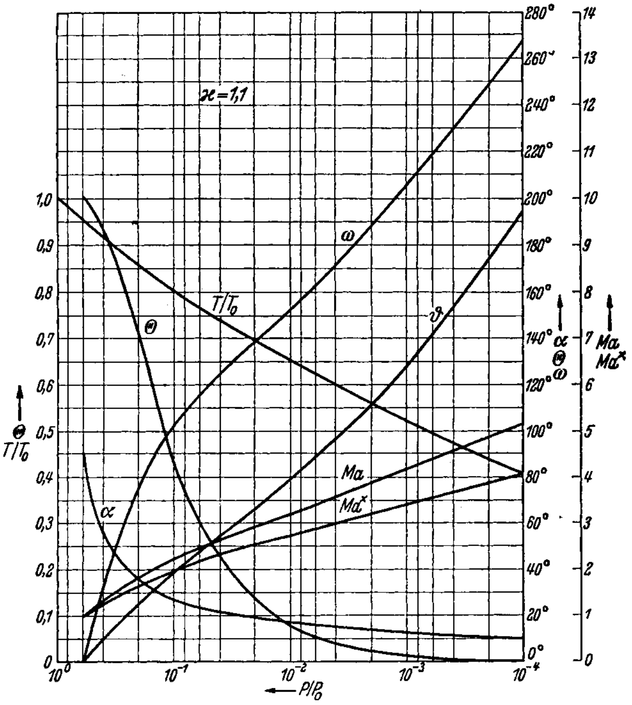

FIG. 1.3.33. Variables of state of organic vapours of high molecular weight ($\varkappa = 1{\cdot}1$) in relation to the expansion ratio p/p_0 (after NÖLLER).

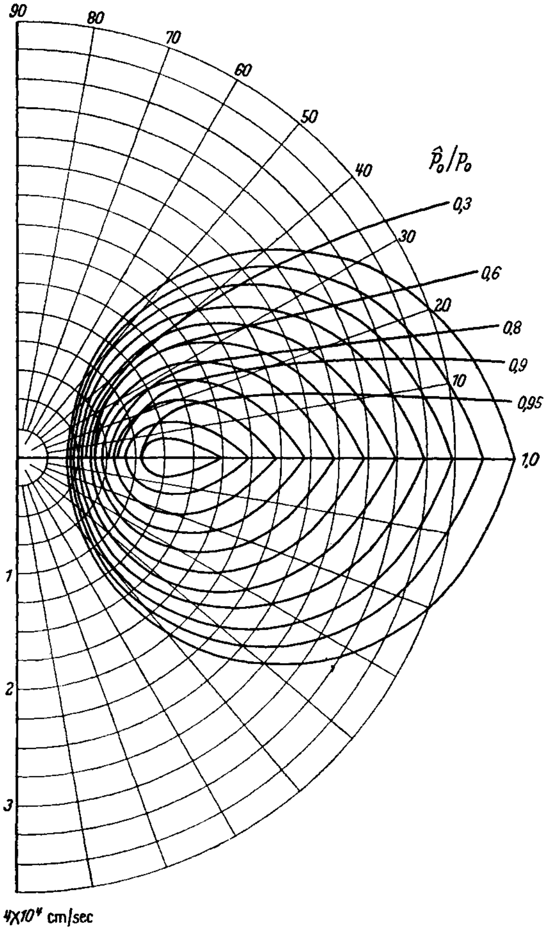

FIG. 1.3.34. Impact polar diagram after BUSEMANN for substances of high molecular weight ($\varkappa = 1{\cdot}1$) (after KUTSCHER).

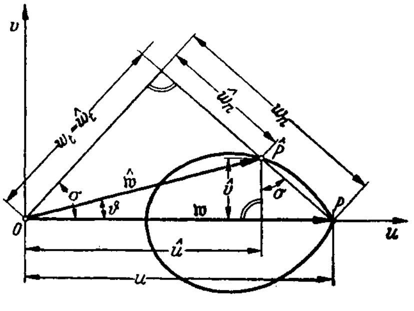

FIG. 1.3.35. Impact polar (after SAUER)

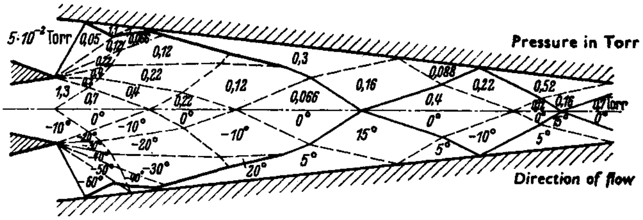

FIG. 1.3.36. Pressure in the surroundings of a booster nozzle mouth ($p_a = 5 \times 10^{-2}$ Torr; low forepressure)

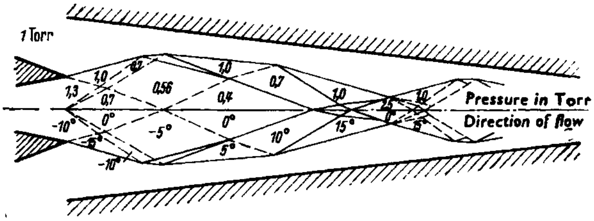

FIG. 1.3.37. $p_a = 1$ Torr; low forepressure.

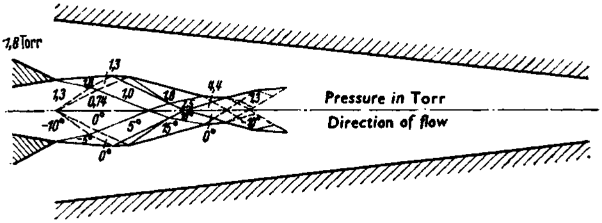

FIG. 1.3.38. $p_a = 1{\cdot}8$ Torr; low forepressure.

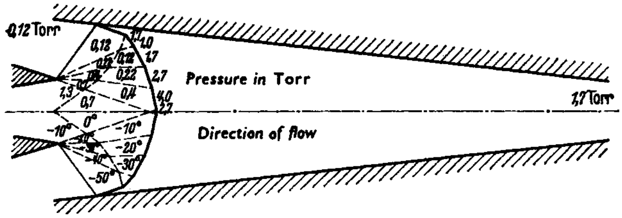

FIG. 1.3.39. $p_a = 0{\cdot}12$ Torr; but high forepressure (1·7 Torr).

The impact polar diagram provides information on the relations between the different values of state for oblique compression impacts.

Impact polar diagram after BUSEMANN (Fig. 1.3.34). If w and σ are known, the impact polar curve (Fig. 1.3.35) gives the values for $\hat{w}$ and $\hat{p}_0/p_0$; if w and $\hat{w}$ are known, the impact polar curve gives the values for σ and $\hat{p}_0/p_0$. It follows from Fig. 1.3.35 that

$$w_t = \hat{w}_t = u \cos\sigma\,, \qquad w_n = u \sin\sigma\,, \tag{1.3.60}$$

$$\hat{w}_n = u \sin\sigma - \frac{\hat{v}}{\cos\sigma}\,, \qquad \tan\sigma = \frac{u - \hat{u}}{\hat{v}}\,. \tag{1.3.61}$$

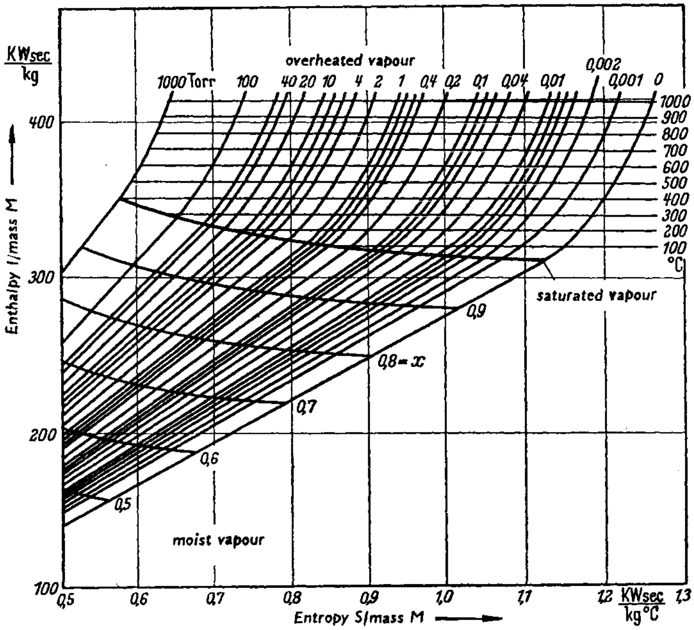

FIG. 1.3.40. IS-diagram for mercury vapour ($\varkappa = 1{\cdot}67$) (after WASSERRAB).

By introducing these values in equation 1.3.56, it is found that

$$\hat{v}^2\left[\frac{c^{*2}}{u} + \frac{2}{\varkappa + 1}u - \hat{u}\right] = (u - \hat{u})^2\left(\hat{u} - \frac{c^{*2}}{u}\right). \tag{1.3.62}$$

The impact polar is valid for $w > c^*$; for $w = w_{\max}$, it changes to a circle.

The diagrams on page 53 for supersonic flow of organic vapours of high molecular weight ($\varkappa = 1{\cdot}1$), issuing out of the mouth of a booster nozzle and entering a conically constricted nozzle, were plotted by applying the methods and numerical values given above. A boiler pressure of $p_0 = 40$ Torr was introduced for all diagrams.*

---

* For details, see H. KUTSCHER: *Z. angew. Phys.* **1**, 229–234 (1955).

TABLE 1.3.7. Characteristic quantities for saturated mercury vapour (0–150 °C) (after WASSERRAB).

(a)

Temperature t °C	Temperature T °K	Saturated vapour pressure p_s Torr	Concentration n cm^{-3}	Diffusion coefficient D cm^2 sec^{-1}	Gas density ϱ g cm^{-3}
0	273	$1{\cdot}49 \times 10^{-4}$	$5{\cdot}3 \times 10^{12}$	$1{\cdot}86 \times 10^{5}$	$1{\cdot}74 \times 10^{-9}$
10	283	$3{\cdot}92 \times 10^{-4}$	$1{\cdot}34 \times 10^{13}$	$7{\cdot}5 \times 10^{4}$	$4{\cdot}40 \times 10^{-9}$
20	293	$9{\cdot}64 \times 10^{-4}$	$3{\cdot}20 \times 10^{13}$	$3{\cdot}2 \times 10^{4}$	$1{\cdot}05 \times 10^{-8}$
30	303	$2{\cdot}23 \times 10^{-3}$	$7{\cdot}18 \times 10^{13}$	$1{\cdot}46 \times 10^{4}$	$2{\cdot}46 \times 10^{-8}$
40	313	$4{\cdot}89 \times 10^{-3}$	$1{\cdot}52 \times 10^{14}$	$6{\cdot}95 \times 10^{3}$	$4{\cdot}99 \times 10^{-8}$
50	323	$1{\cdot}019 \times 10^{-2}$	$3{\cdot}07 \times 10^{14}$	$3{\cdot}5 \times 10^{3}$	$1{\cdot}01 \times 10^{-7}$
60	333	$1{\cdot}99 \times 10^{-2}$	$5{\cdot}80 \times 10^{14}$	$1{\cdot}83 \times 10^{3}$	$1{\cdot}90 \times 10^{-7}$
70	343	$3{\cdot}90 \times 10^{-2}$	$1{\cdot}10 \times 10^{15}$	$9{\cdot}98 \times 10^{2}$	$3{\cdot}61 \times 10^{-7}$
80	353	$7{\cdot}21 \times 10^{-2}$	$1{\cdot}98 \times 10^{15}$	$5{\cdot}7 \times 10^{2}$	$6{\cdot}52 \times 10^{-7}$
90	363	$1{\cdot}285 \times 10^{-1}$	$3{\cdot}44 \times 10^{15}$	$3{\cdot}31 \times 10^{2}$	$1{\cdot}13 \times 10^{-6}$
100	373	$2{\cdot}22 \times 10^{-1}$	$5{\cdot}75 \times 10^{15}$	$2{\cdot}00 \times 10^{2}$	$1{\cdot}89 \times 10^{-6}$
110	383	$3{\cdot}73 \times 10^{-1}$	$9{\cdot}47 \times 10^{15}$	$1{\cdot}23 \times 10^{2}$	$3{\cdot}11 \times 10^{-6}$
120	393	$6{\cdot}11 \times 10^{-1}$	$1{\cdot}51 \times 10^{16}$	$7{\cdot}85 \times 10^{1}$	$4{\cdot}94 \times 10^{-6}$
130	403	$9{\cdot}73 \times 10^{-1}$	$2{\cdot}34 \times 10^{16}$	$5{\cdot}1 \times 10^{1}$	$7{\cdot}67 \times 10^{-6}$
140	413	1·521	$3{\cdot}59 \times 10^{16}$	$3{\cdot}40 \times 10^{1}$	$1{\cdot}18 \times 10^{-5}$
150	423	2·323	$5{\cdot}35 \times 10^{16}$	$2{\cdot}3 \times 10^{1}$	$1{\cdot}75 \times 10^{-5}$

(b)

Sonic velocity c cm sec^{-1}	Mean free path Λ cm	No. of evaporating molecules cm^{-2} sec^{-1}	Velocity of evaporation I g cm^{-2} sec^{-1}	Coefficient of viscosity η g cm^{-1} sec^{-1}	Kinematic viscosity $\nu = \frac{\eta}{\varrho}$ cm^2 sec^{-1}
$1{\cdot}38 \times 10^{4}$	25·9	$2{\cdot}27 \times 10^{16}$	$7{\cdot}46 \times 10^{-6}$	$2{\cdot}62 \times 10^{-4}$	$1{\cdot}50 \times 10^{5}$
$1{\cdot}41 \times 10^{4}$	10·2	$5{\cdot}85 \times 10^{16}$	$1{\cdot}93 \times 10^{-5}$	$2{\cdot}72 \times 10^{-4}$	$6{\cdot}18 \times 10^{4}$
$1{\cdot}43 \times 10^{4}$	4·37	$1{\cdot}42 \times 10^{17}$	$4{\cdot}65 \times 10^{-5}$	$2{\cdot}81 \times 10^{-4}$	$2{\cdot}68 \times 10^{4}$
$1{\cdot}45 \times 10^{4}$	1·91	$3{\cdot}22 \times 10^{17}$	$1{\cdot}06 \times 10^{-4}$	$2{\cdot}91 \times 10^{-4}$	$1{\cdot}18 \times 10^{4}$
$1{\cdot}48 \times 10^{4}$	$9{\cdot}0 \times 10^{-1}$	$6{\cdot}93 \times 10^{17}$	$2{\cdot}28 \times 10^{-4}$	$3{\cdot}00 \times 10^{-4}$	$6{\cdot}02 \times 10^{3}$
$1{\cdot}50 \times 10^{4}$	$4{\cdot}46 \times 10^{-1}$	$1{\cdot}42 \times 10^{18}$	$4{\cdot}68 \times 10^{-4}$	$3{\cdot}10 \times 10^{-4}$	$3{\cdot}07 \times 10^{3}$
$1{\cdot}53 \times 10^{4}$	$2{\cdot}36 \times 10^{-1}$	$2{\cdot}82 \times 10^{18}$	$9{\cdot}25 \times 10^{-4}$	$3{\cdot}20 \times 10^{-4}$	$1{\cdot}68 \times 10^{3}$
$1{\cdot}55 \times 10^{4}$	$1{\cdot}24 \times 10^{-1}$	$5{\cdot}30 \times 10^{18}$	$1{\cdot}74 \times 10^{-3}$	$3{\cdot}29 \times 10^{-4}$	$9{\cdot}11 \times 10^{2}$
$1{\cdot}57 \times 10^{4}$	$6{\cdot}88 \times 10^{-2}$	$9{\cdot}62 \times 10^{18}$	$3{\cdot}18 \times 10^{-3}$	$3{\cdot}38 \times 10^{-4}$	$5{\cdot}19 \times 10^{2}$
$1{\cdot}59 \times 10^{4}$	$3{\cdot}97 \times 10^{-2}$	$1{\cdot}69 \times 10^{19}$	$5{\cdot}58 \times 10^{-3}$	$3{\cdot}48 \times 10^{-4}$	$3{\cdot}08 \times 10^{2}$
$1{\cdot}61 \times 10^{4}$	$2{\cdot}37 \times 10^{-2}$	$2{\cdot}89 \times 10^{19}$	$9{\cdot}50 \times 10^{-3}$	$3{\cdot}58 \times 10^{-4}$	$1{\cdot}90 \times 10^{2}$
$1{\cdot}64 \times 10^{4}$	$1{\cdot}45 \times 10^{-2}$	$4{\cdot}80 \times 10^{19}$	$1{\cdot}58 \times 10^{-2}$	$3{\cdot}67 \times 10^{-4}$	$1{\cdot}18 \times 10^{2}$
$1{\cdot}66 \times 10^{4}$	$9{\cdot}05 \times 10^{-3}$	$7{\cdot}72 \times 10^{19}$	$2{\cdot}55 \times 10^{-2}$	$3{\cdot}77 \times 10^{-4}$	$7{\cdot}64 \times 10^{1}$
$1{\cdot}68 \times 10^{4}$	$5{\cdot}83 \times 10^{-3}$	$1{\cdot}22 \times 10^{20}$	$4{\cdot}01 \times 10^{-2}$	$3{\cdot}86 \times 10^{-4}$	$5{\cdot}04 \times 10^{1}$
$1{\cdot}70 \times 10^{4}$	$3{\cdot}84 \times 10^{-3}$	$1{\cdot}87 \times 10^{20}$	$6{\cdot}18 \times 10^{-2}$	$3{\cdot}96 \times 10^{-4}$	$3{\cdot}35 \times 10^{1}$
$1{\cdot}72 \times 10^{4}$	$2{\cdot}57 \times 10^{-3}$	$2{\cdot}84 \times 10^{20}$	$9{\cdot}35 \times 10^{-2}$	$4{\cdot}05 \times 10^{-4}$	$2{\cdot}32 \times 10^{1}$

TABLE 1.3.8. Decrease of enthalpy $\Delta J/m$ gives velocity w (after WASSERRAB).

$\Delta J/m$	W sec/kg	1×10^{4}	2×10^{4}	3×10^{4}	4×10^{4}	5×10^{4}	6×10^{4}
w	m/sec	100	141	173	200	224	245

$\Delta J/m$	W sec/kg	7×10^{4}	8×10^{4}	9×10^{4}	1×10^{5}	1×10^{6}
w	m/sec	264	283	300	316	1000

1.4. Choice of Pumps

1.4.1 Criteria for Choice of Backing and High-vacuum Pumps

There are three all-important factors to be considered when choosing a pump for a specific purpose:

1. The type of pump, its working range, and its attainable ultimate pressure. With respect to ultimate pressure a distinction must be made between residual gas pressure and residual vapour pressure (vapour pressure of pump fluid and of lubricant).
2. The size of the pump (pumping speed).
3. The size of the backing pump (in the event of the main pump itself not being capable of delivering against atmospheric pressure).

Information on the working ranges of the different pump types is provived by Fig. 1.4.1 (see also Fig. 1.4.19, p. 70/71). Table 1.4.1 gives a review of the physical phenomena in the pressure ranges that correspond to the working ranges. A general rule of thumb for the choice of pumps states that the attainable ultimate pressure of the pump should be at least one order of magnitude better than the working pressure required for the vacuum process.

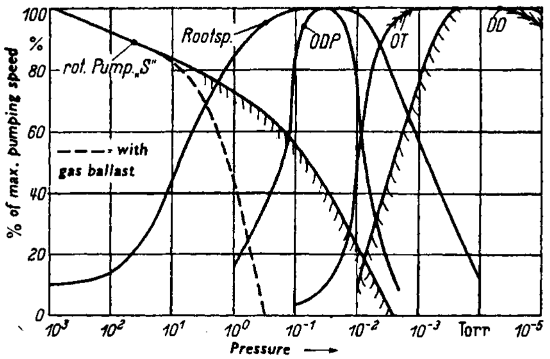

FIG. 1.4.1. Working ranges of different pump types (see also Fig. 1.4.19). Rot. Pump. "S" – single-stage oil-sealed rotary pumps; Rootsp. – Roots pumps; ODP – oil ejectors; OT – boosters; DO – diffusion pumps.

The second characteristic factor that has bearing on the choice of a suitable pump type is the capacity of the pump, which is expressed either in terms of pumping speed, i. e. volume per unit time (litre/sec or m^3/hr) or as throughput or capacity (Torr × litre/sec or g/sec).

The pumping speed or capacity values given for the different pump types refer to standard pressures, viz. for gas ballast pumps: atmospheric pressure, for Roots pumps and ejectors: 10^{-2} Torr, for boosters: 10^{-3} Torr,

TABLE 1.4.1. Pressure ranges of vacuum technology

	Coarse vacuum	Intermediate vacuum	Medium-high vacuum	High vacuum	Ultra-high vacuum
Pressure range in Torr	760–100	100–1	$1–10^{-3}$	$10^{-3}–10^{-7}$	$< 10^{-7}$
No. of particles per cm³ n (air, 20°C)	2.5×10^{19} to 3.3×10^{18}	3.3×10^{18} to 3.3×10^{16}	3.3×10^{16} to 3.3×10^{13}	3.3×10^{13} to 3.3×10^{9}	$< 3.3 \times 10^{9}$
Impingement rate per cm² and sec. A	$10^{23}–10^{22}$	$10^{22}–10^{20}$	$10^{20}–10^{17}$	$10^{17}–10^{13}$	$< 10^{13}$
Differential ionization. No. of ion pairs that an electron produces in 1 cm of its path (electron energy = 100 eV)	$10^{4}–10^{2}$	$10^{2}–10$	$10–10^{-2}$	$10^{-2}–10^{-6}$	$< 10^{-6}$
Corresponding charge in C	$10^{-15}–10^{-16}$	$10^{-16}–10^{-18}$	$10^{-18}–10^{-21}$	$10^{-21}–10^{-25}$	$< 10^{-25}$
Type of flow	continuous flow	continuous flow	transition to molecular flow	molecular flow	practically no flow; only movement of single molecules
Transport phenomena (heat conduction, viscosity, see also chapter 1.2)	independent of pressure	becomes dependent on pressure	dependent on pressure; determining factor is ratio of vessel dimensions to mean free path	proportional to pressure	no transport phenomena
Mean free path Λ [cm] (air, 20°C)	smaller than vessel dimensions $5 \times 10^{-6}–5 \times 10^{-5}$	smaller than vessel dimensions $5 \times 10^{-5}–5 \times 10^{-3}$	smaller than or equal to vessel dimensions $5 \times 10^{-3}–5$	usually larger than vessel dimensions $5–5 \times 10^{4}$	larger than vessel dimensions $> 5 \times 10^{4}$
Factors determining dimensioning of pump	vessel volume; independent of vessel shape	vessel volume; no influence of internal surface condition	vessel volume; dependent on vessel shape; at high pressures volume has greater influence, at low pressures surface condition has greater influence	surface condition	monolayer time (1 sec. to several hours)
Dimensioning of pump	according to curves for pump-down time Fig. 1.4.6 –1.4.8	according to curves for pump-down time Fig. 1.4.6 –1.4.8	nomograms Fig. 1.4.13 and 1.4.14	corresponding to size of surface; approx. formula p. 61	
Suitable pump type	rotary pump, liquid jet pump	rotary pump, Roots pump	ejector pump, Roots pump	diffusion pump	getter-ion pump, diffusion pump, molecular pump

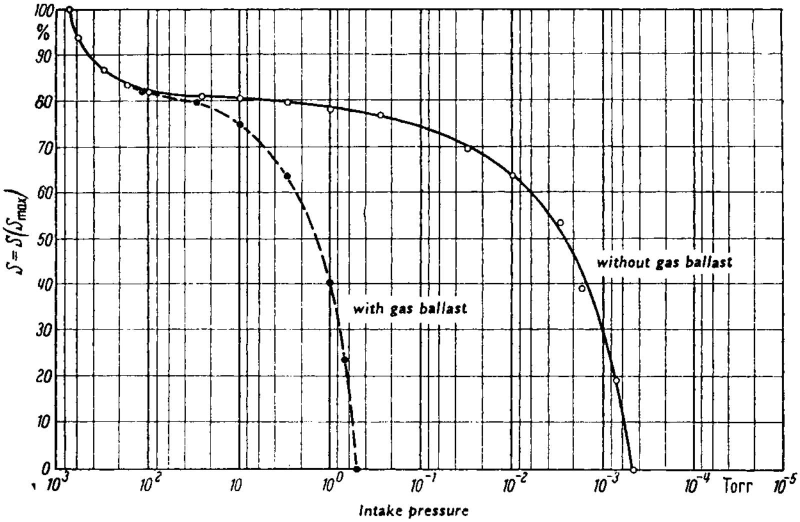

FIG. 1.4.2. Pumping speed (as a percentage of max. pumping speed) of a single-stage rotary vane pump in relation to intake pressure.

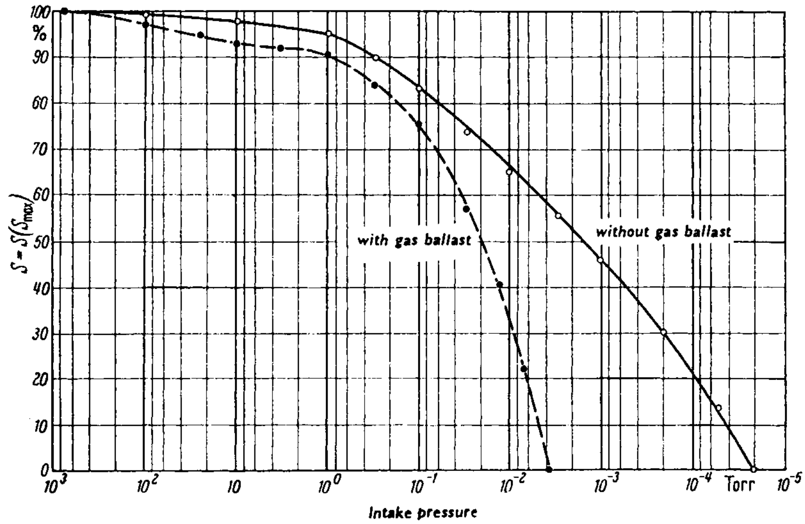

FIG. 1.4.3. Pumping speed (as a percentage of max. pumping speed) of a two-stage rotary vane pump in relation to intake pressure.

for diffusion pumps: 10^{-4} Torr and less. The required capacity or pumping speed depends upon the size of the vessel or the amount of accumulating gas.

In Figs. 1.4.2–1.4.5, the pumping speeds of different types of single-stage and two-stage gas ballast pumps are plotted as a function of the intake pressure for operation with and without gas ballast.

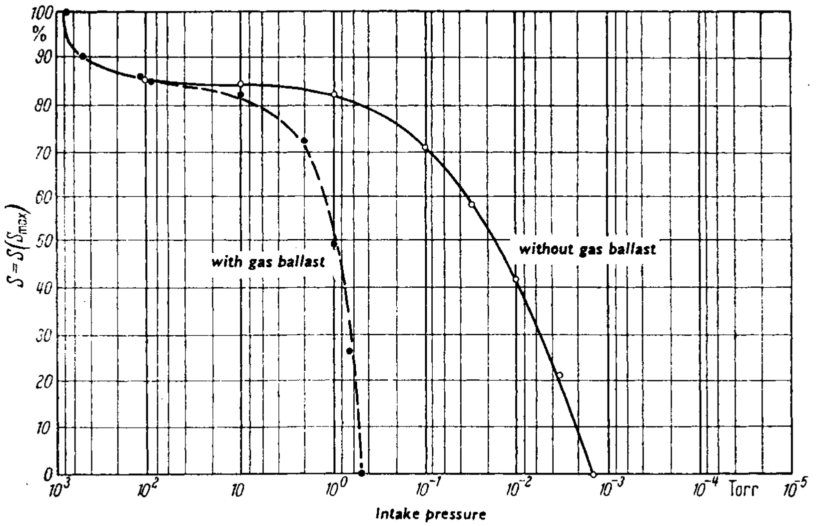

FIG. 1.4.4. Pumping speed (as a percentage of max. pumping speed) of a single-stage rotary piston pump in relation to intake pressure.

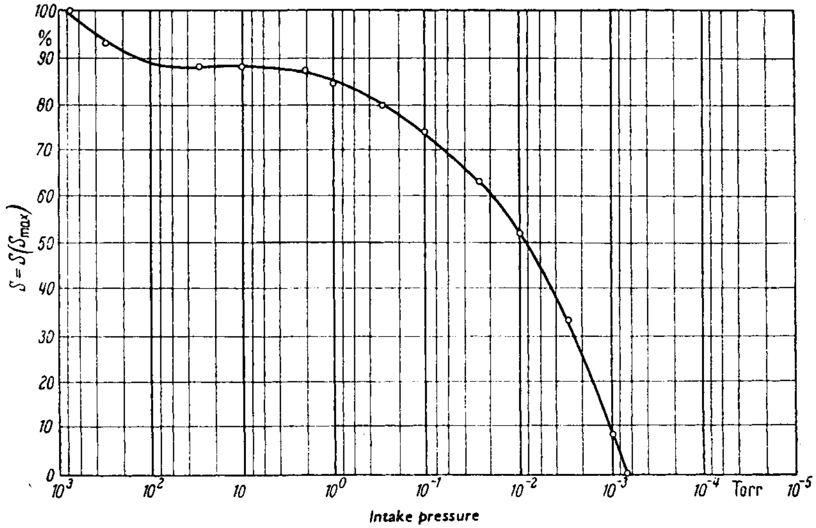

FIG. 1.4.5. Pumping speed (as a percentage of max. pumping speed) of a pump combination, consisting of a large rotary piston pump and a small rotary vane pump, in relation to intake pressure.

In the case of gas ballast pumps, it is also essential to know the time in which a vacuum vessel can be evacuated down to a given pressure by a pump of a certain size. A general indication of the pump-down times involved is provided in Figs. 1.4.6–1.4.8. If a vessel is to be evacuated which has a volume n times larger than that given in the graphs, the

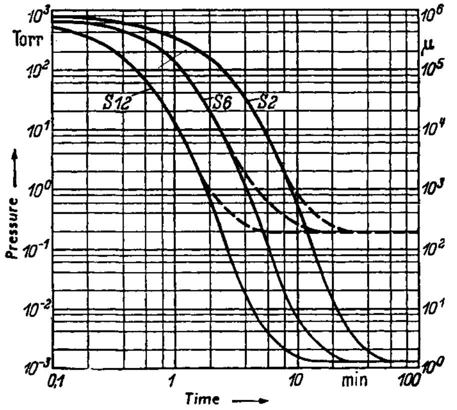

FIG. 1.4.6. Pressure in relation to time for evacuating a 50 litre vessel with single stage gas ballast pumps *S* 2, *S* 6, *S* 12; solid-line curves: without gas ballast; dash-line curves: with gas ballast.

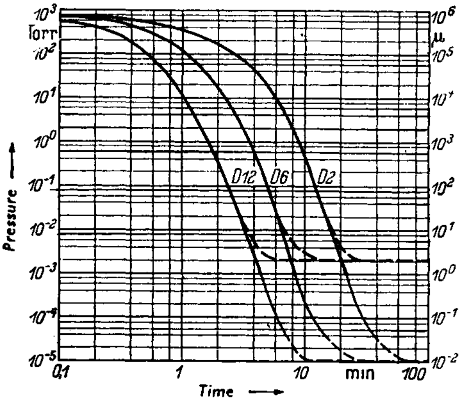

FIG. 1.4.7. Pressure in relation to time for evacuating a 50 litre vessel with two-stage gas ballast pumps *D* 2, *D* 6, *D* 12; solid-line curves: without gas ballast; dash-line curves: with gas ballast.

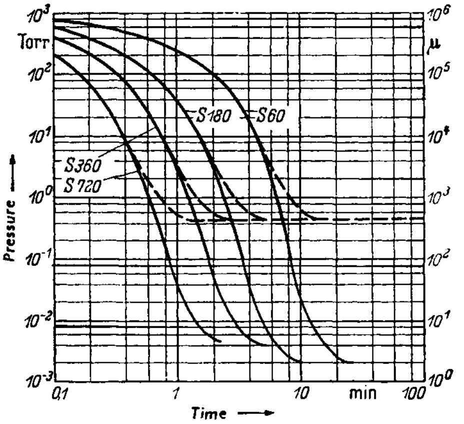

FIG. 1.4.8. Pressure in relation to time for evacuating a 1000 litre vessel with single-stage gas ballast pumps *S* 60, *S* 180, *S* 360, *S* 720; solid-line curves: without gas ballast; dash-line curves: with gas ballast.

required pump-down time will be n times greater. The time taken for pumping down a vessel from 760 to 1 Torr is expressed by the approximate formula

$$t = \frac{6{\cdot}5\,V}{S},$$

where,

V = vessel volume in litres or m^3 t = pump-down time in seconds or hr
S = pumping speed in litre/sec or m^3/hr

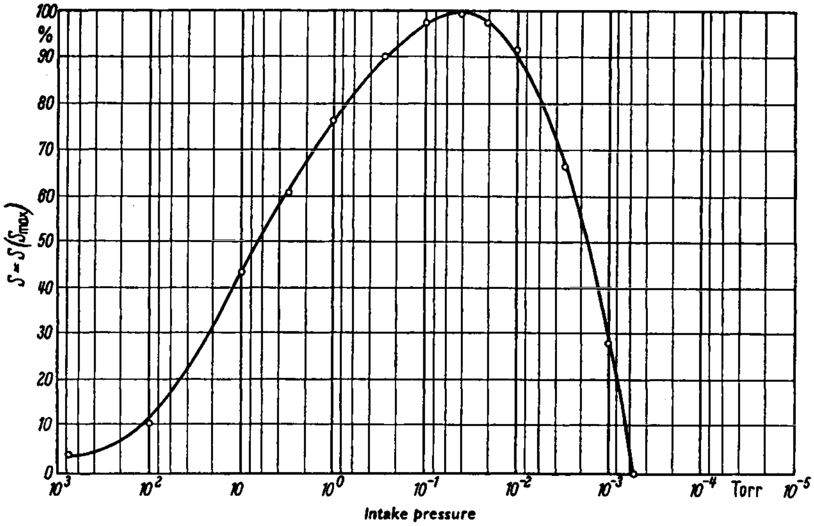

Fig. 1.4.9. Pumping speed (as a percentage of max. pumping speed) of a Roots pump backed by a corresponding forepump in relation to intake pressure.

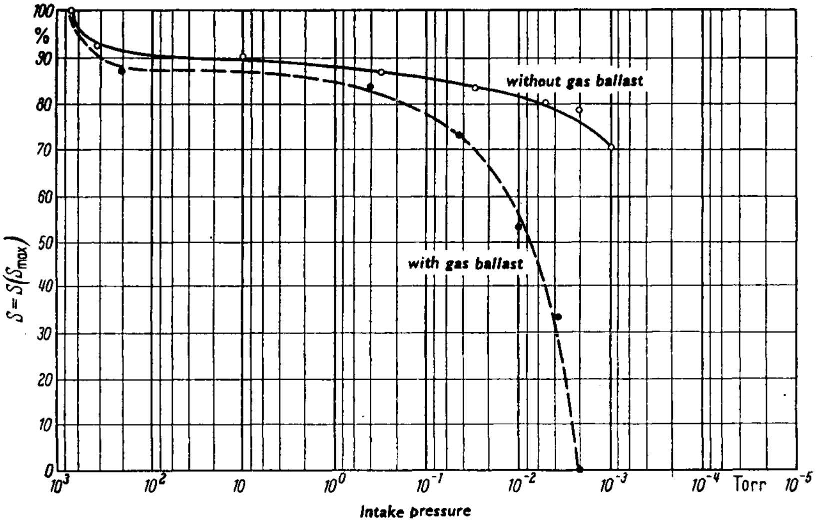

Fig. 1.4.10. Pumping speed (as a percentage of max. pumping speed) of a pump combination, consisting of a rotary piston pump and a Roots pump with comparable pumping speed (Ruta pump), in relation to intake pressure.

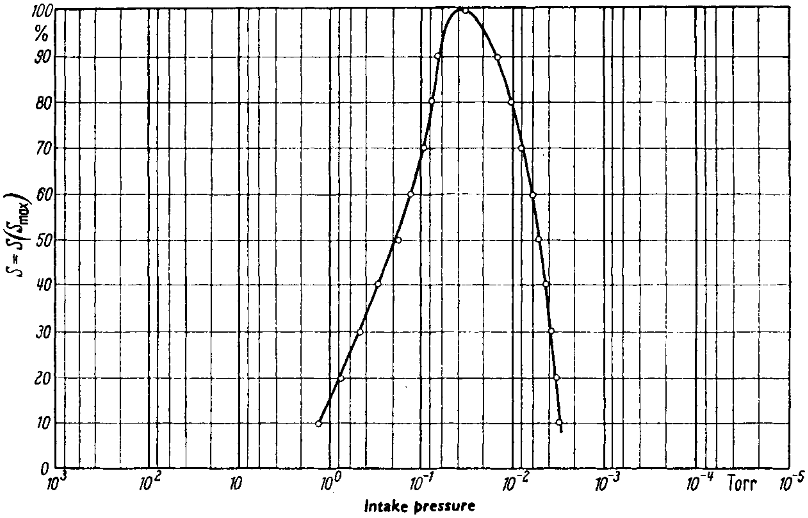

FIG. 1.4.11. Pumping speed (as a percentage of max. pumping speed) of an oil ejector pump in relation to intake pressure.

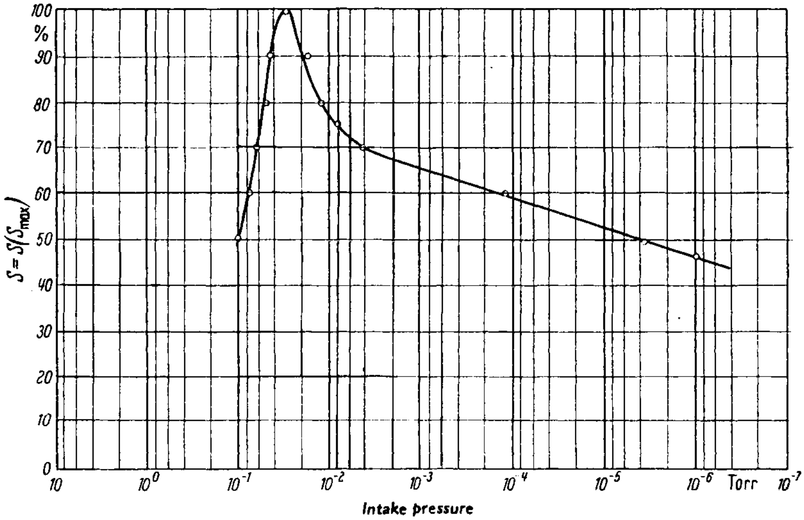

FIG. 1.4.12. Pumping speed (as a percentage of max. pumping speed) of a mercury ejector pump in relation to intake pressure.

In the range of medium-high vacuum, Roots pumps are preferably used, or in special cases oil or mercury ejector pumps; the pumping speed curves for these types are plotted in Figs. 1.4.9–1.4.12. Besides the gas volume of the vacuum vessel, outgassing from the surfaces and thus the shape of the vessel are also influential factors in this pressure range, so that no general curves can be given for pump-down times in medium-high vacuum. Pump sizes suitable for this range can be calculated from the nomograms in Figs. 1.4.13 and 1.4.14.

Whereas in coarse vacuum the pumping speed of the connected pump or the required pump-down time is determined only by the removal of gas molecules from the volume of the system to be evacuated, in high vacuum the amount of gas to be pumped is determined almost exclusively by outgassing from the surfaces, from which, in turn, the pumping speed or pump-down time can be calculated. In medium-high vacuum both factors, viz. gas removal from the volume and outgassing from the surfaces, are influential. For calculations in the range of medium-high vacuum, the nomograms Figs. 1.4.13 and 1.4.14 are provided. Two problems have to be solved. In each case the volume V of the vacuum system is given, likewise the size of the surface F exposed to vacuum.

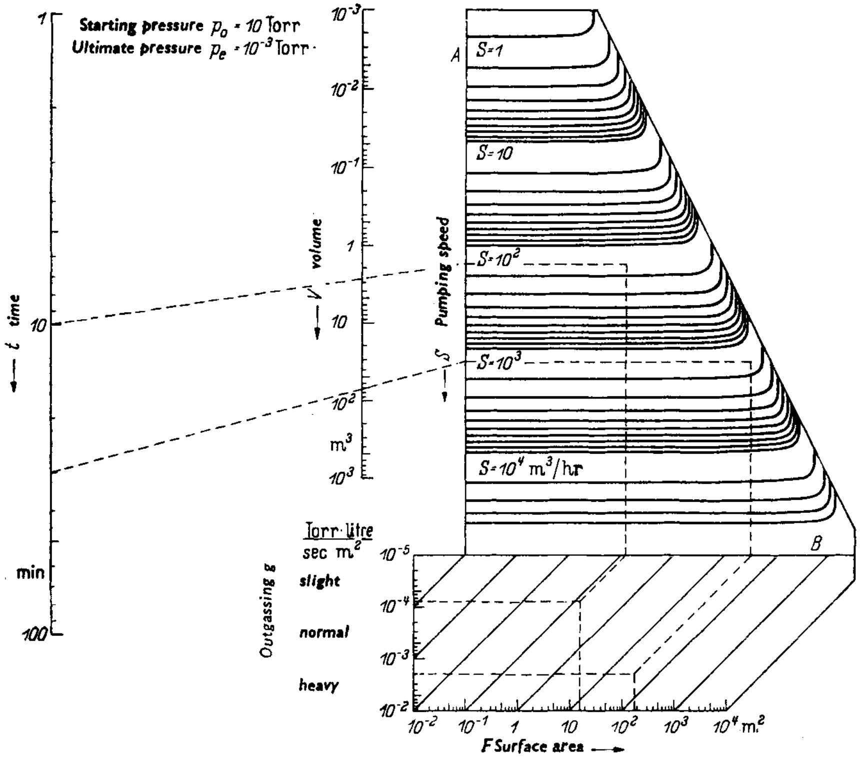

FIG. 1.4.13. Nomogram for choice of pump.

1. If the pumping speed S of the vacuum pump is known, the time t can be calculated which is needed, for instance, for evacuating the system concerned from 10 Torr down to 10^{-3} Torr.

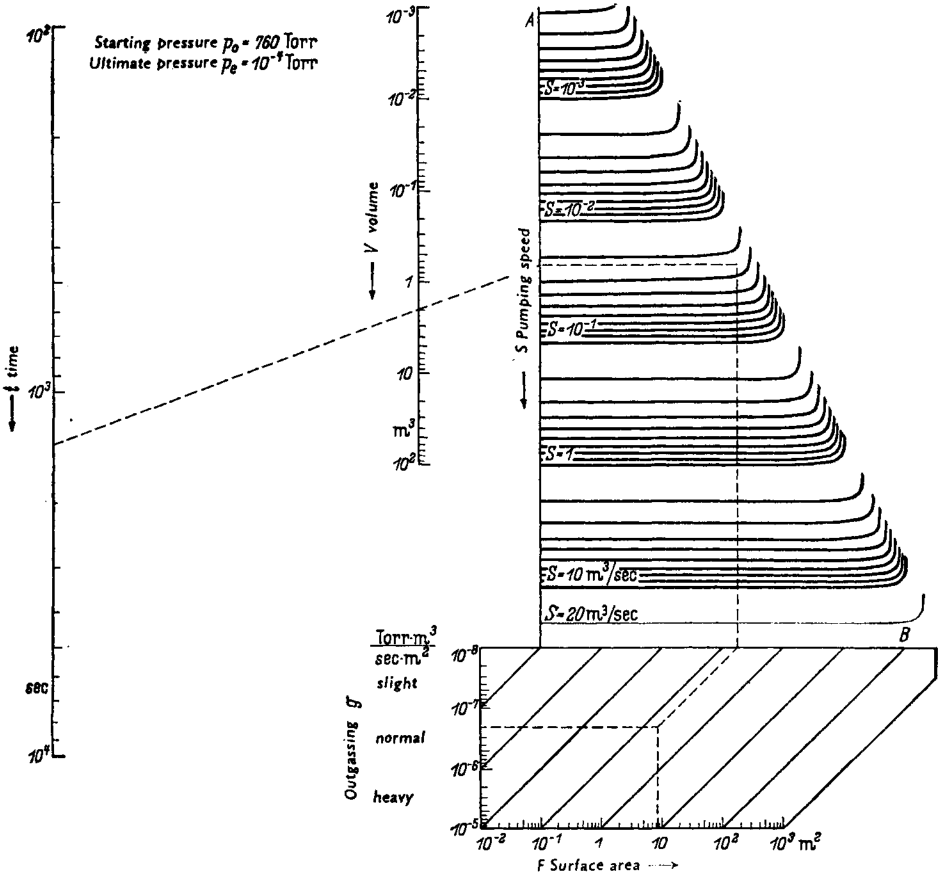

FIG. 1.4.14. Nomogram for choice of pump.

2. If the pump-down time t is known, the pumping speed S which can be calculated is needed for evacuating the system down to a certain pressure.

It is assumed that the vacuum system concerned has a volume V of 70 m^3 and a surface area in vacuum of 180 m^2. It is required to evacuate this system from 10 Torr down to 10^{-3} Torr by means of a pump with a pumping speed of $S = 1.3 \times 10^3$ m^3/hr. What is the time t required for this? The rate of outgassing from the surface will depend upon whether the surface is extremely clean, shows normal contamination or is very dirty. The rate of outgassing g expressed in Torr × litre/sec × m^2, that is to be expected in these three cases, is given by the values in the bottom perpendicular scale (Fig. 1.4.13); its value in the case in question is assumed to be 2×10^{-3} Torr × litre/sec × m^2.

The lines joining the points for 180 m^2 and 2×10^{-3} Torr × litre/sec × m^2 intersect at a point which should first be projected obliquely upwards to line B and from there perpendicularly upwards to the point of intersection with the curve that starts from the point corresponding to the speed of the pump ($S = 1{\cdot}3 \times 10^3$ m^3/hr).

If this projection meets the curve for the pumping speed within the bounded curve section, the pump will be big enough to deal with the rate of outgassing. The respective pump-down time is then given by joining on a straight line the point on scale S ($1{\cdot}3 \times 10^3$ m^3/hr) with the point on scale V (70 m^3), and extending this straight line until it intersects scale t. The found pump-down time t is equal to 30 minutes.

In a second example, it is assumed that a system with a volume V of $2{\cdot}6$ m^3 is to be evacuated from 10 Torr down to 10^{-3} Torr in a time of 10 min. Surfaces of 16 m^2 have a rate of outgassing in vacuum amounting to 8×10^{-5} Torr × litre/sec × m^2. By joining the scale points for $t = 10$ min and $V = 2{\cdot}6$ m^3, it is found that a pump is needed with a speed of $S = 1{\cdot}5 \times 10^2$ m^3/hr.

A horizontal straight line drawn through the point $g = 8 \times 10^{-5}$ Torr × litre/sec × m^2 and a vertical line drawn through the point $F = 16$ m^2, intersect at a point which is projected obliquely upwards to scale B and then perpendicularly upwards to a point on the curve for $S = 1{\cdot}5 \times 10^2$ m^3/hr. This point, too, lies within the bounded curve section. The pumping speed is, therefore, high enough to deal with the outgassing that occurs.

There are two suitable types of pumps for the high vacuum range, viz. boosters for the higher pressures in this range, and diffusion pumps (oil diffusion pumps and mercury diffusion pumps) for the lower pressures. A pumping speed curve for a booster is plotted in Fig. 1.4.15, and for diffusion pumps in Figs. 1.4.16 and 1.4.17. In the working range of boosters and diffusion pumps, outgassing from the surfaces is the only determining factor for the amount of gas to be removed and thus for the choice of the most suitable pump size. The pumping speed of a suitable pump type must, therefore, be high enough for the gas molecules given off from the surfaces to be removed continuously at the required working pressure. This outgassing from surfaces of the same size largely depends upon the condition of the surface and its pre-treatment. A rule of thumb that can be generally applied is that to maintain a pressure of 10^{-4} to 10^{-5} Torr in a vacuum vessel with an overall surface area of 1 m^2, a pump is needed which has a pumping speed of about 20 litre/sec, assuming that optimum conditions prevail (clean surfaces).

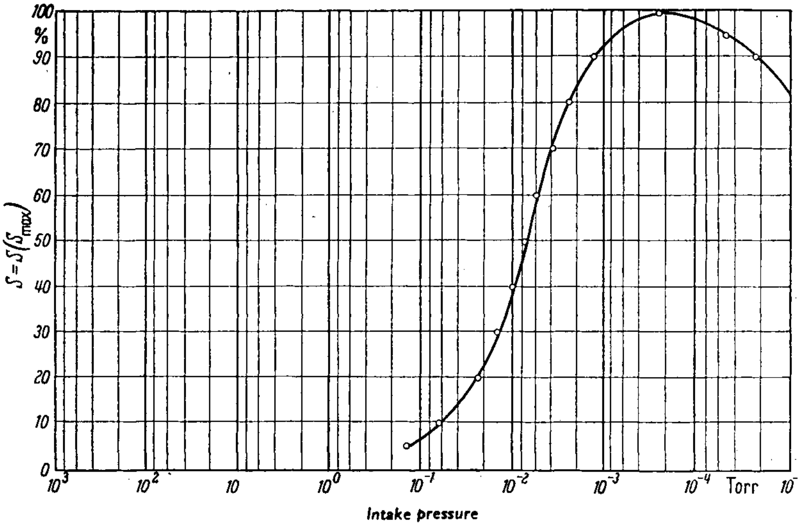

FIG. 1.4.15. Pumping speed (as a percentage of the maximum pumping speed) of a booster in relation to intake pressure.

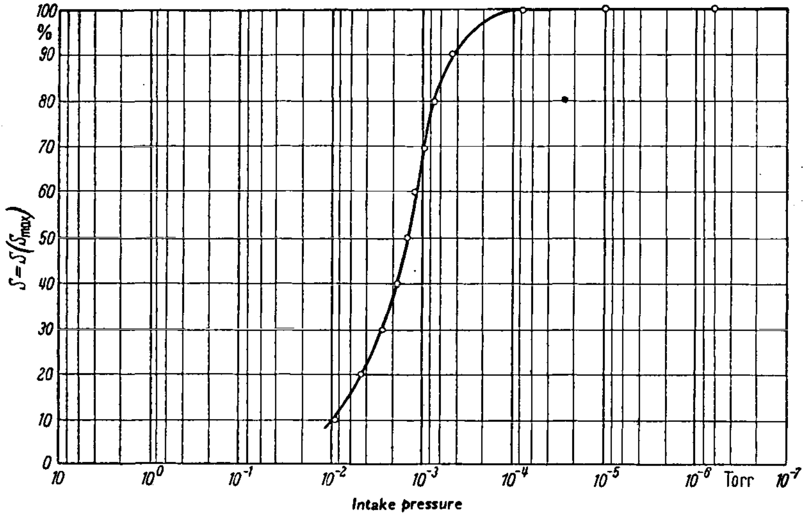

FIG. 1.4.16. Pumping speed (as a percentage of the max. pumping speed) of an oil diffusion pump in relation to intake pressure.

To evacuate such a system down to the required pressure within a few minutes, about ten times the above pumping speed is needed, viz. 200 litre per sec. The given values hold for room temperature; at higher temperatures greater amounts of outgassing must be expected.

Since no compression to atmospheric pressure takes place in Roots pumps, oil ejector pumps, mercury ejector pumps and diffusion pumps, a gas ballast pump must be connected to produce and maintain the forepressure.

The general rule is that the throughput of the backing pump in Torr × litre/sec at forepressure must be at least as high as the throughput of the medium-high or high vacuum pump in Torr × litre/sec at working pressure, as expressed by the equation

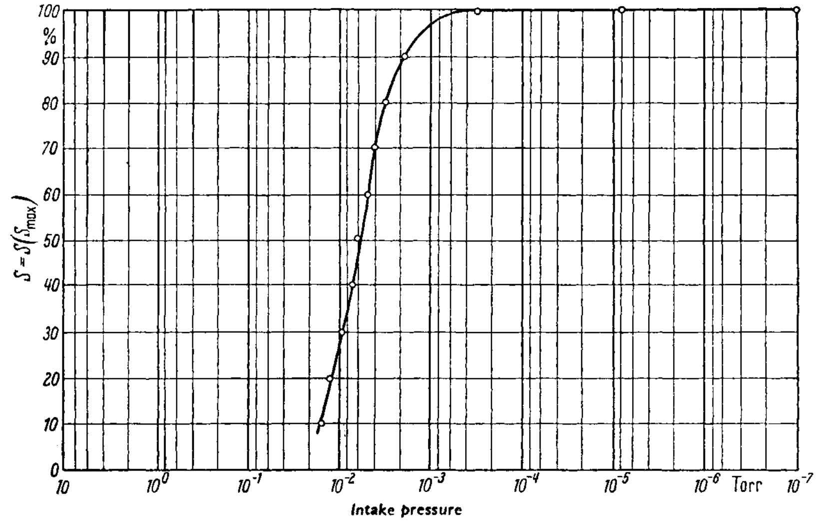

FIG. 1.4.17. Pumping speed (as a percentage of the max. pumping speed) of a mercury diffusion pump in relation to intake pressure.

$$S_H p_H \leqq S_v p_v, \tag{1.4.1}$$

where:

S_H = pumping speed of high vacuum or medium-high vacuum pump in litre/sec
p_H = intake pressure of high vacuum or medium-high vacuum pump in Torr
S_v = pumping speed of backing pump in litre/sec
p_v = forepressure on intake side of backing pump in Torr

Figure 1.4.18 shows a plot of the working ranges of different pump types, i.e. the range between intake pressure and forepressure or compression pressure respectively. The working range of each pump type lies between the diagonals of the coordinate system and the curve plotted for the respective pump type. Diffusion pumps, for instance, are able to compress from any intake pressure that is less than 10^{-1} Torr to a forepressure or compression pressure of 10^{-1} Torr, regardless of whether permanent gases or water vapours are present in the system. Oil ejectors are capable of compressing from intake pressures of more than 10^{-3} Torr and less than about 5 Torr to a forepressure of about 5 Torr.

Two-stage gas ballast pumps are able to compress from intake pressures of less than about 10^{-1} Torr to atmospheric pressure, and single-stage gas ballast pumps from intake pressures of more than 1 Torr to 760 Torr; these values are for operation with gas ballast. Different conditions are encountered for Roots pumps; in their case, the admissible forepressure depends upon the intake pressure. If, for instance, in Fig. 1.4.18 a line is traced

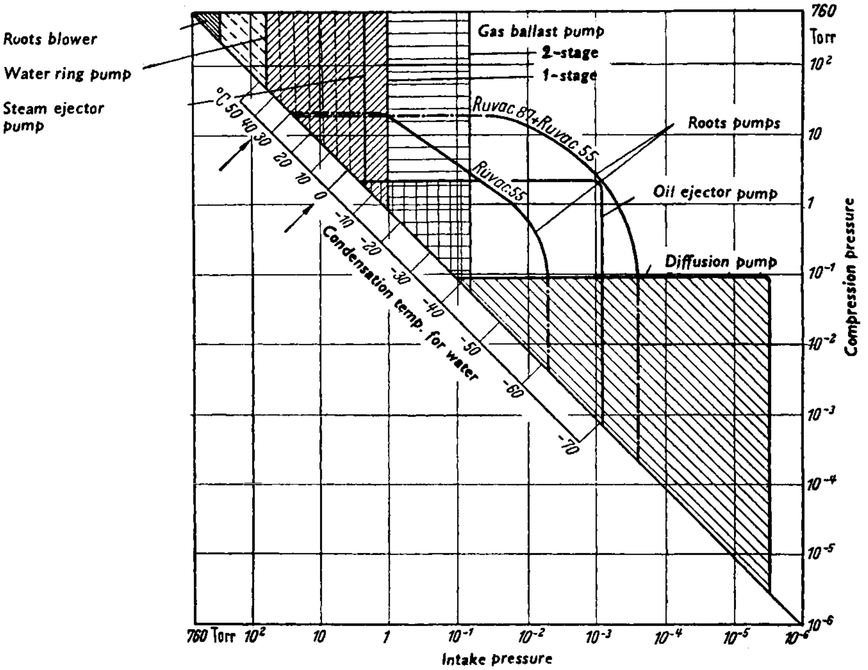

FIG. 1.4.18. Working ranges of different pump types.
Ruvac 54 is a single-stage Roots pump with a speed of 5000 m^3/hr. Ruvac 87 + Ruvac 55 is a combination of two series-connected single-stage Roots pumps with pumping speeds of 30,000 m^3/hr and 6000 m^3/hr, respectively.

vertically upwards from a certain intake pressure to the point of intersection with the curves given for the Roots pumps, it is found that the forepressure determined in this manner varies with the intake pressure. From the curves plotted here for Roots pumps, the attainable intake pressures can be found for a given compression pressure or, alternatively, the required compression pressures can be determined for given intake pressures. Special care must be taken when removing water vapour with Roots pumps because they require a gas ballast pump as backing pump, and the intake pressure for water vapour must not exceed 30 Torr for gas ballast pumps. Therefore, the curves plotted for the working ranges of Roots pumps terminate at a compression pressure of 30 Torr. If, in special instances, the water vapour pressures on the compression side of Roots pumps should be higher, it will be necessary to install a cooled interstage condenser between the Roots pump and the gas ballast pump. For further details, please refer to the chapter on condensers, p. 81.

For calculating the size of a suitable backing pump for use in combination with a Roots pump, the following data are needed:

The accumulating amount of gas, i. e. the product of the speed of the Roots pump times intake pressure ($S_H\,p_H$), and the desired intake pressure p_H.

The size of the required Roots pump is given by the quantity S_H (see, for instance, pump type Ruvac 55 in Fig. 1.4.18). The admissible compression pressure p_v can be determined from the intake pressure p_H by projecting this point vertically upwards until it intersects the curve plotted for the pump type Ruvac 55. Since equation 1.4.1 applies also in this case, the required pumping speed S_v of the backing pump can be calculated from the total value as the product of $S_H\,p_H$ and the now known value p_v.

For boosters and diffusion pumps, the following condition must be satisfied: The backing pump must be so dimensioned that it produces with or without gas ballast the necessary forepressure (p_v) for the high vacuum pump; furthermore, the pumping speed at this forepressure must be adequate to remove completely the amount of gas delivered at the pumping speed of the high vacuum pump at the specified intake pressure (see Figs. 1.4.19—1.4.21). The corresponding capacity ($S_H\,p_H$) of the high vacuum pump is given by the intake pressure p_H according to Fig. 1.4.19. This load must be equal to the capacity ($S_v\,p_v$) of the backing pump at the admissible forepressure p_v, i. e. $S_H\,p_H = S_v\,p_v$; S_v gives the size of the required backing pump. With respect to the values S_v and p_v, a distinction must be made between operation of the backing pump with gas ballast and operation without gas ballast. If water vapour is present on the vacuum side, the values S_v and p_v must be substituted in all cases for operation of the pump with gas ballast. A special point to note is that in such vacuum processes where only a slight amount of water vapour is expected to form on the vacuum side (e. g. when pumping down television tubes), single-stage gas ballast pumps will suffice as backing pumps, whereas in processes where large amounts of water vapour are expected to form (e. g. in drying and distillation processes) two-stage gas ballast pumps should preferably be used as backing pumps.

The curves plotted in Fig. 1.4.19 give the speed of the pumps multiplied by the intake pressure in relation to intake pressure. This quantity, which is expressed by the dimension Torr × litre/sec, and is referred to as capacity, is proportional to the amount of gas removed. Therefore, a scale for the removed amount of air in kg/hr is plotted on the right-hand side of the diagram.

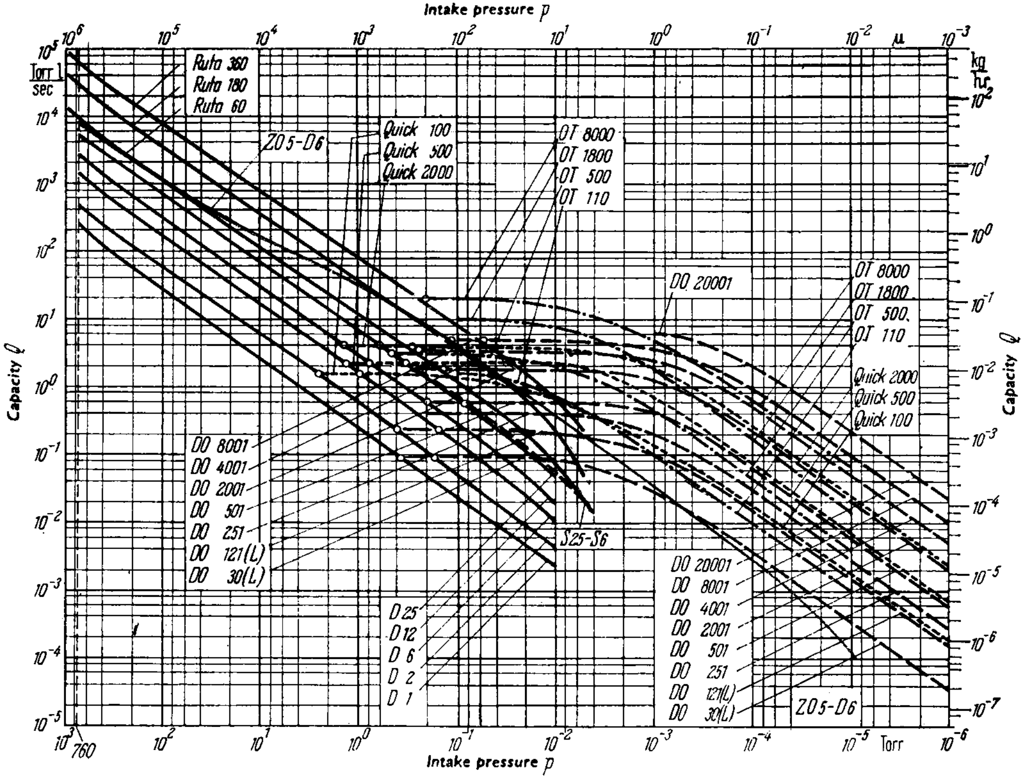

FIG. 1.4.19a. Characteristics of vacuum pumps for air (20 °C) (LEYBOLD).

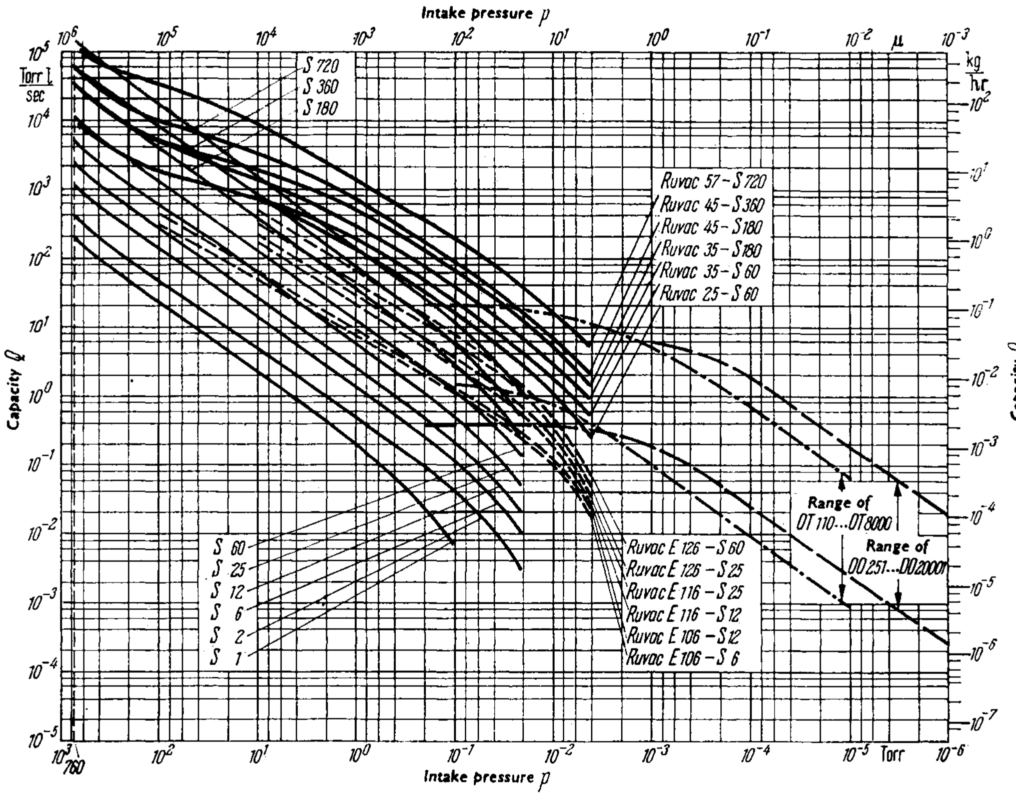

FIG. 1.4.19b. Characteristics of vacuum pumps for air (20°C) (LEYBOLD).

Let us consider the booster OT 1800 as an example. Its working range extends to higher pressures of about 10^{-2} Torr. At this pressure level it delivers about 4×10^{-2} kg of air per hour, an amount which, at a max. forepressure of 0·7 Torr, is removed by the tandem pump type Ruta 180; this pump type is, therefore, suitable for use as a backing pump in the case in question. Another suitable backing pump is the Roots pump Ruvac E 116–S 25. On the other hand, the D 25 type gas ballast pump is just large enough for backing the diffusion pump DO 2001; however, the Ruta 60 tandem pump should preferably be used for work at pressures in the 1×10^{-4} Torr range.

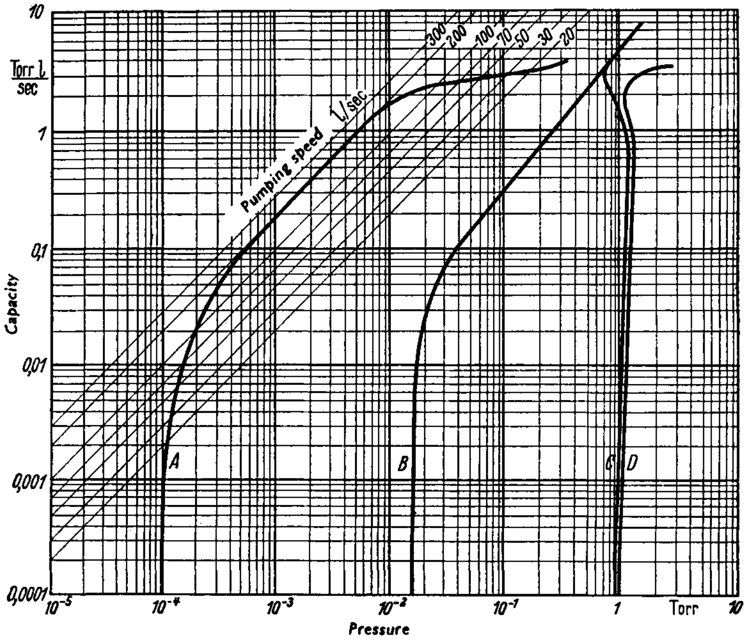

FIG. 1.4.20. Diffusion pump and backing pump (after G. A. SOFER, *Vac. Symp. Trans.*, p. 27, 1954).

A – Capacity resp. pumping speed of diffusion pump in relation to intake pressure in high vacuum; B – Capacity resp. pumping speed of backing pump in relation to intake pressure in fore-vacuum; C – Pressure in fore-vacuum (in relation to capacity), at which intake pressure of diffusion pump rises by 10 per cent; D – Pressure in fore-vacuum (in relation to capacity), at which intake pressure of diffusion pump rises by a factor of 10

The intersection points of the curves marked by circles indicate which pump types are suitable for backing the diffusion pumps. Smaller pumps would be able to remove the amounts of gas delivered by the diffusion pump only at pressures above the maximum admissible forepressure of the booster and diffusion pump. Therefore, use of such smaller backing pumps would reduce the efficiency of the booster and diffusion pump in the higher intake pressure range. The curves also permit the required pump size to be determined. In order to maintain a pressure of 1 Torr at a leakage rate of 1 Torr × litre/sec, at least a gas ballast pump S 6 will be needed. For a pressure of 10^{-1} Torr an S 60 is required, and for a pressure of 10^{-3} Torr an OT 1800.

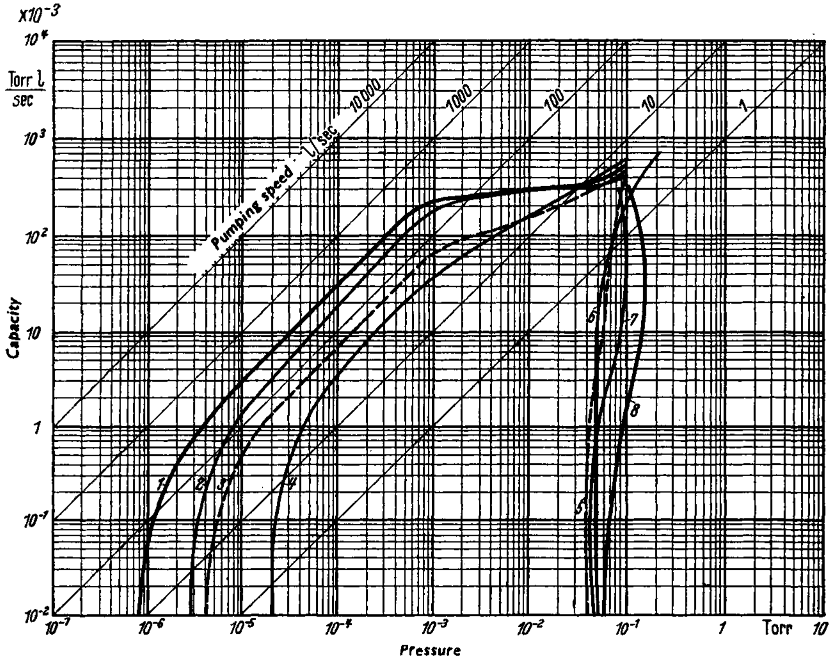

FIG. 1.4.21. Efficiency of the different stages of a (three-stage) diffusion pump (after G. A. SOFER, *Vac. Symp. Trans.* p. 27, 1954).
Curves 1, 2, 3, 4: Capacity or pumping speed respectively of diffusion pump in relation to intake pressure in high vacuum; Curves 5, 6, 7, 8: pressure in fore-vacuum (in relation to capacity or pumping speed respectively), at which intake pressure of diffusion pump rises by 10 per cent; Curves 1, 8: all nozzles operative; 2, 7: top (high vacuum) nozzle switched off; 3, 5: centre nozzle switched off; 4, 6: bottom nozzle switched off.

1.4.2 Water Ring Pumps and Steam Ejectors

There are also other pump types which compress to atmospheric pressure that make suitable backing pumps, above all water ring pumps. They should be used in processes where vapours have to be removed which ruin the oil of rotary pumps. A condition for their use, however, is that the process takes place at several Torr or above, because the ultimate pressure of water ring pumps is in the range of about 20 Torr. At somewhat lower pressures a water ring pump combined with an air ejector will be quite adequate; furthermore in this case no danger of cavitation will arise for the water ring pump, even when the ultimate pressure is attained. In order to reduce the ultimate pressure still further with a water ring pump operating as the backing pump, two or more Roots pumps can be connected in series. But such arrangements are rather costly. A gas ballast pump with oil regeneration in combination with a single-stage Roots pump will often be more favourable.

Steam ejectors also make suitable backing pumps for Roots pumps. According to the number of stages used, very low pressures can be attained, too. The employment of steam ejectors is, however, decided by the operating costs. As a rule they are only economical when cheap exhaust steam is available.

1.5 Removal of Vapours

1.5.1 Gas Ballast

Pure water vapour cannot be removed by mechanical pumps which compress from intake pressure to atmospheric pressure because the working temperature of the pumps is less than 100 °C in most cases, so that the water vapour condenses in the pump during the compression process. To prevent interfering condensation and to eliminate the deficiencies that arise in consequence of such condensation, various methods have been proposed; for instance, centrifuging of pump oil, heating of pumps and continuous oil regeneration. The best method of all has proved to be

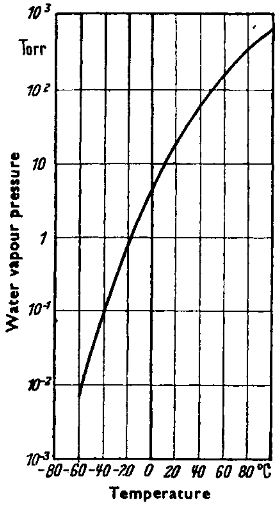

FIG. 1.5.1. Saturation pressure for water vapour vs. temperature.

the gas ballast device, introduced by Gaede, which completely prevents condensation of water vapour in the pumps. The essential feature of the gas ballast technique is that a measured quantity of fresh air (the so-called gas

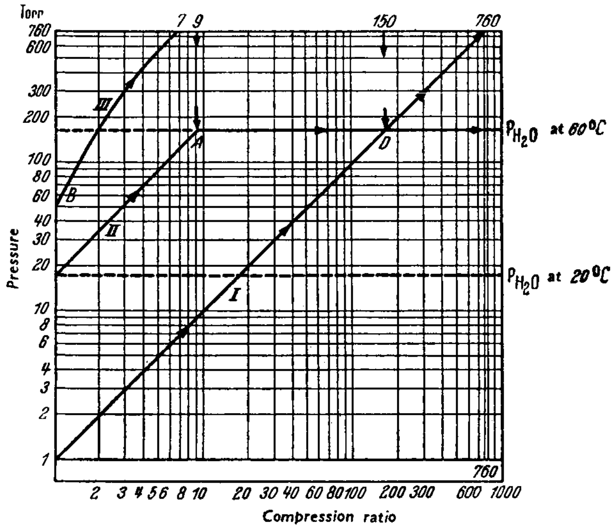

FIG. 1.5.2. Pressure rise during compression process in rotary pumps. Compression ratio equals ratio of the volume of pump chamber, at the instant it is shut off from the intake side, to the instantaneous volume during compression.

Curve I: Removal of permanent gases; pressure (starting pressure of 1 Torr in this example) rises proportionally to compression ratio until exhaust valve opens at 760 Torr.

Curve II and curve III: Removal of vapours: in this example saturated water vapour at 20 °C (saturation pressure of 17·5 Torr, working temperature of pump 60 °C).

Curve II: Removal of vapours with ordinary rotary oil-sealed pumps. Pressure at first rises proportionally to compression ratio until (point *A*) the saturation pressure is reached which corresponds to working temperature of pump (in this example 150 Torr at compression ratio *9*). On further compression, condensation takes place at constant pressure. *A* pressure of 760 Torr is not attained. Exhaust valve remains closed.

Curve III: Removal of vapours with gas ballast pumps. Fresh air (gas ballast) is already admitted into the pump chamber before the compression process begins. Therefore, when compression does begin (point *B*), there is a mixture of vapour and air under increased pressure (in this example 50 Torr) present in the pump chamber. As the compression ratio increases, the pressure rises due, on the one hand, to the compression of the vapour–air mixture and, on the other hand, to the continued admission of gas ballast, until eventually (in this example at compression ratio *7*) a pressure of 760 Torr is attained and the exhaust valve consequently opens. If sufficient gas ballast is admitted, this happens before the vapour is compressed to saturation (in this example at a compression ratio *9*). The vapours are, therefore, ejected from the pump without condensing.

ballast) is continually admitted into the compression chamber of the pump with the result that a pressure of 760 Torr is attained before the water vapour is compressed to the saturation pressure corresponding to the pump temperature, and hence before it can condense. The admission of fresh air into the compression chamber begins immediately the compression chamber has been shut off from the intake port, thus avoiding too large a reduction of the ultimate pressure. To understand the operating principle of the gas ballast device, Fig. 1.5.2 should be studied. By way of comparison, Fig. 1.5.3. illustrates the practical compression process in a gas ballast pump.

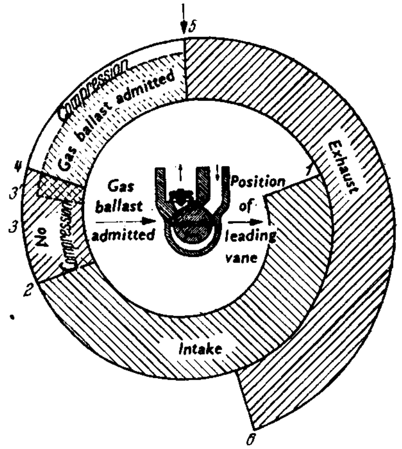

FIG. 1.5.3. Pumping process in a gas ballast pump.
The spiral drawn around the schematically illustrated pump shows the processes that take place in the pump in relation to the position of the leading vane. In *Position 1* the space below this vane is shut off from the intake port, and the space above it gradually increases in volume as the pump continues to rotate. The diagram illustrates what happens to the space *above* the vane in relation to its respective position.
Position 1 to position 2: Intake. *Position 2:* Compression chamber shut off from intake port by the second (rear) vane. *Position 2 to position 3:* Compression chamber continues to increase in volume. *Position 3 to position 4:* Volume of compression chamber is reduced again to value at position 2. *Position 3':* Admission of gas ballast begins. *Position 4 to position 5:* Compression under continued admission of gas ballast. *Position 5:* Exhaust valve opens. *Position 5 to position 6:* Exhaust of delivered vapours and of gas ballast.

According to the calculations of GAEDE, the gas ballast B (expressed in litre/sec related to atmospheric pressure p_{at} in Torr) required to prevent condensation can be calculated from the following equations. The indices refer to the vane position in Fig. 1.5.3. (1 is understood to mean the beginning of the intake period, 5 the beginning of exhaust after atmospheric pressure is reached in the pump chamber).

$$S_1 p_{d,1} = S_5 p_{d,5}\,, \tag{1.5.1}$$

$$S_1 = V_1 \nu = S\,, \tag{1.5.2}$$

$$S_5 = V_5 \nu\,, \tag{1.5.3}$$

$$p_{d,5} \leqq p_s\,, \tag{1.5.4}$$

$$B p_{at} = S_5 p_{g,5}\,, \tag{1.5.5}$$

$$p_{g,5} = p_{at} - p_{d,5}\,. \tag{1.5.6}$$

B – gas ballast (litre/sec) at atmospheric pressure p_{at} (Torr);
p_{at} – atmospheric pressure (Torr);
p_d – partial pressure of vapour to be exhausted (Torr);
p_g – partial pressure of gas to be exhausted (Torr);
p_s – saturation pressure of vapour at working temperature of pump (Torr);
S – pumping speed (litre/sec);
V – pump chamber volume (litre);
ν – rotating speed of vane (sec^{-1}).

It follows therefrom that

$$B p_{at} = S_5 (p_{at} - p_{d,5}) \tag{1.5.7}$$

and hence that

$$B = S p_{d,1} \left[\frac{1}{p_{d,5}} - \frac{1}{p_{at}}\right] \tag{1.5.8}$$

or, with $p_{d,5} \leqq p_s$

$$B \geqq S p_{d,1} \left[\frac{1}{p_s} - \frac{1}{p_{at}}\right] \tag{1.5.9}$$

Hence it follows that the required gas ballast will be all the greater the higher the speed of the pump and the greater the water vapour pressure at the intake port. But it can remain all the smaller, the higher are the values of the saturation pressure of the water vapour at the temperature in the pump. The required gas ballast increases again however, with the barometric pressure. Furthermore, it is evident that the minimum gas ballast becomes equal to zero in the case of the vapour saturation pressure in the pump being equal to the barometric pressure ($p_s = p_{at}$, heated pump). In the case of a mixture of gas and vapour being removed, it follows analogously that

$$B p_{at} = S_5 \left[p_{at} - (p_{d,1} + p_{g,1}) \frac{S}{S_5}\right], \tag{1.5.10}$$

$$B = S_5 \left[1 - \frac{p_{g,1} + p_{d,1}}{p_{at}} \frac{S}{S_5}\right], \tag{1.5.11}$$

$$\frac{S}{S_5} = \frac{p_{d,5}}{p_{d,1}}, \tag{1.5.12}$$

$$B \geqq S p_{d,1} \left[\frac{1}{p_s} - \frac{1 + \dfrac{p_{g,1}}{p_{d,1}}}{p_{at}}\right]. \tag{1.5.13}$$

In this case, too, the required gas ballast similarly depends upon the pumping speed, the water vapour pressure at the intake port and the saturation pressure of the water vapour at the temperature of the pump, just as it is above. But in addition it is also dependent upon the ratio of $p_{g,1}$ to $p_{d,1}$, i. e. upon the amount of gas mixed with the vapour on the intake side; in fact the required minimum gas ballast is all the smaller the larger the amount of gas that is added.

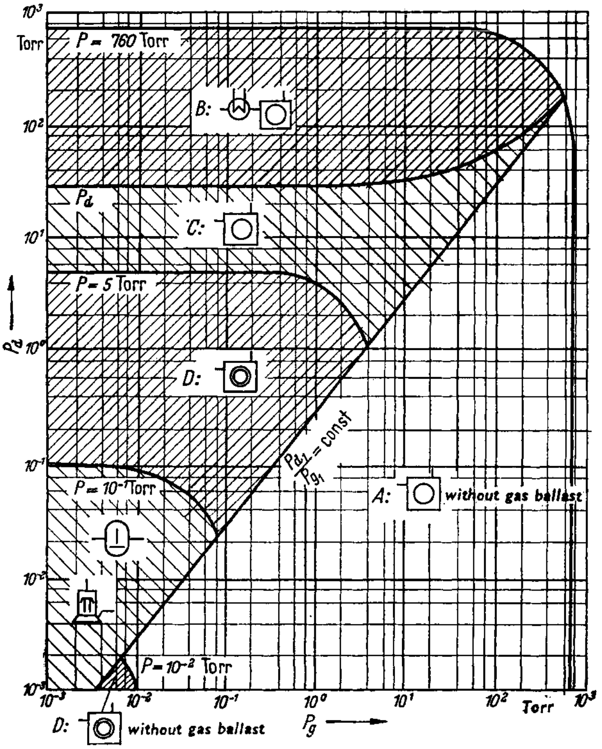

FIG. 1.5.4. Working ranges of single-stage and two-stage rotary vane pumps for removal of gas – vapour mixtures (after THEES, *Vakuum-Technik* **6**, 160 (1957)). $P = p_g + p_d$ = total pressure; the water vapour tolerance is plotted at $p_d = 30$ Torr; A = single-stage rotary vane pump without gas ballast; B = single-stage rotary vane pump with gas ballast and series-connected condenser; C = single-stage rotary vane pump with gas ballast; D = two-stage rotary vane pump without gas ballast.

Assuming we have a certain gas ballast of known value, the admissible water vapour partial pressure $p_{d,1}$ for this pump, according to equation 1.5.13, will be

$$p_{d,1} \leqq \frac{\left(\frac{B}{S}\right) p_{at}\, p_s + p_s\, p_{g,1}}{p_{at} - p_s}. \qquad (1.5.14)$$

For operation of the pump without gas ballast ($B = 0$), the water vapour partial pressure may amount to

$$p_{d,1} \leqq \frac{p_s\, p_{g,1}}{p_{at} - p_s} \tag{1.5.15}$$

(Fig. 1.5.4-1.5.6, range A).

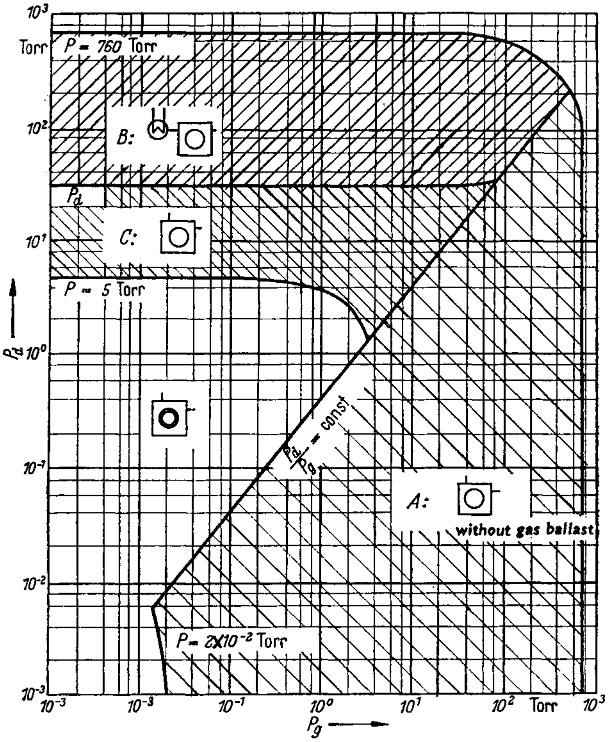

FIG. 1.5.5. Working ranges of rotary piston pumps for removal of gas-vapour mixtures (after THEES, *Vakuum-Technik*, **6**, 160 (1957)). $p = p_g + p_d$ = total pressure; the water vapour tolerance is plotted at $p_d = 30$ Torr; A = single-stage rotary piston pump without gas ballast; B = single-stage rotary piston pump with gas ballast and series-connected condenser; C = single-stage rotary piston pump with gas ballast.

In the LEYBOLD gas ballast pumps, the gas ballast B (equation 1.5.13) is set to a value such that the water vapour tolerance has a value of about 30 Torr (at room temperature).

Thus, the working ranges of the different pumps are given for various mixtures of water vapour and gas (p_d = partial pressure of water vapour, p_g = partial pressure of gas), as shown by Fig. 1.5.4 for single-stage and two-stage rotary vane pumps, by 1.5.5 for single-stage rotary piston pumps, and by 1.5.6. for pump combinations or tandem pumps. For further details on this, please refer to the next chapter on condensers.

In Figs. 1.5.4—1.5.6, the partial pressure of gas p_g and the partial pressure of vapour p_d are plotted on the coordinates. The marked-in ranges indicate

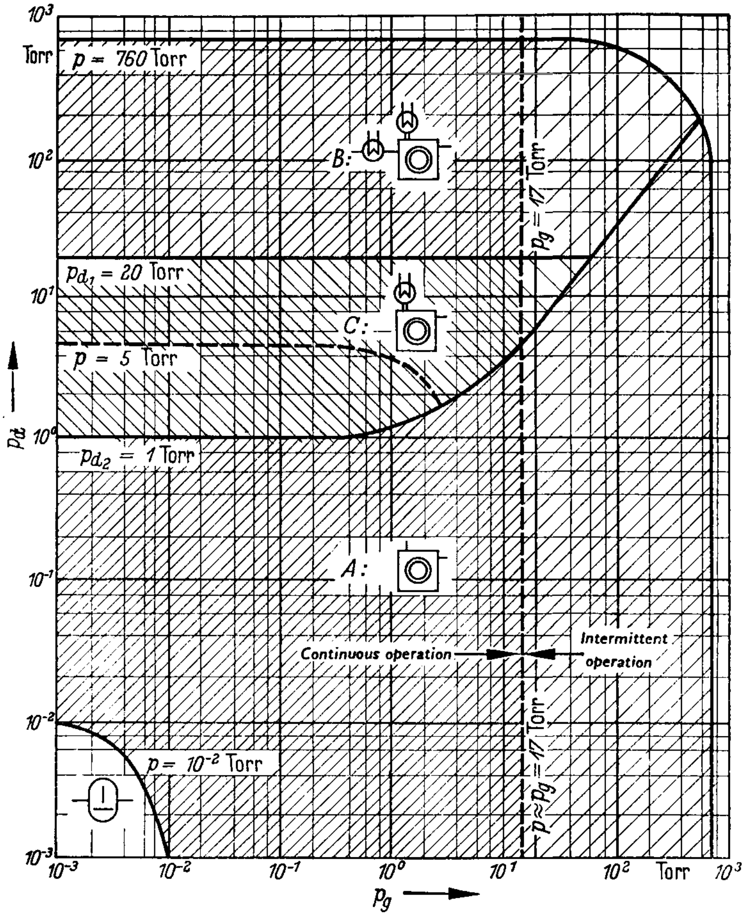

FIG. 1.5.6. Working range of a tandem pump, consisting of a rotary piston pump of high speed backed by a rotary vane pump of low speed, for removal of vapour-gas mixtures (after THEES, *Vakuum-Technik* **6**, 160 (1957)). $p = p_g + p_d$ = total pressure; p_{d1} = water vapour partial pressure on intake side of fore-vacuum stage, determined by temperature of condensate; p_{d2} = water vapour tolerance on intake side of medium-high vacuum stage. At intake pressures of more than 17 Torr, the power consumption of the tandem pump exceeds that of the single pump; A – tandem pump; B – tandem pump with interstage condenser; C – tandem pump with condenser fitted on intake side and interstage condenser.

under which conditions a gas ballast pump must operate without vapours condensing in the pump.

The plotted curves hold for water vapour as the most frequent case of application.

Rotary piston pumps and rotary vane pumps differ only slightly in their working temperatures. The behaviour of the tandem pump is determined by the fact that its two stages are of different sizes, which means that compression takes place between them thus making it necessary to use an interstage condenser (see Fig. 1.5.6, ranges *B* and *C*). In contrast, in two-stage rotary vane pumps no compression can take place between the two stages because of their identical sizes.

Range A (Fig. 1.5.4). The proportion of non-condensable gases is so high that the pump can run without gas ballast.

Range B has the largest proportion of water vapour. The condenser on the intake side of the pump removes the water vapour. The pump operates with gas ballast; no condensation takes place in the pump. The range is limited by the water vapour tolerance ($p_d = 30$ Torr) of a gas ballast pump.

Range C. The proportion of water vapour in this range is so low that the gas ballast pump can be operated without a condenser. A tandem pump, however, requires an interstage condenser. The range is limited on the one side by the water vapour tolerance (p_d) and on the other by the lowest attainable working pressure (5 Torr) of a gas ballast pump.

Range D. A two-stage gas ballast pump should be used in the range below the lowest working pressure (5 Torr) of the single-stage gas ballast pump. The range is limited on the one side by the lowest working pressure (5 Torr) of the single-stage pump and on the other by the lowest working pressure (10^{-1} Torr) of the two-stage gas ballast pump.

At still lower pressures, Ruta pumps (Roots tandem pumps), Roots pumps and diffusion pumps are used.

1.5.2 Condensers

By using gas ballast, vapours can be safely removed with mechanical pumps, in other words without affecting the pumping process; but in all cases where large amounts of vapours have to be exhausted it is uneconomical to use pumps for this purpose (see Fig. 1.5.7). Instead it will prove to be a far easier and cheaper practice to condense the vapours in a condenser. For instance, at temperatures above 10°C the condenser K 100 (K 6) removes more water vapour than even the large rotary piston pump S 720. (For details of the possibility of attaining low temperatures, see Tables 1.5.1—1.5.3). The pump is then left merely with the task of removing noncondensable gases and the residue of vapours not condensed in the condenser.

TABLE 1.5.1. Refrigerating solutions and agents

Substance	g substance per 100 g water								
	Freezing temp.								
	−5°C	−10°C	−15°C	−20°C	−25°C	−30°C	−40°C	−50°C	−60°C
Solutions:									
NaCl	8·44	16·1	22·9	29·4	23·8	–	–	–	–
$MgCl_2$	7·66	13·4	17·7	21·1	–	25·9	–	–	–
$CaCl_2$	9·67	16·6	21·9	26·3	29·9	33·3	38·8	43·8	–
Refrigerating agents:									
Sodium lactate $CH_3CHOHCOONa$	10·5	19	27·5	34	42	49·5	64	80	100
Methyl alcohol CH_3OH	9·3	17	24	31	39	46	43	85	–
Ethyl alcohol C_2H_5OH	11·1	23	34	46	57·5	69·5	104	–	–
Glycerine $C_3H_5(OH)_3$	20·5	42	56	68	80	90·5	113	138	–
Glysantine	13	28	43	57·5	69·5	82	108	144	–

To inhibit corrosion of iron, small quantities of basic substances (e.g. NaOH, Na_2CO_3, $Mg(OH)_2$, $Ca(OH)_2$, $CaCO_3$) are added to refrigerating agents. Reinhartin solution is a mixed solution of $MgCl_2$ and $CaCl_2$ with protective colloids; it can be used at temperatures of down to —52°C.

TABLE 1.5.2. Low temperatures attainable with different refrigeration methods

Refrigeration produced by	Attainable temp. in °C
Refrigeration machine	
single-stage	approx. — 45
two-stage	approx. — 70
Liquid air (fresh)	— 194·5
Liquid nitrogen	— 195·8
Liquid oxygen	— 183·0
Dry ice (solid carbon dioxide)	— 78·5
Mixtures of salts and ice	approx. — 55 (max.)

This applies in principle to all vapours that are not soluble in oil. Water vapour is especially significant. In this respect, a distinction must be made between two characteristic cases:

1. It is assumed that only small quantities of water vapour accumulate; the water vapour is not saturated. It is especially present as a gas-vapour

TABLE 1.5.3. Drying agents for water vapour absorption

Drying agent		H_2O-partial pressure above fresh drying agent at 25°C
P_2O_5		2×10^{-5} Torr
$Mg(ClO_4)_2$		5×10^{-4} Torr
KOH (melted)		2×10^{-3} Torr
Al_2O_3		3×10^{-3} Torr
H_2SO_4	80%	$1{\cdot}24 \times 10^{-1}$ Torr
H_2SO_4	85%	$3{\cdot}9 \times 10^{-2}$ Torr
H_2SO_4	90%	$7{\cdot}7 \times 10^{-3}$ Torr
H_2SO_4	conc.	3×10^{-3} Torr
CaO		2×10^{-1} Torr
$CaCl_2$		$1{\cdot}4$–$2{\cdot}5 \times 10^{-1}$ Torr

mixture (working conditions in physics laboratories). In this case the vapour can be removed in principle with gas ballast, but without a condenser (see chapter 1.5.1, p. 74).

2. It is assumed that large quantities of water vapour accumulate. The water vapour is saturated, in fact, at temperatures above room temperature. In these conditions it is recommended to use a condenser in which so much water vapour should be condensed that water vapour saturated at room temperature forms at the intake port of the pump. The gas ballast of the pump must be so large that it will still be adequate at a water vapour pressure of 20 Torr. For safety the gas ballast, as already mentioned, is adjusted to allow a water vapour pressure of about 30 Torr at the intake part of the pump.

For the pumping of gas-vapour mixtures by means of gas ballast pumps with or without condensers, the following 4 arrangements are of fundamental significance:

1. A single-stage pump without condenser
2. A single-stage pump with condenser fitted on the intake side
3. A two-stage pump system without condenser*
4. A two-stage pump system with interstage condenser*

---

* For arrangements 3.and 4 it is necessary to make a distinction between the following cases:

Case *a* – Two single-stage pumps with identical stage sizes	with and without condenser
Case *b* – Two single-stage pumps with different stage sizes	
Case *c* – A single two-stage pump with identical stage sizes	
Case *d* – A single two-stage pump with different stage sizes	

Cases *a* and *c* can be treated like arrangements 1 and 2. Case *d* has, in comparison with case *c*, considerable disadvantages because when vapours are being exhausted interstage condensation takes place which cannot be influenced from outside. That means the water vapour tolerance is considerably reduced. Case *b*, which can be improved in the most effective way with an interstage condenser, is fully discussed in the comments on arrangement 4.

In all cases a distinction must be made as to whether it is required to remove water vapour ($p_g = 0$) only, or whether vapour-gas mixtures ($p_d \neq 0$) have to be exhausted.

1. The behaviour of single-stage pumps is explained in its essentials by what has been said earlier on gas ballast. Attention will be focused here solely on the case in which a vapour-gas mixture is present. The above equation 1.5.15 showed how large the ratio of the partial pressure of gases p_{g1} to the partial pressure of vapours p_{d1} must at least be for gas ballast to be no longer needed.

A practical outcome which arises from the above formulae is that pure water vapour, without additional gas, can be removed with gas ballast up to a partial pressure of $p_d = 30$ Torr. If the water vapour is mixed with gas, water vapour of still higher pressures can also be exhausted, according to equation 1.5.13. In fact, if there is sufficient additional gas present, it may be possible to dispense with gas ballast completely i. e. $B = 0$. But it is not recommended to enforce the condition given by equation 1.5.15, for $B = 0$, by artificial addition of gas. It is simply a useful point to note for such cases where, due to systems not being completely tight or to heavy outgassing of components in the vacuum system, a high partial pressure of the permanent gases p_g naturally prevails. The artificial addition of gas is not to be recommended if only for the reason that it would very considerably reduce the attainable ultimate pressure.

2. On the other hand, it is recommended to keep the water vapour partial pressure p_d on the intake side as small as possible, at least below 30 Torr. An effective means of achieving this is to fit a condenser on the intake side of the pump; it is essential that the size of the condenser is matched to the amount of water vapour that accumulates. The only suitable condensers for the medium-high vacuum range are those with a very slight flow impedance (pressure gradient along the condenser is negligible), preferably surface condensers with interior cooling coils. For the example of water vapour, a few arrangements of condensers and the corresponding pump sizes are described below.

LEYBOLD manufacture five condenser sizes (see Table 1.5.4). The sole task of the pumps connected to the condenser is to keep the partial pressure of the non-condensable residual gases as low as possible. This pressure depends only upon the quantity of gas which the liquid to be evaporated contains or liberates, and upon the leakage rates of the system. Since the quantity of gas is usually very small (0.1 g gas per kg throughput) and as the leakage rates can be kept at a low value (less than 10^{-2} Torr × litre per sec), a certain ratio of the throughput of water vapour to the accumulating quantity of permanent gases can be given for plants that are kept tight enough to meet the requirements of a medium-high vacuum system, and hence the corresponding pump size can be determined for a certain condenser size (see Table 1.5.4).

Table 1.5.4. Empirical values

Throughput at approx. 10° temperature difference between condensing vapour and cooling water	for gas ballast pump type at a residual gas pressure in condenser of		Main condenser	Protective condenser
	1 Torr	15 Torr		
3 kg/hr	VP 2, S 2 VP 6, S 6	VP 2, S 2	K 05	K 05
15 kg/hr	VP 12, S 12	VP 6, S 6	K 1	K 05
100 kg/hr	S 60	VP 12, S 12	K 6	K 1
300 kg/hr	S 180	60	K 14	K 1
600 kg/hr	S 360	S 180	K 30	K 6
1200 kg/hr	S 720	S 180	(2×) K 30	K 6

Design: Steel* with SB copper pipes according to DIN 1785

Condenser	Condensing surface	Flange connection	
		for system	for pump
K 05	0·5 m^2	NW 50 (EF)	NW 50 (EF) or NW 20 (KF)
K 1	1 m^2	NW 100 (EF)	NW 100 (EF) or NW 32 (KF)
K 6	6·5 m^2	NW 100 (EF)	NW 50 (EF)
K 14	14 m^2	NW 150 (EF)	NW 65 (EF)
K 30	30 m^2	NW 250 (EF)	NW 100 (EF)

EF = unit flange
KF = small flange

* Steel is usually understood to mean wrought and rollable iron.

Figure 1.5.7 shows the relation of the condensed quantity of water to the pressure p_{d1} on the inlet side at different cooling water temperatures for the condenser type K 6†.

It is only in extremely simple cases, as assumed above, that the ratio of the partial pressure of the permanent gases to the water vapour partial pressure is constant throughout the entire evacuation process. The pump must be so dimensioned that it is adequate to deal with the heaviest accumulation of permanent gases during the whole of the process. The condenser must be so dimensioned that it corresponds to the mean quantity of water vapour accumulating during the process. If larger quantities of water vapour form at certain periods in the evacuation process, a valve must be fitted before the condenser to ensure that the quantity of water vapour entering the condenser is never larger than its own capacity. Similarly, a valve should be fitted before the pump, but behind the condenser, for the purpose of reducing the pumping speed if the maximum quantity of permanent gases, for which the pump has been designed, no longer accumulates.

Of the two-stage pump combinations, such arrangements are especially important in which a gas ballast pump of low speed is connected in series

---

† Previously known as K 100.

with a bigger pump without gas ballast; the pump of higher pumping speed can, for instance, be a Roots pump. Such a two-stage pump arrangement can, in turn, be operated with or without an interstage condenser. The following equation* generally holds for such an arrangement: removed quantity on the intake side $S_1(p_{g1} + p_{d1})$ = condensed quantity in condenser $(K = S_K \times p_{d2})$ + quantity removed through backing pump $S_2(p_{d2} + p_{g2})$.

$$S_1(p_{g1} + p_{d1}) = S_2(p_{g2} + p_{d2}) + S_K \times p_{d2}\,. \qquad (1.5.16)$$

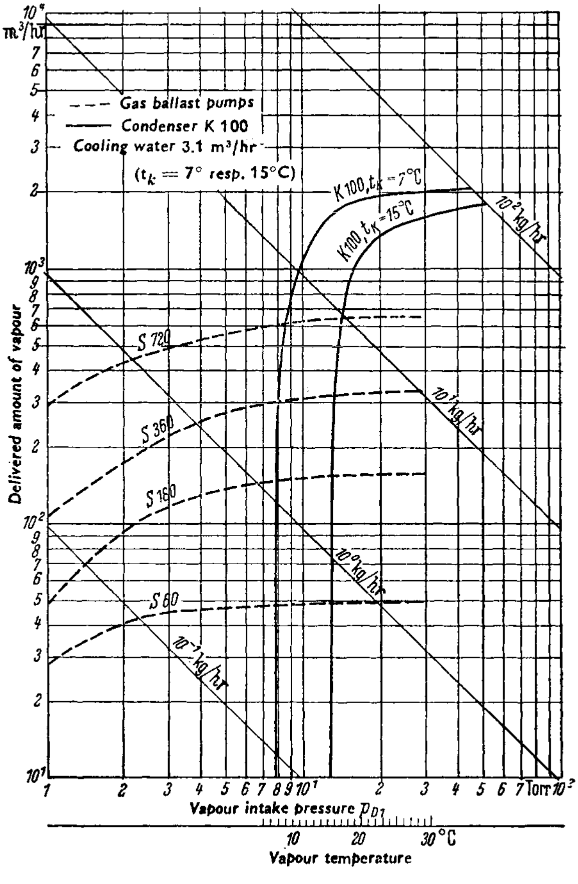

FIG. 1.5.7. Removed quantity of water vapour in relation to intake pressure for gas ballast pumps S 60 to S 720 (dashed-line curve) and condenser K 100 (K 6) (solid line curve), at a cooling water temperature of 7 °C and 15 °C. The ordinate values give the removed quantity of vapour in m³/hr, and the oblique lines of the coordinate system express it in kg/hr. A comparison of the dash-line curves with the solid line curves shows from which pressure onwards the capacity of the condenser is greater than that of the pumps.

---

* In the preceding chapter, index 1 referred to the intake side of the gas ballast (backing) pump; here it refers to the medium-high vacuum stage.

3. Two-stage pump arrangement without interstage condenser, i. e.

$$K = 0.$$

3.1 Pure water vapour without addition of gas ($p_g = 0$):

$$\frac{S_1}{S_2} = \frac{p_{d2}}{p_{d1}} = N, \tag{1.5.17}$$

$$N = \frac{\text{pumping speed of medium-high vacuum stage}}{\text{pumping speed of backing pump}}$$

For the two-stage pumps, N has a value of about 30, and for Roots pumps a value of 10.

p_{d2}, the pressure on the intake side of the gas ballast pump, should not exceed 30 Torr according to what was stated above ($p_{d2} \leqq 30$ Torr); it thus follows from equation 1.5.17 that

$p_{d1} \leqq 30/N$ Torr,
$p_{d1} \leqq 1$ Torr for two-stage pumps,
$p_{d1} \leqq 3$ Torr for Roots pumps.

If the water vapour partial pressure on the intake side of the medium-high vacuum stage is greater than the values given above for p_{d1}, an interstage condenser must be fitted between the two pumps.

3.2 Vapour-gas mixture ($p_g \neq 0$):

$$\frac{S_1}{S_2} = N = \frac{p_{g2} + p_{d2}}{p_{g1} + p_{d1}}. \tag{1.5.18}$$

$$(p_{g2} + p_{d2}) \times \frac{1}{N} = p_{g1} + p_{d1}. \tag{1.5.19}$$

With

$$\frac{p_{g2}}{p_{g1}} = N \tag{1.5.20}$$

then

$$p_{g1} = \frac{1}{N} \times p_{g2}.$$

Since p_{d2} should again be $\leqq 30$ Torr,
it follows that

$$p_{d1} \leqq \frac{30}{N} \text{ Torr}.$$

In the case of $N = 30$, it again follows, therefore, that $p_{d1} \leqq 1$ Torr (see Fig. 1.5.6, range A).

4. Two-stage pump arrangement with interstage condenser ($K \neq 0$);

$$S_1(p_{g1} + p_{d1}) = S_2(p_{g2} + p_{d2}) + S_K \times p_{d2}. \tag{1.5.16}$$

4.1 Let us first consider the case in which the pressure of the permanent gases is very small,

$$p_g \to 0,$$

then

$$S_1 \times p_{d1} = (S_2 + S_K)\, p_{d2}. \tag{1.5.21}$$

Because the permanent gas pressure is small, the pumping speed of the gas ballast backing pump (S_2) can be kept at a very low value:

$$S_2 \ll S_K .$$

It thus follows that

$$S_1 \times p_{d1} = S_K \times p_{d2} \tag{1.5.22}$$

or

$$p_{d1} = \frac{S_K}{S_1} \times p_{d2} = \frac{S_K}{S_2} \times \frac{p_{d2}}{N} .$$

Here

$$p_{d2} = 30 \text{ Torr} ,$$

therefore

$$p_{d1} = \frac{S_K}{S_2} \times \frac{30}{N} . \tag{1.5.23}$$

Since $S_K \gg S_2$, p_{d1} can also thus be kept at $\gg 30/N$. This means that very large water vapour partial pressures are admissible. All water vapour is condensed in the condenser. Only a very small backing pump (S_2) is necessary and admissible.

4.2 Presence of permanent gases ($p_{g1} \neq 0$)

The two following cases require consideration here:
Large condenser and small backing pump:

$$S_K \gg S_2 .$$

Large backing pump and small interstage condenser:

$$S_2 \gg S_K .$$

4.2.1 $S_K \gg S_2$; from this it follows that

$$S_K \times p_{d2} \gg S_2 \times p_{d2}$$

and furthermore, from equation 1.5.15, that

$$S_1(p_{g1} + p_{d1}) = S_2 \times p_{g2} + S_K \times p_{d2} . \tag{1.5.24}$$

Besides, since

$$S_1 \times p_{g1} = S_2 \times p_{g2} ,$$

then

$$S_1 \times p_{d1} = S_K \times p_{d2}$$

or

$$p_{d1} = \frac{S_K}{S_1} \times p_{d2} . \tag{1.5.25}$$

This is the same result as obtained above for a slight addition of permanent gas, because it is only in this case that the backing pump S_2 may be $\ll$condenser S_K. From the equation (1.5.23) follows what water vapour partial pressure p_{d1} is admissible on the intake side at a certain ratio of condenser S_K to backing pump S_2, whereby the backing pump S_2 must be dimensioned according to the amount of permanent gases that accumulates (Fig. 1.5.6, range C). If the accumulating amount of permanent gases becomes smaller during the process, this can be compensated by reducing the speed of the backing pump by means of a valve, with the result that the admissible water vapour partial pressure on the intake side can be raised. The same effect can be brought about by admitting air between the two pumps, as will be shown in the following.

4.2.2 Small condenser, large backing pump:

$$S_K \ll S_2 .$$

This case will be encountered in practice when from the outset the accumulating amount of permanent gases is large in proportion to the amount of vapour.

A transformation of equation 1.5.19 gives

$$p_{d1} = \frac{p_{d2}}{N} - p_{g1} + \frac{p_{g2}}{N},$$

i. e. p_{d1} may not be larger than $30/N$. If larger water vapour partial pressures develop during the course of the process, they can be dealt with by admitting air between the two pumps, and thus raising p_{g2} (Fig. 1.5.6, range C, or possibly an interstage condenser in range B).

1.6 Cold Traps, Baffles and Adsorption Traps

The vapour pressure of the pump fluid is one of the factors that has considerable influence on the total pressure attainable above a diffusion pump of conventional design. This vapour pressure in the vacuum vessel is not determined, as one might assume, by the temperature of the coldest surface above the pump; rather, it is usually somewhat higher. The reason for this is that pump fluid molecules, in keeping with their (thermal) distribution of velocity, break away from the margin of the vapour jet of the top diffusion stage, and stream against the general permitted direction into the vacuum vessel (backstreaming).

Backstreaming of pump fluid vapour is quantitatively checked by inserting cooled or gettering trapping surfaces at a suitable point between the diffusion pump and the vacuum vessel.

It will be readily appreciated that the colder are the surfaces with which the pump fluid vapour comes into contact, the better will be the condensation of the vapour (condensation coefficient).

1.6.1 Cold Traps for Mercury Vapour Pumps

When mercury is used as the pump fluid, a simple overlapping arrangement of the surfaces will not be sufficient. Due to the low condensation coefficient of mercury vapour molecules, provision must be made to ensure that each molecule impinges on cooled surfaces at least 8—10 times on its flight path from the diffusion pump to the vacuum vessel. Besides, the surfaces must be cooled for mercury vapour down to at least — 70 °C either with an alcohol-carbon dioxide mixture or with a two-stage refrigerating machine, or better still with liquid nitrogen down to —196 °C, if the residual vapour pressure in the vacuum vessel is to be kept sufficiently small.

There are several different forms of cold traps in use. Their efficiency is considerably raised following the adsorption of a thin layer of sublimed mercury.

It will be found advantageous to use two identical cold traps connected in series in systems for producing ultra-high vacuum.

1.6.1.1 **Cooling Probe** (Fig. 1.6.1)

This form of cold trap, which is illustrated below, is filled with refrigerant, and inserted from outside into the vacuum.

1.6.1.2 **U-tube**

See Fig. 1.6.2.

1.6.1.3 **Two Concentric Tubes** (Fig. 1.6.3)

In this type of cold trap and in the U-tube, cooling is effected by immersing the U-tube and the two concentric tubes, respectively, in a Dewar vessel filled with liquid air or liquid nitrogen.

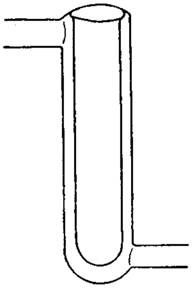

Fig. 1.6.1. Cooling probe

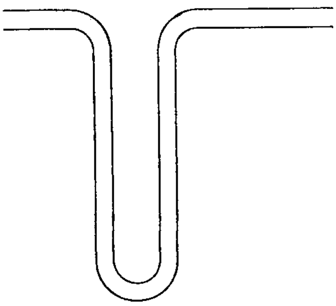

Fig. 1.6.2. U-tube cold trap

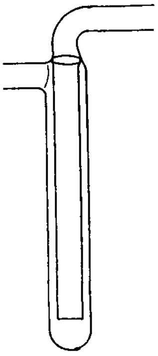

Fig. 1.6.3. Concentric tubes as cold trap

1.6.1.4 **Spherical Cold Trap** (Fig. 1.6.4)

The forms of cold traps described above all have the disadvantage of reducing the pumping speed of the mercury diffusion pump to a relatively large degree. For this reason they are chiefly used on small types of diffusion pumps, especially laboratory pumps.

To overcome this disadvantage, special forms of cold traps with maximum practicable conductivity have been designed for large mercury vapour pumps. By suitably arranging the deflecting plates, reduction of the effective pumping speed will be less than 60 per cent.

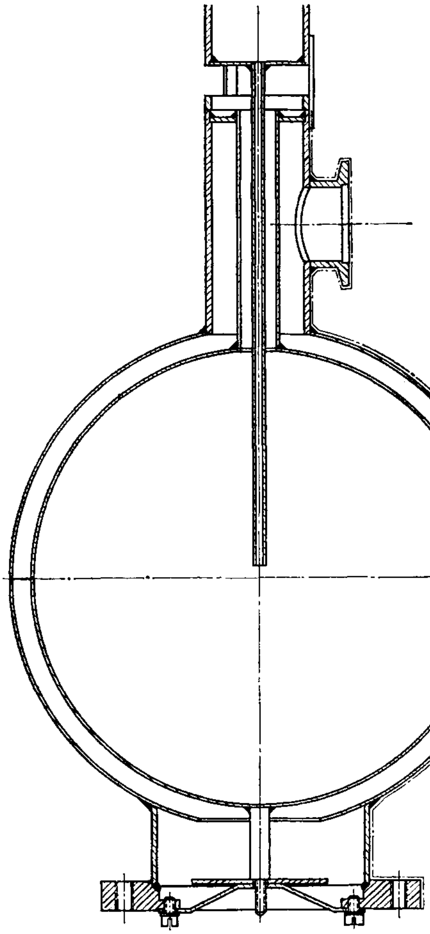

FIG. 1.6.4. Spherical cold trap.

1.6.1.5 Refilling Unit

The refrigerant capacity of the cold traps described above is relatively small (see Table 1.6.1). It is, therefore, recommended to use an automatic refilling unit for replenishing the refrigerant in the cold trap, thus allowing the trap to operate unattended for long periods. Refilling is regulated by a valve which shuts off the stock vessel (Dewar) from the outside air. When

TABLE 1.6.1. Capacity of cold traps.

Cold trap connection NW	65	150	250	Spherical cold trap (after Fig. 1.6.4)
Refrigerant volume (cm^3)	200	500	2000	4000
Cooling time with one filling (hr)	3·5	2·5	7	36

the valve is open, no refilling takes place. But when the valve is closed, the slight excess pressure in the stock vessel, brought about by the continuous evaporation of the refrigerant, forces the cooling liquid through a double-walled pipe with a well-evacuated jacket into the cold trap. A distinction is made between mechanical and electrical refilling units according to the design of the temperature sensing element which opens and closes the valve.

1.6.2 Baffles

The construction of a suitable baffle should satisfy the following requirements:

1. The baffle plates should be so arranged that each straight flight path of a molecule emanating from any point on the uppermost cross-section of the pump terminates on one of the plates (overlapping of two adjacent plates). Spacing between the different baffle plates must also be kept small in relation to the mean free path of the pump fluid molecules.

2. The plates must be assembled so that they are easy to cool (smallest heat losses by heat conduction or convection). Even temperature on all parts of the plates.

3. The entire baffle should be of the smallest possible dimensions, and should not reduce the speed of the diffusion pump by more than 40 to 50 per cent.

4. The baffle plates should be easy to clean (easy to remove).

Requirements 1 and 2 are relatively easy to satisfy. By means of a favourable assembly, heat losses by conduction can be restricted to about $0{\cdot}2\Delta t$ kcal/hr (only important for low-temperature cooling) in the case of small baffles.

Requirement 3, however, needs particular consideration. With a given overall volume of the baffle housing — in many cases the overall height and diameter of the baffle are limited by the design of the system — it is surely wrong to reduce the available cross section still more by additional plates. The ideal answer would be to keep the free passage between the cooled plates constant for each z-section through the baffle. This requirement can easily be met by assembling the baffle from elements cut out of conic section rotary bodies (Fig. 1.6.5). By this means one can, for instance, easily prove that the free passage between concentric spherical plates is constant for each z-section.

Some practical designs are illustrated in Figs. 1.6.6.—1.6.8. For large cross-sectional areas of the intake orifice of diffusion pumps, chevron baffles are especially suitable. See Fig. 1.11.9, p. 131.

The attainable ultimate pressures at different cooling temperatures of the baffles largely depend, *inter alia*, upon the characteristics of the diffusion pump being used. As the vapour pressure curves show, especially for

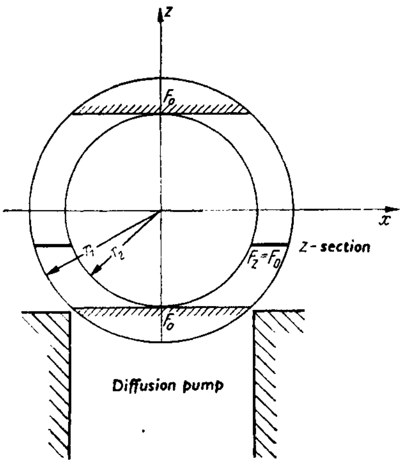

FIG. 1.6.5. Principle of baffle.

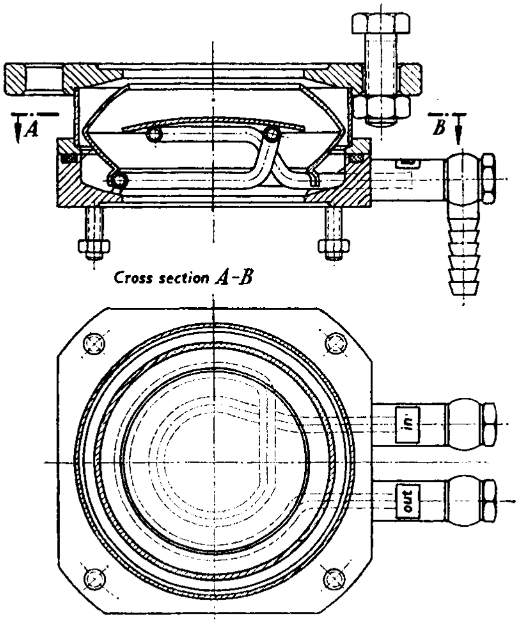

FIG. 1.6.6. Practical design of a baffle.

the lighter hydrocarbons, a condensation of light hydrocarbons is not possible at the usual cooling temperatures, or if so then only to a limited degree. On the other hand, the vapour pressure of heavier molecules (pump fluid molecules) can be considerably reduced by the cooled baffle plates. It is, therefore, necessary to use diffusion pumps in which the pump fluid is effectively degassed and fractionated so that readily volatile hydrocarbons (decomposition products) will be ejected from the pump fluid in the direction of the fore-vacuum side, and will not be able to pass through the baffle into the vacuum vessel.

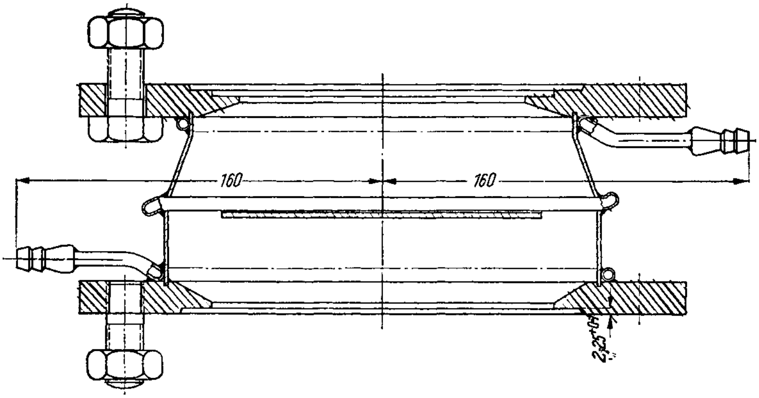

FIG. 1.6.7. Practical design of a baffle.

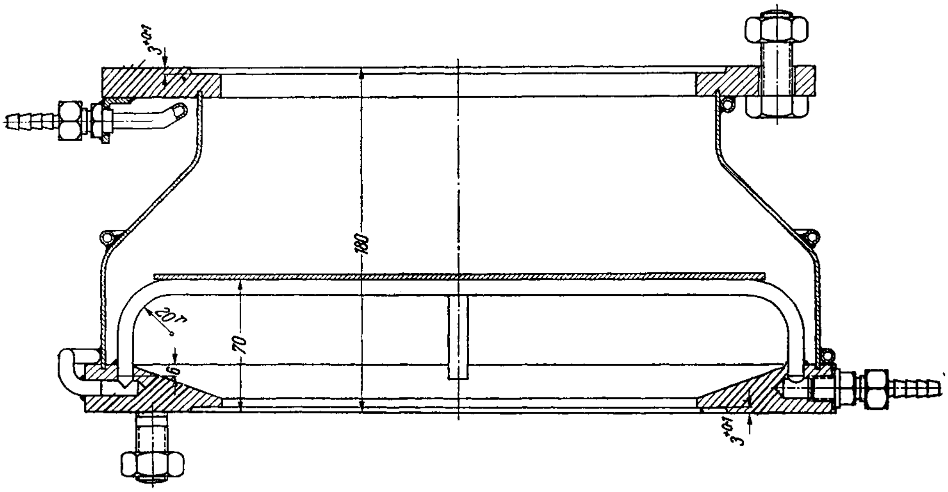

FIG. 1.6.8. Practical design of a baffle.

Such low-temperature cooling of baffles can be accomplished either by using ordinary refrigerating machines or by electrical means by utilizing the PELTIER effect. A mixture of solid carbon dioxide and alcohol also provides a suitable refrigerant for use in laboratories. When such low-temperature cooled baffles are used directly above the pump a certain difficulty arises in that oil molecules freeze on the baffle plates and so cannot flow back into the pump. For this reason, a recommended practice is to insert a second baffle or a deflecting plate (e. g. in the form of a cold cap) between the pump and the low-temperature cooled baffle, especially when a long period of operation is desired; the temperature of this second baffle must be such that the oil molecules will condense but are also allowed to return to the pump.

An indication of the attainable ultimate pressures is furnished by the following data:

Oil diffusion pump of the LEYBOLD DO series with Diffelen Ultra pump fluid and water-cooled baffle (+ 12 °C). Ultimate pressure: approximately 1×10^{-8} Torr.

Oil diffusion pump, as above, but with low-temperature cooled baffle (− 40 °C). Ultimate pressure: several times 10^{-9} Torr.

Oil diffusion pump with water-cooled baffle and with liquid nitrogen cold trap (− 196 °C). Ultimate pressure: approx. $3–4 \times 10^{-10}$ Torr.

Mercury diffusion pump with cold trap (− 70 °C). Ultimate pressure: approx. 10^{-8} Torr.

Mercury diffusion pump with liquid nitrogen cold trap (− 196 °C). Ultimate pressure: less than 5×10^{-8} Torr.

Ultimate pressures of several times 10^{-10}—10^{-11} Torr may also be attained, but this largely depends upon the construction of the cold traps and upon the working technique (e. g. alternate baking of cold traps).

1.6.3 Adsorption Traps

Besides cold traps and baffles, adsorption traps have gained in importance in recent years, especially in ultra-high vacuum technology (see chapter 1.11.3.3, p. 131).

1.6.3.1 Copper Trap

The copper trap described and used by ALPERT (see Fig. 1.6.9) consists of a smooth foil and a corrugated foil of oxygen-free copper (OFHC copper), which are rolled together and inserted in a glass tube. Such a trap operates without cooling if it has been baked out beforehand up to about 400 °C in a good vacuum. Pressures in the range of 10^{-9} to 10^{-10} Torr were attained with this copper trap in bakeable glass systems evacuated by conventional diffusion pumps. A disadvantage of the copper trap is its large flow impedance.

1.6.3.2 Zeolite Trap

Similar results are also obtainable with vapour traps which utilize ceramic materials having a high specific surface area (zeolite). This type of trap seemingly allows constructions with a rather high conductance to be developed.

A common feature of both traps is that they have to be thoroughly baked out before use, and that they become ineffective again after a certain time, i. e. the pressure on the high vacuum side rises slowly. The reason for this is that the back-streaming vapour molecules are adsorbed on the surface of the used material which shows signs of saturation after a time. Nevertheless, if back-streaming from the diffusion pump is slight, this period of time may be very long so that it need not be taken into consideration in many experiments.

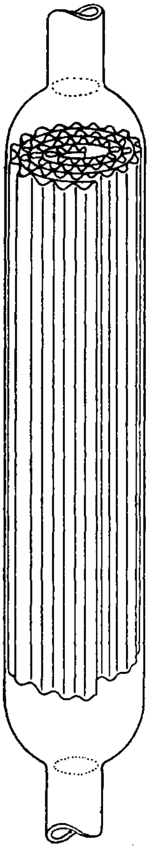

FIG. 1.6.9. Copper trap.

1.7 Getter-Ion Pumps

The term getter-ion pumps includes those devices in which gases are adsorbed on clean metal surfaces in the presence of an electrical discharge. Such an adsorption takes place much more often than is generally assumed. For instance, every clean surface that is free from adsorption layers, e. g. in a vacuum gauge head, is able to adsorb gases in fairly considerable quantities. A mono-molecular adsorption layer consists of a quantity of gas amounting to 2.8×10^{-4} Torr litre per cm^2.

The basic difference between such pumps and other vacuum pumps, viz. diffusion pumps or rotary pumps, is that the gas remains in the vacuum system and is not eventually transferred into the atmospheric air. Consequently the capacity of such pumps, their ultimate pressure or in general their behaviour depends upon the previous history, namely upon the bake-out and upon the nature and quantity of gases already pumped. It must also be appreciated that the reaction of such pumps to different gases will vary considerably; in particular, noble gases will be adsorbed only in slight quantities. In consequence, the uses of such pumps are limited from the very outset to special problems, namely to those in which it is essential to maintain a low pressure in a closed system for a long period with little outgassing.

The combination of the two differing pumping principles, namely the getter pump and the ion pump, has significance insofar as both underlying effects are in a way inseparable. An electrical gas discharge, in which ions are formed, is basically capable of pumping gases, hence one assumes that the formed ions are either bombarded into a metallic collector provided for the purpose, or that these ions, due to a chemisorption effect, are trapped within the surface atoms of such a collector. The maximum pumping speed which can be attained by means of an ionizing current is given by the equation

$$S = \frac{i^+}{e n_0 p} = 0{\cdot}191 \frac{i^+}{p} \quad \text{(litre/sec)},$$

where

i^+ = ionizing current (A),
e = charge of an electron = $1{\cdot}6 \times 10^{-19}$ A sec;
n_0 = number of particles in 1 litre at $p = 1$ Torr (air, 20 °C): $3{\cdot}27 \times 10^{19}$ Torr^{-1} litre^{-1};
p = pressure (in Torr).

In addition a part is also played by adsorption processes which are facilitated by dissociation or excitation of gas particles. Such adsorption is, however, only observed when the system is so well baked out from the start that its own outgassing is less than the pumping speed. Such clean-up, however, is usually accompanied by slight evaporation of the pumping surfaces, resulting in the formation of an active metal film. These phenomena are especially observed in ionization vacuum gauge heads having hot cathodes.

On the other hand, ions arriving at the collector, especially at high energy, are basically capable of sputtering the metal of the ion collector. The sputtered metal will settle on other surfaces where it will then act as active getter material.

This phenomenon is observed, especially at high ion energies, in the well-known PENNING vacuum gauge, and thus partly accounts for the relatively high pumping speeds that are thereby registered. When this principle is utilized for pumping (ion-sputtering pump), an active getter material, e. g. titanium, is used as the cathode to increase the pumping speed. Basically, however, it is a consequence of such sputtering that adsorbed

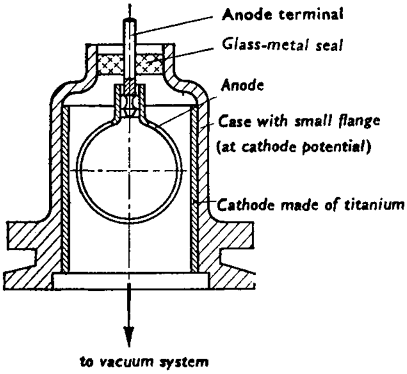

FIG. 1.7.1a. Schematic diagram of an ion-sputtering pump.

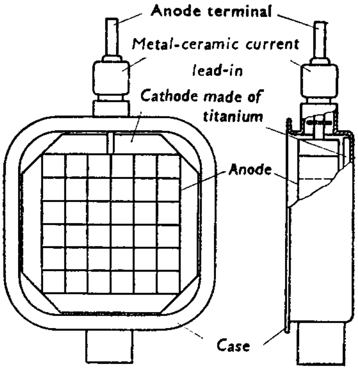

FIG. 1.7.1b. Vac-Ion pump after VARIAN.

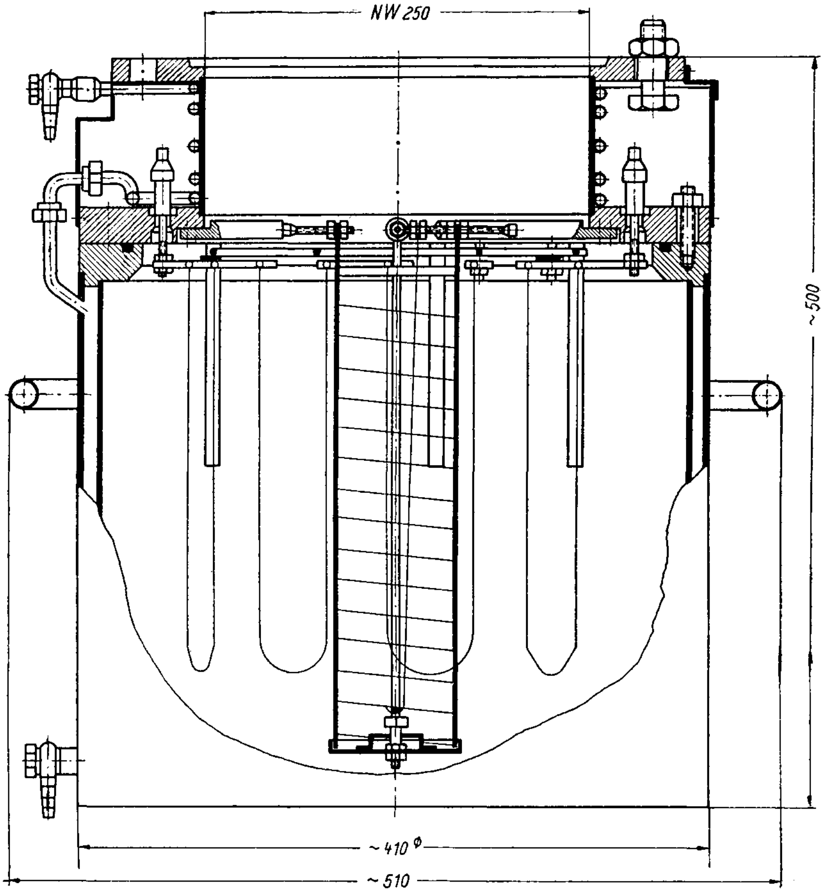

FIG. 1.7.2. Large evaporator-ion pump.

gas particles may be liberated later from the solid material by ion bombardment. This effect may assume considerable significance.

Figures 1.7.1, a and b illustrate typical ion-sputtering pumps that operate with a cold cathode on the principle of the PENNING vacuum gauge. Here the cathode is made of titanium.

Besides the unavoidable sputtering of the getter metal, another characteristic of evaporator-ion pumps is that a getter metal is continuously or intermittently evaporated in some way or other. A typical example of an evaporator-ion pump is illustrated in Fig. 1.7.2.

The getter metal is evaporated by the passage of current through the getter support wire, whereby evaporation is preferably so controlled that a certain given vapour pressure is not exceeded. A centrally arranged hot cathode, in conjunction with a grid and the evaporator elements designed as a second grid, provides for adequate ionization of the gas.

As a result of this discharge, the pumping speed and the capacity are considerably increased for the reason mentioned at the beginning. The speed of the pump illustrated in Fig. 1.7.2, which has an intake port of 250 mm dia., is between 1000 litre/sec for N_2 and 3000 litre/sec for H_2. Here, too, it is seen that, despite continuous regeneration of the getter film, gases already pumped can be liberated again. A special characteristic of such pumps is that light hydrocarbons, in particular methane, and also ethane, can be produced in the pump.

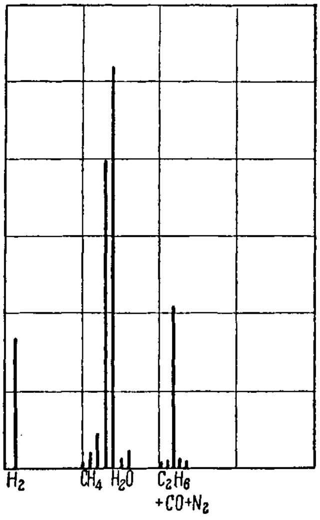

FIG. 1.7.3. Typical gas composition in an evaporator-ion pump fitted with a titanium-evaporator.

A typical gas composition in an evaporator-ion pump is shown in Fig. 1.7.3.

A further procedure of getter evaporation is based on the principle that a continuously fed wire made of getter metal, generally titanium, is continuously evaporated, either by bombarding the end of the wire with an electron beam and thereby heating it to a temperature at which the getter metal can evaporate, or by bringing the wire into contact with an oven which is kept at a temperature sufficient for adequate evaporation by electron bombardment or by direct heating.

A major problem of pumps that utilize intermittent or continuous getter evaporation is that the getter metal film must not exceed a certain thickness, otherwise the film will peel off the wall which is generally cooled. Consequently gases already adsorbed will be liberated due to radiation heating and owing to enlargement of the surface area, limiting the pumping speed and especially the ultimate pressure.

Outgassing and gettering properties of various substances are discussed in chapter 2.4, p. 236.

1.8 Vacuum Gauges

When measuring low pressures the absolute pressure is usually given in Torr (mm Hg). For conversions into other units, see Table 1.8.1. For measuring coarse vacuum, the relative pressure (below atmospheric pressure) is often expressed in %-vacuum.

The most common vacuum gauges are:

1.8.1. *For coarse vacuum:*
  1.8.1.1. Mechanical manometer
  1.8.1.2. Liquid manometer
  1.8.1.3. Swivel-type compression manometer

1.8.2. *For medium-high vacuum:*
  1.8.2.1. High frequency vacuum tester
  1.8.2.2. Alphatron
  1.8.2.3. McLEOD Compression gauge
  1.8.2.4. Thermal conductivity gauge
    1.8.2.4.1. PIRANI gauge
    1.8.2.4.2. Thermocouple gauge
    1.8.2.4.3. Semi-conductor gauge (thermistor gauge)
  1.8.2.5. Viscosity gauge

1.8.3. *For high vacuum:*
  1.8.3.1. PENNING gauge
  1.8.3.2. Ionization gauge (for ultra-high vacuum after BAYARD-ALPERT)
  1.8.3.3. KNUDSEN radiometer gauge

1.8.4. *For ultra-high vacuum*, see chapter 1.11.2.

Table 1.8.2 gives the measuring ranges of the different types of manometers. The different columns in this table also indicate whether the gauge reading depends on the nature of the gas, whether the total pressure (gases + vapours) is measured, or whether only the sum of partial pressures of all non-condensable gases present in the system is measured.

Basically there are two groups of vacuum gauges. In the first group the pressure is compensated by a mechanical force, and the magnitude of this force is indicated by the instrument. This group comprises mechanical manometers, liquid level manometers, compression manometers, and KNUDSEN-type manometers. The pressure indication of these instruments is independent of the gas composition.

The second group comprises instruments in which the pressure is measured indirectly by means of the variation of a pressure-dependent physical quantity, e. g. by thermal or electrical conductivity in thermal conductivity gauges and ionization gauges, Alphatron and PENNING gauges, respectively. In the case of viscosity manometers the pressure-dependence of the viscosity of a gas is utilized.

Some physical quantities are not only a function of pressure but depend also on the nature of the gas, so that the gauge readings of the instruments belonging to the second group are a function of the gas composition. This creates a source of uncertainty, because in the majority of cases the gas composition is not very well known. Further difficulties arise out of the fact that the forces which can be utilized for the purpose of measuring low pressures are extremely small, and that the total range for measuring low pressures extends over more than ten orders of magnitude. The relative accuracy, therefore, is very low. The following sources of error should be mentioned. In compression gauges compression may lead to the condensation of vapours present in the volume. In this case the pressure of these vapours cannot be detected. In the PENNING gauge, gas clean-up is particularly noticeable at very low pressures, so the gauge reading indicates a lower pressure than that actually prevailing in the system. In the ionization gauge certain gas molecules are cracked upon contact with the hot parts (e. g. the filament) of the gauge electrode system, leading to an increase of pressure within the gauge and, consequently, to a false pressure reading.

Finally, it should be noted that in all vacuum systems a pressure gradient exists between the vacuum vessel and the pump. The pressure reading, therefore, depends very much on the location of the gauge in relation to the system (see Chapter 1.3.1 — Flow impedance).

Bearing in mind all potential sources of error, it becomes evident that accuracy of measurement in vacuum technology cannot be claimed to be as high as in other fields of measuring techniques. In many cases, e. g. in industrial vacuum processes, it suffices to know the order of magnitude of pressure.

TABLE 1.8.1. Pressure units

$$\%\text{-Vacuum} = \frac{760 - p_{\text{Torr}}}{760} \cdot 100;$$

	Torr	dyn/cm^2	Millibar	Bar
1 Torr = 1 mm of mercury	1	1·33322 $\times 10^{3}$	1·33322	1·33322 $\times 10^{-3}$
1 dyn/cm^2 = 1 microbar (μb)	0·75006 $\times 10^{-3}$	1	10^{-3}	10^{-6}
1 Millibar (mb) = 10^3 dyn/cm^2	0·75006	10^{3}	1	10^{-3}
1 Bar (b) = 10^6 dyn/cm^2	750·06	10^{6}	10^{3}	1
1 kg/m^2 ≈ 1 mm water column	0·73556 $\times 10^{-1}$	0·980665 $\times 10^{2}$	0·980665 $\times 10^{-1}$	0·980665 $\times 10^{-4}$
1 kg/cm^2 = 1 atm	735·56	0·980665 $\times 10^{6}$	0·980665 $\times 10^{3}$	0·980665
1 atm = 760 Torr	760	1·01325 $\times 10^{6}$	1·01325 $\times 10^{3}$	1·01325
1 lb per sq.inch	5·1715 $\times 10^{1}$	0·68948 $\times 10^{5}$	0·68948 $\times 10^{2}$	0·68948 $\times 10^{-1}$
1 micron (μ) = 1 $\times 10^{-3}$ Torr	10^{-3}	1·33322	1·33322 $\times 10^{-3}$	1·33322 $\times 10^{-6}$
1 inch of mercury	25·400	0·33864 $\times 10^{5}$	0·33864 $\times 10^{2}$	0·33864 $\times 10^{-1}$

Conversion table:

	0	1	2	3	4
0	0	0·75006 $\times 10^{-3}$	0·15001 $\times 10^{-2}$	0·22502 $\times 10^{-2}$	0·30003 $\times 10^{-2}$
10	0·75006 $\times 10^{-2}$	0·82507 $\times 10^{-2}$	0·90007 $\times 10^{-2}$	0·97508 $\times 10^{-2}$	1·0501 $\times 10^{-2}$
20	1·5001 $\times 10^{-2}$	1·5751 $\times 10^{-2}$	1·6501 $\times 10^{-2}$	1·7251 $\times 10^{-2}$	1·8002 $\times 10^{-2}$
30	0·22502 $\times 10^{-1}$	0·23252 $\times 10^{-1}$	0·24002 $\times 10^{-1}$	0·24752 $\times 10^{-1}$	0·25502 $\times 10^{-1}$
40	0·30003 $\times 10^{-1}$	0·30753 $\times 10^{-1}$	0·31503 $\times 10^{-1}$	0·32253 $\times 10^{-1}$	0·33003 $\times 10^{-1}$
50	0·37503 $\times 10^{-1}$	0·38253 $\times 10^{-1}$	0·39003 $\times 10^{-1}$	0·39753 $\times 10^{-1}$	0·40503 $\times 10^{-1}$
60	0·45004 $\times 10^{-1}$	0·45754 $\times 10^{-1}$	0·46504 $\times 10^{-1}$	0·47254 $\times 10^{-1}$	0·48004 $\times 10^{-1}$
70	0·52504 $\times 10^{-1}$	0·53254 $\times 10^{-1}$	0·54005 $\times 10^{-1}$	0·54755 $\times 10^{-1}$	0·55505 $\times 10^{-1}$
80	0·60005 $\times 10^{-1}$	0·60755 $\times 10^{-1}$	0·61505 $\times 10^{-1}$	0·62255 $\times 10^{-1}$	0·63005 $\times 10^{-1}$
90	0·67506 $\times 10^{-1}$	0·68256 $\times 10^{-1}$	0·69006 $\times 10^{-1}$	0·69756 $\times 10^{-1}$	0·70506 $\times 10^{-1}$
100	0·75006 $\times 10^{-1}$	0·75756 $\times 10^{-1}$	0·76506 $\times 10^{-1}$	0·77256 $\times 10^{-1}$	0·78006 $\times 10^{-1}$

Conversion table:

	0	1	2	3	4
0	0	1·3332 $\times 10^{3}$	0·26665 $\times 10^{4}$	0·39997 $\times 10^{4}$	0·53329 $\times 10^{4}$
10	1·3332 $\times 10^{4}$	1·4666 $\times 10^{4}$	1·5999 $\times 10^{4}$	1·7332 $\times 10^{4}$	1·8665 $\times 10^{4}$
20	0·26665 $\times 10^{5}$	0·27998 $\times 10^{5}$	0·29331 $\times 10^{5}$	0·30664 $\times 10^{5}$	0·31997 $\times 10^{5}$
30	0·39997 $\times 10^{5}$	0·41330 $\times 10^{5}$	0·42663 $\times 10^{5}$	0·43996 $\times 10^{5}$	0·45330 $\times 10^{5}$
40	0·53329 $\times 10^{5}$	0·54662 $\times 10^{5}$	0·55995 $\times 10^{5}$	0·57329 $\times 10^{5}$	0·58662 $\times 10^{5}$
50	0·66661 $\times 10^{5}$	0·67994 $\times 10^{5}$	0·69328 $\times 10^{5}$	0·70661 $\times 10^{5}$	0·71994 $\times 10^{5}$
60	0·79993 $\times 10^{5}$	0·81327 $\times 10^{5}$	0·82660 $\times 10^{5}$	0·83993 $\times 10^{5}$	0·85326 $\times 10^{5}$
70	0·93326 $\times 10^{5}$	0·94659 $\times 10^{5}$	0·95992 $\times 10^{5}$	0·97325 $\times 10^{5}$	0·98659 $\times 10^{5}$
80	1·0666 $\times 10^{5}$	1·0799 $\times 10^{5}$	1·0932 $\times 10^{5}$	1·1066 $\times 10^{5}$	1·1199 $\times 10^{5}$
90	1·1999 $\times 10^{5}$	1·2132 $\times 10^{5}$	1·2266 $\times 10^{5}$	1·2399 $\times 10^{5}$	1·2532 $\times 10^{5}$
100	1·3332 $\times 10^{5}$	1·3466 $\times 10^{5}$	1·3599 $\times 10^{5}$	1·3732 $\times 10^{5}$	1·3866 $\times 10^{5}$

(see also DIN 1314)

$$p_{\mathrm{Torr}} = 760\left(1 - \frac{\%\text{-Vacuum}}{100}\right).$$

kg/m² (mm water column)	kg/cm² (atm)	atm (760 Torr)	lb per sq. inch	micron (μ)	inch of mercury
13·5951	$1{\cdot}35951 \times 10^{-3}$	$1{\cdot}31579 \times 10^{-3}$	$1{\cdot}9337 \times 10^{-2}$	10^{3}	$3{\cdot}9370 \times 10^{-2}$
$1{\cdot}01972 \times 10^{-2}$	$1{\cdot}01972 \times 10^{-6}$	$0{\cdot}98692 \times 10^{-6}$	1.4503×10^{-5}	0·75006	$2{\cdot}9530 \times 10^{-5}$
10·1972	$1{\cdot}01972 \times 10^{-3}$	$0{\cdot}98692 \times 10^{-3}$	$1{\cdot}4503 \times 10^{-2}$	$0{\cdot}75006 \times 10^{3}$	$2{\cdot}9530 \times 10^{-2}$
$1{\cdot}01972 \times 10^{4}$	1·01972	0·98692	$1{\cdot}4503 \times 10^{1}$	$0{\cdot}75006 \times 10^{6}$	$2{\cdot}9530 \times 10^{1}$
1	10^{-4}	$0{\cdot}96784 \times 10^{-4}$	$1{\cdot}4223 \times 10^{-3}$	$0{\cdot}73556 \times 10^{2}$	$2{\cdot}8959 \times 10^{-3}$
10^{4}	1	0·96784	$1{\cdot}4223 \times 10^{1}$	$0{\cdot}73556 \times 10^{6}$	$2{\cdot}8959 \times 10^{1}$
$1{\cdot}03323 \times 10^{4}$	1·03323	1	$1{\cdot}4695 \times 10^{1}$	$0{\cdot}760 \times 10^{6}$	$2{\cdot}9921 \times 10^{1}$
$0{\cdot}70307 \times 10^{3}$	$0{\cdot}70307 \times 10^{-1}$	$0{\cdot}68046 \times 10^{-1}$	1	$5{\cdot}1715 \times 10^{4}$	2·0360
$1{\cdot}35951 \times 10^{-2}$	$1{\cdot}35951 \times 10^{-6}$	$1{\cdot}31579 \times 10^{-6}$	$1{\cdot}9337 \times 10^{-5}$	1	$3{\cdot}9370 \times 10^{-5}$
$0{\cdot}34532 \times 10^{3}$	$0{\cdot}34532 \times 10^{-1}$	$0{\cdot}33421 \times 10^{-1}$	0·49115	$2{\cdot}5400 \times 10^{4}$	1

dyn/cm² in Torr

5	6	7	8	9
$0{\cdot}37503 \times 10^{-2}$	$0{\cdot}45004 \times 10^{-2}$	$0{\cdot}52504 \times 10^{-2}$	$0{\cdot}60006 \times 10^{-2}$	$0{\cdot}67506 \times 10^{-2}$
$1{\cdot}1251 \times 10^{-2}$	$1{\cdot}2001 \times 10^{-2}$	$1{\cdot}2751 \times 10^{-2}$	$1{\cdot}3501 \times 10^{-2}$	$1{\cdot}4251 \times 10^{-2}$
$1{\cdot}8752 \times 10^{-2}$	$1{\cdot}9502 \times 10^{-2}$	$0{\cdot}20252 \times 10^{-1}$	$0{\cdot}21002 \times 10^{-1}$	$0{\cdot}21752 \times 10^{-1}$
$0{\cdot}26252 \times 10^{-1}$	$0{\cdot}27002 \times 10^{-1}$	$0{\cdot}27752 \times 10^{-1}$	$0{\cdot}28502 \times 10^{-1}$	$0{\cdot}29252 \times 10^{-1}$
$0{\cdot}33753 \times 10^{-1}$	$0{\cdot}34503 \times 10^{-1}$	$0{\cdot}35253 \times 10^{-1}$	$0{\cdot}36003 \times 10^{-1}$	$0{\cdot}36753 \times 10^{-1}$
$0{\cdot}41253 \times 10^{-1}$	$0{\cdot}42004 \times 10^{-1}$	$0{\cdot}42754 \times 10^{-1}$	$0{\cdot}43504 \times 10^{-1}$	$0{\cdot}44254 \times 10^{-1}$
$0{\cdot}48754 \times 10^{-1}$	$0{\cdot}49504 \times 10^{-1}$	$0{\cdot}50254 \times 10^{-1}$	$0{\cdot}51004 \times 10^{-1}$	$0{\cdot}51754 \times 10^{-1}$
$0{\cdot}56255 \times 10^{-1}$	$0{\cdot}57005 \times 10^{-1}$	$0{\cdot}57755 \times 10^{-1}$	$0{\cdot}58505 \times 10^{-1}$	$0{\cdot}59255 \times 10^{-1}$
$0{\cdot}63755 \times 10^{-1}$	$0{\cdot}64505 \times 10^{-1}$	$0{\cdot}65255 \times 10^{-1}$	$0{\cdot}66006 \times 10^{-1}$	$0{\cdot}66756 \times 10^{-1}$
$0{\cdot}71256 \times 10^{-1}$	$0{\cdot}72006 \times 10^{-1}$	$0{\cdot}72756 \times 10^{-1}$	$0{\cdot}73506 \times 10^{-1}$	$0{\cdot}74256 \times 10^{-1}$
$0{\cdot}78757 \times 10^{-1}$	$0{\cdot}79507 \times 10^{-1}$	$0{\cdot}80257 \times 10^{-1}$	$0{\cdot}81007 \times 10^{-1}$	$0{\cdot}81757 \times 10^{-1}$

Torr in dyn/cm²

5	6	7	8	9
$0{\cdot}66661 \times 10^{4}$	$0{\cdot}79993 \times 10^{4}$	$0{\cdot}93326 \times 10^{4}$	$1{\cdot}0666 \times 10^{4}$	$1{\cdot}1999 \times 10^{4}$
$1{\cdot}9998 \times 10^{4}$	$0{\cdot}21332 \times 10^{5}$	$0{\cdot}22665 \times 10^{5}$	$0{\cdot}23998 \times 10^{5}$	$0{\cdot}25331 \times 10^{5}$
$0{\cdot}33331 \times 10^{5}$	$0{\cdot}34664 \times 10^{5}$	$0{\cdot}35997 \times 10^{5}$	$0{\cdot}37330 \times 10^{5}$	$0{\cdot}38664 \times 10^{5}$
$0{\cdot}46663 \times 10^{5}$	$0{\cdot}47996 \times 10^{5}$	$0{\cdot}49329 \times 10^{5}$	$0{\cdot}50663 \times 10^{5}$	$0{\cdot}51996 \times 10^{5}$
$0{\cdot}59995 \times 10^{5}$	$0{\cdot}61328 \times 10^{5}$	$0{\cdot}62662 \times 10^{5}$	$0{\cdot}63995 \times 10^{5}$	$0{\cdot}65328 \times 10^{5}$
$0{\cdot}73327 \times 10^{5}$	$0{\cdot}74661 \times 10^{5}$	$0{\cdot}75994 \times 10^{5}$	$0{\cdot}77327 \times 10^{5}$	$0{\cdot}78660 \times 10^{5}$
$0{\cdot}86660 \times 10^{5}$	$0{\cdot}87993 \times 10^{5}$	$0{\cdot}89326 \times 10^{5}$	$0{\cdot}90659 \times 10^{5}$	$0{\cdot}91993 \times 10^{5}$
$0{\cdot}99992 \times 10^{5}$	$1{\cdot}0133 \times 10^{5}$	$1{\cdot}0266 \times 10^{5}$	$1{\cdot}0399 \times 10^{5}$	$1{\cdot}0533 \times 10^{5}$
$1{\cdot}1332 \times 10^{5}$	$1{\cdot}1466 \times 10^{5}$	$1{\cdot}1599 \times 10^{5}$	$1{\cdot}1732 \times 10^{5}$	$1{\cdot}1866 \times 10^{5}$
$1{\cdot}2666 \times 10^{5}$	$1{\cdot}2799 \times 10^{5}$	$1{\cdot}2932 \times 10^{5}$	$1{\cdot}3066 \times 10^{5}$	$1{\cdot}3199 \times 10^{5}$
$1{\cdot}3999 \times 10^{5}$	$1{\cdot}4132 \times 10^{5}$	$1{\cdot}4266 \times 10^{5}$	$1{\cdot}4399 \times 10^{5}$	$1{\cdot}4532 \times 10^{5}$

TABLE 1.8.2. Measuring ranges of various types of vacuum gauges

Instrument	Range (Torr)	Reading	dependent or independent on nature of gas
BOURDON tube	720 – 60	Total pressure	independent
Liquid manometer	200 – 1	Total pressure	independent
Swivel-type compression manometer	60 – 0.1 35 – 0,05	Partial pressure	independent
High frequency vacuum tester	10 – 10^{-3}	Total pressure	dependent
Alphatron L (logarithmic scale)	10 – 10^{-3}	Total pressure	dependent
McLEOD compression gauge	10 – 10^{-3} 1 – 10^{-5}	Partial pressure	independent
Thermal conductivity gauge	10 – 10^{-3}	Total pressure	dependent
Alphatron	1000 – 10^{-4}	Total pressure	dependent
Viscosity gauge	10^{-2} – 10^{-5}	Total pressure	dependent
PENNING gauge	10^{-2} – 10^{-6}	Total pressure	dependent
Ionization gauge	10^{-2} – 10^{-7}	Total pressure	dependent
KNUDSEN radiometer gauge	10^{-3} – 10^{-6}	Total pressure	independent
BAYARD-ALPERT ionization gauge	10^{-4} – 10^{-10}	Total pressure	dependent
Magnetron gauge after REDHEAD (for ultra-high vacuum)	10^{-4} – 10^{-12}	Total pressure	dependent
	10^3 10^2 10 1 10^{-1} 10^{-2} 10^{-3} 10^{-4} 10^{-5} 10^{-6} 10^{-7} 10^{-8} 10^{-9} 10^{-10} 10^{-11} 10^{-12}		
	coarse vacuum medium-high vacuum high vacuum ultra-high vacuum		

1.8.1 Gauges for Coarse Vacuum

1.8.1.1 Mechanical Manometer

Design principle: BOURDON tubes or diaphragm manometers.

Range: Atmospheric pressure to 1 Torr, under special technical precautions down to 10^{-2} Torr; when used as a differential pressure gauge down to 10^{-5} Torr.

Measuring principle: Direct pressure measurement.

Measured quantity: Elastic bending of tube or elastic deformation of part of the gauge wall.

Reading: Total pressure.

Advantages: Direct reading, independent of nature of gas.

Disadvantages: Limited accuracy, elastic after-effects, dependent on temperature.

1.8.1.2 Liquid Manometer

Design feature: U-tube manometer, liquid balance manometer.

Range: Atmospheric pressure down to 1 Torr, under special technical precautions down to 10^{-2} Torr.

Measuring principle: Pressure measurement in communicating tubes.

Measured quantity: Level of liquid.

Reading: Total pressure.

Advantages: Direct reading, independent of nature of gas.

Disadvantages: Limited accuracy.

1.8.1.3 Swivel-type Compression Manometer

Design feature: Vacuscope after GAEDE, compression manometer after MOSER, and after VON REDEN.

Pressure measurement is effected by compressing into a small volume a defined amount of gas, which, prior to compression, is enclosed in a large volume. The compression produces a high absolute pressure which can easily be measured. From the pressure reading, assuming the geometry of the device to be known, the true pressure can be calculated. Compression is effected by turning the device on a swivel. The so-called Vacuscope has, besides the compression device, a U-tube manometer. In analogy to the MCLEOD gauge, allowance for possible condensation of vapours, during the operation of the swivel-type compression gauge, has to be made when gauge readings are interpreted.

Measuring range: 80–0·1, and $35\text{–}5 \times 10^{-2}$ Torr.

Measuring principle: Pressure measurement after compression of a well defined amount of gas.

Measured quantity: Level of mercury.

Reading: The sum of the partial pressures of permanent gases.

Advantages: Simple construction and simple operation.

Disadvantages: Condensation of vapours, low accuracy, no continuous pressure indication.

1.8.2 Gauges for Medium-high Vacuum

1.8.2.1 High Frequency (Tesla-coil) Vacuum Tester

Pattern and colour of an electric discharge can be used as a rough indication of pressure. This can be effected in two ways: 1. A small 2-electrode discharge tube is incorporated into the vacuum system and connected to a small inductor. 2. An electrodeless discharge is produced in a glass tube which is part of the vacuum system, by approaching a high frequency Tesla-coil vacuum tester.

Measuring range: 10–10^{-3} Torr total pressure.
Measuring principle: Electrical gas discharge.
Physical quantity: Pattern and colour of the discharge.
Advantages: Simple to operate, continuous indication.
Disadvantages: The Tesla-tester allows only a very rough qualitative pressure indication.

For discharge in air:

Pressure range	*Discharge phenomena*
10–10^{-1} Torr	red or purple glow in the vacuum system, expanding to the full cross section of the tube as the pressure decreases;
10^{-1}–10^{-2} Torr	discharge continues, in addition green fluorescence on the inner glass wall in the vicinity of the high-frequency electrode outside;
10^{-2}–10^{-3} Torr	red glow reduced, at about 10^{-3} Torr only a green fluorescence on the inner wall is visible;
below 10^{-3} Torr	no visible glow.

The colour of the discharge depends on the nature of the gas.

Colour of glow discharge for various gases

Air:	red to purple.
Ammonia:	blue.
Argon:	blue.
Helium:	purple–red to yellow–pink.
Hydrogen:	blue.
Mercury vapour:	greenish blue.
Neon:	red.
Nitrogen:	red–purple.
Oxygen:	lemon-yellow with reddish core.
Water vapour and hydrocarbons:	white–blue, almost white, faint.

1.8.2.2 Alphatron

A radioactive source produces a very constant radiation of α-particles which, in turn, ionizes the gas in an ionization chamber. The corresponding ion current depends on the gas pressure, and is a linear function of pressure over a wide pressure range.

Measuring range: 1000–10^{-4} Torr, 7 ranges.

Principle: Ionization by α-particles.

Measured quantity: Electric current.

Reading: Total pressure.

Advantages: Direct reading (after calibration), remote pressure reading possible. Very consistent calibration curve (in contrast to e.g. thermal conductivity gauges).

Disadvantages: Amplifier required. Reading depends on nature of gas.

1.8.2.3 McLeod Compression Gauge

Pressure is measured by compressing a known volume of gas into a smaller volume by raising a mercury column. From the increased pressure and the known geometry of the gauge, the original pressure can be found.

Measuring range: 10–10^{-5} Torr (see Figs. 1.8.1. and 1.8.2.) depending on gauge dimensions.

Measurin gprinciple: Pressure measurements in communicating tubes after compression.

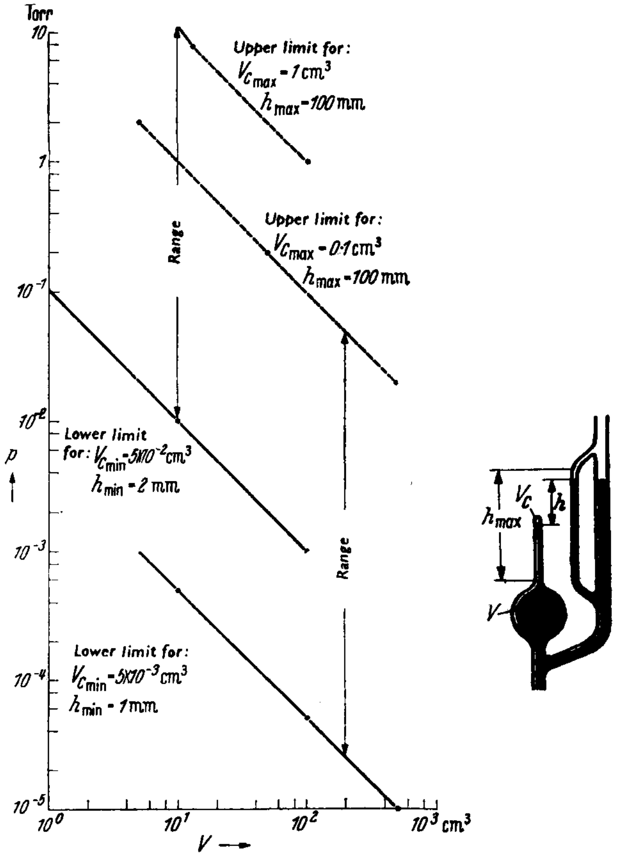

Fig. 1.8.1. Measuring ranges of McLeod gauge with linear scale.

Measured quantity: Level of mercury meniscus.

Reading: Sum of partial pressures of non-condensable gases.

Advantages: Calibration curve can be calculated from dimensions of gauge.

Disadvantages: No continuous pressure indication; condensation of vapour in the gauge prevents measurement of total pressure.

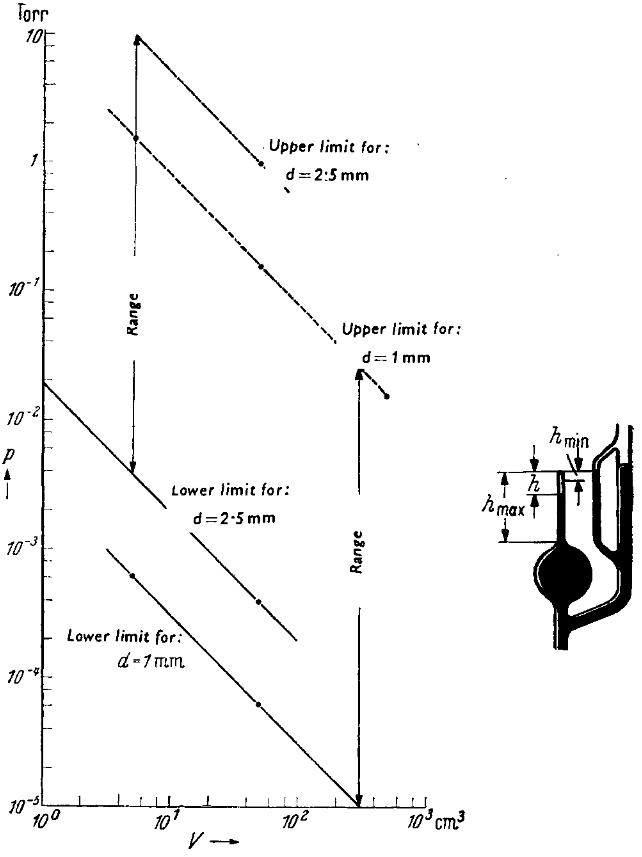

FIG. 1.8.2. Measuring ranges of McLEOD gauge with square-law scale.

Condensable vapours, in particular water vapour, cannot be avoided in chemical work. In such cases the McLEOD gauge should not be used for measurement, but as a reference for the calibration of other vacuum gauges the pressure characteristic of which cannot be calculated from the gauge dimensions.

1.8.2.4 Thermal Conductivity Gauges

In these gauges the dependency of heat conduction of gases on gas pressure is utilized for pressure measurement. At high pressures the heat conductance is independent of pressure. At a few Torr, however, the heat conductance becomes a function of pressure, i. e. when the mean free path of the gas molecules becomes comparable with the dimensions of the heat conducting parts. By making use of convection phenomena, the measuring range can be extended up to 760 Torr. The following types of thermal conductivity gauges are noteworthy:

1.8.2.4.1 PIRANI Gauge

A resistance wire extended in the gauge head forms a branch of a WHEATSTONE bridge, and can be heated by the passage of current. If the pressure in the gauge head alters, the heat transfer will alter accordingly, as will the temperature of the wire and, hence, its ohmic resistance, too. This leads to an alteration of the reading of the instrument in the WHEATSTONE bridge. Another way to operate the gauge is to keep the temperature of the wire constant (by means of appropriate electrical circuitry). In this case the required heating power becomes dependent on the pressure, and hence, is a measure of the pressure. The measuring range is extended to higher pressures.

Measuring range: 10^{-1} to 10^{-3} Torr.
Measuring principle: Thermal conductivity of gases depends on pressure.
Measured quantity: Electrical resistance.
Reading: Total pressure.
Advantages: Remote reading of pressure and continuous pressure indication.
Disadvantages: The calibration curve alters during usage of the instrument, if metal surfaces in the gauge become contaminated and heat radiation alters. Reading depends on nature of gas.

1.8.2.4.2 Thermocouple Gauge

One or more thermocouples are heated with constant input wattage; the pressure-dependent heat transfer in the gauge head alters the temperature of the thermocouples and, hence, their EMF.

Measuring range: Several Torr to 10^{-3} Torr
Measuring principle: Heat conductivity of gases.
Measured quantity: Thermoelectric EMF.
Reading: Total pressure.
Advantages: Large measuring range, remote pressure reading, continuous pressure indication.
Disadvantages: Variation of pressure reading caused by contamination of the thermocouple surface. Artificial surface blackening can reduce the influence of contaminations. Blackening, however, reduces the sensitivity of the gauge. Pressure reading depends on nature of gas.

1.8.2.4.3 Semi-conductor Gauge (Thermistor Gauge)

These gauges are similar to the PIRANI gauge, but instead of a resistance wire a semiconductor is used as the temperature sensing element; the advantage is that the temperature coefficient of the electrical resistance of a semiconductor is much larger than of a metal.

Measuring range: About 50–10^{-3} Torr at constant temperature, about 760–10^{-3} Torr at constant temperature and with forced convection.

Measuring principle: Pressure-dependence of the heat conductivity of gases.

Measured quantity: Ohmic resistance.

Reading: Total pressure.

Advantages: Continuous pressure reading; the influence of surface contamination of the semiconductor element upon gauge calibration is much less than in the PIRANI gauge.

Disadvantages: The semiconductor elements have a greater mass than resistance wires. Thermal delay is, therefore, greater. If the temperature is kept constant, the response time can be reduced to fractions of a second. Reading depends on nature of the gas.

1.8.2.5 Viscosity Gauge

1. The vibrating quartz fibre represents a simple form of this gauge. The damping of the oscillations of the fibre depends on the viscosity of the gas and, hence, on the gas pressure. This design, however, has not achieved technical significance since a gauge built on these lines is very sensitive to vibrations, and it is difficult to keep the oscillations of the quartz fibre free from superimposed oscillations.

Measuring range: Approx. 10^{-2}–10^{-5} Torr, depending on the dimensions of the oscillating parts of the gauge system.

Measuring principle: Pressure-dependence of gas viscosity.

Measured quantity: Damping of oscillation of quartz fibre.

Reading: Total pressure.

Advantages: Gauge system can be made of non-corrosive materials, e.g. glass and quartz. The gauge head contains no hot metal parts, which might otherwise cause cracking of gas molecules, and no cold metal parts that lead to gas clean-up.

Disadvantages: Sensitive to vibrations, superimposed oscillations, no continuous pressure reading, complicated measuring procedure. Reading depends on nature of gas.

2. A different design of viscosity gauge utilizes the influence of gas viscosity on an oscillating ribbon for pressure measurement. The amplitude is kept constant by variation of electric current which is a measure of the pressure prevailing in the gauge head.

Measuring range: 760–10^{-3} Torr.

Measuring principle: Pressure-dependence of gas viscosity.

Measured quantity: Current or amplitude of oscillation.

Reading: Total pressure.

Advantages: Contains neither hot nor cold metal parts which might otherwise cause cracking of gas molecules or gas clean-up, respectively.

Disadvantages: Dirt trap needed against ferro-magnetic particles, need for vibration-free suspension, screening against outer magnetic fields. Reading depends on nature of gas.

1.8.3 High Vacuum Gauges

1.8.3.1 PENNING Gauge (PHILIPS Vacuum Gauge)

If an auxiliary magnetic field is used, a self-sustained gas discharge can be maintained even at pressures below 10^{-3} Torr. The discharge current is a measure of the gas pressure in the gauge head.

Measuring range: 10^{-2} to 10^{-6} Torr.
Measuring principle: Gas ionization.
Measured quantity: Electric current.
Reading: Total pressure.
Advantages: Sturdy system (no hot filament which might burn out during inrush of gas).
Disadvantages: Low sensitivity, measurement hampered by gas clean-up; reading depends on nature of gas.

In spite of the relative inaccuracy of the gauge, so that to all intents and purposes only the order of magnitude of pressure is indicated, the gauge is frequently used in industrial applications because of its insensitivity to inrush of gas.

1.8.3.2 Ionization Gauge

For accurate measurement of pressure in the high vacuum range, a simple triode can be used. The operating principle is as follows: Electrons emitted from a hot filament collide with gas molecules while travelling to a positively charged anode, and in consequence produce positive ions. These ions are collected on a negatively charged grid. The ratio of ion-current i^+ to electron current i^- is a measure of the number of collisions which the electrons undergo during their passage to the anode, and this number is proportional to the gas pressure.

Measuring range: 10^{-2} to 10^{-7} Torr.
Measuring principle: Gas ionization by electron impact.
Measured quantity: Electric current.
Reading: Total pressure.
Advantages: Remote and continuous pressure indication.
Disadvantages: If tungsten filaments are used as an electron source, the filament is likely to burn out during a gas inrush. This can be avoided by using Pt-cathodes coated with ThO_2. The reading depends on the nature of the gas.

Measurement of very high vacuum by means of the BAYARD-ALPERT *gauge*

In the arrangement described above the lower limit of the measuring range is 5×10^{-8} Torr. This limitation is caused by the following mechanism: The electrons which arrive with a certain energy at the anode produce soft X-rays there. A fraction of these X-rays hit the negatively charged ion-collector producing photo-electrons which cannot be distinguished as a current in the measuring circuit from the ion current. This error is avoided in the ionization gauge designed by BAYARD-ALPERT. In their design, the ion collector is only a very thin wire which is not hit by the great majority of all X-rays produced at the anode. Consequently, the lower limit of the BAYARD-ALPERT gauge is very much reduced. Its measuring range is from 10^{-2} to about 10^{-11} Torr.

1.8.3.3 KNUDSEN Radiometer Gauge

A movable vane is positioned between a fixed heated plate and a fixed cold plate. The gas molecules emanating from the heated plate transfer a bigger momentum to the movable vane than the molecules emanating from the cold plate. The movement of the vane is compensated by an elastic force, which is a measure of the difference in momentum and, hence, of the pressure.

Measuring range: According to gauge dimensions about 10^{-3} to 10^{-6} Torr.
Measuring principle: Thermal molecular pressure.
Measured quantity: Deflection of a galvanometer mirror.
Reading: Total pressure.
Advantages: Pressure indication is not dependent on nature of gas.
Disadvantages: Very sensitive to vibrations.

1.9 Partial Pressure Gauges

In many vacuum processes it is essential to obtain not only a knowledge of the total pressure but also of the gas composition. This applies to production line processes as well as to research studies. Partial pressure gauges must satisfy a number of requirements which usually cannot be met by a single instrument. It is, therefore, understandable that various partial pressure measuring methods have been discussed and actually are in use. One of the main features characterizing a partial pressure gauge is that — in contrast to the many designs of well-known mass spectrometers — partial pressure gauges form an integral part of the vacuum system. Moreover the main task of these gauges is to analyse the composition of the gas mixture prevailing in the vacuum system rather than to analyse gases introduced into the system from an outer source. Partial pressure gauges must be simple in design and bakeable, and should be sealed to the vacuum system with as short a connection as possible. These requirements are met by the four partial pressure gauges described below, and also by small cycloidal mass spectrometers.

All partial pressure gauges can of course also be used as leak detectors. Hereby the peak of mass 32 (oxygen) usually serves as the actual leak indicator. In fact a partial pressure gauge, when adjusted to a fixed mass, shows features similar to a leak detector operating on the mass spectrometer principle. Generally the sensitivity obtainable with a partial pressure gauge is less than the sensitivity of actual leak detectors. But partial pressure gauges show no preference for one particular search gas.

The following partial pressure gauges seem to comply with the basic requirements:

1. Omegatron
2. Farvitron
3. Topatron
4. Mass filter after PAUL and STEINWEDEL

These four gauges differ in their physical performance and their application potentialities in vacuum techniques, but are complementary to a certain degree.

1.9.1 Omegatron

Measuring range: 10^{-5}–10^{-11} Torr

Ion sorting principle: Crossed magnetic and electrical high frequency field (similar to cyclotron).

Measured quantity: Ion current.

Response time: Depends on the time constant of the amplifier.

Mass range: 1–200, resolving power depends on mass.

Resolving power: $\frac{M}{\Delta M} = \frac{C}{M}$; $\Delta M = \text{const}\, M^2$.

The constant C depends on the magnetic field strength and the amplitude of the high frequency voltage. It is generally possible to separate completely up to the masses 43 and 44.

Sensitivity: (at 1 μA emission current) 10^{-14} amp/1×10^{-9} Torr.

Emission current: 1–20 μA.

Advantages: The pressure is very accurately proportional to the reading. The resolving power is high, and can be adjusted. High transmission ratio*.

Disadvantages: Because of the high magnetic field strength (3000–4000 gauss) required to operate the Omegatron, a relatively heavy magnet is needed. This limits the possible connections of the Omegatron gauge head.

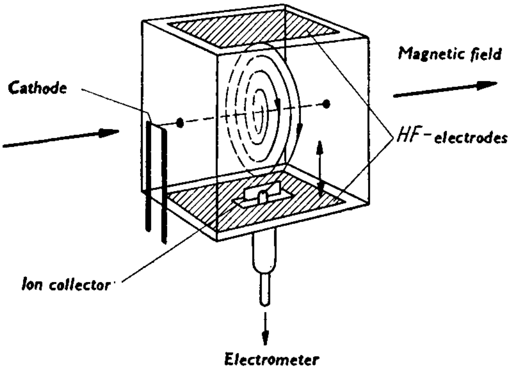

FIG. 1.9.1. Schematic diagram of the Omegatron.

The basic principle of the Omegatron is shown in Fig. 1.9.1. The gas is ionized by an electron beam which originates from a cathode. The divergence of the electron beam is limited by a number of apertures. The direction of the beam coincides with the direction of the magnetic field, which has a focusing action. Under the influence of the constant magnetic field B and the high frequency field perpendicular to B the ions travel along a circular path. But only those ions for which the resonance condition

$$2\pi\nu = \frac{e}{M} B \tag{1.9.1}$$

(ν = high frequency) is satisfied, remain in phase with the high frequency field, i. e. these ions accumulate energy and move on a spiral path, finally

---

* Transmission ratio is the yield of ions, i.e. the ratio of ions collected at the ion collector after separation to the total number of ions produced.

arriving at the ion collector plate. The resultant ion current is amplified and recorded. In order to obtain the complete spectrum, the ion current is recorded whilst the frequency is continuously varied. Figure 1.9.2 shows the mass spectrum of methane, masses between 12 and 16.

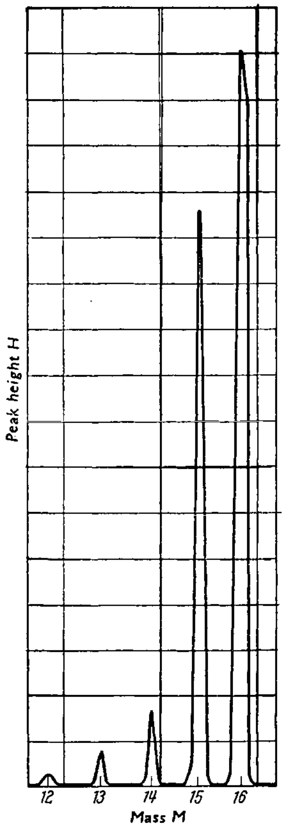

FIG. 1.9.2. Mass spectrum of methane.

1.9.2 Farvitron

Measuring range: 10^{-4} to 10^{-9} Torr

Ion separating principle: Time of passage of ions in a DC-field (harmonic oscillator).

Measured quantity: High frequency signal, representing the whole partial pressure spectrum made visible on an oscilloscope screen.

Response time: 50 c/s.

Mass range: 2–250.

Resolving power: $\frac{M}{\Delta M} = 2\sqrt{M}$; $\Delta M = \frac{1}{2}\sqrt{M}$, i. e. the peak width for mass 16 is two mass units.

Sensitivity: About 5 cm peak height on the screen per 1×10^{-7} Torr.

Emission: 1–2 mA.

Advantages: Direct reading, also of fast-changing processes; small, handy gauge head which needs no adjustment.

Disadvantages: Harmonic peaks. The measuring principle does not allow for quantitative determination of gas composition or for measuring of total pressure. Gas components present in a small proportion can only be detected provided their share of the total pressure is at least 3 per cent.

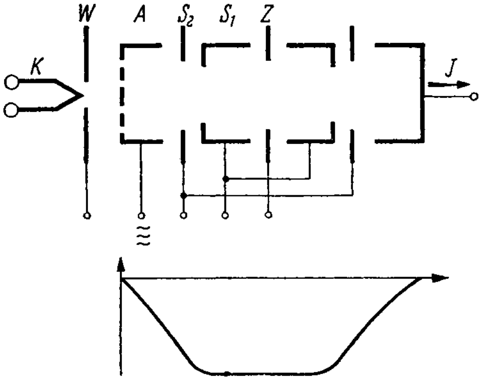

FIG. 1.9.3. Electrode system and potential in the Farvitron gauge.

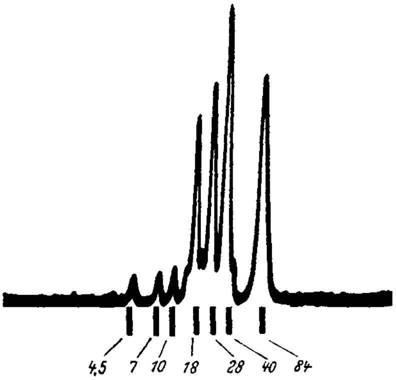

FIG. 1.9.4. Oscilloscope picture of a Farvitron spectrum, showing masses 18, 28, 40 and 84 (see text); the peaks corresponding to mass = 4·5, 7 and 10 are harmonics to mass = 18, 28 and 40, respectively.

The Farvitron is an ion-resonance spectrometer, and works as follows: In a suitable electric field (see Fig. 1.9.3) the ions oscillate, whereby their oscillating frequency is governed by e/M. The frequency is independent of the amplitude. As also shown in Fig. 1.9.3 (upper part), the ions are produced by electrons, which originate from the cathode K and which are accelerated towards the grid-like anode A. The ions thus produced start their path under the influence of the electric field along the logitudinal axis of the electrode system. Around this axis a tubular-shaped ion cloud builds up, in which ions of various frequencies and phase angles relative to the field exist. If, now, by means of the electrode A, the electron current is modulated (frequency ν) and, hence, also the production of ions, then only a certain group of ions will oscillate in phase.

This group of ions develops on the signal electrode J an a. c.-voltage of high frequency, the amplitude of this voltage being proportional to the number of ions oscillating in phase. The high frequency signal thus produced is amplified, demodulated and recorded by means of a suitable instrument. In order to record continuously the whole spectrum, the modulating frequency of the electron current is wobbled at a rate of 50 c/s over the total frequency range, i. e. mass range. The low frequency signal obtained after the demodulating stage, which represents the mass spectrum, is reproduced on the oscilloscope screen.

Figure 1.9.4 shows a spectrum with the masses 18 (H_2O), 28 (N_2), 40 (A), 84 (Kr) present, and some harmonics.

1.9.3 Topatron

Pressure range: 1×10^{-3} to 1×10^{-7} Torr.

Ion separating mode: High frequency time-of-flight principle.

Measured quantity: Ion current.

Speed of response: Given by the time constant of the amplifier.

Mass range: 2–100.

Resolving power: $\frac{M}{\Delta M} = \text{const}$; $\Delta M = \text{const} \times M$; the constant depends on the setting of sensitivity and is between 10 and 30.

Sensitivity: 1×10^{-9} amp/1×10^{-4} Torr.

Emission current: 10 mA.

Advantages: Instrument reading proportional to pressure. Total pressure indicated simultaneously. Max. permissible total pressure is high; no adjustments required.

Disadvantages: Low transmission, high constancy of electrical data necessary.

Figure 1.9.5 shows a schematic diagram of the Topatron gauge head. The gas mixture becomes ionized in the positively charged ionization chamber A by means of an electron beam which is emitted from the cathode K and accelerated through A. The positive ions thus formed are extracted from the ion source by means of the negatively charged grid G_1. The following grids which make up the ion separator section of the gauge head, are negatively charged in relation to the cathode. The actual ion separation is effected by a high frequency field between the grids G_2 to G_{12}. Ions which are in the correct phase and which have the correct value of e/M according to the prevailing high frequency, are able to pick up energy between two grids, resulting in acceleration of these particular ions. This process is repeated between the next grids in stages. On the end of the grid system a further grid G_{13} is situated, which is positively charged. Only those resonant ions which have gained sufficient energy, are able to penetrate the analyser grid G_{13}. These ions are collected on T causing an ion current in the external circuit.

A negatively charged grid G_{14} is situated between the decelerating grid G_{13} and the collecting electrode T. Its function is to screen the electrode T from secondary electrons, which can be produced by the impact of fast ions on the last grid of the separating system. A typical spectrum as obtained with the HF time-of-flight spectrometer is shown in Fig. 1.9.6.

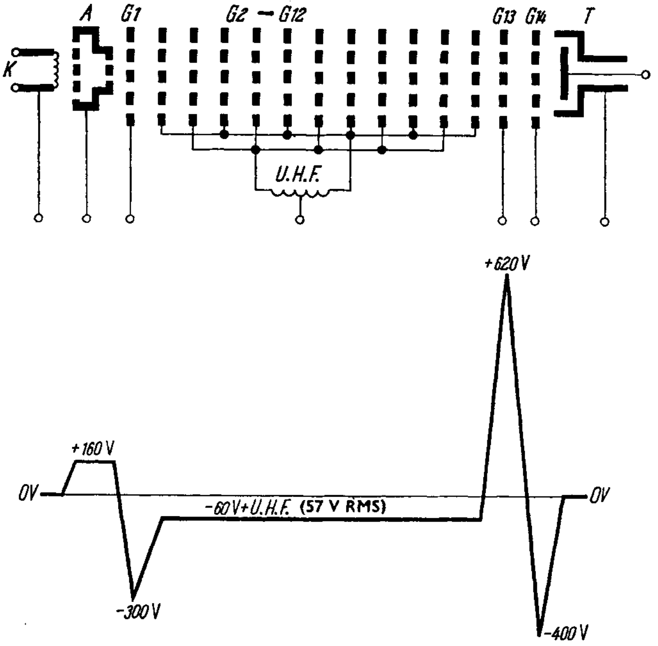

FIG. 1.9.5. Electrode system and axial potential distribution of Topatron.

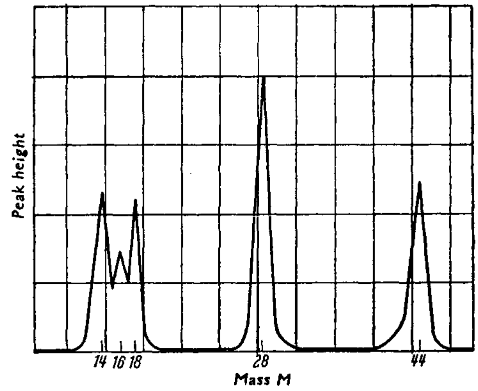

FIG. 1.9.6. Mass spectrum showing H_2O, CO, and CO_2.

1.9.4 Mass Filter after Paul and Steinwedel

Pressure range: 10^{-3} to 10^{-8} Torr.

Ion separating principle: Amplitude limitation of resonant ions in a 4-pole electrical field.

Measured quantity: Ion current.

Speed of response: Depending on time constant of amplifier

Mass range: 2–100.

Resolving power: $\frac{M}{\Delta M} = \frac{\text{const}}{M}$; $\Delta M = \text{const} = 1$.

Sensitivity: 1×10^{-9} amp/1×10^{-4} Torr.

Transmission: 0·2.

Advantages: Large mass range; no adjustments.

Disadvantages: Extremely high consistency of the h.f. voltage in relation to the d.c. voltage is essential.

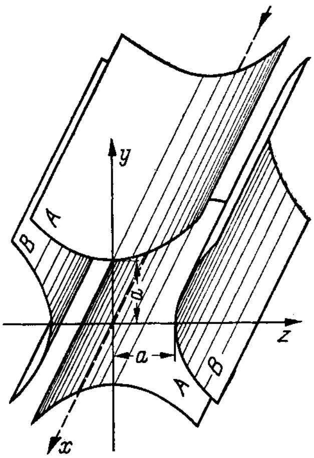

Fig. 1.9.7. Schematic diagram of the 4-pole field.

Figure 1.9.7 shows a schematic diagram of the 4-pole field, whereby a d.c. voltage is applied between the poles *AA* and *BB*, and with a superimposed h.f. voltage. The ions, which enter the system in the direction of the arrow pointing in the *x*-direction, are produced by an ion source positioned beyond the 4-pole system. The ions oscillate during their passage through the system, and the separation of ions is obtained by the following means: The stable or resonant ions have a limited amplitude, whilst all other ions show increasing amplitudes causing them to impinge on the surrounding electrodes. The ion collector picking up the resonant ions, is situated in the direction of the *x*-axis. For a given set of electrical values the stability of the ion path is determined only by the value of e/M of the ions.

1.10 Leaks and Leak Detection

It has become customary to indicate the leak (leak rate) of a vacuum system quantitatively in Torr × litre/sec, corresponding to the amount of atmospheric air entering the system, if normal atmospheric pressure prevails outside the system whilst the pressure inside the system is below 1 Torr. At a temperature of 20 °C, 1 Torr × litre/sec corresponds to a rate of 3.27×10^{19} gas molecules per sec. For practical applications the following comment might be useful:

If the leak rate of a clean system is 10^{-5} Torr litre/sec, a pumping speed of 1 litre/sec is sufficient to maintain a vacuum of 10^{-5} Torr in the system; in similarly a pumping speed of 10 litre/sec maintains a vacuum of 10^{-6} Torr.

List of permissible leak rates for the various vacuum ranges:

Coarse vacuum: 1 Torr litre/sec.
Medium-high vacuum: 10^{-2} Torr litre/sec.
High vacuum: 10^{-5} Torr litre/sec.
Ultra-high vacuum: $\leqq 10^{-9}$ Torr litre/sec.

In order to measure the leak rate in a vacuum system and to locate the leak, a number of leak-hunting methods have been introduced.

1.10.1 Bubble Method with Water

The plant (or part of it) is pressurized (e. g. with air) and immersed in water. Leaks are indicated by gas (air) bubbles, emerging through the leak into the surrounding liquid.

Sensitivity: 1 Torr litre/sec.
Test period for detecting the leak: A few minutes.
Advantage of the method: Simplicity.
Disadvantage: Low sensitivity.

1.10.2 Painting with Nekal or Erkantol or Soap Solution

Plant (or part of it) is pressurized and suspected areas are painted outside with foam-producing substances (soap solution, Nekal, Erkantol). Leaks indicated by formation of bubbles.

Sensitivity: 0·1 Torr litre/sec.
Test period: Minutes.
Advantages: Simplicity; the method can be used both on single components as well as on assembled vacuum systems.
Disadvantages: Low sensitivity.

1.10.3 Ammonia plus Ozalid-paper

Plant is pressurized with ammonia (only slight overpressure is required), and suspected areas are covered on the outside with wet Ozalid-paper. Leaks are shown by black spots on the Ozalid-paper.

Sensitivity: 10^{-11} Torr litre/sec.
Test period: Several hours.
Advantages: High sensitivity.
Disadvantages: Long testing times; danger of inner parts of vacuum system being corroded by the wet ammonia.

1.10.4 Pressure Rise Method

The plant is first evacuated to the lowest possible pressure and then isolated from the pump by an isolating valve. The pressure rise is measured. The leak rate U is calculated from the basic formula:

$$U = \frac{\Delta p\, V}{t} \quad \text{(Torr litre/sec)}$$

Δp pressure rise in Torr during time t (sec).
V volume of the system in litres.

Pressure range: About 760 Torr down to lowest pressures.
Sensitivity: Depends on the time available for the test and on test conditions. In extreme cases leak rates of the order of 10^{-13} Torr litre/sec can be detected.
Test period: Seconds to months.
Advantages: Simple and applicable within very wide limits.
Disadvantages: The pressure rise caused by actual leaks can be superimposed by a pressure rise caused by gas desorption from the inner walls of the system and/or from inner parts, also from liquid residues, falsifying the true leak rate perhaps considerably as the case may be.

1.10.5 Use of Vacuum Gauges for Leak Detection

1.10.5.1 Heat Conductivity Gauges and Viscosity Manometers

The pressure indication of both types of gauges depends on the nature of the gas. If, therefore, suspected areas are sprayed with a gas which is different from the main component gases of the atmospheric air, the pressure reading will alter as soon as the spray touches a leaky portion of the system or of one of its components. Test gases used in this procedure are hydrogen, helium or neon. The method can also be modified in that instead of using a gas for spraying suspected areas a volatile liquid is applied, e.g. alcohol, trichlorethylene or carbon tetrachloride. These liquids will enter any leaks and so penetrate the container wall; on arrival on the inner surface the liquids evaporate, causing a different atmosphere which in turn causes an alteration of the gauge reading. It is also possible to seal leaks with a vacuum sealing wax or a vacuum cement. This also leads to an alteration of the gauge reading.

Pressure range: 20–*ca.* 10^{-3} Torr.
Sensitivity: About 10^{-4} Torr litre/sec.
Test period: Seconds.
Advantages: Simplicity and short test periods.
Disadvantages: Low sensitivity.

1.10.5.2 Penning Gauge and Standard Ionization Gauge

The procedure is identical to that described in section 1.10.5.1.

Pressure range: 10^{-2}–10^{-6} Torr.
Sensitivity: 10^{-6} Torr litre/sec.
Test period: Seconds.

1.10.5.3 Bayard–Alpert Ionization Gauge

The procedure is identical to that described in section 1.10.5.1.

Pressure range: 10^{-4}–10^{-10} Torr.
Sensitivity: 10^{-10} Torr litre/sec.
Test period: Seconds.
Advantages: Reasonable sensitivity; fairly simple.
Disadvantages: The test procedure can only be started after a pressure of about 10^{-4} Torr or less is obtained in the system.

1.10.6 Penning or Ionization Gauge in Combination with Palladium Barrier; Hydrogen Test Gas

The monitoring gauge head is isolated from the vacuum system proper by a palladium disk which can be heated. The vacuum system or parts thereof are sprayed with hydrogen. Any hydrogen infiltrating through a leak will arrive at the heated palladium disk and thus enter the gauge causing an alteration of the gauge reading.

Pressure operating range: 10^{-2}–10^{-6} Torr.
Sensitivity: 10^{-7} Torr litre/sec.
Test period: Minutes.
Advantages: Simple testing, cheap test gas.
Disadvantages: Limited sensitivity; danger of poisoning the heated palladium disk by oxygen.

1.10.7 Halogen Diode Detector

The gauge consists of a heated platinum wire surrounded by a cylindrical cathode. Several hundred volts are applied between the two electrodes of the diode system. When heated, the positive platinum wire emits alkali ions; this ion current is very sensitive to traces of organic halides. The vacuum system, therefore, is sprayed with a gas containing an organic halide, e. g. freon. Any trace of organic halide entering the system through a leak or porosity, gives rise to a large increase of the diode current, which can be indicated either by an instrument or by a speaker.

Pressure operating range: 760–10^{-6} Torr.
Sensitivity: 10^{-7} Torr litre/sec.
Test period: Seconds.
Advantages: The pressure range starts at 760 Torr.
Disadvantages: Misleading readings when vacuum system is contaminated by halide containing substances.

1.10.8 Use of Partial Pressure Gauges

In the methods described in this section, basically any search gas can be used which is not already present in appreciable quantities in the atmospheric air. In particular, hydrogen and the noble gases helium, neon and argon are suitable. Special attention should be given to helium. The element sensitive to the search gas is a small mass spectrometer adjusted for the particular search gas to be used.

Details are given in the corresponding section on p. 112, where the application of mass spectrometers as specific indicators for certain gases is described.

1.10.8.1 Omegatron-type Mass Spectrometer

Pressure operating range: 10^{-5}–10^{-11} Torr.
Sensitivity: 10^{-9} Torr litre/sec.
Test period: Seconds.

1.10.8.2 Farvitron-type Mass Spectrometer

Pressure operating range: 10^{-4}–10^{-9} Torr.
Sensitivity: 10^{-7} Torr litre/sec.
Test period: Seconds.

1.10.8.3 Topatron-type Mass Spectrometer

Pressure operating range: 10^{-3}–10^{-7} Torr.
Sensitivity: 10^{-7} Torr litre/sec.
Test period: Seconds.

1.10.8.4 Conventional Mass Spectrometer

Pressure operating range: 10^{-4}–10^{-10} Torr
Sensitivity: 10^{-10} Torr litre/sec.
Test period: Seconds.

1.10.8.5 Mass Filter after PAUL and STEINWEDEL

Pressure operating range: 10^{-3}–10^{-8} Torr.
Sensitivity: 10^{-9} Torr litre/sec.
Test period: Seconds.

Common features:

Advantages: High sensitivity and quantitative indication.
Disadvantages: Complicated test rig and low starting pressure required in the system.

In all methods using partial pressure gauges the deflection A of the mass spectrometer is a direct measure of the leak rate U. The deflection and its function of time depend on the leak rate

$$U = p_0 L\,, \quad \text{where } p_0 = 760\,\text{Torr}, \ L \text{ conductivity of the leak,}$$

and also on

$$\frac{\text{Pumping speed}}{\text{Volume of plant under test}} = \frac{S}{V}\,.$$

It is evident that the period of time between the instant of spraying the leak and the readiness for a repetition of the test is a function of S/V, because when the spray gun points to a leak, this leak becomes flooded with the search gas. The partial pressure p of the search gas inside the mass spectrometer gauge and, hence, the gauge reading depends on the time. The flow of search gas into the plant under test (volume V) is given by

$$d(pV) = (p_0 L - pS)\,dt.$$

It follows for

$$t < T:\quad p_t = \frac{L}{S}\,p_0\left(1 - e^{-\frac{S}{V}t}\right),$$

$$t > T:\quad p_t = \frac{L}{S}\,p_0\left(1 - e^{-\frac{S}{V}t}\right)e^{-\frac{S}{V}(t-T)},$$

$$T \to \infty,\quad t \to T:\quad p_\infty = \frac{L}{S}\,p_0,$$

T = time during which the leak is sprayed.

In Fig. 1.10.1 the mass spectrometer reading (strength of signal) is given as a function of time for $T = 1$ sec and for various values of S/V as a percentage of the reading for equilibrium, $p_\infty = \frac{L}{S}\,p_0$. In order to obtain instant readiness for the repetition of the test and for large deflections, S/V should be as large as possible. If, in addition to the pumping system of the mass spectrometer rig, a roughing pump is used, then the response time will be determined by the effective pumping speed S of the mass spectrometer *and* the effective pumping speed of the roughing pump.

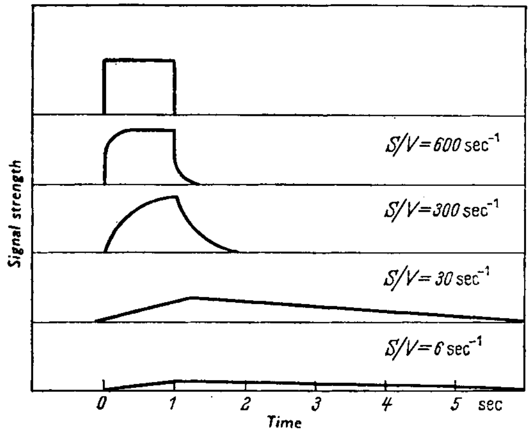

FIG. 1.10.1. Signal of a mass spectrometer leak detector as a function of time and ratio S/V (parameter). S effective speed of the pumping system attached to the test piece of volume V. The leak was exposed to spray for the period of 0–1 sec.

1.11 Ultra-high Vacuum Technology

Studies of ultra-high vacuum started after ALPERT 1951 had shown how to measure pressures as low as 10^{-11} Torr by using the novel vacuum gauge named after him and his colleague BAYARD [*1*]*. Very low pressures of similar order of magnitude no doubt had been obtained prior to ALPERT's work, but no measuring facilities existed, because all gauges used hitherto had a lower limit of 10^{-8} Torr.†

1.11.1 Experimental Preliminaries for the Production of Ultra-high Vacuum

The pumping system must be capable of producing very low pressures. The gas desorption from the inner walls of the vacuum system must be kept to a minimum. The degassing rate should not exceed 10^{-7} Torr litre/sec after baking at temperatures of up to 400—500 °C. The gas tightness should be of the order of 10^{-10} to 10^{-8} Torr litre/sec or better. When measuring pressures in an ultra-high vacuum system attention should be given to the following complexities:

We already find in the high vacuum pressure range — assuming there is a state of equilibrium between gas desorption from the walls and pumping speed — that the result of the pressure measurement is dependent on the site at which the measurement is carried out in the vacuum system because of the flow impedance of the pipelines. In the ultra-high vacuum range, however, not only gas desorption and pumping speed, but also adsorption and solubility of gas in solid parts of the vacuum system have a remarkable influence upon the state of equilibrium. The two latter mechanisms contribute to additional pressure gradients in the system, which is particularly annoying when an alteration of pressure in the system, e. g. due to start of pumping, has already previously taken place. Based on these experiences the pressure measuring system of the gauge head should be mounted in an unrestricted way inside the vacuum system; intermediate pipes or tubular connections should be avoided in both glass and metal ultra-high vacuum systems.

---

* Figures in brackets refer to the list of references at the end of this chapter (page 139).

† It had been suggested, therefore, to use this value as a marker between the high vacuum and ultra-high vacuum measuring range. We prefer, however, to divide the whole vacuum range into subdivisions as per table 1.4.1 (page 57). Accordingly the lower limit of the high vacuum range is 10^{-7} Torr, which simultaneously is the upper limit of the ultra-high vacuum range; no lower limit of this latter range is suggested.

1.11.2 Pressure Measurement

1.11.2.1 Use of Bayard–Alpert Gauge

For the measurement of pressures down to 10^{-10} Torr the ionization gauge after Bayard-Alpert [2, 3] (see page 111) is widely used. For pressures below 10^{-10} Torr the following considerations apply: By means of low temperature cooling, by ionic pumping action of the Bayard-Alpert gauge itself or by use of mercury diffusion pumps, pressures can be obtained which are below the threshold of the Bayard–Alpert gauge (10^{-11} Torr). Special measuring methods have been developed for these low pressures. The lower limit of any ionization gauge — as is well known — is caused by the soft X-rays which liberate electrons from the ion collector, and thus simulate an ion current. This so-called X-ray limit is independent of pressure. If therefore, at very low pressures, the ion current is of the magnitude of the X-ray limit, then accurate pressure measurement will only be possible provided the X-ray limit is taken into account. The first attempts made in this direction aimed to discriminate, by means of voltage variations, between the ion current proper, which is virtually independent of electrode voltages, and the X-ray limit, which shows a marked dependance on voltage. This method, however, is complicated and not very accurate. A simpler procedure has, therefore, been suggested, in which a strongly negative voltage is temporarily fed to an auxiliary electrode, so that the ions produced in the gauge reach the auxiliary electrode and not the actual ion collector (Fig. 1.11.1).

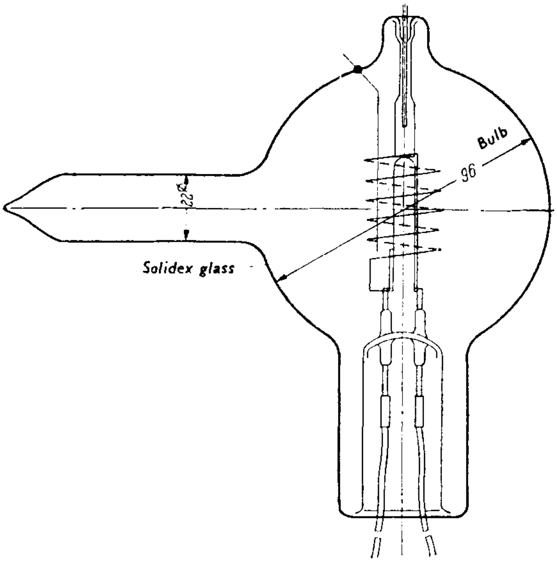

Fig. 1.11.1. Ionization gauge with auxiliary electrode.

In consequence, the collector current which flows during this time represents the X-ray limit. If the auxiliary electrode is then made positive, relative to the potential of the ion collector, the ions will flow to the collector. The difference between this collector current and the X-ray limit as measured previously is the ion current proper and, hence, the pressure in the gauge.

1.11.2.2 Use of the Magnetron Gauge

For the measurement of very low pressures, the magnetron gauge [*4*] (Fig. 1.11.2) has been recently introduced. This is a cold cathode discharge tube which ignites at the lowest pressures so far obtained, and which yields relatively high ion currents. Figure 1.11.3 shows a calibration curve. Because of the high ion current the gauge acts as a pump of fairly high pumping speed (a value of 0·15 litre/sec was measured for He). The advantages of this gauge are: Relatively high sensitivity and large measuring range (10^{-4} to 10^{-12} Torr). Disadvantages: Relatively inaccurate

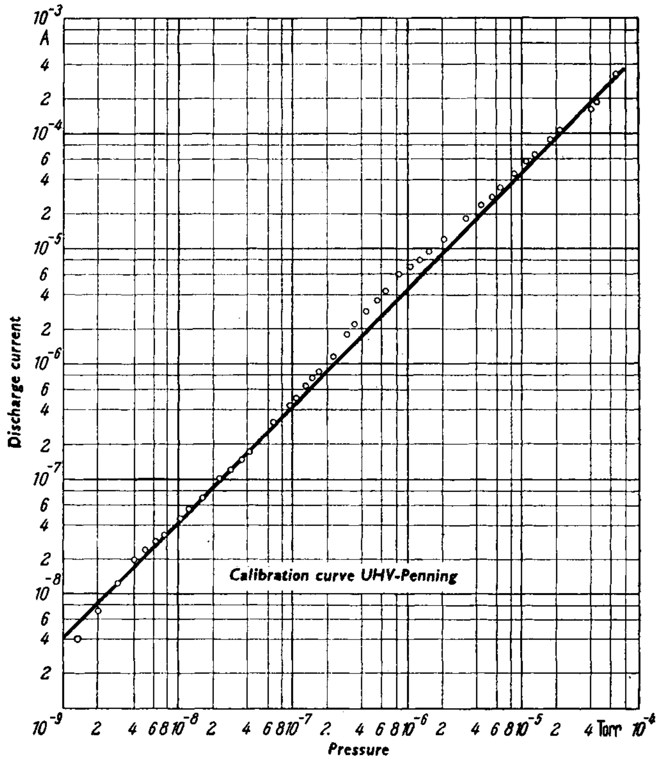

FIG. 1.11.3. Calibration curve of a magnetron gauge.

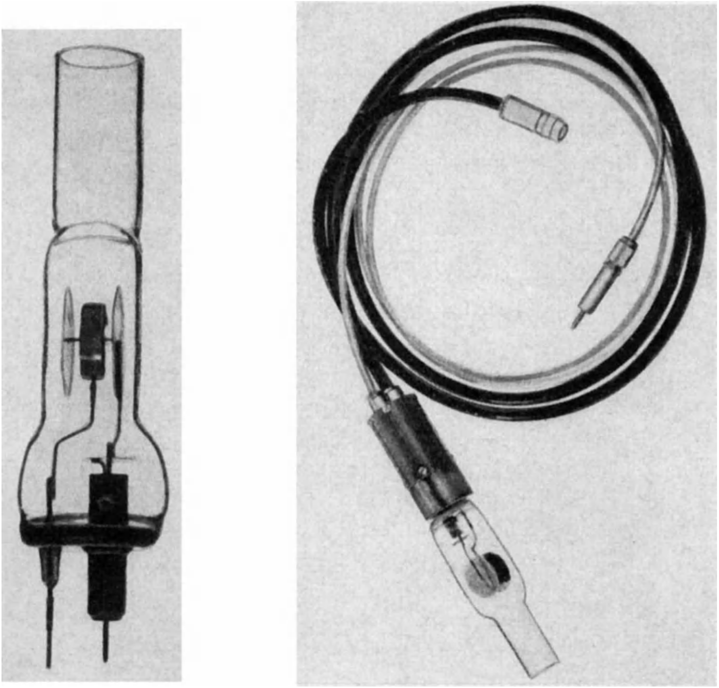

FIG. 1.11.2a. and b. Magnetron gauge head.

owing to pumping action and electrode surface conditions, the need for a magnet, and high operating voltage.

1.11.2.3 Flash-filament Method

A completely different method for measuring very low pressures is the so-called flash-filament method [5]. A metal surface situated inside the vacuum system is first cleaned by heating at about 2000 °C. A so-called cold time follows during which molecules of active gases adsorb on the surface at a rate proportional to the prevailing gas pressure.

In the actual device a tungsten or molybdenum filament is used which, after degassing (cleaning) and a given cold time, is reheated. The adsorbed gases become desorbed and cause an increase of pressure which is a measure of the pressure of the active gases (Fig. 1.11.4).

Saturation occurs when a monolayer is reached. From the cold time

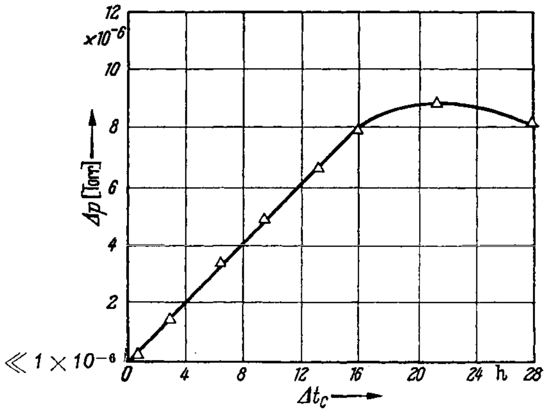

FIG. 1.11.4. Pressure increase as a function of cold time.

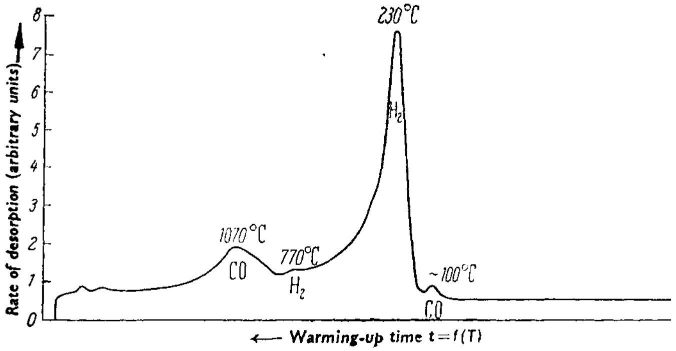

FIG. 1.11.5. Desorption spectrum of a gas atmosphere containing CO and H_2.

required to obtain a monolayer, the pressure of the adsorbed gases can be evaluated. More accurate results, however, can be obtained if one uses shorter cold times and hence lower pressure increases, and by calibrating with known gases. The method can be elaborated so that discrimination between adsorbed gases of different nature can be achieved. For this, the filament is reheated at a definite rate; at certain temperatures, pressure peaks are observed. The diatomic gases N_2, H_2 and CO each show two characteristic desorption temperatures which correspond to two states of adsorption. Figure 1.11.5 shows the desorption spectrum for a gas mixture containing CO and H_2.

1.11.3 The Production of Ultra-high Vacuum

1.11.3.1 In Glass Systems (volume of a few litres)

A typical arrangement is shown in Fig. 1.11.6 [*6*]. Two mercury diffusion pumps D_1 and D_2, connected in series, operate on the container via the series-connected cold traps F_1 and F_2 and the valve V_2. For larger systems oil diffusion pumps are also used. In this case F_1 is a water-cooled baffle.

The fore-vacuum is produced by the rotating pump R via the valve V_1 and the fore-vacuum tank B. The total pressure is measured by the BAYARD–ALPERT gauge IV (see gauges), and partial pressures (see page 112) by the Omegatron gauge O. The valve V_3 provides the facility for gas inlet into the container. The parts inside the dotted square can be baked up to 450°C. The valves V_2 and V_3 are, therefore, made entirely of metal. Proven designs are shown in Figs. 1.11.16 and 1.11.17.

Pumps, traps and the best part of the rest of the system are made of Duran (*Pyrex*-type) glass or of equivalent borosilicate glasses. The pumping procedure is as follows:

1. The container is evacuated down to about 10^{-6} Torr by means of backing pump and diffusion pumps; the cold trap F_1 is filled with liquid nitrogen.
2. The device is baked for about 15 hrs at 450°C.
3. After removing the baking oven, the metal parts of the gauge head IV are degassed at about 1300°C.
4. The cold trap F_2 is filled with liquid N_2. The pressure then drops below 10^{-9} Torr within several hours.

It is now possible to shut valve V_2 and the pressure will not rise when the gauge head *IV* is switched on and operated at a relatively high electron current (10 mA.). The gauge head acts as an ion pump with a pumping speed of several ccs/sec. This speed is sufficient for atmospheric Helium, which penetrates the glass walls of the system, to be removed at a pressure of about 10^{-11} Torr.

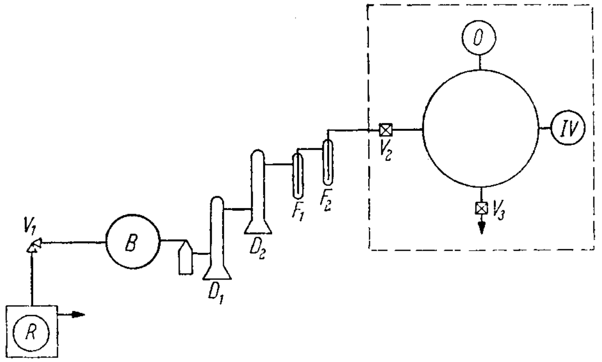

FIG. 1.11.6. Device for the production of ultra-high vacuum.

1.11.3.2 In Metal Systems

Metal systems used are assembled from components which can all be baked up to 400—500 °C. Such systems are usually constructed with relatively large overall dimensions. The main difficulties involved are, besides

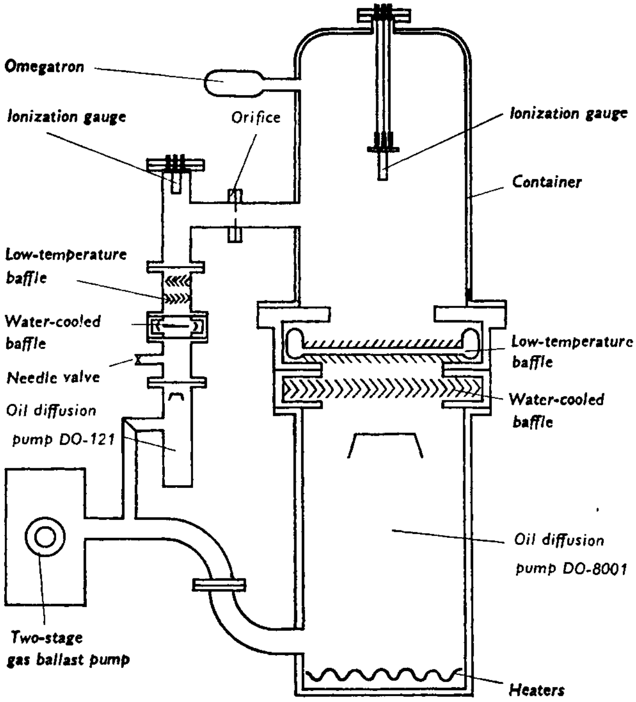

FIG. 1.11.7. High speed pumps and baffle arrangement for the production of ultra-high vacuum.

those outlined for glass systems in the previous sections, the heavy gas desorption from the large surface areas of the walls of the system. The use of suitable materials is, therefore, most essential. Stainless steel is widely used, sometimes combined with ceramic materials. Suitably designed vacuum lines, flanges and valves are also essential in large systems (see section 1.11.4).

Diffusion pumps of high pumping speed in conjunction with suitable vapour traps seem to be the answer in large systems. Oil diffusion pumps with liquid-nitrogen-filled traps are especially suitable. Figure 1.11.7 shows, by way of example, a pump with a speed of 8000 litre/sec. The ultimate pressure is 10^{-9} Torr; the effective pumping speed for air and hydrogen is shown in Fig. 1.11.8. Measurements of speed were carried out down to pressures of 10^{-9} Torr, and no appreciable decrease was observed [7].

To avoid creeping of oil from the diffusion pump at ambient tempe-

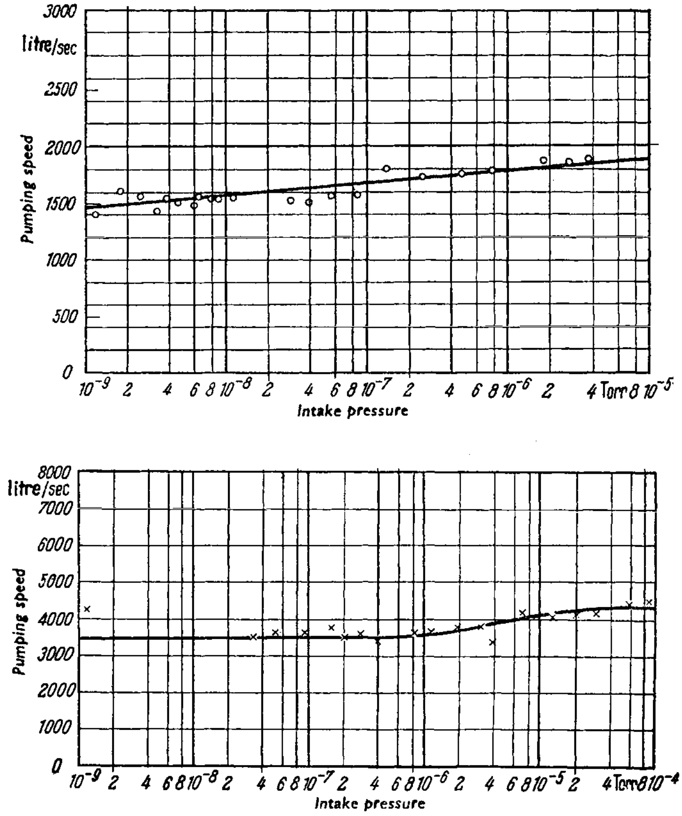

FIG. 1.11.8. Pumping speed for air (top) and for hydrogen (bottom) of oil diffusion pump DO 8001 with water-cooled and low temperature baffle. Pumping fluid: DIFFELEN ultra.

rature along the inner walls of the vacuum vessel, a piece of metal sheet must be appropriately inserted, to be connected to the low temperature parts of the baffle or cold trap (see Fig. 1.11.9).

Metal systems for ultra-high vacuum are sometimes designed as a double bell jar; the outer jar is equipped with normal high-vacuum flanges, using metal gaskets, whilst the inner jar features no gaskets at all. This is possible because of the evacuation of the interspace between the two jars; only one set of high vacuum joints is required [*8*].

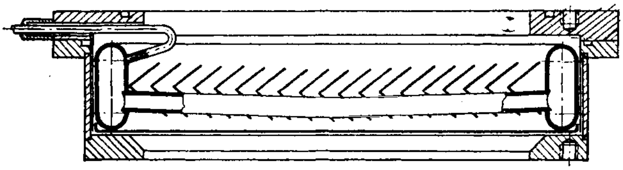

FIG. 1.11.9. Chevron baffle with oil creep barrier.

1.11.3.3 Adsorption Traps

The systems described above are sometimes modified insofar as the cold traps are replaced by so-called adsorption traps [*9*]. As already mentioned on page 95 (Chapter 1.6.3), these traps have attained particular significance in ultra-high vacuum techniques, and are now widely used.

ALPERT used oil diffusion pumps with copper traps instead of mercury diffusion pumps with cold traps. The cross section of a copper trap (see also Fig. 1.6.9) is shown in Fig. 1.11.10. This trap consists of a smooth copper sheet and a second corrugated copper sheet which are rolled on top of each other as shown in Fig. 1.11.10. OFHC copper is used. It is important to keep the copper surface clean, i. e. free of grease. The completed copper sheet roll should, therefore, be heated in a hydrogen atmosphere.

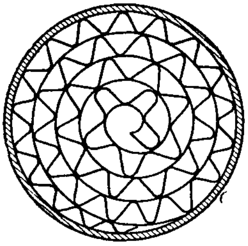

FIG. 1.11.10. Cross section of a copper trap.

ALPERT used in the first place a diffusion pump made of glass, although a pump made of metal cum baffle is equally suitable, provided this pump has good fractionating and oil degassing properties. Above the baffle, glass is joined to the pumping system via a Kovar glass-to-metal seal. The copper trap is baked together with the rest of the vacuum system. The pumping procedure consists of the following stages:

1. Pump-down to 10^{-6} Torr by means of backing pump and diffusion pump.
2. Baking for 15 hrs at 450 °C.
3. After removal of baking oven, degassing of the metal parts of the gauges at 1300 °C.

After a few hours the pressure drops below 10^{-9} Torr. It then slowly increases again, and will reach a value of 10^{-9} Torr after days or weeks according to the design of the copper trap. This pressure increase stops as soon as the ultimate pressure of the diffusion pump is reached. The copper trap operates on the principle that the oil molecules backstreaming from the pump to the vacuum vessel are bound to impinge very frequently on the clean uncharged copper surface en route. As a result, adsorption takes place. It is still unknown whether chemical reactions also take place besides adsorption.

By using the copper trap system, the design and the mode of operation of the ultra-high vacuum rig can be very much simplified (no liquid nitrogen!). But pressure increase has to be tolerated instead, although the nature of gases causing this increase cannot be anticipated with certainty. Recent reports seem to indicate that CO is present.

Instead of copper, the use of ceramic materials (aluminium oxide or so-called molecular sieves, Zeolite) has recently been suggested. The advantage of these materials is that traps of rather high conductivity (100 litres per sec and more) can be built.

The use of charcoal which, however, has to be cooled down to low temperatures, has been known for a long time.

1.11.3.4 Getters

A further means for producing ultra-high vacuum is the application of getters [*10*] (see chapter 2.4). Certain precautions however, are required because sufficiently low ultimate pressures can only be obtained provided the getter material is extremely well degassed. The usual procedure is to produce a metallic film by evaporation of the getter; the fresh surface of this film adsorbs active gases (see chapter 1.7, Getter-ion-pumps). A tungsten wire forms the core of a spiral that is made of the getter material to be evaporated.

For degassing, the tungsten wire is slowly heated to a temperature just high enough for no evaporation of the getter spiral to take place. It is advisable to check the pressure during heating. The degassing is finished as soon as the original pressure has again been obtained. The temperature is now further increased, whereby the pressure drops rapidly owing to the evaporation of the getter material. If titanium is used there will be marked evaporation below the melting point, so temperature is critical and should not exceed the melting point of the titanium. Therefore, a second tungsten wire of similar dimensions is usually spiraled around the tungsten core; this prevents the formation of titanium droplets in the event of the melting point being exceeded. Titanium has become a very common getter material because of its affinity for almost all gases except the noble gases. Zirconium, molybdenum and other materials known in connection with the manufacture of electron tubes, are also used.

1.11.3.5 Cryogenic Pumps

Finally, we have to discuss the application of very low temperatures for the production of ultra-high vacuum. If inside a vacuum vessel is inserted a surface which can be cooled down to the temperature of boiling hydrogen (20.4° abs.) or of boiling helium (4.2° abs.), vapours and so-called permanent gases (N_2, O_2, CO, CO_2, etc.) will condense on this surface, i. e. this surface acts as a pump (cryogenic pump or cryopump).

Figure 1.11.11 shows the saturation pressures of light gases at low temperatures; at 20.4° abs. these pressures are between 10^{-11} and 10^{-17} Torr for the gases N_2, O_2, CO and argon. For neon and helium the corresponding figures are 40 and several hundred Torr, respectively. But at 4.2° abs. no other gas can be detected than H_2 and He. The pressures of these gases are several times 10^{-7} Torr and 760 Torr respectively. This shows that by using cold surfaces only, no low ultimate pressures can be attained; for in the normal atmospheric air which fills any vacuum system prior to pumping, H_2, He and Ne are present at a rate which produces partial pressures of 3.8×10^{-4} Torr, 4×10^{-3} Torr and 1.4×10^{-2} Torr, respectively. In order to be able to produce extremely low pressures by cryogenic pumping, these gases first have to be rarefied by means of conventional pumps.

The pumping speed of a cryogenic pump depends on the shape and size of the condensing element (cryo-condenser), on the orientation of the latter to the vacuum chamber, and on the condensation coefficient of the gas to be pumped. The pumping speed is proportional to the surface area, if the condenser has a plane surface and is mounted inside the vacuum vessel.

The kinetic theory of gases shows that the volume V (litre) of a gas which penetrates in t seconds a plane F (cm²) in high vacuum or which impinges on the same plane, is given by

$$\frac{V}{t} = 10^{-3} F \frac{\bar{w}}{4} \quad \text{(litre/sec)},$$

where $\bar{w}$ is the mean velocity $= \sqrt{\frac{8kT}{\pi m}}$ (cm/sec).

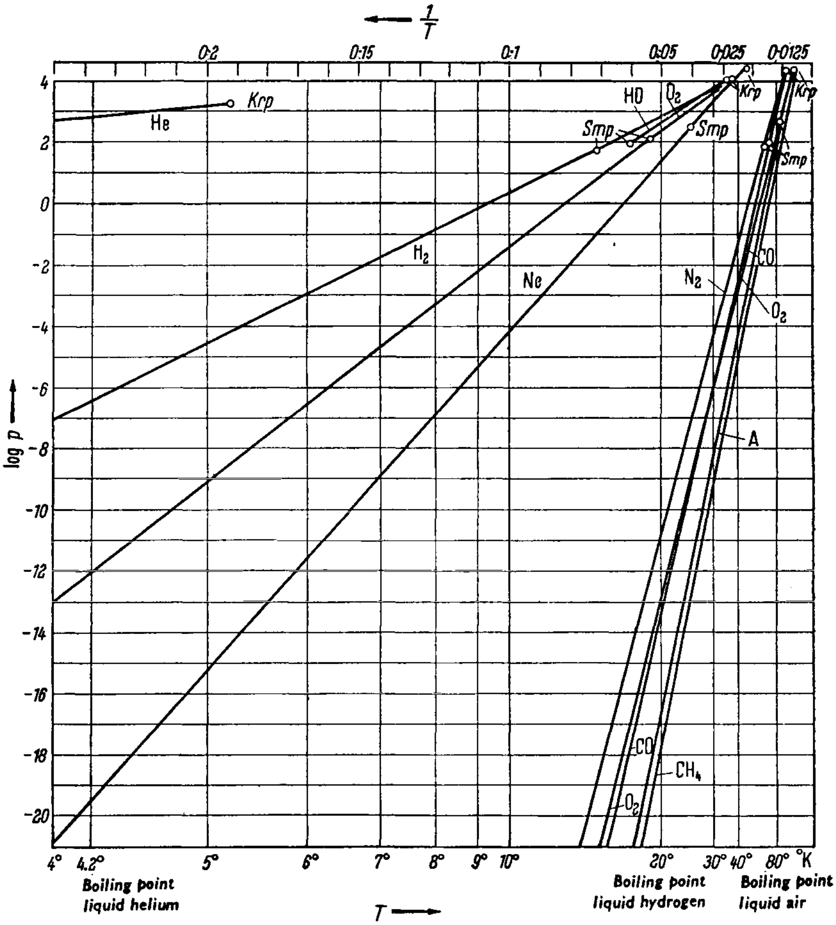

FIG. 1.11.11. Saturation pressures of lightweight gases at low temperatures. Krp = Critical point Smp = Melting point; p in Torr

If the plane is cooled down to a very low temperature and if all impinging molecules condense, i. e. the condensation coefficient $\alpha = 1$, then $\frac{V}{t} = S$, and S is the pumping speed of the condenser.

For a wall temperature of the vacuum vessel of 20 °C,

$$\bar{w} = 4.64 \times 10^4 \text{ cm/sec for air}$$

$$\bar{w} = 17.54 \times 10^4 \text{ cm/sec for } H_2$$

Hence:

$$S = 11.6 \times F \text{ (litre/sec) for air}$$

$$S = 43.8 \times F \text{ (litre/sec) for } H_2.$$

There are several alternatives for the design and the type of cooling of a cryogenic condenser. For smaller pumps a properly insulated cold trap (cryostat) can be used, filled with liquid He or liquid H_2.

For larger pumps which are intended to work for a longer period of time, the cryo-condenser is virtually a spiral made of copper tubing through which the cooling agent is sucked by means of a mechanical pump [*11*]. In the spiral the cooling agent evaporates, causing additional cooling. By means of a control valve which is regulated by a temperature sensing element, the temperature of the condensing surface can be kept constant within 1/10 to 1/100 deg. Ultimate pressures between 10^{-11} and 10^{-12} Torr can be obtained.

1.11.4 Components

1.11.4.1 Flanges [*12*]

A flange connection suitable for ultra-high vacuum work must satisfy a number of requirements, notably the leak rate must be extremely low and repeated baking cycles up to a temperature of 450 °C must not impair the quality of the joint. A host of designs have been suggested. It is important to note that the stringent requirements cannot be satisfied by using rubber or rubber-like gasket materials. The only alternative is to use metal gaskets. Several conditions have to be fulfilled: The flange must be of a design that is easy to make, the gasket seating should be proof against mechanical damage, and the flange connection must remain vacuum-tight even at the highest admissible baking temperature. An inherent disadvantage of all joints which use metal gaskets is that individual gaskets can only be used a few times. This has to be borne in mind with regard to costs.

From the great many suggestions that have been published within recent years, a few typical examples are given below. No forecast is possible as to the type of design which eventually will be generally adopted. To date it seems to be impossible that a single design could represent an optimization of the various requirements. Opinions as to the most suitable gasket material differ widely. The following materials are under discussion: Indium, copper, gold, soft iron, stainless steel, silver, platinum, nickel and aluminium.

The following systems will now be discussed in more detail (gasket material in brackets):

1. Unit flange connection (Al, Cu, Au)
2. Knife edge seal (Cu, Ag)
3. Stepped seal (Cu)
4. Edge seal (Au)

The simplest procedure no doubt is just to replace the rubber ring by a metal ring. This suggestion has been followed up successfully for unit flange systems (Fig. 1.11.12a), in which the rubber ring has been replaced by an aluminium ring. The advantage of such a procedure is that ordinary standard components can be used; its disadvantage is however, that considerable force is required to tighten the joint. This can lead to a distortion of the flange itself; the use of aluminium as a gasket material limits the max. permissible bake-out temperature to 200 °C. An improvement is brought about by making, close to the circle of holes for the bolts of the flange, a circular groove (see Fig. 1.11.12 b) to fit the gasket ring now made of copper or gold. By using temperature-resistant external spring washers, the mechanical forces required to maintain the joint vacuum-tight are retained during the whole bake-out cycle (400 °C max. baking temperature).

The well-known knife edge seal (Fig. 1.11.13) is basically successful, but has the disadvantage that the knife edges must be worked with great care, and that the finished edges are not protected against mechanical damage. Many metals have been suggested for use as gasket materials in this type of seal, in particular, copper and silver.

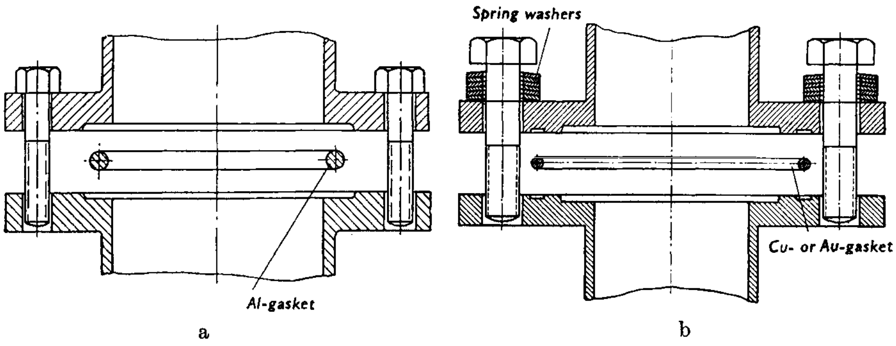

Fig. 1.11.12a and b. Unit flange connection. (a) – normal flange with Al-gasket; (b) – normal flange with additional groove and Cu- or Au-gasket.

The stepped seal (Fig. 1.11.14) uses an annular flat copper gasket made of OFHC copper, squeezed between the flanges. The copper gasket must be annealed at 850–900 °C, which is inconvenient for large size gaskets.

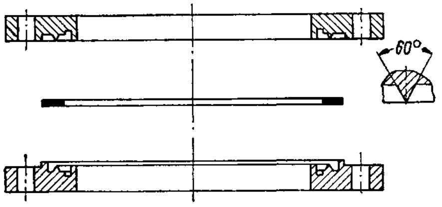

Fig. 1.11.13. Knife edge seal with copper gasket.

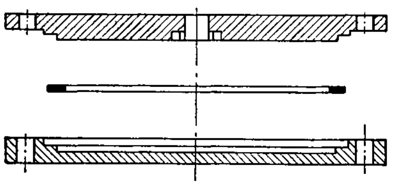

Fig. 1.11.14. Stepped seal with annular copper gasket.

The now most common type of seal is the edge seal (Fig. 1.11.15); a gold ring is used as the gasket. The cross section of the gold ring is between 0·5 and 1 mm², so that little material is involved, and it can always be recovered. All flange systems, except the unit flange system, have the disadvantage that to make up a joint two non-identical flanges must be used; this does not facilitate the assembly of a vacuum system.

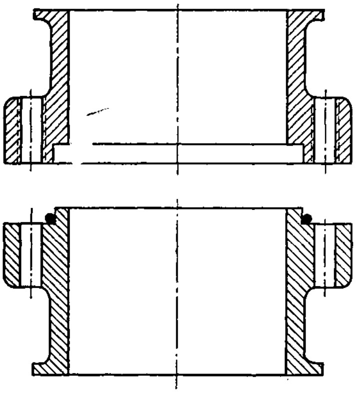

FIG. 1.11.15. Edge seal with gold gasket.

A further frequently discussed type of ultra-high vacuum flange is the soldered flange. In order to effect the seal a solder is used that starts to flow at a temperature above the maximum bake-out temperature, and one which has a sufficiently low vapour pressure also at elevated temperatures. Indium belongs to this category of solders.

A not very practical, but otherwise very safe type of joint is the welding flange, which is also easily applicable for large diameters. Thin metal rings of a diameter exceeding the outer diameter of the flange are fitted to the ends of the flange. After fitting the flanges, the metal rings are welded on their outer rim. In order to open the joint the weld is ground off. This type of joint can be used up to five times, provided it is appropriately designed.

1.11.4.2 Valves [*13*]

The same requirements have to be met for bakeable valves and for bakeable flange connections. The foremost problem here is to obtain an adequate seal between the valve plate and the valve seat. The procedure is to press the valve plate by force on to the valve seat. Bakeable valves suitable for 100—1000 operating cycles are so far commercially available only for small diameters; see Figs. 1.11.16 and 1.11.17.

The valve seat usually is made of a hard material, e. g. stainless steel, whilst the valve plate is made of a softer material, e. g. copper, monel or silver. The valves are characterized by the maximum torque required for closing the valve, and the maximum bake-out temperature. Bake-out with the valve closed is generally not possible or only up to moderate baking temperatures. The problem with valves of larger dimensions is to ensure that the valve plate meets the valve seat at exactly the same spot each time the valve closes, otherwise a perfect seal cannot be expected.

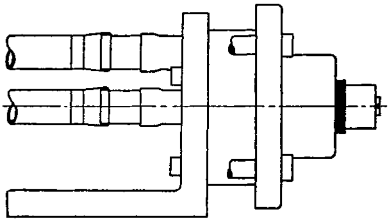

FIG. 1.11.16. Granville–Phillips valve.

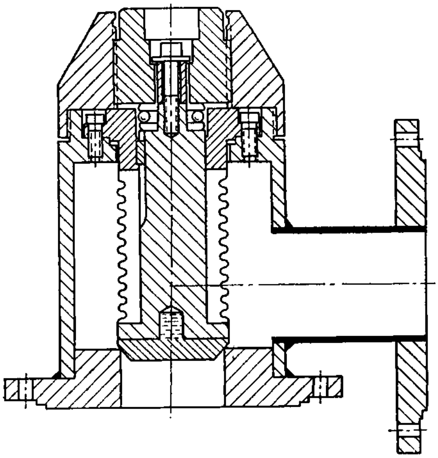

FIG. 1.11.17. Westinghouse valve NW 25.

In glass systems, valves are sometimes used which are made entirely of glass; sealing is achieved by pressing two greaseless spherical or plane glass surfaces against each other; these valves however, are only effective in sealing the ultra-high vacuum against pressures not higher than 10^{-4} Torr. Glass valves can be baked and sealed directly to the glass system.

In analogy to the flanges sealed with solder as described above, valves can also be designed on the same principle. For this the solder is in a groove which can be heated. The valve plate sinks into the groove.

1.11.4.3 Inspection Windows

Inspection windows for vacuum containers can be made by sealing a plain glass disk to a piece of Kovar tubing, which in turn is welded into a stainless steel flange (Fig. 1.11.18). For observation in the ultra-violet

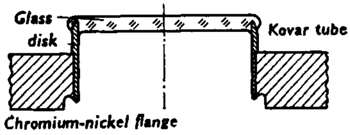

Fig. 1.11.18. Flange with inspection window.

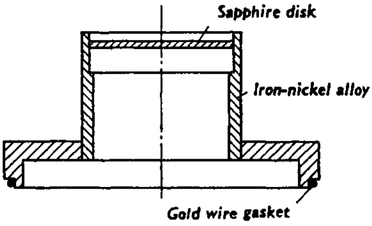

Fig. 1.11.19. Sapphire inspection window.

range sapphire windows are used [*14*] (Fig. 1.11.19). The sapphire disks are metallized with titanium-hydride and brazed into a seamless iron-nickel tube.

References

[*1*] Alpert, D., New development in the production and measurement of ultra-high vacuum. *J. Appl. Physics*, **24**, 860 (1953).
[*2*] Carter, G., *Brit. J. Appl. Physics* **10**, 364 (1959).
[*3*] Mizushima, Y., and Z. Oda, *Rev. Sci. Instrum.*, **30**, 12, 1037–1041 (1959).
[*4*] Hobson, J. P., and P. A. Redhead, *Canad. J. Physics* **36**, 3, 271 to 288 (1958).
[*5*] Baker, F. A., and J. Yarwood, *Vakuum-Technik* **6**, 147 (1957).
[*6*] Hobson, J. P., and P. A. Redhead, *Proc. First Internat. Congr. Vac. Techn.* pp. 384–388 (1960).
[*7*] Nöller, H. G., G. Reich and W. Bächler, *Vac. Symp. Trans. 1960*, pp. 72–74.
[*8*] Moll, J., and H. Ehlers, *Z. angew. Phys.* **7**, 324–328 (1960).
[*9*] Carmichael, J. H., and W. J. Lange, *Vac. Symp. Trans. 1958*, pp. 137–139.
[*10*] Milleron, N., and E. C. Popp, *Vac. Symp. Trans. 1958*, pp. 153–159.
[*11*] Klipping, G., *Kältetechnik* **13**, 250–252 (1961).
[*12*] Henry, R. P., and J. C. Blaive, *Proc. First Internat. Congr. Vac. Techn.* pp. 345-348 (1960).
13] Lange, W. J., *Rev. Sci. Instrum.* **30**, 602 (1959).
14] Greenblatt, M. H., *Rev. Sci. Instrum.* **29**, 738 (1958)

2 Vacuum

2.1 Vacuum

(dimensions

Item		Fig. no. (see pp. 142, 143)	Dimension
2.1.1 Pipelines	Precision tubing made of steel		outer dia. wall thickness
2.1.2 Rigid Joints	Bearing ring with ○-ring seal	2.1.3	
2.1.2.1 Components using Unit Flanges (see also Table "Flanges after DIN 2572" Fig. 2.1.1. and Fig. 2.1.2)	Flange with pipe connection	2.1.4	pipe dia. d H
	Flange with male ground joint	2.1.5	pipe dia. H NS
	Flange with female ground joint NS 14. 5/35	2.1.6	D H
	Flange with female ground joint NS 19/38	2.1.6	D H
	Pipe bend	2.1.7	E
	Flexible connection	2.1.8	H
	T-piece	2.1.9	E
	Reducing piece		
	20–10	2.1.10	H
	32–20	2.1.10	H
	50–32	2.1.10	H
	65–50	2.1.10	H
	100–65	2.1.10	H
	100–50	2.1.10	H
	Cross-piece with 2 lateral DIN flanges NW 10 (unit flange) offset by 180°	2.1.11	H_1 H_2 D
	Cross-piece with 2 lateral small flanges NW 10, offset by 180°	2.1.12	H_1 H_2 D
	Cross-piece with 2 lateral small flanges NW 10, offset by 90°	2.1.13	H_1 H_2
	Cross-piece with 1 small flange NW 10 and 1 small flange NW 32, offset by 90°	2.1.14	H_1 H_2
	Blind flange	2.1.15	

Technology

Accessories

in mm)

NW 10	NW 20	NW 32	NW 50	NW 65	NW 100	NW 150	NW 250
15	25	38	55	75	108	159	255
2·5	2·5	3	2·5	2·5	4	4·5	3

available for NW 10 up to NW 250

NW 10	NW 20	NW 32	NW 50	NW 65	NW 100	NW 150	NW 250
15	25	38	55	75	108	159	255
2·5	2·5	3	2·5	2·5	4	4·5	3
110	110	110	112	112	114	114	115
	30	30	60				
	130	100	87				
	29/42	29/42	60/46				
20							
100							
20							
155							
50	60	77	85	105	130	170	290
			120	120	120	200	
50	60	77	85	105	130	170	290
	100						
		100					
			100				
				100			
					100		
					100		
40	50	50					
50	60	70					
10	10	10					
40	50	50					
50	60	70					
10	10	10					
			50				
			85				
				50	50		
				95	120		

available for NW 10 up to NW 250

Unit flange connections DIN 2572 (UF = unit flange)

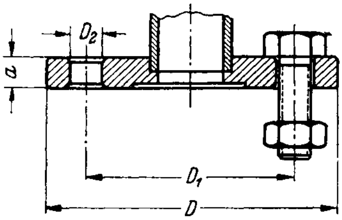

Fig. 2.1.1. Flange (UF) after DIN 2572.

(dimensions in mm)

i. d. (NW)	D	D_1	D_2	No. of D_2	a	Nuts and bolts thereto DIN 933
10	75	50	11·5	4	10	M10 × 30
20	90	65	11·5	4	10	M10 × 30
32	120	90	14	4	10	M12 × 35
50	140	110	14	4	12	M12 × 35
65	160	130	14	4	12	M12 × 35
100	210	170	18	8	14	M16 × 45
150	265	225	18	8	14	M16 × 45
250	375	335	18	12	15	M16 × 45
350	490	445	23	12	22	M20 × 60
500	645	600	23	20	22	M20 × 60

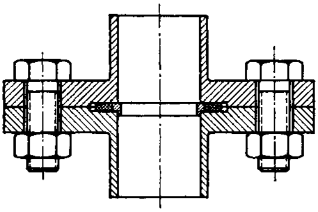

Fig. 2.1.2. Unit flange connection (2 flanges with pipe connection and bearing ring with ○-ring seal).

Fig. 2.1.3. Bearing ring with ○-ring seal.

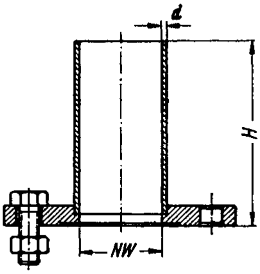

Fig. 2.1.4. Flange with pipe connection.

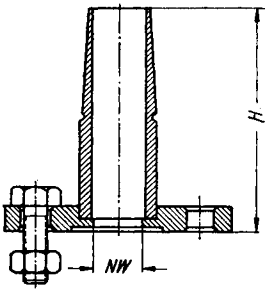

Fig. 2.1.5. Flange with male ground joint.

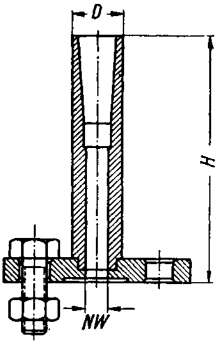

Fig. 2.1.6. Flange with female ground joint.

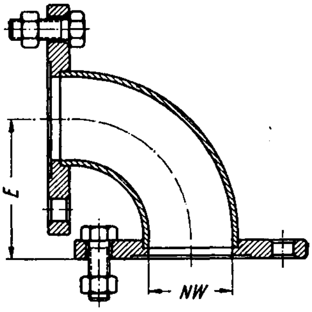

Fig. 2.1.7. Pipe bend.

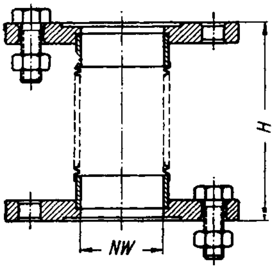

FIG. 2.1.8. Flexible connection.

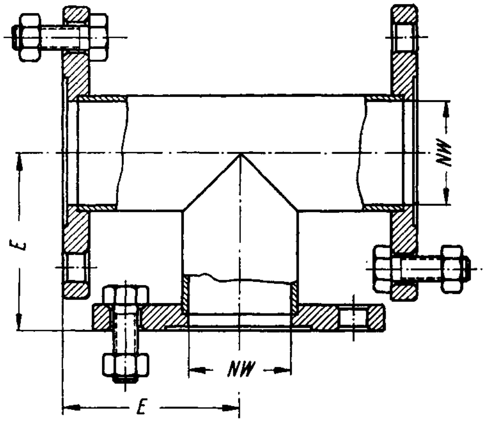

FIG. 2.1.9. T-piece.

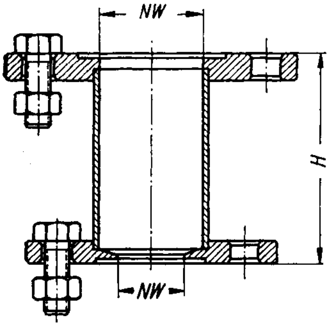

FIG. 2.1.10. Reducing piece.

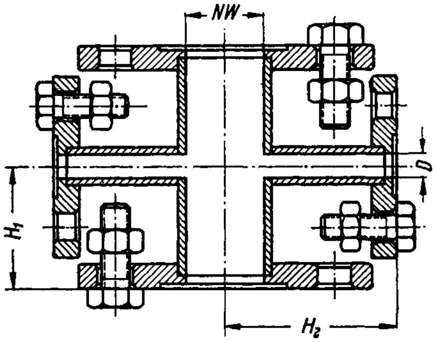

FIG. 2.1.11. Cross-piece with 2 lateral DIN-flanges NW 10 (UF).

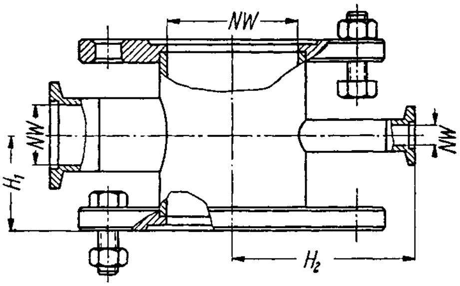

FIG. 2.1.14. Cross-piece with small flange NW 10 and small flange NW 32, offset by 90°.

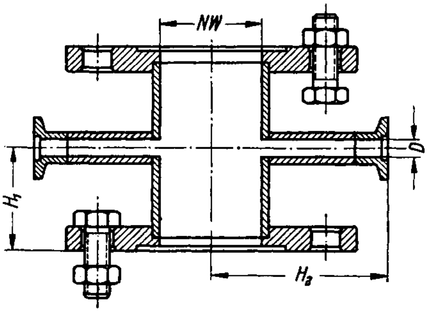

FIG. 2.1.12 and 2.1.13. Cross-piece with 2 lateral small flanges NW 10;
2.1.12: offset by 180°;
2.1.13: offset by 90°.

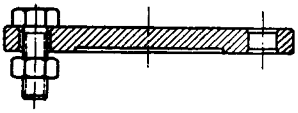

FIG. 2.1.15. Blind flange.

	Item	Fig. no. (see pp. 146. 147)	Dimension
2.1.2.2 Assembly Parts with Small Flanges	Centring ring	2.1.16	D h
	Clamping ring	2.1.17	D B H
	Small flange with pipe connection	2.1.18	D_1 D_2 H
	Small flange with hose nipple	2.1.19	D_1 D_2 H
	Small flange with male ground joint	2.1.20	D_1 D_2 H NS
	Small flange with female ground joint NS 14·5/35	2.1.21	D_1 D_2 H
	Small flange with female ground joint NS 19/38	2.1.21	D_1 D_2 H
	Pipe bend	2.1.22	D H
	Flexible connection	2.1.23	D_1 H
	T-piece	2.1.24	D H, H_1 L
	Reducing piece 20–10	2.1.25	D_1 D_2 D_3 H
	Reducing piece 32–30	2.1.25	D_1 D_2 D_3 H
	Cross-piece with 2 lateral small flanges NW 10, offset by 180°	2.1.26	D_1 D_2 D_3 H_1 H_2
	Adapter flange (small flange on unit flange NW 10, NW 20, NW 32)	2.1.27	A/B C/D E/F
	Blind flange	2.1.28	D S

NW 10	NW 20	NW 32	NW 50	NW 65	NW 100				
30	40	55							
3·9	3·9	3·9							
44	55	70							
62	73	80							
16	16	16							
30	40	55							
15	25	38							
16	20	25							
30	40	55							
7	7	7							
40	40	40							
30	40	55							
12·2	22	34							
50	55	65							
19/38	29/42	45/50							
30									
18									
65									
30									
22									
65									
30	40	55							
30	50	50							
30	40	55							
70	80	100							
30	40	55							
30	50	50							
60	100	100							
30									
10									
40									
40									
	40								
	20								
	55								
	40								
30	40	55							
30	30	30							
10	10	10							
25	30	35							
35	35	35							
30/12·2	26/ 75	30/10							
40/22·2	36/ 90	30/10							
55/34·2	52/120	30/10							
30	40	55							
5	5	5							

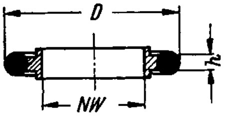

FIG. 2.1.16. Centring ring with ○-ring seal.

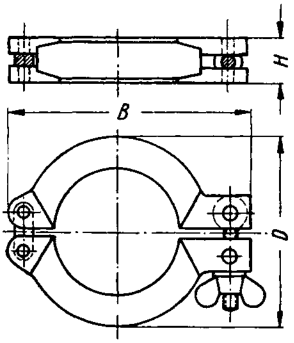

FIG. 2.1.17. Clamping ring.

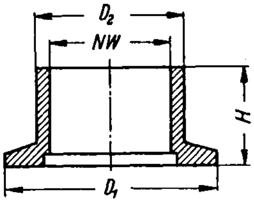

FIG. 2.1.18. Small flange with pipe connection.

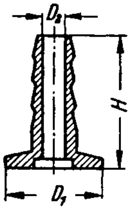

FIG. 2.1.19. Small flange with hose nipple.

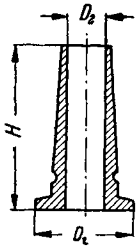

FIG. 2.1.20. Small flange with male ground joint.

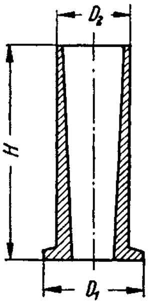

FIG. 2.1.21. Small flange with female ground joint.

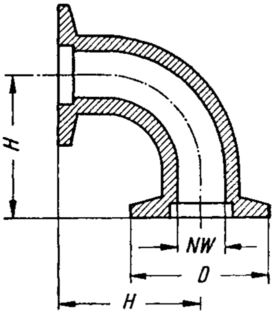

FIG. 2.1.22. Pipe bend.

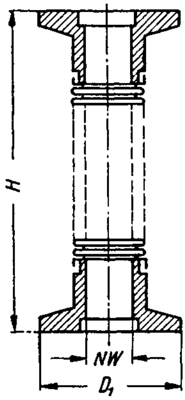

FIG. 2.1.23. Flexible connection.

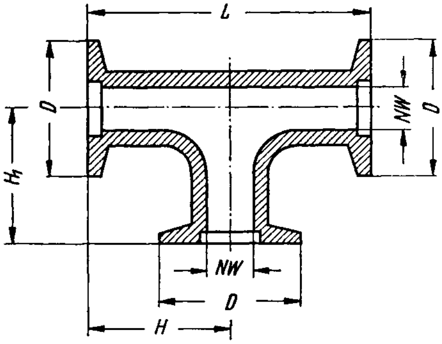

FIG. 2.1.24. T-piece.

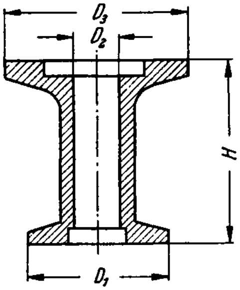

FIG. 2.1.25. Reducing piece.

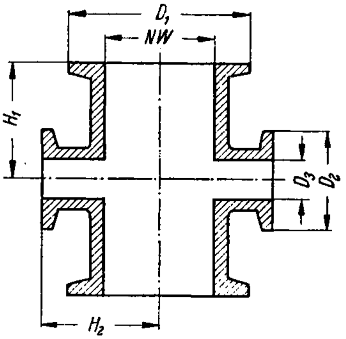

FIG. 2.1.26. Cross-piece.

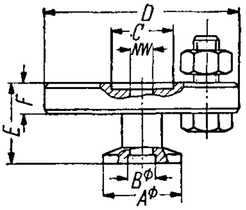

FIG. 2.1.27. Adapter flange (small flange on unit flange NW 10, NW 20, NW 32).

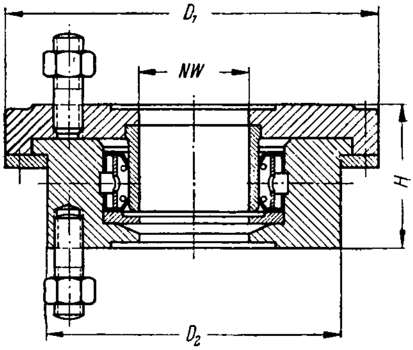

FIG. 2.1.29. Rotary flange.

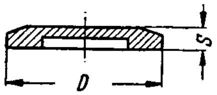

FIG. 2.1.28. Blind flange.

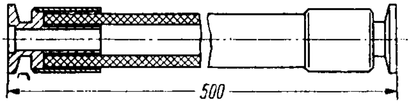

FIG. 2.1.30. PVC-tubing.

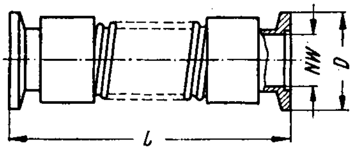

FIG. 2.1.31a. Tombac pipe with small flanges.

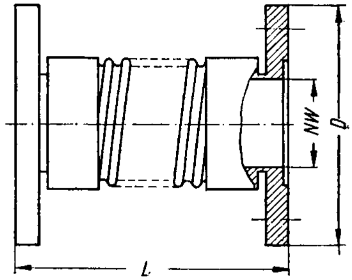

FIG. 2.1.31b. Tombac pipe with unit flanges.

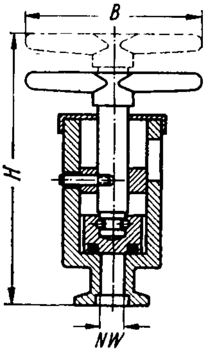

FIG. 2.1.32. Air-inlet valve NW 10.

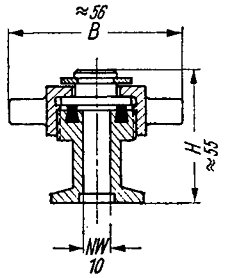

FIG. 2.1.33. Air-inlet valve, simple design.

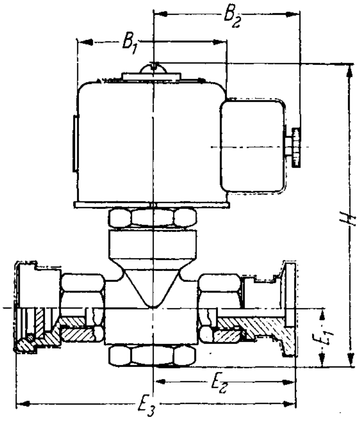

FIG. 2.1.34. Electromagnetic air-inlet valve.
$B_1 = 48$ mm $E_1 = 20$ mm $E_3 = 86$ mm
$B_2 = 48$ mm $E_2 = 45$ mm $H = 95$ mm

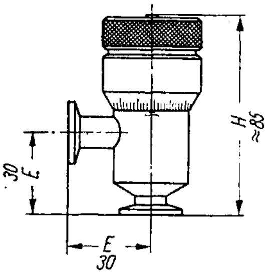

FIG. 2.1.35. Variable leak.

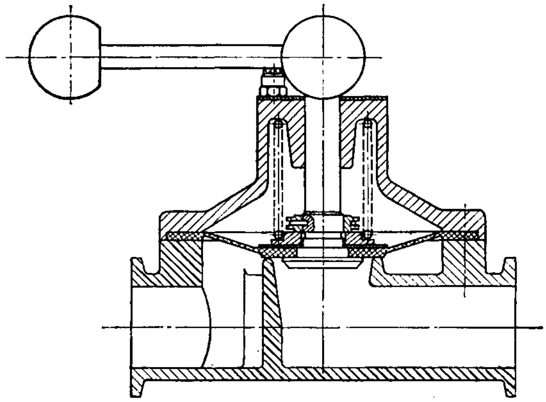

FIG. 2.1.36. Packless diaphragm valve.

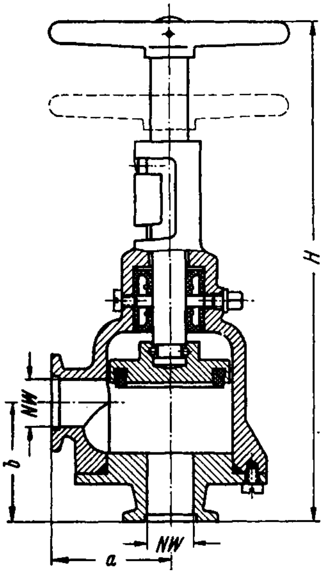

FIG. 2.1.37a. Right-angle valve with small flanges.

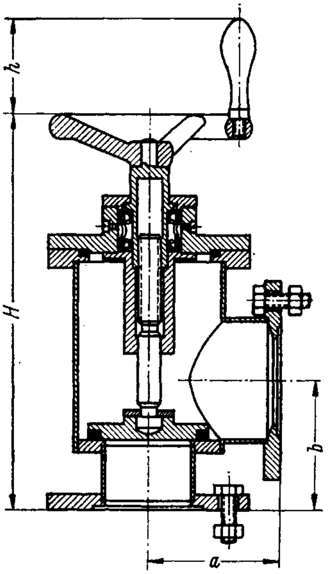

FIG. 2.1.37b. Right-angle valve with unit flanges.

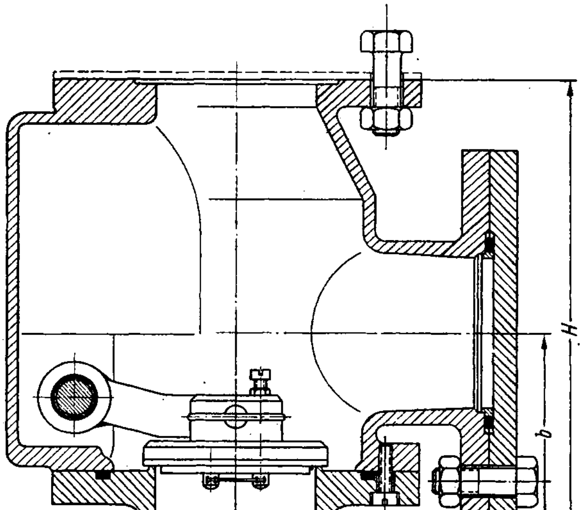

FIG. 2.1.38. Flap valve.

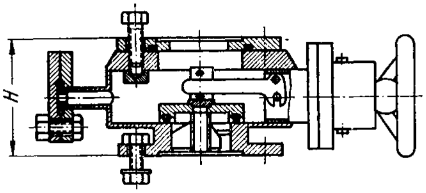

FIG. 2.1.39. Plate valve, low overall height.

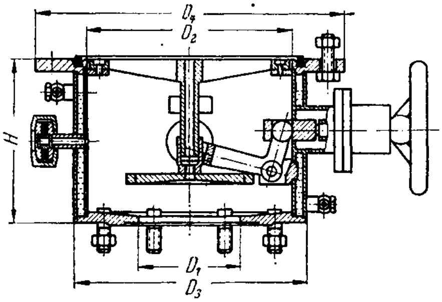

FIG. 2.1.40. Plate valve of low impedance.

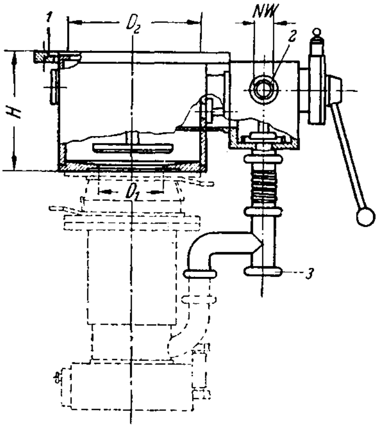

FIG. 2.1.41. Valve block with baffle and diffusion pump;
1 – high-vacuum connection;
2 – fore-vacuum connection;
3 – connection for holding pump.

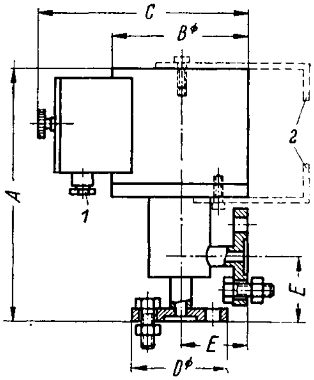

FIG. 2.1.42. Electromagnetic right-angle valve NW 10 (unit flange) and NW 20 (unit flange);
1 – Cable lead-in 7 mm (for 220 V~, 50 c/s);
2 – Two possibilities for applying retaining brackets.

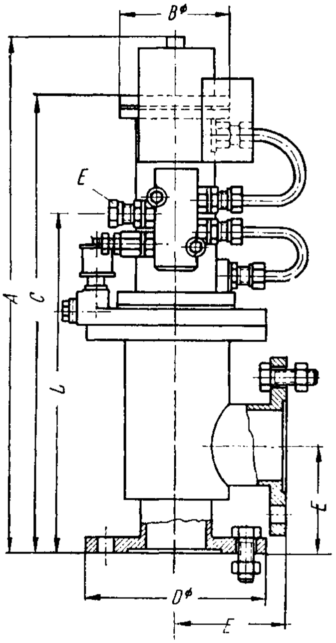

FIG. 2.1.44. Electro-pneumatic right-angle valve; E – screw coupling; DL 8 DIN 2353 for compressed-air connection.

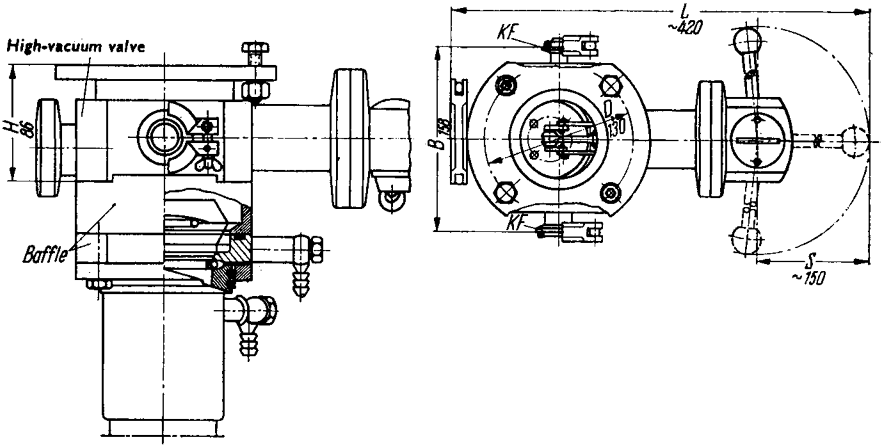

FIG. 2.1.43a. Bellows-sealed valve NW 65, mounted.

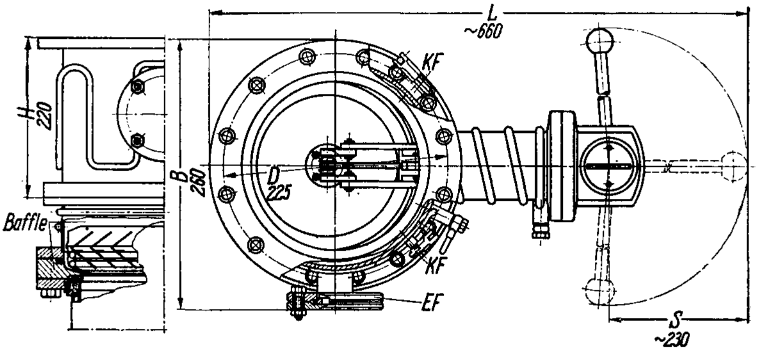

FIG. 2.1.43b. Bellows-sealed valve NW 150, mounted.

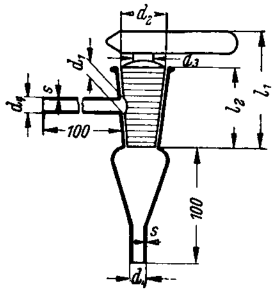

FIG. 2.1.45. Right-angle glass cone tap.

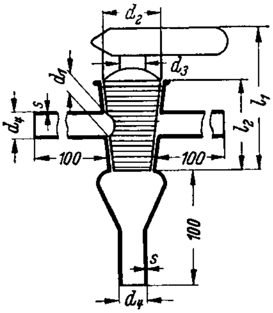

FIG. 2.1.46. Two-way tap, made of glass.

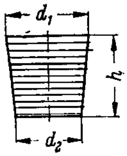

FIG. 2.1.47. Standard-type ground joint.

	Type	Fig. no. (see pp. 147 to 150)	Dimensions
2.1.3 Flexible Connections	Rotary flange (unit flange)	2.1.29	D_1 D_2 H
	Tombac pipe with small flanges L = 25, 50, 100 cm	2.1.31a	D smallest bending radius
	Tombac pipe with unit flanges L = 50, 100 cm	2.1.31b	D smallest bending radius
	PVC tubing with small flanges L = 50, 100 cm	2.1.30	D smallest bending radius
2.1.4 Valves	Air-inlet valve with small flange NW 10	2.1.32	H B
	Air-inlet valve, simple design, with small flange NW 10	2.1.33	B H
	Electromagnetic air-inlet valve with small flange NW 10 (opens if power supply fails)	2.1.34	
	Variable leak with small flanges NW 10	2.1.35	E H
	Packless diaphragm valve with small flanges	2.1.36	length
	Right-angle valve with small flanges	2.1.37a	a, b H
	Right-angle valve with unit flanges	2.1.37b	a b H h
	Flap valve with unit flanges	2.1.38	a, b H
	Plate valve, low overall height, with unit flanges	2.1.39	H
	Plate valve, low impedance, with unit flanges (on pump side NW is lower by one stage than indicated)	2.1.40	D_1 D_2 D_3 D_4 H
	Valve block	2.1.41	
	1-high-vacuum connection		NW
	pump connection		NW

NW 10	NW 20	NW 32	NW 50	NW 65	NW 100	NW 150	NW 250	NW 350	NW 500
		142	164						
		110	130						
		65	65						
30	40	55							
60	125	200							
			140	160	210				
			450	600	800				
30	40								
25	50								
110									
70									
56 closed: 42 open: 55									
30 open: 85									
100	120	150							
30	50	50							
144	210	210							
50	60	77	85	105	130	170			370
50	60	77	85	105	130	170			270
150	190	250	275	319	390	460			720
–	–	64	64	80	80	80			–
				110	135	170			
				220	270	340			
		105	105						
					70		125	250	
					110		250	350	
					210		280	400	
					210		375	490	
					150		200	260	
					100(UF)		250(UF)		
					65(UF)		150(UF)		

	Type	Fig. no. (see pp. 150/151 and 156/159)	Dimensions
	2-fore-vacuum connection		NW
	3-connection for holding pump		NW
	(UF = unit flange)		D_1
	(SF = small flange)		D_2 H
	Electromagnetic right-angle valve with unit flanges	2.1.42	A B C D E
	Electro-pneumatic right-angle valve with unit flanges	2.1.44	A B C D E L
	Bellows-sealed valve	2.1.43 a, b	
2.1.5 Taps and Ground Joints			
(a) Glass cone taps	Right-angle tap	2.1.45	d_1 l_1
	Two-way tap	2.1.46	l_2 d_2 d_3 d_4 s
(b) Standard type ground joints	Made of Ruhrglas (male and female ground joints) Made of Jena glass (female ground joint) Made of steel (male and female ground joint)	2.1.47	NS d_1 h d_2
(c) Ground-in ball-and-socket joints	Made of glass	2.1.48	code no. ball dia. tube i.d.
	Capillary ground joints		code no. ball dia. tube i.d.
	Forked clamp		code no. for ground-in ball-and-socket joint
(d) Surface grinding		2.1.49	flange dia. tube dia.
(e) Joint combination		2.1.50	

NW 10	NW 20	NW 32	NW 50	NW 65	NW 100	NW 150	NW 250	NW 350	NW 500
					20 (SF)		32 (SF)		
					20 (SF)		20 (SF)		
					70		125		
					100		250		
					210		230		
195	260	300							
105	125	125							
160	190	—							
75	90	120							
50	60	77							
		405	425	455	515	595			
		75	95	118	165	165			
		312	345	400	510	505			
		120	140	160	210	265			
		77	85	105	130	170			
		240	260	292	352	425			
Sizes									
6	8	12	20	35					
60	80	100	125	165					
40	50	70	80	100					
20	30	40	50	75					
10	14	20	25	35					
9·25	11	15·2	25	40					
1·25	1·5	2	2·5	2·5					
14·5/35	19/38	29/42	45/50	60/46	75/72				
14·5	19	29	45	60	75				
35	38	42	50	46	52				
11	15·2	24·8	40	50·8	64·6				
12/5	18/7	18/9	28/12	28/15	35/20	35/25	40/25	50/30	65/45
12	18	18	28	28	35	35	40	50	65
5	7	9	12	15	20	25	25	30	45
12/1	12/2	12/3							
12	12	12							
1	2	3							
1	2	3	4	5	6	7			
12/1 to 12/5	18/7, 18/9	28/12, 28/15	35/20, 35/25	40/25	50/30	65/45			
28	50	65							
13	26	40							

Type		Fig. no. (see pp. 157/158)	Dimensions
2.1.6 Transmissions			
2.1.6.1 Rotary Transmissions		2.1.51 2.1.52	code no. connection boring shaft dia. r. p. m. torque (mkg)
2.1.6.2. Current Lead-ins (see also Fig. 2.1.59–2.1.64)	Casting resin, 4-pole	2.1.53	
	Casting resin, 2-pole	2.1.54	
	Glass-to-metal seal	2.1.55	
	Glass-to-metal seal	2.1.56	
	Perbunan-insulated current lead in (with cooling water system)	2.1.57	
	Porcelain-to-metal current lead in (with cooling water system)	2.1.58	

* Maximum value for current lead-in at atmospheric pressure. Naturally, in the tensions.

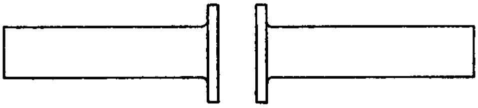

FIG. 2.1.49. Surface grinding.

Sizes				
G 27 threads M 26 × 1	G 27 K threads M 26 × 1	F 45 flange with groove	F 45 K flange with groove	F 65 K unit flange N W 65
27	27	45	45	70
8	8	12	10	24
100	3000	100	3000	3000
0·2	0·2	1	0·5	10

Load capacity to		High-vacuum connection	Boring
A	V		
4 × 1	220*	screw coupling	27
2 × 15	220*	screw coupling	27
35	3000*	flange with groove	45
120	3000*	screw coupling	46
250	40	screw coupling	27
800	500*	flange with groove	70

pressure range between 100 and 10^{-2} Torr, discharges occur at considerably lower

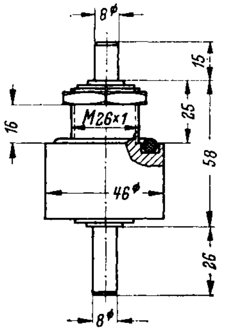

FIG. 2.1.51. Rotary transmission G 27.

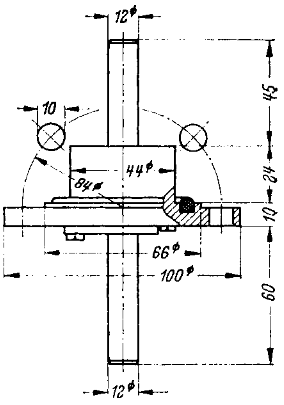

FIG. 2.1.52. Rotary transmission F 45.

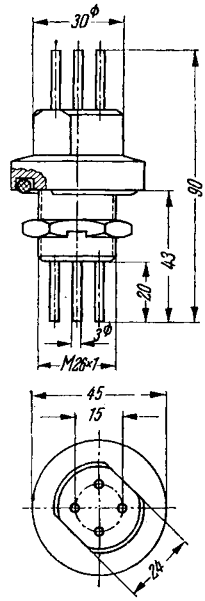

Fig. 2.1.53. Current lead-in of casting resin, 4-pole.

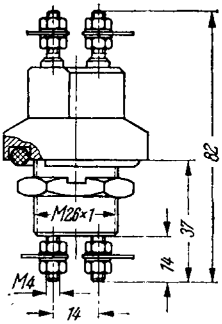

Fig. 2.1.54. Current lead-in of casting resin, 2-pole.

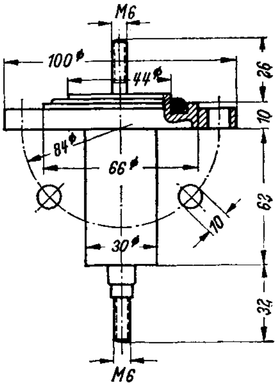

Fig. 2.1.55. Glass-to-metal seal for 35 amp.

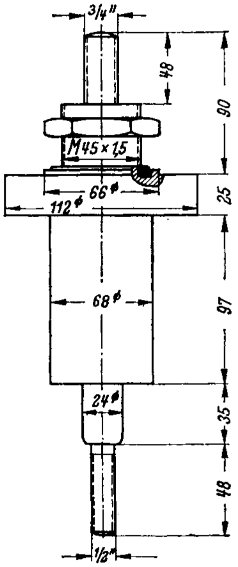

Fig. 2.1.56. Glass-to-metal seal for 120 amp.

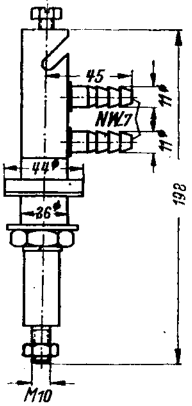

Fig. 2.1.57. Perbunan-insulated current lead-in (water cooled) for 250 amp.

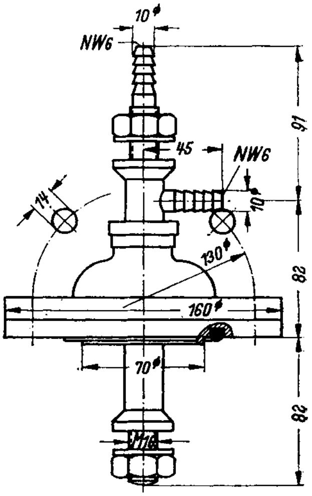

Fig. 2.1.58. Porcelain-to-metal current lead-in (water cooled).

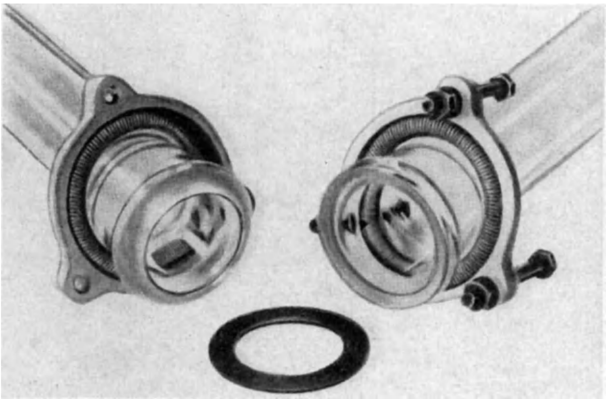

FIG. 2.1.48. Ground-in ball-and-socket joint (Schott).

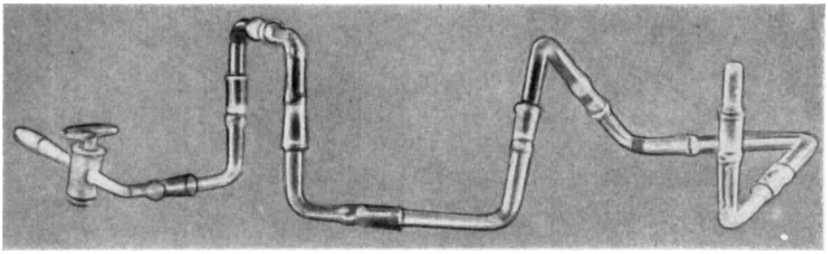

Fig. 2.1.50. Joint combination.

LVH.

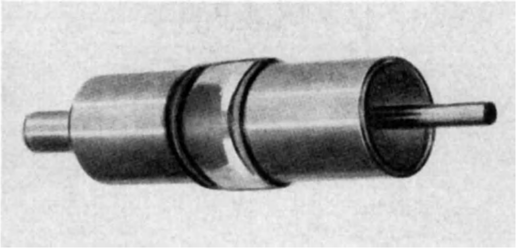

FIG. 2.1.59. Metal-to-glass current lead-in.

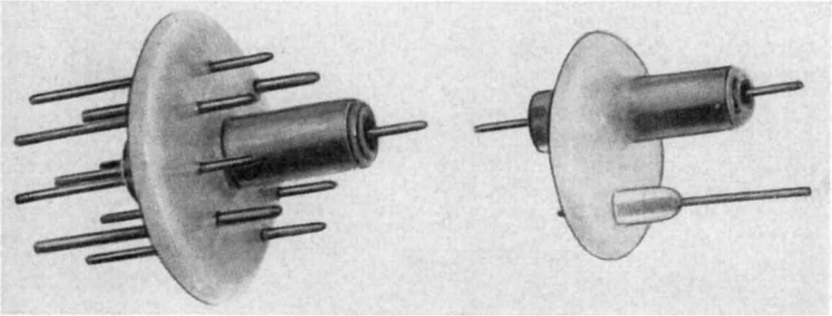

FIG. 2.1.60. Multiple current lead-ins using sintered glass: bakeable; suitable for high-vacuum work.

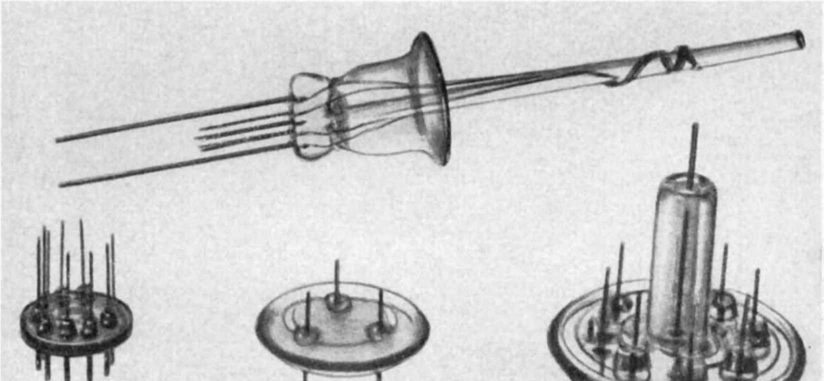

FIG. 2.1.61. Pinch seal (top) and various designs of pressed glass seals.

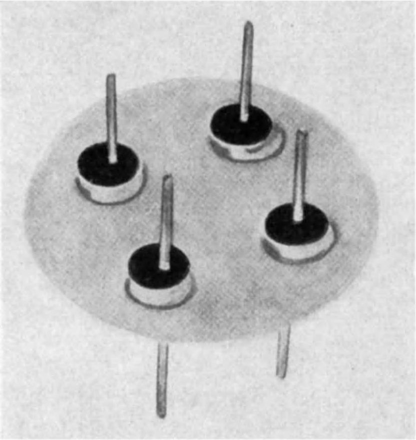

FIG. 2.1.62. Metal base with four glass-insulated current lead-ins.

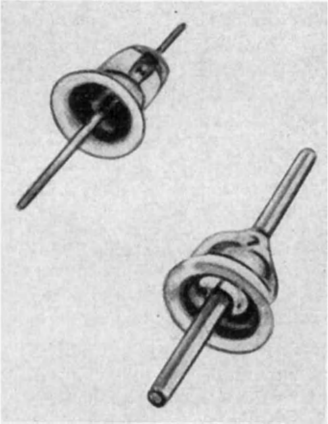

FIG. 2.1.63. Glass-insulated current lead-ins for soldering or brazing.

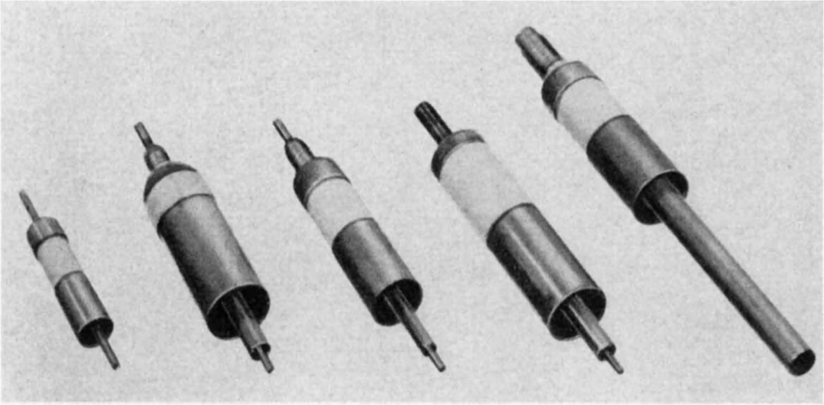

FIG. 2.1.64. Metal-to-ceramic current lead-ins with high insulation resistance. ($20°C \geqq 10^{14}\,\Omega$, $400°C \geqq 10^{10}\,\Omega$)

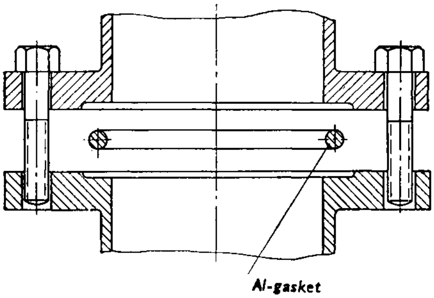

FIG. 2.1.65. Unit flange seal. Normal flange with aluminium ring.

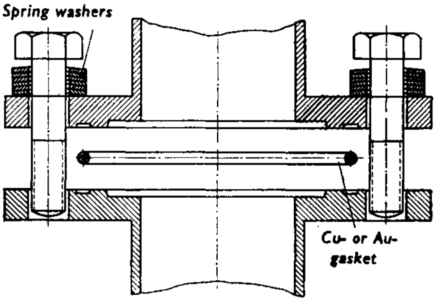

FIG. 2.1.66. Unit flange seal. Normal flange with additional groove and copper or gold ring gasket.

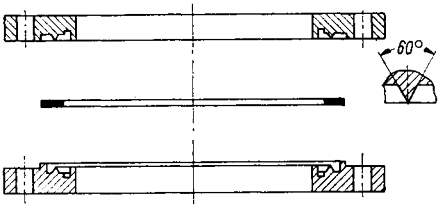

FIG. 2.1.67. Knife edge seal with flat copper ring gasket.

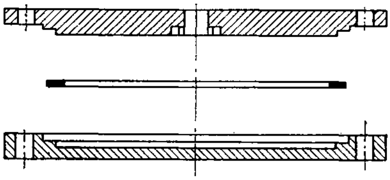

FIG. 2.1.68. Stepped seal with flat copper ring gasket.

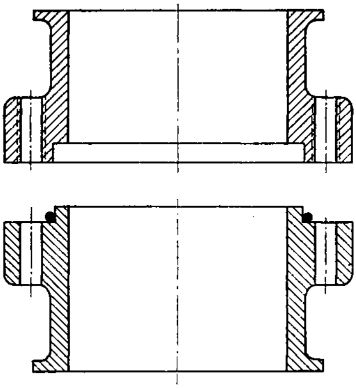

FIG. 2.1.69. Right-angle seal with gold ring gasket.

Type	Fig. no.
2.1.7 Sealing Rings (Gaskets)	
2.1.7.1 Metal Seals (see also chapter 1.11.4.1, page 135)	2.1.65–2.1.69 (see page 159)
2.1.7.2 Rubber Seals *○-ring seals* *for standard connections* 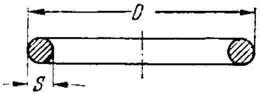 Fig. 2.1.70. ○-ring (sectional view).	2.1.70
Trapezoidal gaskets 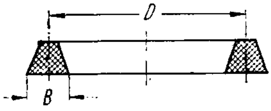 Fig. 2.1.71. Trapezoidal gasket (sectional view).	2.1.71

D×S in mm	For centring rings on small flanges NW	For bearing rings on unit flanges NW	For groove on DIN-flanges NW
16×3		10	
26×3		20	
25×5	10		
30×5			10
35×5	20		
40×5			20
45×5		32	
50×5	32		
60×5			32
63×5		50	
78×5		65	
85×5			50
95×5			65
107×5		100	
130×5			100
175×5			150
160×6		150	
266×8		250	
275×8			250

D×B in mm	For flanges NW
16× 4	10
26× 4	20
32× 4	25
42× 6	32
50× 7	40
60× 7	50
85× 8	65
105× 9·5	90
115× 9·5	100
140× 9·5	125
165× 9·5	150
220×10	200
270×10	250
330×10	300
380×10	350
416×10	400
550×10	500
640×10	600
820×12	800

Groove dimensions for DIN-flanges with ○-ring gaskets (see Fig. 2.1.72).

NW		DA	S	DI	B	D	DM	T
DIN flange	small flange							
	10	25	5	15	6	14	20	3·6
10		30	5	20	6	19	25	3·6
	20	35	5	25	6	24	30	3·6
20		40	5	30	6	29	35	3·6
	32	50	5	40	6	39	45	3·6
32		60	5	50	6	49	55	3·6
50		85	5	75	6	74	80	3·6
65		95	5	85	6	84	90	3·6
100		130	5	120	6	119	125	3·6
150		175	5	165	6	164	170	3·6
250		275	8	259	9·5	257·5	267	5·9

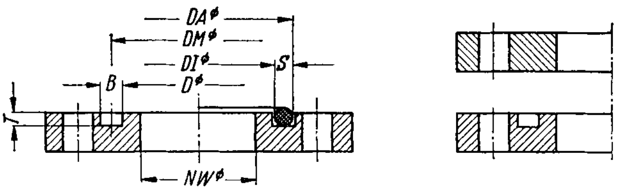

FIG. 2.1.72. Groove for ○-ring gasket.

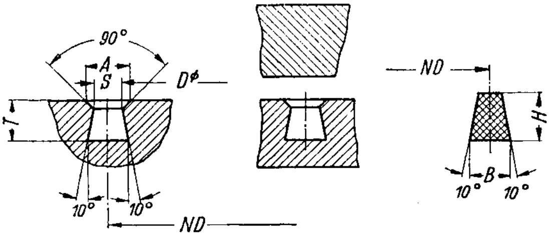

FIG. 2.1.73. Groove for dove-tail gasket.

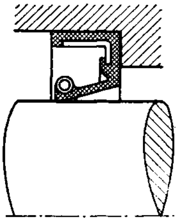

FIG. 2.1.74. Radial sealing gasket for shafts.

Groove dimensions for DIN-flanges with dove-tail gaskets (see Fig. 2.1.73).

NW	ND	Groove				Ring	
		A	D	S	T	H	B
10	16	5	13	3	4	4·8	4
20	26	5	23	3	4	4·8	4
25	32	5	29	3	4	4·8	4
32	42	7·5	37·6	4·4	6	7·2	6
40	50	9·5	44·7	5·3	7	9	7
50	60	9·5	54·7	5·3	7	9	7
65	85	10	79	6	8	9·6	8
90	105	11	97·7	7·3	8	10	9·5
100	115	11	107·7	7·3	8	10	9·5
125	140	11	132·7	7·3	8	10	9·5
150	165	11	157·7	7·3	8	10	9·5
200	220	13	212·5	7·5	10	12	10
250	270	13	262·5	7·5	10	12	10
300	330	13	322·5	7·5	10	12	10
350	380	13	372·5	7·5	10	12	10
400	416	13	408·5	7·5	10	12	10
500	550	13	542·5	7·5	10	12	10
600	640	13	632·5	7·5	10	12	10
800	820	14·5	811·2	8·8	12	14·5	12

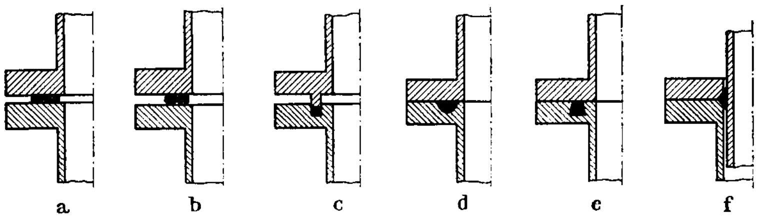

FIG. 2.1.75a-f. Various flange seals.
(a) – flat seal; (b) – Sicromal seal; (c) – seal with rectangular groove; (d) – seal with semi-circular groove; (e) – seal with dove-tail groove; (f) – seal with triangular groove.

2.2 High Vacuum Process Technology

(See Bibliography)

2.3 Materials, Vapour Pressures, Boiling Points, Melting Points, Gas Permeability, etc.

2.3.1 Materials

2.3.1.1 Materials Testing

(See Bibliography)

2.3.1.2 Metals

TABLE 2.3.1. Suitability of various materials for vacuum systems. Temperature range: —30 to + 100 °C. Materials, suitable for the construction of vacuum containers, are listed in column 1–5; for inner parts used in vacuum systems up to operating pressures of 10^{-5} Torr, metals generally can be used.

Pressure range	Materials			
	Forged and drawn iron, alloyed steels, no-cast iron, stainless steel 1	Grey pig iron 2	Copper, copper alloys, rolled and drawn 3	Non-iron castings 4
Coarse vacuum	+	+	+	+
Medium vacuum	+	+	+	+
High vacuum up to 10^{-5} Torr	+	+	+	—
High and ultra-high vacuum ($\leq 10^{-6}$ Torr)	special degassing procedures required	only after highly specialized treatment	special degassing procedures required	—

Pressure range	Materials						
	Aluminium 5	Quartz 6	Ceramics 7	Resins 8	Rubber and rubber-like sealing materials 9	Wood and Iporka for inner parts 10	Graphite for inner parts 11
Coarse vacuum	+	+	+	+	+	+ —	+
Medium vacuum	for inner parts; for containers only by special welding methods	+	+	+	+	—	+
High vacuum up to 10^{-5} Torr		conical greased joints	only dense material can be used	—	gas free special types	—	only after careful degassing
High and ultra-high vacuum ($\leq 10^{-6}$ Torr)	special degassing procedures	permanently sealed	permanently sealed after metallizing	—	gas free special types	—	—

TABLE 2.3.2. Gas contents in commercial materials (examples taken from very pure samples)

	H_2	CO	CO_2	N_2	SO_2	Total amount in ccs (NTP) per 100 g metal
	per cent of total amount of gas					
"Mond"-nickel*	24·7	72·4	2·9	–	–	113
Cubic-nickel*	3·5	90	2·3	4·2	–	482
Electrolytic nickel*	78·9	21	0·00	–	–	7·9
Electrolytic copper*	39·5	49·7	–	–	10·9	8·0
Electrolytic zinc†	100	–	–	–	–	20–60††
Tungsten**	small amount	30–40	–	50–60	–	0·05
Molybdenum**	small amount	30–40	–	50–60	–	0·5
Tin*	47	45	8	–	–	5–12
Aluminium*	71·7	15·4	2·5	10·4	–	7·03

* After W. HESSENBRUCH, *Z. Metallk.* **21**, 46 (1929).

† After RÖNTGEN and MÖLLER, *Metallwirtsch.* **11**, 685 (1932) and BURMEISTER and SCHLOETTER, *Metallwirtsch.* **13**, 115 (1934).

** NORTON and MARSHALL, *Trans. Amer. Inst. Min. Metallurg. Engrs.*, February, 1932.

†† The hydrogen content in electrolytic zinc is proportional to the square root of the electrolytic current.

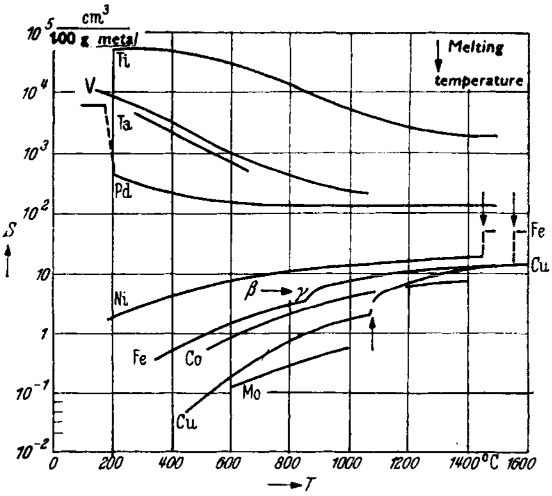

FIG. 2.3.1. Hydrogen sorption of metals as a function of temperature at atmospheric pressure (Gas amount S in ccs (NTP) per 100 g).

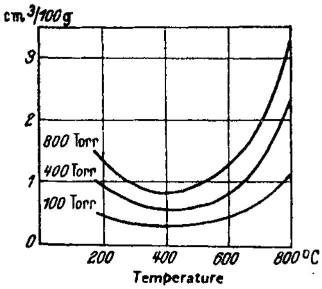

FIG. 2.3.2. Solubility of oxygen in silver for various temperatures and pressures (after STEACIE and JOHNSON).

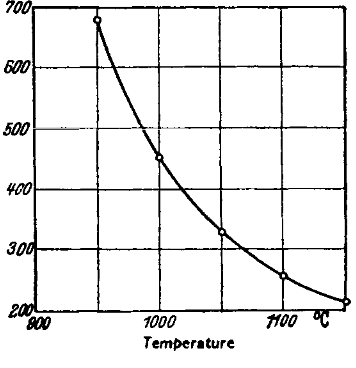

FIG. 2.3.3. Solubility of nitrogen in molybdenum at 760 Torr as a function of temperature (after SIEVERTS and BRUNING).

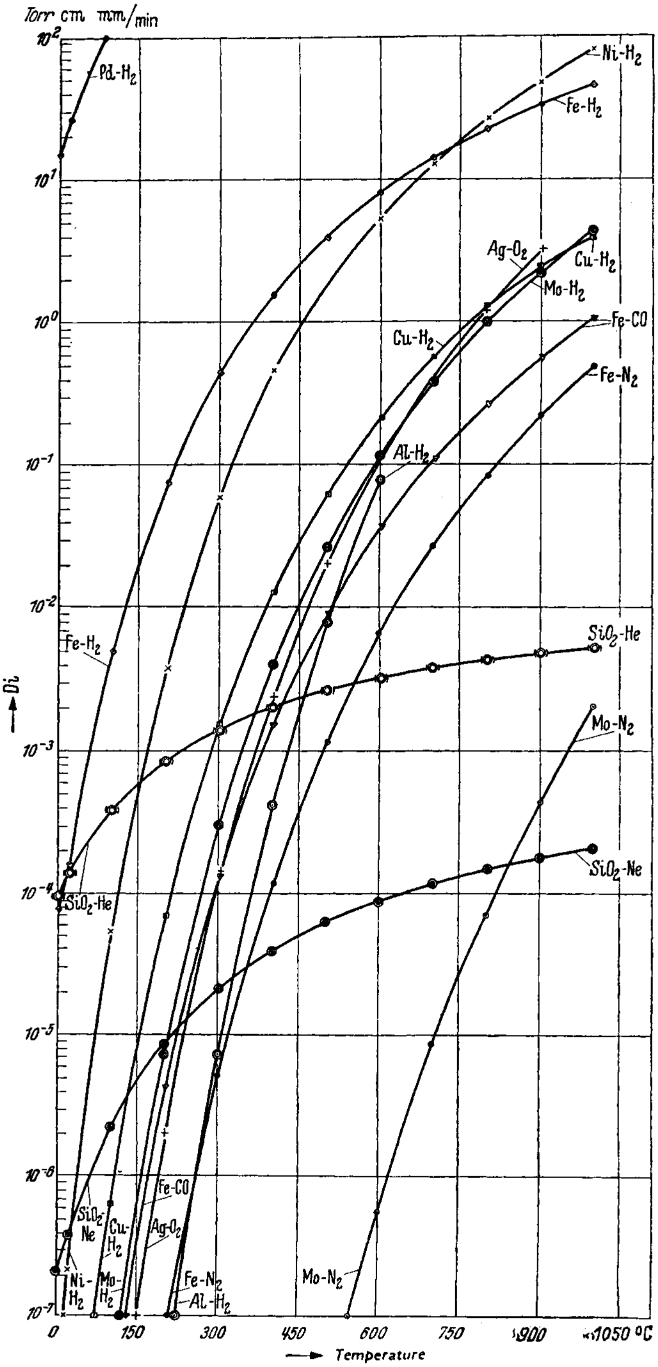

FIG. 2.3.4. Gas permeability for walls made of different materials as a function of temperature, represented by the function

$$D_i = f(T);$$

D_i is the pressure increase in a closed container of 1 cc volume, 1 mm wall thickness, when the gas permeates through 1 cm² surface area (after H. SCHWARZ).

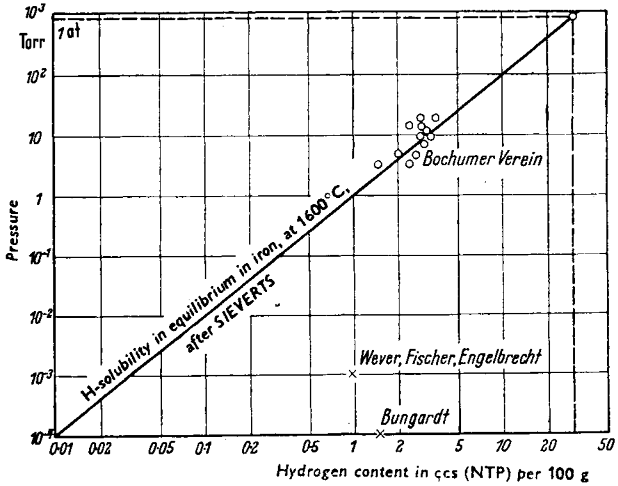

FIG. 2.3.5. Hydrogen content of iron after vacuum treatment as a function of pressure (after various authors, taken from a summary by TIX).

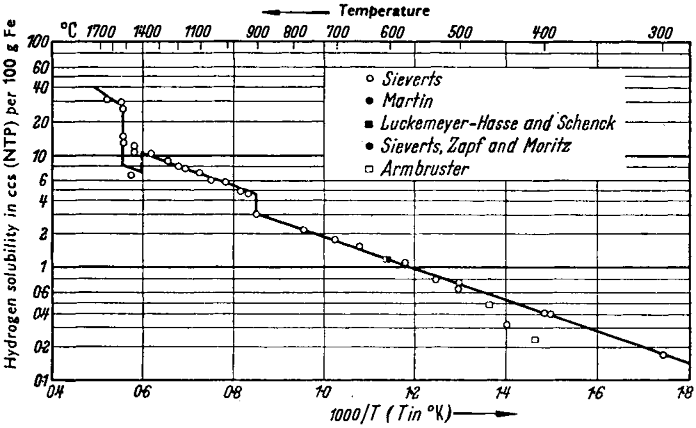

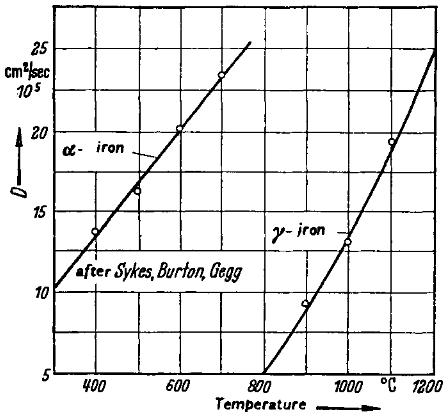

FIG. 2.3.6. Solubility and rate of diffusion D of hydrogen in iron as a function of temperature (after several authors as named in the graph).

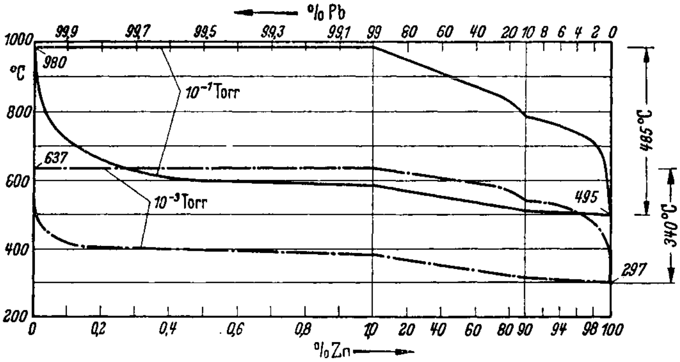

FIG. 2.3.7. Evaporation and dew point curve for lead-zinc alloys (after A. LANGE and L. MÜLLER). The lower curve of each group shows the composition of the melt, whilst the upper curve shows the composition in the vapour phase at the pressure of 10^{-3} Torr and 10^{-1} Torr, respectively. The graph shows that, for example at a pressure of 10^{-1} Torr and at 700 °C with a lead content of 99·9 per cent in the liquid phase the lead content in the vapour phase is only about 1 per cent, whilst at a pressure of 10^{-3} Torr and at a temperature of 400 °C with lead content in the liquid phase of 99·8–99·5 per cent the lead content in the vapour phase is extremely small and cannot be measured. In this way, therefore, practically absolutely clean zinc can be evaporated.

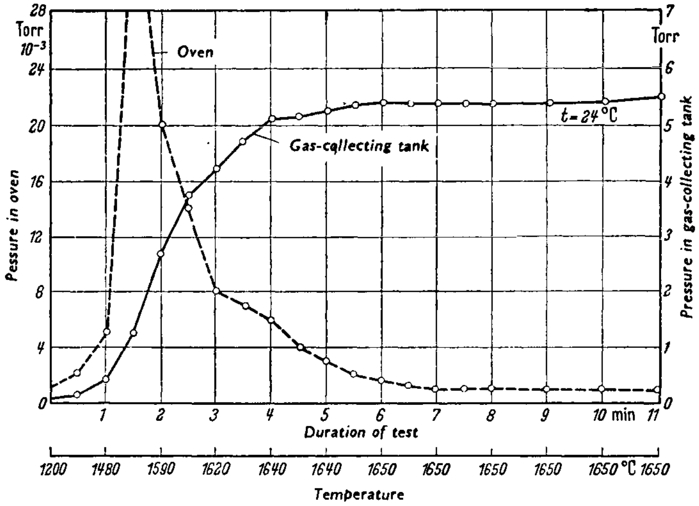

FIG. 2.3.8. Temperature and evolution of gases (after KORDON and SCHMID). In order to determine the amount of gas dissolved in a metal, the so-called hot extraction method is frequently applied, i.e. the metals are melted in an evacuated container; the partial pressure of the gas increases at first in the oven. The evolved gases are pumped by a diffusion pump and forced into a gas collecting tank. Here the gas pressure increases and the collected gases can be separately analysed. The graph shows the pressure and temperature in the oven and in the gas-collecting tank during one single hot extraction procedure.

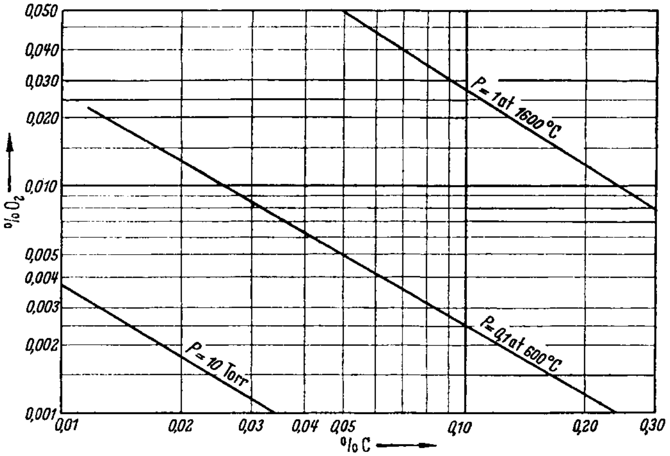

FIG. 2.3.9. Carbon–oxygen equilibrium in steel (after WINKLER).

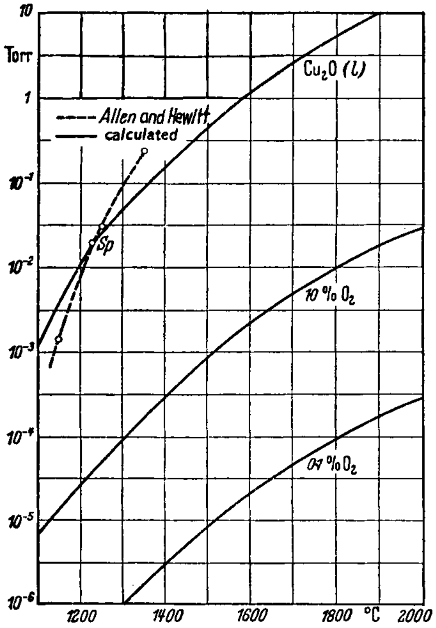

FIG. 2.3.10. Dissociation pressures of Cu_2O and solubility of Cu_2O in Cu (after WINKLER) as a function of temperature.

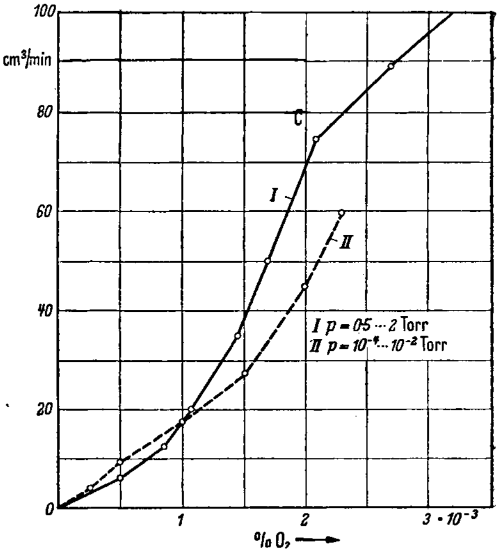

FIG. 2.3.11. Gas desorption as a function of the O_2-content of Cu in different pressure ranges (after WINKLER). Crucible material: graphite; weight of melt: 10 kg; temp. = 1200 °C.

Metal	Type of metal and composition in % weight	Degassing temperature [°C]	Approx. gas content* $\left[\frac{cm^3 (NTP)}{100 g metal}\right]$
Al	97·6 Al; 1·2 Fe; 1·2 Si	1200	4·6
	99 Al; 0·65 Fe; 0·07 Si	1200	12–17
C	Graphite, non-degassed	2150††	> 27
	Graphite, first predegassed in H_2 at 1500 °C, then in vacuum at 1800 °C	up to 1300	
		1300–1600	
		1600–1900	
		1900–2110	
		2150	0·15–1·23
Cu	Refined Cu	1250	0·7–2·7
	Electrolytic Cu	1250	7·9
	Electrodes	degassed by h. f.	0·4–2·2
	OFHC-Cu†††		O_2: 0·35 H_2: 1·3
	Vacuum melted Cu		O_2: 0·27 H_2: 0·11
Fe	Electrolytic 0·02 C; 0·02 Mn; 0·02 Si	1550	21
	Armco-0·02 C; 0·05 Mn; —Si	1550	54
	Swedish Fe 0·02 C; —Mn; —Si	1550	122
	Swedish iron	1380	23
	Cast iron (0·17 C; 0·37 Si; 0·47 Mn; 1·74 Cr; 0·69 Mo)	1370	15·5
	New iron (0·05 C; 0·008 Si; 0·18 Mn)†	1370	8·2
	Ingot iron with small C-content		O_2: 56–84
	Ingot iron after H_2-degassing at 1500 °C		O_2: 2·8
	Electrolytic iron		O_2: 25–34
	Sintered iron		O_2: ca. 17
	Vacuum melted pure iron		O_2: 4·2–8·4
	Fe with 0·25 % Al		O_2: 2·8
	Fe with 0·5 % Al		O_2: trace
Mo	Sheet, degassed in H_2 or in vacuum at 1150 °C		1·5
	Sheet, non-degassed		6·0
	Chemically cleaned electrodes	< 1000	
		1000–1200	
		≧ 1200	
		1760††	0·09–0·8
Ni	Cube, commercial	1470	482
	"Mond"-Ni	1470	113
	Electrolytic Ni	1470	7·9
	Electrolytic Ni	1090 (7 hrs)	0·028
		1100 (15 hrs) + 1200 (4 hrs)	1·93
	Electrodes	degassed by h. f. ***	4–10
	Commercial "Grade A"-nickel		O_2: 1·4–2·8
Sn	—	—	5–12
W		2300–2430††	0·03

* Total gas content, related to 760 Torr and 0 °C, if not otherwise stated. † Molten by h. f. ** Frequently obtained. *** Max. degassing temperature in vacuum without appreciable evaporation (gettering effect):

of metals (see also Dushman)

Approx. gas content* $\left[\frac{cm^3 (NTP)}{cm^3 metal}\right]$	Approx. gas composition [%-vol] H_2	CO	N_2	O_2	CO_2	Author
0·13	72**	12	11	1	5	Hessenbruch
0·34–0·46	77–88**	8–17	–	–	3–6	
> 0·6						
	52	44	–	–	4	Norton
	30	48	–		6	
	11	13	71		5	
		9	87		4	
0·003–0·027	mostly H_2, CO, N_2			–	little CO_2	
0·07–0·24	7–29	20–38	5–14	SO_2: 33–61	–	Hessenbruch
0·7 (–1·2)	39·5	49·7	–	SO_2: 10·9	–	
0·04–0·2	62–100				0 to 38	Andrews
						Morse
						Morse
1·7	0·0010*		0·0037*	0·01*		Hessenbruch
4·3	0·0007*		0·0035*	0·06*		
9·6	0·0012*		0·0029*	0·15*		
1·8	little H_2	mostly CO and N_2			little CO_2	Norton
1·3	little H_2	mostly CO and N_2			little CO_2	
0·65	little H_2	mostly CO and N_2			little CO_2	
						Wise
						Larsen
						Wise
	ca. 73				27	Andrews
	ca. 86				14	
	mostly H_2	mostly CO	mostly N_2			Norton
0·01–0·1	0–17	0–76	22–98		0–9	[ ] = frequently cited values
	[0]	[15–36]	[> 60]		[3–6]	
43	3·5	90	4·2		2·3	Hessenbruch
10	24·7	72·4	–		2·9	
0·7	78·9	21	–	–	0·00	
–	2–40	–	6–11		60–90	Norton
0·03–0·18						
0·3–0·9	88–94				6–12	Andrews, Smithells
						Wise
–	47	45	8	–		Hessenbruch
0·004–0·008	3	30	67			Norton

as a consequence of reaction of H_2O upon Al. †† Temperature for which practically complete degassing is 1050 °C. ††† Oxygen-free copper.

TABLE 2.3.4. Predegassing temperatures and predegassing timesin vacuum and in hydrogen of the more important electrode materials (after ESPE)

Material	Form	Used for	High vacuum (8 hrs degassing) [°C]	Hydrogen normal		Complete degassing †† at [°C]
				[°C]	[min]	
W	shaped pieces*	anti-cathodes (prior to sealing-in into copper)	*ca.* 1800	–	–	2300-2430 (high vacuum)
	wire	springs, hot cathodes and grids	should not be predegassed			
Mo	sheet	anodes	950	1200	30 ⸸⸸	1760 †
	wire	grids	900	1000	30 ⸸⸸	1900 §
		springs	should not be predegassed			
Ta	sheet wire	anodes grids	$>$ 1800 ($<10^{-3}$ Torr)	H_2-degassing not permissible		$>$ 2000 ††† §§ (high vacuum)
	wire	springs	should not be predegassed			
Pt	sheet	–	900-1000	950	5–10	
(Pt–Ir, Pt-Ni)	wire	oxide-cathodes	should not be predegassed			
Ni and Ni-alloys without Cu		all electrodes, except support rods for low operating temperatures	750–950***	950–1050	10–15	
Fe and Fe-alloys without Cu		as above	950–1000	950**, ⸸⸸	5–10	
		with dense packing (danger of sticking)		750	5–10	
Fe, Kovar		glass-to-metal seals	850	800- 900 900–1000	127 37 ⸸	
Cu and Cu-alloys without Zn or Sn		electrodes and parts thereof, except supports and copper anodes exposed to the atmosphere	500–550	should be avoided for normal Cu (permissible for OFHC copper)		

TABLE 2.3.4. (continued)

Material	Used for	High vacuum (8 hrs degassing) [°C]	Hydrogen normal		Complete degassing †† at [°C]
			[°C]	[min]	
Cu, Constantan	lead-ins	up to 600	up to 900	15	
Cu-alloys with low melting components (Zn, Sn)	non sealed-off vessels on vacuum pump	should not be predegassed			
Al	cold cathodes	should not be predegassed			
Carbonized Ni	anodes	950	H_2 to be avoided (formation of hydrocarbons!)		
P2-sheet (Al-clad Fe)	anodes, cooling fins	should not be predegassed			
Chromium oxidized metals (W, Ni)	grids and anodes	–	950	15	
Graphite	anodes	1500–1800	H_2 to be avoided		2150

* Non-copper-plated tungsten targets should not be degassed when C is present (formation of carbide!). C may be present in the graphite copper-casting oven.

† $^1/_2$–1 hr in extremely pure H_2 or longer in high vacuum.

** Components up to 1370°C.

†† After NORTON.

*** Max. degassing temperature of Ni in vacuum 1050°C, otherwise Ni volatilizes.

††† All Ta-parts should be kept at the same temperature.

⸸ In moist H_2, then degassing in vacuum shortly before sealing into glass.

⸸⸸ In pure dry hydrogen.

§ For extremely pure electrodes, as used in glow-discharge stabilizers, filled with extremely pure noble gas (and deliberate sputtering of the electrodes for the purpose of gettering). Mo-material must be degassed by means of h. f. at a temperature of 1900°C in a high vacuum of less than 5×10^{-5} Torr for not less than 6 hrs (TODD).

§§ After MAMULA, VACEK:

Desorption of H_2 at 600–1200°C,
Desorption of CO at 1700–2000°C,
Desorption of N_2 at 1900–2400°C.

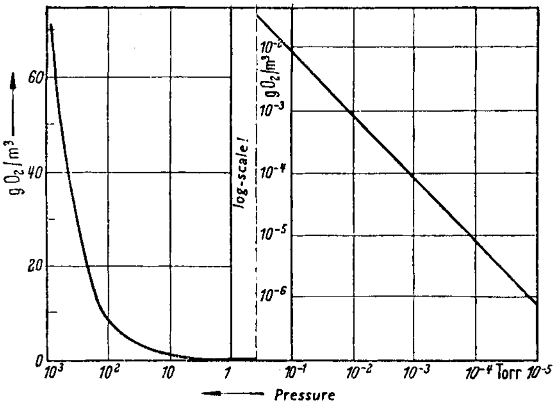

FIG. 2.3.12.

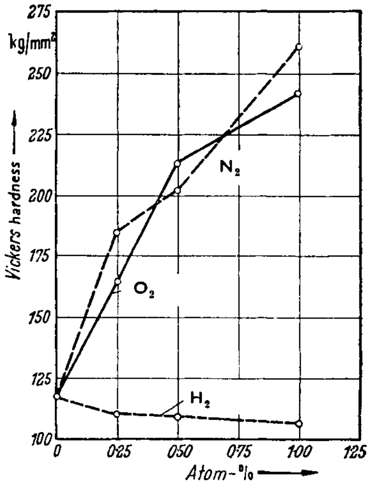

FIG. 2.3.13.

FIG. 2.3.12. Reactive amount of O_2 as a function of pressure at 1000 °C in the oven (after DEISINGER). The protection of metals against undesired oxidation during temperature treatment in vacuum depends on the amount of oxygen available, which may be detrimental.

FIG. 2.3.13. The influence of O_2, N_2 and H_2-content on the hardness of titanium (after R. J. JAFFEE and I. E. CAMPBELL).

TABLE 2.3.5. Purification of metals by evaporation in vacuum (after CRITES)

Mode and degree of separation	Basic metal	Liberated impurities
(a) Separation almost complete. Impurities in the distillate	Be	Ca, Ba, Mg
	Fe	S, P, Cu, Mn
	Cu	Ag, Bi, Pb, Zn, Co
	Al	Mn, Ag, Mg, Na
(b) Separation almost complete, but impurities in the residue	Fe	W
	Be	C, Fe, Ni
	Cu	Au
	Al	Fe, Ti, Cu
(c) Separation incomplete. Impurities in the distillate	Ni	Cu
	Fe	Cr
	Cr	Al, S
	Cu	S, Sb
(d) Separation incomplete. Impurities in the residue	Ni	Cr
	Fe	Ni, Co, C, Si
	Be	
	Al	Si
	Cr	Fe
	Cu	Ni, O_2

TABLE 2.3.6. Oxygen partial pressures above metal-oxides (after CRITES)

$2\,MnO_2 = Mn_2O_3 + {}^1/_2\,O_2$

655 °K	22·8 Torr
751	200
1213	760

$3\,Mn_2O_3 = Mn_3O_4 + {}^1/_2\,O_2$

1213 °K	159 Torr
1363	760

$3\,Fe_2O_3 = 2\,Fe_3O_4 + {}^1/_2\,O_2$

1373 °K	5 Torr
1473	9
1573	59
1673	353
1773	454

$NiO = Ni + {}^1/_2\,O_2$

1273 °K	2 Torr
1373	5·5
1473	13

$SiO_2 = Si + O_2$

2000 °K	10^{-12} Torr

$TiO_2 = Ti + O_2$

2000 °K	10^{-18} Torr

$Al_2O_3 = 2\,Al + {}^3/_2\,O_2$

2000 °K	10^{-50} Torr

TABLE 2.3.7. Gas-sorption of vacuum-melted Ni at different gas pressures

O_2-pressure (Torr)	O_2 (%)	N_2-pressure (Torr)	N_2 (%)	H_2-pressure (Torr)	H_2 (%)
0·001	$1{\cdot}5 \times 10^{-3}$	27	$1{\cdot}7 \times 10^{-4}$	2·2	7×10^{-5}
0·02	4·0	50	3·0	6·7	22
0·10	15·0	760	8·0	33·2	34

2.3.1.3 Glass and Quartz

Devices and large systems used in modern vacuum technology must be mechanically rigid. This deserves special attention in the case of individual constructional elements of large dimensions. Vacuum systems, therefore, are built completely of metals. Glass (and other insulation materials) is used for vacuum tight lead-ins and supports. It also finds wide application in the design of vacuum gauge heads (e.g. MCLEOD manometers, ionization gauges, etc.) which, in turn, are joined to the metal system by means of suitable glass-to-metal seals. More recently, however, particularly in connection with the production and measurement of extremely low pressures in ultra-high vacuum technique, small systems made entirely of glass seem to have assumed more importance. In such systems all joints are made as permanent seals.

In line with such applications as those just mentioned, vacuum technology can confine itself — in contrast to other glass users, e. g. in the valve and lamp industry — to comparatively few types of glasses. For economic reasons commercially available standard glasses are used as much as possible, and special glasses should be avoided.

In Table 2. 3.8, a number of glasses are listed, which are of interest in vacuum technology. No claim is made to completeness.

TABLE 2.3.8. Glasses of importance in vacuum technology

	Type of glass	Code no.	Make	$\alpha \times 10^7/^\circ C$ (temperature range in °C)	Transformation temperature °C	Softening point * °C	Working point † °C
Apparatus and bulb sealing glasses	Duran 50	8330	Schott	32 (20–300)	530	815	1260
	Supremax	2955	Schott	37 (20–300)	715	938	1220
Essentially tungsten sealing glasses	Suprax	3891	Schott	40 (20–300)	553	793	1195
	Supremax 56	8409	Schott	41 (20–300)	745	960	1245
	Lead-wrapping glass	8212	Schott	41 (20–300)	495	742	1138
	Tungsten glass	1646	Schott	42 (20–300)	515	754	1095
	Wrapping glass for W-seals	362 a	Osram	42 (0–300)	480	850	1230
	Bulb glass	742 c	Osram	44 (0–300)	770	1027	1260
	Wrapping glass for W-seals	712 b	Osram	44 (0–300)	530	875	1240
Essentially sealing glasses for Molybdenum and for Fe–Ni–Co alloys	Sealing glass	EW	Wertheim	44 (20–400)	505	565	
	Universal glass ††	8447	Schott	48 (20–300)	465	720	1031
	Apparatus glass	2877	Schott	49 (20–300)	560	794	1190
	Mo-sealing glass	906 c	Osram	49 (0–300)	510	810	1100
	Mo-glass	1639	Schott	50 (20–300)	531	736	1025
	Mo- and Fe-Ni-Co-glass	1447	Schott	51 (20–300)	528	725	1080
	Sealing glass	8482	Schott	51·5 (20–300)	488	738	1058
	Mo- and Fe-Ni-Co-glass	8243	Schott	52 (20–300)	485	715	1040
	Kovar-sealing glass	911 b	Osram	53 (0–300)	500	766	1060

* $\eta = 10^{7.6}$ P † $\eta = 10^4$ P

** TWB = thermal shock resistivity

(in the order of increasing thermal expansion coefficients)

$T_{\varkappa 100}$ § °C	Chemical Resistivity hydrol. class (DIN 12111)	acid class (DIN 12116)	caustic class (DIN 52322)	Density g/cm^3	Chemical composition	Application and special properties
248	1	1	2	2·23	Pure borosilicate glass	For thick-walled containers, TWB** high, working temperature up to 490°C
517	1	–	3	2·47		Continuous operation up to 700°C. For working use oxidizing flame.
245	1	1	2	2·31		Suitable for sealing to tungsten and certain ceramic materials
616	1	3	3	2·59		For tungsten sealing; $T_{\varkappa 100}$ is high!
401	2	1	3	2·31	Lead-borosilicate glass	Wrapping glass for tungsten seals. High electrical insulation
252	3	2	3	2·27		Wrapping glass for W-seals, but $T_{\varkappa 100}$ low
380	1	3	3	2·33	Lead-borosilicate glass	
580	1	3	3	2·67	Borophosphate glass	High thermal resistivity
306	1	2	3	2·29	Borosilicate glass	
320	1					For sealing to Mo, Fernico and Kovar; for vessels for storage of liquid He
264	–	3	3	2·26		
195	1	1	2	2·40	Borosilicate glass	High chemical resistivity, TWB ** high, universal glass, working temperature up to 500°C
274	1	3	3	2·56	Contains lead	
232	4	2	3	2·30		(Soft) wrapping glass for Mo
197	1	1	3	2·48		Only for low electrical insulation
416	4	3	3	2·34		For sealing to Mo, Nilo-K, Vacon 10/12; $T_{\varkappa 100}$ high, but chemical resistivity medium
342	–	–	–	2·26		High electrical insulation
360	5	3	3	2·31	Lead-free	Vacon sealing glass, high electrical insulation

†† Between Schottglass 2877 and Fe-Ni-Co-alloys.

§ $T_{\varkappa 100}$ temperature for $\varrho = 10^8\ \Omega$ cm.

TABLE 2.3.8.

	Type of glass	Code no.	Make	$\alpha \times 10^7$/°C (temperature range in °C)	Transformation temperature °C	Softening point* °C	Working point† °C
Soft glasses for chemical apparatus and for sealing to metals and ceramics	Apparatus glass	R	Wertheim	63 (20–400)	570	620	
	Standard glass for thermometers	NW	Wertheim	89 (20–400)	540	600	
	Standard glass	16^{III}	Schott	90 (20–300)	543	712	1000
	Apparatus glass	AR	Ruhrglas	91 (20–300)	512	716	
	Lead glass	8095	Schott	95 (20–300)	425	628	974
	Apparatus glass	GW	Wertheim	95 (20–400)	525	580	
	Glass for tubes	AW	Wertheim	95 (20–400)	525	580	
	Sealing glass	LW	Wertheim	97 (20–400)	520	570	
	Lead glass 28%	123a	Osram	97 (20–300)	410	670	970
	Sealing glass	MW	Wertheim	99 (20–400)	420	460	
	Bulb glass	584d	Osram	102 (0–300)	512	743	1020
	Standard glass	905c	Osram	102 (0–300)	500	730	1012
		MGR	Ruhrglas	106 (20–300)	481	671	
	Glass for tubes	LR-weiß	Ruhrglas	109 (20–300)	487	669	

* $\eta = 10^{7.6}$ P † $\eta = 10^4$ P

(continued)

$T_{\kappa 100}$**	Chemical Resistivity			Density	Chemical composition	Application and special properties
°C	hydrol. class (DIN 12111)	acid class (DIN 12116)	caustic class (DIN 52322)	g/cm^3		
256	1	—	—			Sealing-in glass for Vacon 10, 12, 20, Frequenta 221 (Steatite)
165	3	—	—			Standard glass for thermometers, and sealing glass for Pt, Vacovit 501, Steatite Gl 9
165	3	1	2	2·58		For thermometers and for sealing to Pt, Ni-Fe-alloys, and ceramics
—	3	1	2			
311	3	3	3	3·02		Sealing glass for Pt and the Vacovit alloys 485, 426
205	3	—	—			Sealing glass for CR 25, Vacovit 501, 511, Steatite Gl 9
230	3	—	—			General glass for apparatus, glass for tubes
250	3	1	1		Pb-free	Glassware, sealing glass for CR 25, Vacovit 426, 511, 025, 540
322	1	3	3	3·03		Sealing glass for Dumet-wire, high electrical insulation
280	3	—	—		contains Pb	Sealing glass for Pt, Pt-"Substitute", Ni-Fe-alloys, Dumet-wire
230	3	2	2	2·56		Soda lime glass
175	4	2	2	2·54		
169	4	1	2			
165	(5)	2	2			

** $T_{\kappa 100}$ temperature for $\varrho = 10^8\ \Omega$ cm.

TABLE 2.3.9. Properties of glasses used in valve technology

Designation	Soft glass		Hard glass a) Borosilicate glass b) Alumoborosilicate glass	Quartz
	Pb-glass	a) Soda glass b) Thuringia glass		
SiO_2-content	55–60 %	~ 70 %	~ 70–80 %	100 %
Important constituent	up to 30 % PbO	a) alkali and alkali-earth oxides (~ 20 %) b) as a) + 4 % Al_2O_3	a) up to 20 % B_2O_3 b) as a) + Al_2O_3	
Application	sockets	bulbs apparatus	sockets bulbs	
$\alpha \times 10^7$ deg^{-1} (20–300 °C)	80–90		30–50	6
Transformation temperature in °C	400–450	500–600	450–750	1050
$T_{\varkappa 100}$ in °C	300–350	150–250	200–600	600
Dielectric constant (20 °C)	7–16	7–8	~ 5	3·8
$\tan \delta \cdot 10^4$ at 1 Mc/s (20 °C)	5–120			2
λ in cal/(deg cm sec) (20 °C)	0·0016–0·0030			0·0033
Tensile strength in kg/mm² (20 °C)	3·5–8·5			7–12
Compression strength in kg/mm² (20 °C)	60–120			160–200
Electrical breakdown strength in kV/mm (20 °C)	16–40			25–40

TABLE 2.3.10. Some glass solders

Make	Solder no.	Composition in %						$\alpha \times 10^7$ deg^{-1}	Soldering temperature in °C
		PbO	B_2O_3	ZnO	Al_2O_3	SiO_2	Na_2O		
Telefunken	T 209	78	14·8	–	1	5	1·2	90	410
Gen. El. Co., Wembley, England	GSS 38	80	20	2·5	–	–	–	96	475
	GSS 34	70	30	2·5	–	–	–	80	525
	GSS 1	84	16	8	–	2	–	92	500
Fischer	F 3	73·8	11·2	–	0·2	14·3	0·5	90	540
Schott	8435	Alumoborosilicate glass containing Li- and Pb-oxide						58 (20–300 °C)	549*
	8461	Lead-borate glass + SiO_2						83 (20–300 °C)	485*
	8468	Lead-borate glass + zinc oxide						124 (20–300 °C)	330*

* Softening point ($\eta = 10^{7 \cdot 6}$ P) in °C.

TABLE 2.3.11. Metals for glass-to-metal seals

Glass	Soft glass						Hard glass				
Metal	Pt	Pt-clad core: Ni 48 Fe 52	Cu-clad* core: Ni 42 Fe 58	Ni 47–54 bal. Fe	Cr 6 Ni 42 bal. Fe	Cr 23–30 bal. Fe	Pure sintered iron	Cu	W	Mo	Kovar Fe 54 Ni 28 Co 18
Wire dia. in mm	< 1	< 3	< 1	< 5	yes	< 12	< 3	–	< 12	< 15	< 15
Ring seals	–	–	–	all dim.	all dim. (feather edge)	all dim. (feather edge)	yes	all dim. edge 0·05 mm	–	–	all dim.
$\alpha \times 10^7$ deg^{-1} (20–100 °C)	90	≈ 90	80–100 rad. 60–65 axis	80–110	80–100	95–100	125	165	40–45	48–52	48–60 depending on type of alloy
ϱ in $\frac{\Omega\,\text{mm}^2}{\text{m}}$ (20 °C)	0·11	0·5	0·04–0·06	0·50–0·35	0·34	0·72	0·11	0·017	0·06	0·06	0·49
λ in $\frac{\text{cal}}{\text{deg cm sec}}$	0·17	0·03	$\approx 0{\cdot}4$	0·03–0·05	0·03	90·0	0·18	0·92	0·38	0·35	0·09
inflection point °C	–	core: 450	core: 340–370	425–500	–	–	–	–	–	–	~ 425
Notes	simple sealing technique to soft glass			Oxide peels off easily for pure NiFe. Doping required: e.g. Cu-coating to prevent Pb-reduction in glass	Oxide sticks well, prior to soldering Ni-plating required (10μ thick)	simple sealing technique, soldering and welding difficult; silver coating required		electrically excellent, mechanically poor, special sealing technique required	seals well to appropriate type of glass: yellow to orange colour	seals well to appropriate type of glass: chocolate-brown colour	seals well to appropriate type of glass: grey colour (black could be porous)

* So-called CuFeNi-wire, or Dumet-wire.

TABLE 2.3.12. Quartz (after W. ESPE)

Net density	g/cm^3	crystall. 2·65 fused silica 2·2 quartz ware 2·1–2·2	
Tensile strength	kg/mm^2	fused silica: 7–9	
Compression strength	kg/mm^2	fused silica: 160–200	
YOUNG's modulus	kg/mm^2	fused silica: 6200–7200	
Shear modulus	kg/mm^2	fused silica: 2400–3150	
Thermal expansion coefficient	deg^{-1}	crystall. (0–567 °C) $\parallel$ axis: 140×10^{-7} $\perp$ axis: 240×10^{-7}	
		fused silica: 0–100 °C: $5{\cdot}2 \times 10^{-7}$; 0–1000 °C: $5{\cdot}6 \times 10^{-7}$	
Heat conductivity	$\frac{\text{cal}}{\text{deg cm sec}}$	crystall. (20 °C) $\parallel$ axis: 32×10^{-3}; $\perp$ axis: 17×10^{-3}	
		fused silica: 20 °C: $3{\cdot}5 \times 10^{-3}$; 350 °C: $6{\cdot}4 \times 10^{-3}$	
Transformation point	°C	fused silica: 1220–1250	
Electrical resistivity at 20 °C	Ω cm	crystall.: $\parallel$ 10^{13}–10^{15}; $\perp$ 10^{18}–10^{20} fused silica: 10^{17}–10^{18}	
$T_{\varkappa 100}$	°C	crystall. (very pure): ≈ 800 fused silica: 600–700	
Dielectric constant		crystall.: $\perp$ 4·3–4·4; $\parallel$ 4·6–4·7 fused silica, pure 3·5–3·8	
Dielectric loss factor tan δ ($\lambda = 300$ m–60 cm)		crystall.: 1×10^{-4}; quartz ware: 5–10×10^{-4} fused silica (20 °C): 2–3×10^{-4}; (400 °C): 5–6×10^{-4}	
Electric breakdown voltage	$\frac{\text{kV}}{\text{cm}}$	20 °C 250–400 500 °C: 40–50	

Applications: for fused silica: Insulation material of high thermal strength in transmitter valves, also envelopes for such valves, electrode supports in short wave tubes, inserts in switching tubes; cathode inserts in mercury arc rectifiers; diffusion pumps, ultraviolet lamps.

For crystallized quartz: quartz oscillator plates.

References

(a) *Fused silica and quartzware:*

Espe, W., and M. Knoll, *Werkstoffkunde der Hochvakuumtechnik*, Berlin 1936, p. 193 (Quarzglas und Quarzgut).

Singer, F., Geschmolzener Quarz in M. Pirani, *Elektrothermie*, Berlin 1930.

(b) *Quartz oscillators:*

Beckerat, H. V., and W. Arens, Der Schwingquarz in der Nachrichtentechnik; *Elektr. Nachr.-Techn.* **19**, 3/4 and 12 (1942).

Scheibe, A., *Die Piezoelektrizität des Quarzes*, Berlin 1938.

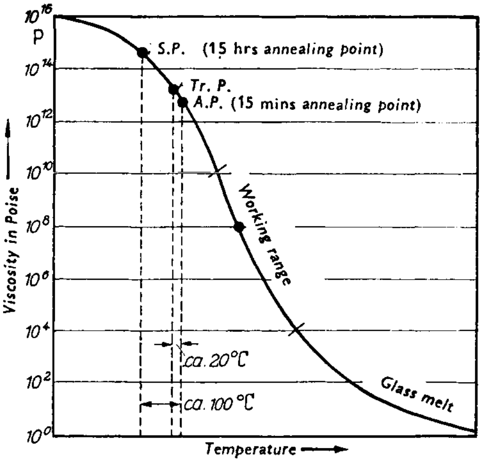

Fig. 2.3.14. Viscosity of glasses vs. temperature.
S. P. — Strain point; $10^{14.5}$ P
Tr. P. — Transformation point; $10^{13.3}$ P
A. P. — Annealing point; 10^{13} P
(after W. Espe).

2.3.1.4 Mica

TABLE 2.3.13. Mica (after W. ESPE)

Net density	g/cm^3	range 2·15–3·2 muscovite 2·65–3·2		
YOUNG's modulus	kg/mm^2	16,000–21,000		
Yield point	kg/mm^2	muscovite: 35–39	amber: 20–28	
Tensile strength	kg/mm^2	thickness 0·07 mm: 40–75		
Shear strength	kg/mm^2	muscovite: 23·5–26·5	amber: 10–13	
Thermal expansion coefficient (0–100 °C)	deg^{-1}	muscovite: 85×10^{-7}	phlogopite: 135×10^{-7}	
Heat conductivity	$\frac{\text{cal}}{\text{deg cm sec}}$	0·8–1·4 · 10^{-3}		
Calcination temperature	°C	muscovite: 550–600	amber: 750–900	
Melting point	°C	muscovite: 1130	amber: 1030	
Electrical resistivity	Ω cm	at 20 °C: between 10^{15}–10^{17}	single measurement 20 °C: 3×10^{17} 100 °C: 3×10^{16}	
Dielectric constant		6–8		
Dielectric loss factor tan δ between 50 and 10^7 c/s		20 °C: 1·6–2×10^{-4}		
		120 °C: 20–200×10^{-4}		
		micanite (20 °C): 2–10×10^{-4}		
Breakdown voltage	$\frac{\text{kV}}{\text{cm}}$	0·1 mm thick: 1000–2000	1 mm thick: 250–720	micanite 1 mm: 350

Applications: dielectric material in condensers, where high constancy of capacity and small losses are required; resilient insulating disks in electronic valves.

References

EBINGER, A., and L. LINDER, Glimmer für Kondensatoren, *Elektrotechn. u. Masch.-Bau*, **59**, 286 (1941).

ESPE, W., and M. KNOLL, *Werkstoffkunde der Hochvakuumtechnik*, p. 216. Springer, Berlin 1936.

SCHRÖDER, K., in H. SCHEERING, *Die Isolierstoffe der Elektrotechnik*, Berlin 1924.

STÄGER, H., *Elektrotechnische Isoliermaterialien*, Stuttgart 1931.

Standard specifications: DIN 40 612-1942; VDE 0332-IX, 38; VDE 614-1939; ČSN ESČ 127-1947.

2.3.1.5 Ceramic

TABLE 2.3.14. Ceramic materials data after DIN and VDE –

Group as per DIN 40685	Trade name		Net density	Water absorption	Tensile strength	Compression strength	Bending strength	Coefficient of linear thermal expansion	Thermal conductivity
			g/cm³	(%)	kg/mm²	kg/mm²	kg/mm²	10^{-7}/°C	cal / deg cm sec
IA1 Porcelain fired at high temperature, turned, cast, pressed	Hescho hard porcelain	glazed	2·4	0	3–5	45–55	9–10	35–45	3·6 to $3{\cdot}9 \times 10^{-3}$
		unglazed	2·4	0	2·5–3·5	40–45	5–7		
	Melalith	glazed	2·3–2·5	0	3–5	45–55	6–10	35–45	3·6 to $3{\cdot}9 \times 10^{-3}$
		unglazed			2·5–3·5 [2.3.15]*	40–45 [2.3.15]	4–7 [2.3.15]		
IA2 Porcelain fired at high temperature, wet pressed	Hescho hard porcelain	glazed	2·4	—	—	30–40	—	35–45	3·6 to $3{\cdot}9 \times 10^{-3}$
		unglazed	2·4	0·1–0·5	—	30–45	3–6		
IB Clay-like material, pressed	100 F Ardorit VI		2·5	0·4–0·8	—	25–35	4–7	47	$3{\cdot}9 \times 10^{-3}$
IIA Materials containing Mg silicate, fired at low temperatures	Ardorit XII		2·8	0·1–0·8	—	80–90	10–12	68	$4{\cdot}5 \times 10^{-3}$
IIB1 Steatite, normal	Steatite	glazed	2·6–2·8	0	6–9·5	85–95	12–14	70–90 60–65	$5{\cdot}4 \times 10^{-3}$ 5·3 to $6{\cdot}1 \times 10^{-3}$
		unglazed			4·5–6	85–95	12–14		
IIB2 Steatite, special brands	Calite		2·7–2·8	0	glazed 6·5–9·5 unglaz. 4·5–6	glazed 95–100 unglaz. 90–100	14–16	60–80	5·3 to $6{\cdot}1 \times 10^{-3}$
	Frequenta		2·6–2·8	0	glazed 6–10 unglaz. 4·5–6	90–100	14–16	60–80	5·3 to $6{\cdot}1 \times 10^{-3}$
Porous materials	Ergan		1·9–2·1	≈ 20	—	10–20	3·5–6	85–95	$3{\cdot}9 \times 10^{-3}$
	Q 5		1·9–2	10–15	1–1·5	20–25	4–5	60–70	$2{\cdot}8 \times 10^{-3}$
Natural mineral	Natural soapstone		2·6–2·8	≈ 3	—	40–80	≈ 10	90–100	—
IIIA1 Materials containing titanium oxide (rutile): $\varepsilon > 50$	Condensa C		3·9	0	—	—	—	75–85	8·3 to $9{\cdot}7 \times 10^{-3}$
	Condensa F		3·9	0	—	—	—	75–85	8·3 to $9{\cdot}7 \times 10^{-3}$
	Kerafar U		3·5–3·9	0	3–8	30–90	9–15	60–80	8·3 to $9{\cdot}7 \times 10^{-3}$

---

* Figures in brackets refer the diagrams on pp. 188 to 192.

Materials

standard specifications (after W. Espe)

Resistivity Ωcm		Dielectric constant ε	Temperature coefficient of dielectric constant at 10^6 c/s 10^{-6}/°C	$\tan\delta \times 10^4$ at 50 c/s (800 c/s)	$\tan\delta \times 10^4$ at 10^6–10^7 c/s	Electric breakdown strength kV/mm	Special properties	Applications
at 20°C	at 600°C							
10^{11}	10^4–10^5	5·5–6	(at 50 c/s: +550 to 600)	170–250	70–85	30–35	Good mechanical, thermal and electrical properties; can be manufactured with very thick wall	High- and low voltage insulators, vacuum envelope e.g. for mercury switches, cathode bowl in large mercury arc rectifiers, tubes for carbon resistors
10^{11} [2.3.17]	10^4–10^5 [2.3.16]	≈6 [2.3.19]	(at 50 c/s. +550 to 600)	170–250 100°C: 1200 [2.3.20]	60–120 [2.3.20]	30–35 [2.3.13–15]		
10^{11}	10^4–10^5	—	—	—	—	—	Medium mechanical and thermal properties	Low voltage insulators
200°C: 10^7	10^4 [2.3.17]	—	—	—	—	—		
200°C: 10^9	10^5 [2.3.17]	—	—	—	—	—	Can be made within small tolerances; great mechanical strength	Low voltage insulators
10^{12} [2.3.16]	10^5–10^6 [2.3.17]	≈6 [2.3.19]	+500 to +600	25–30 100°C: 650	15–20 25–30 [2.3.20]	20–30 30–35 [2.3.12–13]	Small dielectric loss factor, small tolerances, great mechanical strength	High- and low voltage insulators, in particular for h.f.
10^{12} to 10^{13}	10^7–10^8 [2.3.17]	6·5 [2.3.19]	+90 to +180	8–15	3–5 [2.3.20/21]	30–45		
10^{12} to 10^{13}	10^7–10^8	≈6	+120 to +160	10–15 100°C: 150	3–5 100°C: 6–8 [2.3.21]	30–45		
400°C: 10^8	10^7	≈4·5	—	—	2–4 100°C: 3–6	—	Can be machined after firing; small dielectric losses	Vacuum tube spacers; ceramic models
—	—	4	—	—	30	—	Small tolerances	Insulating component parts in vacuum (discs, rings), replacing mica
200°C: 10^{11}	10^7	≈6	—	—	20–30	—	Can be machined like metal; afterwards sintering	Ceramic models
200°C: 7×10^8	2×10^5	80 [2.3.19]	−680 to −860	{30–120}	5–10 [2.3.21]	10–20	High dielectric constant, small loss factor	Condensers, in particular for h.f.
200°C: 4×10^9	3×10^5 [2.3.17]	80 [2.3.19]	−680 to −860	{4–15}	1·5–5 [2.3.20]	10–20		
10^{11} to 10^{12}	10^5	64	−650 to −750	{3–10}	3–5 100°C: 3–8 [2.3.20]	10–20		

TABLE 2.3.14.

Group as per DIN 40685	Trade name	Net density g/cm³	Water absorption (%)	Tensile strength kg/mm²	Compression strength kg/mm²	Bending strength kg/mm²	Coefficient of linear thermal expansion 10^{-7}/°C	Thermal conductivity cal / deg cm sec
IIIA2 Materials containing titanium oxide $\varepsilon < 50$	Condensa N	3·7	0	—	—	—	65–70	7 to $8{\cdot}3 \times 10^{-3}$
	Kerafar W	3·5–3·9	0	3–8	30–90	9–15	60–80	7 to $8{\cdot}3 \times 10^{-3}$
IIIB	Tempa S	3·1	0	—	—	—	77–82	$8{\cdot}9 \times 10^{-3}$
Materials containing Mg-titanate	Diacond	3·1–3·2	0	6–7	50–60	8–11	60–100	$8{\cdot}9 \times 10^{-3}$
IVA Materials containing clay, dense	Ardostan	2·2	0	2·5–3·5	30–50	5–11	100–140	4·7 to $5{\cdot}6 \times 10^{-3}$
	Sipa H	2·1–2·2	0	2·5–3·5	30–50	5–8·5	110	4·7 to $6{\cdot}1 \times 10^{-3}$
IVB Materials containing clay, not fully dense	Sipa 14	2·1	1–5	1·5–2·5	30–50	5–6·5	120–170	$4{\cdot}5 \times 10^{-3}$
V Porous products, containing clay	Thermisol	1·5–1·7	14–18	1·5–2·5	8–10	2·5–3	25–30	2 to $3{\cdot}6 \times 10^{-3}$
	Calodur	2·4	10–14	1–1·5	6–7	1·5–2	40–45	3·1 to 5×10^{-3}
	St G	1·8–1·9	15–20	0·9–1	5–8	1·5–2	30–40	2·5 to $2{\cdot}8 \times 10^{-3}$
	Sipalox	2·0–2·1	10–15	1–1·5	25–30	4–5	35–45	$3{\cdot}6 \times 10^{-3}$
IX Pure aluminium oxide, porous	—	3–3·9	—	—	—	—	15 to 1000°C: 62	1·6 to 8×10^{-3}
Pure aluminium oxide sintered at high temperature	Sinterkorund	3·9	—	3·5	51–62	12	20–100°C: 46 20–400°C: 68	20°C: 47×10^{-3} 400°C: 19×10^{-3}

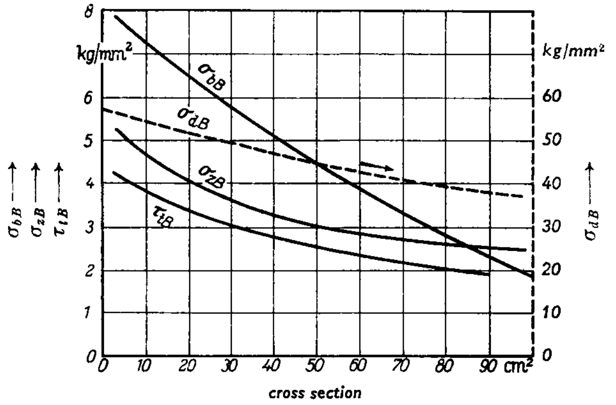

FIG. 2.3.15. Tensile (σ_{zB})-, compression (σ_{dB})-, bending (σ_{bB})- and shear (τ_{tB})-strength of porcelain, as a function of cross section Q of the probe. *Note*: compression strength (right-hand ordinate) approx. 10 times higher than tensile strength.

(continued)

Resistivity Ω cm		Dielectric constant ε	Temperature coefficient of dielectric constant at 10^6 c/s 10^{-6}/°C	tan $\delta \times 10^4$ at 50 c/s (800 c/s)	tan $\delta \times 10^4$ at 10^6–10^7 c/s	Electric breakdown strength kV/mm	Special properties	Applications
at 20°C	at 600°C							
—	[2.3.17]	40 [2.3.19]	−360 to −480	{30–65}	5–20 [2.3.20]	10–20	High dielectric constant; low loss factor	Condensers, in particular for h.f.
10^{11} to 10^{12}	10^5	32	−350 to −450	{3–10}	3–5 100°C: 3–8	10–20		
200°C: 2×10^{10}	3×10^7 [2.3.17]	14 [2.3.19]	+30 to +90	{3–50}	0·5–1 [2.3.20/21]	10–20	Dielectric constant almost independent of temperature, very low loss factor	Condensers, in particular for h.f.
10^{12} to 10^{13}	10^6–10^7	16	+30 to +50	{3–20}	0·5–3 100°C: 1–5 [2.3.21]	10–20		
3×10^{11}	1×10^5 [2.3.17]	5·5 [2.3.19]	+500 to +600	150–200	80–100	10–20	Low thermal expansion, high thermal shock resistivity	Arc protection, insulators of high thermal shock resistance
10^{11}	10^4–10^5	≈5	+500 to +600	200	40–70	10–20		
200°C: 10^{10}	10^6 [2.3.17]	—	—	—	—	—		Supports for heater elements
300°C: 10^8–10^9	10^5–10^6	—	—	—	—	—	High thermal shock resistivity and high operating temperature	
300°C: 10^8–10^9	10^5–10^6	—	—	—	—	—		
300°C: 10^8	10^5 [2.3.17]	—	—	—	-	—		
300°C: 10^8	10^6 [2.3.17]	—	—	—	—	—		
at 1000°C: 5 to 8×10^6	at 1600°C: 4 to 5×10^3	[2.3.18]	—	—	[2.3.18]	—	Can be easily degassed, high melting point	Insulating tubes for indirectly heated cathodes
$1{\cdot}3 \times 10^{11}$	10^{10}	9·5	—	32–77	—	15 (20°C) 6 (400°C)	High thermal and electrical stress resistance	Spark plugs, hot insulation parts for high voltage

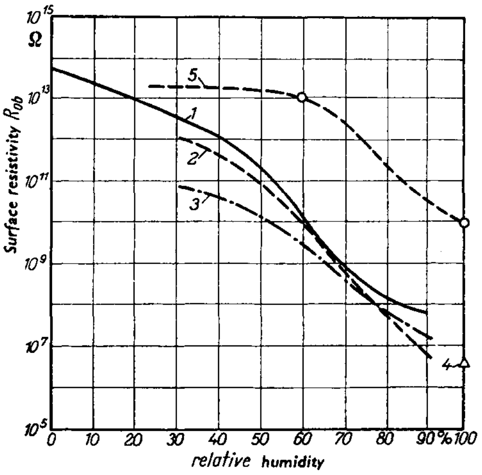

FIG. 2.3.16. Surface resistivity R_{ob} of ceramic materials as a function of the relative humidity F of the ambient air.

1 – glazed porcelain;
2 – unglazed porcelain;
3 – Lavite;
4 – unglazed steatite;
5 – unglazed steatite, but with silicon coating "dry film".

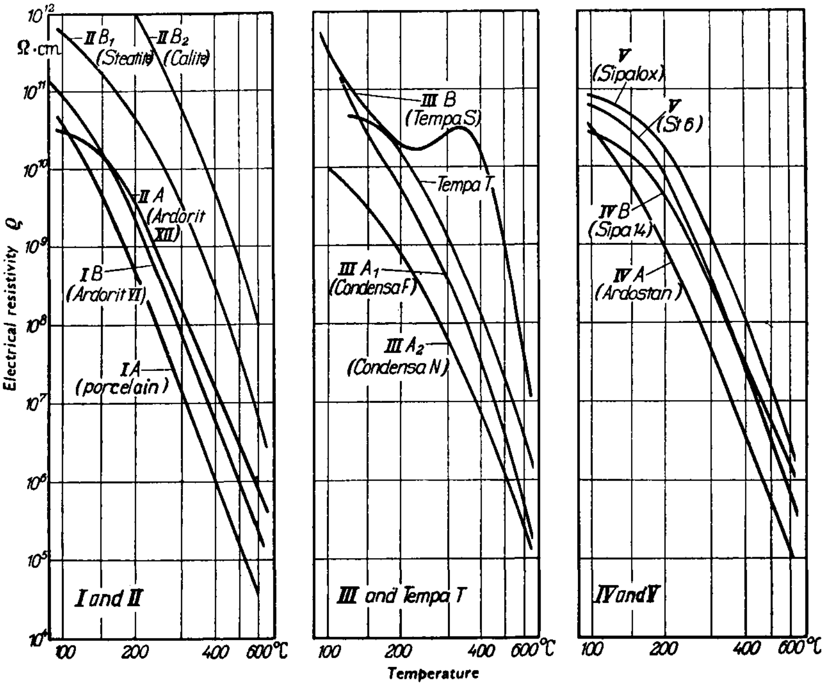

FIG. 2.3.17. Electrical resistivity of ceramic materials of DIN groups I–V, as a function of temperature (100 V a.c., 50 c/s).

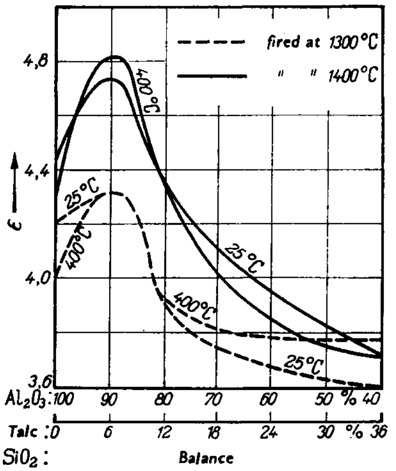

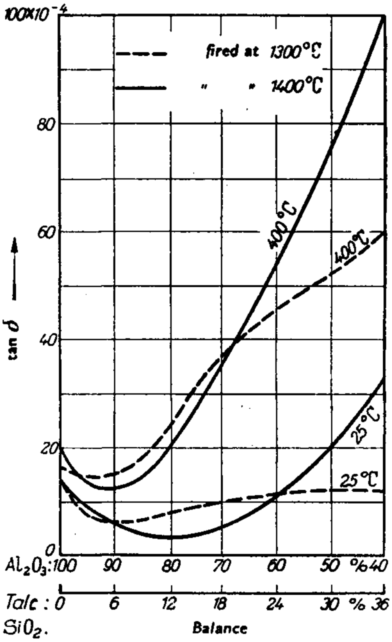

FIG. 2.3.18. (left and right): Dielectric constant ε and dielectric loss factor tan δ of ceramic materials measured at 6×10^7 c/s and at 25 °C and 400 °C resp., as a function of composition (weight per cent).

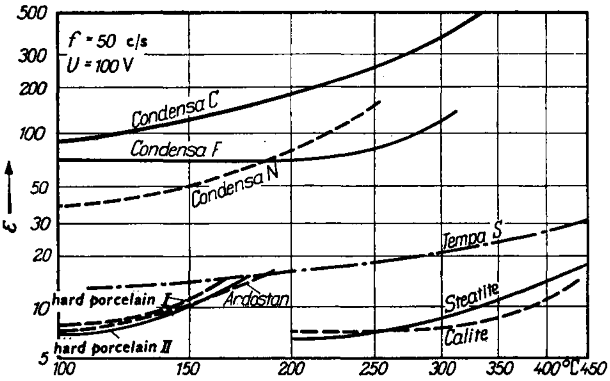

FIG. 2.3.19. Dielectric constant ε of commercial dense ceramic materials, as a function of temperature T (50 c/s, 100 V).

Material	Curve no.
Calite	3
Condensa C	8
Condensa F	4
Condensa N	6
Hard porcelain (average)	7
Steatite, normal (average)	5
Tempa S	2
Titanium oxide, ceramically bonded	9
Zirkonium oxide + titanium oxide, ceramically bonded (e. g. Kerafar U)	1

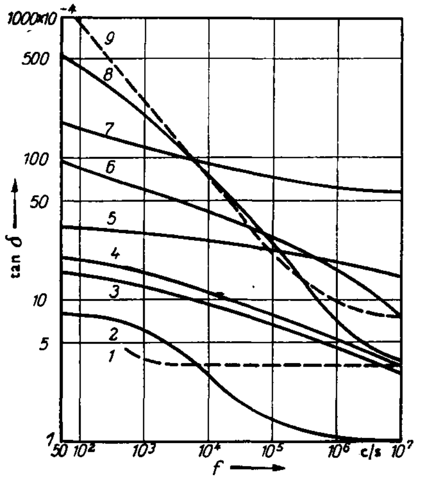

FIG. 2.3.20. Dielectric loss factor tan δ of commercial ceramic insulating materials at room temperature vs. frequency.

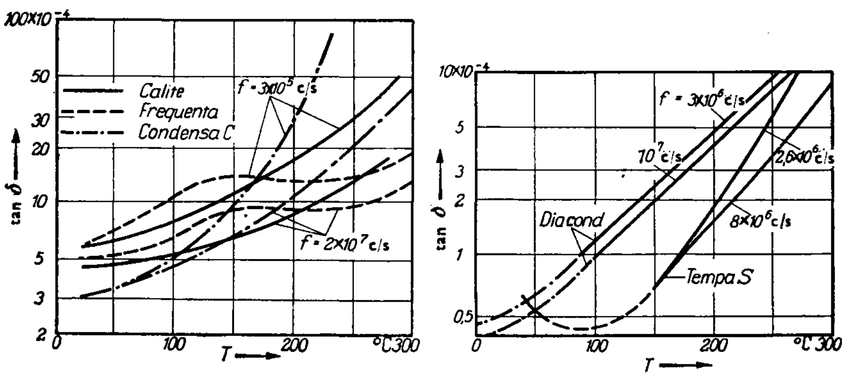

FIG. 2.3.21. Dielectric loss factor tan δ of commercial ceramic insulating materials at different frequencies vs. temperature.

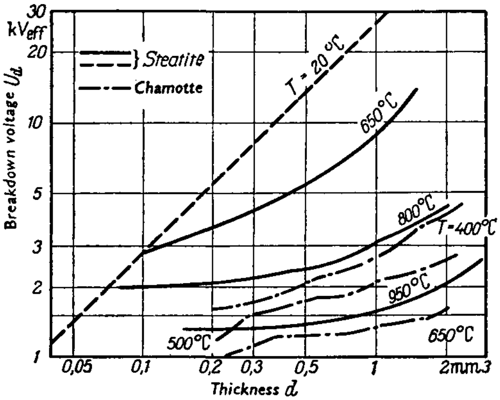

FIG. 2.3.22. Breakdown voltage U_d of Steatite (———, – – – –) and of clay (kaolin) with 12 per cent porosity and 1 per cent K_2O (– · – · –), for various temperatures vs. thickness *d*.

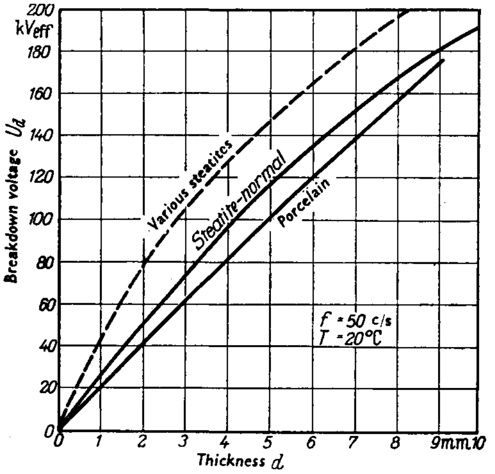

FIG. 2.3.23. Breakdown voltage U_d of porcelain and various steatites vs. wall thickness *d*.

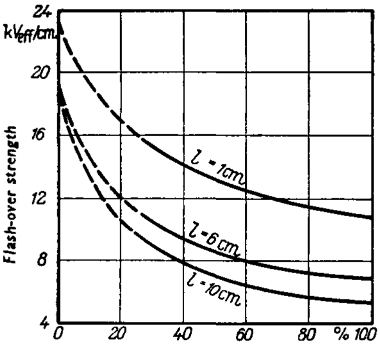

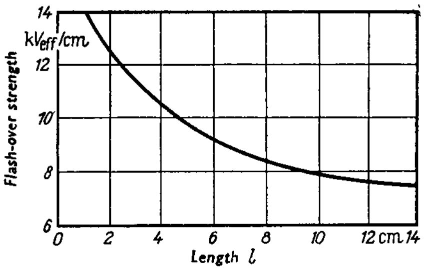

FIG. 2.3.25. Flash-over strength of porcelain cylinders at a relative humidity of 40 per cent vs. length of insulator, *l*.

FIG. 2.3.24. Flash-over strength of cylindrical porcelain insulators of various lengths *l*, as a function of the relative humidity F_{rel} of the surrounding air (in high vacuum the flash-over strength is equal to 100 kV/cm for porcelain and Calite).

TABLE 2.3.15. Constants of ceramic materials

re: Sintered corundum °C a 46 (20—100) b 68 (20—400) c 80 (20—800) d 0.23 (0—300) e 0.28 (0—1500) f 0.047 (20) g 0.019 (400) h 0.013 (900)	Density (g/cm³)	MOHS' hardness	Micro hardness	Melting point (°C)	Softening temperature (°C) under a load of 2 kg/cm²	Mean linear coefficient of thermal expansion $\alpha \times 10^7 (\text{deg}^{-1})$	Specific heat (cal/g degree)	Heat conductivity (cal deg⁻¹ cm⁻¹ sec⁻¹)	Electrical resistivity (Ω cm) at 20°C	(Ω cm) at 800°C	(Ω cm) at 1200°C	(Ω cm) at 1600°C	Electrical breakdown strength (kV/mm) at 20°C	Dielectric constant	Max. working temperature (°C)
Mica	2·15—3·2				975	85—135			$>10^{15}$				25—70	6—8	
Unglazed hard porcelain glazed	2·3—2·5	7		1670—1730	1410—1550	25—55	0·2—0·25 (20—100°C) 0·3 (1000°C)	0·0019—0·0037	10^{18}				30—35	5·4—6·4	
Natural soapstone baked	2·6—2·8	7—8			1500	90—100		0·0033—0·0067	10^{14}—10^{15}				5—10		
Steatite	2·65	7—8			1440	76 (20—100°C) 85 (20—800°C)	0·19—0·20	0·0054	10^{14}—10^{15}				20—30	5·5—6·5	
Calite	2·6—2·8	7—8			1310	78							35—45	6·5	
Frequenta					1440	70—80	0·194	0·0061	10^{14}—10^{15}				35—45	≈ 5·6	
Calan	2·6—2·8	7—8			1250	76							35—45	6·5	
Ergan					1460	85—95			$>10^{12}$				10—20	4·5	
MgO	3·2—3·7			2800		127 (15—1000°C)	0·26	0·00145—0·0030		3×10^{6}	5×10^{4}	10^{3}			
Al_2O_3	3·03—3·9	9		2050		62 (15—1000°C)	0·2	0·00160—0·0084			10^{5}	5×10^{3}			
Sintered corundum	3·9	9		2050	1730	a b c	d e	f g h					15	9·5—9·9	
BeO	2·8—2·9	9		2530		6	0·24								
ZrO_2	3·4—4·1			2700		irregular	0·3								
ThO_2	9·2			3000		87	0·0614								
Titanium carbide	4·9—5·1		3000	>3000		80			9×10^{5}	$1·2\times10^{4}$	$1·5\times10^{4}$	$1·8\times10^{4}$			2000
Zirconium boride	5·3—5·5		2300	ca. 3000		60			3×10^{5}	7×10^{5}	9×10^{5}	$1·2\times10^{4}$			2000

TABLE 2.3.16. Reaction temperatures (°C) of materials in vacuum (after STEYSKAL)

	W	Mo	ThO_2	ZrO_2	MgO	BeO
BeO	2000	1900	2100	1900	1800	–
ZrO_2	1600	2200	2200	–	–	–
MgO	2000	1600	2200	2000	–	–
ThO_2	2200	1900	–	–	–	–
C	1500	1500	2000	1600	1800	2300

TABLE 2.3.17. Constituents and characteristic data of zirconium-ceramic and alkaline-earth porcelain

Item	Zirconium ceramic 2618	Zirconium ceramic	Alkaline-earth porcelain
Constituents of the original material (weight, %)	Zr_2SiO_2 (53), talc (32), BaF_2 (5) clay (7), Betonit (3)	Zr_2SiO_2 (55), ZrO_2 (10), talc (22), clay (4), $BaCO_3$ (6), borosilicate glas frit (3)	Florida Kaolin (40), $MgCO_3$ (15), $CaCO_3$ (15), $SrCO_3$ (15), $BaCO_3$ (15)
Firing temperature °C	1325 (2 hrs)	1370–1400	1200–1250 (3 hrs minimum)
Coefficient of thermal expansion 10^{-7}/deg (temperature range)	55·4 (25–300 °C) 58·7 (25–300 °C)	56 (25–500 °C)	33 (25–300 °C) 41 (25–600 °C)
Electrical resistivity Ω cm (Temperature)			10^{14} (125 °C) 10^{13} (175 °C) 10^{12} (225 °C) 10^{11} (275 °C)
Dielectric loss factor tan $\delta \times 10^4$	26 (10^{10} c/s)	5·9–7·6 (10^6 c/s)	$\left.\begin{array}{l}5{\cdot}4\ (25\,^\circ C)\\62{\cdot}5\ (250\,^\circ C)\\250\ (350\,^\circ C)\end{array}\right\}$ (10^5c/s) $\left.\begin{array}{l}4{\cdot}6\ (25\,^\circ C)\\33{\cdot}4\ (250\,^\circ C)\\111\ (350\,^\circ C)\end{array}\right\}$ (10^6c/s)
Dielectric constant ε	7·51 (10^{10} c/s)	7·4–7·8 (10^6 c/s)	

TABLE 2.3.18. Constants of high-grade Al_2O_3 ceramics of different Al_2O_3-content

Al_2O_3-content		weight, %	85%	95%	99·5%	99·5%	100%
Structure		–	dense	dense	dense	porous	dense
Specific weight		g/cm³	3·40–3·53	3·61–3·75	3·7 (–3·97)	2·4–3·4	3·79–3·87
Porosity		%	< 1	< 1	< 1	7·2	–
Absorption of water		%	0·00–0·02	0·00	0·00	7–1·8	–
MOHS' hardness		–	8·5–9	9	9	–	–
Max. operating temperature		°C	1300–1400	1600–1700	1950	1400–1800	1800
Tensile strength		kg/mm²	12–16	17·5–24·5	26·3–27	–	26·5
Compression strength		kg/mm²	98–280	175–280	300	7–87	300
Bending strength		kg/mm²	21–32	32–35	30–33	7–15	33
YOUNG's modulus		kg/mm²	21,700–24,500	27,300–30 000	36,400	–	34,800–38,500
Specific heat		$\frac{\text{cal}}{\text{g °C}}$	0·18	0·188–0·190	0·22	–	0·26 (1000 °C)
Thermal conductivity	100 °C	$10^{-3} \frac{\text{cal}}{\text{°C cm sec}}$	31–40	45–52	47	40	47–90
	870 °C		(79)	(107)	–	–	≈ 12 (1000 °C)
Mean thermal expansion coefficient	25– 200 °C	10^{-7}/°C	54–57	57–67	–	51	(54)
	25– 700 °C	10^{-7}/°C	76–79	81	77	–	76
	25–1000 °C	10^{-7}/°C	77–79	85–91	84	–	85

TABLE 2.3.18. (continued)

Al_2O_3-content		weight, %	85%	95%	99·5%	99·5%	100%
Electrical breakdown strength	25 °C	kV/cm	82–140	100–160	152	20	≈ 150
	500 °C	kV/cm	–	40–48	–	–	–
	1000 °C	kV/cm	–	8–12	–	–	–
Electrical resistivity	300 °C	Ω cm	$(1-5)\times 10^{10}$	$5{\cdot}3\times 10^{12}$	$1{\cdot}2\times 10^{13}$	$10^{10}-10^{11}$	$10^{12}-10^{13}$
	500 °C	Ω cm	$10^{8}-7{\cdot}5\times 10^{9}$	$(1{\cdot}2-4{\cdot}5)\times 10^{10}$	$1{\cdot}3\times 10^{11}$	$7{\cdot}5\times 10^{7}-10^{9}$	$2\times 10^{10}-3\times 10^{11}$
	700 °C	Ω cm	$3{\cdot}7\times 10^{6}$	6×10^{8}	–	$3{\cdot}6\times 10^{6}$ to $3{\cdot}0\times 10^{7}$	$3\times 10^{8}-5\times 10^{9}$
	900 °C	Ω cm	$4{\cdot}5\times 10^{5}$	–	–	$5{\cdot}6\times 10^{5}$	$10^{7}-2\times 10^{8}$
Te-Value (10^6 Ω cm)		°C	750–1000	800–1100	1100	835–1100	1000–1200
Dielectric constant ε	10^6 c/s, 25 °C	–	7·4–8·95	8·81–9·6	–	5·5	9·5–12
	10^6 c/s, 500 °C	–	8·87	9·03	–	–	–
	10^{10} c/s, 25 °C	–	8·08–8·77	8·4–9·36	–	7·07	–
	10^{10} c/s, 500 °C	–	8·26	9·03	–	–	–
Dielectric loss factor tan α $\times 10^4$	10^6 c/s, 25 °C	–	7–12	2·5–3·5	–	5	–
	10^6 c/s, 500 °C	–	240	120	–	–	–
	10^{10} c/s, 25 °C	–	27	8–15	–	–	(5×10^7 c/s) 10–20
	10^{10} c/s, 500 °C	–	33	21	–	(1·1)	–

TABLE 2.3.19. Hydrogen permeability of ceramic tube materials (i. d. 3 mm, length of hot zone 180 mm, pressure 300 Torr gauge; see BAUKLOH [9])

Temperature	Permeability [cm^3 (NTP) per hr]			
°C	unglazed porcelain wall thickness 0·11 mm	glazed porcelain wall thickness 0·15 mm	K-paste* 16 mm	sintered corundum† 1·6 mm
22	0·00	0·00	0·00	23·5
500	0·27	0·31	0·86	18·2
1000	0·33	0·23	1·18	–
1100	0·37	0·30	0·83	10·27
1200	0·33	0·36	1·07	–
1300	0·43	0·33	0·92	–

* Manufacturer: Staatliche Porzellan-Manufaktur, ceramic with high Al_2O_3 content with little glass phase.

† DIN-Typ 710, pure sintered Al_2O_3, without glass phase.

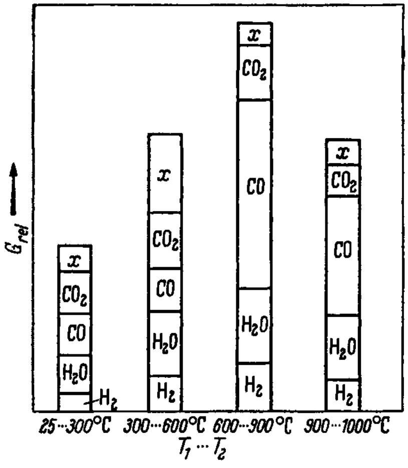

FIG. 2.3.26. Gas desorption G_{rel} of a Forsterite-ceramic used as envelope of electronic tubes in different degassing ranges $T_1 \ldots T_2$. The various gases were found by the method of mass spectrometry (after GRIESSEL [10]).

References

[1] ESPE, W., *Werkstoffkunde der Hochvakuumtechnik*, Bd. II, *Silikatwerkstoffe. VEB Deutscher Verlag der Wissenschaften*, Berlin 1960.

[2] ESPE, W., *Werkstoffe der Elektrotechnik in Tabellen und Diagrammen*, *Akademie-Verlag*, Berlin 1954.

[3] STEYSKAL, H., *Arbeitsverfahren und Stoffkunde der Hochvakuumtechnik*, Physik-Verlag, Mosbach, 1955.

[4] VON HIPPEL, A. R., *Dielectric Materials and Applications*, New York, 1954.

[5] SALMANG, H., *Die physikalischen und chemischen Grundlagen der Keramik*, 4th. ed. Berlin/Göttingen/Heidelberg, Springer 1958.

[6] *American Lava, Corp. Techn. Inform.* Chart No. 501 Mechanical and Electrical Properties of Alsimag-Ceramics. Chattanooga, Tenn. (USA) 1954.

[7] LEBEDINSKY, M. A., *Elektrovakuumnye materialy*, Moscow, 1956.

[8] NAVIAS, L. J., *Amer. Ceram. Soc. Bull.* **37**, 329–350 (1954).

[9] BAUKLOH, W., and A. HOFFMANN, *Ber. dtsch. keram. Ges.* **15**, 424 (1934).

[10] GRIESSEL, R. W., in *ASTM, Techn. Publ. No. 246*, p. 91, Philadelphia, 1959.

2.3.1.6 Plastic

TABLE 2.3.20. Mechanical and

Material (trade mark)	Tensile strength	Elongation	Compression strength	YOUNG's modulus	Thermal expansion $\alpha \times 10^6$	Thermal conductivity $\lambda \times 10^4$	MARTENS' temperature
	kg cm^{-2}	%	kg cm^{-2}	kg cm^{-2}	deg^{-1}	$\frac{\text{cal}}{\text{deg cm sec}}$	°C
Cellulose ether (Trolit) Bc (α)	300–500	5–20	400–500	20,000–25,000	80–150	4–6	50–55
Cellulose ester (Cellit T 3d 25% plasticizer.)	150–500	35–45	100–1000	—	120–180	4–6	50–70
Polyethylene (Lupolen, Alkathene, Polythene)	100–200	50–500	—	1000–2000	150–250	6–8	50
Polyisobutylene (Oppanol 3, Vistanex)	20–50	800–1000	—	5–15	200	6–8	—
Polytetrafluoroethylene (Teflon, Fluon, Gaflon)	100–200	50–150	50–150	4000–4500	60–120	5–6	100–150
Polymonochlortrifluoroethylene (Hostaflon, Kel-F, Fluorothene)	400–550	10–50	1500	10,000–20,000	70–90	4–6	—
Polyvinylchloride (PVC, Igelit PCU, Koroseal)	500–700	10–50	700–900	15,000–35,000	60–80	4–5	60–70
Polyvinylchloride-Vinylacetate (Igelit MP, Vinylite VY)	500–700	20–100	700–800	25,000	60–70	4	—
Polyvinylidenechloride (Saran A)	300–400	<10	400–500	35,000–45,000	160–170	3	—
Polyvinylbenzene (Polystyrol, Trolitul, Polystyrene, Styron)	400–700	1–4	800–1200	10,000–30,000	60–80	2–4	65–75
Polystyrene (impact resistant)	250–500	10–90	—	10,000–30,000	50–200	3–4	70
Polydichlorostyrene, (Styramaic HT)	300–600	—	—	35,000–60,000	—	—	—
Polyvinylcarbazole (Luvican, Polectron)	200–400	<1	—	30,000–45,000	40–80	6	125–175
Polymethylmethacrylate (Plexiglas D, Perspex)	400–800	1–10	600–1200	30,000–35,000	70–110	4–6	70–90
Polyacrylonitrile-methyl-methacrylate (Plexiglas)	900–1000	30–50	—	45,000	—	—	70–80
Polyamide (Durethan BK)	650–750	50–100	1000	10,000–25,000	110	7–9	55–65
Polyurethane (Durethan U)	550	15	640	—	110–130	11	50
Polymethane (Vulkollan)	300–600	700	—	—	—	—	—

Materials

electrical data of plastic materials

Continuous operating temperature °C	Water absorption in 24 hr wt., %	Electrical resistivity Ω cm	Dielectric constant ε		tan δ × 10^4		Electric breakdown strength kV cm^{-1}	Surface resistivity [Ω]	
			10^2 c/s	10^6 c/s	10^2 c/s	10^6 c/s		a) dry	b) after 24 hrs in water
45–75	0·2–0·4	10^{14}–10^{15}	3–3·5	3–3·5	50–100	50–100	150–350	10^{13}	10^{9}
60–75	1–2	10^{12}–10^{15}	3·5–4	3·3–3·6	50–150	100–300	150–200	10^{13}	10^{9}
70–100	$<$0·05	10^{15}–10^{18}	2·2–2·3	2·2–2·3	2–5		150–250	$>10^{14}$	$>10^{14}$
100	$<$0·01	10^{16}	2·2–2·3		4–10		250	$>10^{14}$	$>10^{14}$
200–250	$<$0·01	10^{15}–10^{16}	2		1–5		150–200	—	—
150–200	$<$0·01	10^{15}–10^{18}	2·8–2·9	2·5	50–200	100	200–250	—	—
50–80	0·1–0·5	10^{14}–10^{16}	3·4	3·1	200	150	200	$>10^{13}$	$>10^{13}$
50–65	$<$0·1	10^{13}–10^{16}	3·2–3·3	3·0–3·1	50–100	150–200	150–200	$>10^{13}$	$>10^{13}$
80	$<$0·1	10^{14}–10^{16}	6	4	300–800	500–1000	100–150	$>10^{13}$	$>10^{13}$
70–85	$<$0·05	10^{17}–10^{20}	2·5–2·7		1–5		200–300	$>10^{14}$	$>10^{14}$
60–80	—	10^{13}–10^{17}	2·5–4·8	2·4–3·8	3–200	4–200	120–240	$>10^{13}$	$>10^{13}$
100–110	$<$0·05	—	2·65	2·6	3–10	2	150–200	—	—
125–175	$<$0·1	10^{15}–10^{17}	3·0–3·1		2–10		300	—	—
60–80	$<$0·5	10^{14}–10^{18}	3·5–4·5	2·7–3·5	500–700	200–400	200	$>10^{15}$	$>10^{15}$
75	—	—	4·5		500–1000		200	—	—
80–120	2–3	10^{12}–10^{15}	—	3·5–5	—	200–1000	200–250	10^{14}	10^{11}
(180)	2	10^{14}	—	3·4	—	470	380	10^{14}	10^{12}
—	—	10^{10}	—	—	—	—	100–150	10^{14}	10^{12}

Table 2.3.20.

Material (trade mark)		Tensile strength kg cm^{-2}	Elongation %	Compression strength kg cm^{-2}	Young's modulus kg cm^{-2}	Thermal expansion $\alpha \times 10^6$ deg^{-1}	Thermal conductivity $\lambda \times 10^4$ $\frac{\text{cal}}{\text{deg cm sec}}$	Martens' temperature °C
Aniline resin (Iganil, Cibanit)		600–800	1–2	1200–1600	20,000–50,000	50–60	3	110–115
Phenolic resin (pure) (Bakelite, Dekorit, Trolon)		300–800	0·5–2	800–2000	25,000–90,000	20–100	3–6	75–150
Phenolic resin + Mica		300–500	—	—	—	20–30	10–15	—
Phenolic resin + asbestos		250–750	0·2–0·5	1000–2000	130,000–170,000	15–30	10–15	150–175
Melamine resin (Ultrapas, Melmac)		400–800	0·5–1	2000–3000	70,000–110,000	20–60	7–10	>150
Melamine resin + glass fibre		1500	—	2000–7000	—	—	—	—
Urea and carbonic resins (Pollopas, Resopal, Beetle, Cibanoid)		250–800	0·4–0·8	1500–2500	50,000–100,000	25–50	7–10	100–125
Silicone rubber	DC 120	35	150	—	—	—	—	—
	DC 150	28	300	—	—	—	—	—
	DC 160	42	200	—	—	—	—	—
	DC 180	49	75	—	—	—	—	—
Silicone rubber	R 20	65–75	200–280	—	—	—	3·5	—
	R 30	70–85	250–300	—	—	—	4·1	—
	R 40	55–65	190–220	—	—	—	4·2	—
	R 50	45–55	130–170	—	—	—	4·4	—
	R 60	55–60	110–130	—	—	—	4·6	—

(continued)

Continuous operating temperature °C	Water absorption in 24 hr wt., %	Electrical resistivity Ω cm	Dielectric constant ε		tan $\delta \times 10^4$		Electric breakdown strength kV cm^{-1}	Surface resistivity [Ω]	
			10^2 c/s	10^6 c/s	10^2 c/s	10^6 c/s		a) dry	b) after 24 hrs in water
80–90	<0·1	10^{15}–10^{17}	3·5–3·8	3·4–3·6	20–200	500–1000	200–250	—	—
100–150	0·1–0·2	10^{10}–10^{12}	5–6·5	4·5–5	500–1000	100–300	100–200	10^{12}	10^{12}
120–150	0·01–0·1	10^{11}–10^{15}	4·5–7·5	4–5·5	100–500	50–300	150–300	10^{12}	10^{12}
150–200	0·1–0·3	10^{9}–10^{12}	6–50	5–10	1000–5000	500–2000	50–150	—	—
100–150	0·1–1	10^{8}–10^{13}	6–10	4–8	300–1000	200–600	100–200	>10^{10}	>10^{10}
130	1–3	—	—	6–8	—	100	150	—	—
70–90	0·2–2	10^{12}–10^{14}	7–10	5–7·5	300–1000	200–400	100–200	10^{11}	10^{11}
—	after 7 days 1·4	—	5·78	7·5(–5·7)	51	10–(8)	190	—	—
—	after 7 days 2·6	—	5·87	5·4	43	270	200	—	—
—	after 7 days 0·9	—	8·8	9	50	300	150	—	—
—	after 7 days 0·5	—	4·60	4·6	67	30	260	—	—
—	—	5×10^{14}	2·5	—	4	—	>200	—	—
—	—	5×10^{14}	2·8	—	9	—	>200	—	—
—	—	—	3·2	—	25	—	>200	—	—
—	—	—	4·2	—	210	—	>200	—	—
—	—	—	3·15	—	230	—	>200	—	—

Table 2.3.21. Mechanical and

Material	Make	Tensile strength kg cm^{-2}	Elongation %	Compression strength kg cm^{-2}	Young's modulus kg cm^{-2}	Thermal expansion $\alpha \times 10^6$ deg^{-1}	Thermal conductivity $\lambda \times 10^4$ $\frac{\text{cal}}{\text{deg cm sec}}$	Martens' temperature °C
Ethoxyline resin (pure)		600–800	—	1000–1500	25,000–40,000	60–65	5	105–120
Araldite B	Ciba	650–800	—	—	30,000–40,000	60–65	—	110–120
Araldite F	Ciba	500–800	—	1300–1400	40,000–45,000	60	—	115–125
Araldite D	Ciba	550–800	—	900–1000	30,000–35,000	90–95	—	50–60
Lekutherm × 50	Bayer	700	—	—	—	57	7	120
Lekutherm × 60	Bayer	700	—	—	—	56	6	120
Hortacoll	Farbwerke Hoechst	500–600	—	—	—	—	—	40
Polyester resins		250–700	—	700–2000	10,000–60,000	50–150	4–6	400–700
P_3	BASF	400	—	>1800	29,000	—	—	45
P_4	BASF	400	—	>1800	33,500	—	—	54
P_5	BASF	400	—	>1500	31,800	—	—	45
Leguval N 30	Bayer	840	6	1400	30,000–37,000	106	6·1	60
Leguval W 30	Bayer	200	2	1900	33,000–42,000	73	5·8	130
Leguval W 50	Bayer	650	3·5	1280	34,000–41,000	90	4·7	74
Leguval F 10	Bayer	300	2·5	1475	40,000–33,000	81	4·7	85
Leguval K 25 R	Bayer	500	3·8	1560	29,000–36,000	122	5·4	58
Allyl-ester resins (Kriston)	B.F. Goodrich	350–450	—	1300–1600	20,000–45,000	50–100	4–5	—
Polyether-cyclo-acetal resin		750–800	—	800–1100	25,000–35,000	75–140	5	45–90
Ultralon T	Bayer	≈750	—	800	26,000–28,000	75	5	45–55
Ultralon S	Bayer	≈750	—	1100	32,000–33,000	140	5	70–90
Phenolic resin		400–650	—	1000–2000	20,000–35,000	50–150	3–5	40–80
Polymethylmethacrylate (Plexiglas)	Röhm & Haas	400	—	700–1000	20,000–40,000	70–90	4–6	70
Polystyrene		600–700	—	800–1200	35,000–45,000	60–80	2–4	60–80

electrical constants of resins for casting

Continuous operating temperature C°	Water absorption in 24 hours wt., %	Electrical resistivity Ω cm	Dielectric constant ε		tan $\delta \times 10^4$		Electric breakdown strength kV cm^{-1} 50—60 c/s	Surface resistivity [Ω]
			10^2 c/s	10^6 c/s	10^2 c/s	10^6 c/s		
—	0·1—0·5	5×10^{14} to 10^{17}	3·7	3·6	10	200—300	150—360	—
—	7 × 24 hrs 0·1—0·14	10^{16}—10^{17}	3·7	3·5	7—9	260—270	0·5 mm: 700	10^{12}—10^{13}
—	10 × 24 hrs 0·3—0·35	$>3\times10^{15}$	3·5	—	35—45	—	≈2 mm: 200	$>10^{11}$
—	10 × 24 hrs 0·3—0·5	10^{12}	4	—	100	—	≈2 mm: 200	—
—	0·1—0·14	10^{16}	—	3	—	100	800	10^{10}—10^{14}
—	0·1—0·14	10^{16}	—	3	—	100	700	10^{10}—10^{14}
—	7 × 24 hr 0·2	10^{10}	3·6	—	1·00	—	—	—
—	0·1—0·6	10^{13} to 5×10^{15}	3·0—4·5	2·8—3·7	70—300	100—300	150—300	—
—	—	10^{14} (10^{13})	3·5 (8·3)		110 (1140)		—	—
—	—	$1·8\times10^{14}$ ($1·4\times10^{13}$)	3·5 (4·5)		200 (300)		—	—
—	—	$1·6\times10^{14}$ (1×10^{12})	3·8 (5·5)		170 (550)		—	—
—	0·8	5×10^{15}	—	3·4	—	310	285	9×10^{13} (after 24 hrs in water)
—	1·6	6×10^{15}	—	3·1	—	170	330	3×10^{14}
—	0·5	3×10^{16}	—	3·2	—	140	420	2×10^{13}
—	0·55	$>10^{16}$	—	2·9	—	120	310	1×10^{14}
—	0·7	3×10^{15}	—	3·1	—	170	310	4×10^{13}
—	0·5	$>10^{14}$	3·4—5	3·2—4·5	50—200	200—600	150—200	—
—	7 × 24 hrs 0·2—2	$>10^{15}$	3·5—4·0		30	300	150—200	—
—	7 × 24 hrs 0·3—0·55	$>10^{15}$	3·8	3·5	30	300	160	73×10^{13} } 2×10^{11} (after 24 hrs in water)
—	7 × 24 hrs 0·3—0·7	$>10^{15}$	4·0	3·7	30	300	180	$>10^{13}$
—	0·4	10^{10}—10^{13}	5—10	4—7	500—5000	300—1000	100—150	—
—	0·2—0·5	$>10^{15}$	3·5—4·5	2·7—3·3	200—600	200—300	150—200	—
—	<0·1	10^{15}—10^{19}	2·5—2·7		5—10		150—250	—

TABLE 2.3.22. Electrical data of Desmodur-Desmophen lacquer films* at 20°C

No.	Lacquer system, mixing ratio in brackets	Temperature for drying the films† °C	Storage condition of Probe**	Electrical resistivity ϱ Ω cm	Surface resistivity R_0††; figure of merit	Dielectric constant ε for 50 c/s	Dielectric loss factor tan δ for 50 c/s	Electrical breakdown E_d*** kV/cm
1	Desmophen 800 + Desmodur T	180	indoors	$2–3 \times 10^{15}$	13	4·4–4·5	0·01	1270
	(100:60)		moist	$2–3 \times 10^{15}$	13	4·4–4·5	0·01	1100
2	Desmophen 800 + Desmodur T	180	indoors	1×10^{16}	13	4	0·01	1410
	(100:45)		moist	1×10^{16}	13	4	0·01	1220
3	Desmophen 800 + Desmodur T	24 hrs at air	indoors	3×10^{15}	13	4·6–5·0	0·012	1300
	(100:60)	5 hrs: 50	moist	2×10^{15}	13	4·7–5·1	0·015	1030
4	Desmophen 800 + Desmodur TH	180	indoors	$1 \times 10^{15}–1 \times 10^{16}$	13	3·7–3·9	0·012–0·014	1370
	(0 %) (100:300)		moist	1×10^{15}	13	3·9–4·2	0·015–0·02	1300
5	Desmophen 1100+DesmodurTH	80	indoors	3×10^{15}	13	4·0–4·3	0·013–0·015	1220
	(50 %) (100:225)		moist	2×10^{13}	13	4·0–4·4	0·014	1090
6	Desmophen 1100+DesmodurTH	80	indoors	2×10^{15}	13	4·0–4·3	0·013	1200
	(50 %) (100:170)		moist	3×10^{15}	13	4·4	0·014	1040
7	Desmophen 1100+DesmodurTH	24 hrs at air	indoors	$2–4 \times 10^{15}$	13	4·0	0·013	1040
	(50 %) (100:225)	5 hrs: 50	moist	4×10^{14}	13	4·1–4·3	0·017	1040

* Desmodur and Desmophen are registered trade marks of FARBENFABRIKEN BAYER A. G., Leverkusen, for the intermediates supplied for manufacturing lacquers based on polyurethane. Polyurethanes are polyaddition products obtained by chemical reactions of two components. By suitable combination lacquers are obtained with versatile properties and a wide range of variation.

† The lacquer film (three coatings) was stored at the given temperature; where times are not given, the first and second coatings were each stored for 15 mins, and the third for 1 hr.

** Indoors is understood to mean that the measurement was made after storage in normal conditions indoors (i.e. without predrying). Moist is understood to mean that ϱ, ε and tan δ were measured on samples after 48 hrs of storage in 80 per cent r.h., R_0 and E_d on samples after 24 hrs of storage in water.

†† Measured in accordance with German spec. VDE 0303. Figure of merit 13 for R_0 means $\geqq 10^{13}$ to $< 10^{14}$ Ω.

*** Measured in accordance with German spec. VDE 0303 in arrangement ball-plate.

TABLE 2.3.23. Permeability $P = Dh$ of various gases through plastics and natural rubber

Permeated mass of gas: $G = DhF \frac{p_1 - p_2}{d} t$.

h solubility [Torr litre/cm³ Torr] or [ccm NTP/cm³ Atm.]

d thickness of membrane [cm]

t time [sec]

p pressure [Torr]

F surface area of membrane [cm²]

G [Torr litre] or [cc NTP]

Permeability $P = D\,h$ [10^{-8} cm² sec^{-1}]

Diffusion coefficient D [10^{-7} cm² sec^{-1}]

Temperature of material (°C)	H_2		O_2		N_2		CO_2		He	
	D h	*D*	*D h*	*D*	*D h*	*D*	*D h*	*D*	*D h*	*D*
Natural rubber										
17	28	79	12	12·5	4·1	8·0	72	6·7	16·5	—
25	39	105	18	17·5	6·6	11·5	102	10·5	23	—
35	58·5	140	28·5	27	11·0	20	145	17	33	—
43	77	185	39	36	16	28	185	25	44	—
50	97	220	49·5	49	22·5	37	220	3 2	—	—
Buna S										
17	22·5	80	9·0	9·6	3·0	7·2	71	6·8	13	—
25	30·5	100	13	14	4·8	10	94	10	17·5	—
35	44	135	20	20	7·8	14·5	130	15·5	25	—
43	59·5	165	27·5	28	11·5	21	165	23	33	—
50	74	200	34·5	34	14·5	28	195	29	42	—
Perbunan										
17	7·6	31	2·0	2·4	0·50	1·45	15	1·0	5·8	—
25	11·5	42	3·2	3·6	0·89	2·3	23	1·7	8·7	—
35	17·5	64	5·3	6·3	1·65	4·1	37	3·1	12·5	—
43	25·5	86	7·7	9·1	2·5	6·2	52	4·7	16·5	—
50	31·5	110	10·5	13	3·7	8·6	66	7·0	21	—
Neoprene G										
17	6·8	29	1·75	2·5	0·53	1·55	12·4	1·3	—	—
25	10·3	38	3·0	3·8	0·89	2·4	19·5	2·3	—	—
35	16	56	5·1	6·2	1·65	4·4	31	4·2	—	—
43	23	74	7·7	10·0	2·55	7·2	43·5	6·8	—	—
50	28·5	94	10·1	13	3·55	9·4	56·5	9·1	—	—
Oppanol B 200										
17	3·0	10	0·54	0·50	0·11	0·27	2·3	0·32	3·8	—
25	4·9	14	0·90	0·78	0·22	0·43	3·8	0.54	5·6	—
35	8·3	21	1·6	1·55	0·44	0·84	6·6	1·05	8·5	—
43	12	31	2·6	2·4	0·78	1·5	10·0	1·8	12	—
50	16·5	38	3·7	3·4	1·15	2·1	14	2·5	15·5	—
Butadiene rubber										
17	23	75	10·1	11	3·4	8·1	80	7·6	—	—
25	32	96	14·5	15	4·9	11	105	10·5	—	—
35	46	125	21	22	7·8	16	140	16	—	—
43	60	160	28	30	11	22	175	22	—	—
50	77	180	36	37	14·5	29	200	28	—	—
Methyl-rubber										
17	9·0	27	0,93	0·88	0·20	0·46	3·0	0·36	8·1	—
25	13	39	1·6	1·4	0·36	0·79	5·7	0·63	11	—
35	20	61	3·1	2·5	0·78	1·7	10·5	1·3	16	—
43	29	80	5·0	4·1	1·3	2·8	17	2·2	22	—
50	38	105	7·1	6·1	2·2	4·1	24	3·6	27	—
Mipolam MP										
17	2·9	15	0·41	0·90	—	—	2·3	0·23	—	—
25	4·4	20	0·70	1·3	0·2	—	4·0	0·44	—	—
35	7·3	30	1·4	2·4	0·4	—	7·6	0·83	—	—
43	10·5	39	2·1	3·9	0·7	—	11·5	1·4	—	—
50	14	50	3·2	5·2	—	—	15	1·9	—	—
Thiokol B										
17	0·71	7·8	0·11	—	—	—	1·3	0·43	—	—
25	1·2	10·5	0·22	—	—	—	2·4	0·81	—	—
35	2·2	18	0·49	—	—	—	4·8	1·7	—	—
43	3·3	26	0·85	—	—	—	7·7	2·8	—	—
50	4·6	35	1·3	—	—	—	11·0	4·0	—	—

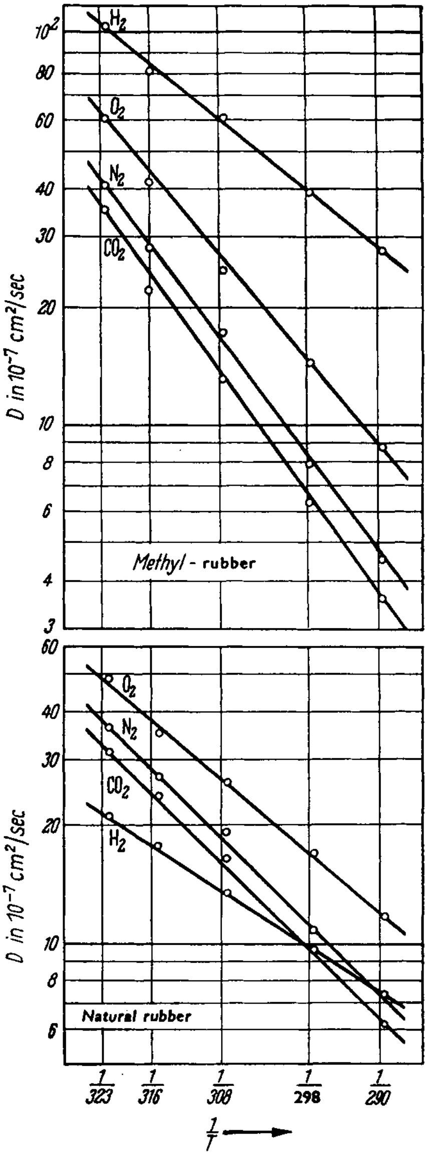

FIG. 2.3.27. Diffusion constant D for H_2, N_2, O_2 and CO_2 in methyl-rubber and natural rubber as a function of temperature T(°K). Top graph: Divide ordinate by 10 for O_2, N_2 and CO_2. Bottom graph: Multiply ordinate by 10 for H_2.

TABLE 2.3.24. Permeability relative to natural rubber (= 100)

	H_2	O_2	N_2	CO_2	CH_4	He
Natural rubber	100	100	100	100	100	100
Butadiene rubber	82	80	74	103	–	–
Buna S	78	72	73	92	73	76
Methyl-rubber	33	9	5·5	5·6	2·7	48
Perbunan	29	18	14	23	11	38
Neoprene G	26	17	14	19	11	–
Oppanol B 200	12	5	3·3	3·7	2·5	24
Mipolam MP	11	4	3	3·9	–	–
Thiokol B	3	1·2	–	2·4	–	–

Permeability for different gases ($H_2 = 100$)

	H_2	O_2	N_2	CO_2	CH_4	He
Natural rubber	100	46	17	260	56	59
Butadiene rubber	100	45	15	330	–	–
Buna S	100	43	16	310	52	57
Methyl-rubber	100	12	2·8	44	4·6	85
Perbunan	100	28	7·7	200	21	76
Neoprene G	100	29	8·6	190	24	–
Oppanol B 200	100	18	4·5	77	11	114
Mipolam MP	100	16	4·5	91	–	–
Thiokol B	100	18	–	200	–	–

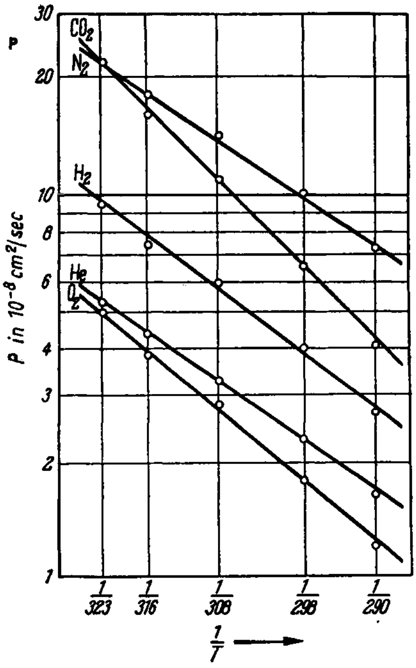

FIG. 2.3.28. Permeability P of H_2, O_2, He, N_2, CO_2, through natural rubber as a function of temperature T (°K). Multiply ordinate by 10 for H_2, O_2, CO_2 and He.

TABLE 2.3.25. Permeability of water vapour through plastics, at 25 °C. Pressure difference of the water vapour 23·8 Torr.

	Permeability $g\,hr^{-1}\,cm^{-1}\,Torr^{-1}$
Polyisobutylene-soot mixture	$0{\cdot}006–0{\cdot}08 \times 10^{-8}$
Paraffin	$0{\cdot}02 \times 10^{-8}$
Polyethylene $s = 0{\cdot}96$	$0{\cdot}06 \times 10^{-8}$
Polyisobutylene	$0{\cdot}14 \times 10^{-8}$
Polyethylene $s = 0{\cdot}92$	$0{\cdot}22 \times 10^{-8}$
Polyvinylchloride	$0{\cdot}8 \times 10^{-8}$
Bitumen fillers	$1{\cdot}1 \times 10^{-8}$
Cellophane, weather-proof	$1{\cdot}5 \times 10^{-8}$
Ebonite (hard rubber)	$1{\cdot}5 \times 10^{-8}$
Polystyrene	$3{\cdot}3 \times 10^{-8}$
Polycarbonate (Makrolon)	$2{\cdot}6 \times 10^{-8}$
Phenol casting resin	$4{\cdot}7 \times 10^{-8}$
Polymethylmethacrylate	$5{\cdot}7 \times 10^{-8}$
Polyvinylchloride plus plasticizer	$2–10 \times 10^{-8}$

TABLE 2.3.26. Application

Designation	Thermo setting			Cold setting
	I	VIII	XV	101
Supplied as	Sticks, powder (for tablets) colour: amber or silvery	Amber colour thixotropic paste	Amber colour resin solution with liquid hardener XV	Amber colour liquid resin with liquid hardeners 951, 930 or 936
Storage time of resin ready for use	2 years	1 year	1 month	1–6 hrs
Mode of application	Powder sprinkling; sticks rubbed over warm surfaces; flame spraying	By spatula or spraying under pressure	Brushing, spraying or dipping	By spatula
Curing	130 °C: 10 hrs 200 °C: 30 mins	130 °C: 10 hrs 200 °C: 30 mins	130 °C: 14 hrs 200 °C: 30 mins	According to type of hardener: 20 °C: 24 hrs 100 °C: 30 mins 60 °C: 2 hrs
Uses	Joining of metals and non-metals	Joining of metals and non-metals, filling up of gaps of varying widths, and of cavities	Joints of large surface area, packets of films and sheets, sealing of porosities in cast components	Joining of small metallic surfaces

TABLE 2.3.25. (continued)

	Permeability $\mathrm{g\,hr^{-1}\,cm^{-1}\,Torr^{-1}}$
Benzylcellulose	16×10^{-8}
Cellulosetriacetate	$80\text{-}100\times10^{-8}$
Cellulosehydrate film	$80\text{-}100\times10^{-8}$
Novodur W	6×10^{-8}
Leguval	$1\text{-}4\times10^{-8}$
Lekutherm	$0{\cdot}2\text{-}0{\cdot}6\times10^{-8}$

$$G' = D'\,h\,F\,\frac{p_1 - p_2}{d}\,t'.$$

$$G' = P'\,F\,\frac{p_1 - p_2}{d}\,t'.$$

The dimensions are the same as in the equation on page 205 except:

$P' = D'h$: g $\mathrm{hr^{-1}\,cm^{-1}\,Torr^{-1}}$;

t' = time: hrs;

G' = mass: g

of Epoxy-type resins (Araldite)

Cold setting			
102	103	121	123
Amber colour resin solution with liquid hardeners 951 or 936	Amber colour liquid resin with liquid hardeners 951 and 930 and paste hardeners 953 and 954	Paste resin black, white, brown or grey. With liquid hardeners 951 and 930 and paste hardeners 953 and 954	White paste resin. With liquid hardeners 951 and 930 and paste hardeners 953 and 954
$1^1/_2$–7 hrs, according to hardness and thinning	1–2 hrs	1–2 hrs	1–2 hrs
By brushing, spraying or dipping, to be predried	By brushing, spraying, dipping, by spatula as per type of hardener	By spatula	By spatula
According to type of hardener: 20°C: 24 hrs or 60°C: 2 hrs	20°C: 24–36 hrs 100°C: 30 mins 200°C: 5 mins	20°C: 24 hrs 100°C: 30 mins 200°C: 5 mins	20°C: 24 hrs 100°C: 30 mins 200°C: 5 mins
Joining of materials, one of which must be porous; of materials of fine granular structure; for the impregnation of paper, cardboard and porous cast components	Joining of metals and non-metals with thin gaps According to type of hardener used the gap is hard or flexible	Joining of metals, ceramics and hardened plastics with thick gaps. Filling up of cavities, sealing of in-cast components According to type of hardener used the gap is hard or flexible	Joining of metals, glass, ceramics and hardened plastics with large and widely varying joints. Filling up of pits to obtain smooth surfaces

2.3.1.7 Natural Rubber

TABLE 2.3.27. Natural rubber

Density	g/cm^3	slightly vulcanized		0·92–0·93
		vulcanized with filler		0·95–2·0
		hard rubber (DIN 7711)		1·2 –1·7
Bulk density	g/cm^3	foam rubber		0·06–0·09
Tensile strength	kg/mm^2	natural rubber 0·8–2·5	hard rubber 2–8	–
Elongation	%	350–1000	2–8	–
Bending strength	kg/mm^2	–	$> 7-10^2$	–
Impact strength	cm kg/cm^2	–	$> 4-10^2$	–
YOUNG's modulus	kg/mm^2	0·1–0·7	200–500	–
Water absorption after 7 days in water at 20 °C	% weight	soft rubber according to filler content		0·6 – 5 %
		hard rubber without filler		0·11–0·16 %
		hard rubber with much filler		0·16–0·27 %
Mean linear thermal expansion coefficient; 20–120 °C	deg^{-1}	natural hard rubber: $1400-1950 \times 10^{-7}$		
Volume thermal expansion coefficient	deg^{-1}	rubber with 3 % sulphur: $\approx 7000 \times 10^{-7}$ rubber with 31 % sulphur: $\approx 2000 \times 10^{-7}$		
Thermal conductivity	$\frac{\text{cal}}{{}^\circ\text{C cm sec}}$	$3\text{-}5 \times 10^{-4}$		
MARTENS' temperature	°C	natural rubber		67–68
		rubber, vulcanized		55–80
Electr. resistivity	Ωcm	rubber: $10^{13}-10^{16}$		–
		hard rubber: $10^{12}-10^{18}$		
Dielectric constant		rubber: 2·4–3		–
		hard rubber: 3		
		caoutchouc: 2–3		
Dielectric loss factor tan $\delta \times 10^4$		rubber: 60–150 (10^3 c/s)		–
		caoutchouc: 90–200 (10^3 c/s)		
		hard rubber: 65–110 (10^6 c/s)		
Electrical breakdown strength	kV/cm	1 mm: 400	4 mm: 150–200	hard rubber (according to purity): 100–1200

TABLE 2.3.28. Natural rubber (critical load in industrial applications at 20 °C)

Mode of load	Max. permissible load in kg/mm²		Permissible deformation at max. load in %
Pressure (metal enclosed buffer rubber)	at rest	0·5	max.: 50; normal: 20–30
	slowly moved (spring buffer)	0·2	
	slow continuous movement	0·1	
	oscillations > 100 c/s	0·05	
Shear load	for soft rubber	0·1	
	for springs, couplings	0·05*	
Tension	at rest, constant load	†	100
	continuously changing	0·1	

* Related to the surface with maximum momentum.

† For larger cross sections dependent on tension on the edges (surface conditions), hardly dependent on tensile strength.

Examples of use: gasket rings, cooling water pipes, buffers, protecting caps, cable sheathings.

References

EHLERS, G., Gummi als Konstruktionswerkstoff, *Kunststoffe 31*, 422 (1941).
ESPE, W., a. M. KNOLL, *Werkstoffkunde der Hochvakuumtechnik*, Springer, Berlin 1936, p. 221.
LUFF-SCHMELKES, *Chemie des Kautschuks*, Berlin, 1925.
MEMMLER, K., *Handbuch der Kautschukwissenschaft*, Leipzig, 1930.

2.3.1.8 Oils and Greases

(See bibliography)

2.3.2 Vapour Pressures, Melting and Boiling Points

TABLE 2.3.29. Vapour pressures of pump fluids.

Diffusion pump fluid	Chemical composition	M	B	A	T_{-5} in °C*	T_{-2} in °C*	p at 25 °C [Torr] †	Ref.
Butylphthalate	di-*n*-butylphthalate	278	11·215	4680	18	81	$3{\cdot}3^{-5}$	[*1*]
Octylphthalate	di-*n*-octylphthalate	391	12·94	6035	65	128	$4{\cdot}0^{-8}$	[*5*]
Nonylphthalate	di-*n*-nonylphthalate	419	13·41	5690	73	146	$1{\cdot}0^{-8}$	[*5*]
Octoil (35/*9*)**	di-2-ethylhexylphthalate	390	12·116	5590	54	128	$2{\cdot}3^{-7}$	[*1*]
			12·90	6157	67	134	$3{\cdot}3^{-8}$	[*5*]
Narcoil 40	di-(3·5·5-trimethylhexyl)-phthalate	418	12·88	5936	57	124	$6{\cdot}0^{-8}$	[*5*]
Amoil (35/*3*)	di-*iso*-amylphthalate	306	10·60	4610	22	93	$1{\cdot}3^{-5}$	[*1*]
Amoil S (32/*1*)	di-*iso*-amylsebacate	343	11·40	5190	25	114	$1{\cdot}0^{-6}$	[*4*]
Octoil S	di-2-ethylhexylsebacate	426	11·26	5514	50	142	$2{\cdot}0^{-8}$	[*3*]
m-Cr (32/*4*, *5*)	tri-*m*-cresylphosphate	368	10·982	5373	50	141	$9{\cdot}0^{-8}$	[*2*]
p-Cr	tri-*p*-cresylphosphate	368	12·223	5926	52	144	$2{\cdot}0^{-8}$	[*2*]
b-S (32/*9*)	di-benzylsebacate	–	12·775	6320	64	155	$4{\cdot}0^{-9}$	[*2*]
Apiezon A (35/*4*)	mixture of hydrocarbons	350	–	–	37	110	$2{\cdot}0^{-6}$	[*3*]
Apiezon B (32/*2*)		350	–	–	50	127	$4{\cdot}0^{-7}$	[*3*]
Apiezon C (35/*11*)		450	11·67	5925	77	160	$1{\cdot}0^{-8}$	[*6*]
Arochlor (35/*2*)	similar to pentachlordiphenyl	326	–	–	27	93	$8{\cdot}0^{-6}$	[*3*]
Littonoil (32/*3*)	hydrocarbon chains with even numbers, C_nH_{2n}	–	–	–	57	132	$1{\cdot}4^{-7}$	[*3*]

Chlophen A 40 (35/*1*)	chlorinated benzene	205	10·15	4135	0	67	2·0^{-4}	[*6*]
Silicone DC 703 (35/*12*)	semi-organic compound of silicon	570	12·32	6165	83	153	5·0^{-9}	[*6*]
Silicone oils normal (35/*5*)	by trimethylsiloxy-groups derived from siloxane with phenyl-groups on the silicon bonds	—	14·01	6410	64	127	3·2^{-8}	[*7*]
Silicone oils ultra (35/*6*)		730	14·49	6667	69	131	1·3^{-3}	[*7*]
Diffelen L (35/*7*)	mixture of saturated hydrocarbons	335	12·70	6098	71	142	1·8^{-8}	[*7*]
Diffelen N (35/*8*)		435	13·15	6329	76	145	8·5^{-9}	[*7*]
Diffelen U (35/*10*)		450	12·92	6410	85	156	2·6^{-9}	[*7*]

* The table shows the figures for the constants A and B in the equation $\log p = B - A/T$ for the vapour pressure in Torr. T abs. temperature. T_{-5} and T_{-2} are the temperatures *in* °*C*, for which the corresponding vapour pressure is 10^{-5} and 10^{-2} Torr, resp. The next column shows the vapour pressure in Torr at room temperature (25 °C).

† Abbreviation: x^{-n} stands for $x \times 10^{-n}$. Example: $3{\cdot}3^{-5}$ stands for $3{\cdot}3 \times 10^{-5}$.

** Figures in brackets refer to the vapour pressure curves on pp. 217—220 (35/9) means: Fig. 2.3.35, curve 9.

References

[*1*] Hickman, K. C. D., J. C. Hacker and N. D. Embree, *Industr. Engng. Chem.*, **9**, 264 (1937).
[*2*] Verhoek, F. H., and A. L. Marshall, *J. Amer. Chem. Soc.*, **61** 2737 (1939)
[*3*] Metropolitan Vickers (1946).
[*4*] Values of constants deduced by S. F. Kapff of Distillation Products, Inc.
[*5*] Peperle, W., and H. Hoyer, *Z. Elektrochem.*, **62**, 61 (1958)
[*6*] Herlet, A., and G. Reich, *Z. angew. Phys.*, **9**, 14 (1957).
[*7*] Struck, B. D., Not yet published.

TABLE 2.3.30. Silicone oils

Formula: $[(CH_3)_3\,SiO_{1/2}]\,[(CH_3)_{x-2}]\,[(CH_3)\,SiO_{1/2}]$

Vapour pressures of linear silicon polymers* (see Fig. 2.3.32).

x	B	A	T_{-5} (°C)†	T_{-1} (°C)†	p at 25°C (Torr)
12	11·60	5350	49	152	$4{\cdot}4 \times 10^{-7}$
13	12·06	5710	62	165	$7{\cdot}6 \times 10^{-8}$
14	12·48	6070	74	177	$1{\cdot}3 \times 10^{-8}$
15	12·93	6430	86	189	$2{\cdot}2 \times 10^{-9}$
16	13·37	6790	97	200	$3{\cdot}8 \times 10^{-10}$
17	13·81	7150	107	210	$6{\cdot}5 \times 10^{-11}$
18	14·25	7510	117	294	$1{\cdot}2 \times 10^{-11}$

* WILCOCK, D. F., *J. Amer. Chem. Soc.*, **68**, 691 (1946).

† See footnote * in Table 2.3.29.

TABLE 2.3.31. Greases and cements for vacuum sealings* †

Material	vapour pressure [Torr]	
	at 20 °C	at 90 °C
Ramsay grease	10^{-4}–10^{-5}	
Apiezon grease M, fresh	10^{-5}	
Apiezon grease M, degassed	10^{-8}–10^{-9}	6×10^{-6}
Apiezon grease L, fresh	5×10^{-6}	
Apiezon grease L, degassed	ca. 10^{-10}	10^{-7}
Apiezon grease P	ca. 10^{-10}	10^{-7}
Apiezon grease R	ca. 10^{-10}	10^{-7}
Apiezon grease S	ca. 10^{-10}	10^{-7}
Apiezon, soft wax	10^{-4}	
Apiezon wax Q	10^{-4}	2×10^{-4} (70 °C)
Sealing wax, white	10^{-3}	
Silicone grease	$< 10^{-10}$	10^{-8}
Picein	3–4×10^{4}	

* ESPE, W., *Werkstoffe der Elektrotechnik in Tabellen und Diagrammen*, Akademie-Verlag 1954, Berlin.

† HERLET, A., and G. REICH, *Z. angew. Phys.*, **9**, 14 (1957).

TABLE 2.3.32. Various organic substances

Phthalicesters		$\log p_{\text{liquid}} = B - A/T$ (p_{liquid} in Torr)
Dimethylphthalate (33/*6*)*	$C_6H_4(CO_2CH_3)_2$	11·50–4122/T
Diethylphthalate (33/*11*)	$C_6H_4(CO_2C_2H_5)_2$	12·51–4614/T
Dibutylphthalate	$C_6H_4(CO_2C_4H_9)_2$	13·83–5204/T
Di-*n*-octylphthalate	$C_6H_4(CO_2C_8H_{17})_2$	12·94–6035/T
Di-2-ethylhexylphthalate	$C_6H_4(CO_2C_8H_{17})_2$	12·90–6157/T
Di-*n*-nonylphthalate	$C_6H_4(CO_2C_9H_{19})_2$	11·41–5690/T
Di-(3·5·5-trimethylhexyl)-phthalate	$C_6H_4(CO_2C_9H_{19})_2$	12·88–5936/T
Butylphenylphthalate (33/*13*)	$C_6H_4CO_2C_6H_5CO_2C_4H_9$	11·12–4745/T

* See footnote ** in Table 2.3.29.

TABLE 2.3.32. (continued)

Aromatic hydrocarbons			log $p_{solid} = B - A/T$ (p_{solid} in Torr)
Naphthalene	(33/*1*)	$C_{10}H_8$	10·75–3616/T
Azulene	(33/*5*)	$C_{10}H_8$	11·00–3958/T
Acenaphthene	(33/*8*)	$C_{12}H_{10}$	11·50–4264/T
Anthracene	(30/*11*)	$C_{14}H_{10}$	11·15–5401/T
Phenanthrene	(30/*3*)	$C_{14}H_{10}$	16·00–5008/T
9·10-Dihydroanthracene		$C_{14}H_{12}$	12·73–4878/T
9·10-Diphenylanthracene		$C_{14}H_8(C_6H_5)_2$	14·57–7500/T
Fluoranthene	(34/*5*)	$C_{16}H_{10}$	12·67–5357/T
Chrysene	(31/*7*)	$C_{18}H_{12}$	13·07–6340/T
Pyrene	(30/*9*)	$C_{16}H_{10}$	12·00–5248/T
5·12-Benzanthracene	(30/*14*)	$C_{18}H_{12}$	13·68–6250/T
Triphenylene	(30/*15*)	$C_{18}H_{12}$	12·89–6154/T
5·12-Dihydrotetracene	(30/*16*)	$C_{18}H_{14}$	12·35–6060/T
1·4-Diphenylbenzene	(34/*11*)	$C_6H_4(C_6H_5)_2$	13·65–6298/T

Alphatic hydrocarbons			log $p_{solid} = B - A/T$ (p_{solid} in Torr)
n-Tetradecane	(33/*3*)	$CH_3(CH_2)_{12}CH_3$	16·82–5401/T
n-Hexadecane	(33/*10*)	$CH_3(CH_2)_{14}CH_3$	18·13–6154/T
n-Tetradecene-1	(33/*2*)	$CH_3CH:CH(CH_2)_{10}CH_3$	14·40–4636/T
n-Octadecene-1	(34/*1*)	$CH_3CH:CH(CH_2)_{14}CH_3$	15·33–5648/T

Alcohols			log $p_{solid} = B - A/T$ (p_{solid} in Torr)
Lauryl alcohol	(33/*12*)	$CH_3(CH_2)_{10}CH_2OH$	21·29–7205/T
Myristyl alcohol	(34/*3*)	$CH_3(CH_2)_{12}CH_2OH$	24·08–8484/T
Cetyl alcohol	(34/*6*)	$CH_3(CH_2)_{14}CH_2OH$	23·47–8681/T
Stearyl alcohol	(34/*10*)	$CH_3(CH_2)_{16}CH_2OH$	23·63–9075/T

Carboxylicacids			log $p_{solid} = B - A/T$ (p_{solid} in Torr)
Lauric acid	(34/*4*)	$CH_3(CH_2)_{10}CO_2H$	19·98–7369/T
Myristic acid	(34/*7*)	$CH_3(CH_2)_{12}CO_2H$	20·35–7828/T
Palmitic acid	(34/*9*)	$CH_3(CH_2)_{14}CO_2H$	22·65–8878/T

Benzene derivates			log $p_{solid} = B - A/T$ (p_{solid} in Torr)
1·4-Diphenylbenzene	(31/*3*)	$C_6H_4(C_6H_5)_2$	13·65–6298/T
1·3-Diphenylbenzene	(31/*1*)	$C_6H_4(C_6H_5)_2$	15·01–6213/T
1·3·5-Triphenylbenzene	(34/*12*)	$C_6H_3(C_6H_5)_3$	15·40–7500/T

TABLE 2.3.32. (continued)

Benzene derivatives			$\log p_{\text{solid}} = B - A/T$ (p_{solid} in Torr)
o-Nitroaniline	(30/*1*)	$O_2NC_6H_4NH_2$	12·50–4701/T
m-Nitroaniline	(30/*6*)	$O_2NC_6H_4NH_2$	13·00–5095/T
p-Nitroaniline	(30/*10*)	$O_2NC_6H_4NH_2$	13·69–5707/T
2·3-Dinitrophenol	(30/*8*)	$(O_2N)_2C_6H_3OH$	12·58–5171/T
2·4-Dinitrophenol	(30/*7*)	$(O_2N)_2C_6H_3OH$	13·95–5466/T
2·5-Dinitrophenol	(30/*4*)	$(O_2N)_2C_6H_3OH$	12·45–4876/T
2·6-Dinitrophenol	(30/*5*)	$(O_2N)_2C_6H_3OH$	15·38–5860/T
3·4-Dinitrophenol	(30/*13*)	$(O_2N)_2C_6H_3OH$	14·25–6451/T
Resorcinol	(30/*2*)	$C_6H_4(OH)_2$	12·30–4876/T
2-Nitroresorcinol	(33/*4*)	$O_2NC_6H_3(OH)_2$	11·05–3892/T
Perylene	(31/*11*)	$C_{20}H_{12}$	13·95–7260/T
Coronene	(29/*4*)	$C_{24}H_{12}$	12·62–7675/T
Rubrene	(29/*5*)	$(C_6H_5)_2C_9H_4:C_9H_4(C_6H_5)_2$	13·71–8397/T
9·9′-Biantryl	(29/*3*)	$C_{28}H_{18}$	11·42–6679/T
Phenanthrenequinone	(31/*8*)	$C_{14}H_8O_2$	14·37–6895/T
4-Hydroxybenzaldehydanil	(30/*17*)	$C_6H_5N:CHC_6H_4OH$	14·03–6679/T
Salicylaldehydanil	(34/*2*)	$C_6H_5N:CHC_6H_4OH$	16·20–6057/T
Fluorol 5 G		$C_{23}H_{10}O$	14·61–7219/T
1·5-Dipiperidylanthraquinone, red	(31/*13*)		17·13–9053/T
Triglycol-œnanthicester	(30/*12*)	$C_{13}H_{26}O_5$	10·60–4876/T
Tricresylphosphate		$PO_4(C_6H_4CH_3)_3$	13·28–6278/T

Hydroxyanthraquinones			$\log p_{\text{solid}} = B - A/T$ (p_{solid} in Torr)
Anthraquinone	(31/*5*)	$C_{14}H_8O_2$	14·31–6604/T
1-Hydroxyanthraquinone	(31/*2*)	$C_6H_4\begin{smallmatrix}CO\\CO\end{smallmatrix}C_6H_3OH$	13·84–6298/T
2-Hydroxyanthraquinone	(31/*12*)	$C_6H_4\begin{smallmatrix}CO\\CO\end{smallmatrix}C_6H_3OH$	15·23–7999/T
1·2-Dihydroxyanthraquinone	(31/*10*)	$C_6H_4\begin{smallmatrix}CO\\CO\end{smallmatrix}C_6H_2(OH)_2$	12·57–6473/T
1·4-Dihydroxyanthraquinone	(31/*6*)	$C_6H_4\begin{smallmatrix}CO\\CO\end{smallmatrix}C_6H_2(OH)_2$	13·70–6451/T
1·5-Dihydroxyanthraquinone	(31/*9*)	$HOC_6H_3\begin{smallmatrix}CO\\CO\end{smallmatrix}C_6H_3OH$	13·10–6619/T
1·8-Dihydroxyanthraquinone	(31/*4*)	$HOC_6H_3\begin{smallmatrix}CO\\CO\end{smallmatrix}C_6H_3OH$	13·82–6422/T
2·6-Dihydroxyanthraquinone	(29/*6*)	$HOC_6H_3\begin{smallmatrix}CO\\CO\end{smallmatrix}C_6H_3OH$	14·74–9075/T
1·4·5·8-Tetrahydroxyanthraquinone	(31/*14*)	$(HO)_2C_6H_2\begin{smallmatrix}CO\\CO\end{smallmatrix}C_6H_2(OH)_2$	14·42–7916/T

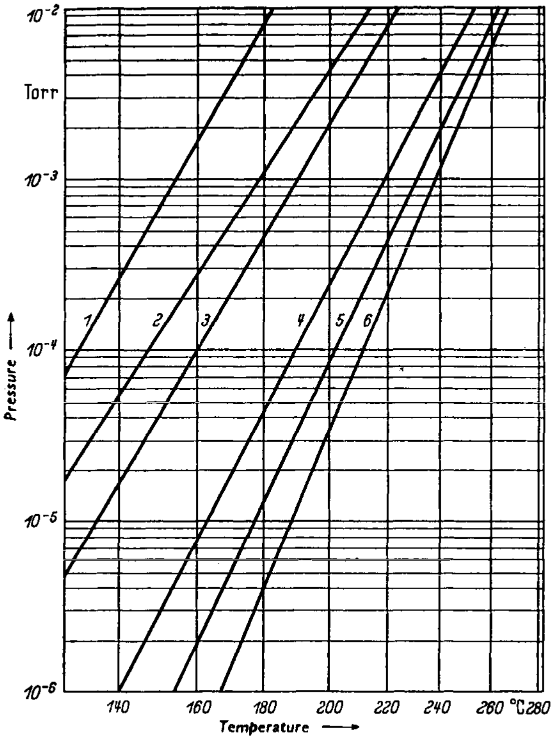

FIG. 2.3.29. Vapour pressure curves of *1* – 9·10-Diphenylanthraquinone, *2* – Lithium grease, *3* – 9·9′-Biantryl, *4* – Coronene, *5* – Rubrene, *6*–2·6-Dihydroxyanthraquinone.

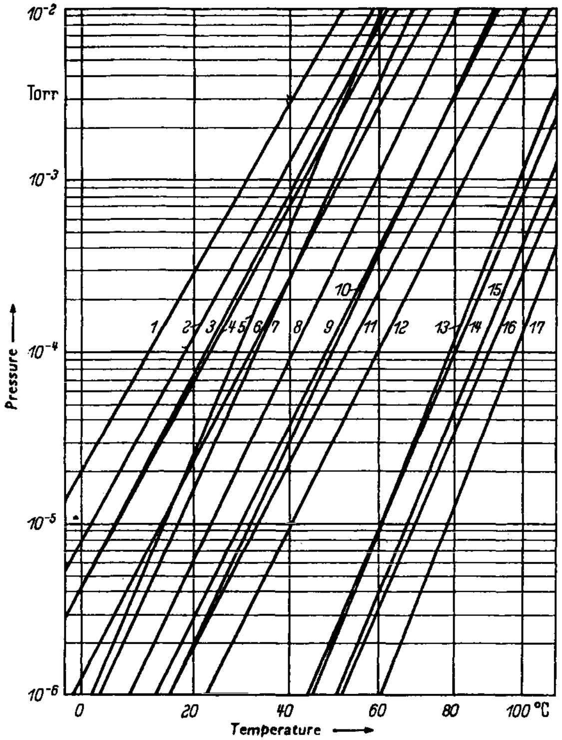

FIG. 2.3.30. Vapour pressure curves of *1* — ŏ-Nitraniline, *2* – Resorcinol, *3* – Phenanthrene, *4* — 2·5-Dinitrophenol, *5* — 2·6-Dinitrophenol, *6* – *m*-Nitraniline, *7* — 2·4-Dinitrophenol, *8* — 2·3-Dinitrophenol, *9* – Pyrene, *10* – *p*-Nitraniline, *11* – Anthracene, *12* – Triglycolœnanthicester, *13* — 3·4-Dinitrophenol, *14* — 1·2-Benzanthracene, *15* – Triphenylene, *16* — 5·12-Dihydrotetracene, *17* — 4-Hydroxybenzaldehydanil

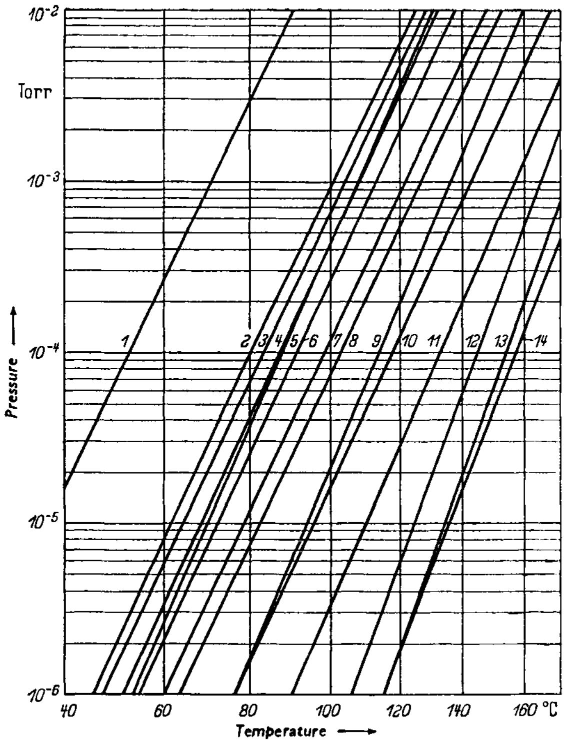

FIG. 2.3.31. Vapour pressure curves of *1* – 1·3-Diphenylbenzene, *2* – 1-Hydroxyanthraquinone, *3* – 1·4-Diphenylbenzene, *4* – 1·8-Dihydroxyanthraquinone, *5* – Anthraquinone, *6* – 1·4-Dihydroxyanthraquinone, *7* – Chrysene, *8* – Phenanthrenquinone, *9* – 1·5-Dihydroxyanthraquinone, *10* – Alizarin, *11* – Perylene, *12* – 2-Hydroxyanthraquinone, *13* – 1·5-Dipiperidylanthraquinone, *14* – 1·4·5·8-Tetrahydroxyanthraquinone.

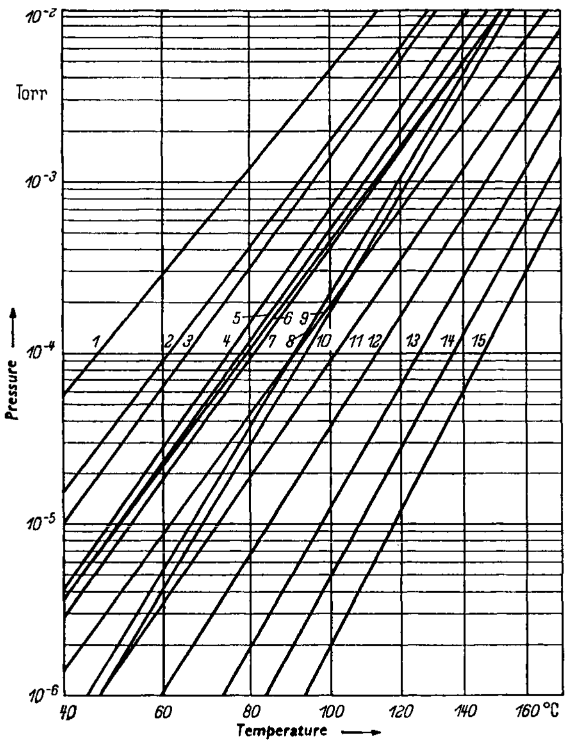

FIG. 2.3.32. Vapour pressure curves of *1* – Amoil-S, *2* – Apiezon-B, *3* – Litton oil, *4* – *m*-Cr(1), *5* – *m*-Cr(2), *6* — Silicone oil $[(CH_3)SiO_{1/2}](CH_3)_{10}$, *7* – Octoil, *8* – Silicone oil $[(CH_3)SiO_{1/2}](CH_3)_{11}$, *9* – b-S, *10* – Di-*n*-ethylphthalate, *11* – Silicone oil $[(CH_3)SiO_{1/2}](CH_3)_{12}$, *12* — Silicone oil $[CH_3)SiO_{1/2}](CH_3)_{13}$, *13* – Silicone oil $[(CH_3)SiO_{1/2}](CH_3)_{14}$, *14* – Silicone oil $[(CH_3)SiO_{1/2}](CH_3)_1^9$ *15* – Silicone oil $[CH_3)SiO_{1/2}](CH_3)_{16}$.

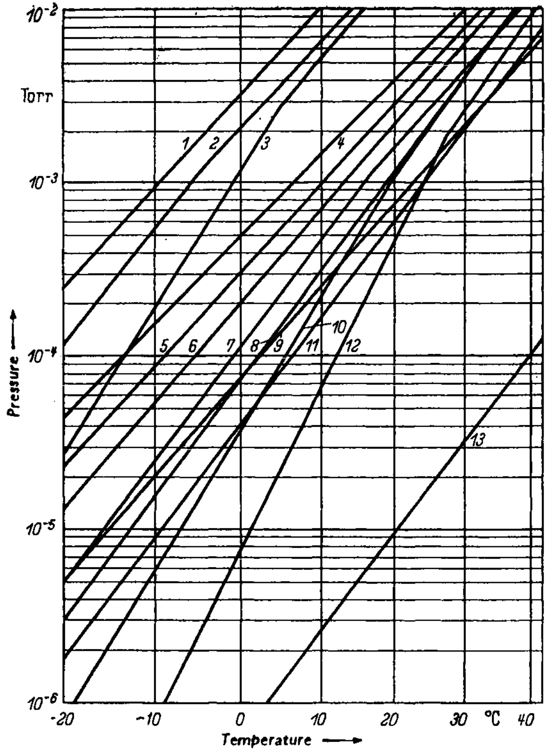

FIG. 2.3.33. Vapour pressure curves of *1* – Naphthalene, *2* – *n*-Tetradecene-1, *3* – *n*-Tetradecane, *4* – 2-Nitroresorcinol, 5 – Azulene, *6* – Dimethylphthalate, *7* – *n*-Hexadecene, *8* – Acenaphthene, *9* – Capro-Lactam, *10* – *n*-Hexadecane, *11* – Diethylphthalate, *12* – *n*-Laurylalcohol, *13* – Butylbenzylphthalate.

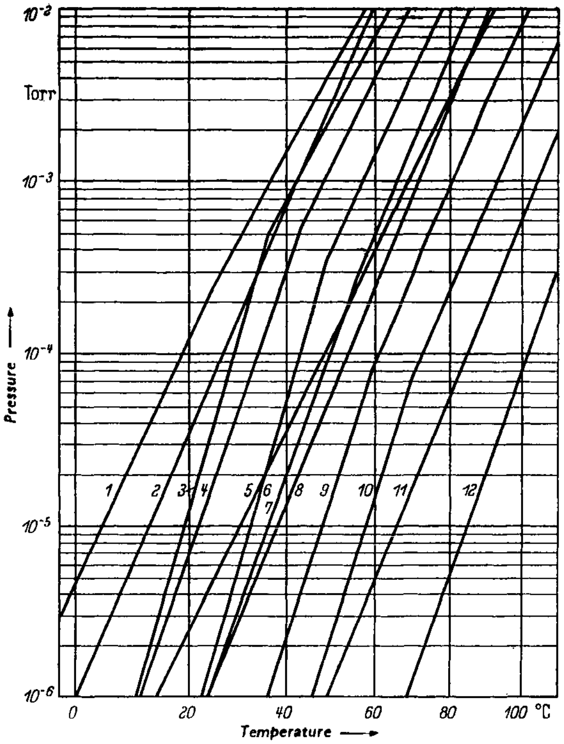

FIG. 2.3.34. Vapour pressure curves of *1* – n-Octadecene-1, *2* – Salicylaldehydanil, *3* – Myristyl alcohol, *4* – Lauric acid, *5* – Fluoranthene, *6* – *n*-Cetyl alcohol, *7* – Myristic acid, *8* – 1·3-Diphenylbenzene, *9* – Palmitic acid, *10* – Stearyl alcohol, *11* – 1·4-Diphenylbenzene, *12* – 1·3·5-Triphenylbenzene.

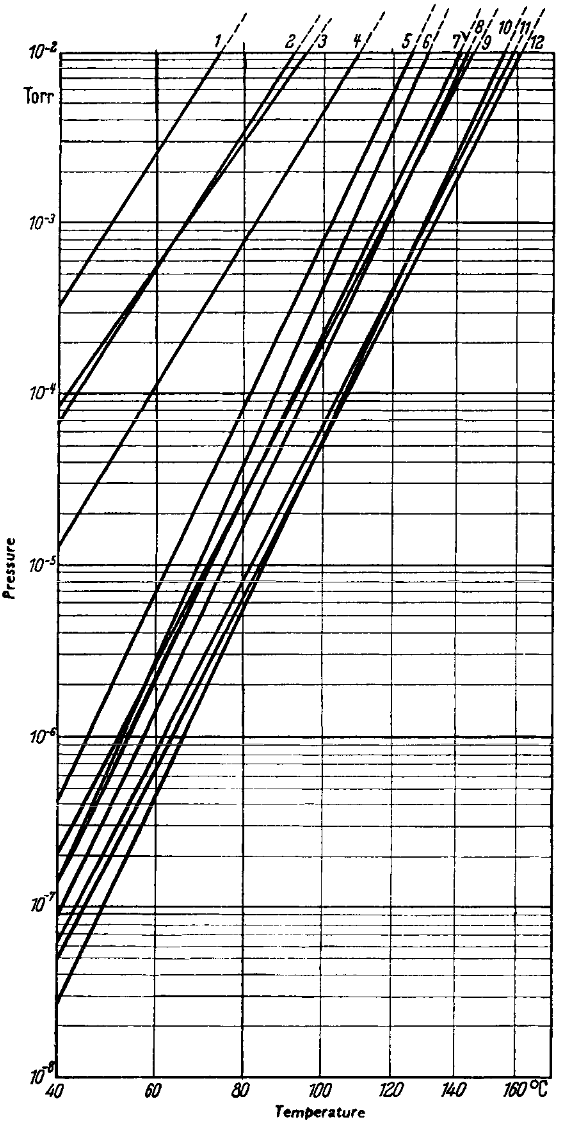

FIG. 2.3.35. Vapour pressure curves of *1* – Clophen A 40, *2* – Arochlor, *3* – Amoil, *4* – Apiezon A, *5* – Silicone oil normal, *6* – Silicone oil ultra, *7* – Diffelen L, *8* – Diffelen N, *9* – Octoil, *10* – Diffelen U, *11* – Apiezon C, *12* – Silicone oil DC 703.

Table 2.3.33. Metals *

Element	Melting point °C	Boiling point °C	Temperature T (°K) for vapour pressure p_s [Torr]			
			10^{-8}	10^{-5}	10^{-2}	10
Ag	960·8	2210	852	1030	1305	1830
Al	659	2300	950	1155	1480	2050
Au	1063	2970	1045	1260	1605	2240
B	2300	2600	1650	1960	2430	3300
Ba	704	1640	560	690	900	1310
Be	1284	2510	972	1175	1485	2060
Bi	271	1630	590	723	934	1330
Graphite	≈ 3700	$1{\cdot}8 \times 10^{10}$	1950	2250	2700	3420
Ca	849	1450	555	675	865	1240
Cd	321	765	346	422	540	759
Ce	775	2400	1080	1280	1680	2070
Co	1495	3000	1200	1435	1790	2440
Cr	1890	2500	1125	1335	1665	2240
Cs	28	690	256	319	425	646
Cu	1083	2600	1005	1215	1545	2140
Fe	1535	2740	1150	1380	1740	2370
Ga	29·8	2070	845	1030	1330	1870
Ge	959	(2700)	1085	1310	1680	2350
Hg	— 38·87	357	199	245	318	456
In	156	≈ 2000	770	943	1220	1730
Ir	2454	≈ 5300	1720	2070	2580	3440
K	63	762	294	364	481	715
La	866	4340	1260	1535	1970	2730
Li	186	1370	505	621	806	1155
Mg	650	1110	462	560	715	1000
Mn	1244	≈ 2150	807	970	1220	1700
Mo	2622	4800	1855	2260	2900	4040
Na	97·7	890	350	431	563	818
Nb	2500	≈ 5000	2080	2470	3010	3900
Ni	1453	2730	1185	1415	1770	2400
Os	≈ 2700	≈ 5500	1980	2370	2930	3860
Pb	327·4	1740	617	760	992	1435
Pd	1555	≈ 3000	1180	1430	1820	2560
Pt	1773	4400	1560	1875	2350	3210
Rb	39	≈ 690	270	337	449	665
Re	3176	5900	2200	2640	3330	
Rh	1966	> 4000	1550	1860	2300	3120
Ru	2500	≈ 4900	(1840)	2190	2700	3540
Sb	630	1620	550	655	815	1250
Se	220	680	357	417	505	702
Si	1414	2480	1200	1450	1820	2430
Sn	231·9	2270	937	1155	1500	2160
Sr	771	1380	499	615	804	1170
Ta	2996	(4100)	2230	2670	3340	
Te	452	1390	451	534	656	906

(continued p. 227)

---

* After W. Espe: *Werkstoffkunde der Hochvakuumtechnik I*, Berlin, 1959.

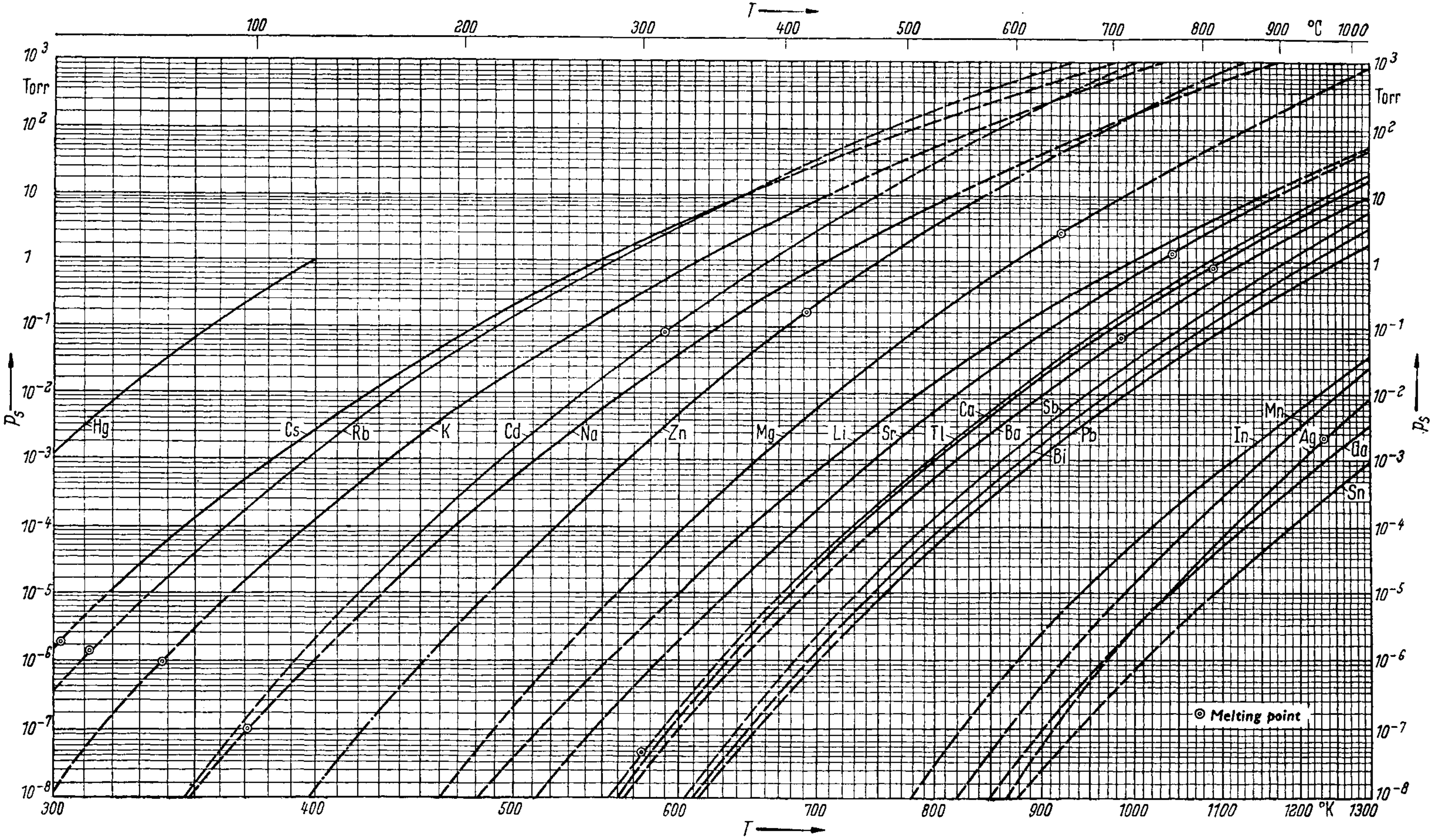

FIG. 2.3.36a. Saturation pressure p_s of metals for temperatures of 300–1300°K (after ESPE: *Werkstoffkunde der Hochvakuumtechnik I*, Berlin, 1959).

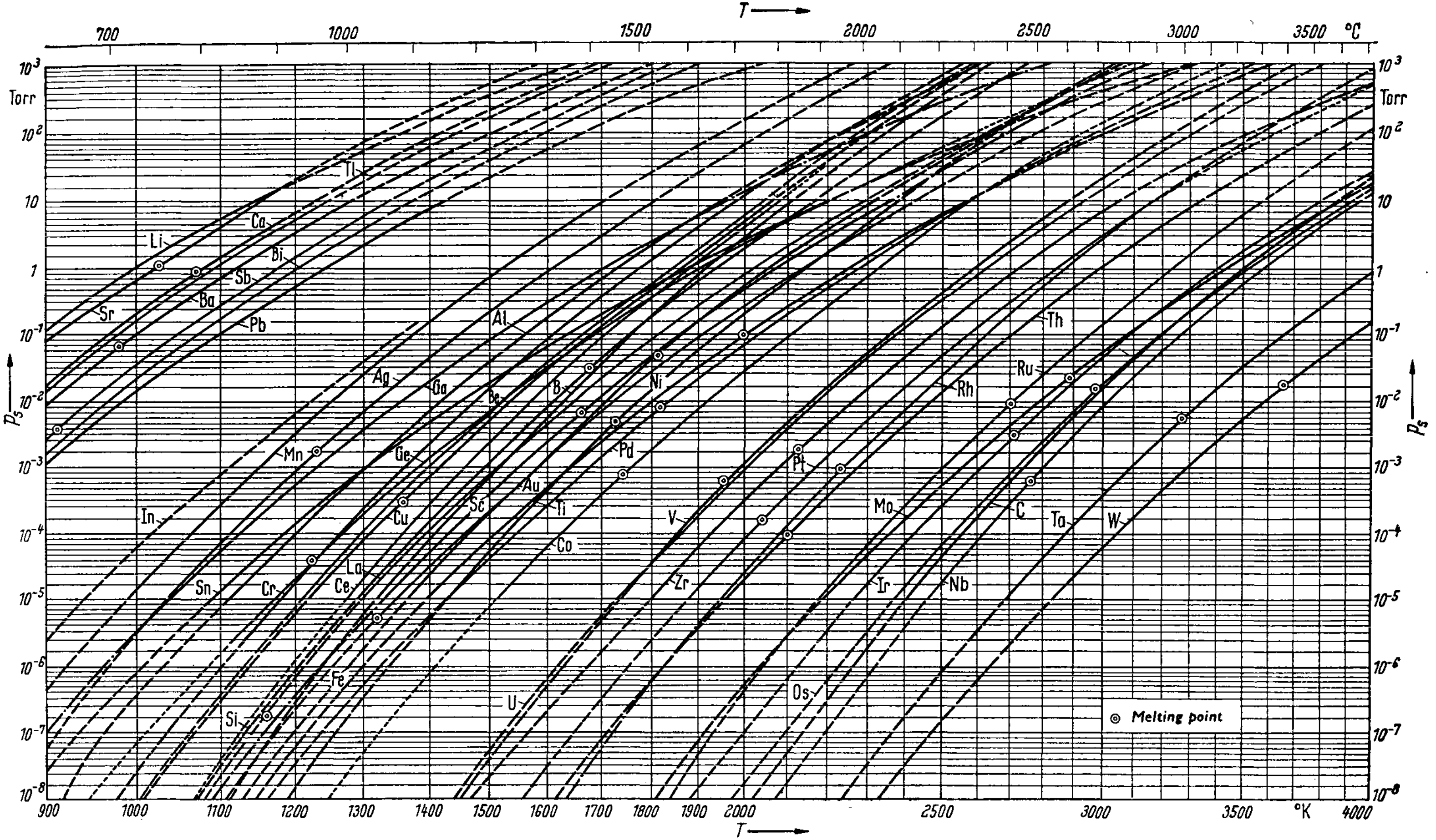

FIG. 2.3.36b. Saturation pressure p_s of metals for temperatures of 900–4000°K. (after ESPE: *Werkstoffkunde der Hochvakuumtechnik I*, Berlin, 1959).

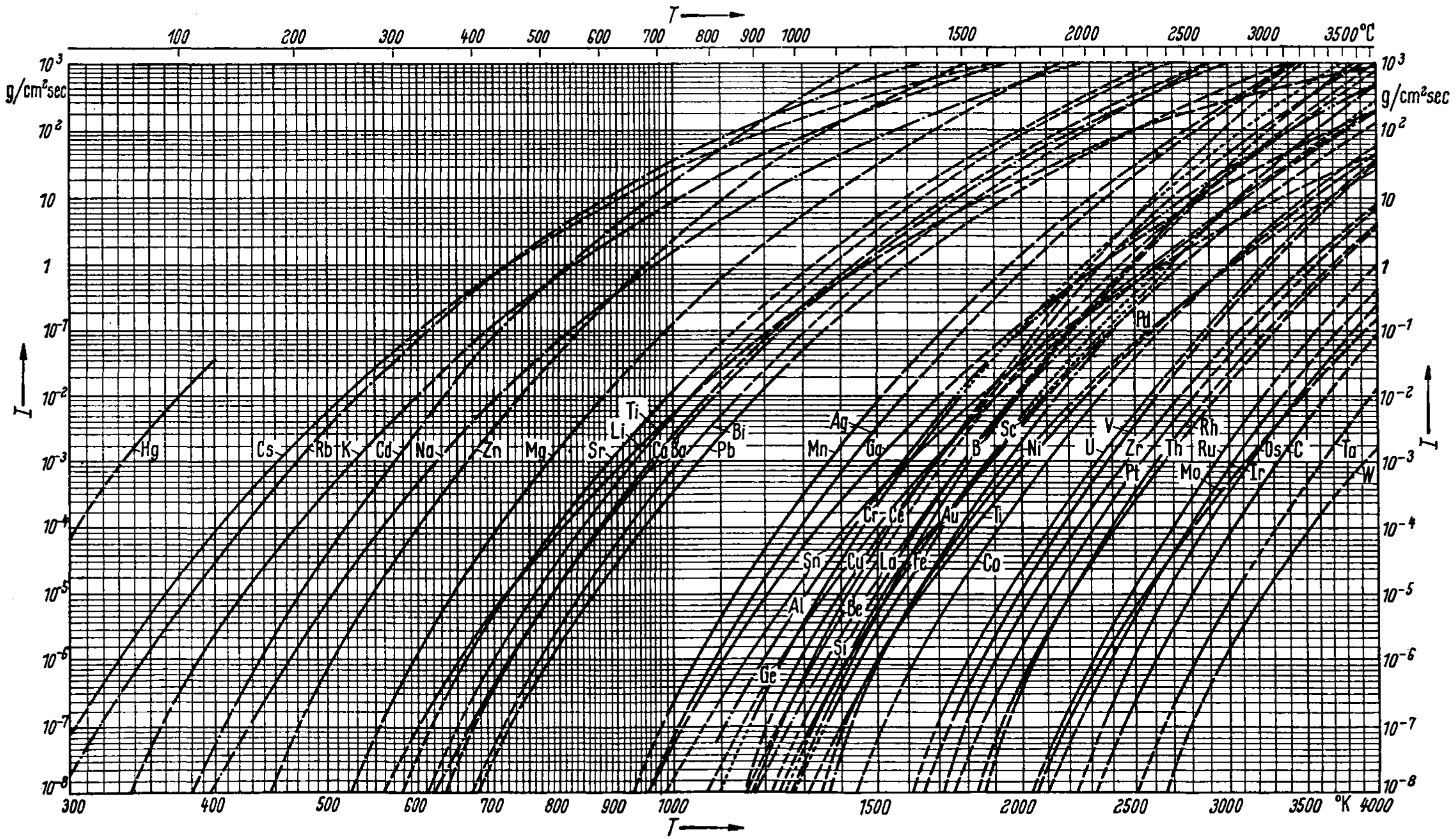

FIG. 2.3.37. Rate of evaporation I of metals for temperatures of 300–4000 °K. (after ESPE: *Werkstoffkunde der Hochvakuumtechnik I*, Berlin, 1959).

TABLE 2.3.33. (continued)

Element	Melting point °C	Boiling point °C	Temperature T (°K) for vapour pressure p_S [Torr]			
			10^{-8}	10^{-5}	10^{-2}	10
Th	1690	≈ 4200	1620	1960	2470	3330
Ti	1690	3535	1330	1600	2000	2750
Tl	300	1460	558	685	888	1270
U	≈ 1133	3900	1405	1715	2200	3070
V	1900	≈ 3400	1428	1705	2120	2840
W	3382	5900	2340	2820	3570	
Zn	419·4	907	396	481	615	864
Zr	1857	3700	1745	2110	2670	3620

2.3.3 Gas Permeation and Diffusion through Vitreous Silica and Glass

The permeation of gas through vitreous silica and different kinds of glass was first discovered by VILLARD [*1*]* in 1910, and has since been investigated in numerous studies. A summary of this work up to 1938 can be found in the publication of BARRER [*2*], which includes measuring procedures and results. More recent investigations are listed in references [*14*] to [*27*].

The permeation of gas through a membrane shows the following features:

(a) The steady flow is governed by FICK's first law [*3, 4, 6*]

$$j = -D \operatorname{grad} n \tag{2.3.1}$$

where

j density of the gas flow
D diffusion constant
n gas concentration inside the membrane

(b) The rate of permeation is proportional to the pressure (i. e. without dissociation of the molecules) and inversely proportional to the thickness of the membrane [*7*].

(c) On membranes made of glass no activation energy for the absorption and the desorption process was observed. The speed of permeation is governed by the diffusion of the gas inside the membrane.

(d) HENRY's law governs the solubility of gases in vitreous silica and glass.

The majority of measurements were made in cylindrically or spherically shaped membranes. A schematic diagram of a typical arrangement is illustrated

---

* Figures in [ ] refer to the list of references at the end of chapter 2.3.3 (i.e. p. 233).

in Fig. 2.3.38. In older studies pressure was measured with the McLeod gauge or with the Pirani gauge. In more recent studies, in which the methods of ultra-high vacuum techniques are largely used, pressure is measured either with the Bayard–Alpert gauge [*20, 23, 24*] or with mass spectrometers [*17, 18, 19, 21, 22*].

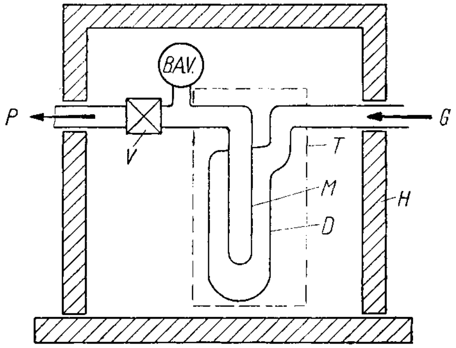

Fig. 2.3.38. Experimental set-up for measuring the diffusion constant for gases in glass.
D – diffusion cell; M – membrane; T – thermostat for experiments at different temperatures; G – gas inlet; BAV – Bayard–Alpert gauge; V – bakeable metal valve; P – to diffusion pump, H – oven.

The total mass of a noble gas, G, which, without any dissociation, penetrates the membrane, is – according to [*14*] – given by:

$$G = K F t \frac{p_1 - p_2}{d} \quad (\mathrm{cm^3\,(NTP)}), \qquad (2.3.2)$$

where

K – permeation rate;
F – area of membrane ($\mathrm{cm^2}$);
t – time (sec);
p_1, p_2 – pressures on each side of the membrane (Torr),
d – thickness of membrane (mm).

The permeation rate K indicates how many cm³ of gas (NTP, i.e. at 0 °C, 760 Torr) per cm² area, per sec and at a gas pressure difference of 1 Torr penetrate a membrane of 1 mm thickness. The dimension of K, therefore, is:

$$(K) = (\mathrm{cm^3\,(NTP)\,mm\,cm^{-2}\,sec^{-1}\,Torr^{-1}})\,.$$

The permeation rate K for helium, neon, argon, hydrogen and nitrogen through vitreous silica are given in Tables 2.3.34 and 2.3.35.

TABLE 2.3.34. Permeation rate K of helium through vitreous silica

Temperature (°C)	$K \times 10^{10}$ [cm^3 (NTP) mm cm^{-2} sec^{-1} $Torr^{-1}$]			
	BRAATEN and CLARK [7]			BURTON, BRAATEN and WILHELM [8]
—200	–	–	–	0·0028
—180	–	–	–	0·0035
—160	–	–	–	0·0038
—140	–	–	–	0·0044
—120	–	–	–	0·0053
—100	–	–	–	0·0066
— 80	0·00070	–	–	0·0084
— 70	0·00176	–	–	0·0101
— 60	0·00315	–	–	0·0121
— 50	0·0052	–	–	0·0145
— 40	0·0077	–	–	0·0179
— 30	0·0109	–	–	0·0224
— 20	0·0174	–	–	0·028
— 10	0·022	–	–	0·037
0	0·035	0·029	0·028	0·050
10	0·051	0·046	0·040	0·073
20	0·070	0·062	0·055	0·104
30	0·090	0·080	0·073	–
40	0·114	0·106	0·095	–
50	0·135	0·132	0·119	–
70	0·205	0·198	0·176	–
90	0·304	0·29	0·264	0·274
110	0·44	0·42	0·39	0·45
130	0·62	0·59	0·52	0·55
150	0·79	–	–	0·55

TABLE 2.3.35. Permeation rate K of various gases through vitreous silica

Temperature (°C)	$K \times 10^{10}$ [cm^2 (NTP) mm cm^{-2} sec^{-1} Torr^{-1}]								
	Ne T'SAI and HOGNESS [9]	A BARRER [10], JOHNSON and BURT [11]	H_2 BARRER [10]	H_2 WILLIAMS and FERGUSON [4]	H_2 WILLIAMS and FERGUSON [4]	H_2 WÜSTNER [3]	H_2 JOHNSON and BURT [11]	N_2 JOHNSON and BURT [11]	N_2 JOHNSON and BURT [11]
200	—	—	0·022	—	—	—	—	—	—
300	—	—	0·099	—	—	—	0·051	—	—
400	—	—	0·366	0·48	0·44	—	0·275	—	—
500	0·139	—	0·70	0·92	0·84	—	0·58	—	—
600	0·282	—	1·43	1·75	1·54	2·0	0·81	—	—
650	—	—	—	—	—	—	—	0·065	0·066
700	0·50	—	2·52	3·1	2·7	2·76	1·7	0·137	0·146
750	—	—	—	—	—	—	—	0·286	0·271
800	0·81	—	4·25	4·8	4·4	4·5	2·53	0·43	0·39
850	—	0·0161 [10]	—	—	—	—	—	0·80	0·64
900	1·18	0·58 [11]	6·4	—	7·0	—	3·6	1·19	0·95
950	0·062 0·031 [10]	—	—	—	—	—	—	—	1·44
1000	1·63	—	10·0	—	—	—	5·1	—	—

The Tables 2.3.36 and 2.3.37 give examples of the permeability of Pyrex glass for helium.

TABLE 2.3.36. Permeation rate K of helium through Pyrex glass

Temperature (°C)	$K \times 10^{10}$ [cm^3 (NTP) mm cm^{-2} sec^{-1} Torr^{-1}]	
	URRY [6]	VAN VOORHIS [12]
0	0·0037	—
20	0·0064	—
50	0·0128	—
100	0·0264	—
150	0·058	—
200	0·124	0·69
250	0·229	—
300	0·38	2·43
400	—	7·0
500	—	15·7

TABLE 2.3.37.
Permeation rate K of helium through Pyrex glass (after NORTON [17, 18, 19])

$K \times 10^{10}$ [cm^3 (NTP) mm cm^{-2} sec^{-1} Torr^{-1}]			
Temperature (°C)	$K \times 10^{10}$	Temperature (°C)	$K \times 10^{10}$
—78	0·000049	110	0·14
—23	0·0016	160	0·35
0	0·004	205	0·71
25	0·0091	230	1·1
25	0·015	260	1·9
100	0·084	265	1·7
107	0·10		

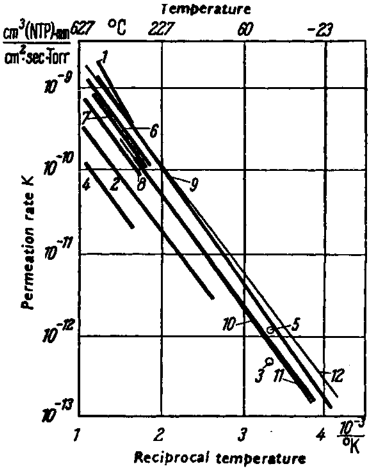

FIG. 2.3.39. Permeability of hard glasses for helium after various authors.

1 – VAN VOORHIS [*12*]
2 – URRY [*6*]
6 – RAYLEIGH
4 – TAYLOR and RAST [*13*]
5 – BAXTER
6 – SMITH and TAYLOR,
1. probe [*15*] (Pyrex)
7 – SMITH and TAYLOR,
2. probe [*15*]
8 – NEWKIRK and TOOLEY [*16*]
9 – NORTON [*17, 18, 19*]
10 – ALPERT [20]
11 – ESCHBACH [*24*] (Duran)
12 – LEIBY and CHEN [*23*] (Vycor)

The results obtained by various authors for the permeability of Pyrex glass for helium are summarized in Fig. 2.3.39. In the same graph the permeabilities of Duran glass [*24*] and Vycor glass [*23*] for helium are also plotted. The composition of these two glasses is not very much different from that of Pyrex glass (see Table 2.3.39).

NORTON [*18*] found a marked dependence of the permeation rate of various gases through vitreous silica on the atomic or molecular radius. This is shown in Table 2.3.38.

TABLE 2.3.38. Permeation rate K of various gases through vitreous silica (after NORTON [*18*])

	K [cm^3 (NTP) mm cm^{-2} sec^{-1} Torr^{-1})	
	at 700°C	at 600°C
Helium	$2{\cdot}1 \times 10^{-9}$	–
Hydrogen	$2{\cdot}1 \times 10^{-10}$	$1{\cdot}25 \times 10^{-10}$
Deuterium	$1{\cdot}7 \times 10^{-10}$	–
Neon	$4{\cdot}2 \times 10^{-11}$	$2{\cdot}8 \times 10^{-11}$
Argon	below 10^{-16}	–
Oxygen	below 10^{-16}	–
Nitrogen	below 10^{-16}	–

The relations between glass composition and gas permeability were also investigated [*12, 15, 16, 17, 18, 19, 24*].

Table 2.3.39 shows the composition of a number of glasses.

TABLE 2.3.39. Composition of some glasses (in per cent) for which the permeability for helium was measured at various temperatures (see Fig. 2.3.40)

Glass	1	2	3	4	5	6	7 (Pyrex)	8 (Vycor)	9 (Quartz)	10 (Duran)
SiO_2	–	31	62	72	–	90	81	96	100	76·1
B_2O_3	22	–	5	–	5	–	13	3	–	16·0
P_2O_5	–	–	–	–	77	–	–	–	–	–
Al_2O_3	–	–	18	1	11	3	2	1	–	1·75
CaO MgO	–	–	15	10	–	–	–	–	–	–
BaO	–	8	–	–	–	–	–	–	–	–
PbO	78	61	–	–	–	–	–	–	–	–
ZnO	–	–	–	–	7	–	–	–	–	–
Na_2O K_2O	–	–	–	17	–	7	4	–	–	5·5 0·6
SiO_2 B_2O_3 P_2O_5	22	31	67	72	82	90	94	99	100	92·1

The permeability of glasses 1—9 for helium was measured as a function of temperature by NORTON [*17, 18, 19*], (see Fig. 2.3.40). As the glass formers ($SiO_2 + B_2O_3 + P_2O_5$) decrease (100 per cent for glass 9 and 22 per cent for glass 1) the permeation rate also decreases by several orders of magnitude.

The dependence of gas permeation on temperature is expressed by the following equation:

$$K = K_0 \exp\left(-\frac{E}{RT}\right), \tag{2.3.3}$$

K_0 constant, E activation energy,
R general gas constant, T absolute temperature.

The activation energies can be calculated from the slope of the straight lines in Fig. 2.3.40. The result is shown in Fig. 2.3.41.

Very similar results to those shown in Fig. 2.3.40 for the permeation rates were obtained by ESCHBACH [*24*] for the diffusion coefficient. The activation energies calculated from these experiments are also plotted in Fig. 2.3.41.

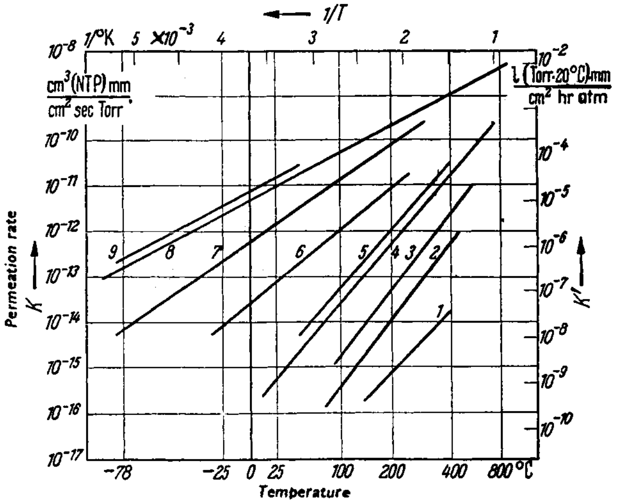

FIG. 2.3.40. Permeation rate of helium through various glasses as a function of temperature (after NORTON).
The numbers refer to the glasses listed in Table 2.3.39.

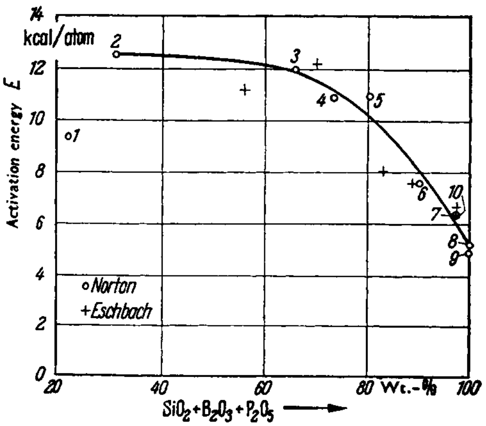

FIG. 2.3.41. Activation energy for the permeation of helium through various glasses (○ NORTON, + ESCHBACH).
The numbers refer to the glasses listed in Table 2.3.39.

The activation energies for the permeation of gases through glasses as obtained by various authors are listed in Table 2.3.40.

Table 2.3.40. Activation energies for the permeation of gases through glasses

Gas	Glass	E (cal/mol)	Author
Helium	Quartz	5,390	Braaten and Clark [7]
Helium	Quartz	5,600	T'sai and Hogness [9]
Helium	Quartz	5,700	Barrer [10]
Helium	Pyrex	8,700	Van Voorhis [12]
Helium	Pyrex	7,150 6,920 6,480	Taylor and Rast [13]
Helium	Pyrex	6,500 6,200	Rogers, Buritz and Alpert [20]
Helium	Pyrex	7,100	Smith and Taylor [15]
Helium	Pyrex	6,400	Norton [17]
Helium	Vycor	4,900	Norton [17]
Helium	Vycor	5,900	Leiby and Chen [23]
Helium	Duran	6,400	Eschbach [24]
Neon	Quartz	9,500	T'sai and Hogness [9]
Hydrogen	Quartz	9,300 10,000 10,800	Williams and Ferguson [4]
Hydrogen	Quartz	10,900	Barrer [10]
Hydrogen	Quartz	12,000	Wüstner [3]
Hydrogen	Quartz	9,200	Johnson and Burt [1]
Hydrogen	Duran	13,700	Eschbach [24]
Nitrogen	Quartz	26,000	Johnson and Burt [1]
Nitrogen	Quartz	22,000 29,900	Barrer [10]
Oxygen	Quartz	31,200	Barrer [10]

For the non-steady flow of gas through a membrane Fick's second law is valid:

$$\frac{\partial c}{\partial t} = D \Delta c. \tag{2.3.4}$$

If the boundary conditions and the conditions at $t = 0$ are known, this equation can be solved [20]. Two approximations can be obtained, one of which describes the steady state and is valid for large values of t. By extrapolating the curve of pressure rise the diffusion coefficient of the gas in the membrane can be found directly [2].

The second approximation is for small values of t [20], and it expresses the build-up mechanism of gas permeation. Here, too, the diffusion constant can be evaluated directly. Furthermore the solubility S for gases in glass [20, 23, 24] can be found. The results obtained by various authors are summarized in Table 2.3.41.

TABLE 2.3.41. Solubility S of various gases in glass

Gas	Glass	$S \times 10^3 \left[\frac{\text{cm}^3\ (\text{NTP})}{\text{cm}^3_{\text{glass}}\ (760\ \text{Torr})}\right]$	Author
Helium	Pyrex	8·0	WILLIAMS and FERGUSON [5]
Helium	Pyrex	7·9 6·5	ROGERS, BURITZ and ALPERT [20]
Helium	Pyrex	5·3	MCAFEE [21]
Helium	Vycor	4·3 4·6 at 26 °C	CHEN and LEIBY [23]
Helium	Vycor	9·4 at 100 °C	CHEN and LEIBY [23]
Helium	Duran	6·9	ESCHBACH [24]
Hydrogen	Duran	4·3	ESCHBACH [24]
Hydrogen	Vycor	7·0	CHEN and LEIBY [23]
Neon	Vycor	6·0	CHEN and LEIBY [23]
Nitrogen	Vycor	0·01–0·1	CHEN and LEIBY [23]

The solubility of helium in Pyrex [*20*] and of hydrogen and helium in Duran glass [*24*] seems to be independent of temperature. The rather high permeability of glasses and vitreous silica for helium can be utilized for cleaning and for accumulation of helium [*23, 26, 27*]. Furthermore the dependence of permeability on temperature allows very fine variable leaks to be produced for the admittance of helium.

References

[*1*] VILLARD, P., *C. R. Acad. Sci., Paris,* **130**, 1752 (1900).
[*2*] BARRER, R. M., *Diffusion in and through solids.* Cambridge University Press, 1951.
[*3*] WÜSTNER, H., *Ann. Phys.,* **46**, 1095 (1915).
[*4*] WILLIAMS, G. A., and J. B. FERGUSON, *J. Amer. Chem. Soc.* **44**, 2160 (1922).
[*5*] WILLIAMS, G. A., and J. B. FERGUSON, *J. Amer. Chem. Soc.,* **46**, 635 (1924).
[*6*] URRY, W., *J. Amer. Chem. Soc.* **54**, 3887 (1932).
[*7*] BRAATEN, E. O., and C. G. CLARK, *J. Amer. Chem. Soc.* **57**, 2714 (1935).
[*8*] BURTON, E. E., E. O. BRAATEN and J. O. WILHELM, *Canad. J. Res.,* **21**, 497 (1933).
[*9*] T'SAI, L. S., and T. HOGNESS, *J. Phys. Chem.,* **36**, 2595 (1932).
[*10*] BARRER, R. M., *J. Chem. Soc.,* 378 (1934).
[*11*] JOHNSON, J., and R. BURT, *J. Opt. Soc. Amer.,* **6**, 734 (1922).
[*12*] VAN VOORHIS, C. C., *Phys. Rev.,* **23**, 557 (1924).
[*13*] TAYLOR, N. W., and W. RAST, *J. Chem. Phys.* **6**, 612 (1938).
[*14*] VAN AMERONGEN, G. J., *J. Appl. Phys.,* **17**, 972 (1946).
[*15*] SMITH, P. L., and N. W. TAYLOR, *J. Amer. Ceram. Soc.,* **23**, 139 (1940).
[*16*] NEWKIRK, T. F., and F. V. TOOLEY, *J. Amer. Ceram. Soc.,* **32**, 272 (1949).
[*17*] NORTON, F, J., *J. Amer. Ceram. Soc.* **36**, 90 (1953).
[*18*] NORTON, F. J., *Vacuum Symp. Trans.* 47 (1954).
[*19*] NORTON, F. J., *J. Appl. Phys.* **28**, 34 (1957).
[*20*] ROGERS, W. A. R. S. BURITZ and D. ALPERT, *J. Appl. Phys.,* **25**, 868 (1954).
[*21*] MCAFEE, K. B. JR., *J. Chem. Phys.,* **28**, 218 (1958).
[*22*] MCAFEE, K. B. JR., *J. Chem. Phys.,* **28**, 226 (1958).

[23] Leiby, C. C., and C. L. Chen, *J. Appl. Phys.*, **31**, 268 (1960).
[24] Eschbach, H. L., *Advances in Vacuum Science and Technology*, Pergamon Press, vol. I, 373 (1960).
[25] Work, R. H., *Vacuum Symp. Trans.* 126 (1958).
[26] *Oil Gas J.*, **20**, 107 (1958).
[27] *Chem. Engng. News* **36**, 64 (1958).

2.4 Gas Desorption and Gettering

2.4.1 Gas Desorption of Solids

When evacuating a container one has to differentiate between the pumping of free gas, which is present in the container at the very beginning of the pumping procedure, and the pumping of gas which is liberated at low pressures from the inner surfaces of the container (Fig. 2.4.1).

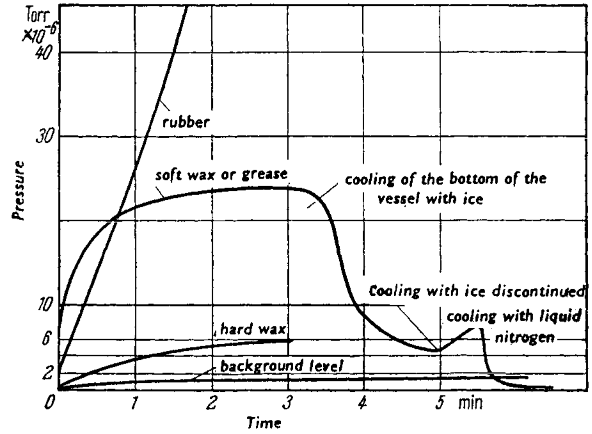

Fig. 2.4.1. Pressure increase in an isolated vacuum vessel with various materials present.

The rate of desorption determines for a given pumping system the vacuum which can be obtained in the container or vacuum plant within a certain time.

The desorption is made up of gases which

(a) adhere to the inner surface prior to the start of pumping;
(b) migrate from the inner parts of the container wall to the surface;
(c) permeate the wall from the outer atmosphere.

The properties of the material and the state of its inner surface determine the adsorption of gases and vapours. Rough and corroded surfaces are capable of adsorbing much more than smooth surfaces. Unsuitable surface coatings, e. g. a copper coating sprayed at normal atmospheric pressure, show a gas desorption which is twenty times greater than the desorption figure for the pure metal. Hygroscopic surfaces contain large amounts of adsorbed water, which are difficult to remove when attempted at normal temperatures.

Gas occlusions or gassy chemical compounds dissolved in materials, such as found in plastics that are extended or plasticized with vaporizable substances, cause high gas desorption. Materials which absorb water vapour from the natural humidity of the atmospheric air are bound to lead to poor vacuum. Porous substances should not be used in vacuum plants – except where adsorption is specially required.

The gas desorption of materials can have unwanted detrimental effects on the materials themselves. It is known, for instance, that the mechanical properties of a substance alter when one component has a very much higher evaporation rate under vacuum than other components, leading to structural changes in the substance.

In sealing materials containing plasticizers, this leads to loss of the sealing properties of these materials, when the plasticizing component evaporates in vacuum.

The rate of gas desorption during evacuation of the vacuum system depends very much on the past history of the materials used. High humidity is always detrimental. It is, therefore, preferable to admit dry permanent gases, e. g. dry nitrogen, rather than atmospheric air if the system has to be opened for a short period and is then to be evacuated again. Even so, short-time exposure to atmosphere leads to much shorter pump-down times than are required for the very first evacuation of the system or plant.

The quantity of gas, $G = \int g\,F\,dt$ in Torr × litre, which is desorbed from a probe during evacuation, can be found in different ways. Assuming that no other sources of gas, except the probe (surface area F in cm^2) itself, are present in the container of volume V (litre) and that the desorbed gas is pumped through a conductance of known value L [litre/sec], whereby the pressure difference $p_1 - p_2$ [Torr] across the impedance is measured, then the following equation for the conservation of mass is valid:

$$gF = V\frac{dp_1}{dt} + C \times F \times h(\Theta)\frac{n\bar{w}}{4} + L(p_1 - p_2) \quad \text{(Torr litre/sec)}$$

Total amount		alteration		adsorption		amount of	(2.4.1)
of gas	=	of pressure	+	on F	+	gas pumped	
desorbed		in V					

$h(\Theta)$ is the sticking probability at F,

Θ coverage,

C proportionality factor.

$$\frac{n\overline{w}}{4} = p_1\, 1333\, (2\pi m k T)^{-\frac{1}{2}} = p_1\, a(T)\,. \tag{2.4.2}$$

$$p_1 \gg p_2: \quad gF = V\frac{dp_1}{dt} + C \times F \times h(\overline{\Theta})\, p_1\, a(T) + L p_1\,, \tag{2.4.3}$$

$$p_1 = \frac{gF - V\dfrac{dp_1}{dt}}{L + C \times F \times h(\Theta)\, a(T)}\,; \tag{2.4.4}$$

For different surfaces F_m and for n different types of gas this equation can be written as follows:

$$p_n = \frac{\sum\limits_m g_{n\,m} F_m - V\dfrac{dp_n}{dt}}{\sum\limits_m L_n + C F_m h(\Theta)_{n\,m}\, a(T)_{n\,m}}\,. \tag{2.4.5}$$

For the measurement of gas desorption various experimental arrangements can be used, whereby certain terms in equation (2.4.1) can be omitted.

(1) A probe with a large surface is introduced straight from the atmosphere into an already evacuated container, which is pumped continuously. The pressure changes slowly.

Terms in equation (2.4.1), which can be omitted:

$\dfrac{dp_1}{dt} \approx 0$, because of very slow pressure change.

$C \times F \times h(\Theta)\dfrac{n\overline{w}}{4} \approx 0$, because of adsorption on container walls.

The gas desorption is therefore given by: $g\,F = L(p_1 - p_2)$.

(2) The same applies when a probe with a small surface is introduced into an already evacuated container.

(3) The probe is introduced into a container which can be isolated by a valve. With the container isolated the pressure in the volume increases because of gas desorption of the probe. When the pressure has reached a certain value, the container is pumped down, then isolated again, and the cycle is repeated several times, so that a series of pressure increases dp_1/dt can be measured.

In (2.4.1) the following can be omitted:

$L(p_1 - p_2) = 0$, because of isolation.

$C \times F \times h(\Theta)\dfrac{n\overline{w}}{4} \approx 0$, because of adsorption on container walls.

Therefore:

Gas desorption is given by: $g\,F = V\dfrac{dp_1}{dt}$.

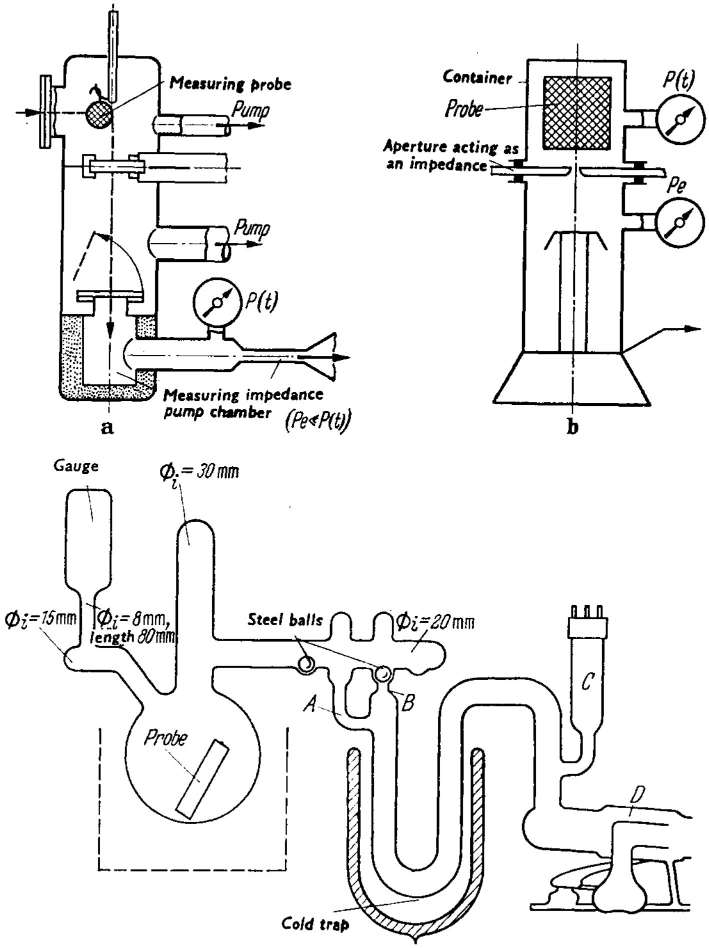

FIG. 2.4.2a–c. Experimental rigs for measuring gas desorption. (a) after JAECKEL and SCHITTKO [30], (b) after GELLER *et al.* [29], (c) after DAYTON *et al.* [37].

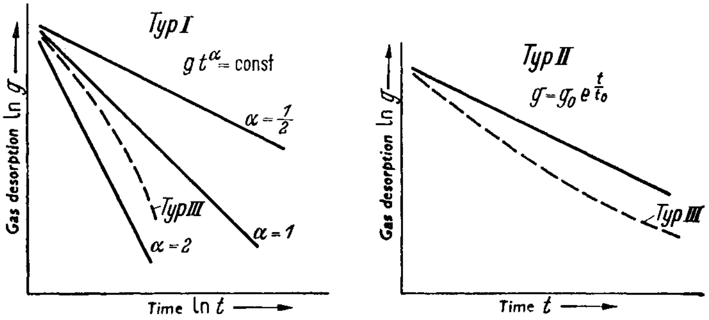

FIG. 2.4.3. Typical gas desorption curves at 20°C.

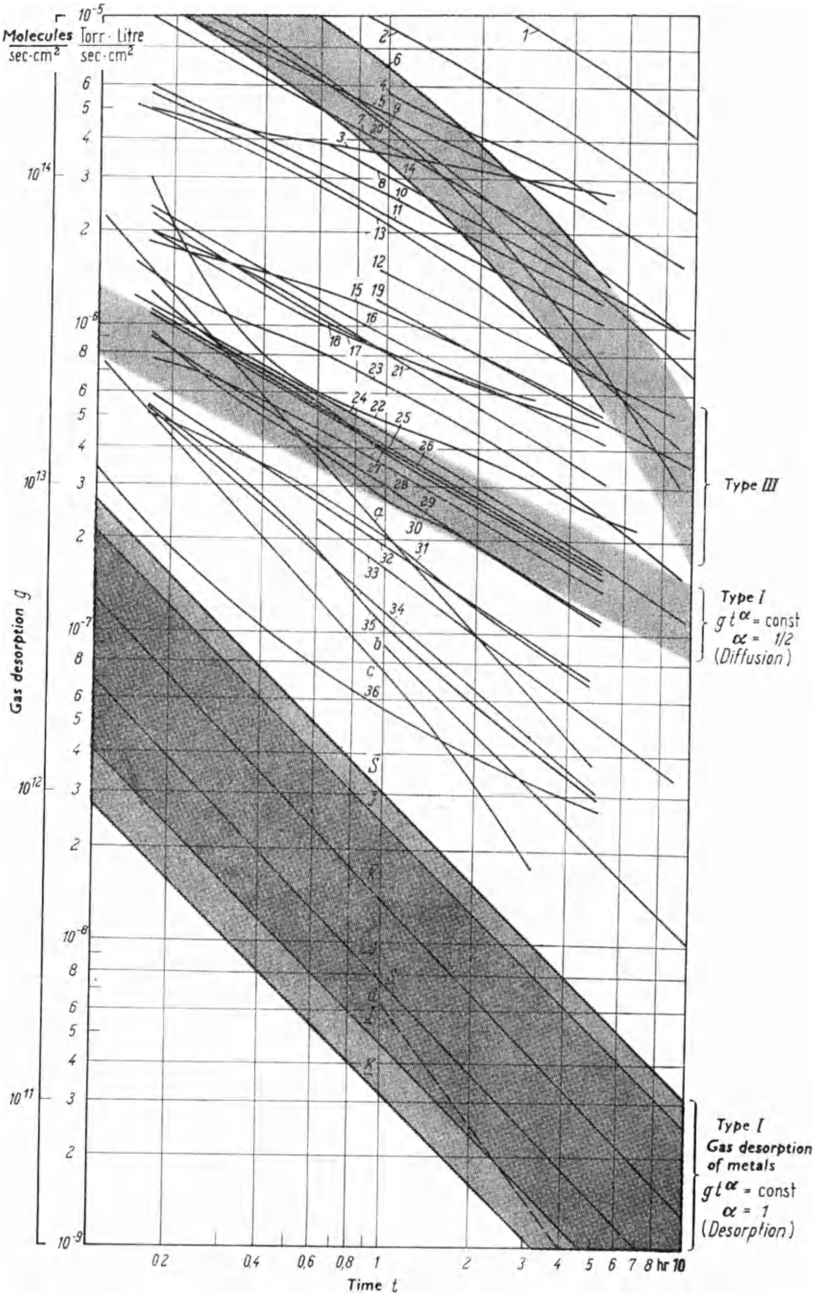

FIG. 2.4.4. Gas desorption of various substances (see notes on next page).

Curve	Material	Type	α	Author*
1	Vulkollan	I	1/2	B
2	Perbunan + Buna	I	1/2	B
3	Mowital	(I)	(1/2)	J
4	Mowilith	(I)	(1/2)	J
5	Neoprene (45/Ne 747)	I	1/2	B
		(for long periods III)	—	
6	Silicone rubber	III	—	J
7	Natural rubber	I	1/2	B
		(for long periods (III)	—	
8	Perbunan	I	1/2	S
9	Perbunan	III	—	B
10	Perbunan	I	1/2	J
11	Polyamide	I	1/2	G
12	Araldite	I	1/2	G
13	Neoprene (35/Ne 746)	III	—	B
14	Silicone rubber (O-Ring)	III	—	J
15	Plexiglas	I	1/2	J
16	Polyvinylcarbazole	I	1/2	J
17	Polyvinylcarbazole	I	1/2	J
18	Polycarbonate	I	1/2	J
19	Araldite	I	1/2	S
20	Silicone (37/Si 502)	III	—	B
21	Ultramide	I	1/2	J
22	PVC	I	1/2	J
23	Viton (25/Vi 575)	I	1/2	B
24	Teflon (3/Tf 528)	I	1/2	B
25	Araldite	I	1/2	J
		(for long periods II)	—	
26	Polymethane	I	1/2	J
27	Viton	I	1/2	J
28	Viton	I	1/2	J
29	Polystyrene	I	1/2	J
30	Polystyrene	I	1/2	J
31	Polystyrene	I	1/2	J
32	Teflon	I	1/2	J
33	Teflon	I	1/2	S
34	Polyethylene	I	1/2	J
		(for long periods II)	—	
35	Polyethylene	I	1/2	J
		(for long periods II)	—	
36	Hostaflon	I	1/2	J
a	Pyrophylite	I	1	J
b	Steatite (Al_2O_3)	I	1	G
c	Degussit (Al_2O_3)	I	1	J
d	Pyrex glass	I	1	S

* Continuation and footnote see p. 240.

(4) As under (1) and (2), but L is altered so that p_1 in V remains constant. In this case is

$$\frac{dp_1}{dt} = 0; \quad C \times F \times h(\Theta) \frac{n\overline{w}}{4} = 0\,.$$

Therefore: $gF = L(p_1 - p_2)$.

The methods according to (1), (2) and (3) were used for investigations of gas desorption (see Fig. 2.4.2). The accuracy can be increased, if in methods (1) and (2) a changeover to different impedance is provided. In this case it becomes possible to check whether and by how much the gas desorption rate depends on the pressure p_1 [*10, 17*]*.

The time functions for the rate of gas desorption at room temperature differ according to the material as shown schematically in Fig. 2.4.3. Rubber probes have a time-function between type I and II (type III in Fig. 2.4.3). Various authors [*1, 6, 13, 19*] have attempted to establish a relation between the various time-functions and the diffusion or desorption mechanism. There is a tendency to assume that type I with $\alpha = 1$ and $\alpha = 2$ as well as type II correspond to a desorption mechanism, whilst type I with $\alpha = 1/2$ corresponds to the diffusion mechanism.

Figure 2.4.4 shows the gas desorption vs. time functions for various materials.

For detailed investigations determination of the gas composition during desorption is important. This can be done by using a mass spectrometer. If possible the spectrum should be obtained by means of an oscilloscope, so that the intensities of the various masses present can be found simultaneously.

* The numbers in brackets refer to the list of references at the end of this chapter (p. 250).

Continuation and footnote from p. 239;

$$\left.\begin{array}{ll}\overline{J} & \text{upper limit}\\ \underline{J} & \text{lower limit}\end{array}\right\} \text{of gas desorption after } J$$

$\overline{LS}$ empty rig after J

$$\left.\begin{array}{ll}\overline{K} & \text{upper limit}\\ \underline{K} & \text{lower limit}\end{array}\right\} \text{of gas desorption after } K$$

$$\left.\begin{array}{ll}\overline{S} & \text{upper limit}\\ \overline{V} & \text{lower limit}\end{array}\right\} \text{of gas desorption after } S$$

* Authors: B = Beckmann, W., not published; G = Geller, R., [*18*]; J = Jaeckel, R., and F. J. Schittko, partly published in [*30*]; K = Kraus, Th., not published; S = Schram, A., [*1*]

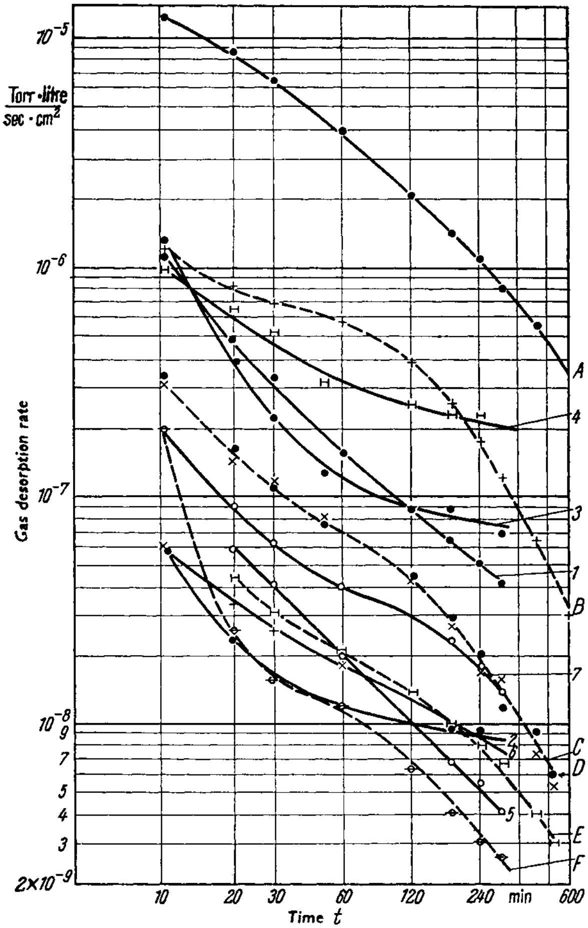

FIG. 2.4.5. Gas desorption of plastic materials after drying in warm air (after JAECKEL and SCHITTKO [30]).

- *A* – Silicone rubber (without pre-treatment)
- *B* – Silicone rubber (1 hr at 200 °C)
- *C* – Silicone rubber (2 hrs at 200 °C)
- *D* – Silicone rubber (1 hr at 250 °C)
- *E* – Silicone rubber (9 hrs at 200 °C)
- *F* – Silicone rubber (12 hrs at 200 °C)
- *1* – Perbunan (3 hrs at 150 °C)
- *2* – Araldite (3 hrs at 150 °C)
- *3* – Rubber (20 hrs at 150 °C, decomposition)
- *4* – Polycarbonate (7 hrs at 45 °C)
- *5* – Polycarbonate (48 hrs at 150 °C)
- *6* – Lupolen (1/2 hrs at 80 °C)

TABLE 2.4.1. Gas desorption of plastic materials

Material	Make	Class*	Conductance L† $\left[\frac{\text{litre}}{\text{sec}}\right]$	Measured pressure p_t [× 10^{-6} Torr] after t hours pumping time							
				$t = 1/6$	$1/3$	$1/2$	1	2	3	4	5
				$p_{1/6}$	$p_{1/3}$	$p_{1/2}$	p_1	p_2	p_3	p_4	p_5
Lupolen	BASF	1111	0·08	85	48	35	17	9	7	5·8	5
Polystyrene	Dynamit-A. G.	121	0·123	100	55	45	28	21	17	14	—
Polyvinylcarbazole	BASF	126	0·225	110	75	60	45	35	30	26	—
PVC	BASF	131	0·520	70	22	16	11·5	8·8	7·5	6·8	6·2
Astralon	Dynamit-A. G.	131	0·225	130	88	72	49	36	32	—	—
Viton	Freudenberg	135	0·08	80	49	40	24	16·3	13	11	10
Teflon	Dupont	1351	0·08	80	60	48	30	18	15	11	7
Hostaflon	Farbwerke Hoechst	1352	0·1	25·4	15·4	11	7·6	5	4·3	3·8	3·4
Mowilith	Farbwerke Hoechst	151	0·225	—	—	—	300	210	180	150	135
Mowital	Farbwerke Hoechst	154	0·225	310	230	200	170	150	140	140	—
Plexiglas	Röhm& Haas	263	0·1	220	190	170	127	98	81	70	63
Polycarbonate	Bayer	2411	0·08	350	230	180	130	95	80	70	66
Araldite	Ciba	233	0·08	160	110	90	60	40	32	28	25
Polyamide	Bayer	261	0·123	480	380	320	220	160	130	110	100
Ultramide	Bayer	261	0·1	240	170	150	100	67	52	44	40
Polyurethane	Bayer	262	0·085	110	87	71	52	35	28	25	—
Perbunan	Bayer	323	0·52	140	100	83	60	44	34	29	25
Silicone rubber	Wacker	38	0·52	—	500	340	250	120	83	62	46
Silicone rubber	Freudenberg	38	0·08	850	490	327	200	104	67	47	35

* Classification after SAECHTLING-ZEBROWSKI: Kunststoff-Taschenbuch, 15th ed. Munich, 1961.

TABLE 2.4.2. Gas desorption of plastic materials after drying in warm air

Material	Make	Class*	Conductance L† $\left[\frac{\text{litre}}{\text{sec}}\right]$	Measured pressure p_t [× 10^{-6} Torr] after t hours pumping time							
				$t = 1/6$	$1/3$	$1/2$	1	2	3	4	5
				$p_{1/6}$	$p_{1/3}$	$p_{1/3}$	p_1	p_2	p_3	p_4	p_5
Lupolen H 1300	BASF	1111	0·08	30	14	9·8	6·8	4·8	4	3·2	2·5
Araldite	Ciba	233	0·08	10	9·2	6·7	3·5	2·9	1·4	1·2	1·1
Araldite	Ciba	233	0·08	9	3·8	2·8	2	1·9	1·7	1·7	1·5
Polycarbonate	Bayer	2411	0·08	150	100	80	48	39	35	35	31
Polycarbonate	Bayer	2411	0·08	9	5·4	4·3	3·1	2·4	2	1·8	1·6
Perbunan	Bayer	323	0·39	36	16	11	5·5	3·4	2·7	2·3	2
Silicone rubber	Wacker	38	0·16	950	670	510	300	160	110	82	62
Silicone rubber	Wacker	38	0·16	93	63	53	44	29	19	13	9·2
Silicone rubber	Wacker	38	0·16	26	12·5	8·4	6	3·5	2·4	1·7	1·4
Silicone rubber	Wacker	38	0·16	24	11	9	6·3	3·5	2·2	1·5	1·4
Silicone rubber	Wacker	38	0·16	—	3·5	2·5	1·8	1·2	0·95	0·8	0·7
Silicone rubber	Wacker	38	0·16	15	2	1·4	1·1	0·68	0·5	0·43	0·4

* Classification after SAECHTLING-ZEBROWSKI: Kunststoff-Taschenbuch, 15th ed. Munich, 1961.

(after JAECKEL and SCHITTKO [*30*])

Rate of gas desorption g_t [$\times 10^{-9}$ Torr litre/sec cm^2] at time t [hr]								
$t = {}^1/_6$	${}^1/_3$	${}^1/_2$	1	2	3	4	5	
$g_{1/6}$	$g_{1/3}$	$g_{1/2}$	g_1	g_2	g_3	g_4	g_5	
588	316	233	108	55·8	41·6	35	30	
974	540	340	266	192	154	125	—	
2080	1390	1110	832	640	540	466	—	
300	915	660	483	383	305	275	241	
2410	1640	1330	916	658	583	—	—	
1260	770	630	280	254	200	170	152	
525	382	316	200	170	96	77	(42)	
210	126	90	61·5	40	33·8	32	27	
—	—	—	5580	3910	3330	2830	2500	
5830	4330	3750	3750	3160	2830	2620	—	
1811	1570	1410	1050	808	660	575	517	
2330	1500	1165	857	625	525	458	433	
1040	725	604	392	262	208	283	162	
5000	4080	3250	2250	1610	1300	1100	973	
2000	1410	1250	824	550	425	358	325	
774	615	500	358	233	187	166	—	
6000	4330	3620	2580	1870	1440	1220	1040	
—	15800	10600	8000	3830	2620	1950	1430	
13600	7500	5200	3200	1600	1006	740	540	

† Conductance of the line, which was used to evacuate the test chamber (see FIG. 2.4.2a)

(after JAECKEL and SCHITTKO [*30*], see Fig. 2.4.5.).

Rate of gas desorption g_t [$\times 10^{-9}$ Torr litre/sec cm^2] at time t [hr]								
$t = {}^1/_6$	${}^1/_3$	${}^1/_2$	1	2	3	4	5	
$g_{1/6}$	$g_{1/3}$	$g_{1/2}$	g_1	g_2	g_3	g_4	g_5	
195	90	63	40	30	23	18	14	${}^1/_3$ hr dried at 180°C
66·5	60	42	20	16	6·8	5·5	4	20 hrs dried at 150°C
60	25·3	16·5	11·4	10·6	9·4	9·4	8	3 hrs dried at 150°C
1000	660	530	320	257	230	230	205	7 hrs dried at 45°C
60	34	26	18	13	10	8·6	7·5	48 hrs dried at 150°C
1150	497	335	156	87·7	65	52	42	3 hrs dried at 150°C
12700	8940	6800	4000	2130	1460	1090	820	without pre-treatment
1230	840	706	587	486	253	173	120	1 hr dried at 200°C
346	165	110	77	44	29	20	12	2 hrs dried at 200°C
315	144	117	81	44	27	17·3	16	1 hr dried at 250°C
—	44	31	21·3	13·4	11·5	8	6·7	9 hrs dried at 200°C
200	26	16	12	6·4	4	3	2·6	12 hrs dried at 200°C

† Conductance of the line, which was used to evacuate the test chamber (see FIG. 2.4.2a)

TABLE 2.4.3. Gas composition during gas desorption of plastic materials

Material	Make	Class*	Main constituents	Ion current					
				1	2	12	14	15	16
Lupolen	BASF	1111	N_2, H_2O, CO, O_2, CO_2	6	20	10	15	5	10
Polystyrene	Dynamit-A.G.	121	H_2O, N_2, CO, CO_2, O_2	60	60	20	10	–	90
Polyvinylcarbazole	BASF	126	H_2O, CO, CO_2, N_2	60	50	8	7	–	30
PVC	BASF	131	H_2O, CO, CO_2, N_2	70	10	20	4	3	30
Teflon	Dupont	1351	N_2, CO, O_2, H_2O	2	2	10	45	–	1
Plexiglas	Röhm & Haas	263	H_2O, CO, CO_2	230	60	30	4	3	100
Polyamide	Bayer	261	H_2O, CO, CO_2	40	5	10	5	–	20
Ultramide	Bayer	261	H_2O, CO, CO_2	260	100	40	7	15	140
Polyurethane	Bayer	262	H_2O, CO, CO_2	140	79	20	3	–	60
Siliconerubber	Wacker	38	CO, H_2O	10	35	4	2	4	10

* Classification after SAECHTLING-ZEBROWSKI: Kunststoff-Taschenbuch, 15th ed. Munich 1961.

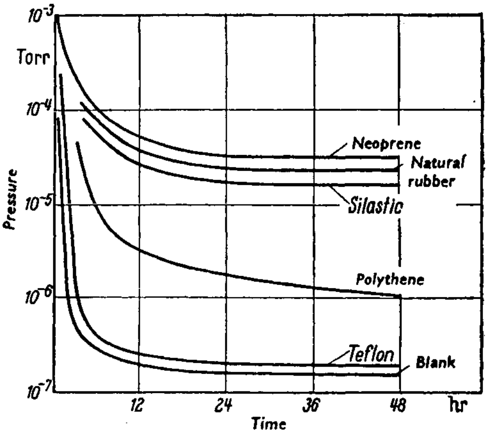

FIG. 2.4.6. Pressure vs. time for the gas desorption of rubber type gasket materials (after DAYTON *et al.* [*37*]).

(after JAECKEL and SCHITTKO [*30*]).

[$\times 10^{-14}$ A] for masses (mass numbers)																	
17	18	19	20	22	26	27	28	29	32	39	40	41	42	43	44	55	57
22	100	—	2	—	—	3	200	5	12	2	10	8	—	7	10	4	4
300	1200	—	7	—	7	10	300	17	13	20	10	20	20	20	110	—	—
140	520	1	3	—	—	—	180	5	2	—	—	—	—	—	56	—	—
300	1000	3	4	2	2	7	360	10	2	4	—	10	—	6	30	10	9
10	40	—	4	1	—	1	400	5	33	—	16	—	—	—	15	—	—
700	2700	4	7	—	—	—	700	13	1	—	—	—	—	—	10	—	—
170	700	—	—	—	—	—	200	—	—	—	—	—	—	—	—	—	—
820	3000	—	—	—	—	5	560	18	—	1	—	—	—	—	200	—	—
500	2200	5	7	1	1	1	700	13	—	3	—	6	—	3	35	3	2
30	120	—	—	—	5	10	30	10	20	—	20	5	15	14	—	—	—†

† After drying in air.

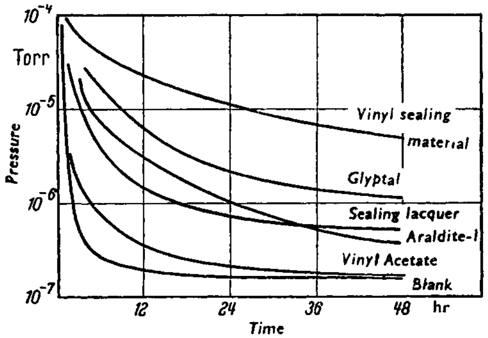

FIG. 2.4.7. Pressure vs. time for the gas desorption of sealing materials (after DAYTON *et al.* [*37*]).

TABLE 2.4.4. Pressure and gas desorption of metals, Degussit and Pyrophylite

	Impedance L* [litre/sec]	Measured pressure p_t [$\times 10^{-7}$ Torr] after t minutes pumping time								
		$t = 5$	10	15	20	25	30	60	120	180
		p_5	p_{10}	p_{15}	p_{20}	p_{25}	p_{30}	p_{60}	p_{120}	p_{180}
Cu	0·07	250	140	100	85	72	60	34	18	—
Ni	0·07	270	120	80	62	52	43	20	8	5
Fe	0·07	200	60	35	23	18	14	7	5	—
Ag	0·07	200	80	50	35	27	22	10	6	5
Ta	0·07	260	24	75	53	41	33	13	7	5
W	0·07	220	76	44	30	22	18	8	6	5
Zr	0·07	250	73	40	27	20	16	8	6	3
Mo	0·07	350	120	85	68	72	33	14	7	—
Al	0·07	320	160	110	72	51	42	21	11	7
Degussit	0·028	5450	2540	1630	1220	1000	800	380	150	95
Degussit	0·028	6700	1700	780	530	410	330	160	90	—
Pyrophylite	0·08	6000	1350	820	605	470	385	192	93	61

* Impedance of the line, which was used to evacuate the test chamber (see

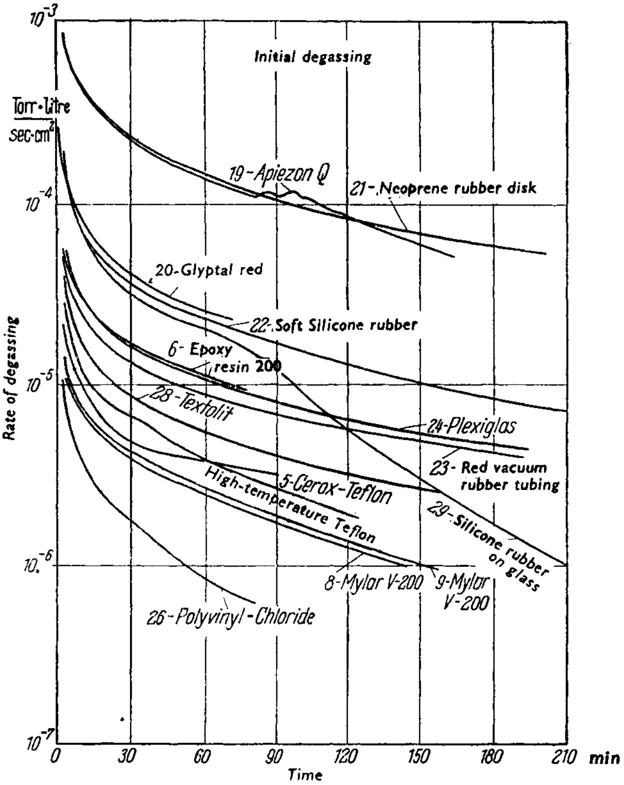

FIG. 2.4.8a.

FIG. 2.4.8a and b. Gas desorption of plastic materials I (after SANTELER [21]).

(after JAECKEL and SCHITTKO [*30*]).

Rate of gas desorption g_t [$\times 10^{-9}$ Torr litre/sec cm^2] at time t [min]								
$t = 5$	10	15	20	25	30	60	120	180
g_5	g_{10}	g_{15}	g_{20}	g_{25}	g_{30}	g_{60}	g_{120}	g_{180}
141	79	56·7	47·5	38	33·4	18·3	8·7	–
158	67·5	45	33·4	28·3	23·3	10	(3)	–
113	33·4	18·3	11·7	8·7	(2·3)	(1·2)	–	–
113	46	26	18·3	14	11	4·2	(1·7)	–
145	67·5	40	29	22·5	17·5	5·8	(2·3)	–
125	41	23·4	23	11	8·7	2·9	(1·7)	–
140	40	22	14	10	7·5	2·9	(1·7)	–
200	67·5	48·4	38·4	41	17·5	8	–	–
182	91·7	62·5	41	29·4	22·5	10·5	6·4	–
1070	506	320	242	196	156	75	30	17·8
1356	336	153	103	80	64	30	17	–
3430	1430	856	630	484	405	197	96	61

FIG. 2.4.2a)

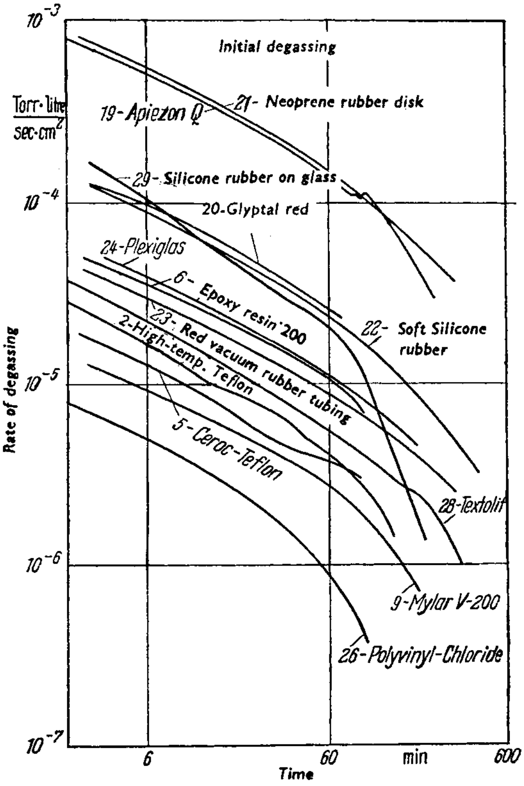

FIG. 2.4.8b.

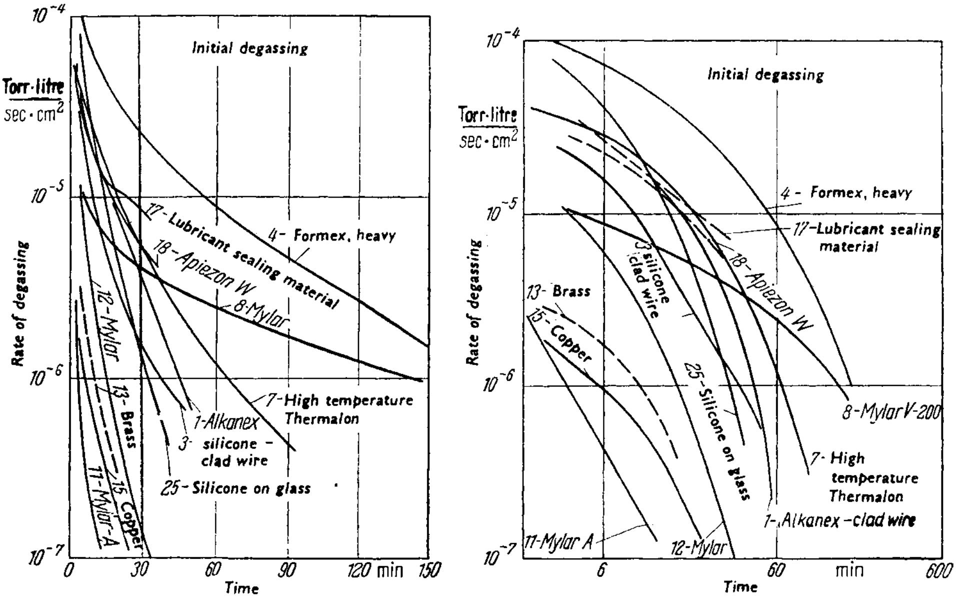

FIG. 2.4.9a and b. Gas desorption of plastic materials II (after SANTELER [21]).

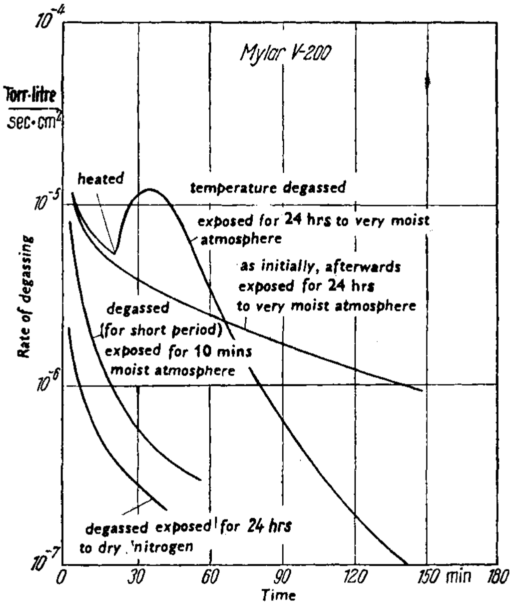

FIG. 2.4.10. Gas desorption of Mylar V-200 after various pre-treatments (after SANTELER [21]).

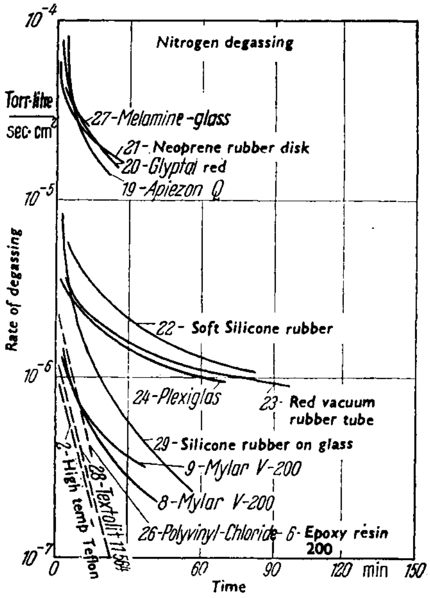

FIG. 2.4.11. Gas desorption of materials filled with nitrogen (after DAYTON *et al.* [37])

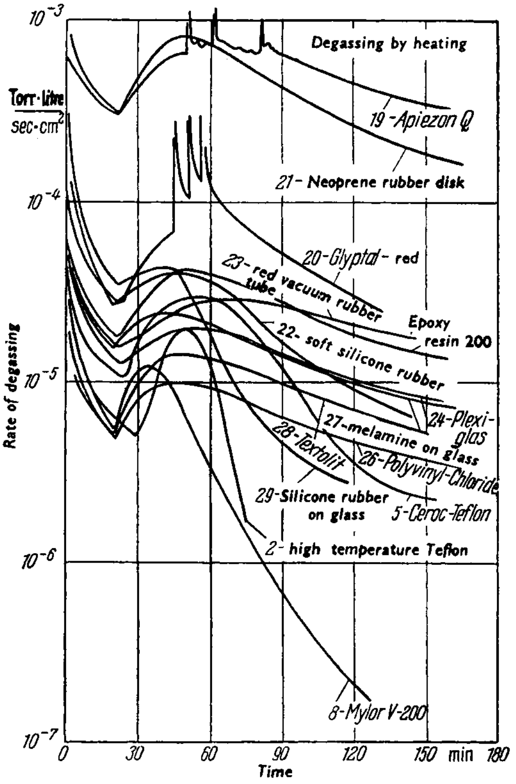

Fig. 2.4.12. Gas desorption during heating of plastic materials, which were exposed for 24 hrs to moist air (after Santeler [*21*]).

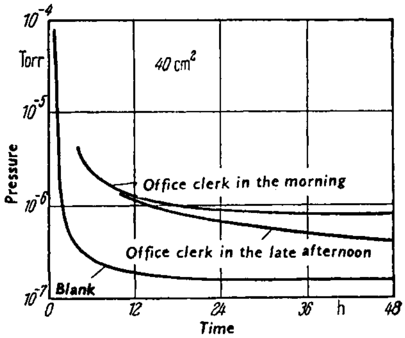

Fig. 2.4.13. Pressure-time curves for the gas desorption of finger prints on glass (after Dayton *et al.* [*37*]).

References

[*1*] Schram, A., *Citav, Paris* (1961).
[*2*] Farkass, I., and E. J. Barry, *Vac. Symp. Trans. 1960*, pp. 35–38.
[*3*] Redhead, P. A.. *Vac. Symp. Trans. 1960*, pp. 108–111.
[*4*] Todd, B., J. L. Lineweaver and J. T. Kerr, *J. Appl. Physics*, **31**, 51 (1960).
[*5*] Varadi, P. F., *Vac. Symp. Trans. 1960*, pp. 149–154.
[*6*] Dayton, B. B., *Vac. Symp. Trans. 1959*, pp. 101–119.
[*7*] Boulassier, J. C., *Vide*, **14**, 80, 39 (1959).
[*8*] Dayton, B. B., *Report Cons. Vac. Corp.* (1959).
[*9*] Fish, I. P. S., *Rev. Sci. Instrum.* **30**, 889, (1959).
[*10*] Henry, R. P., *Vide*, **14**, 82, 226–240 (1959).
[*11*] Kelly, J. C., *J. Sci. Instrum.* **36**, 89–90 (1959) and *Vacuum*, **9** 3/4, 241 (1959).
[*12*] Kraus, Th., *Vac. Symp. Trans. 1959*, p. 204.
[*13*] Kraus, Th. *Vakuum-Technik* **8**, 2, 39–43 (1959) and *Vacuum*, **9**, 3/4, 234 (1959).
[*14*] Redhead, P. A., *Vac. Symp. Trans. 1959*, pp. 12–15.
[*15*] Blears, J., E. J. Greer and J. Nightingale, *Proc. First Internat. Congr. Vacuum Technique*, pp. 473–480, *1960*, Pergamon Press, London.
[*16*] Basalaeva, N. I. *Soviet Physics-Technical Physics* **3**, 4, 1027–1031 (1958).
[*17*] Benichuo, R., J. C. Blaive and R. P. Henry, *Vide*, **13**, 79, 353–363 (1958).
[*18*] Geller, R., *Vide*, **13**, 74, 71–76 (1958).
[*19*] Kraus, Th., *Naturwissenschaften*, **45**, 22, 538 (1958).
[*20*] Power, B. D., and D. J. Crawley, *Proc. First Internat. Congr. Vacuum Technique*, p. 206, *1960*, Pergamon Press, London.
[*21*] Santeler, D. J., *Proc. First Internat. Congr. Vacuum Technique*, pp. 98–109, *1960*, Pergamon Press, London.
[*22*] Santeler, D. J., *Vac. Symp. Trans.* 1958, pp. 1–8.
[*23*] Trendelenburg, E. A., and J. H. Carmichael, *Proc. First Internat. Congr. Vacuum Technique*, 1960, pp. 657–660, Pergamon Press, London.
[*24*] Amoignon, J., and J. Mongodin, *Vide*, **12**, 337 (1959) and *Phys. Abstr.* (Nr. 2866), **61**, 274 (1958).
[*25*] Dawton, RHVM, *Brit. J. Appl. Physics*, **8**, 414 (1957) and Reports U. K. Atom. En. Res. Establ. G/R-393.
[*26*] Geller, R., *Vide*, **12**, 69, 194 (1957).
[*27*] Taylor, K. C., *Vac. Symp. Trans. 1957*, pp. 157–160.
[*28*] Geller, R., *Vide*, **12**, 69, 194 (1957).
[*29*] Geller, R., R. Barre and G. Mongodin, *Vide*, **12**, 69, 195–201 (1957).
[*30*] Jaeckel, R., and F. J. Schittko, *Forsch. Ber. Nordrh.-Westf.*, 369 (1957).
[*31*] Amphlett, C. B., and T. F. Williams, *J. Sci. Instrum.* **33**, 64–65 (1956) and *Vacuum*, **6**, 195 (1956).
[*32*] Haefer, R., and O. Winkler, *Vakuum-Technik*, **5**, 7, 149–155 (1956).
[*33*] Higalsburger, M., *Acta Phys. Austr.* **10**, 3, 181–185 (1956) and *Phys. Abstr.* (No. 6938), **60**, 635, (1957).
[*34*] Hoffmann, K., and L. Fischer, *Chem. Ing. Techn.* **27**, 10, 604–607 (1955).
[*35*] Todd, B. J., *J. Appl. Physics*, **26**, 10, 1238–1244 (1955).
[*36*] Alpert, D., and R. S. Buritz, *J. Appl. Physics*, **25**, 202 (1954).
[*37*] Dayton, B. B., F. Trabert, G. Gerow, R. B. Morse and B. B. Dayton, Rep. Cons. Vac. Corp., Rochester, N. Y.
[*38*] Eckardt, A., and C. Eden, *Glas- und Hochvakuumtechnik*, 2, 15–19 (1952).
[*39*] Britt, J. R., Naval Research Laboratory Rep. 3827 (1951).
[*40*] Fernand, F., *Canad. J. Research*, **27 F**, 318 (1949).

2.4.2 Gas Desorption of Liquids with High Boiling Point

For many applications of vacuum technology, e. g. for the design of degassing plants, for the impregnation of condensers etc., it is important to know the amount of gas and/or vapour dissolved in the liquid. In practically all cases only liquids with a high boiling point are encountered; so the following tables and graphs refer only to those liquids. For other liquids reference should be made to the publications listed on page 251 and also to the corresponding tables in the *Taschenbuch für Chemiker und Physiker* by J. D'ANS and E. LAX.

For the absorption of gases which cannot be liquefied under normal conditions, HENRY's law applies at partial pressures below 760 Torr:

$$c = k(T) \times p_g, \tag{2.4.6}$$

c — concentration of gas dissolved in the liquid,
$k\,(T)$ — constant, dependent on temperature;
p_g — partial pressure of gas dissolved in the liquid.

Gases which — when dissolved in a liquid — cannot be further considered as perfect gases obey the generalized form of HENRY's law:

$$c = k(T) \times p_g^n \tag{2.4.7}$$

In the diagrams, showing the absorption isotherms (see Figs. 2.4.14 and 2.4.15), the concentration c is given in milligram gas per gram liquid. In Table 2.4.5 and in the diagrams (Figs. 2.4.16 and 2.4.17), showing the absorption isobars, the solubility coefficient Γ (after OSTWALD) is used. The coefficient Γ is defined by the ratio of volume concentration of gas in solution in the liquid to volume concentration of the same gas in the gas phase:

$$\Gamma = \frac{c_{Fl}}{c_g}. \tag{2.4.8}$$

Since $p_g = c_g \times RT$, the coefficient Γ is independent of pressure at constant temperature, provided that HENRY's law is valid.

$\Gamma = 0{\cdot}01$ therefore means that e. g. in 100 litres of liquid there is 1 litre of gas in solution, in relation to the prevailing partial pressure of this gas.

The solubility coefficient after OSTWALD is particularly suitable for the plotting of absorption isobars since, for the temperature dependence at constant pressure, the equation (2.4.9) holds which is analogous to the CLAUSIUS-CLAPEYRON equation:

$$\frac{d(\ln \Gamma)}{dT} = -\frac{E_A(T)}{RT^2}, \tag{2.4.9}$$

E_A is the heat of absorption.

From thermodynamics it follows that

for $\Gamma > 1$, $E_A > 0$, and Γ decreases with increasing temperature and
for $\Gamma < 1$, $E_A < 0$, and Γ increases with increasing temperature.

Equation (2.4.9) is valid only if no adsorption compounds are present. If adsorption compounds are present, the additional heat H of adsorption has to be taken into account, and the equation for the absorption isobars will therefore, then read

$$\frac{d(\ln\Gamma)}{dT} = -\frac{E_A(T)}{RT^2} - \frac{H}{RT^2}. \qquad (2.4.10)$$

Table 2.4.5 shows the solubility coefficient after Ostwald; the corresponding figures for the heat of dissolution are shown in Table 2.4.6. Finally, Table 2.4.7 shows a few characteristic physical data for liquids.

References

[1] Landolt-Börnstein, HW 774; Eg. Bd. I, 309; Eg. Bd. IIa, 499; Eg. Bd. IIIa, 715.a.

[2] Markham, A. E., and K. A. Kobe, *Chem. Rev.*, **28**, 519 (1941).

[3] Burrows, G., and F. H. Preece, *J. Appl. Chem.*, **3**, 451 (1953).

[4] Oetjen, G. W., and F. Gross, *Chemie-Ing.-Techn.*, **26**, 9 (1954).

[5] Jaeckel, R., and F. Gross, Forschungsbericht Nr. 404 des Wirtschafts- u. Verkehrsministeriums Nordrhein-Westfalen, 1957.

[6] Gross, F., *Z. angew. Phys.*, **9**, 606 (1957).

[7] Luther, H., and W. Hiemenz, *Chemie-Ing.-Techn.*, **29**, 530 (1957).

Table 2.4.5. Solubility coefficient (after Ostwald)

Liquid	Solubility coefficient for								at T(°C)
	Air	N_2	O_2	A	He	H_2O-vapour	CO_2	H_2	
Apiezon oil "GW"	0·088	–	–	–	0·015	*	–	–	25
Silicone oil DC 200	0·16	–	–	–	0·032	–	–	–	25
Silicone oil DC 702	0·098	–	–	–	0·016	–	–	–	25
Dibutylphthalate	0·080	0·060	–	0·16	–	120 (0·13 Torr)	–	–	20
Trichlordiphenyl	–	0·031	–	0·07	–	9·2 (10 Torr)	–	–	20
Glycerine	–	0·006	–	–	–	–	–	–	80
Paraffin oil	–	0·074	–	0·16	–	2·6 (17 Torr)	–	–	20
Shell oil	–	0·073	–	0·102	–	3·5 (9 Torr)	–	–	23
Vaseline	–	0·075	–	0·14	–	1·7 (17 Torr)	–	–	70
Transformer oil	–	0·092	0·171	–	–	–	1·083	–	25
Transformer oil	–	0·119	0·193	–	–	–	–	–	80
Heavy lubricating oil	–	0·065	0·129	–	–	–	–	–	21
Light lubricating oil	–	0·092	0·171	–	–	–	–	–	21
Aircraft engine oil	–	0·224	0·359	–	–	–	–	–	21
Kerosene	0·143	0·122	0·227	–	–	–	–	–	18
Kerosene	–	0·126	0·232	–	–	–	–	–	25
Kerosene	0·155	0·134	0·238	–	–	–	–	–	42
Naphthenic oil (A)	0·047	–	–	–	–	–	–	–	20
Naphthenic oil (B)	0·040	–	–	–	–	–	–	–	20
Naphthenic oil (C)	0·090	–	–	–	–	–	–	–	20
Naphthenic oil (D)	0·095	–	–	–	–	–	–	–	20

* Henry's law does not apply.

Table 2.4.6. Heat of dissolution

Liquid	Heat of dissolution in kcal/mol for						at T(°C)
	Air	N_2	O_2	He	H_2O vapour	CO_2	
Apiezon oil "GW"	–	–	–	—3·79	–	–	25
Silicone oil DC 200	–	–	–	—3·08	–	–	25
Silicone oil DC 702	–	–	–	—2·45	–	–	25
Dibutylphthalate	–	–	–	–	+ 4·1	–	20
Trichlordiphenyl	–	—1·65	–	–	+ 4·0	–	20
Glycerine	–	–	–	–	–	–	–
Paraffin oil	–	0·46	–	–	+ 0·50	–	20
Shell oil K 8	–	0	–	–	+ 0·82	–	23
Vaseline	–	–	–	–	–	–	–
Transformer oil	–	— 1·07	—0·57	–	–	+ 1·17	25
Heavy lubricating oil	–	—1·4	—0·92	–	–	–	21
Light lubricating oil	–	—0·91	—0·52	–	–	–	21
Aircraft engine oil	–	+ 0·34	+ 0·57	–	–	–	21
Kerosene	–	—0·49	—0·18	–	–	–	25

Table 2.4.7. Physical data of liquids

Liquid	Density (g/cm³)	at °C	Viscosity (cP)	at °C	Surface tension (dyn/cm)	at °C	Molecular weight (average value)	Remarks
Apiezon oil "GW"	0·878	20	160·5	20	31·7	20	450	–
Silicone oil DC 200	0·971	20	104·4	20	26·7	20	400	–
Silicone oil DC 702	1·072	20	39·8	20	29·1	20	530	–
Dibutylphthalate	1·035	20	20·8	20	–	–	278	–
Trichlordiphenyl	1·49	20	–	–	–	–	256	(Clophen A 40)
Glycerine	1·263	20	1499	20	64·7	30	92	OH-number: 1823
Paraffin oil	0·889	20	242	20	24	20	430	Refractive index $n_{D20} = 1{\cdot}479$
Shell oil K 8	0·891	20	26·8	20	25·2	20	–	$n_{D20} = 1{\cdot}543$
Vaseline	0·840	70	16·3	70	–	–	–	Setting point: ≈50°C
Transformer oil	0·840	25	–	–	29·5	25	300	–
Heavy lubricating oil	0·882	25	–	–	29·4	25	400	–
Light lubricating oil	0·838	25	–	–	25·4	21	300	–
Aircraft engine oil	0·692	25	–	–	17·8	21	120	–
Kerosene	0·776	25	–	–	25·0	25	180	–
Cyclohexane	0·779	18	–	–	26·5	20	–	–
Naphthenic oil (A)	–	–	≈ 90	60	–	–	–	50 c/s 60°C } tan δ = 0·0016
Naphthenic oil (B)	–	–	≈200	60	–	–	–	id. = 0·0011
Naphthenic oil (C)	–	–	≈ 20	60	–	–	–	id. = 0·0005
Naphthenic oil (D)	–	–	≈ 7	60	–	–	–	–

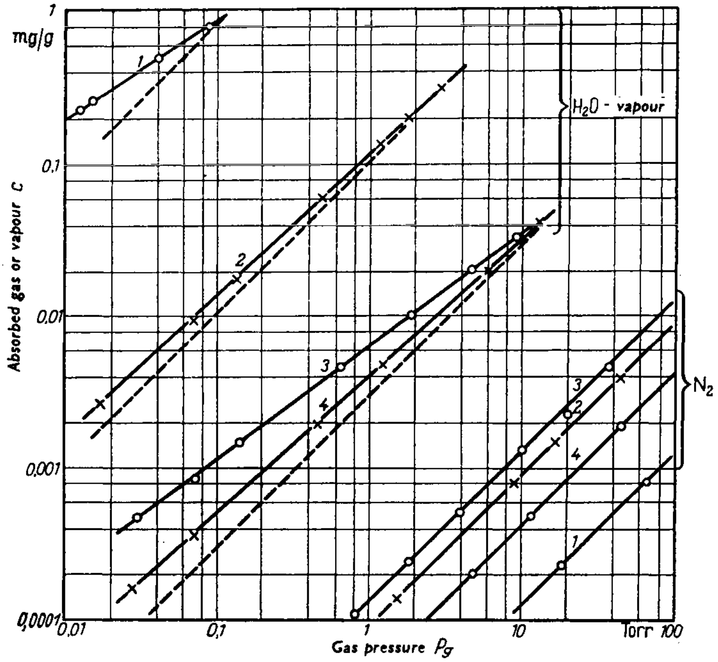

FIG. 2.4.14. Absorption isotherms for N_2 and water vapour.

Curve	Liquid	Temperature	Curve	Liquid	Temperature
1	Glycerine	80°C	*3*	Shell oil K 8	23°C
2	Dibutylphthalate	20°C	*4*	Clophen A 40	55°C

Molar fractions at 1 Torr water vapour partial pressure:
Glycerine: 2×10^{-2} (extrapolated) Shell oil K 8: $1{\cdot}2\times10^{-4}$
Dibutylphthalate: $1{\cdot}8\times10^{-3}$ Clophen A 40: $5{\cdot}7\times10^{-5}$

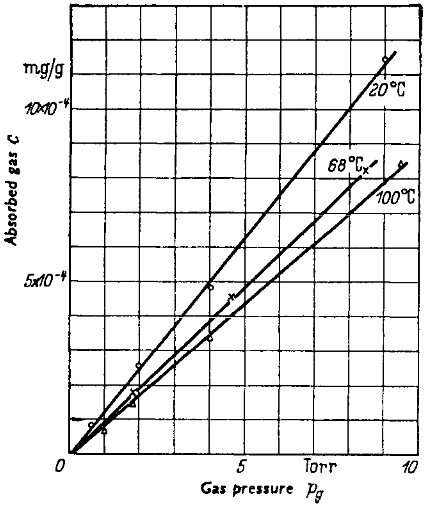

FIG. 2.4.15. Absorption isotherms of atmospheric air in dibutylphthalate at various temperatures.

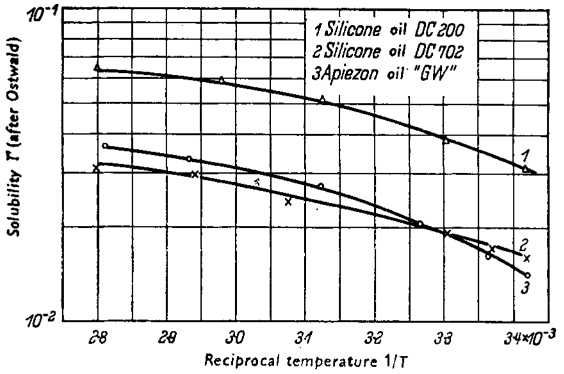

FIG. 2.4.16. Absorption isobars of He in pump fluids ($p = 760$ Torr).

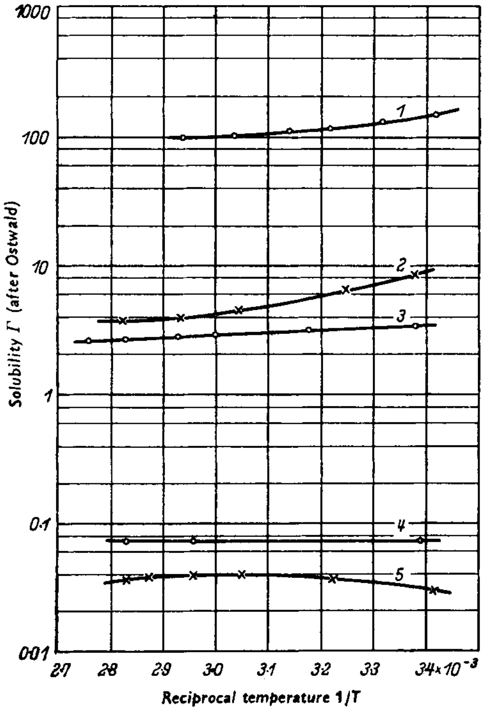

FIG. 2.4.17. Absorption isobars for nitrogen and water vapour

Curve	Liquid	Gas	Pressure (Torr)
1	Dibutylphthalate	H_2O vapour	0·13
2	Clophen A 40	H_2O vapour	10·5
3	Shell oil K 8	H_2O vapour	9
4	Shell oil K 8	N_2	4
5	Clophen A 40	N_2	10

2.4.3 Sorption of Gas by Getters

In order to maintain or to improve the vacuum in an evacuated sealed-off container, but also for the production of high vacuum without diffusion pumps, so-called getters have successfully been used. Getter materials take up large amounts of gas by sorption (absorption and/or adsorption), by chemical reactions, and by similar processes. Getters are classified in three main groups: Flash getters, bulk getters, and coating getters.

For the production of bulk and coating getters the elements tantalum, niobium, zirconium, titanium, and thorium, and to a lesser extent also tungsten and molybdenum are used. These refractory metals are mounted in the vacuum vessel in the form of small pieces of wire, foil, strip, and rod or, alternatively, are applied as a powder forming a layer of large surface area. When mounted appropriately in the container, these getters reach an operating temperature, at which the efficiency of the getters is an optimum and which depends on the system getter material-gas. In many cases where the getter material cannot be suitably fixed to the electrodes, separate getter mounts, which can be electrically heated, have to be provided inside the container.

Bulk and coating getters are particularly suitable for use in containers where a high standard of electrical insulation is required, because these getters have a low vapour pressure and their physical size inside the vessel is — in contrast to flash getters — well defined.

These types of getters take up the gases mainly by sorption; only a small fraction is chemically sorbed (e. g. tantalum reacts under certain conditions with oxygen).

The technical data of common getter materials are listed in Table 2.4.8.

Tantalum. The working temperature of tantalum when used as a getter is between 600 and 1200 °C. It sorbs a volume of hydrogen 740 times that of its own volume. Tantalum retains its oxide film up to 2000 °C and should, therefore, be degassed at this temperature. Tantalum is applied in the form of thin strips, which are fitted to the electrodes, or more economically in the form of a powder sintered to electrodes made of tungsten or molybdenum.

Niobium is similar to tantalum.

Zirconium. The maxima of sorption for the various gases are not in the same temperature range, i. e. the maximum sorption for nitrogen occurs at 1530 °C, for oxygen at 1100 °C. The corresponding temperatures for hydrogen, as reported in the literature, vary very much. This may be explained by the fact that zirconium, like tantalum, is covered with an oxide layer which has a strong influence upon sorption. Carbon dioxide is not sorbed by zirconium.

Zirconium is a frequently used getter material. It is used in the form of wire, sheet, or powder. According to the nature of gases present in the

TABLE 2.4.8. Data for the application of typical getters (after STEYSKAL)

Bulk and coating getters	Ta	Nb	Zr	Th	Ceto
Form of getter	sheet, powder	pellets	sheet wire, powder	powder	powder
Degassing temperature in °C	1600–2000	1650	700–1300 (up to 1700 in compound wires)	for metal base 800–1000 (for graphite base 1500–1600)	800–1200
Operating temperature in °C	700–1200	300	800 (up to 1600 in compound wires)	400–500	200–500
Applications reported	*D, E, M*	*D, E*	*C, D, E, F, I, K, L, M, N*	*C, D*	*P*

Flash getters	Mg	Al–Mg	Ba	Bato	Batalum	$BaBeO_2$
Form of getter	ribbon wire	powder-paint	metal-clad pellets	Ni-clad pellets	$BaCO_3$ painted on Ta	$BaBeO_2$ painted on Ta
Degassing temperature in °C	400	400	600–700	–	800–1100	900–1000
Flashing temperature in °C	500	–	900–1300	780–900	1200–1300	1300
Operating temperature in °C	absorbs gases only during flashing		maximum 200		maximum 200	
Applications reported	*I, K*	*A, F*	*A, B, D, F, G, H, I, N*	*D, M*	*A, F*	*A, F*

A – Small receiving tubes
B – Miniature tubes
C – UHF-tubes
D – Medium size transmitting tubes
E – High power transmitting tubes
F – Oxide cathode tubes
G – Cathode-ray tubes
H – Photocells
I – Gaseous discharge tubes
K – Hg-vapour tubes
L – X-ray tubes
M – High power vacuum tubes
N – Tubes with thoriated cathodes
P – Vacuum tubes in which neither flash getters nor the high temperature necessary for Ta and Zr may be used.

system (tube), it is sometimes necessary to mount two zirconium getters, which operate at different temperatures. Zirconium powder is readily inflammable.

Titanium has similar properties to tantalum or niobium. It sorbs much greater quantities of hydrogen than does tantalum. It is especially important as a metal for use in getter-ion pumps.

Thorium. The best temperature range for sorption and chemisorption is between 400 and 500 °C. Except in special cases thorium is used in the form of powder and coated on the appropriate part of the vacuum tube electrodes made of nickel or iron. Like zirconium, thorium powder is ignited readily by friction. A getter material consisting of 80 per cent Th and 20 per cent "Mischmetall" (cerium, lanthanum, *et al.*), the so-called *Ceto*-getter, getters at 200 up to 500 °C.

Tungsten. This material reacts at high temperatures with oxygen and H_2O where by oxides are formed. These oxides evaporate even at low temperatures and form deposits on glass walls. If nascent H is present, the oxides will be reduced and H_2O is produced again. On account of this cyclic process (LANGMUIR), water vapour has to be carefully avoided wherever tungsten electrodes are used, because even small amounts of water vapour will destroy them.

Nitrogen and carbon dioxide are sorbed only at temperatures above 2300 °C. Because of these high gettering temperatures tungsten is generally not used as a getter material.

Barium, magnesium, aluminium, thorium and suitable mixtures and compounds of these materials are used for the production of flash getters. The getter material is evaporated within a container, e. g. an electron tube, when the deposit forms a large surface area which facilitates gas sorption and chemical reaction.

The resulting compounds of low vapour pressure condense on the coldest spot of the container. When barium is evaporated in a gas atmosphere containing oxygen, barium oxide is formed. But chemical reactions are not solely responsible for the gas sorption which takes place; a number of other mechanisms, the nature of which is not fully understood, also seem to play an important part.

The deposit should be porous. Porosity facilitates contact gettering, i. e. gas sorption by the condensate. Table 2.4.9 shows how much the gettering rate depends on the appearance and hence the surface structure of the getter deposit. The getters referred to in this table were produced in ultrahigh vacuum after thorough predegassing. It appears that a diffuse getter film can absorb 10 to 20 times more gas than a shiny getter film. These differences are particularly pronounced in the case of barium and "Mischmetall"; both getters are frequently used in the valve industry. The table also includes the materials uranium and thorium. These materials, however, are not widely used in gettering techniques, because of their high evaporation temperature. Thorium is sometimes added to other gettering materials (barium).

TABLE 2.4.9. Gas sorption by contact gettering
(after EHRKE and SLACK).
The figures in the table show the amount of gas in litre/mg getter material sorbed at 10^{-3} Torr.

Getter	Gas	Getter film		Getter	Gas	Getter film	
		bright mirror	diffuse			bright mirror	diffuse
Al	O_2	7·5	38·6	U	O_2	10·56	9·26
	N_2, H_2,	–	–		H_2	8·9	21·5
	CO_2	–	–				
Mg	O_2	20	202	"Misch-metall"	O_2	21·2	50·9
	CO_2	–	little gas sorption at 200 °C		H_2	46·1	63·9
					N_2	3·18	16·1
	N_2, H_2	no gas sorption at room temperature			CO_2	2·2	44·8
Th	O_2	7·45	33·15				
				Ba	O_2	15·2	45
	H_2	19·45	53·7				
					H_2	87·5	73·0
					N_2	9·5	36·1
					CO_2	5·2	59·5

To a small extent noble gases are also sorbed by flash gettering. It is assumed that noble gas atoms which are near the wall are occluded by the condensate film.

Flash getters are inexpensive and are easy to handle. Such getters are used in small containers, e. g. oxide cathode and discharge tubes, when extreme electrical insulation is not required. The common types of flash getters are described below, and are also listed in Table 2.4.8.

Aluminium. Aluminium plated on iron displays a considerable coating getter effect. It is frequently alloyed with barium and magnesium; because of its higher evaporation temperature aluminium does not evaporate during the evaporation of the alloy.

Magnesium. This material reacts with oxygen, but only during evaporation. Magnesium is used as a getter occasionally in mercury arc rectifiers and in gas discharge tubes. A magnesium-aluminium alloy is called "Formier"-getter.

Barium getters oxygen, nitrogen, hydrogen, and carbon dioxide, both during evaporation and as a condensate film. Oxide cathodes are not poisoned by Ba-getter. Its relatively high vapour pressure is a disadvantage, so this getter cannot be used in high power valves running at high operating temperatures. Barium oxidizes when exposed to air; therefore, it has to

TABLE 2.4.10. Capacity of various getters (after WAGENER)

Getter	Weight of film in mg/cm^2	Temperature °K	Getter capacity in 10^{-3} Torr litre/cm^2				
			O_2	CO	CO_2	H_2	N_2
Barium	≈ 0·1	325	2·5	0·25	0·5	–	0·5
		375	–	0·5	–	–	–
		425	–	0·75	–	–	–
Thorium	2·5	350	0·2	–	–	0·04	–
		500	–	–	–	0·27	–
		630	–	–	–	0·53	–
		740	–	–	–	0·50	–
		950	6·5	–	–	0·08	–
Zirconium	4	300	1·5	0·0	0·0	0·36	–
		625	–	–	–	53	–
		675	8·0	–	–	–	–
		775	–	1·7	2·3	–	3·5
		1075	–	14·6	12·2	–	5·8

TALBE 2.4.11. Total sorption capacity of frame-shaped barium getter and of sintered ring getter at normal valve operating temperature (after DELLA PORTA)

Gas	Frame getter	Sintered ring getter
O_2	50×10^{-3} Torr litre/mg	50×10^{-3} Torr litre/mg
H_2O	35×10^{-3} Torr litre/mg	61×10^{-3} Torr litre/mg
H_2	$4{\cdot}48 \times 10^{-3}$ Torr litre/cm^2	13×10^{-3} Torr litre/cm^2
CO_2	$0{\cdot}60 \times 10^{-3}$ Torr litre/cm^2	$1{\cdot}8 \times 10^{-3}$ Torr litre/cm^2
CO	$0{\cdot}72 \times 10^{-3}$ Torr litre/cm^2	$3{\cdot}7 \times 10^{-3}$ Torr litre/cm^2
N_2	$0{\cdot}33 \times 10^{-3}$ Torr litre/cm^2	$2{\cdot}25 \times 10^{-3}$ Torr litre/cm^2
dry air	$0{\cdot}64 \times 10^{-3}$ Torr litre/cm^2	$2{\cdot}6 \times 10^{-3}$ Torr litre/cm^2

TABLE 2.4.12. Total sorption capacity of

Gas	Quantity of gas sorbed at		
	20°C	100°C	200°C
O_2	50×10^{-3} Torr litre/mg	–	–
H_2O	35×10^{-3} Torr litre/mg	–	–
H_2	$4{\cdot}48 \times 10^{-3}$ Torr litre/cm^2	5×10^{-3} Torr litre/cm^2	$5{\cdot}5 \times 10^{-3}$ Torr litre/cm^2
CO_2	$0{\cdot}60 \times 10^{-3}$ Torr litre/cm^2	2×10^{-3} Torr litre/cm^2	$3{\cdot}3 \times 10^{-3}$ Torr litre/cm^2
CO	$0{\cdot}72 \times 10^{-3}$ Torr litre/cm^2	4×10^{-3} Torr litre/cm^2	$4{\cdot}4 \times 10^{-3}$ Torr litre/cm^2
N_2	$0{\cdot}33 \times 10^{-3}$ Torr litre/cm^2	$0{\cdot}48 \times 10^{-3}$ Torr litre/cm^2	$3{\cdot}4 \times 10^{-3}$ Torr litre/cm^2
dry air	$0{\cdot}64 \times 10^{-3}$ Torr litre/cm^2	$1{\cdot}60 \times 10^{-3}$ Torr litre/cm^2	$4{\cdot}6 \times 10^{-3}$ Torr litre/cm^2

TABLE 2.4.13. Adsorption by 1 cm³ coconut charcoal (after DEWAR)

Gas	Adsorbed gas volume in ccs (NTP)	
	0°C	−185°C
A	12	175
H_2	4	135
CO_2	21	190
He	2	15
N_2	15	155
O_2	18	230

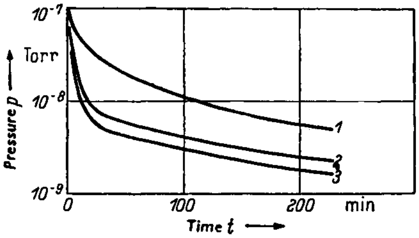

FIG. 2.4.18. Pressure vs. time in valves with Ba- and Th-getters (after WAGENER). Curves 1—3, see text.

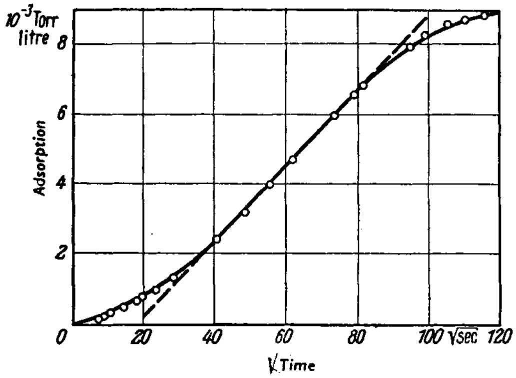

FIG. 2.4.19. Adsorption of nitrogen by Ba-film as a function of time (after DELLA PORTA).

bright barium mirrors (after DELLA PORTA)

Quantity of gas sorbed at	
300°C	400°C
57×10^{-3} Torr litre/mg	—
72×10^{-3} Torr litre/mg	—
9×10^{-3} Torr litre/cm² (90×10^{-3} Torr litre/mg)	10×10^{-3} Torr litre/cm² (100×10^{-3} Torr litre/mg)
$5{\cdot}8\times10^{-3}$ Torr litre/cm² (58×10^{-3} Torr litre/mg)	$6{\cdot}6\times10^{-3}$ Torr litre/cm² (66×10^{-3} Torr litre/mg)
9×10^{-3} Torr litre/cm² (90×10^{-3} Torr litre/mg)	10×10^{-3} Torr litre/cm² (100×10^{-3} Torr litre/mg)
5×10^{-3} Torr litre/cm² (50×10^{-3} Torr litre/mg)	$5{\cdot}1\times10^{-3}$ Torr litre/cm² (51×10^{-3} Torr litre/mg)
$5{\cdot}6\times10^{-3}$ Torr litre/cm² (56×10^{-3} Torr litre/mg)	$5{\cdot}6\times10^{-3}$ Torr litre/cm² (56×10^{-3} Torr litre/mg)

be protected by a metal casing or a protective layer of wax, which is destroyed by predegassing of the getter.

The so-called Kemet-getter consists of a Ba-Mg-Al alloy, which is enclosed in a sealed thin steel cylinder. When heated to 850 °C, the barium permeates through the thin wall of the steel envelope.

In the case of *Batalum*-getter, barium and strontium carbonate are sprayed on to a heater spiral made of tantalum. When heated up to 800 to 1000 °C, the carbonates dissociate into oxides, and on further heating up to 1200 °C these oxides are reduced by the tantalum to metallic barium and strontium.

Alba-getters are produced by reduction of barium oxide by aluminium.

From barium-beryllate metallic barium can be obtained when a tantalum wire is heated up to 1300 °C.

The *Bato*-getter becomes operative through a chemical reaction between a Ba-Al alloy, iron oxide and thorium powder, in the course of which barium evaporates.

The presence of mercury vapour makes barium getters ineffective and moreover may cause desorption of already sorbed gases, because of the amalgamation of barium.

For both types of getters the gettering capacity depends very much on the pretreatment. Prior to flashing, thorough degassing by preheating of the getter is essential. At normal degassing temperatures (400—500 °C) the vapour pressure of the getter material should be relatively low.

Table 2.4.10 shows the capacities of several getters. At low temperatures the total absorption capacity of barium getters is larger than the total capacity of bulk and coating getters. These become superior to barium getters only at higher temperatures. As stated by WAGENER, diffusion into deeper regions of the film is possible at higher temperatures.

Effectiveness of a getter implies, apart from a large total capacity, a high initial gettering speed and lasting contact gettering, so that gases desorbed from electrodes during operation can be sorbed by gettering. Figure 2.4.18 shows the pressure as a function of time in electronic tubes, in which two getters were operative: a barium getter was deposited on the glass wall and a thorium getter was mounted inside the anode. The curves 1—3 show the influence of the predegassing time upon the end pressure. The degassing temperature was 535 °C. Predegassing time for curve 1 was 30 mins, for curve 2 it was 45 mins, and for curve 3 it was 75 mins. The pressures shown in Fig. 2.4.18 refer to an operating temperature of 325 °C.

A recent application of getters is formed in the so-called getter pumps; these clean up residual gases in vacuum systems which are not permanently sealed-off. Titanium is the preferred gettering material in these pumps; in the form of vapour or freshly deposited as a film it getters large amounts of gas (see p. 99).

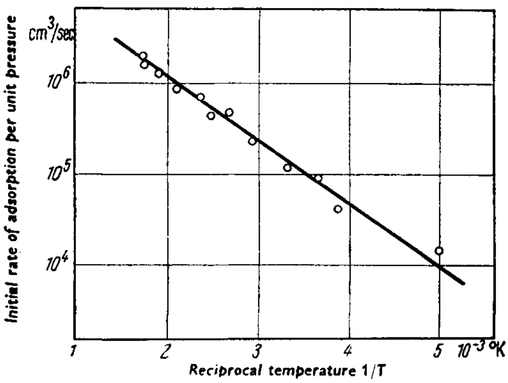

FIG. 2.4.20. Rate of adsorption for nitrogen on Ba-film as a function of temperature (after DELLA PORTA).

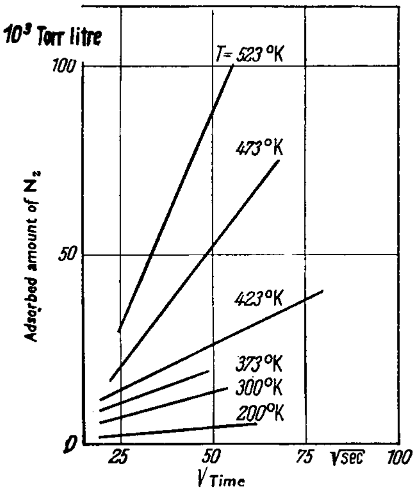

FIG. 2.4.21. Adsorption of nitrogen on Ba-films as a function of time for various temperatures (after DELLA PORTA).

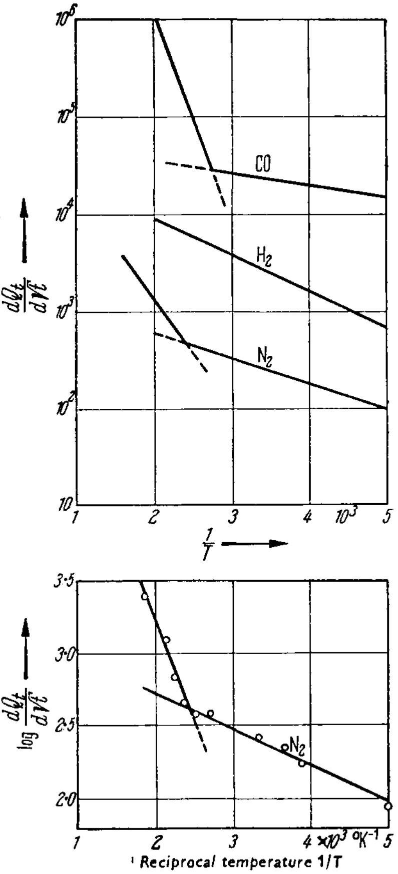

FIG. 2.4.22. Diffusion of N_2, H_2 and CO in Ba-films as a function of temperature (after DELLA PORTA).
The resulting activation energies are given in Table 2.4.14.

TABLE 2.4.14. Activation energies calculated from Fig. 2.4.22

	N_2	H_2	CO
Critical temperature T_k (°C)	≈ 140	–	≈ 100
Activation energy for $T < T_k$ (cal)	≈ 2300	–	< 1000
Activation energy for $T > T_k$ (cal)	$\approx 11\,000$	≈ 3000	≈ 9000

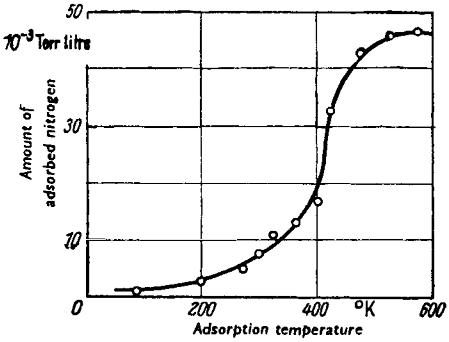

FIG. 2.4.23. Total amount of nitrogen adsorbed on Ba-films as a function of adsorption temperature (after DELLA PORTA).

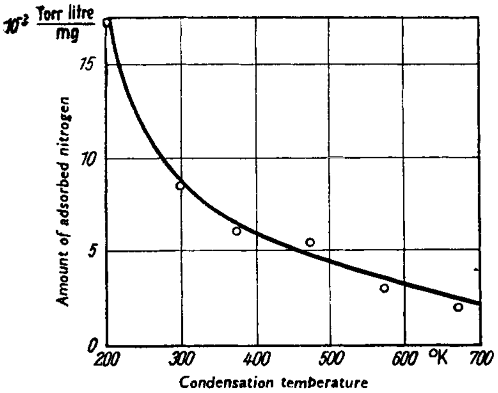

FIG. 2.4.24. Nitrogen adsorbed on Ba-films as a function of the condensation temperature of the films (after DELLA PORTA).

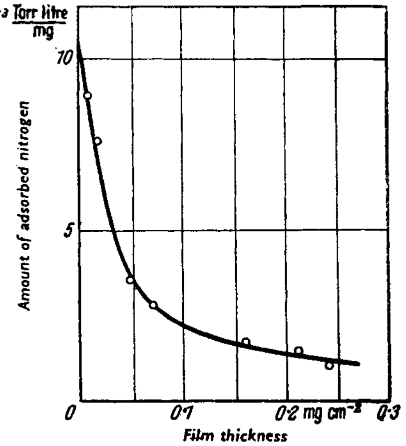

FIG. 2.4.25. Nitrogen adsorbed on barium as a function of the film thickness.

2.4.4 Evaporation, Condensation, Sublimation

(See Bibliography)

2.5 Applications

(See Bibliography)

Bibliography

Note: This vacuum handbook has been duly kept short. The bibliography including many original papers published between 1948 and 1959, partly up to 1961, is provided as a guide to those who are interested in further details. Older papers – except a few outstanding ones – are not listed, because it is felt that the main contents of these papers are included in standard text books and referred to in the publications given in our list. In order to save space, the references are arranged in the form of a table. The sequence follows the contents of this book. The following abbreviations which are not included in the international register, are used:

AEC	US-Atomic Energy Commission Report
AECD	Office of Technical Services Department of Commerce
AERE	U. K. – Atomic Energy Research Establishment Reports
ATM	Archiv für technisches Messen
Brit JAP	British Journal of Applied Physics
CR	Comptes Rendus (Hebdomaires des Séances de l'Académie des Sciences)
ETZ	Elektrotechnische Zeitschrift
Gl und HVT	Glas- und Hochvakuumtechnik
IEC	Industrial and Engineering Chemistry
invest Phys	Investigations Physicae (Australia)
J	Journal
JAP	Journal of Applied Physics
JSI	Journal Scientific Instruments
Namur Ber.	Proceedings of the First International Congress on Vacuum Technique; London, Pergamon Press, 1960.
NBS	National Bureau of Standards (Technical News Bulletin)
Rdsch	Rundschau
RSI	Review of Scientific Instruments
Trans ASME	Transactions American Society of Mechanical Engineers
Z	Zeitschrift
Zbl	Zentralblatt

If a paper has been abstracted in another publication, the list first gives the reference of the original paper and below the reference of the abstract, marked: ref.

Text Books and Monographs of Vacuum Technology

BUCH, S.	Einführung in die allgemeine Vakuumtechnik Stuttgart: Wissenschaftliche Verlagsgesellschaft 1962
CHAMPEIX, R.	Eléments de Technique du Vide, vol. I Paris: Dunod 1958
DAVY, J. R.	Industrial High Vacuum London: I. Bitman & Sons 1951
DUNOYER, L.	Le vide et ses applications Paris: Presses Univ. de France 1951
DUSHMAN, S.	Scientific Foundation of Vacuum Technique New York and London: J. Wiley & Sons Second edition by Lafferty 1962
GUTHRIE and WAKERLING	Vacuum Equipment and Techniques New York/London/Toronto: McGraw Hill 1949

Heinze, W.	Einführung in die Vakuumtechnik, Bd. I Berlin: VEB Verlag Technik 1955
Holland-Merten	Handbuch der Vakuumtechnik, 3. Aufl. Halle: Knapp 1953
Jaeckel, R.	Kleinste Drücke, ihre Messung und Erzeugung Berlin/Göttingen/Heidelberg: Springer 1950
Jaeckel, R.	Vakuumtechnik in "DECHEMA-Erfahrungsaustausch" Frankfurt/M. 1956
Jaeckel, R.	Allgemeine Vakuumphysik in ,,Handbuch der Physik", Bd. 12, edited by S. Flügge Berlin/Göttingen/Heidelberg: Springer 1958
Jaeckel, R.	Erzeugung von Vakuum und Arbeiten mit Unterdruck in ,,Houben-Weyl: Methoden der organischen Chemie, Bd. I/2" Stuttgart: Georg-Thieme-Verlag 1959
Laporte, H.	Hochvakuum, seine Erzeugung, Messung und Anwendung Halle: Knapp 1951
Leblanc, M.	La Technique du Vide Paris: Librairie Armand Colin 1951
Mönch, G. Ch.	Hochvakuumtechnik, 2. Aufl. Pößneck: Rudolf A. Lang Verlag 1950
Mönch, G. Ch.	Neues und Bewährtes aus der Hochvakuumtechnik Berlin: VEB Verlag Technik 1961
Morand, N.	Traité pratique de Technique du Vide Paris: Soc. G. E. P. 1958
Oetjen, G. W.	Kapitel: Vakuumtechnik Ullmanns Enzykl. der techn. Chemie, 3. Aufl., Bd. 1
Pirani, M. and Yarwood, J.	Principles of Vacuum Engineering London: Chapman & Hall 1961
Pupp, W.,	Vakuumtechnik. Teil I: Grundlagen München: Thiemig KG, 1962
Reimann, A. L.	Vacuum Technique London: Chapman & Hall 1952
Turnbull, Barton and Riviere	An Introduction to Vacuum Technique, London: Newnes Ltd. 1962.
Wagner, G.	Erzeugung und Messung von Hochvakuum Aufbau und Betrieb von Hochvakuumapparaten Wien: Franz Deuticke 1950
Yarwood, J.	High Vacuum Technique London: Chapman & Hall 1955 New York: J. Wiley & Sons 1955
Yarwood, J.	Hochvakuumtechnik Berlin: Rudolf A. Lang Verlag 1955

Congress Reports on Vacuum Technology

CVT	Committee on Vacuum Techniques, Inc. Boston 9, Mass. Vacuum Symposium Transactions 1953, 1954, 1955, 1956, 1957, 1958, 1959, 1960, 1961
–	Proceedings of the First International Congress on Vacuum Technique London: Pergamon Press 1960
–	Cambridge High Vacuum Symposium 1947, 1948, 1949 (NRC)

– French Lick Meeting 11.–14. May 1952
Amer. Inst. Chem. Engrs.
Ref.: Vacuum II, 1952, 2, 147–150 by L. A. Bromley

– Transactions of Instruments and Measurements
Conference Stockholm 1952
Svenska Teknolofören

– High Vacua Convention, Pertshire
Ref: Chem. and Ind. Oct. 1948 by Dushman

– Symposium Institute of Physics Birmingham 27.–28. June 1950
J. Sci. Instr. Suppl. 1, 1951
Ref: Engineering 170, 1950, 4409, 95/96

– Congrès national des Sciences Bruxelles 1950

– Symposium Institute of Biology
Freeze and Drying, London Sept. 1951
Ref: Vacuum I, 1951, 4, 294 by R. J. C. Harris

Books dealing with important Vacuum Problems

Ardenne, M. von — Tabellen der Elektronenphysik, Ionenphysik und Übermikroskopie
Berlin: VEB Deutscher Verlag der Wissenschaften 1956

Auwärter, M. — Ergebnisse der Hochvakuumtechnik und der Physik dünner Schichten
Stuttgart: Wissenschaftliche Verlagsgesellschaft 1957

Bachman, Ch. — Techn. in Exp. Electronics
London: Chapman & Hall 1948

Barret, A. S. D. — Progress in Vacuum Science and Technology
London: Pergamon Press 1959

Bunshah, R. F. — Vacuum Metallurgy
New York: Reinhold Publishing Corp. 1957
London: Chapman & Hall 1957

Bunshah, R. F. — Transactions of the Vacuum Metallurgy Conference 1959
New York U. P.

Dayton, B. B. — Physikalische Methoden bei chemischen Analysen, Bd. II: Technik und Analysen unter Vakuum
New York: Academic Press 1951

Delafosse, J., Mongodin, G. — Les Calculs de la Technique du Vide
Special issue "Le vide", 1961

Eschbach, H. L. — Praktikum der Hochvakuumtechnik
Leipzig: Akademische Verlagsgesellschaft 1961

Espe, W. — Zirkonium, seine Herstellung, Eigenschaften und Anwendungen in der Hochvakuumtechnik
Füssen 1953

Espe, W. — Werkstoffe der Elektrotechnik in Tabellen und Diagrammen
Berlin: Akademie Verlag 1954

Espe, W. — Werkstoffkunde der Hochvakuumtechnik
Berlin: VEB Deutscher Verlag der Wissenschaften 1960

Flossdorf, Earl W. — Freeze Drying
New York: Reinhold 1949

Harris, R. J. C. — Biological Applications of Freezing and Drying
New York: Academic Press 1954

Heiss, R. — Kapitel: Gefriertrocknung
Ullmanns Enzykl. der techn. Chemie, 3. Aufl., Bd. 1

HIPPEL, A. R. VON	Dielectric Materials and Applications New York 1954
HOLLAND, L.	Vacuum Deposition of Thin Films London: Chapman & Hall 1956
JAECKEL, R.	Destillation und Sublimation im Fein- und Hochvakuum in „HOUBEN-WEYL: Methoden der organischen Chemie, Bd. I/1“ Stuttgart: Thieme 1958
KNOLL, M.	Materials and Processes of Electron Devices Berlin/Göttingen/Heidelberg: Springer 1959
LEBEDINSKY, M. A.	Electrovacuumnye materialy Moscow 1956
	American Lava Corp. Techn. Inform. Cart No. 501 Mechanical and Electrical Properties of Alsimag-Ceramics Chattanooga, Tenn. (USA)
LUFF-SCHMELKES	Chemie des Kautschuks Berlin 1925
MARTIN, L. H., HILL, R. D.	A Manual of Vacuum Practice Melbourne: Univ. Press 1949
MAYER, H.	Physik dünner Schichten, Bd. I Stuttgart: Wissenschaftliche Verlagsgesellschaft 1960
MAYER, H.	Physik dünner Schichten, Bd. II Stuttgart: Wissenschaftliche Verlagsgesellschaft 1955
MEMMLER, K.	Handbuch der Kautschukwissenschaft Leipzig 1930
METHFESSEL, S.	Dünne Schichten Halle: Knapp 1953
MÜLLER, K. G.	Vakuumtechnische Berechnungsgrundlagen Weinheim: Verlag Chemie 1961
PFLEIDERER, C.	Die Kreiselpumpen für Flüssigkeiten und Gase, 5. Aufl. Berlin/Göttingen/Heidelberg: Springer 1961
PIRANI, M.	Elektrothermie, 2. Aufl. Berlin/Göttingen/Heidelberg: Springer 1960
SALMANG, H.	Die physikalischen und chemischen Grundlagen der Keramik, 4. Aufl. Berlin/Göttingen/Heidelberg: Springer 1958
SAUER, R.	Einführung in die theoretische Gasdynamik, 3. Aufl. Berlin/Göttingen/Heidelberg: Springer 1960
SMITHELS, C. J.	Metal Reference Book London 1949
STÄGER, H.	Werkstoffkunde der elektrischen Isolierstoffe. 5. Aufl. Berlin: Borntraeger 1961
STEYSKAL, H.	Arbeitsverfahren und Stoffkunde der Hochvakuumtechnik Mosbach (Baden): Physik-Verlag 1955

1.1 Vacuum Physics and Technology, general

Author	Journal	Volume	Month and Year	Issue No.	Page
Yarwood, J.	Brit JAP	10	59	9	383–391
—	Nuovo Cim	XII	59	X	297–329
Pollard, J.	Rep Progr Phys	22	59		33–73
Lyubimov, M. L., Shakov, K. P., Yukhvidin, Ya.A.	Vacuum	IX	59		108
Günther, K. G.	Chem Ing Techn	31	59	6	379–387
Santeler, D. J.	Gen Engng Lab Rep 58 GL 146		May 58		
Reich, H.	Vac Symp Trans		58		279–282
Müschenborn, G.	Chem Ing. Techn	30	58	12	796–798
Günther, K. G.	Z VDI	100	58	28	1376
Blank, R.	Chem Ing Techn	30	58	4	265
Gould, C. L.	Vac Symp Trans		58		105–109
Brown, F. C.	Vac Symp Trans		58		89–93
—	Brit Chem Engng Pract	3	58	1	26–28
Edwards, F. D.	Financial Times		1. 7. 57		93
	ref. Vacuum publ. 1959	7/8	57/58		111
Hix, P.	Glato prondy Obsor	17	56	12	727–735
	ref. Phys Abstr 5115	60	57		472
Doré, R.	Galvano	229	56		35–39
	ref. Vacuum publ. 1959	7/8	57/58		113
Doré, R.	Ing Tech		56		79–89
	ref. Vacuum	VI	56		183
—	Chem Ing Techn	28	56	10	661–663
Degras, D. A.	Vide Analogie: Vakuum-Elektrizität	11	56	64	155–162
Jaeckel, R.	Chem Ing Techn Neue Forschungsergebnisse	28	56		201
Mercier, C.	J Phys Radium Theorie der Molekularpumpen	17	March 56	3	1A–11A
Degras, D. A.	Genie Chimique	73	55	2	25–30
Becker, J. A.	Bell Labor Rec Ionisationserscheinungen und Vakuumtechnik	33	55	1	
Alpert, D.	Science Versuche bei sehr niedrigen Drucken	122	Oct. 55		729–733
Hiesinger, L.	Vak Techn	4	55	4/5	73–78
Prevot, F.	Genie Chimiquc	73	55	1	1–7
Stürmer, W.	Umschau	55	55	10	293–296
Ennons, A. E.	Brit JAP	5	54	1	27–31
Johnston, A. R., Nebber, H. V.	RSI Technische Hinweise	25	May 54		517/18

Author	Journal	Volume	Month and Year	Issue No.	Page
Adam, H.	Gl und HVT	2	53	9	179–185
				11	222–227
Aitken, M. J.	Brit JAP	4	53	6	188
		4	53	11	350
—	Chem Engng Progr	49	53		3–7, 8–14
Kistenmaker, J.	Ingenieur Nederl	65	53	27	29–32
	ref. Vide	10	55	55	403
Stoddardt, C. K.	Chem Engng Progr	49	53	4	197–202
Mooz, W. E.					
Jaeckel, R.	Techn Mitt	46	53	10	304
Bunt, E. A.,	Ind Chemist		Oct. 52		460–465
McCulloch, R. J.			Nov. 52		503–508
Ebert, H.	Z Glaskunde	25	52	9	286–291
		25	52	10	324-332
		25	52	11	361–370
Ebert, H.	Gl und HVT		52	6	101–105
Busch, W. E.	Oak Ridge Tenn		52		(4)
	UCLR-1887				
	Fehlerquellen bei Vakuumsystemen				
Laporte, H.	Chem Techn	4	52	8	359–366
Martin, S. L.	Chem Process Engng	33	52	7	370–373
Stempfler, R.	Chim et Ind	67	52	4	584–592
Thormann, K.	Chem Ing Techn	24	52	12	653–715
Adam, H.	Feinwerktechnik	55	51	1	11–19
Andrade, E. N.	Vacuum	I	51	1	3–10
Baxter, A. S.	Vacuum	I	51	3	185–190
Blears, J.	JSI (Vakuum Physik)	36	51		
Ebert, H.	Z Glaskunde	24	51	6	152–157
Engel, A. von	Vacuum	I	51		257
Turnbull, A. H.	U.K. AERE Rep Nr. G/R	752	31. 8. 51		
Turnbull, A. H.	JSI	28	51	1	
Jaeckel, R.	Umschau		1. 10. 50		
Ebert, H.	Z Glaskunde	23	50	10	273–279
—	J techn Phys	19	Dec. 49		1341–1369
Bendict, M.	Nat Nucl Energy Ser Div. I, Vol. I		49		
Loevinger, R.	Nat Nucl Energy Scr Div. I, Vol. I		49		
Dushman	IEC	40	48		778
Oetjen, G. W.	Elektrotechnik	B 2	48	12	333–340

1.2 Kinetic Theory of Gases

Burrows, G.	Vacuum publ. 1959	7/8	57/58		3–18
Corrucini, R. J.	Vacuum publ. 1959	7/8	57/58		19–29
Dunoyer, L.	Vacuum	IX	59	1	36–40
German, O.	Soviet Physics JETP	34	Dec. 58	6	1016–1019
	ref. Vacuum	IX	59		154

Author	Journal	Volume	Month and Year	Issue No.	Page
Liu, V. C.	JAP	29	58		1188–1189
	ref. Vacuum	IX	59		154
Muckenfuss, C.	J Chem Phys	29	58		1257
Waldmann, L.	Z Naturforschg	11a	56	6	523
Mori, Y.	J Sci Res Inst	48	Dec. 54	1372	272–280
Schottky, W. F.	Z Elektrochem Ber Bunsengesellsch	58	54	7	442–454
Sugiura, Y.	J Phys Soc Japan	9	54	2448	
Takayanagi, K.	Progr theor Phys	11	June 54	6	557–594
Caro, D. E., Martin, L. H.	Proc phys Soc	66B	Sept. 53		760–768
Folsom, R. G.	Trans Amer Soc mech Engrs	74	52		915–918
Hiby, J. W.	Z Naturforschg	7a	52	8	533–553
Pahl, M.	Electrical Engng		July 51		46
Pahl, M.	Vide	7	52	38	
Boyer, A.	J acoust Soc Amer	30	51		176–178
	ref. Phys Ber	30	51	11	
Dunoyer, L.	Vide	5	Nov. 50		881–886
	ref. Vacuum	I	April 51	2	
Hiby, J. W., Pahl, M.	Z Phys	729	51		517–529

1.3 Flow (Supersonic Flow)

Amoignon, J.	Vak Techn	8	59	8	220–223
Hurlbut, F. C.	JAP	30	59	3	273
Kirchner, F.	Z angew Phys	11	59	5	167–169
Strauss, W. A., Edse, R.	RSI	30	59		258
Abraham, S. Berman	JAP	29	58	1	71
Amoignon, J.	Vide	13	58	78	277
Dayton, B.	Vak Techn	7	58	1	7
Grove, D. M., Ford, M. G.	Nature	182	58	4641	999–1000
Klumb, H., Schmitt, K. H.	Vak Techn	7	58	1	7–13
Manov, M. G.	ref. Vacuum	IX	59		154
Maslach, G. L., Latz, R. N.	Namur-Ber		58		809–812
Nerken, A.	Vak Techn	7	58		116–118
Rothstein, J.	RSI	29	58		243/44
Shirokov, M. F.	Soviet Phys, V	34	Dec. 58	6	1029–1032
Deyagin, B. V.,	Zh tekh Fiz	27	57		2056
Bakanov, S. P.	ref. Phys Abstr 4552	62	59		405
Kemp, J. F.	JSI	34	57		411
Jaeckel, R., Kutscher H.	Forschungsbericht NRW			683	

Author	Journal	Volume	Month and Year	Issue No.	Page
Kondo, Y.	J Jap Vac Soc	7	57		168–175
Kunkel, W. B., Hurlbut, F. C.	JAP	28	57		827–835
Oatly, C. W., Steckelmacher, W.	Brit JAP	8	57		494
Oatley, C. W.	Brit JAP	8	57	1	15–19
Stark, D. S.	Brit JAP	8	57		210–213
Dong, W.	AEC-Rep UCRL 3353		56		
Hiby, J. W., Pahl, M.	Z Naturforschg	11a	56	1	80
Monroe, A. G.,	Nature		56		197/98
Gaffee, D. I.	ref. Vacuum	VI	56		298
Maslach, G. J.,	RSI		55		751–754
Frisch, J.	ref. Vacuum	VI	56		186
Kutscher, H.	Z angew Phys	VII	55	5	229–240
Greenhalgh, R. E.,	Chem Engng	63	56	1	222
Miller, J. W.	Nomogramme zum Lösen von Vakuumproblemen				
Zeller, H.	Forschungsbericht NRW		55	175	5–119
Günther, K. G.	Vak Techn	4	55	3	49/50
Jaeckel, R. Günther, K. G., Oetjen, G. W.	Z angew Phys	VII	55		71
Nöller, H. G.	Z angew Phys	VII	55		218–229
Santeler, D. I., Norton, J. F.	Vacuum	IV	54		176
Oatly, C. W.	JAP	25	54		358
Sears, G. W.	J Chem Physics	22	54	7	1252/53
Kyte, J., Madden, A. J., Piret, E.	Chem Engng Progr	49	53	12	653–662
Lauer, O.	Z angew Phys	V	53	3	81
Trevoy, D. J., Torpey, W. A.	RSI	24	53	8	676–682
Folsom, R. G.	Chem Engng Progr	48	52		542–548
Alancraig, C.	Chem Engng Progr	48	52		357–361
Huggil, J. A. W.	Proc Roy Soc, Lond	221A	52		123–136
James, D. H., Phillips, C. S. G.	JSI	29	52		362/63
Strong, J.	Vacuum	II	52	2	
Harries, W.	Z angew Phys	III	51		296
Wasserrab, T.	BBC-Nachr	33	51	1 u. 2	
Dunoyer, L.	Vide	5	50	30	881
Harries, W.	Chem Ing Techn	21	49	7/8	139–142
Mellen, G. L.	Chem Engng	56	May 49		
Andersen, J. W., Friedmann, R.	RSI	20	49		61

Author	Journal	Volume	Month and Year	Issue No.	Page
Sheriff, E. V.	JSI	26	49	2	43–45
Witty, R.	JSI	26	49	9	316–318
Dayton, B. B.	IEC	40	48		795

1.4 Vacuum Pumps, general

Armbruster, W.	Chem Ing Techn	31	59	5	338–342
	ref. Vacuum	IX	59	3/4	238
Foresti, R.	RSI	30	59	11	1067
Knight, G. B.	Chem Engng	66	59		171–174
Pagel, H. J., Schwarz, W., Simon, W.	JSI	36	59		53
Venema, A.	Vide	14	59	81	113–120
Vratny, F., Graas, B.	RSI	30	59	7	597
Amoignon, J.	Namur-Ber		58		311–314
Andrade, E. N.	Namur-Ber		58		14–20
Baquet, E. H.	Vide	13	58	75	123
Beecher, N., Hnilicka, M. P.	Vac Symp Trans		58		94–100
Degras, A.	Vide	13	58	78	268
Diels, K.	Vide	13	58	75	143–153
Florescu, N. A.	Appl Sci Res	B 7	58	1	63
	ref. Phys Abstr	61	58	86	909
Kraus, Th.	Vac Symp Trans		58		38–40
Haefer, R., Wild, H.	Namur-Ber		58		626–631
Reich, G., Nöller, H. G.	Namur-Ber		58		93–97
Baum, H.	Vak Techn	6	57	7	
Knechtli, R. C.	Vac Symp Trans		57		83–87
Hänlein, W.,	Z angew Phys	8	56	12	603–607
Günther, K. G.	ref. Phys Abstr Nr. 9035	60	57		828
Urry, G.,	RSI	27	56	10	819/20
Urry, W. H.	ref. Phys Abstr Nr. 1118	60	57		106
Thomas, E.	Vide	11	56	63	88–98
Delcher, J., Geller, R., Mongodin, G., Prevot, F.	Vide	11	56	62	78–90
Düsing, W.	Telefunkenztg	28	55	108	71–84
Günther, K. G.	Vak Techn Saugleistung	4	55	3	49/50
Hochhäusler, P.	ETZ Treibdampf- und Molekularpumpen	7	55	11	417–423

Author	Journal	Volume	Month and Year	Issue No.	Page
Nöller, H. G.,	Z angew Phys	VII	55		218–234
Kutscher, H.	Die phys. Vorgänge in Diff.- u. Dampfstrahlpumpen				
Seel, F.	Chem Ing Techn	27	55	8/9	542
Sofer, G. A.	Vac Symp Trans		54		27
Venema, A.	Vacuum	IV	54	3	272–283
Jaeckel, R.,	Vak Techn	3	54	1	1
Nöller, H. G.,	Die phys. Vorgänge in Diff.- u. Dampfstrahlpumpen				
Kutscher, H.					
Oatly, C. W.	JAP	25	54		358
Florescu, N. A.	Invest Phys (Theorie)		53	1	
Jackson, D. H.	Chem Engng Progr	49	53	2	102–104
Lorenz, C. W.	Techn Wiss Ber Osram	27	54	10	320
	Mechanische Hochvakuumpumpe				
Leake	JSI	30	53	11	434
Mukherjèe, S. K.	Indian J Phys	27	53		137–144
Florescu, N. A.	Invest Phys (Theorie)		52	2	20
	ref. Vak Techn	3	54	3/4	72
Jaeckel, R.,	Z VDI	94	52	24	797–803
Nöller, H. G.					
Kumagai, H.,	RSI	23	52	1	56/57
Sibata, H.,					
Tuzi, Y.					
Laporte, H.	Gl und HVT		52	5	97
	Prüfung von Pumpen				
Lawrence, R. B.	Chem Engng Progr	48	52		537–542
Strong, J.	Vacuum	II	52	2	
Goddart	JSI	28	51	1	1–7
Cecchine, L. P.,	RSI	22	51	11	836/37
Bronson, J. F.					
Kerner, H.	Chem and Ind (Glaspumpen)		13. 1. 51		24
Lawrence, R. B.	NRC-Mitt		51/52		
Henry, R. M.	Vide	5	50	28/29	859–865
Hicks, T. J.	Chem Engng	57	50		108–110
Johnson, E. F.	Chem Engng	57	50	9	125
	ref. Vacuum	I	51	1	49
Dushman, S.	RSI	20	49		131
	Kurven für Pumpgeschwindigkeiten				
Kohl, W. H.	Iron Age	164	49		59–63
Mellen, G. L.	Electronics, N. Y.	22	49		90–95
Blears, J.,	RSI	19	48		847
Hill, R. W.					
Fluke, D.	RSI	19	48		665/66
Neumann, R.	Electronic Engng	20	Jan. 48		3

Author	Journal	Volume	Month and Year	Issue No.	Page
Neumann, R.	Electronic Engng	20	Febr. 48		44
Neumann, R.	Electronic Engng	20	March 48		79
Neumann, R.	Electronic Engng	20	April 48		122
Neumann, R.	Electronic Engng	20	May 48		163
Witty, R., Grindley, J.	JSI	25	Oct. 48	10	
Risch, R.	Schweiz Arch	14	48		279–285
Dayton, B. B.	IEC	40	48		795

1.4.1 Mechanical pumps

Lorenz, A.	Vide	14	59	81	121
Klumb, H., Wagner, F.	Vak Techn	7	58	8	191–193
Lorenz, A.	Vac Symp Trans		58		79–82
	Namur-Ber		58		177–180
Steckelmacher, W.	Namur-Ber		58		159–163
Bürger, H.	Chem Techn	8	56		218–232
	ref. Vacuum	VI	56		237
Thees, R., Treupel, H.	ETZ		55		321
Hockley, D. K.	Vacuum	IV	54	1	40–47
	ref. Phys Abstr	60	57		16
Schunk, H.	Chem Ing Techn	24	52	3	156/57

1.4.2 Roots pumps

Armbruster, W., Lorenz, A.	Vak Techn	7	58	4	81–85
Thees, R.	Namur-Ber		58		784–788
Thees, R.	Namur-Ber		58		164–167
Winzenburger, E. A.	Vac Symp Trans		58		83–85
Winzenburger, E. A.	Vac Symp Trans		57		1–5
Nöller, H. G., Thees, R.	Z VDI	99	57	14	613–619
Ziock	Vak Techn	6	57	5	98
Thees, R.	Vacuum	V	55		25–34

1.4.3 Vapour jet pumps

Kilpatrick, P. W.	Control Engng	6	59	8	109
Barret, A. S. D., Dennis, N. T. M.	Namur-Ber		58		212–218
Ishii, H., Ito, A.	J Jap Vac Soc	1	58	2	
Linck, C. G.	Chem Engng	13	Jan. 58		
Power, B. D., Dennis, N. T. M.	Namur-Ber		58		197–201

Author	Journal	Volume	Month and Year	Issue No.	Page
Power, B. D.,	Vide	13	58	75	129
Dennis, N. T. M.					
Reinhardt, H. G.	Siemens Z	32	58		351–354
Trabert, F. W.	Vac Symp Trans		58		101–104
Fondrk, V. V.	Vac Symp Trans		57		88–94
Florescu, N. A.	Invest Phys		55	2	
Florescu, N. A.	Vacuum	IV	54	1	30–39
	ref. Phys Abstr	60	57		16
George, J. S.	RSI	26	55	3	303
Nöller, H. G.	Z angew Phys	VII	55		218
	Phys. Vorgänge				
Stokes-Machine Co.	Chem Engng	62	55	3	250
Berkley, F. D.	Chem Engng	61	54	11	164–168
Lifshic,	Zh tekh Fiz USSR	22	54	8	362–375
Rozenevejg	(Theorie)				
Takashima, Y.,	Chem Engng Japan	18	54		427–438
Hasegawa, M.					
Fondrk, V. V.	Chem Engng Progr	49	53	1	3–7
Power, B. P.	Vacuum	IV	54	4	415–437
	ref. Phys Abstr Nr. 9034	60	57		828
Tajima,	RSI	24	53	4	323
Kaneko, K.,	Charakteristiken				
Katajama, A.					
Tallman, J. C.	Chem Engng		Jan. 53		176–179
	ref. Vacuum	III	53	2	191
	Untersuchung der Kostenfrage				
Zimmermann, L	Chem Ing Techn	11	53		655–671
	Graph. Berechnungsverfahren				
Catlin, J. R.,	AERE-Rep Nr. C/M	152	52		
Coward, L.,	ref. Vacuum	III	April 53	2	191
Darling, D.,					
Spragg, W. T.,					
Webb, C. G.					
Simonin, R. F.	J Phys Radium		Febr. 52		
Power, B. D.,	US-Pat 2696344		21. 8. 51/		
Latham, D.	Ölrücklauf		7. 12. 54		

1.4.4 Diffusion pumps

Jaeckel, R.	Vacuum	IX	59	3/4	209–218
Amoignon, J.,	Vide	13	58	76	204
Mongodin, G.,					
Moreau, J.					
Borovyk, Y. S.,	Ukrayin fiz Zh	2	57	1	87 94
Lazaryev, B. H.,	ref. Phys Abstr Nr. 7754	61	58	73	712
Fedorova, M. F.,					
Tsyn, N. M.					
Jaeckel, R.	Namur-Bcr		58		21–30

Author	Journal	Volume	Month and Year	Issue No.	Page
Landfords, A. A., Hablanian, M. H.	Vac Symp Trans		58		22–24
Komiya, S.,	J Jap Vac Soc	7	57		131–147
Ikeda, T.	ref. Vacuum publ. 1959	7/8	57/58		167
Nöller, H. G.	Vacuum	V	55		59–76

1.4.4.1 Mercury diffusion pumps

Author	Journal	Volume	Month and Year	Issue No.	Page
Bailleul-Langlais, J.	Vide	14	59	79	19
Haak, W., Vratny, F.	RSI	30	59	4	
Bailleul-Langlais, J.	Namur-Ber		58		329–331
Hiesinger, L.	Phys Blätter Versuch zur Erklärung der Wirkungsweise	12	56	4	156–162
Mönch, G. Ch.	Naturwissenschaften	43	56	5	103
Reichard, M. von	Z angew Phys	VII	55	6	297–301
Mönch, G. Ch.	Z angew Phys	VI	54	2	59
Reichard, M. von	Z angew Phys	VI	54	2	61
Reichard, M. von	Z angew Phys	VI	54	3	104
Lind, E. R.,	AEC-Rep Nr. MTA 14		53		
Steinhaus, J. R.	ref. Vacuum 50000 l-Pumpe	III	53	2	190
Fluke, D.	RSI	19	48		665/66
Dayton	RSI	19	48		793–804

1.4.4.2 Oil diffusion pumps

Author	Journal	Volume	Month and Year	Issue No.	Page
Allabia, S.	Namur-Ber		58		202–204
Bächler, W.	Namur-Ber		58		182–185
Kobayashi, S., Otake, H.	Namur-Ber		58		193–195
Komiya, S., Ikeda, T.	Namur-Ber		58		323–328
Power, B. D., Crawley, D. J.	Namur-Ber		58		206–211
Bächler, W., Nöller, H. G.	Z angew Phys	9	57	12	612–616
Hiesinger, L.	Vak Techn	6	57	4	65–70
Nöller, H. G., Reich, G., Bächler, W.	Vac Symp Trans		57		6–12
Reich, G., Nöller, H. G.	Z angew Phys	9	57	12	617
Reich, G.	Z angew Phys	9	57	1	23–29
Delcher, J.,	Vide	11	56		78–80
Geller, R., Mongodin, G., Prevot, F.	ref. Vacuum	VI	56		184

Author	Journal	Volume	Month and Year	Issue No.	Page
Coe, R. F., Riddiford, L.	JSI	32	55	6	207–213
Nöller, H. G.	Z angew Phys	VII	55		218
Coe, R. F., Riddiford, L.	JSI (Theorie)	31	54		33–36
Frank, R.	Gl und HVT	2	53	14	294–296
Gaviola	Rev Un Nat Argent (einfache Theorie)		52	3	101–127
Nöller, H. G.	Gl und HVT		52	6	113–118
Parat, L. G., Jossem, E. L.	RSI Rückdiffusion	23	52		188
Azam, Orthel	Vide	6	51		1063
Hickman, K. C. D.	RSI	22	51		146
Oyana, S.	J Phys Soc Japan	5	May 50		192–197
Witty, R.	Brit JAP	1	50		232
Berry, C. E.	RSI	20	49		835
Harrington, E. L.	RSI	20	49		761/62
Sears, G. W.	RSI	20	49		485–489
Dayton, B. B.	RSI Sauggeschwindigkeit	19	48		533
Gibson, R.	RSI Sauggeschwindigkeit	19	48		276
Pollard, J., Sutton, R. W., Alexander, P.	JSI	25	48		401–403
Dayton, B. B.	US-Pat 2639086				
	ref. Vak Techn	3	54	3/4	72
Lawrence, R. B.	Brit Pat 686659				
	ref. Vacuum	III	53	2	190
Lawrence, R. B.	US-Pat 2630266		13. 4. 51/ 3. 3. 53		
Vogt, A.	Brit Pat 691434				
	ref. Vacuum	III	53	3	316
Hickman, K. C. D.	US-Pat 2465590				
Nakaji, E. M.	US-Pat 2207256		5. 8. 52/ 15. 2. 55		

1.4.5 Molecular pumps

Author	Journal	Volume	Month and Year	Issue No.	Page
Pupp, W.	Vak Techn	8	59	6	158–162
Becker, W.	Vak Techn	7	58	7	149–152
	ref. Vacuum	IX	59	3/4	239
Becker, W.	Namur-Ber		58		173–176
Mercier, C.	J Phys Radium	17	56		1A–11A
	ref. Vacuum	VI	56		239
Mercier, C.	J Phys Radium	17	56		182A/83A
	ref. Phys Abstr Nr. 5923	60	57		546

1.5 Removal of Vapours, Gas Ballast Device, Condensers

Author	Journal	Volume	Month and Year	Issue No.	Page
Rose, W.	Chem Ing Techn	31	59		101–105
Reylander, H.	Vak Techn	7	58	4	78–81
Lawrence, E.	US-Pat 2737779				
	ref. Vacuum publ. 1959	7/8	57/58		186
Burleigh, Th. E.,	Vak Techn	6	57	1	11
Frye, W. C.	Erklärung des Gasballastprinzips				
Thees, R.	Brennstoff-Wärme-Kraft	9	57	7	315–319
Thees, R.	Vak Techn	6	57	7	160
Power, B. D.	Vacuum	V	55		35–58
Dunoyer, M.	Vide	8	53	43	1280–1294
Kirschbaum, E.	Z VDI	95	53	27	927–932
Oetjen, G. W.	Vacuum	II	52	2	148
Stempfler, R.	Chim et Ind	67	52		484–492
Mitchell, T. J.	Chim et Ind		25.12.50		741–743
George, J. S.	JSI	29	52		413

1.6 Cold Traps, Vapour Traps (Baffles) and Adsorption Traps

Author	Journal	Volume	Month and Year	Issue No.	Page
Gamblin, R. L., Goldberg, E., Scay, D. T.	RSI	30	59		371
Flinn, I.,	JSI	36	59		374
Moore, P.	Constant level device				
Miller, L. D., Petersen, P. N.	Vacuum	IX	59	3/4	231/32
Purser, K. H., Richards, J. R.	JSI	36	59		142
Richelmann, B.	RSI	30	59		598
McFarland, R. H.,	RSI	29	58	6	530/31
McDonald, D. G.	Kupferfalle für Hg-Dampf				
Maltagliati, M., Menicalli	Namur-Ber		58		341–344
Carmichael, J. H., Lange, W. J.	Vac Symp Trans		58		137–139
Ochert, N., Heppel, T. A.	Vac Symp Trans		58		247–253
Walther, H.	Z angew Phys	10	58		272
Zinsmeister, G.	Namur-Ber		58		335–340
Buehler, E.	RSI	28	57		453–460
	ref. Vacuum publ. 1959	7/8	57/58		186
Burns, J.	RSI	28	57	6	469/70
Conn, G. K. T., Daglish, H. N.	JSI	34	57		245
Henshaw, D. E.	JSI	34	57		207
Kunzler, S.	RSI	27	56	10	879
	ref. Phys Abstr Nr. 1965	60	57		185

Author	Journal	Volume	Month and Year	Issue No.	Page
Probyn, H. C.	JSI	33	56		322
	ref. Vacuum	VI	56		255
Feld, M., Klein, F. S.	JSI	31	54		474
Hino, J., Stevens, D. K., Strauss, H. E.	RSI	24	53		445
Alpert, D.	RSI	24	53	10	1004/05
Riddiford, L.	Vacuum	III	53	1	49–51
Miller, G. H.	RSI	24	53		549
Pollard, J.	RSI	24	53		996
Thomas, E., Destappes, J., Dupont, J.	Vacuum	III	53	4	413/14
Evans, E. C., Babelay, E. F.	RSI	23	52	5	249/50
Barton, R. S., Turnbull, R. H	Vacuum	I	51		171
Longini, R. L.	RSI	22	51		345/46
Skvarla, J. E., Evans, R. C.	RSI	22	51	5	341/42

1.7 Getter-ion Pumps, Gas Absorption

Author	Journal	Volume	Month and Year	Issue No.	Page
Bartholomew, C. Y., LaPadula, A. R.	JAP	31	60	2	445
Baker, F. A.,	Vak Techn	8	59		77/78
Yarwood, J.	ref. Vacuum	IX	59	3/4	238
Carter, G.	Vacuum	IX	59	3/4	190–200
Carter, G.	Nature	183	59		1619
	ref. Vacuum	IX	59	3/4	238
Comsa, G.	Vak Techn	8	59		76/77
	ref. Vacuum	IX	59	3/4	238
Comsa, G.	Vak Techn	8	59		194–200
Degras, L. A.	Vide	14	59	81	128
Herb, R. G.	Vacuum	IX	59		97
Holland, L., Laurenson, L.	Vide	14	59	81	141
Holland, L.	JSI	36	59		105–116
	ref. Vacuum	IX	59	3/4	239
Huber, H., Schroff, A. M., Warnecke, M.	Vide	14	59	82	214–225
Jepsen, R. L.	Vide	14	59	80	80
Klopfer, A., Emmrich, W.	Vak Techn	8	59		162–167
Schürer, P., Eckertova, L.	Czechoslovak J Phys	9	59	6	753/54

Author	Journal	Volume	Month and Year	Issue No.	Page
Strotzer, G.	Z angew Phys	11	59		223
Adam, H.	Vak Techn	7	58	2/3	29–34
Blodgett, K. G.	J chem Physics	29	58	1	39
	ref. Phys Abstr	62	59		115
Hall, L. D.	Science	128	58		279–285
	ref. Vacuum	IX	59		154
Herb, R. G.	Namur-Ber		58		45–55
Holland, L., Laurenson, L., Holden, J. T.	Nature	182	58		851
Huber, H., Warnecke, M.	Namur-Ber		58		457–462
Klopfer, A., Ermrich, W.	Namur-Ber		58		427–429
Kumagai, H., u.a.	Namur-Ber		58		433–438
Leck, J. H., Carter, G.	Namur-Ber		58		463–467
Markali, J.	Namur-Ber		58		450–452
Prugne, P., Garin, P.	Namur-Ber		58		439–442
Reich, G., Nöller, H. G.	Namur-Ber		58		443–445
Schram, A.	Namur-Ber		58		446–449
Sibata, S., Hayashi, C., Kumagai, H.	Namur-Ber		58		430–432
Strotzer, G.	Z angew Phys	10	58		207
	ref. Phys Abstr Nr. 7755	61	58		712
Thomas, E., Steenbrughe, R. v.	Vide	13	58	76	208
Winogradoff, M. I.	Namur-Ber		58		453–456
Brigoli, B., Cerrai, E., Silvestri, M.	JSI	34	57		291
Comsa, G.,	JSI	34	57	7	291/92
Musa, G.	ref. Phys Abstr Nr. 8457	60	57		772
Reich, G., Nöller, H. G.	Vac Symp Trans		57		97–99
Thomas, E.	Bull Acad Roy Belg		7. 7. 56		778
Thomas, E.	Vide	11	56	63	88–98
Alexeff, I., Peterson, E. C.	Vac Symp Trans		55		87
Swartz, J. C.	Vac Symp Trans		55		83
Varnerin, L. J.	US Dept Air Force Rep 71, F 191—R 3		55		
	ref. Vacuum	VI	56		184
Young, J. R.	JAP	27	56	8	926–928

Author	Journal	Volume	Month and Year	Issue No.	Page
Harris, D. J., Hawkins, P. O.	Nature	177	56		285/86
Bina, M. J., Alexeff, I., Sanders, R. M.	Phys Rev	98	55	1	251
Brown, E., Leck, J. H.	Brit JAP	6	55	5	161–164
Solanet, P.	Chim et Ind	74	55	1	116/17
Varnerin	JAP	26	55		782
Davis, R. H.	RSI	25	54		1193
Gurewitsch, A. M., Westendorp, W. F.	RSI	25	54		389
Schwarz, H.	RSI	25	54		924
Varadi, P. F.	Acta techn Acad Sci Hunguericae	9	54	3/4	343–353
Wagener, S.	Nature	173	54		684
Bloomer, R. N., Haine, M. E.	Vacuum	III	53	2	128–135
Foster, J. S., Lawrance, E. O., Lofgren, E. J.	RSI	24	53		388/89
Schwarz, H.	RSI	24	53		371
Ebert, H.	Gl und HVT		Jan. 52	1	
Florescu, N. A.	Invest Phys		52	1	8
Foster, J. S., Lofgren, E. J.	Vacuum	II	52		257
Reddan, M. J., Rouse, C. F.	Electronic Engng	71	52		159
Riddiford, L.	Vacuum	II	52		151

1.8 Vacuum Gauges, Control Systems

Blaha, A.	Slaboproudy Obzor	20	59	4	222–230
	ref. Phys Abstr Nr. 7853	62	59	740	751
Hiesch, E. H.	JSI	36	59	11	477
André, P.	Namur-Ber		58		290–294
Berthaud, M.	Namur-Ber		58		302–304
Bottomley, G. A.	JSI	35	58		254
Mirgel, K. H.	Namur-Ber		58		491/92
Antal, J.,	Periodica polytech	1	57	3	297–300
König, A.	Electronic Engng				
	ref. Phys Abstr Nr. 3780	61	58	727	355
Farquharson, J., Kermisch, H. A.	RSI	28	57	5	324
Klumb, H., Baum, H.	Vak Techn	6	57	2/3	29–33
Varicak, M.	Nuovo Cim	6	57		723
	ref. Phys Abstr	61	58	50	538
Kirchner, F.	Z angew Phys	8	56	10	478–481
Slack, G. A.	RSI	27	56		241

Author	Journal	Volume	Month and Year	Issue No.	Page
Leck, J. H.	Proc Inst Electronics	32	55		25–34
	ref. Vacuum publ. 1959	7/8	57/58		171
Nagahama, M., Kukihara, T.	RSI	26	55		727
Lynn, S.	RSI	27	56		368/69
Sancier, K. M., Richeson, W.	RSI	27	56		134–136
Garfunkel, M. P., Wexler, A.	RSI	25	54		170
Kenneth, R., Roach, K.	Instr and Automation	27	54	11	1792
Sugiura, Y.	J Phys Soc Japan	9	54		244–248
Williams, N. T., Johnson, J. B.	RSI	25	54		393
Reynolds, F. H.	JSI	30	53	3	92–96
Uyeda, R.,	J Phys Soc Japan	8	53		99–103
Sugiura, Y.	ref. Vak Techn	3	54	1	17
Coffin, E. K. P., Bauer, G. H.	RSI	23	52		115–118
Schwarz	ATM	7	52		
Sedding, M., Haase, G.	Z angew Phys	IV	52		105
Ziock, K.	Gl und HVT	1	52	3/4	57
Alpert, D.	RSI	22	51		370
Schopper, E., Schumacher, B.	Z Naturforschg Gasdichten Korpuskularstrahlen	6a	51		700–705
Carlton, F., Johnson, J. B.	RSI (Elektromagnetisch)	20	49		364
Gulbransen, E. A., Andrew, K. F.	IEC Neue Meßmethode	41	49	12	2762
Kersten, J. A.	Physica	14	48		567
Makinson, R. E., Treacy, P. B.	JSI	25	48		298
Mellen, G. L.	IEC	40	48		787
Child, P. G., Penfold, J.	RSI	26	55	2	235
Dobley, H. E., Atkins, D. F.	RSI	26	55	6	568–571
Starzmann, F.	Gl und HVT		52	8	162
Young, C. G., Mallard, T. M., Craig, B. M.	Canad J Technol	29	51	10	447–450
Clark, J. W., Witts, G. H.	Electronics, N. Y.	23	50		108–110
Allwood, H. J. S.	J Sci Inst Phys Ind	25	48		207
Lewis, I. A. D.	J Sci Inst Phys Ind	25	48		205
Roberts, C. C.	Product Engng		53		190

Author	Journal	Volume	Month and Year	Issue No.	Page
Jaeckel, R.	Transactions of Instruments and Measurements Conference — Svenska Teknologfören		52		227–235
Schwarz, H.	New Research Techniques in Physics		52		411
Schwarz, H.	ATM V 1342-2		51		
Steckelmacher	JSI	28	51	1	9/10
Dunoyer, L.	CR	227	48		1147
Dunoyer, L.	CR	228	49		372
Dunoyer, L.	CR	230	50		57/58
Dunoyer, L.	Vide	4	49		571
Dunoyer, L.	Vide	4	49		603
Dunoyer, L.	Vide	4	49		643
Gaffer, D. E.	Nature	174	54		756
Hurd, D. Z., Corrin, M. L.	RSI	25	54		1126
Lawrance, R. B.	Chem Engng Progr	50	54	3	155–160
Alpert, D.	JAP	24	53	7	860
Roberts, C. C., O'Hara, W. W.	Product Engng		53		190
Akobjanoff, L.	RSI	23	52		447
Riddiford, L.	Vide	7	52	39	5
Gomer, R.	J Chem Physics	19	51	8	1072/73
Monk, G. W.	RSI	19	48		485

1.8.1 Coarse vacuum gauges (see also under 1.8)

Honick, K. R.	JSI	24	51	5	140–142
	ref. Vacuum	I	51	4	322
Meakin, R.	JSI	28	51	12	372/73
	ref. Vacuum	II	52	2	79
	Bestimmung der Hg-Niveaus in Metallmanometern				

1.8.1.1 Pointer vacuum gauges (spring-loaded pressure gauges)

Drawin, H. W.	Namur-Ber		58		274–284
Drawin, H. W.	Vak Techn	7	58	8	177–185
Kramer, A. G., Platzmann, P. M.	RSI	29	58	10	897/98
Opstelten, J. J., Warmoltz, N.	Namur-Ber		58		295–298
Crompton, R. W., Elford, M. T.	JSI	34	57		405–407
De Crescente, M., Sanz, G. S.	RSI	28	57	6	468
Millazzo, G.	Z Elektrochem	60	56		185–188
Rogers, M. T., Malik, J. G., Bradford, H.	RSI	26	55	7	730

Author	Journal	Volume	Month and Year	Issue No.	Page
Warmoltz, N.,	Appl Sci Res Sect B	4	55		329–336
Opstelten, J. J.					
Baxter, I. G.	JSI	30	53		358–360
Baxter, I. G.	JSI	30	53		456/57
Cook, D. B.,	JSI	30	53		238/240
Danby, C. J.					
Lorant, M.	Electronic Engng	24	53		80/81
	ref. Vak Techn		55	6/7	137
Perls, T. A.,	News Bull NBS	37	53	9	140–142
Kaechele, W. H.,	ref. Vacuum	III	53	2	192
Goalwin, D. S.					
Pressy, D. C.	JSI	30	53		20–24
Pringle, D. H.,	RSI	24	53		877
Kidd, R. M.					
Becker, E. W.,	Z angew Phys	IV	52	1	20–22
Steel, O.	ref. Vide	8	53	43	
Alpert, D., Matland, McCombry	RSI	22	51		370
Dibelier	J Res NBS	15	51		46
Los, J. M.,	RSI	22	51		805–809
Morrison, J.					
Heavens, R.,	RSI	21	50	7	596–598
La Gow, H.,					
Kroll, R.					
Hett, J. H.,	RSI	21	50		150–153
King, R. W.					
Nisbeth, J. S.	JSI	26	49	8	620
	ref. Vide	5	50	30	

1.8.1.2 Liquid level vacuum gauges

Zigman, P.	RSI	30	59	11	1060–1062
Bottomley, G. A.	JSI	35	58		254-257
	ref. Vacuum	IX	59		159
Nester, R. G.	RSI	28	57	7	577
Ross, S. M.	RSI	27	56		409
	ref. Vacuum	VI	56		241
Sancier, K. M.,	RSI	27	56		134–136
Rickeson, W.	ref. Vacuum	VI	56		241
Camburian, A.	Chim et Ind	73	55		541/42
Engel, L.,	Regelungstechnik	1	53	11	264
Lechner, H.	ref. Vak Techn	3	54	2	43
Handley, L. R.	RSI	25	54		94
Nester, R. G.	RSI	25	54	11	1136/37
Ayer, I. I.	RSI	21	50		496
Laternser, A.	US-Pat 2564116		19. 3. 47/ 14. 8. 51		

Author	Journal	Volume	Month and Year	Issue No.	Page
1.8.1.3 Compression vacuum gauges					
Buch, S., Voigt, W.	Vak Techn	8	59		189–193
Bültemann, H. J.	Vak Techn	8	59	4	104–108
Jansen, C. G. J., Venema, A.	Vacuum	IX	59	3/4	219–229
Haase, G.	Chemische Technik Beiblatt Glas-Apparate-Technik	10	59		37–39
Cochran, C. N.	RSI	29	58		69/70
	ref. Vacuum publ. 1959	7/8	57/58		169
Florescu, N. A.	RSI	29	58		528/29
	ref. Vacuum publ. 1959	7/8	57/58		169
Ebert, H.	Namur-Ber		58		260–262
Goto, M.	Namur-Ber		58		266–270
Griffith, L. J.	Namur-Ber		58		263–265
Groszkowski, J.	Namur-Ber		58		288/89
Barnard, J. A.	JSI	34	57		511
Ishii, H.	J Jap Vac Soc	7	57		113–120
	ref. Vacuum publ. 1959	7/8	57/58		169
Moser, H., Poltz, H.	Z Instrumentenkunde	65	57	3	43–46
Lott, P.	Analyt Chem	28	56		276/77
	ref. Vacuum	VI	56		240
Wyllie, H. A.	JSI	33	56		317
	ref Vacuum	VI	56		240
Reynolds, M. B.	J Chem Educat	32	55		621
	ref. Vacuum	VI	56		240
Hartel, W.	Z VDI Feststellen von Wasserdampf in Vakuumbehältern	95	56	7	215–218
Bradley, R. S.	JSI	31	54		129
Flossdorf, W.	Instr et Automation	27	54		1795/96
Sveo, H. J., Gibbs, D. S.	RSI	24	53	3	302
Gould, F. A., Wickers, T.	JSI Kapillardepression	29	52		85
Kenty, C.	RSI	23	52		217/18
Mielenz, K. D.	Gl und HVT	1	52	7	139
Thom, H. G.	Gl und HVT	1	52	8	159
Axelbank, A.	RSI	21	50		511
Grosskowski	Vide	4	49		668
1.8.2. Fine vacuum gauges (see also under 1.8)					
1.8.2.1 Vacuum measuring by discharge (high frequency vacuum tester)					
Haefer, R.	Acta Phys Austr	IX	55	3/4	200–215
Burger, A.	Exp Techn Phys	2	54	1	38/39

1.8.2.2 Alphatron

Author	Journal	Volume	Month and Year	Issue No.	Page
Akishin, A. I.	Pribory i Tekh Eksper		59	2	78–80
	ref. Phys Abstr Nr. 9313	62	59	741	891
Sibley, C. B.	Electronics, N. Y.	26	53		176/77
	ref. Vak Techn	4	55		137
Cousisine, D. M.	Chem Engng	59	52		162–172
Tunnicliff, P. R., Ward, A. G.	Proc Phys Soc	65	52		233
Gimenez, G.,	J Phys Radium	12	51		64A
Labeyrie, J.	ref. Vide	7	Nov. 52		
Steckelmacher, W.	JSI	21	50		195
Mellen, G. L., Glenn, L.	IEC	40	48		787

1.8.2.3 Compression vacuum gauges after Mc Leod (see also under 1.8.1.3)

1.8.2.4 Heat conductivity gauges

Author	Journal	Volume	Month and Year	Issue No.	Page
Praxmayer, W.	Nachrichtentechnik	7	57	2	61–65
	ref. Phys Abstr Nr. 7660	60	57		699
Hamilton, A. R.	Vac Symp Trans		57		112–114
Hamilton, A. R.	RSI	28	57		693/94
	ref. Vacuum publ. 1959	7/8	57/58		172
Leck, J. H.,	RSI	28	57		119–121
Martin, C. S.	ref. Vacuum publ. 1959	7/8	57/58		126
McMillan, J.,	RSI	28	57		881/82
Buch, T.	ref. Vacuum publ. 1959	7/8	57/58		172
Ubisch, H. v.	Vak Techn	6	57	8	175–181
Schwarz, H.	ATM 1341 — 3. Lieferung	192	52		
Wirth, H.,	Monatsh	83	52		879–882
Klemenc, A.	ref. Vacuum	III	53	1	102
Peck, R. E., Fagan, W. S.	Trans Amer Soc Mech Engrs	73	51		281–287
Ubisch, H. v.	Appl Sci Res	A 2	51		364–403

1.8.2.4.1 Vacuum gauges after Pirani

Author	Journal	Volume	Month and Year	Issue No.	Page
Smith, A. W.	RSI	30	59		485
Veis, S.	Vacuum	IX	59	3/4	186–189
Leck, J. H.	JSI	35	58		107
	ref. Vacuum publ. 1959	7/8	57/58		171
Leck, J. H.,	JSI	33	56		181–183
Martin, C. S.	ref. Vacuum	VI	56		242
Morgan, P. G.	Electr J	156	56		1999–2000
	ref. Vacuum	VI	56		241
Marsden, D. G. H.	RSI	26	55		1205
Ubisch, H. v.	Analyt Chem	24	52		931
Litting, C. N. W.	JSI	32	55	3	91/92
Leck, J. H.	JSI	31	54		226

Author	Journal	Volume	Month and Year	Issue No.	Page
Mielenz, K. D.	Z angew Phys bis zu Drücken von 1,7 · 10^{-5}	VI	54	3	101-104
Auwärter, M.	Brit Pat 692232				
	ref. Vacuum	III	53	3	320
Dardel, G. von	JSI	30	53	4	114–117
Pilny, M. J.	NACA-Rep Nr. TN 2946		53		
	ref. Vacuum	III	53	3	
Reynolds, F. H.	JSI	30	53		92
Glockler, G., Ven Horst, H.	Science	116	52		364–367
Gruber, H.	Gl und HVT	1	52	15/16	302
Leck, J. H.	JSI	29	52		258
Brown, D. R. H., Chasmar, R. P., Fellgatt, P. B.	JSI	28	51	6	195
Blasco, E., Miranda, L.	RSI	21	50		494
Blears, J.	Brit JAP	1	50		301
Spears, L.,	Brit JAP	1	50		132/33
Jolly, W. P.	ref. Vacuum	I	51	1	
Ubisch, H. v.	Arkiv För Mathematik, Astronomi Och Physik K Svenska Vetenskapsakademien	34A	46	14	
Ubisch, H. v.	Arkiv För Mathematik, Astronomi Och Physik K Svenska Vetenskapsakademien	35A	47	28	
Ubisch, H. v.	Arkiv För Mathematik, Astronomi Och Physik K Svenska Vetenskapsakademien	36A	48	4	

1.8.2.4.2 Thermoelectric vacuum gauges

Author	Journal	Volume	Month and Year	Issue No.	Page
Rivera, M. P., Leriche, R. P.	Vac Symp Trans		58		118–122
Schlitt, H.	Z angew Phys	8	56	5	216/17
	ref. Vacuum	VI	56		242
Degras, D. A.	Vide	7	52	38	1153
Florescu, N. A.	JSI	29	52		298
Pupp, W.	Gl und HVT	1	52	3/4	66

1.8.2.4.3 Semiconductor vacuum gauges (thermistors)

Author	Journal	Volume	Month and Year	Issue No.	Page
Degras, D. A., Andrieux, P.	Vide	14	59	80	45–58
Varicak, M., Saftic, B.	RSI	30	59		891
Varicak, M., Saftic, B.	Namur-Ber		58		285–287
Seiden, P. E.	RSI	28	57		657/58
	ref. Vacuum publ. 1959	7/8	57/58		172

Author	Journal	Volume	Month and Year	Issue No.	Page
Varicak, M.	CR	243	56		893–895
	ref. Vacuum	VI	56		242
Lortie, J.	J Phys Radium	16	55	4	317–320
	ref. Phys Abstr	58	55		876

1.8.2.5 Viscosity vacuum gauges

Author	Journal	Volume	Month and Year	Issue No.	Page
Anderson, J. R.	RSI	29	58	12	1073–1078
	ref. Vacuum	IX	59	3/4	239
Heiligenbrunner, O.	Vak Techn	5	56	7	133–139
Klumb, H., Kollmannsberger	Gl und HVT	2	53	11	211–213
Klumb, H., Heiligenbrunner, O.	Gl und HVT	2	53	13	269–271
Heiligenbrunner, O.	Gl und HVT	1	52	8	162
Schwarz, H.	ATM V 1341 — 4. Lieferung	194	52		
Eberhard, E., Kern, H., Klumb, H.	Z angew Phys	III	51		209–211
Kohler, M.	Z Phys	125	49		715

1.8.3 High vacuum gauges (see also under 1.8)

1.8.3.1 Vacuum gauges after Penning

Author	Journal	Volume	Month and Year	Issue No.	Page
Conn, G. K. T.	Vacuum publ 1959	7/8	57/58		72–79
Redhead, P. A.	Canad J Phys	37	59	11	1260–1271
Grigoriev, A. M.	Namur-Ber		58		308–310
Paty, L.	Czech J Phys	7	57	1	113
	ref. Phys Abstr Nr. 7851	62	59		751
Leck, J. H.,	Brit JAP	7	56		153–155
Riddoch, A.	ref. Vacuum	VI	56		243
Moesta, H.	Z angew Phys	8	56		598–603
Dumas, G.	Rev gen Electr	65	55	7	331–350
Haefer, R.	Acta Phys Austr	9	55	3/4	200–215
Varicak, M., Vosicki, B.	JSI	32	55		346
Beer, O.	Vak Techn	3	54	1	15
Conn, G. K. T., Daglish, H. N.	JSI	31	54		433
Phillips, K.	JSI	31	54	3	110/11
	ref. Vide	10	55	55	408
	ref. Vak Techn	4	55	6/7	138
Varicak, M., Vosicki, B., Saftic, B.	Period math phys astr Zagreb	10	55	1/2	89–96
Bobenried, A.	Vide	8	53		1302–1304
Conn, G. K. T., Daglish, H. N.	Vacuum	III	53	1	24–34

Author	Journal	Volume	Month and Year	Issue No.	Page
Haefer, R.	Acta Phys Austr	7	53	1	52–90
Haefer, R.	Acta Phys Austr	7	53	3	251–277
Leck, J. H., Brown, E.	JSI	30	53	8	271–274
Bergmann, W. H.	Acta Phys Austr	5	52		415
Vermonde, J.	Vide	7	52		1145–1152
Evans, E., Burmaster, K. E.	Proc Inst Radio Engrs N.Y.	38	50		69–75
Leduc, P.	Vide	4	49		684

1.8.3.2 Ionization vacuum gauges

Author	Journal	Volume	Month and Year	Issue No.	Page
Benton, H. B.	RSI	30	59		887
Opitz, P., Schneider, F., Voisichi, B.	Vak Techn	8	59		171
Penchko, E. A.,	Pribory i Tekh Eksper		59	1	128/29
Khavkin, L. P.	ref. Phys Abstr Nr. 7854	62	59	740	751
Robinson, N. W., Berz, F.	Vacuum	IX	59	1	48–53
Habanec, J.	Slaboproudy Obzor	19	58	3	140
	ref. Phys Abstr Nr. 3781	61	58		355
Henry, R. P.	Namur-Ber		58		299–301
Kobayashi, S.	Namur-Ber		58		271–273
E. Leybold's Nachf.	Chem Ing Techn	30	58		364
Robinson, N. W., Berz, F.	Namur-Ber		58		378–383
Hall, L. D.	RSI	28	57	8	653/54
Ishii, H.,	J Jap Vac Soc	7	57		176–188
Nakayama, K.	ref. Vacuum publ. 1959	7/8	57/58		172
Moesta, H., Renn, R.	Vak Techn	6	57	2/3	35
Okamoto, H.	Proc Jap Vac Soc	7	57		71–89
	ref. Vacuum publ. 1959	7/8	57/58		172
Reece, M. P.	JSI	34	57		513
Schulz, G. J.,	RSI	28	57		1051–1054
Phelps, A. V.	ref. Vacuum publ. 1959	7/8	57/58		172
Schutten, J.	Appl Sci Res Sect B	6	57		276–284
Beynon, J. H.,	JSI	33	56		376–380
Nicholson, G. R.	ref. Vacuum publ. 1959	7/8	57/58		173
Harikaran, P.,	JSI	33	56	12	488–491
Bhalla, M. S.	ref. Phys Abstr Nr. 3387	60	57		314
Henry, R. P.	Vide	11	56		54–63
	ref. Vacuum	VI	56		242
Khavkin, L. P.	Zk tekh Fiz	26	56	10	2356–2360
	ref. Phys Abstr Nr. 4026	60	57	713	372
Young, J. R.	JAP	27	56		926
Bouwmeester, E.,	Phil Techn Rev	17	55		121–125
Warmoltz, N.	ref. Vacuum	VI	56		243
Peters, I. L.	Vac Symp Trans		55		71

Author	Journal	Volume	Month and Year	Issue No.	Page
Varnerin, L. J., Carmichael, J. H.	JAP	26	55		782
Ainsworth, J., La Gow, H. E.	RSI	27	56	8	653
Leck, J. H., Riddoch, A.	Brit JAP	7	56	4	153–155
Peters, J. L.	Vak Techn	5	56		65–69
Boillinger, L. E.	Instr and Automation	28	55	9	1507
Bouwmeester, F.	Philips techn Rdsch	17	55	3	107–112
Raible, R. W., Testermann, M. R.	Electronics, N. Y.	28	55		210–218
Hiby, J. W., Pahl, M.	Z Naturforschg	9a	54	10	906/07
Conn, G. K. T., Daglish, H. N.	JSI	31	54		412–416
Murata, S.	J Inst Electr Comm Engrs Japan	37	54		865–870
	ref. Phys Abstr		55		705
Redhead, R. A., MacNarry, L. R.	Canad J Phys	32	54		167–174
Reynolds, J. H., Lipson, J.	RSI	25	54		1029
Riddiford, L.	JSI	31	54	3	111
Varnerin, L. D., White, D.	JAP Gasaufzehrung	25	54	9	207
Versnel, A., Jonker, J. L. H.	Phil Res Rep	9	54	6	458/59
Auwärter, M.	Brit Pat 692232				
	ref. Vacuum	III	53	3	320
Branson, S. M.	Instr Practice	7	53		425
Dardel, G. von	JSI	30	53		114–117
Dobke, G., Schröder, B.	Gl und HVT	2	53	14	285–292
Fitz, F. J.	Canad J Phys	31	53	1	111–114
	ref. Vacuum	III	53	2	193
Stinnet, A. J.	RSI	24	53		985
Burrows, J. H., Mitchel, E. W.	JSI	29	52	1	27/28
Hibbert, F. H.	JSI	29	52		280
Pupp, W.	Gl und HVT	1	52	1	13
Redhead, P. A.	NRC Canada Rep ERB	275	52		
	ref. Vacuum	III	53	1	81
Sibata, H., Tuzi, Y., Kumagai, H.	RSI	23	52		54/55
Tsukakshi, O.	J Sci Inst Japan	46			247–254
Valle, G.	Nuovo Cim	9	52		145
Weinreich, O. A., Bleecher, H.	RSI	23	52		56

Author	Journal	Volume	Month and Year	Issue No.	Page
Bashkin, S.	US-Pat 2548283				
Biondi, M. A.	Westinghouse Res· Lab Sci Paper Pittburgh		51		1579
Goldschwarz, J.M.	Vide	6	51	31	955/56
Riddiford, L.	JSI	28	51		375–379
	ref. Vide	7	52		
Warmoltz, N.	Appl Sci Res Sect B	2	51		273–276
Washburn, H. W.,	US-Pat 2406419				
Wily, H. (CEC)	ref. Vacuum	I	51	2	
Filosofo, L., Merlin, M., Rostagni, A.	Nuovo Cim	7	50		69–75
Kelly, F. M.	RSI	21	50		673
Lander, J. S.	RSI	21	50		672
Metson, G. H.	Brit JAP	1	50		73–77
	ref. Vacuum	I	51	1	66
Valle, G.	Nuovo Cim	7	50		174
Milner, C. J., Watt, I. M.	JSI	26	49		159
Apker, L. R.	IEC	40	48		846/47
Brisbane, A. D.	Vacuum	II	52	2	
Beck, A. H.	Vide	9	54	49	1454–1461
Hariharan, P., Bhalla, M. S.	RSI	27	56	7	448/49

1.8.3.3 Radiometer vacuum gauges

Author	Journal	Volume	Month and Year	Issue No.	Page
Bailleul-Langlais, J.	Vide	14	59	80	59
Klumb, H.,	Vak Techn	7	58		133–135
Fuchs, D.	ref. Vacuum	IX	59	3/4	239
Biette, A.	Vide	13	58	76	211
Vanderschmidt, G.F., Simons, J.C.	Namur-Ber		58		305–307
Kiefer, H., Ziegler, B.	Z angew Phys	VII	55		48
Weissmann, E.	Vak Techn	4	55	8	152–155
Klumb, H., Weissmann, E.	Gl und HVT	2	53	12/13	266–269
Mielenz, K. D., Schönheit, E.	Z angew Phys	III	53		90–94
Jensen, H. G.	Vacuum	II	52	4	388/89
Weissmann, E.	Gl und HVT	1	52	8	160
Witman, C. I.	J Chem Physics	20	52		161–163
	ref. Vacuum	II	52		188
Steckelmacher, W.	Vacuum	I	51	4	166–182
Assmussen, R. W., Bushman-Olsen, B.	Trans Danish Acad Techn Sci		48	5	

Author	Journal	Volume	Month and Year	Issue No.	Page
Meers, J. T.,	Phys Rev	74	48		119
Parduis, L. A.					
Blears, J.	Brit Pat 664788				
Steckelmacher,W.	Brit Pat 630885				
	ref. Vacuum	I	51	1	49

1.9 Partial Pressure Measuring Instruments

Author	Journal	Volume	Month and Year	Issue No.	Page
Kaljabin, I. A.,	Vacuum	IX	59		117
Yukhvidin, Y. A.					
Tretner, W.	Z angew Phys	11	59		395
Amoignon, J.,	Vide	12	57		377
Rommel, G.	ref. Phys Abstr Nr. 2867	61	58		274
Bishop, J.	Namur-Ber		58		484–490
Diels, K.,	Vac Symp Trans		58		115–117
Moesta, H.					
Garbe, S.	Namur-Ber		58		404–409
Hintenberger, H.,	Vak Techn	7	58	5	121–130
Dörnenburg, E.					
Hintenberger, H.,	Vak Techn	7	58	7	159–171
Dörnenburg, E.	ref. Vacuum	IX	59	3/4	241
Johnson, C. Y.	JAP	29	58		740
Kaljabin, I.,	Namur-Ber		58		418–426
Yukhvidin, Y. A.					
Klopfer, A.	Namur-Ber		58		397–400
McNarry, L. R.	Canad J Phys	36	58		1710
Paul, W.,	Z Phys	152	58		143–182
Reinhard, H. P.,					
Zahn, U. v.					
Schütze, H. J.,	Namur-Ber		58		125–133
Varadi, P. F.					
Varadi, P. F.,	Vak Techn	7	58	1	13–16
Sebestyen, L. G.,					
Rieger, E.					
Varadi, P. F.,	Vak Techn	7	58	2/3	46–51
Sebestyen, L. G.,					
Rieger, E.					
Peper, J.	Phil Tech Rev	19	57/58	7/8	218–220
	ref. Vacuum publ. 1959	7/8	57/58		179
Edwards, A. G.	Research	10	57		288/89
	ref. Vacuum publ. 1959	7/8	57/58		180
Falk, G.,	Vak Techn	6	57	2/3	34
Schwering, F.					
Gutbier	Z Naturforschg	12a	57	6	
Perkins, G. D.,	Vac Symp Trans		57		125–128
Charpentier, D. E.					
Wagener, J. S.,	JAP	28	57	9	1027
Marth, P. T.					

Author	Journal	Volume	Month and Year	Issue No.	Page
Edwards, A. G.	Vacuum	V	55		93–108
Roberts, R. H.,	AEC-Rep Nr. AECD-3149		55		
Earnshaw, K. B.	ref. Vacuum	VI	56		257
Wiley, W. C., McLaren, I. H.	RSI	26	55	12	1150–1157
Wherry, T. C., Karazek, F. W.	JAP	26	55		682
Brubaker, W. M., Perkins, G. D.	RSI	27	56		720
Cannon, W. W., Testermann, M. K.	JAP	27	56		1283
Reynolds, J. H.	RSI	27	56		928–934
Robinson, C. F.	RSI	27	56		88/89
	ref. Vacuum	VI	56		244
Woodford, H. J., Gardner, J. H.	RSI	27	56		378
Bennet. W. H.	JAP	21	50	2	143–149

1.10 Leaks and Leak Detectors

Drawin, H. W., Kronberger, K.	Vak Techn	8	59		128–137
Drawin, H. W.	Vak Techn	8	59	8	215–219
Paty, L.	Vacuum publ. 1959	7/8	57/58		80–86
Thiel, A.	Atomenergie	4	59	2	75–80
Botden, Th. P. J.	Namur-Ber		58		241–244
Briggs, W. E., Jones, A. C., Roberts, J. A.	Vac Symp Trans		58		129–136
Choumoff, S.	Vide	13	58	76	193
Choumoff, S., Laplume, J.	Namur-Ber		58		133–140
Ehlers, K. W.	RSI	29	58		72
	ref. Vacuum publ. 1959	7/8	57/58		110
Glueckauf, E., Kitt, G. P.	JSI	35	58		220
Gordon, S. A.	RSI	29	58		501–504
	ref. Vacuum publ. 1959	7/8	57/58		188
Ishii, H.	Namur-Ber		58		245–247
Jean, R.	Vide	13	58	76	188
Jean, R.	Namur-Ber		58		223–228
Jenkins, R. O.	JSI	35	58		428
Kobayashi, S., Yada, H.	Namur-Ber		58		248–250
Kronberger, H.	Brit Chem Engng	3	58	7	393
Minter, C. C.	RSI	29	58	9	793
Mongodin, G.	Namur-Ber		58		229–232

Author	Journal	Volume	Month and Year	Issue No.	Page
Warnecke, R. J.	Namur-Ber		58		251–256
Warmoltz, N.	Namur-Ber		58		257–259
Work, R. H.	Vac Symp Trans		58		126–128
Biram, J. G. S.	AERE CE/R 2066		57		
Kobayashi, S.,	J Jap Vac Soc		57	7	189–196
Yada, K.	ref. Vacuum publ. 1959	7/8	57/58		188
Moody, R. F.	Vak Techn	6	57	4	80
Sack, W.	Energie	8	57		305
Schumacher, B. W.	Vak Techn	6	57	6	119
Torney, F. L.	Vac Symp Trans		57		115–119
Warmoltz, N., Grefte, H. A. M.	Vide	12	57	69	202–207
Bell, R. L.	JSI	33	56		269–272
	ref. Vacuum	VI	56		258
Leuwen, J. A. v., Oskam, H. J.	RSI	27	56	5	328
Niviere, P.	Genie Chimique	75	56		122/23
	ref. Vacuum	VI	56		188
Verkamp, J. P.,	Nucleonics	14	56		54–57
Williams, S. L.	ref. Vacuum	VI	56		187
Varadi, P. F.,	JSI	33	56		392/93
Sebestyen, L. G.	ref. Vacuum publ. 1959	7/8	57/58		193
Varicak, M.	RSI	27	56		655
	ref. Vacuum	VI	56		259
Levina, L. E.	Uspekhi Fizicheskikh Nauk	55	55	1	101–110
	ref. Vacuum	VI	56		187
Jakobs, R. B.	Ind Engng Chem	40	48		791–794
Neck, H.	Bull schweiz elektrotechn Ver	46	55	8	392/93
Reiss, K. H.	Z angew Phys	VII	55	9	473
Benson, F. A., Seaman, M. S.	Electronic Engng		55		360
Leyer, E. C.	Canad J Technol	32	54	6	199–205
Lindberg, D. A.	Electronic Engng	26	54		436–440
White, W. C.	Electronic Engng		54		806
Alars, G. A., Jakobs, J. A., Malmberg, P. R.	RSI	24	53	5	399–400
Babelay, E. F., Smith, L. A.	RSI	24	53		508
Blommer, R. N., Heine, M. E.	JSI Ventil	30	53	10	385/86
Forman, R.	RSI (Ventil)	24	53	4	326/27
Gassignoll, C. H., Geller, R., Norceau, J.	Vide Spektrometer	8	53	48	1415–1421
Gemant, A.	JAP	24	53		93
Harrison, E. R.	JSI	30	53		170/71

Author	Journal	Volume	Month and Year	Issue No.	Page
Lecomte, J., Taieb, J., Thebault, J.	Vide	8	53	48	1422–1427
Morrison, J.	RSI	24	53		230/31
	ref. Vacuum	III	53	2	176
Ochert, N., Steckelmacher, W., Reiss, T. H.	Vacuum	III	53	2	125–136
Stinnet, A. J.	RSI	24	53	9	883/84
Weber, A.	Gl und HVT	2	53	7	216
Ziock, K.	Phys Verh	4	53	7	216
Leck, J. H.	Vacuum	II	52	4	382
Nief, G.	Brit JAP	3	52	1	29
Ochert, N.	Vacuum	II	52	2	125–136
Kloepper, F. H., Seagondollar, L. W., Smith, R. K.	RSI	23	52		245
Stern, L. E.	Automat Industr	107	52		52
Ubisch, H. v.	Analyt Chem	24	52		931
Leck, J. H.	Brit JAP	3	52		227–232
Hutton, J. G., Usher, T. E.	Gen Electr Rev	54	51		18–23
Jenkins, W.	RSI	22	51		845
	ref. Vacuum	II	52	1	66
Martin, S. L.	IEC	32	51		221–229
Ochert, N., Steckelmacher, W.	Brit JAP	2	51		332/33
	ref. Vacuum	II	52	2	186
Reinders, M. E., Schutten, J., Kistemaker, J.	Appl Sci Res	B2	51		66–70
Riddiford, L., Coe, R. F.	JSI	28	51	11	352/53
	ref. Vide	7	52	38	
Romand, J., Schwetzoff, V., Vodar, B.	Vide	6	51	34/35	1046–1051
Ubisch, H. v.	Appl Sci Res	A2	51		429
Volker, E.	Z Naturforschg	6a	51	9	512/13
Warmoltz, N.	Appl Sci Res	B2	51		429
Deutsch, Z. G., Raible, F.	Chem Engng	27	50	4	279–284
Guthrie, A.	Electronics, N. Y.	23	50		96–101
Hagstrum, A. G., Weinhart, H. W.	RSI	21	50	4	394
Lloyd, J. T.	JSI	27	50		376
McFee, R. H.	RSI	21	50		100/01
Penning, F. M., Nienhuis, K.	Phil Tech Rev	11	49		116–122
Saxon, D., Richards, J.	RSI	20	49	10	

1.11 Ultra-high Vacuum Technology

Author	Journal	Volume	Month and Year	Issue No.	Page
Alpert, D.	Vacuum	IX	59	2	89
Munday, G. L.	Nucl Instr Methods		59	4	367–375
Yarwood, J.	JSI	34	57		297–304
	ref. Vacuum publ. 1959	7/8	57/58		107
Alpert, D.	Namur-Ber	I	58		31–38
Diels, K.	Namur-Ber	I	58		90–92
Florescu, N. A.	Namur-Ber	I	58		367–372
Schweitzer, J.	Vide	14	59	82	165–182
Yarwood, J.	JSI	34	57	8	297–304
	ref. Phys Abstr		57	9036	828
Simon, H.	Exp Techn Phys	4	56	1	8–26
Alpert, D.	Science	122	55		729–733
	ref. Vacuum	VI	56		185

1.11.2 Measuring of pressures

Müller, K. G.	Vide	14	59	82	250–259
Redhead, P. A.	Namur-Ber	I	58		410–413
Schutten, J.	Namur-Ber	I	58		414–417

1.11.2.1 Measuring of pressures with Bayard-Alpert tube

Carter, G., **Leck**, J. H.	Brit JAP	10	59		364
Gavriluk, V. M.	Pribory i Tekh Eksper	2	59	83	
Kucherov, Y. M.	ref. Phys Abstr	62	59	9314	
Mizushima, Y., **Oda**, Z.	RSI	30	59	12	1037–1041
Schulz, G. J.	JAP	28	57		1149–1152
	ref. Vacuum publ. 1959	7/8	57/58		172
Allenden, D.	Vide	13	58	77	247

1.11.2.2 Measuring of pressures with magnetron vacuum gauge

Hobson, J. P., **Redhead**, P. A.	Canad J Phys	36	58	3	271–288

1.11.2.3 Flash-filament method

Baker, F. A., **Yarwood**, J.	Vak Techn	6	57	7	147

1.11.3 Production of ultra-high vacuum

Redhead, P. A., **Kornelsen**, E. V.	Vak Techn.	10	61	2	31–39
Nöller, H. G., **Reich**, G., **Bächler**, W.	Vac Symp Trans		60		72–74

Author	Journal	Volume	Month and Year	Issue No.	Page
Moll, J., Ehlers, H.	Z angew Phys	12	60		324–328
Mongodin, G.	Vide	14	59	80	95
Trendelenburg, E. A.	Vide	14	59	80	74
Venema, A.	Vacuum	IX	59	1	54–57
Venema, A., Bandringa, M.	Philips techn Rdsch	20	59	6	153–160
Hall, L. D.	RSI	29	58		367–370
	ref. Vacuum publ. 1959	7/8	57/58		165
Hall, L. D.	Vac Symp Trans		58		158–163
Hobson, J. P., Redhead, P. A.	Namur-Ber (Glas)		58		384–388
Milleron, N.	Vac Symp Trans		58		140–147
Redhead, P. A.	Vac Symp Trans		58		148–152
Venema, A.	Namur-Ber		58		389–392
Reich, G., Nöller, H. G.	Vac Symp Trans		57		97–99

1.11.3.3 Adsorption traps

Biondi, M. A.	RSI	30	59		831
Carmichael, J. H., Lange, W. J.	Vac Symp Trans		58		137–139
Mickelsen, W. R., Childs, J. H.	RSI	29	Oct. 58		871–873
Venema, A.	Namur-Ber		58		389–392
Grove, D. J.	AEC Res Dev Rep Proj Matterhorn Tech Memo NYO-7883	40	57		

1.11.3.4 Getters

Milleron, N., Popp, E. C.	Vac Symp Trans		59		153–159

1.11.3.5 Deep-freeze processes (cryopumps)

Klipping, G., Mascher, W.	Vak Techn	11	62	3	81–85
Klipping, G.	Kältetechnik	13	61		250–252
Caswell, H. L.	RSI	30	59		1054
—	Franklin Inst	267	59		97/98
	ref. Vacuum	IX	59	3/4	234
Bailey, B. M., Chuan, R. L.	Vac Symp Trans		58		262–267
Bailey, B. M.	Chem Engng News	36	58	45	60–62
Little, A. D.	Chem Engng	65	58	26	30

Author	Journal	Volume	Month and Year	Issue No.	Page
Lasarew, B. G., Borowik, E. S., Fedorowa, N. M., Zin, N. M.	UPN	2	57		175

1.11.4 Assembly parts

1.11.4.1 Flange connections

Boulloud, J. P., Schweitzer, J.	Vide	14	59	82	241–249
Henry, R. P., Blaive, J. C.	Namur-Ber		58		345–348

1.11.4.2 Valves

Axelrod, N. N.	RSI	30	59		944/45
Carmichael, J. H., Trendelenburg, E. A.	RSI	30	59		494
Lange, W. J.	RSI	30	59		602
Paty, L.,	RSI	28	57		654/55
Schürer, P.	ref. Vacuum publ. 1959	7/8	57/58		111
Vogl, T. P.,	RSI	27	56		657
Evans, H. D.	ref. Vacuum	VI	56		254
Bills, D. G., Allen, F. G.	RSI	26	55		654–656

1.11.4.3 Inspection windows

Roberts, V.	JSI	36	59	36	99
Greenblatt, M. H.	RSI	29	58	8	738
Hauser, V., Kerler, W.	RSI	29	58	5	380
Strad, A. R.	RSI	29	58		533
	ref. Vacuum publ. 1959	7/8	57/58		191
Sterzer, F.	RSI	28	57		208/09
	ref. Vacuum publ. 1959	7/8	57/58		191
Perry, J. T.	RSI	27	56		759–762
	ref. Vacuum	VI	56		256
Koops, R., Zeiss, C.	German Pat Appl No. Z 4921 V 1/48 b				
	ref. Vacuum	VI	56		256

2.1 Vacuum Accessories

Warmoltz, N., Bouwmeester, E.	Philips techn Rdsch	21	59/60	6	170–175
Sloan, L. G.	RSI	27	56	12	1019–1021
	ref. Vacuum publ. 1959	7/8	57/58		118
Wyllie, H. A.	JSI	33	56		360

Author	Journal	Volume	Month and Year	Issue No.	Page
2.1.1 Pipelines					
Henry, R. P.	Namur-Ber		58		349–352
Pollard, J.	JSI	30	53	1	25/26
Reichard, H. F.	Chem Engng	59	Jan. 52		161
	ref. Vacuum	II	April 52	2	186
2.1.2 Rigid connections					
Brymner, R., Steckelmacher, W.	JSI	36	59		278
Gaunt, A. J., Redford, R. A.	JSI	36	59		377
Green, L. A., Miles, H. T., Richardson, A. C.	JSI	36	59		324
Moore, H. R.	RSI	29	58	8	737/38
Adam, H. A.,	JSI	34	57		123/24
Kaufman, S., Liley, B. S.	ref. Vacuum publ. 1959	7/8	57/58		190
Drowart, J., Goldfinger, R., Steenwinkel, R. van	JSI	34	57		248
Foote, T.,	RSI	28	57		585/586
Harrington, D. B.	ref. Vacuum publ. 1959	7/8	57/58		189
Gore, G. W.	JSI	34	57		459
Yonts, O. C., Morgan, H. W.	RSI	26	55	6	619/20
Pattee, H. H. jr.	Phys Rev	98	55	1	283
Adam, H.	Trans Soc Glas Technol	38	54		285–296
Brannen, E., Ferguson, H. I. S.	RSI	25	Aug. 54		836/37
Lee, F. R. N., Young	JSI	31	54	2	70
McKnight, W. H.	Material and Methods		Oct. 54		94
Nester, R. G.	RSI	25	Jan. 54	1	95
Pattee, H. H. jr.	RSI	25	54	11	1132/33
Rawson, H., Renton, E. P.	Brit JAP	5	Oct. 54		352
Elson, L.	JSI	30	53		140
Duesing, W.	Telefunkenztg	26	March 53		110–120
Duesing, W.	Glastechn Ber		Aug. 53		232–238
Garbe, H. W.	Amer Mach N. Y.	97	6. 3. 53	6	131–135
Herrmann, H.	Gl und HVT	2	June 53	10	189–200
Kent, P. J. O.	JSI	30	53	12	485
Schriever, W. W.	RSI	24	May 53	5	402/03
	ref. Vide	9	54	49	1470

Author	Journal	Volume	Month and Year	Issue No.	Page
HAYWARD, A. G.	Vacuum	II	52	2	262–264
—	Amer Export Ind.	149	Aug. 51		31
	ref. Vacuum	I	51	4	341
DVOREK, H. R., LITTLE, R. N.	RSI	22	51		1027/28
KARMAUS	Glas-Email-Keramotechn		May 51	5	
STROHTER, F. B., GRANBERRY, H.	RSI	22	June 51		432
ECKSTEIN, N. A.,	RSI	21	April 50	4	398/99
FITZGERALD, J. W., BOYD, C. A.	ref. Vacuum	I	Jan. 51	1	67
STANWORTH, J. E.	JSI	27	Oct. 50		282–284

2.1.3 Flexible connections

(a) elastic joints

KERNER	Z angew Phys	V	53	5	168
	ref. Vide	10	55	55	404
FREMLIN	JSI	29	52		267
SANCIER, K. M.	RSI	20	49	12	958

(b) other flexible joints

FRENCH, E. P.	Nucleonics	10	March 52		66
NEWTON, A.	ref. Vacuum	II	52	2	186
HAYWARD	JSI	29	52	12	410
KNUDSEN, A. W.	RSI	23	Oct. 52	10	566/67
MCCUISTION, T. J.	India Rubber World	125	52		575
NORBURY, J.	JSI	29	52	6	204
SMITH, J. R. W.	JSI	29	52	4	131
GARROD, J. R.	JSI	28	51	6	187
RETZLOFF, O.	RSI	20	April 49	4	324
GARROD, J. R.	JSI	25	48		378–383
GARROD, J. R.	JSI	26	49		279

2.1.4 Valves

(a) miscellaneous valves

GOROWITZ, B., MOSES, K., GLOERSEN, P.	RSI	31	60	2	146–148
LAMB, W. R., RHOADS, F. A., APPLEBAUM, P. S.	Vacuum	IX	59		147
MOREAU, J.	Vide	14	59	79	3
PRESTON, J.	JSI	36	59		98
ROBERTS, V.	JSI	36	59		99
SALMON, D.	Instr and Control Systems	32	59		1026/27
SHPIGEL, I. S.	Pribory Tekh eksper	1	59		151

Author	Journal	Volume	Month and Year	Issue No.	Page
Smith, H. A., Posey, J. C., Thomas, C. O.	RSI	30	59	3	202/03
Thiele, K.	Vak Techn	8	59	8	223–226
Almond, J.	JSI	35	58		70
Blanaru, L.	JSI	35	58		184
	ref. Vacuum publ. 1959	7/8	57/58		187
Cope, J. O.	RSI	29	58		232–234
	ref. Vacuum publ. 1959	7/8	57/58		187
Forst, J. A.	JSI	35	July 58		268
McFarland, R. H., Anderson, R., Wells, J.	RSI	29	58		529/30
Moreau, J.	Namur-Ber		58		332–334
d'Amico, C., Hagstrum, H. D.	RSI	28	57	1	60
Bottomley, G. A.	JSI	34	57		369
Fetz, H., Schiefer, K.	Z angew Phys	9	57	1	13
Franks, A.	JSI	34	57		122
Raats, E., Harley, J.	JSI	34	57		510
Toby, S.,	RSI	28	57		470/71
Kutschke, K. O.	ref. Vacuum publ. 1959	7/8	57/58		187
Barrow, C.	JSI	33	Febr. 56		83
Biddulph, R. H.,	Chem Ind		56		569
Plesch, P. H.	ref. Vacuum	VI	56		186
Block, H.	Nature	178	56		1307/08
	ref. Vacuum publ. 1959	7/8	57/58		187
Buck, H. M.	JSI	33	56		361
Haul, H. W., Swart, E. R.	JSI	33	56		243
Horseling, J.	Philips techn Rdsch	17	56	7	217–219
Moore, H. R.	JSI	33	56		282
Nestler, R. G.	RSI	27	56	10	874/75
	ref. Phys Abstr	60	57	1964	185
Wyllie, H. A.	JSI	33	56		360
Bills, D. G.	RSI	26	July 55	7	654–656
Holland, R. E., Mooring, F. P.	RSI	26	55		989
Roberts, R. H., Walsh, J. V.	RSI	26	Sept. 55	9	890
—	Chem Engng News	32	54		2972
Richards, R. J.	RSI	25	May 54	5	520/21
Stanier, H. M.	JSI	29	54		165
Stein, F. S.	RSI	25	May 54	5	515/16
Reinders, H. E., Kistemaker, J.	Appl Sci Res	B 2		1	71/72

Author	Journal	Volume	Month and Year	Issue No.	Page
Forman, R.	RSI	24	April 53	4	326/27
	ref. Vacuum	III	July 53	3	302
Harrison, E. R.	JSI	30	July 53	5	170/71
	ref. Vacuum	III	July 53	3	302
Mallet, W.	Analyt Chem	25	Jan. 53		116–119
Gerds, A. F., Griffith, G.	ref. Vacuum	III	April 53	2	209/10
Speed, F. L.	AERE-Rep Nr. ED/R 1302		53		
	ref. Vacuum	III	June 53	3	325
Stevans, C. M.	RSI	24	53	2	148–151
Yarwood, J.	Vacuum	III	53	4	398–411
Black, S., Bryson Inc.	Chem Engng	59	52	10	207
Buchman, K. C.	Analyt Chem	23	Nov. 51		1724
	ref. Vacuum	II	Jan. 52	1	82
Wahl, J. S., Forbes, C., Nyer, W. E.	RSI	23	52	7	379
Kenty, C.	RSI	22	51	11	844/45
	ref. Vide	7	52		
Riddiford, L., Lilley, H.	JSI	29	52		296
Shatford, P. A.	JSI	29	52		336
Smith, R. K.	RSI	23	52		767/68
Stanier, H. M. Beynon, J. M.	JSI	29	52		165
Yergin, P. F.	RSI	23	52		310
Jennings, B.	RSI	20	49		366
Norton, J.	RSI	20	49		620
	ref. Vide	5	50	30	
King, L. D. P.	RSI	19	48		83
Kurie, F. N. D.	RSI	19	48		585
Lockenwitz, A. E.	RSI	19	48		242
Giese, H.	Wiss Z Uni Halle math nat	II	52	9	

(b) glass valves

Author	Journal	Volume	Month and Year	Issue No.	Page
Fuller, J.	JSI	33	56		161
Sill, R. C.	RSI	27	56	8	657
Greene, St. A.	RSI	26	55	7	731
Krisliss, S. S., Asmanes, C.	RSI	26	55	7	615
Decker, R. W.	JAP	25	Nov. 54	11	1441/42
McCutchen, C. W.	RSI	25	54		1220
Holton, P.	JSI	29	52		300
—	Instruments	24	June 51		656–659
Stern, J.	RSI	22	51	9	703/04
	ref. Vide	7	March 52	38	

Author	Journal	Volume	Month and Year	Issue No.	Page
(c) metal valves					
Koppen, H. M. van	Appl Sci Res	3b	53		116–119
Reilly, E. G.	RSI	24	53		875/76
Brown, S. C., Coyle, J. E.	RSI	23	Oct. 52	10	570/71
Shatford, P. A.	JSI	29	Oct. 52	10	207
Sears, G. M., Hopke, E. R.	RSI	21	50		570
Cameron, A. E.	RSI	25	Oct. 54	10	1027/28
Rueger, L. J.	RSI	24	53		551
Robin, S.	J Phys Radium	13	July 52	2	116
	Vide	7	52	40/41	
Alpert, D.	RSI	22	51	7	536/37
Arkins, W. F., Jenkins, G. C. H.	Machinery		9. 3. 50		351/52
	ref. Vacuum	I	Jan. 51	1	53
Garrod, R. I.	JSI	27	July 50		205
	ref. Vacuum	I	Jan. 51	1	54
McIntosh, R. O., Coltman, J. W.	RSI	20	49		135
Gerrod, R. T., Coyle, R. A.	JSI	27	50	8	228/29
(d) control valves					
Fisher, P.	RSI	27	May 56	5	271
Knudsen, A. W.	RSI	27	March 56	3	148–150
Glaister, R. M.	JSI	32	Jan. 55	1	34/35
Prugne, P.	J Phys Radium	12	Oct. 51		66A
	ref. Vacuum	II	Jan. 52	1	82
2.1.5 Stopcocks and ground joints					
Crocker, A.	JSI	36	59		447
Amoignon, J., Delcher, J., Geller, R.	Vide	12	57		176–183
Horseling, J.	Philips Techn Rev	17	55		184–186
	ref. Vacuum	VI	56		255
2.1.6. Lead-ins					
(a) general					
Adam, H.	Vak Techn	8	59		59–62
	ref. Vacuum	IX	59	3/4	251
Haas, N. de	RSI	30	59		594
Hearst, J. R., Ahn, S. H., Strait, E. N.	RSI	30	59	3	200
Davis, E. J.	JSI	35	58		308

Author	Journal	Volume	Month and Year	Issue No.	Page
Lewin, G., Mark, R.	Vac Symp Trans		58		44–49
Lewin, G., Mark, R.	AEC-Rep NYO-8749				
Mariner, T. H.	Product Engng		57		188–192
	ref. Vacuum publ. 1959	7/8	57/58		250
Kleinteich, R.	Glas-Email-Keramotechn	9	56		355–357
	ref. Vacuum publ. 1959	7/8	57/58		250
Weiss, W.	Glastechn Ber Z Glaskunde	29	56	10	386–392
(b) welding and soldering connections					
McGuire, J. C.	RSI	26	55	9	893
Espe, W.	Vak Techn	4	55	3	51–64
Espe, W.	Feinwerktechnik	57	53		309
Müller, M. A.,	Weld J		Febr. 53		116–118
Russel, A. S.	ref. Vacuum	III	April 53	2	179
Vanderveer, W. R.	Vacuum	III	53		86
Laboulaye	Vide	7	May 52	39	1199
Wallace, R. A.	Materials and Methods	36	52		117–119
2.1.6.1 Rotary transmission seals					
Irland, M. J., Schermer, E. B.	RSI	30	59		743/44
Billet, E. A.,	JSI	35	58		70
Bishop, J.	ref. Vacuum publ. 1959	7/8	57/58		189
Ubisch, H. v.	JSI	33	May 56		200/01
Howe, P. G.	RSI	26	55	6	625
Diefenbach, G.	Chem Ing Techn	26	54	7	397–400
Sikorski, J., Woods, H. S.	JSI	30	Nov. 53	11	342
Sitney, R., Garrod, J. R.	RSI	23	52	9	505/06
2.1.6.2 Current lead-ins					
Edwards, W. D.	JSI	35	58		111
Meedchan, C. J., Sosín, A.	RSI	29	58		323
Viliéres, J. M.	RSI	29	58	6	527/28
Wieder, H., Smith, A. W.	RSI	29	58	9	794
Noggle, T. S., Oslewitt, T. H., Coltman, R.	RSI	28	57	6	464
Gomer, R.	RSI	27	July 56	7	544
Einstein, P. A., Pesterfield, E.	JSI	32	55		77
Harrower, G. A., Best, F. S., Machalett, A. A.	RSI	26	April 55	4	404/05

Author	Journal	Volume	Month and Year	Issue No.	Page
Lorenz, A.	Gl und HVT Quarz	2	Sept. 55	12/13	247
McKnight, W. H.	Materials and Methods		Oct. 54		94
Rawson, H.	Brit JAP	5	Oct. 54		352
Elson, L.	JSI	30	53		140
Schwarz-Bergkamp, F.	Gl und HVT	2	Sept. 53	12/13	254
Adam, H.	Gl und HVT	1	Dec. 52	7	123–134
Adam, H.	Gl und HVT	1	52	2	29–40
Bleuze, J., Dussanssoy, P.	Verres et Ref	6	52	6	347–355
Hoch, M.	RSI	23	52		651
Turnbull, J. C.	RCA-Rev	13	Sept. 52		291–299
Dvorek, H. R., Lihle, R. N.	RSI	22	51		1077
Karmaus	Glas-Email-Keramotechnik		May 51	5	
Taylor, R. C.	RSI	20	49		457

2.1.7 Gaskets

Higatsberger, M. J.	Phys Verh	6	55		221
Schwarz, E.	JSI	32	55		445
Barton, D. M.	Vacuum	III	Jan. 53	1	51–53
Carlotta, E. L.	Material and Methods	38	53	6	104–107
	ref. Vide	12	55	57	82
Gale, R. F., Machin, C. E.	JSI	30	53	3	97/98
Bartel, A.	Erdöl und Kohle	5	52		724
Evans, E. C., Babelay, E. F.	RSI	23	52		249/50
Hayward, A. G.	Vacuum	II	52		262–264
Knudsen, A. G.	RSI	23	52		566
Lord, R. C., McDonald, R. S.	RSI	23	52		442
Medicus	RSI	23	52		647/48
Stops, D. W.	JSI	29	April 52	4	
Cloud, R. W., Philp, S. F.	RSI	21	50		731
Heller, R. B.	Nucleonics	6	Febr. 50		81/82
Wexler, A., Corak, W. S., Cunningham, S. J.	RSI	21	50		259/60
Taylor, R. C., Ward, C. W.	RSI	20	49		457

2.1.7.1 Metal seals

Holden, J., Holland, L., Laurenson, L.	JSI	36	59		281

Author	Journal	Volume	Month and Year	Issue No.	Page
Henry, R. P., Blaire, J. C.	Vide	13	58	75	172
Adam, H. A., Kaufmann, S., Liley, B. S.	JSI	34	57		123
Fook, T., Harrington, D. B.	RSI	28	57	7	585/86
Lange, W. J.,	RSI	28	57		726
Alpert, D.	ref. Vacuum publ. 1959	7/8	57/58		189
Spees, A. H.,	RSI	28	57		1090
Reynolds, C. A., Boxer, A.	ref. Vacuum publ. 1959	7/8	57/58		189
Milleron, N.	Vac Symp Trans		57		38–41
Higatsberger, M. J., Erbe, W. W.	RSI	27	56		110
Heerden, P. J. van	RSI	26	55		1130/31
	ref. Vacuum	VI	56		255
Ruthberg, St., Creedon, J. E.	RSI	26	55		1208
Hees, G. W.,	Vacuum	IV	54		438–444
Eaton, W., Leck, J.	ref. Phys Abstr	60	57	9033	828
Hintenberger, H.	Z Naturforschg	6 A	51		459–462
	ref. Vacuum	VI	56		255

2.1.7.2 Rubber seals

Author	Journal	Volume	Month and Year	Issue No.	Page
Doty, W. R.	RSI	30	59	11	1053/54
Young, J. R.	RSI	30	59		291
	ref. Vacuum	IX	59	3/4	240
Davies, A. J.	JSI	35	58		378
Heinrich, J. T.	RSI	29	58	11	1053/54
Prior, A. C.	JSI	35	Oct. 58	9	795/96
Dawton, R. H. V. M.	Brit JAP	9	58		414

2.2 High Vacuum Process Engineering

Author	Journal	Volume	Month and Year	Issue No.	Page
Charlton, M. G., Perkin, G. M. C.	JSI Breaking Open Sealed Electronic Devices in Vacuum	36	59		49/50
Wadsworth, N. J.	JSI Vacuum Fatigue Apparatus	36	59		274
Baronetzky, E.	JSI Vacuum Grinding of Solids	35	58		427
Bas, E. B.	Namur-Ber Elektronenbeschuß im Hochvakuum		58		691–697
Batel, W.	Chem Ing Techn	30	58		651–660
	ref. Vacuum Pulverisation in Vibratory and Rotory Mills	IX	59	3/4	234

Author	Journal	Volume	Month and Year	Issue No.	Page
BERNHARD, F.,	Vak Techn	7	58		153–158
BUMM, H.	ref. Vacuum	IX	59	3/4	251
	Soldering in Vacuum				
HOLLAND-MERTEN, E. L.	Chem Techn	9	58	9	520–522
	Vakuumbereiche der Verfahrenstechnik				
SCHAEFER, K.	Vak Techn	7	58	1	21/22
	Vakuumbereiche der Verfahrenstechnik				
TANTAM, D. H.,	Namur-Ber		58		792–797
FARRAR, F.	Transfer Line for Liquefied Gases				
BOETTCHER, A.	Chem Ing Techn	29	57	3	169
	Hochreaktive, reine Metalle				
BOGERT, O.	Product Engng		57		141–145
	Atmospheric Pressure as a Process Tool				
ESPE, W.	Vak Techn	6	57	6	123–129
	Schweißen				
FUHRMANN, H.	Chem Ing Techn	29	57	4	256–258
	Selektive Gasspurenmessung				
KLUMB, H.,	Vak Techn	6	57	1	1–5
DÜMMLER, S.	Molekulargewichtsbestimmung				
Anon.	Galvano				35–38
	ref. Vacuum	VII	57		190
	Finishing of Metal				
BROWN, W. B.	Vacuum publ. 1959	VII	57		75–87
	Fumigation				
SCHNEIDMESSER, B.	Vacuum	IV	54	4	489/90
	Abschmelzen von Quarzbehältern				

2.2.1 Evaporation of thin layers, cathodic sputtering

Author	Journal	Volume	Month and Year	Issue No.	Page
HEAVENS, O. S.,	Vacuum	IX	59	1	17–20
BROWN, M. M.,	Iron Films				
HINTON, V.					
MEISSNER, C. R.	Vak Techn	8	59		93–100
	Metallische und dielektrische Substanzen				
ROSS, A.	Vak Techn	8	59		1–11
	ref. Vacuum	IX	59	3/4	242
	Thin Films of Inorganic Materials				
SCHOSSBERGER, F.,	Vacuum	IX	59	1	28–35
FRANSON, K. D.	Adhesion of Evaporated Metal Films				

Author	Journal	Volume	Month and Year	Issue No.	Page
Scott, V. D., Owen, L. W.	Brit JAP Titanium and zirconium for tritium targets	10	59	2	91
Chandra, S., Scott, G. D.	Canad J Phys Condensation Coefficients of Ag, Au, Cu	3b	58		1148
Gnaedinger, R. J.	Vac Symp Trans Transistor Fabrication		58		235–241
Hänlein, W., Günther, K. G.	Namur-Ber Mehrkomponentenschichten		58		727–733
Hanszen, K. J.	Z Phys Oberflächenfremdschichten und Strukturveränderungen	150	58		527–550
Hart, D. M.	Vac Symp Trans Ferromagnetic Films		58		230–234
Henschke, E. B.	JAP Cathode Sputtered Copper	29	58		1495–1502
Koehler, W.	Sonderdr. Metalloberfläche Oberflächenveredlung	12	58	9	262–267
Kövesligethy, R. de	Nanur-Ber Evaporation de Tungstène		58		803–806
Maddocks, F. S., Behrndt, K. H.	Vac Symp Trans Contamination Film Prior to the Evaporation of Nickel-Iron		58		225–229
Moriya, Y.	Namur-Ber Graphite Evaporator for Al		58		744–748
Nassauer, W. D.	Kunststoffe Metallisierung von Kunststoffen	48	58	4	165/66
Prugne, P., Garin, P., Lechangette, O.	Vide Films Minces de Nickel	13	58	74	82/83
Reichelt, W.	Namur-Ber Spezielle Probleme		58		737-743
Alderson, R. H., Ashworth, F.	Brit JAP Film of Nickel-Chromium Alloy	8	57		205
Alphen, P. M. van	Philips techn Rdsch Interferenz an dünnen Schichten	19	57	2	55–64
Cuckow, F. W.	JSI Deposition Apparatus	34	57		36
Ennos, A. E.	Brit JAP Highly-Conducting Gold Films	8	57		113
Gerharz, R.	Z angew Phys Aluminiumschichten in kurzen Bedampfungszeiten	9	57	2	95–98

Author	Journal	Volume	Month and Year	Issue No.	Page
Groton, Clay, H.	JAP	28	57	2	279
	Unusual Ring Structure of				
	Thallium-Doped Selenium				
Patzke, H.	Feingeräte-Technik	6	57	12	535–538
	HV-Bedampfungsapparatur				(B. 1464/
	HBA 1 des VEB Carl Zeiss				46)
	Jena				
Tabata, S.,	Vacuum publ. 1959	7/8	57/58		88
Jwata, M.,	Evaporation Source of Aluminium				
Sawaki, T.					
Clough, P. J.,	Iron Age		56		91–94
Durant, J. H.	ref. Vacuum	VI	56		190
	New Markets for Metallisers				
Hänlein, W.	Congress Intern Verre		July 56		
	ref. Vacuum	VI	56		266
	Thin, Flexible Glass Films				
Hiesinger, L.	German Pat		56		765–915
	ref. Vacuum	VI	56		189
	Thin Layers				
Holland, L.	Chapman & Hall, London		56		
Holland, L.	Nature		56	178	328
	ref. Vacuum	VI	56		263
	Electric Arc Evaporation				
Holland, L.	Vacuum publ. 1959	VI	56		161–172
	Continuous Al-Evaporation				
Feldmann, C.	RSI	26	56		463–466
Henry, R. O.	Vide	11	56	57	50–63
Reichelt, W.	Z Metallkde	46	56	4	268–271
Vodar, B.,	J Phys Radium	16	55		811/12
Minn, S.,	ref. Vacuum	VI	56		190
Offret, S.	Intermittent Arc Evaporation				
Biram, J. S. P.	AERE (Harwell) Rep		54		1394–1398
Kelly, R. L.,	RSI	25	54	4	391/92
Rice, P. J.					
Nandy, K. P.	RSI	25	54	5	523/24
Bateson, S.	Vacuum	III	53	1	35–42
Cross, J.	ref. Vak Techn	2	53	6/7	143
	Metal Finishing				
Engel, O. G.	J Res NBS	50	53		249–261
	ref. Vak Techn	2	53	8	162
Heritage, R. J.	Metallurgia	47	53		171–174
Balmer, J. R.	ref. Vacuum	III	53	4	464
Güntherschulze, A.	Vacuum	III	53	4	360–374
Holland, L.	Vacuum	III	53	3	245–253
Siddal, G.	Vacuum	III	53	4	375–391
Holland, L.	J Opt Soc Amer	43	53		376–380
	ref. Vacuum	III	53	3	308

Author	Journal	Volume	Month and Year	Issue No.	Page
Lafourcade, L.	CR	236	53		2220/21
Laporte, H.	Chem Ing Techn	5	53	11	632–634
Methfessel, S.	Gl und HVT	2	53	9	167–175
	Vacuum	III	53	3	327
Schrover, K., Rosen, J., MacDonald, A., Broder, J.	JAP	24	53		513
Schwager, J. E., Cox, C. A.	RSI	24	53		986
Tyler, J. E.	J Opt Soc Amer	43	53		708
	ref. Vacuum	III	53	4	464
Biram, J.	Vacuum	II	52	2	152–154
Clegg, P. L.,	JSI	II	52		201
Crook, A. W.	Torsionswaage zur Kontrolle der Aufdampfung				
Belser, R. B.	Res Engng		52		721
Ellis, C. E.,	JAP	23	52		31–34
Scott, G. D.	ref. Vacuum	II	52	2	194
Greenland, K. M.	Vacuum	II	52	3	216–230
Gruber, H.	Gl und HVT	1	52	8	160/61
Heavens, O. S.	Proc phys Soc	65B	52		788–793
	ref. Vacuum	III	53	1	89/90
Holland, L.	RSI	23	52	11	642/43
Newman, N. J.	ref. Vacuum Apparate	III	53	1	91
Methfessel, S.	Gl und HVT	1	52	1	6–8
Prugne, P.,	J Phys Radium	13	52	7	129/30A
Leger, P.	ref. Vacuum	III	53	2	202
Russel, S. O.	Bell System techn J	31	52		104
Seiter, J. G.	Amer Elektropl Soc Proc	39	52		141–151
Uzan, R.	Vide	7	52		1139/40
	ref. Vacuum	III	53	1	88
Vernon, E. V.	JSI	29	52		292
Dunoyer, L.	CR	233	51	17	919–921
	ref. Vacuum	I	52	1	86
Brochard, J.	J Phys Radium	12	51		632
Giacomo, P., Jaqinot, Roizen, S.	ref. Vacuum	I	51	4	329
Cline, J. E.,	J Elektrochem Soc	98	51		385–387
Wulff, J.	ref. Vacuum	II	52	2	180
Erdmann, R.	Metalloberfläche	5	51		133–135
	ref. Vacuum	II	52	2	172
Goldstaub, M.	CR	232	51		1843–1845
Michel, P.	ref. Vacuum	II	52	2	192
Hiesinger, L.	100 Jahre Heraeus		51		355–375
Holland, L.	JSI		51	1	59–61
	ref. Vacuum	II	52	1	85

Author	Journal	Volume	Month and Year	Issue No.	Page
Holland, L.	Vacuum	I	51	1	23
Hudswell, G., Mandleberg, G.J.	AERE-Rep C/R	861	51		
Schöpper, H.	Z Phys	130	51	5	562–585
	ref. Vacuum	II	52	2	
Bacquet, M. E. H.	Vide	5	50		916/17
	ref. Vacuum	I	51	2	145
Boettcher, A.	Z angew Phys	II	50	5	
	Al-Ag-, Al-Mg-Legierungen				
Crank, J.	Proc Phys Soc		50		484-491
Greenland, K.M., Billington, C.	Proc Phys Soc	63 B	50		359-363
Hass, G., Scott, N. W.	J Phys Radium		50		394-402
Heavens, O. S.	J Phys Radium		50		355
Heinmets, F.	JAP	20	49		384–389
Levinstein, H.	JAP	20	49		306
Mostovetch	CR	229	49		1850–1852
Rohn, K.	Z Phys	126	49		20-26
Stahl, H.	JAP	20	49		1–14
Tolanski, S.	Nature	163	49		885
Daub, E.	Z angew Phys	I	49	12	545
Williams, R. C., Birks, L. S.	JAP	20	49		98–106

2.2.2 Metallurgy, vacuum furnaces, vacuum melting

Author	Journal	Volume	Month and Year	Issue No.	Page
Anon.	Engineer	39	59	5371	207
	ref. Vacuum	IX	59	3/4	248
	Vacuum Arc Furnace				
Anon.	Engineer	207	59	5390	779
	ref. Vacuum	IX	59	3/4	248
	Vacuum Furnace				
Allenden, D.	JSI	36	59		60–70
	ref. Vacuum	IX	59	3/4	240
	Electron Bombardment Furnaces				
Anon.	Metal Progr	75	59		119/20
	ref. Vacuum	IX	59	3/4	248
	Electron Beam welding				
Bas, E. B., Cremonsik, G.	Vak Techn	8	59	7	
	Schweißen mit Elektronenstrahlen				
Begley, R. T., Comenetz, G., Flinn, P. A., Salatka, J. W.	RSI	30	59		38
	Levitation Melting				

Author	Journal	Volume	Month and Year	Issue No.	Page
Coupette, W.	Vak Techn	8	59	8	101–103
	Gießstrahl-Stahlentgasungsverfahren				
Dyracz, W. W.	Metal Progr	75	59		138–144
	ref. Vacuum	IX	59	3/4	248
	Stainless Steels and Superalloys				
Franks, A. E.	Progr Vac, Sci Techn		59		59–74
	Vacuum Metallurgy in USA				
Kornelson, E. V.,	RSI	30	59		290
Weeks, J. O.	ref. Vacuum	IX	59	3/4	241
	High Temperature Vacuum Furnace				
Loding, W.,	RSI	30	59		885
Hammell, L.	Vacuum Furnace				
Moore, R. A.,	RSI	30	59		837
Seagondollar, L. W., Smith, R. B.	Target Preparation				
Ogiermann, G.	Nickel-Ber	17	59	12	403–411
	Nickelhaltige Werkstoffe				
Samarin, A. M.,	Vacuum	IX	59		134
Novik, L. M.	Molten Steel Treatment				
Scheibe, W.	Z Metallkde	48	57		91–100
	ref. Vacuum publ. 1959	7/8	57/58		115
	Techniques in Metallurgy				
Anon.	Brit Chem Engng	3	58	2	99
Bangert, L.	Namur-Ber		58		577–587
	Stahl im Vakuum				
Bernhard, F.,	Vak Techn	7	58		153–158
Bumm, H.	Vakuum-Löten				
Bussard, A.	Namur-Ber		58		571–576
	Vakuum-Sinteröfen				
Candidus, E. S.,	Vac Symp Trans		58		86–88
Simons, J. C.	Electron Bombardment Furnace				
Carnaham, D. R.	Metal Progr	74	58		100–102
	ref. Vacuum publ. 1959	IX	59		165
	Discaloy by Vacuum Arc Melting				
Danforth, W. E.,	J Franklin Inst	265	58	4	303
Bleecher, H.	ref. Phys Abstr	61	58	3624	342
	Electrical Conduction Studies up to 2000 °C				
Dickinson, J. M.	Vac Symp Trans		58		192–197
	Resistance Furnace (3000 °C)				
England, P. G.,	JSI	35	58		66
Jones, H. N.	ref. Vacuum publ. 1959	7/8	57/58		220

Author	Journal	Volume	Month and Year	Issue No.	Page
Eudier, M.	Namur-Ber Frittage des Métaux Ordinaires		58		604–608
Facaros, G. N., Carnaham, D. R., Bianchi, L. M.	Vac Symp Trans Skull Furnace		58		168–174
Gross, R. C.	Vac Symp Trans Vacuum Brazing		58		175–180
Hardung-Hardung, H.	Vak Techn Uranium Melting Furnace	7	58		135–137
Huschke, E. G.	Vac Symp Trans High Temperature Vacuum Brazing		58		50–57
Levaux, J., Hannon, L.	Namur-Ber Coulée sous Vide des Gros Lignots de Forge		58		611–615
Marton, L., Suddeth, J. A.	RSI Temperature-Gradient Furnace	29	58	5	440
Merril, J. H.	Vac Symp Trans High Vacuum Heat Treat Plant		58		254–257
Nagashima, T.	Namur-Ber High Vacuum Furnace		58		593–595
Ortel, Y., Ollier, H.	Namur-Ber Fusion sous Vide de l'Uranium		58		545–552
Remy, F., Rosen, B.	Namur-Ber Fusion sous Vide Gaz Occlus dans les Métaux		58		609/10
Samarin, A. M.	Vac Symp Trans Vacuum-Treated Bessemer Steel		58		198–203
Samarin, A. M., Karasev, R. A.	Vac Symp Trans Gas-Evolution from Liquid Metal under Vacuum		58		35–37
Samarin, M., Novik, L. M.	Namur-Ber Molten Steel Vacuum Treatment		58		588–592
Scheibe, W. H.	Namur-Ber Nickel- und Chromstähle mit O_2N_2C		58		559–561
Scheibe, W. H.	Namur-Ber Vakuum Metallurgie		58		557/58
Sibley, C. B.	Vac Symp Trans High Temperature Vacuum Sintering Furnace		58		181–184
Smith, H. R.,	Vac Symp Trans		58		164–167

Author	Journal	Volume	Month and Year	Issue No.	Page
Hunt, C. D.,	Electron Bombardment				
Hanks, C. W.	Melting				
Stohr, J. A.,	Namur-Ber		58		536–545
Briola, J.	Soudure des Métaux sous				
	Vide				
Stohr, J. A.	Vide	13	58	75	163
Taylor, K. C.	Vac Symp Trans		58		185–191
	Vacuum Stream Degassing				
Tix, A.,	Namur-Ber		58		562–567
Coupette, W.	Vakuum-Stahlentgasungs-				
	strahlverfahren				
Linden-Bouwens,	Namur-Ber		58		553–556
N. van der	Bombardment Ionique				
Winkler, O.,	Namur-Ber		58		568–570
Kraus, Th.	Vakuumentgasung von flüs-				
	sigem Stahl				
Yasukawa, S.	Namur-Ber		58		596–603
	Heat Insulators of Vacuum				
	Furnace				
Anon.	Steel		22. 7. 57		137, 139
					140, 142
	ref. Vacuum publ. 1959	7/8	57/58		117
	Vacuum Melted Alloys				
Aksoy, A. M.	Vac Symp Trans		57		168–176
	Vacuum Melting Processes				
Calverley, A.,	JSI	34	57		142/43
Davis, M.,	ref. Vacuum publ. 1959	7/8	57/58		229
Lever, R. F.	Refractory Metals by Elec-				
	tron Bombardment				
Carpenter,	JSI	34	57		110
Mair, W. N.	Low Pressure Oxidation Ki-				
	netics of Hot Metals				
Damare, F. N.,	Vak Techn	6	57	2/3	50–54
Huntington, J. S.	Vakuumschmelzen von				
	Nickel-Legierungen				
Destribats, M. T.	Vide	12	57	68	184–187
	Four sous Vide				
Giler, R. R.	Vac Symp Trans		57		161–167
	Vacuum Heat-Treating				
Hiester, N. K.,	Chem Engng	64	57		237–252
Ferguson, F. A.,	ref. Vacuum publ. 1959	7/8	57/58		148
Fishman, N.	High Temperature Techno-				
	logy				
Ley, H.	Chem Ing Techn	29	57	7	460–468
	Reine Uran-Verbindungen				
Matthews, J. C.	JSI	34	57	2	62/63
	ref. Phys Abstr	60	57	3874	358
	ref. Vacuum publ. 1959	7/8	57/58		119

Author	Journal	Volume	Month and Year	Issue No.	Page
MEYERING, J. L.	Acta Metallurgica	5	57		257–264
	Nickel-Chromium-Copper Phase Diagram				
NOESEN, S. J.	Vac Symp Trans		57		150–156
	Vacuum Arc Melting				
VUCHT, J. H. N. VAN	Z Metallkde	48	57		253–258
	System Cer-Aluminium				
WILLIAMS, A. E.	Metal Ind	91	57	12	233–237
	Vacuum Metallurgy				
ADAMS, K. B.,	J Opt Soc Amer	46	56		36–38
BURNS, K.	ref. Vacuum	VI	56		209
	Interferometer and Cadmium Oven				
Anon.	Compr Air Mag		May 56		
	ref. Vacuum	VI	56		205
	High Vacuum Brazing				
CHASTON, J. C.	Metal Progr	69	56		64–67
	ref. Vacuum	VI	56		193
	Metals of High Purity				
EVANS, R. M.	Battelle Techn Rev	5	56		8–12
	ref. Vacuum	VI	56		204
FOLEY, E.,	Inst Min Metal		March 56		
WARD, M.,	ref. Vacuum	VI	56		228
HOCK, A. L.	High Purity Vanadium Metal Symposium on Extraction Metallurgy				
FRANKS, A. E.	Vacuum	VI	56		59–74
	Vacuum Metallurgy USA				
GRUBER, H., SCHEIDIG, H.	Z Metallkde	47	56		149–160
HALL, N.	Metal Finish; Technical Developments of 1955	54	56		43–52
HARDERS, F.,	Stahl u. Eisen	76	56	26	1721–1728
KNUPPEL, H.,	ref. Vacuum publ. 1959	7/8	57/58		227
BROTZMANN, K.	Steel Melts under Reduced Pressure				
HOPKINS, B. E.	Metal Rev	1	56		117–155
	ref. Vacuum	VI	56		235
	High-Purity Iron				
IVERSON, F. K.	PMM	14	56		130–135
	ref. Vacuum	VI	56		226
	Vacuum Alloys				
KIEFFER, R., BENESOVSKI, F.	Z Metallkde	47	56		160–164
LANGE, M. H. DE	IV^e Congres du Verre, Paris		56		148–152
	Glass Furnace				(1957)

Author	Journal	Volume	Month and Year	Issue No.	Page
Lorenz, F. R.,	J Metals	8	56		1076–1080
Haynes, W. B.	ref. Vacuum	VI	56		227
	Binary Uranium Alloys				
Mascré, C.,	Fonderie		56		496–508
Lefebre, A.	ref. Vacuum publ. 1959	7/8	57/58		115
	Degassing of Light Alloys				
Newitt, J. H.	Steel		56		107/08
	ref. Vacuum	VI	56		204
	Brazing in a Vacuum				
Powell, A. R.	Chem Ind	31	56		809–812
	ref. Vacuum	VI	56		194
	Some hitherto Rare Metals				
Rengstorff, G. W.	Battelle Techn Rev	5	56		3–6
	ref. Vacuum	VI	56		192
	Metals melting in a Vacuum				
Scheibe, W.	Gießerei		56		8–17
	ref. Vacuum	VI	56		229
	Melting and Casting of Titanium				
Schumann-Horn, L., Mager, A., Deisinger, W.	Z Metallkde	47	56		
Seaman, F. D.	Iron Age		56		64–66
	ref. Vacuum	VI	56		205
	Titanium Welding a Shop Tool				
Southern, R. L.	US-Pat 2734241 Vakuum-Gießeinrichtung		22.11.54/14.2.56		
Tix, A.	Hüttenzeitung	3	54	Transl. by Bisra	
	Stahl u. Eisen	76	56		
	Iron Steel		56		81–85
	ref. Vacuum	VI	56		193
	Bochumer Verein Process				
Tix, A.	Hüttenzeitung Bochumer Verein	25	56	4	2
	Bochumer Verein — Vakuumstahl				
Unterweiser, P.M.	Iron Age		56		67–72
	ref. Vacuum	VI	56		192
	Big Money behind Vacuum Metals				
Winkler, O.	Z Metallkde	47	56		133–144
	ref. Vacuum	VI	56		275
	State of Industrial Vacuum Melting Process				

Author	Journal	Volume	Month and Year	Issue No.	Page
Zeitz, E.	VDI-Nachr	10	56	23	
	Große Hochvakuum-Glühöfen				
Bain, E. C.	J Iron Steel Inst		55		193–212
	ref. Vacuum	VI	56		191
	Metallurgical Research in the US				
Blumenthal, B.	J Metals		55		2–8
	ref. Vacuum	VI	56		227
	High-Purity Uranium				
Chesnut, F.	Metal Progr		55		118–123
	ref. Vacuum	VI	56		275
	Vacuum Melting Furnaces (Interim Report)				
Crites, G. J.	Vak Techn	4	55	8	176–179
	Vakuum-Metallurgie				
Diels, K.	Berg- u Hüttenm Mh		55	7/8	
	Vakuummetallurgische Probleme				
Dyrkacz, W. W.	Iron Age	176	55	17	75–77
	Hochwarmfeste Legierungen besserer Qualität				
Edman, E.,	ASEA J	28	55		84–96
Victor, A.	ref. Vacuum	VI	56		227
	Vacuum Furnace for High Temperature Heat Treatment				
Gyorgak, C. A.,	NACA-Rep TN 3450		55		
Francisco, A. C.	ref. Vacuum	VI	56		205
	High Temperature Brazed Joints Processed in Vacuum or in Molten Salt				
Tix, A.	Bericht Nr. 587 des Stahlwerksausschusses des Vereins Deutscher Eisenhüttenleute		55		
	Stahlentgasung im Vakuum bei großen Schmiedeblöcken				
Gen. Electric	Chem Engng News	32	54	47	4666
Heldt, K.,	Z angew Phys	VI	54	4	157–160
Haase, G.	ref. Vacuum	VI	56		235
	Electr. Resistance of Pure Vacuum — Sintered Al				
Powell, R. L.	Chem Engng Progr	50	54		578–581
	ref. Vacuum	VI	56		230
	Titanium Metal Production				
Winkler, O.	Technica		54	24–26	1–16
Coupette, W.	DBP 866231		54		
	Entgasen und Gießen von Stahl				

Author	Journal	Volume	Month and Year	Issue No.	Page
Kramers, W. J., Dennard, F.	Vacuum Hochtemperaturwiderstandsgeheizter Hochvakuumofen	III	53	2	151–158
Winkler, O.	Stahl u Eisen	73	53		1261
Caule, E. J., Cook, M. A.	Canad J Technol	30	52		63–65
Wartmann, F. S.	US Dept of the Interior Bureau of Mines Invest 4837		52		
Davoine, F., Bernhard, R.	J Phys Radium	13	52		(50)
Gilbert, H. L., Aschoff, W. A., Brennan, W. F.	J Electrochem Soc	99	52	5	191–193
Jaffee, R. I., Blocher, J. M. jr.	Mod Metals	8	52		62–68
Lange, A., Müller, L.	Metallkundliche Ber Entzinkung von Parkes-Blei	50	52		
Miller, Gl.	Vacuum	II	52	2	19–32
Winkler, O.	Wiss Beihefte Gießerei Techn		52	9	435–437
Wroughton, D., Ockress, E. C., Brace, P. H., Comentz, G., Kelly, J. C. R.	J Electrochem Soc	99	52	5	205–211
Kroll, W. J.	Brit Pat 633117		51		
	ref. Vacuum	I	51	1	60
	Engng Min J		51		134
Malcolm, E. D.	JSI	28	51	1	63–66
	ref. Vacuum	II	52	1	93
Parke	Metal Progr	60	51		81
Fast, J. D.	Philips Techn Rev	11	50		241–244
	ref. Vacuum	I	51	1	61

2.2.3 Impregnating

Beyer, M.	Namur-Ber Trocken- und Imprägnieranlagen/Chargenzeiten		58		813–816
Wanser, G.	CEG-Ber Trocknung von Hochspannungskabeln		April/ June 56		
Hochhäusler, P.	ETZ Verbesserung des Kondensatordielektrikums	11	51		357–361

2.2.4 Vacuum distillation

Neumann, F.	Chem Ing Techn Rektifikation bei 1 bis 20 Torr	31	59	8	540
Preuss, L. E.	Vacuum Vacuum Distillation Source	IX	59	3/4	233

Author	Journal	Volume	Month and Year	Issue No.	Page
Hashimoto, K.	Namur-Ber Compounds having High Melting Points		58		701–704
Kirschbaum, Dieter, K.	Chem Ing Techn Dünnschichtverdampfen	30	58	11	715–720
Martin, A. J.	Vacuum publ. 1959 Purification of Beryllium	7/8	57/58		38–45
Matz, G.	Chem Ing Techn Fließbett-Sublimation	30	58	5	319–329
Nakagawa, H.	Namur-Ber Falling Film Molecular Still		58		705–708
Watt, P. R.	Namur-Ber Laboratory Molecular Still		58		709–711
Williams, F. E.	Vak Techn Kontinuierliche Vakuumdestillation	7	58	2/3	41–46
Günther, K. G.	Z Phys Kondensationsverhalten hochsiedender Substanzen	149	57		538–549
Keunecke, E.	Chemiker-Ztg Fein- und Hochvakuumdestillation	81	57	8	
Kirschbaum, E.	Chem Ing Techn Rektifiziertechnik	29	57	3	159/60
Kirschbaum, E.	Chem Ing Techn Rektifiziertechnik	29	57	3	133–220
Kretschmar, G., Pictet, J.	Chem Ing Techn Techn. Molekulardestillation	29	57		16–19
Kuhn, W.	Chem Ing Techn Präzisions-Destillationskolonne	29	57		6–16
Mair, B. J., Krouskop, N. C., Rossini, F. D.	Analyt Chem ref. Vacuum publ. 1959 Rotary Concentric Tube Distilling Column	29 7/8	57 57/58		1065–1068 230
Spendlove, M. J.	Vak Techn Vakuumdestillation von NE-Metallen und -Legierungen, 1. Teil	6	57	1	15
Spendlove, M. J.	Vak Techn Vakuumdestillation von NE-Metallen und -Legierungen, 2. Teil	6	57	2/3	36
Stephenson, J. L., Smith, G. W., Trantham, H.	RSI ref. Vacuum publ. 1959 Weight- and Temperature Record for Vacuum Sublimation Studies	28 7/8	57 57/58		381/82 239

Author	Journal	Volume	Month and Year	Issue No.	Page
Stephenson, J. L., Smith, G. W., Trantham, H.	Chem Ing Techn VDI-Fachgruppe Verfahrenstechnik — Interne Fachsitzung des Ausschusses Destillation, Rektifikation und Extraktion am 24. 4. 1956 in Bingen/Rhein	28	56	8/9	587–589
Danko, J. C., Griest, A. J.	J Metal Trans AIME	8	56		515/16
	ref. Vacuum Cu, Zn, Ni-Sublimation Figures	VI	56		235
Jaeckel, R.	Allgemeine Laboratoriumspraxis I Georg Thieme Verlag Destillation und Sublimation im Fein- und Hochvakuum: Methoden der organischen Chemie Bd. I/1, Houben-Weyl		56	1. Teil	901–956
Junge, C.	Chem Techn Absatzweise Rektifikation	8	56	10	579–588
Keunecke, E.	Dechema-Monographie Hochvakuumdestillation	31	56		233–240
Kirschbaum, E., Buch, W., Billet, R.	Chem Ing Techn Rektifikation in Füllkörpersäulen	28	56	7	475–480
Kirschbaum, E.	Z VDI Rektifiziertechnik	98	56	32	1797–1804
Kuhn, W.	18. Kolloquium des Dechema-Institutes für Apparate und Stoffkunde gemeinsam mit dem Arbeitskreis Verfahrenstechnik des Frankfurter VDI-Bezirksvereins am 13. 4. 1956 (Basel) Präzisions-Destillationskolonne				
Lee, C. A.	Chem Engng	63	56		189–194
	ref. Vacuum Fatty Acid Destillation	VI	56		219
Martin, A. J.	Metal Ind	88	56	I. Theory II. Practical	473–477 495–498
	ref. Vacuum Vacuum Distillation of Metals	VI	56		284
Röck, H.	Chem Ing Techn Gaschromatographie und extraktive Destillation	28	56	7	489–495

Author	Journal	Volume	Month and Year	Issue No.	Page
Watt, P. R.	Vacuum Molecular Distillation	VI	56		113–160
Dufour, A., Pariaud, J. C.	Bull Soc Chim France Sublimation Moleculaire Fractionnée	3	55		419/20
Jaeckel, R.	Fortschritte der Verfahrenstechnik Molekulardestillation		55		29–43
Kraus, Th.	Chem Ind Kurzwegdestillation		55/56		
Lawroski, S.	Chem Engng Progr	51	55		461–466
	ref. Vacuum Separation Processes	VI	56		218
Mair, B. J., Pignocco, A. J., Cossini, F. D.	Analyt Chem	27	55	2	190–194
Melpoloer, F. W., Warshall, T. A., Alexander, J. A.	Analyt Chem	27	55		974–976
Mullin, J. W.	Ind Chemist Sublimation	31	55		540–546
Schneider, R.	Chem Ing Techn	27	55	5	257–261
	Chem Process Engng	35	55	3	91–93
	Chem Age	96	55	1797	1268–1272
Burrows, G.	Trans Inst Chem Engrs	32	54		23–34
Jantzen, E., Wieckhorst, O.	Chem Ing Techn	26	54	7	392–396
Sims, R. P. A.	Canad Chem Process	39	54		(29)
	Battelle Techn Rev	4	54	2, 80a	1738
Trevoy, D. J., Torpey, W. A.	Analyt Chem Falling Stream Still	26	54	3	492–494
Aldershoff, W.G., Booy, H., Langendijk, S. L., Philippi, G. Th., Waterman, H. I.	Inst Petroleum	39	53		688–694
Baker, P. S., Duncan, F. R., Greene, H. B.	Science	118	53		778–780
Burrows, G.	Metrovic Gaz G. B.	25	53	Nr.409	40–43
	ref. Vacuum	III	53	4	
	ref. Vide	8	53	55	405
Gorritz, A. M., Garcia, D. M.	An Real Soc Espan Fisica Quim Ser	B 49	53		19–22
Valle, F.S.C. del	ref. Vak Techn	2	53	3/4	78
Hausschild, W.	Chem Ing Techn	25	53	10	573/74
Hickman, K. C. D.	IEC	45	53	I	44–46
Mason, A. C. F.	Analyt Chem	25	53	3	533

Author	Journal	Volume	Month and Year	Issue No.	Page
Nieman, C.	Chem Pharm Techn	9	53	2	1–16
Schurig	Chem Ing Techn	25	53	11	672–676
Benedict, O. E.	Petr Refiner	31	52	1	103–106
Bliss, H.	Chem Engng Progr	48	52		627–632
Eshaya, A. M., Frisch, N. W.	ref. Vacuum	III	53	1	98
Gorritz, A. M., Garcia, Valle, F. S. C. del	An Real Soc Espan Fisica Quim Ser	48	52	II I	841–850 825–840
Hickman, K. C. D., Trevoy, D. C.	IEC	44	52	8	1882–1888
Hickman, K. C. D., Trevoy, D. J.	Vacuum	II	52	1	3–18
Kelly, E. J.	Chem Engng Progr	48	52		589–593
	ref. Vacuum	II	52	2	149
Simms, R. P. A.	Vacuum Micromolekular-Destillationsanlage	II	52	2	245–256
Thormann, K.	Chem Ing Techn	24	52	12	673–750
Henry, R.	Vide	7	52	39	
Hickman, K. C. D.	IEC	43	51		62–69
Jaeckel, R.	Erdöl und Kohle	4	51		175/76
Madorski, S. L.	Int Chem Engng	32	51	2	82
	J Res NBS	44	51	2	135
Simpson, D. A.	Analyt Chem	23	51		1345/46
Sutherland, M. D.	ref. Vacuum	I	51	4	335
Williamson, L.	J Appl Chem		51		33–40
	Vacuum	II	52	1	96
Brenner, F. C., Dinardo, A.	IEC	42	50	9	1930–1934
Dixon, O. G.	J Soc Chem Ind	69	50		191/92
	ref. Vacuum	I	50	2	149
Hickman, K. C. D.	IEC	42	50		36–38
	ref. Vacuum	1	50	1	61
Jaeckel, R.	Chem Techn	2	50	9	
Masch, L. W.	Chem Ing Techn	22	50		141–164
Noyce, W. R.	Analyt Chem	22	50	12	1581
Smith, C. C.	Nature	165	50		613
Matalon, R.	ref. Vacuum	I	50	1	62
Spence, L. U.	IEC	42	50		1926
Biehler, R. M., Hickman, K. C. D.	Analyt Chem	21	49	5	638–640
Helin, A. F., Vanderwerf, C. A.	Analyt Chem	21	49		1284/85
Gold, M. H.	Analyt Chem	21	49		636/37
Jaeckel, R., Oetjen, G. W.	Chem Ing Techn	21	49	9/10	169–176
Roper, J. N. jr.	Analyt Chem	21	49		1575

Author	Journal	Volume	Month and Year	Issue No.	Page
Wylie, G.	Proc Roy Soc, Lond	197	49		383
Breger, I. A.	Analyt Chem	20	48		980/81

2.2.5 Drying and freeze-drying

Author	Journal	Volume	Month and Year	Issue No.	Page
Grant, P. M.,	JSI	36	59		133/34
Ward, R. B.	ref. Vacuum Freeze-Drying Apparatus	IX	59	3/4	248
Neumann, K.	Vide Lypphilisation de Denrees Alimentaires	14	59	81	151–157
Verma, N. S., Rowe, T. W. G.	Vacuum Freeze-Drying of Glass-Ampoules	IX	59	1	21–27
Dietrich, N.	Chem Ing Techn Trocknungsverhalten von Weizen	30	58		511–513
Ginette, L. F., Graham, R. P., Morgan, A. I.	Vac Symp Trans Freeze-Drying Rates		58		268–273
Hauduroy, P., Piguet, J. D.	Namur-Ber Collections de Types Microbiens		58		721–723
Hopkins, A. L.	Namur-Ber Dielectric Heating in Drying Biological Materials		58		724–726
Hörter, R.	I Org Überlebensraten nach Gefriertrocknung Zentralblatt für Bakteriologie, Parasitenkunde, Infektionskrankheiten und Hygiene	171	58		526–541
Müller, H.	Chem Ing Techn Hochfrequenz-Vakuum-Trocknung	30	58		133–137
Munden, H. R.	Vacuum publ. 1959 Vacuum Desiccator	7/8	57/58		87/88
Neumann, K.	Gefriertrocknungslabor der LHA-ELN Gefriertrocknung		58		
Neumann, K.	Linde-Ber Gefriertrocknung	3	58		70–78
Neumann, K., Oetjen, G. W.	Vac Symp Trans Automatic Freeze Drying of Food Products		58		258–261
Neumann, K. H.	Namur-Ber Regelprobleme bei Gefriertrocknung		58		712–717

Author	Journal	Volume	Month and Year	Issue No.	Page
SCHNELL, W.	Chem Ing Techn Vakuumtrockner auf der ACHEMA	30	58		812/13
SMITH, A. V.	Nature Freezing and Drying Biological Materials	181	58		1694–1696
	ref. Vacuum publ. 1959	7/8	57/58		119
FIXARI, F.,	Chem Engng Progr	53	57	3	110, 112,
CONLEY, W.,	Verfahrenstechnik	B			115, 116,
VIALL, K. G.	Kontinuierliche Vakuumtrocknung	1396 56			118
GÖRLING, P.	Chem Ing Techn Forschungsergebnisse/Trocknungstechnik	29	57		170–176
KUPRIANOFF, J.	Der Ingenieur	10	57		
	Chemische Technik „Trocknen in der Lebensmittelindustrie“	4			
ZIEGLER, L.	Chem Ing Techn Wärmelufttrockner	29	57	7	466–468
NEUMANN, K. H.	Chem Ing Techn	29	57		267–275
	ref. Vacuum publ. 1959	7/8	57/58		119
OETJEN, G. W.	Vac Symp Trans Vacuum Drying and Impregnation		57		129–135
BRINKMANN, K., BEYER, M.	ETZ Dielektrische Trocknung von Hochspannungskabeln	77	56	24	
EVANS, P.	Electrical World		56		82–84
	ref. Vacuum Field Vacuum Drying of Large Power Transformers	VI	56		275
FLOSDORF, E. W., TEASE, S. C.	Vacuum Vacuum Drying	VI	56		89–112
KIRSCHER, O., KRÖLL, K.	Trocknungstechnik Berlin/Göttingen/Heidelberg: Springer		56		1
SCHULZ, R., SABEL, A.	Chem Ing Techn	28	56	4	296
BAKER, P. R. W.	J Hygiene	53	55		426–435
	ref. Vacuum Residual Moisture in Freeze-Dried Biological Materials	VI	56		223
COCHRAM, D. L.	Refrig Engng		55	63, 8	49–56
HAY, J. M., GOODING, E.	J Sci Food Agric		55	6	427–438
MATZ, G.	Vak Techn	4	55	6/7	109–123

Author	Journal	Volume	Month and Year	Issue No.	Page
Neumann, K., Matz, G.	Chem Ing Techn	27	55		5
Neumann, K.	Vak Techn	4	55	6/7	123–129 130–137
Kerwick, R. A.	Chem Proc Engng	35	54	1	14
Mellor, J. D.	Vacuum — Protecting the Surface of some Materials in Freeze Drying	4	54		341
Call, F.	Nature	172	53	4368	126
Marshall	IEC	45	53		47
Oetjen, G. W.	Chemische Industrie: Ausgabe Gefriertrocknungsanlagen				
	Chem Engng	59	52	4	240
	Chem Process Engng	33	52	9	505
Nord, M.	Chem Ing Techn	24	52	6	364/65
	Food Manuf				452
Haas, H.	Z VDI	94	52	13	357
Zamsow, W. H.	Chem Engng Progr	48	52	1	21–32
Marshall, W. R.	ref. Vide	7	52	42	
Beckett, G.	JSI Vacuum Physics	28	51		66
Dunoyer, L.	CR	232	51	11	1080–1082
	Vide	6	51	34/35	1025–1040
	Vide	6	51	36	1077–1090
Friedman, S. J.	IEC	43	51		70
Harris, R. C.	Vacuum	I	51	1	11–21
Kramers, H., Stemerding, S.	Appl Sci Res	A 3	51	1	73–82
Niedergall	Chem Ing Techn	23	51		113
Walker, L. H., Patterson, D. C.	IEC	43	51		534–536
Wittenberg, D.	ref. Vacuum	I	51	4	337
	Int Chem Engng	32	51		365–367
	Chem Engng	58			141
Bruce, E. W.	Chem Engng Soc	6	50–52		39–51
	ref. Vacuum	III	53	3	304
Schroeder, A. L., Schwarz, H. W.	Chem Engng Progr		51		370
Morse, R. S.	Chem and Ind		48		27
	Hochvakuumtrocknung und -destillation				
	Chem Rdsch	8	48	7	129/30

2.2.6 Vacuum technology in elementary particle and nuclear physics

Author	Journal	Volume	Month and Year	Issue No.	Page
Blears, J., Greer, E. J.	Proc Instr Elect Engrs Paper		59	2904	
	ref. Phys Abstr	62	59	4358	405
	Vacuum System Design in Zeta I				

Author	Journal	Volume	Month and Year	Issue No.	Page
Dore, R.	Vide Isotope Separation by Gaseous Diffusion	14	59	82	183–196
Gould, C. L.	Vacuum Vacuum System for a 30 GeV Particle Accelerator	IX	59	1	63–68
Marker, R. C.	Vacuum Continuously Pumped Linear Electron Accelerator	IX	59		128
Sledziewski, Z., Torossin, A.	Vide Vide Ultra Pousse Fusion Controllee	14	59	81	107
Vekshinsky, S. A., Menshikov, M. I., Rabinovich, I. S.	Vacuum HV-Pumps and Units for Accelerators	IX	59	3/4	201–205
Gates, W. C., Reitzer, B. J.	Vac Symp Trans Altitude Temperature Environmental Chamber		58		274–278
Geiger, K. A.	Vac Symp Trans An Altitude Chamber Control		58		110–114
Gould, C. L.	Namur-Ber Vacuum System for a 30 GeV Particle Accelerator		58		514–519
Grove, F. J.	Vac Symp Trans Ultra-High Vacuum Techniques Controlled Thermonuclear Devices		58		9–17
Haefer, R.	Namur-Ber Automatisation von Zirkularbeschleunigern		58		508–513
Hall, R. L.	Vac Symp Trans System Cambridge Electron Accelerator		58		41–43
Hardung-Hardung, H.	Namur-Ber HV-Techniques for Reactor Materials		58		59–62
Marker, R. C.	Namur-Ber Continuously Pumped Linear Electron Accelerator		58		493–498
Meyer, H.	Namur-Ber Automatische Pumpstände für Teilchenbeschleuniger		58		520–525
Mongodin, G.	Vide Technique du Vide et Fusion Thermonucleaire	13	58	77	217
Monnier, B.	Namur-Ber Le Système à Vide d'un Synchrotron à Protons		58		504–507

Author	Journal	Volume	Month and Year	Issue No.	Page
Munday, G. L.	Namur-Ber Vacuum System of the CERN Proton Synchrotron		58		499–503
Vekshinsky, S. A., Menshikov, M. I., Rabinovich, I. S.	Namur-Ber HV-Pumps and Units for Accelerators		58		63–68
Auwaerter, M.	Vac Symp Trans High Vacuum Technique for Nuclear Physics		57		143–147
Schubert, W.	Die Atomwirtschaft Vakuumanlage für das CERN-Synchro-Zyklotron		57		332–334
Laock, B. G.	AERE (Harwell) Rep. EL/R		56		229
Seiden, J.	J Phys Radium	16	55		917–925
	ref. Vacuum Diffusion of Protons through the Residual Gas	VI	56		212

2.2.7 Miscellaneous vacuum systems and accessories

Vacuum apparatus

Author	Journal	Volume	Month and Year	Issue No.	Page
Amariglio, I., Benarie, M. M.	JSI Vacuum Controller	35	58		385
Hamilton, A. R.	Vac Symp Trans A Pressure Responsive Relay Control Circuit		58		123–125
Conrad, J.	CR	244	57	1	52/54
	ref. Phys Abstr	60	57	5924	546
Penther, C. S.	RSI Vactroller	28	57	6	460–463
Ullmann, J. R.	Vac Symp Trans Low Base Pressure in a large Metal System		57		95/96
Childs, B. G., Penfold, J.	RSI Vacuum Pump Control Circuit	26	55		235
Nahagama, M., Kukihara, T.	RSI Vacuum Control	26	55		727

Cooling-water control devices

Author	Journal	Volume	Month and Year	Issue No.	Page
Thiele, K.	Vak Techn Kühlwasser-Sicherheitsschalter	7	58	1	23/24
Steel, C., Smith, R. F., Sunners, B.	JSI Water Failure Guard	34	57		125
Wutz, M.	Vak Techn Kühlwasser-Kontrollschalter	6	57	8	193
Houghton, G.	JSI Water Failure Guard	33	56		199

Author	Journal	Volume	Month and Year	Issue No.	Page
Mercury vapour detection					
Ely, T. S.	AEC-Rep No. WASH	744	57		
	ref. Vacuum publ. 1959	7/8	57/58		181
	Mercury Vapour Detector				
Wintersteen, C. R.	AEC-Rep No. UCRL	3714	57		
	ref. Vacuum publ. 1959	7/8	57/58		181
	Control of Mercury Vapour				
Wyllie, H. A.	JSI	34	57		410
	A Mercury in Glass Burette				
Vacuum balances					
Cochran, C.	RSI	29	58		1135
	ref. Vacuum	IX	59	3/4	247
	Vacuum Microbalance				
Cordes, J. F.	Chem Ing Techn	30	58		342–346
	ref. Vacuum publ. 1959	7/8	57/58		180
	Vacuum Balance				
Espe, M. I.	JSI	34	57		229
	Vacuum Balance				
2.3.1 Materials					
Johnson, Vaughn, G. W.	JAP Schmierung mit MoS_2	27	56	10	1173–1178
Espe, W.	Vak Techn	4	55	1	10–24
Espe, W.	Vak Techn	4	55	2	34–40
	Kohlenstoff				
Frank, K., Stow, R. L.	RSI Kochsalzfenster	25	54		514
Michaelson, H. B.	Materials and Methods		Dec. 53		110
	Material für hohe Temperaturen				
Schwarz-Bergkampf, E.	Gl und HVT Eisenhaltige Einschmelzleg.	2	Sept. 53	12/13	254
Martin, S. L.	Chem Process Engng	33	52	7	370–373
Mönch, G. Ch.	Wiss Z Uni Halle	2	52/53	H 9	
	Das Löten von Glas-Keramik und Metallteilen mit Glasuren, niedrig schmelzenden Gläsern und Metalllegierungen				
Sited, J. R., Baldock, R.	AEC-Rep Nr. ORNL 1405				
	ref. Vacuum	III	53	1	
	Massenspektroskopische Untersuchungen von Werkstoffen der Hochvakuumtechnik				
Labeyrie, J., Leger, P.	Vide	6	Jan. 51	31	951/52

Author	Journal	Volume	Month and Year	Issue No.	Page
Taylor	Eng Exp Station News	23	51		52
Labeyrie, J.	J Phys Radium	11	50		
	Vakuumdichte Kittung von Glimmer auf Glas				
Bush, W. E.	Nat Nucl Energy Ser Div I	I	49		146-189
Hoog, B. G.,	RSI	19	48		331
Dushworth, H. E.	Synthetische Dielektrika				
Kroll, W. J.,	Trans Electrochem Soc	93	48		147-158
Schlechten, A. W.	Kohlenstoff und Metalloxyde				

2.3.1.1 Materials testing

Author	Journal	Volume	Month and Year	Issue No.	Page
Johnson, V. R.,	RSI	27	56		611-613
Vaughn, G. W.,	ref. Vacuum	VI	56		217
Lavik, M. T.					
Fleischmann, W. L.	AEC-Rep KAPL-M-AJH-2		Oct. 55		
	ref. Vacuum	VI	56		205

2.3.1.2 Metals (see also under 2.4.1)

Author	Journal	Volume	Month and Year	Issue No.	Page
Rain, N.	JSI	36	59	11	479
Jänecke, D.	Vak Techn	7	58	2/3	52-55
Espe, W.	Nachrichtentechnik	6	56	8	355-364
	Kupfer				
Espe, W.	Nachrichtentechnik	6	56	9	401-408
	Kupfer				
Fuschillo, N.	RSI	27	56		410/11
	ref. Vacuum	VI	56		249
	Hg-Reinigung				
Rowe, G. W.	Brit JAP	7	56		152/53
	ref. Vacuum	VI	56		218
Spengler, H. F.	Z VDI	98	56		381-383
Espe, W.	Vak Techn	4	55		51
Espe, W.	Nachrichtentechnik	5	55	2	69-74
Reynolds, F. L.	UCRL 2989		May 55		
	Indium				
Rüdiger, O.,	Techn Mitt Krupp	13	55	2	23-38
Kann, H. van,	Titan				
Knorr, W.					
Heyding, R. D.,	Canad J Chem	32	54		591/92
Flood, E. A.	ref. Phys Abstr		Oct. 54		1137
	Indium zur Entfernung von Hg-Dampf				
Hintenberger, H.	Werkstoffe und Korrosion		53	6	225
Jones, D. A.	Times Rev Ind		May 53		38
Gudzow, H. T.,	Z techn Phys	22	52		905-920
Losinski, M. T.					
Neumann, K.,	Naturwissenschaften	39	52	6	132
Schmoll, K.	Verdampfungskoeffizient von Kalium				

Author	Journal	Volume	Month and Year	Issue No.	Page
Neumann, K.	Naturwissenschaften	39	52	5	107/08
	Theorie der Verdampfungsgeschwindigkeit fester Körper				
Palm, R.	Gl und HVT	1	52	7	132
	Wolfram und Molybdän				
Seary	J Amer Chem Soc	74	52	10	4789–4791
Alan, W.	Germanium (Dampfdruck)				
Nineuil, P.	Vide	5	May 50		807–813
Johnson, P. D.	J Amer Ceram Soc	33	May 50		168–171
	ref. Vacuum	I	51	1	53
Morse, R. S.	Ind Eng Chem	30	47		1064
Norton, F. J.	Trans Amer Inst Min Metallurg Engrs	156	44		351–371
Langmuir, D. B., Malter, L.	Phys Rev	55	39		748
Wise, E. M.	Proc IRE	25	37		714
Smithells, C. J. Ransley, C. E.	Proc Roy Soc, London	(A) 155	36		195–212
Reimann, A. L., Grand, C. K.	Phil Mag	22	36		34
Kelley, K. K.	Bureau Mines Bull	383	35		
Larsen B. M.	Trans Amer Inst Min Metallurg Engrs	113	34		61
Sieverts, A., Bruning	Arch Eisenhütt	7	33		641
Winkler, O.	Z techn Phys	14	33		319
Andrews, M. R.	J Franklin Inst	211	31		689
Hessenbruch, W.	Z Metallkde	21	29		46
Jonas, H. A., Langmuir, I., Mackay, G. M.	Phys Rev	30	27		201
Jonas, H. A., Langmuir, I.	Gen Electr Rev	30	27		354
Steacie, E. W. R, Johnson, F. M. G.	Proc Roy Soc, London	(A) 112	26		542

2.3.1.3 Glass and quartz

Espe, W.	Vak Techn	8	59		209–214
Long, B.	Chem Ing Techn	31	59	12	812
Putner, T.	Brit JAP	10	59		332
Stevels, J. M.	Vetro e Silicati	3	59		23–30
Espe, W.	Vak Techn	7	58	4	65–77
Espe, W.	Vak Techn	7	58	5	101–110
Holland, L.	Brit JAP	9	58	10	410
Tuzi, Y., Okamoto, H.	J Phys Soc Japan ref. Vacuum	13 IX	58 59	8	960 155
Knapp, O.	Silikattechnik	5	54		51–54
Norton, F. J.	Vac Symp Trans		54		47

Author	Journal	Volume	Month and Year	Issue No.	Page
Rogers, W. A., Burritz, R. S., Alpert, D.	JAP	25	54		868
Briggs, L. J.	JAP	24	53		488–490
	ref. Vacuum	III	53	3	318
Harrison, E. R.	JSI Glass-bursting Stoppers	30	53		97
Manners, M.	Electronic Engng	25	53		512
Norton, F. J.	J Amer Ceram Soc	36	53		90
Adam, H.	Feinwerktechnik Die theoretischen Grundlagen der Druckglaseinschmelzungen und ihre praktischen Folgerungen	56	52	2	29–40
Adam, H., Espe, W., Schwarz-Bergkampf, E.	Gl und HVT Druckglaseinschmelzungen, Prinzip, Herstellung und technische Anwendungen	1	52	7	123–134
Dietzel, A.	Glastechn Ber	24	51	11	263–268
Wüstner, H.	Ann Phys	46	51		1095
Newkirk, T. F., Tooley, F. V.	J Amer Ceram Soc	32	49		272
Amerongen, G. J. Van	JAP	17	46		972
Smith, P. L., Taylor, N. W.	J Amer Ceram Soc	23	40		139
Beckerat, H. V., Arens, W.	ENT	19	42	3/4, 12	
Johnson, J., Burt, R.	J Opt Soc Amer	6	38		612
Taylor, N. W.	J Chem Physics	6	38		612
Braaten, E. O., Clark, C. G.	J Amer Chem Soc	57	35		2714
Barrer, R. M.	J Chem Soc		34		378
Burton, E., Braaten, E. O., Wilhelm, I. O.	Canad J Res	21	33		497
Tsai, L. S., Hogness, T.	J Phys Chem	36	32		2595
Urry, W.	J Amer Chem Soc	54	32		3887
Voorhis, C. C. Van	Phys Rev	23	24		557
Williams, G. A., Ferguson, J. B.	J Amer Chem Soc	44	22		2160

2.3.1.4 Mica

Espe, W.	Vak Techn	8	59		15–19
Espe, W.	Vak Techn	8	59		29–38
Espe, W.	Vak Techn	8	59		67–75

Author	Journal	Volume	Month and Year	Issue No.	Page
Ebinger, A., Linder, L.	E und M	59	41		286
2.3.1.5 Ceramic materials					
Navias, L. J.	J Amer Ceram Soc	37	54		329–350
Baukloh, W., Hoffmann, A.	Ber dtsch keram Ges	15	34		424
Griessel, R. W.	ASTM — Techn Publ		59	246	91
2.3.1.6 Plastic materials					
Kolenko, E. A., Yurev, V. G.	Zh tekh fiz ref. Phys Abstr Nr. 7860	28 62	58 59	10 740	2259 752
Luy, H., Schumacher, K.	Z angew Phys		56	5	222–226
Bockhoff, Neumann	Chem Engng	62	55	9	228
Geronimi, M.	Industr Plast Mod Teflon	7	55	4	4/5
Duncan, J. F.	Brit JAP	5	54		66–69
Beatty, J.	Trans ASME	75	53		605
Henry, H. G.	Materials and Methods	38	53	4	114/15
Keen, N. W.	Trans ASME	75	53		891
Sites, J. R.	Oak Ridge ORNL-1405		52		
Cloud, R. W., Philp, S. F.	RSI	21	50		731
Adams, G. D., Scherwin, W.	RSI	20	49		957
2.3.1.7 Rubber					
Bénichou, R., Blaive, J. C., Henry, R. P.	Namur-Ber		58		353–363
Smith-Johansen, R.	Gen Electr Rev	55	52		54
Frank, Ch. E., Kraus, G., Haefener, A. J.	IEC	44	52		1600
Beatty, J.	Trans ASME	75	53		605
Cloud, R. W., Philp, S. F.	RSI	21	50		731
Ehlers, G.	Kunststoffe	31	41		422
2.3.1.8 Oils and greases					
Simmler, W., Bächler, W.	Vak Techn	8	59	6	155–158
Ames, J.	JSI	35	58		1
Herrmann, O.	Techn wiss Abh Osram	7	58		369–375
Ishii, H.	Namur-Ber		58		186–192

Author	Journal	Volume	Month and Year	Issue No.	Page
Huntress, A. R., Smith, A. L., Power, B. D., Dennis, N. T. M.	Vac Symp Trans		57		104–111
Payne, J. N. W.	Petroleum		57		221–224
	ref. Vacuum publ. 1959	7/8	57/58		232
Melpoder, F. W.,	Analyt Chem	28	56		1936–1945
Brown, R. A., Washall, T. A., Doherty, W., Headington, C. E.	ref. Vacuum publ. 1959	7/8	57/58		231
Herlet, A., Reich, G.	Z angew Phys	9	57	1	14–23
Wilcock, D. F.	J Amer Chem Soc	68	46		691

2.3.2 Vapour pressures, melting and boiling points

Author	Journal	Volume	Month and Year	Issue No.	Page
Klumb, H.,	Vak Techn	8	59		62–66
Lückert, J.	ref. Vacuum	IX	59	3/4	234
Pratt, J. N., Aldred, A. T.	JSI	36	59	11	465–468
Günther, K. G.	Z Glaskunde	31	58	1	9–15
Hoyer, H., Peperle, W.	Z Elektrochem	62	58	1	61–66
Kansky, E., Jeric, S.	Namur-Ber		58		672–675
Nakayama, K., Ishii, H.	J Jap Vac Soc	1	58	6	222–227
Paty, L., Schürer, P.	Czech J Phys	8	58		
Richards, L. A., Gen Ogata	Science	128	58	3331	1089/90
Herlet, A., Reich, G.	Z angew Phys	9	57		14–23
Othmer, D. F.,	Industr Engng Chem	49	57		125–137
Maurer, P. W., Molinary, C. J. Kowalski, R. C.	ref. Vacuum publ. 1959	7/8	57/58		191
Amsel, O.,	Z angew Phys	8	56	1	20–24
Wittwer, G.	ref. Vacuum	VI	56		260
Groth, W., Ihle, H., Murrenhoff, A.	Angew Chem	68	56	20	644–648
Groth, W., Ihle, H., Murrenhoff, A.	Angew Chem	68	56	19	605–611
Jensen, N.	JAP	27	56		1460–1462
	ref. Vacuum publ. 1959	7/8	57/58		184

Author	Journal	Volume	Month and Year	Issue No.	Page
Milazzo, G.	Chem Ing Techn	28	56	10	646–654
	ref. Vacuum publ. 1959	7/8	57/58		191
Milazzo, G.	Rend Ist Super Sanita Fehler bei Dampfdruckmessungen (elektrostatisch)	19	56		313–321
Ernsberger, F. M., Pittmann, H. F.	RSI Manometer für Dampfdruckmessungen	26	55	6	584–589
Kiefer, H., Ziegler, B.	Z angew Phys Dampfdruckmessung mit Knudsenmanometer	VII	55		48
Myers, H. S., Fenske, M. R.	IEC	47	55	8	1562–1568
Burrows, G.	J Appl Chem	4	54		394–400
Yarwood, Rossman	Brit JAP	5	54		7
Waldschmidt, E.	Z angew Phys Empirische Näherungsformel für den Sättigungsdampfdruck	VI	54	7	313–318
Brandt, H., Röck, H.	Chem Ing Techn Druck- und Temperaturregelung bei Rektifikationen und der Messung von Verdampfungsgleichgewichten	25	53	8/9	511
Mahnert	Techn-wiss Abh Osram		53	6	
Hersch, H. N.	J Amer Chem Soc Dampfdruck von Kupfer	75	53		1529–1531
Histake, K., Mastuda, K.	J Phys Soc Japan	8	53		416–423
	ref. Vacuum Massenspektroskopische Untersuchung von Diffusionspumpenöl, Gasanalyse bei Endvakuum	III	53	3	317
Holland-Merten, Reuter, H., Slivinski, S.	Chem Techn Silikonöl	5	53		301–303
Reich, G.	Phys Verhandl Schreibendes Gerät zur Messung kleiner Dampfdrücke	4	53	7	213
Latham, P., Power, B. D., Dennis, N. T. M.	Vacuum Treibmittel für Diffusionspumpen	II	52	1	33–49
Nozakura, S.	J Chem Soc Japan Ind Chem Lab 55 Alkylphenyl		52		458–460

Author	Journal	Volume	Month and Year	Issue No.	Page
TAKAO, M.,	J Chem Soc Japan	55	52		98–100
TOMIYAMA, S.	Herstellung von Diffusionspumpenölen aus höheren Alkoholen				
TREVOY, D. J.	IEC	44	52		1888–1892
CARPENTER	Proc Phys Soc, Lond	64	51		57
CASADO, F. L., MASSIE, D. S., WHYTLAW-GRAY	Proc Roy Soc, Lond ref. Vacuum	(A)207 I	51 51	 4	483–495 319
EDWARDS, J. W.,	J Amer Chem Soc	73	51		172
JOHNSTON, H. L., BLACKBURN, P.	Dampfdrucke anorganischer Substanzen				
HERLET, A.,	Dissertation Bonn		51		
JAECKEL, R.	Dampfdruckmessungen unter 10^{-2} Torr				
HOPKE, E. R., SEARS, G. W.	J Chem Physics	19	51	11	1345–1351
JOHNSON, E. W.	RSI	22	51		240–244
NASH, L. K.	Vacuum	I	51	4	320
LEMPICKI, A.,	Nature	167	51		813/14
MCFARLANE, A.	Silikonöldämpfe und Sekundärelektronenemission				
NASH, L. K.	Analyt Chem ref. Vacuum	13 I	51 51	 1	168–170 71
RIDDIFORD, L.	JSI	28	51	1	47
CLANCEY, V. J.	Nature	166	50		275
DORSTEN, A. C. VAN, NIEUWDORP, H., VERHOEFF, A.	Philips techn Rdsch	12	50		33
SPEISER, R.,	Trans Amer Soc Metals	1	50		283–307
JOHNSTON, H. L.	Dampfdruckbestimmung von Metallen				
PERRY, E. S., WEBER, W. H., DANBERT, B. F.	J Amer Chem Soc	71	49		3720
VERHOEK, F. H., MARSHALL, A. L.	J Amer Chem Soc	61	39		2737
HICKMAN, K. C. D., HACKER, J. C., EMBREE, N. D.	Industr Engng Chem	9	37		264

2.3.3 Gas permeability and diffusion for quartz and glass

Author	Journal	Volume	Month and Year	Issue No.	Page
LEIBY, C. C., CHEN, C. L.	JAP	31	60	2	268
DARBY, J. B., TOMIZUKA, C. T., BALLUFFI, R. W.	JAP	30	59	1	104
OSBORNE, A. D.	JSI	36	59		370

Author	Journal	Volume	Month and Year	Issue No.	Page
Whet, N. R., Yong, J. R.	RSI	30	59		472
Compaan, K., Haven, Y.	Trans Faraday Soc	54	58		1498–1508
Eschbach, H. L.	Namur-Ber		58		373–377
Fara, H., Balluffi, R. W.	JAP	29	58	7	1133
Francis, J., Norton	JAP	29	58	7	1122
Frank, R. C.	JAP	29	58	8	1262
Frank, R. C., Swets, D. E., Fry, D. L.	JAP ref. Vacuum publ. 1959	29 7/8	58 57/58	8	892–898 157
Frank, R. C., Lee, R. W., Williams, R. L.	JAP ref. Vacuum publ. 1959	29 7/8	58 57/58	8	898–900 157
Grove, D. M., Ford, M. G.	Nature	182	58	4641	999–1000
Klumb, H., Dauscher, R.	Vak Techn	7	58	2/3	35–41
Penning, P.	Phys Rev	110	58	2	586/87
Silberg, P. A., Bachmann, C. H.	J Chem Physics ref. Vacuum	29 IX	58 59		777 155
Simmons, J., Dorn, J. E.	JAP	29	58	9	1308
Cayles, M. A., Forster-Brown, A. D.	Brit JAP	8	57		380
Compaan, K., Haven, Y.	Philips techn Rdsch	20	58	1	31
Compaan, K., Haven, Y.	Disc Faraday Soc	23	57		105–112
Edwards, A. G.	Brit JAP	8	57		406
Ferro, A.	JAP	28	57	8	895
Frank, R., Swets, D. E.	JAP	28	57	3	380
Gross, F.	Z angew Phys	9	57	12	606–612
Karstensen, F.	J Electron Control	3	57	3	305
Kendall, J. K.	Vac Symp Trans		57		120–124
Kucherov, R. Y.	Zh tekh fiz ref. Phys Abstr Nr. 4353	27 62	57 59		2158 405
Logan, R. A., Peters, A. J.	JAP	28	57	7	819
Mallet, M. W., Albrecht, W. M.	J Elect Chem Soc ref. Vacuum publ. 1959	104 7/8	57 57/58		142–146 161
Meijering, J. L.	Rev Metall	14	57		520
Norton, F. J.	JAP ref. Vacuum publ. 1959	28 7/8	57 57/58		34–39 237

Author	Journal	Volume	Month and Year	Issue No.	Page
Westenberg, A.A.,	J Chem Physics	26	57	6	1753/54
Walcher, R. E.	ref. Phys Abstr Nr. 8454	60	57		772
Millican, R.	AEC-Rep No. KY-166		56		1–5
	ref. Vacuum publ. 1959	7/8	57/58		188
Harrison, E. R.	RSI	26	55		305
Waldschmidt, E.	Metall		Oct. 54	19/20	
	ref. Vacuum publ. 1959	7/8	57/58		113–115
Schmellenmeier, H.	Exp Techn Phys	2	54	1	27
	ref. Phys Abstr Nr. 4356	62	59		405

2.4 Outgassing and Gettering

Author	Journal	Volume	Month and Year	Issue No.	Page
Todd, B., Lineweaver, J. L., Kerr, J. T.	JAP	31	60	1	51
Boulassier, J. C.	Vide	14	59	80	39
Fish, I. P. S.	RSI	30	59		889
Henry, R. P.	Vide	14	59	82	226–240
Kelly, J. C.	JSI	36	59		89/90
	ref. Vacuum	IX	59	3/4	241
Kraus, Th.	Vak Techn	8	59	2	39–43
	ref. Vacuum	IX	59	3/4	234
Geller, R.	Vide	13	58	74	71–76
Kraus, Th.	Naturwissenschaften	45	58	22	538
Santeler, D. J.	Namur-Ber		58		98–109
Santeler, D. J.	Vac Symp Trans		58		1–8
Trendelenburg, E. A., Carmichael, J. H.	Namur-Ber		58		657–660
Amoignon, J.,	Vide	12	57		377
Mongodin, J.	ref. Phys Abstr Nr. 2866	61	58		274
Geller, R.	Vide	12	57	69	194
Taylor, K. C.	Vac Symp Trans		57		157–160
Geller, R.	Vide	12	57	69	194
Geller, R., Barre, R., Mongodin, G.	Vide	12	57	69	195–201
Jaeckel, R., Schittko, F. J.	Forschungsberichte Nordrhein-Westfalen		57	369	
Amphlett, C. B.,	JSI	33	56		64/65
Williams, T. F.	ref. Vacuum	VI	56		195
Haefer, R., Winkler, O.	Vak Techn	5	56	7	149–155
Higalsburger, M.	Acta Phys Austr	10	56	3	181–185
	ref. Phys Abstr Nr. 6938	60	57		635
Hoffmann, K.,	Chem Ing Techn	27	55	10	604–607
Fischer, L.	Bestimmung kleiner Wassermengen in Folien und organischen Flüssigkeiten				

Author	Journal	Volume	Month and Year	Issue No.	Page
Todd, B. J.	JAP Entgasung von Glas	26	55	10	1238–1244
Alpert, D., Buritz, R. S.	JAP Grenzen des erreichbaren Vakuums	25	54		202
Eckardt, A., Eden, C.	Gl und HVT Entgasung optischer Gläser mit Ultraschall		52	2	15–19
Britt, J. R.	Naval Research Laboratory Report 3827		51		
Fernand, F.	Canad J Res	27 F	49		318

2.4.1 Outgassing of solid substances

Author	Journal	Volume	Month and Year	Issue No.	Page
Schram, A.	CITAV Paris		61		
Farkass, I., Barry, E. J.	Vac Symp Trans		60		35–38
Redhead, P. A.	Vac Symp Trans		60		108–111
Varadi, P. F.	Vac Symp Trans		60		149–154
Dayton, B. B.	Vac Symp Trans		59		101–119
Kraus, Th.	Vac Symp Trans		59		204
Redhead, P. A.	Vac Symp Trans		59		12–15
Heavens, O. S.	JSI	36	59		95
	ref. Vacuum	IX	59	3/4	243
Holland, L.,	JSI	36	59		81–84
Putner, T.	ref. Vacuum	IX	59	3/4	243
Tix, A., Bandel, G., Coupette, W., Sickbert, A.	Stahl u Eisen	79	59	8	472–477
Blears, J., Greer, E. J., Nightingale, J.	Namur-Ber		58		473–480
Carmichael, J. H.,	JAP	29	58	11	1570–1577
Trendelenburg, E. A.	ref. Vacuum	IX	59		155
Blonn, W. A.	Vac Symp Trans		58		31–34
Bills, D. G.	Phys Rev	107	57	4	994
Basalaeva, N. I.	Soviet Physics-Technical Physics	3	58	4	1027–1031
Benichou, R., Blaive, J. C., Henry, R. P.	Vide	13	58	79	353–363
Power, B. D., Crawley, D. J.	Namur-Ber		58		206
Dawton, RHVM	Brit JAP (AERF-G/R-393) Report	8	57		414

Author	Journal	Volume	Month and Year	Issue No.	Page
Dayton, B. B. Trabert, F. Gerow, G. Morse, R. B., Dayton, B. B.	Report Cons Vac Corp Rochester 3, N. Y.				
Campbell, J. E.	Vak Techn	6	57	1	12
Hanin, M.	Vide	68	57		148–161
Jaeckel, R., Junge, H.	Ann Phys	20	57		331–336
Milleron, N.	Vac Symp Trans		57		148/49
Espe, W.	Vak Techn	3	56		39–53
	ref. Vacuum	VI	56		283
Espe, W.	Vak Techn	3	56		69–82
	ref. Vacuum	VI	56		283
Todd, B. J.	JAP	27	56		1209/10
	ref. Vacuum publ. 1959	7/8	57/58		110
Winkler, O.	Rev Metall	52	55		934–942
	ref. Vacuum	VI	56		282
Harris, B. L.	IEC	47	55	3, II	161–164
Hackermann, Lee, E. A.	J Phys Chem Gasadsorption und Kontaktpotential	59	55	9	900
McMickle, Kubu	JAP — Diffusion	26	55	7	838
Seifert, H., Buhl, R., Seifert, K. F.	Kolloid Z Adsorption an Quarz	141	55	3	146–159
Schmellenmeier, H., Germey, K.	Exp Techn Phys Der Einfluß einer ionisierten Gasatmosphäre auf feste Oberflächen	3	55	3	109–116
Clauss, A.	CR	239	54		25–27
	ref. Phys Abstr Nr. 9680	57	54		1226
Dillon, J. A., Farnsworth, H. E.	RSI	25	55	1	96
Fast, J. D.	J Iron Steel Inst	176	54	1	24–27
Verrijp, M. B.	Philips techn Rdsch — Diffusion	17	55	2	74
Wasilewski, R. J., Kehl	J Inst Met Diffusion	83	54/55	P 3	94–104
Wilson, M. K.	RSI Abgabe von adsorbiertem Wasser in Vakuumanlagen	25	54	11	1130/31
Day, A. G.	JSI Mikrowaage zur Messung adsorbierter Gase	30	53		260–263
Kitchner, J. A., Bockris, J. O., Evans, J. W.	Acta Metalurgia		53	1	93–101
	ref. Vacuum Löslichkeit von Sauerstoff in γ-Eisen	III	53	2	187/88

Author	Journal	Volume	Month and Year	Issue No.	Page
ANTROPOFF, A. VON	Kolloid Z	129	52		1–10
BOETTCHER, A.	Glastechn Ber	25	52		347–353
DAYTON	Vacuum	II	52	2	147
	Gasabgabe von Kunststoffen				
HEDVAL, J. A.	Gl und HVT	1	52	3/4	50–56
HIGUCHI, I.,	J chem Soc Japan pure	73	52		400–405
CHIBA	chem section				
	ref. Vak Techn	3	54	3/4	81
NORTON, F. J.	Gen Electr Rev	55	52	5	28/29
	Diffusion				
TÖDT, F.	Gl und HVT	1	52	6	109
BARRER, R. M.,	Trans Farady Soc	47	51		826
GROVE, D. M.					
RUDNAY, A. DE	Vacuum	I	51	3	204/05
DUNOYER, J. M.	Vide	5	50	11	905–911
	ref. Vacuum	I	51	2	150
HÜTTIG, G. F.,	Kolloid Z	199	50		69–73
THEIME, O.	Adsorptionstheorie				
ALLANDER,	Trans Roy Inst Techn	70	53		
CLAES, G.	ref. Vak Techn	3	54	1	17
BADGER, W. L.,	IEC	45	53	1	15–98
LINDSAY, R. A.					
BECKER, J. A.,	J Phys Chem	57	53		153–159
HARTMANN, C. D.	Adsorption und Feldelektronenemission				
HARRIS, B.	IEC	44	53		24–31
HOLLAND, L.	Plast Inst Trans G B	21	53	45	65–85
KIRCHNER, F.,	Z angew Phys	V	53	8	281–283
KIRCHNER, H.	Adsorption und Feldelektronenemission				
WALDSCHMIDT, E.	Metall	8	54	19/20	749–758
	Gasabgabe und Gasdurchlässigkeit metallischer Vakuumbaustoffe				
BURMEISTER,	Metallwirtsch	13	34		115
SCHLOETTER					
NORTON, F. J.,	Trans Amer Inst Min		Febr. 32		
MARSHALL	Metallurg Engrs				
RÖNTGEN,	Metallwirtsch	11	32		685
MÖLLER					
HESSENBRUCH, W.	Z Metallkde	21	29		46

2.4.2 Outgassing of high-temperature boiling liquids

Author	Journal	Volume	Month and Year	Issue No.	Page
LUTHER, H.,	Chem Ing Techn	29	57		530
HIEMENZ, W.					
GROSS, F.	Z angew Phys	9	57		606
JAECKEL, R.,	Forschungsberichte		57	404	
GROSS, F.	Nordrhein-Westfalen				

Author	Journal	Volume	Month and Year	Issue No.	Page
Manser, H., Kortüm, G.	Z Naturforschg Thermodynamik der Lösungen von Gasen und festen Stoffen in Flüssigkeiten	10a	55	1	42-47
Burrows, G., Preece, F. H.	Trans Int Chem Engrs	32	54	2	99-114
Hayashi, C.	J Phys Soc Japan	9	54		287-290
Knödler, E. L., Bonilla, C. F.	Chem Engng Progr	50	54	3	125-133
Oetjen, G. W., Gross, F.	Chem Ing Techn	26	54	1	9-13
Seed, J. B.	US-Pat 2668598 Apparat zur Entgasung einer Flüssigkeit		26. 9. 50/ 9. 2. 54		
Smith, A. L., Taylor, J. C.	Vac Symp Trans		54		
Burrows, G., Preece, F. H.	J Appl Chem	3	53	10	451-462
Howard, W. B.	Petroleum Refiner	32	53	12	97-99
Matsuyama, T.	Chem Fac Engng Kyoto Univ	15	53		142-162
Mahnert	Techn wiss Abh Osram		53	6	
Eckardt, A., Eden, C.	Gl und HVT Entgasen von Flüssigkeiten	1	52	2	15-19
Kelly, E J.	Chem Engng Progr	48	52		589-593
	ref. Vacuum	II	52	2	149
Russel, S. O.	Bell Syst techn J	31	52		104
Steele, F. M.	Vacuum	II	52	2	148
Stringer, J. E. C.	Nature	169	52	4297	412
Weil, L.	CR Soc Franc Phys			29	30
	Beilage zu J Phys Radium	13	53	4	
Wirth	Österr Chem Ztg	63	52	17/18	212/13
	ref. Vide	9	54	49	1470
	Gasadsorption durch Hochvakuumfett				
Kirkwood, J. G.	J Chem Physics	18	50		901
Normand, C. E.	Oak Ridge (Y-642 Rev)		50		
Fürth, R.	Science Progress	37	49		202-218
Kirkwood, J. B.	J Chem Physics	17	49		988
Markham, A. E., Kobe, K. A.	Chem Rev	28	41		519

2.4.3 Gas absorption by gettering

Author	Journal	Volume	Month and Year	Issue No.	Page
Della Porta, P.	Vac Symp Trans		59		
Della Porta, P., Agano, E.	Vacuum	X	60	1/2	229-236
Della Porta, P., Origlio, S.	Vacuum	X	60	1/2	227-230

Author	Journal	Volume	Month and Year	Issue No.	Page
Ricca, F., Della Porta, P.	Vacuum	X	60	1/2	215–222
Della Porta, P., Origlio, S., Argano, E.	Vacuum	X	60	1/2	194–198
Della Porta, P.	Vacuum	X	60	1/2	181–187
Jepsen, R. L., Mercer, S. L., Callaghan, M. J.	RSI	30	59		377
Della Porta, P.	Vacuum	VI	56		41–58
Fransen, J.J.B., Perdijk, H. J. R.	Philips techn Rdsch	19	57/58	10	321–332
Ames, I., Christensen, R. L., Teale, J.	RSI	29	58	8	736/37
Bailleul-Langlais, J.	Namur-Ber		58		652–657
Baronetzky, E.	Namur-Ber		58		646/47
Berthaud, M.	Vide	13	58	78	293
Bills, D. G., Carleton, N. P.	JAP	29	58	4	692
Gregg, S. J., Jepson, W. B., Bloomer, R. N.	Brit JAP	9	58	10	417
Haine, M. E., Francis, E.W.R., Bloomer, R. N.	Nature	182	58	4640	931/32
Ichima, T., Mizichuma, Y., Oda, Z.	Namur-Ber		58		641–645
Della Porta, P., Ricca, F.	Namur-Ber		58		661–666
Della Porta, P., Ricca, F.	Vac Symp Trans		58		25–29
Schlier, R. E.	JAP	29	58	8	1162–1168
	ref. Vacuum	IX	59		154
Todd, B. J.	JAP	29	58	2	232
Todd, B. J.	JAP	29	58		1143
Yazawa, K. M.	Namur-Ber		58		648–651
Bloomer, R. N.	Brit JAP	8	57		352–355
	ref. Vacuum publ. 1959	7/8	57/58		108
Bloomer, R. N.	Brit JAP	8	57	8	321–329
	ref. Vacuum publ. 1959	7/8	57/58		108
Bloomer, R. N.	Brit JAP	8	57		40–43
	ref. Vacuum publ. 1959	7/8	57/58		109
Bloomer, R. N.	Nature	180	57		249/50
	ref. Vacuum publ. 1959	7/8	57/58		108

Author	Journal	Volume	Month and Year	Issue No.	Page
CARPENTER, L. G., MAIR, W. N.	Nature	179	57		212/13
	ref. Vacuum publ. 1959	7/8	57/58		109
CLOUD, R. W.,	RSI	28	57		889–892
BECKMAN, L., TRUMP, J. G.	ref. Vacuum publ. 1959	7/8	57/58		108
GOMER, R., HULM, J. K.	J Chem Physics	27	57	6	1363
HAYASHI, C.	Vac Symp Trans		57		13–26
TUZI, Y., OKAMOTO, H.	J Jap Vac Soc	7	57		216–230
	ref. Vacuum publ. 1959	7/8	57/58		184
VARNERIN, L., CARMICHAEL, J. H.	JAP	28	57		913–919
	ref. Vacuum publ. 1959	7/8	57/58		109
BLOOMER, R. N.	Nature	178	56		1000/01
	ref. Phys Abstr Nr. 3057	60	57		284
FLECHSIG, W.	Brit Pat 783485				
	ref. Vacuum	VI	56		185
GUNDRY, P. M., TOMPKINS, F. C.	Trans Faraday Soc	52	56		1609–1618
	ref. Vacuum publ. 1959	7/8	57/58		144
STOLL, S. J.	Brit JAP	7	56		94–96
ZIJLSTRA, P.	Vide	12	56		248–250
	ref. Vacuum publ. 1959	7/8	57/58		109
MORRISON, J., ZETTERSTROM, R.B.	JAP	26	55		437–442
STOUT, V. L., GIBBONS, M. D.	JAP	26	55	12	1488–1492
	ref. Vide		55	57	86
SUHRMANN, R., SCHULZ, K.	Z Naturforschg	10a	55	7	517–521
OETJEN, G., GROSS, F.	Chem Ing Techn	26	54	1	9–13
DE BOER, F., NIKLAS, W. F.	Brit JAP	5	54	5	341/42
DELLA PORTA, P.	Vacuum	IV	54	4	464–475
				3	284–302
STOUT, V. L., GIBBONS, M. D.	Phys Rev	96	54		(3)
WAGENER, S.	Z angew Phys	VI	54	10	433–442
WAGENER, S.	Nature	173	54	4406	684/85
KINGTON, G. L.	Trans Faraday Soc	49	53		417–425
OCKERT, C. E.	Chem Engng	60	53		374
TSUKAKOSHI, O.	J Sci Res Inst	47	53		132–148
ARIZUMI, T., KOTANI, S.	J Phys Soc Japan	7	53		300–307
WAGNER, S.	Vacuum	3	53		11–23
TAUERN, D.	Gl und HVT		52	8	161
WAGENER, S.	Proc Inst Electr Engrs	99	52	III	59
ALLEN, J. A., MITCHEL, J. W.	Disc Faraday Soc		50	8	309–340

Author	Journal	Volume	Month and Year	Issue No.	Page
Espe, W., Knoll, M., Wilder, M. P.	Electronics, N. Y. Getter Material	23	50		80–86
Haase, G.	Z angew Phys	II	50		188–191
Schreiner, H.	Dtsch Z anorg Chem	262	50	1–5	113–121
Wagener, S.	Brit JAP	1	50		225–231
Ehrke, L. F., Slack, Ch. M.	JAP	11	40		129

2.4.4 Evaporation, condensation, sublimation

Anthony, C. E., Preuss, L. E.	Vacuum	IX	59	3/4	232
Gutbier, H. B.	Z Naturforschg	14a	59	1	32–36
Algermissen, J.	Chem Ing Techn	30	58	8	502–510
Behrndt, K. H., Jones, R. A.	Vac Symp Trans		58		217–224
Bressler, R.	Z VDI	100	58	15	630–638
Leniger, I. H. A., Veldstra, I. J.	Chem Ing Techn	30	58	10	636–642
Poocza, A.	Chem Ing Techn	30	58	10	648–650
Miller, R. J., Bachmann, C. H.	JAP	29	58	9	1277
Burrows, G.	J Appl Chem	7	57		375–384
Patzke, H.	Feingerätetechnik	6	57	12	535–538
Sherwood, T. K.	Amer Inst Chem Engrs J	3	57		37–42

2.5 Applications

2.5.1 Chemical industry

Cayless, M. A.	Brit JAP Gasanalysen bei niedrigen Drucken	7	Jan. 56	1	13–16
Fabian, D. J., Robertson, A. J. B.	Proc Roy Soc, Lond Ser A	237	56	1208	1–16
Gäbler, H.	Seifen, Fette, Anstrichmittel Kontinuierliche Seifenverarbeitung unter Vakuum	58	56		286–292
Andrew, T. R.	Vide Bestimmung des Schwefelgehalts von Nickel	10	Jan. 55	55	394–400
Feichtinger, H.	Arch Eisenhüttenw Mikroschnellanalysen	20	55	3	127–130
Griffith, J. H., Phillips, C. S. G.	J Chem Soc Detektor für automatische Gasanalysengeräte		54		3646–3653

Author	Journal	Volume	Month and Year	Issue No.	Page
YOKOMIZO, H.,	Chem Ind Res Report, Tokyo	49	54	6	209 236
FUJITA, E.	Reinstdarstellung von Kalzium				
DUNCAN, J. F.,	JSI	30	Dec. 53		462–464
WARREN, D. T.	ref. Phys Abstr		Febr. 54		232
	ref. Vak Techn		54	3/4	72
KOLLMANNSPERGER, H.	Z angew Phys	V	53	7	213
	Molekulargewichtsbestimmung von Gasen und Dämpfen im Druckbereich von 10^{-6} Torr				
PANETH, F. A.	Endeavour	12	Jan. 53		5–17
	ref. Vacuum	III	53	2	184
	Mikroanalysen				
TURNBULL,	JSI	30	53		260
HARRISON	Bestimmung geringer Wasserstoffmengen in Stickstoff				
YEATON, R. A.	Vacuum	III	53		115–124
	Vakuumschmelztechnik und Gasanalysen				
ALBERT, ADRIEN,	J Chem Soc		52		4985–4993
HAMPTON, A.	Sublimieren unter Vakuum				
BURROWS, G.,	Vacuum	II	52	1	50–55
JACKSON, R.	Molekulargewichtsbestimmung von Ölen und Fetten				
HORTON, W. S.	US-AEC-Rep KAPL	666			
	ref. Vacuum	II	52	2	196
	Analysen				
HOLT, W. R.	Analyt Chem	24	Nov. 52		1870
	Vakuumpipette				
MACDONALD, F.S.	J Chem Soc		52		4184–4192
	Synthesen von Pyrrolen				
MAGEL, T. T.	AECD-Rep Nr. 3321		Febr. 52		
	Reduktion von Metalloxyden				
VYNER, E. M.	Brit Gel and Glue R.A.		Nov. 52		(14)
	ref. Vacuum	III	53	1	95
	Leim- und Gelatineindustrie				
SLOMAN, H ,	J Metals	80	52	7	391–404
HARVEY, C. A.,	ref. Vacuum	II	52	2	197
KUBASCHEWSKI, O.	Reaktionen zur Bestimmung von O_2, N_2 und H_2 in Mo, Th, Ti, U, V, Zr				
—	Light Metals	14	March 51		149/50
	Analytische Destillation				
JAECKEL, R.	Chimia	5	June 51		129
	Anwendung der Hochvakuumtechnik in der Chemie				

Author	Journal	Volume	Month and Year	Issue No.	Page
MURRAY, K. E.	J Amer Oil Chem Soc	28	June 51		235–239
	ref. Vacuum II Fraktionierung bei niedrigen Drucken	II	52	1	95
ROGERS, R. R., **VICUS, G. E.**	Canad Min Metal Bull Lithiumdarstellung	44	Jan. 51		15–20
STANLEY, J. K., **HOENE, J. VON,** **WIENER, G.**	Analyt Chem Bestimmung von O_2 in Zr	23	Febr. 51		377
CARNEY, D. J., **CHIPMAN, J.,** **GRANT, N. J.**	Trans Amer Inst Min Metallurg Engrs Zinnschmelzmethode zur Bestimmung von H_2 in Stahl	188	50		397–403
NASH, L. K.	Analyt Chem	22	Jan. 50		108–18
	ref. Vacuum Gasanalyse	I	51	1	64
PUGH, W.	South African ind Chemist Hochvakuumtechnik für die chemische Forschung	4	Febr. 50		22–26
ARROWSMITH	Trans Inst Chem Engrs G.B.	27	49		101–112
	ref. Vide Vakuumtechnik in der chemischen Industrie	7	March 52	38	
EBERT, H.	Die Vakuumtechnik bei chemischen Arbeiten	1	July 49	1	
LEYLAND	Trans Inst Chem Engrs Anwendung der Vakuumtechnik in der chemischen Industrie	27	49		83–100
RODDEN, C. J.	Nat Nucl Energy Ser VIII I				
KRAFT, W. W.	IEC Vakuumdestillation von Erdölrückständen	46	48		807

2.5.2 Electrical industry

Author	Journal	Volume	Month and Year	Issue No.	Page
HOCHHÄUSLER, P.	ETZ B	7	55	08	293–296
	Erzeugung. . . . hoher Vakua in der Elektrotechnik			07	255–259
BECKER, E., **AWENDER, A.,** **SANN, K.**	Telefunkenztg Schwingquarzherstellung	28	March 55	107	34/35
SEITER	Electronics, N. Y. Selengleichrichterbau	28	Nov. 55	11	258
FISCHER, A.	Z Naturforschg Halbleiterschichten auf Glas	9a	Jan. 54		7–21

Author	Journal	Volume	Month and Year	Issue No.	Page
Weigelt, W.,	Mitt. aus dem Institut für angew. Physik der Univ. Frankfurt/Main				
Haase, G.	Ber. dtsch keram Ges	31	54	2	45–48
	Der elektrische Widerstand von hochvakuumgesintertem Magnesiumoxyd				
Bayer, K.	Elektrotechn u. Masch-Bau	70	53	17	386
	Aufbereitung und Konservierung von Isolierölen				
Forest, J. S.	Brit JAP		53	2	37–39
	ref. Vacuum	III	53	2	179
	Erhöhung der Oberflächenleitfähigkeit				
Reichelt, W.	Gl und HVT		Sept. 53	12/13	256
	Herstellung elektrischer Widerstände durch Aufdampfen				
Brinkmann, K.,	ETZ	73	52	14	449/50
Marderwald, E.	Dielektrische Trocknung der Papierisolation von Hochspannungskabeln				
Cline, J. E.,	J elektrochem Soc	98	Oct. 51		385–387
Wulff, J.	ref. Vacuum	II	52	2	180
Hochhäusler, P.	ETZ	72	51	11	357–361
	Die Verbesserung von Kondensatordielektrika durch Hochvakuumbehandlung				
Latham, D.,	Brit Inst Radio Engrs	11	51		561–568
Power, B. D.	ref. Vacuum	II	52	1	
	Anwendung der Vakuumtechnik in der Radio- und Elektroindustrie				
Maleady, N. R.	Gen Electr Rev		Aug. 51	54	52–54
Reichelt, W.	Gl und HVT		52	8	152–159
Dufour, Ch.	Vide	5	July 50		837–841
Hochhäusler, P.	Der Elektrotechniker	2	50	10	297
	Clophenkondensator				
	Elektrotechnik		49	6	166
	Kondensatorbau				

2.5.3 Electron microscopy

Author	Journal	Volume	Month and Year	Issue No.	Page
Williams, R. C.,	Exp Cell Res	4	Febr. 53		188–202
Brettschneider, L. H.	ref. Vacuum	III	53	2	194/95
Elbers, P. F.	Proc Acad Soc Amsterdam	55	52		88–92

2.5.4 Precision mechanics industry

Author	Journal	Volume	Month and Year	Issue No.	Page
Reichelt, W.	Z Metallkde	46	April 55	4	268–271
	Veredlung und Korrosionsschutz von Oberflächen				
Crites, G. H.	Instrumentation	7	54	2	14/15
	Tempern von Uhrenfedern				
Johnson, R. O.	Precision Metal Molding	.	Febr. 54		45–48, 66
	Automobiltechnik	7	54	8	225
—	Industr Finish	5	March 53		546–561
	ref. Vacuum	III	53	3	330
Shepard, M.	Materials and Methods		June 53		97
Brown, R. W.	Canad Chem Process		Nov. 52		38–40
	ref. Vacuum	III	Jan. 31	1	88
Seiter, J. G.	Electr Manufact	50	52		148
Warring, R. H.	Mech World Engng Rec	132	52		276–280
	ref. Vacuum	III	Jan. 53	1	88

2.5.5 Incandescent lamps, valves and tubes industry

Author	Journal	Volume	Month and Year	Issue No.	Page
Engel, F.	Vak Techn	8	59		44–47
Harries, J. O. H.	Electronics, N. Y.	32	59	25	78–81
Almer, F. H. R., Perdijk, H. J. R., Zanten, P. G. van	Namur-Ber		58		676–678
Bailleul-Langlais, L.	Namur-Ber		58		632–635
Huber, H.,	Ann Radioelectr	13	58	53	230–252
Warnecke, M.	ref. Vacuum	IX	59		154
Kohl, W. H.	Namur-Ber		58		635–640
Robinson, N. W.	Namur-Ber		58		616–621
Seehof, J., Smithberg, S., Armstrong, M.	RSI	29	58	9	776–778
Tachihara, Y., Hata, T., Onizuka, M.	Namur-Ber		58		679–682
Yazawa, K. M.	Namur-Ber		58		622–625
Zincke, A.	Vak Techn	7	58		93–100
	ref. Vacuum	IX	59	3/4	240
Espe, W.	Vak Techn	6	57	5	91
Curnow, H. J.	JSI	34	57		73
Edens, A. H.	Philips techn Rdsch	19	57/58	8/9	271–277
Morrison, J.	Vac Symp Trans		57		100–103
Robinson, N. W.	Vacuum	VI	56		21–40
Stoll, S. J.	Brit JAP	7	56	3	94
Dobke, G.	Gl und HVT		Sept. 53	12/13	249
	Die Vakuumtechnik des Hg-Dampf-Eisengleichrichters				
	ref. Vacuum	III	53	4	438

Author	Journal	Volume	Month and Year	Issue No.	Page
Luchsinger, W.	Techn Rdsch Bern	45	53		25–27
	ref. Vak Techn		55		142/43
	Pumpenlose Hg-Dampf-Gleichrichter mit Stahlgefäß und Edelgasfüllung				
Behne, R.	SEG-Nachrichten	1	53		26
	Bildröhren in Fließfertigung				
Gladitz, F. A.	Gl und HVT		52	8	162
	Herstellung von Glasteilen für Vakuumröhren				
Günther-Schulze, A.	Elektron Wiss Techn	5	Febr. 52		390–395
	Vakuum und Glasgleichrichter				
Latham, D.,	J Brit Inst Radio Engrs	11	Dec. 51		561–568
Power, B. D.	ref. Vacuum	II	Jan. 52	1	
Metson, G. H.	Vacuum	I	51	4	283–292
	Hochvakuum-Oxydkathodenröhren				

2.5.6 Plastics industry

Author	Journal	Volume	Month and Year	Issue No.	Page
—	Brit Plastics	28	55	9	358–372
	Vakuumformen				
—	Mod Plastics	31	54	9	87–97
	Vakuumformen				183
Hulpert, G. C.	Research	6	53		54–60
	ref. Vak Techn		(55) 54	8	160
Edwards, E. G.	US-Pat 2503251		28. 1. 46/ 11. 4. 52		
Reynolds, R. J. W.	Herstellung von Fäden, Fasern und Formkörpern aus Polyestern				

2.5.6.1 Treatment of plastics

Author	Journal	Volume	Month and Year	Issue No.	Page
—	Industr Finish	5	March 53		546–561
	ref. Vacuum	III	53		330
	Metallisieren von Kunststoffen				
Bancroft, G. H.	Mod Plastics	31	53	4	122/23
	Metallisieren von Kunststoffen				210
Giegerl, E.	Der Plastikverarbeiter		53	10	
	Metallische Überzüge auf Kunststoffen				
Hiesinger, L.	Kunststoffe	43	53	12	547/48
	Metallisieren von Kunststoffen				
Holland, L.	Plastics Progr		53		361–380

Author	Journal	Volume	Month and Year	Issue No.	Page
Sutherland, N.	Vacuum	III	53	3	331
	Metallisieren von Kunststoffen				
Seiter, J. G.	India Rubber World	128	53	4	493–496
	Metallisieren von Kunststoffen				
Brown, R. W.	Canad Chem Process		Nov. 52		38–40
	ref. Vacuum	III	Jan. 53	1	88
	Metallisieren				
Seiter, J. G.	SPEJ		Oct. 52		12/13
	ref. Vacuum	III	53	1	89
	Metallisieren				
Hartmann, H.,	Metal Finish	49	Sept. 51		64–70
Schneider, M.	ref. Vacuum	II	52	1	85
	Metallisieren				
Hiesinger, L.	Kunststoffe	41	51	12	444–446
	Chem Ing Techn	24	52	1	34
	Metallisieren				
Holland, L.	Brit Plastics	24	March 51		96–102
	ref. Vacuum	I	51	4	331
	Metallisieren				
Navoy, T. M.	Metal Finish		Nov. 51		
	Metallisieren				
Swallow, J. S.,	Chem and Ind	9	Oct. 48		9–13
Gourlay, J. S.	Anwendungen von Hochvakuum in der Lack- und Kunststoffindustrie				
Kraus, Th.	Jahrb Kunststoffe — Plastics		54/55		

2.5.7 Medical-biological applications

Author	Journal	Volume	Month and Year	Issue No.	Page
Neumann, K.	Vak Techn		55	6/7	24
	Gefriertrocknung von Mikroorganismen, Zellen und Geweben				
Butler, L.,	Nature	171	53	4361	941/42
Bell, L. G.					
Eastcott, H. H. G.	Vacuum	III	53	3	279–286
Levin, J.	Vide	8	53	44	1307–1319
	ref. Gl und HVT		54	15/16	319
Scheer, K. E.	Zbl Bakteriol., Parasitenkunde Infektionskrankh, Abt I	159	53		311–313
	Laborgerät zum Gefriertrocknen				
Stevenson, J. L.	Bull Math Biophys	14	53		411–429
	ref. Vacuum	III	53	4	437
	Theorie der Trocknung gefrorener Gewebe				

Author	Journal	Volume	Month and Year	Issue No.	Page
Wright, L. J.	J Med Lab Techn		April 53		73–86
	ref. Vacuum	III	53	3	340
—	Nature	171	53		1047–1049
	ref. Vacuum	III	53	3	311
Beckett, L. G.	Malay Pharm J		April 52		88–92
	Canad Chem Process		May 52		110–114
Priestly, F. W.	Pharm Acta Helv	27	52		125–135
Sager, H.	Pharm Acta Helv	27	52		121
Fry, R. M.,	J Hygiene	49	Sept. 51		220–246
Greaves, R. I.					
Desh, J. B.,	IEC	42	50	7	1376–1380
Schultz, K.,	ref. Vacuum	I	51	1	59
Porsche, J. D.	Fraktionierung von Blutplasma				
Craight, J.	Brit J Cancer		49	3	250
Gye, W. E.,	Brit J Cancer		49	3	259
Begg, A. M.,					
Mann, I.,					
Craigie, J.					

2.5.8 Metallurgical industry

Hoffmann, W.,	Z Metallkde	47	56		231–239
Maatsch, J.	Heißentgasungsversuche an Bleischmelzen				
Goto, H.,	Sci Rep Res Inst Tohoku, Ser A	8	56	1	24–30
Suzuki, S.,					
Omma, A.					
Amoignon, M. J.	Vide		Jan. 55	49	1462–1469
Feichtinger, H.	Berg- u Hüttenm Mh	100	55	7/8	
Scheibe, W.	Vak Techn		54	3/4	67–71
Winkler, O.	Vak Techn		54	5	87–96
—	Light Metals	16	April 53		130
	ref. Vacuum	III	53	3	314
Griffith, G. B.,	Analyt Chem	25	July 53		1085–1087
Mallet, M. W.	ref. Vacuum	III	53	4	450
Horton, W. S.,	AEC-Rep Nr. KAPL 874				
Brady, J.	ref. Vacuum	III	53	3	333
Torrisi, A. F.,	Analyt Chem	23	June 51		928/29
Kernahan, J. L.	ref. Vacuum	I	51	4	333
Gulbransen, E.A.,	IEC	41	49		2762
Andrew, K. F.					
—	IEC	48	56		77A, 80A
Crites, G. J.	Vak Techn	5	56	8	176–179
Scheibe, W.	Gießerei	1	56		
	Schmelzen und Gießen von Titan				
—	Industrie-Anz	77	55	14	415
Adams, G. D.	Aviat Age	23	Jan. 55		66–73

Author	Journal	Volume	Month and Year	Issue No.	Page
Balluf, R. W., Seigle, L. L.	Acta Metallurg	3	55	2	170–177
Deuble, N. L.	Metal Progr	62	55	5	89–92
Dyrkaz, W. W.	Iron Age	176	55	17	75–77
Gilbert, H. L., Morrison, C. R.	Chem Engng Progr	51	55	7	320–325
Jenkins, I.	Nature	175	55	4450	276–279
Wigram, P. W.	Engineering	180	55	4671	172/73
—	VDI-Nachr	8	54	26	2
Baukloh, R.	Orion Warum Hochvakuummetallurgie?	9	54	19/20	
Benesowski, E.	Metall	8	54	9/10	378–385
Clark, H. T., Catlin, J. P., Gregg, W. E.	Mech Engng	76	54	9	716–720
Kroll, W. J.	Z Metallkde	45	54	2	67–75
McKechnie, R. K., Green, D. W., Moore, W. F.	J Metals	6	54	12	1364–1367
Mahla, E. M.	J Metals	6	54	12	1370/71
Miller, G. L.	Ind Chemist	30	54		577–588
Moore, J. H.	J Metals	2	54	12	1368/69
Osborn, A. B.	J Inst Met	83	54/55	P 5	185–188
Boettcher, A.	Forschung und Produktion		53		7–31
	ref. Vacuum	III	53	3	313
Brockmeier, K. H.	Gl und HVT	2	Sept. 53		234–240
Cook, M.	J Inst Met	82	53/54		93–106
	ref. Vacuum	III	53	4	451
Crites, J. G.	Metal Progr	63	May 53		161–166
	ref. Vacuum	III	53	3	332
Fast, J. D., Lips, E. M. H.	Metal Progr		Jan. 53		109–112
Scheibe, W.	Metall	7	53		751–757
—	Light Metals	15	Aug. 52		176/77
			Sept. 52		308/09
			Oct. 52		339–341
	ref. Vacuum	III	53	1	97
Bishop, T.	Metal Progr	61	52		75–81
Holland, L.	Electrodep Techn Soc Adv Copy	4	52		(12)
Pearsall, C. S.	US AEC — Publ MJT —	1104	52		(7)
Rengsdorf, G. W. P., Fischer, R.	J Metals	4	Febr. 52		157–160
Sully, A. H.,	J Inst Met	81	52/53		569–572
Brendes, E. A., Proven, A. G.	ref. Vacuum	III	53	4	469

Author	Journal	Volume	Month and Year	Issue No.	Page
Tolansky, S.	Electrodep Techn Soc Adv Copy	3	52		(11)
Hartmann, K., Schneider, M.	Metal Finish	49	Sept. 51		1843–1845
Kroll, W. J.	Vacuum	I	51	3	163–184
Riley, R. V.	Iron Coal Tr Rev	162	51		1083–1089
	ref. Vacuum	I	51	4	334
Fast, J. D.	Philips Techn Rev	II	Febr. 50		241–244
Flemming, H. W.	Metall	5	May 51	9/10	188
			July 50	13/14	
Navoy, T. M.	Metal Finish		Nov. 50		
Schlechten, A. W.	Engng Min J	151	July 50		71–73
	ref. Vacuum	I	April 51	2	
Spendlove, M.,	J Metals		Sept. 49		553–560
St. Clair, H. W.	ref. Vacuum	I	51	1	61

2.5.9 Food industry

Author	Journal	Volume	Month and Year	Issue No.	Page
Bochmann, G.	Die Müllerei Wassergehaltsbestimmung von Getreide		55		48/49
Bungartz, H.	Z VDI Getreidetrocknung	97	55	11/12	363–367
Hayes, H. P.	Refrig Engng	62	54	9	47–49
—	Food Investigation Board DSTR Special Rep 57		53		98–110
	Vacuum Trockenfleisch	III	53	2	216/17
Horneman, H., Hussong, R. W., Quam, S. N., Hammer, B. W.	US-Pat 2630388 ref. Vacuum Fettkonzentrate	III	53	3	335
Strashun, S. I., Taburt, W. F.	Food Engng Trocknen von Fruchtsäften	25	53		59
Carrier Corp.	Mech Engng Fruchtsaft	74	52	5	57
Coulter, S. T., Jennes, R.	J Dairy Sci Milch	35	Jan. 52		675
—	Food Engng	23	Febr. 51		125/26
	ref. Vacuum	I	51	4	318
Eskew, R. K.	IEC	43	Oct. 51		2397–2403
	ref. Vacuum	I	51	4	318
Gilmont, R.	US-Pat 2563233				
	ref. Vacuum	I	51	4	337
Jones, C. R.	J Sci Food Agric	2	Dec. 51		565–571
	ref. Vacuum	II	52	1	90
—	Food Industr	22	June 50		124
	ref. Vacuum	I	51	1	63
Cloud, H. R.	Food Industr	22	50		1891–1894

2.5.10 Pharmaceutical industry

Author	Journal	Volume	Month and Year	Issue No.	Page
Masch, L. W.	Chem Ing Techn	22	50		141
	ref. Vacuum Bedeutung der Molekulardestillation für die Pharmazeutische Industrie	I	51	2	
Chumbers, M., Nelson, J. W.	J Amer Pharm Ass	39	June 50		323–326
Kay, W. A.	Manufact Chem	22	May 51		188/89
	ref. Vacuum	I	51	4	332
Pupp, W.	Pharm Ind	15	53		162–164

2.5.11 Toy and jewelry industry

Author	Journal	Volume	Month and Year	Issue No.	Page
Gigerl, E.	Der Plastverarbeiter Dekorative Metallische Überzüge auf Kunststoffen durch Bedampfung im Hochvakuum		53	10	
Hiesinger, L.	Kunststoffe Praktische Erfahrungen bei Metallisieren von Kunststoffartikeln	43	53	12	547/48
Seiter, J. G.	Amer Electroplaters' Soc Proc	39	52		141–151
Jacques, T. A. J.	Vacuum	I	51	1	51

Miscellaneous applications

Author	Journal	Volume	Month and Year	Issue No.	Page
—	Chem Engng		June 53		134–136
	Vacuum Neue Anwendungsmöglichkeiten der Hochvakuumtechnik	III	53	3	310
Dunoyer, J. M.	Vide	10	55		42–49
Gooch, N.	Civ Engng Vakuumbeton	50	55		586
Haas, H.	Chem Ing Techn Anwendung von Vakuum in der Trocknungstechnik	27	55		357
—	Z Naturforschg Tiegelfreies Ziehen von Si-Einkristallen	9a	54		64
Geach, G. A.	Metallurgia	42	May 53		269–271
Harper, M. E.	Vacuum Schmelzen von nichtmetallischem Material im Lichtbogen	III	53	3	323
Gibaldo, F.	Chem Engng	60	53	5	235
Ziock, K.	Hausmitteilungen Jos. Schneider, Opt. Werke Kreuznach	5	53	7/8	

Author	Journal	Volume	Month and Year	Issue No.	Page
Gibbs,	Iron and Steel	25	52	4	141/42
Smith, A. J.	Neue Entwicklung auf dem Festland über das Schmelzen im Hochvakuum				
Laporte, H.	Chem Technik	4	52	8	
	Methoden der Fein- und Hochvakuumtechnik in Industrielaboratorien				
Leviant, I.	Structural Engr	30	Nov. 52		149–158
	Vakuumbeton				
Millen, T. S.	JSI Suppl	1	51		7–10
	Industrielle Vakuumanlagen				
Oetjen, G. W.	Techn Mitt	44	51	4	
	Industrielle Hochvakuumanlagen				
Subowitsch, S.	Hydrotechn Bau (russ.)	20	51	2	6–10
	ref. Vak Techn		55	8	160
	Vakuumbeton				
Blasco, E.	Anales de Mécanica y eletricidad Nr. 208				
Miranda, L.	Industrielle Anwendungen der Hochvakuumtechnik				
Walter, R.	Chem Ing Techn	21	49	3/4	49–88
	Neuere Entwicklung und Anwendung aus dem Gebiet der Hochvakuumtechnik				
Aitken, P. B.,	RSI	25	54	10	967
Boxall, H. L.,	Vakuumkalorimeter				
Cook, L. G.					
Fortescue, R. L.	Vacuum	III	53	1	47
Gold, N.	US-Pat 2636915				
	ref. Vacuum	III	53		314
	Dental-Bedarf				
Holland, L.,	Plastics Progr		53		361–380
Sutherland, N.	ref. Vacuum	III	53	3	331
Rowland, P. R.	Vacuum	III	53	2	136–150
Shover, K.,	RSI	24	53		652
Soled, J., Koch, R.,	Kristallziehen im Vakuum				
McDonald, A.,					
Sterns, C.					

Index